Respiratory Medicine
Series Editors: Sharon I.S. Rounds · Anne Dixon · Lynn M. Schnapp

Nishant Gupta
Kathryn A. Wikenheiser-Brokamp
Francis X. McCormack *Editors*

Diffuse Cystic Lung Diseases

We help the world breathe®
PULMONARY • CRITICAL CARE • SLEEP

Humana Press

Respiratory Medicine

Series Editors

Sharon I. S. Rounds
Alpert Medical School of Brown University
Providence, RI, USA

Anne Dixon
University of Vermont, Larner College of Medicine
Burlington, VT, USA

Lynn M. Schnapp
University of Wisconsin - Madison
Madison, WI, USA

More information about this series at http://www.springer.com/series/7665

Nishant Gupta
Kathryn A. Wikenheiser-Brokamp
Francis X. McCormack
Editors

Diffuse Cystic Lung Diseases

ATS
We help the world breathe®
PULMONARY • CRITICAL CARE • SLEEP

Humana Press

Editors
Nishant Gupta
University of Cincinnati
Cincinnati, OH
USA

Francis X. McCormack
University of Cincinnati
Cincinnati, OH
USA

Kathryn A. Wikenheiser-Brokamp
Cincinnati Children's Hospital
Medical Center
Cincinnati, OH
USA

University of Cincinnati
Cincinnati, OH
USA

ISSN 2197-7372 ISSN 2197-7380 (electronic)
Respiratory Medicine
ISBN 978-3-030-63364-6 ISBN 978-3-030-63365-3 (eBook)
https://doi.org/10.1007/978-3-030-63365-3

This Humana imprint is published by the registered company Springer Nature Switzerland AG
The registered company address is: Gewerbestrasse 11, 6330 Cham, Switzerland

Preface

The inspiration for this textbook derives from our firmly held belief that the diffuse cystic lung diseases (DCLDs) are a family of lung disorders with a unique differential diagnosis that is distinct from the interstitial lung diseases (ILDs) and worthy of separate classification. There are multiple differences in the epidemiology, presentation, disease mechanisms, and therapeutic approaches that also suggest the DCLDs belong in their own category. For instance, the DCLDs more commonly present with pneumothorax and typically affect younger age groups compared to the typical fibrotic ILDs. The etiopathogeneses of the DCLDs also differ from the ILDs in that they range from one-way check valve formation due to small airway inflammation to protease-mediated cystic lung destruction, in contrast to the epithelial senescence, repeated microinjury, and aberrant repair mechanisms that characterize the fibrotic ILDs. As a group, the DCLDs tend to progress more slowly than the fibrotic ILDs and have a better long-term prognosis. Lastly, the molecular insights that have emerged from the study of some DCLDs such as lymphangioleiomyomatosis (LAM) have resulted in powerful diagnostic biomarkers, such as VEGF-D, and exquisitely targeted, FDA-approved treatment options, such as sirolimus, that meaningfully impact patient lives. We submit that gratification derived from the proper diagnosis and treatment of DCLDs is among the most rewarding experiences in all of pulmonary medicine.

Our fascination with DCLDs first arose from our longstanding interest in LAM, the prototypical DCLD that typifies the progressive cystic remodeling of the pulmonary parenchyma that is common to this group of disorders. Through the LAM Foundation, we created a network of 36 LAM clinics around the United States to enable patients with LAM to receive care from expert clinicians close to home. Patients referred with suspected LAM often turned out to have other cystic lung diseases such as Birt-Hogg-Dubé syndrome (BHD), Sjögren's related cystic lung disease, or pulmonary Langerhans cell histiocytosis (PLCH), which captured our interest, and ultimately those disease communities asked to become part of our network and list our LAM clinics on their own websites. The LAM clinic network was expanded to include 28 international clinics, was rebranded as the Rare Lung Disease Consortium Clinic Network, and became the platform for clinical trials

including MILES and TRAIL for LAM and questionnaire-based studies for BHD and PLCH. As a group, we conduct conference calls and share case studies with one another quarterly. We routinely discuss novel and unclassifiable DCLDs, some of which will almost certainly emerge as new diseases as our collective experiences grow.

We are finding that insights from LAM are informing our understanding of the molecular pathogenesis in other rare lung diseases. Collaborative efforts by clinicians, physician-scientists, basic science investigators, and a highly engaged patient community led to our current understanding of LAM as a low-grade metastasizing neoplasm driven by mutations in tuberous sclerosis complex genes. This paradigm-shifting mechanism was most recently proven to also apply to PLCH, which has been shown to be an inflammatory neoplasm driven by MAPK mutations in circulating myeloid cells. We are curious about the possibility that cystic changes that occur in lymphoid interstitial pneumonia (LIP) may also be related to transforming mutations, given the occasional neoplastic conversion of that lesion to lymphoma.

The study of LAM has also informed our approach to the radiologic assessment of the DCLDs. When the diffusely distributed, smooth, round, and uniform cysts of LAM are compared to those of other DCLDs, we have noted important distinctions that can lead to the correct diagnosis. For instance, although cysts in follicular bronchiolitis (FB) and LIP are also diffusely distributed, they are often bordered by eccentric vessels and contain internal structures and septations, which are rare findings in LAM. Other DCLDs have distinctive craniocaudal cyst distributions and morphological cyst features. For instance, the cysts in PLCH tend to be upper lobe predominant and to exhibit irregular or bizarre shapes with varying wall thicknesses, while cysts in BHD are most commonly basilar and subpleural in distribution and oval/lentiform in shape compared to the round cysts seen in LAM. Our ability to assign the correct DCLD diagnosis based on high-resolution CT alone has improved over time, and we are often able to tailor the clinical evaluation of the patient to a few diagnoses in the differential based on radiologic features.

Although collectively LAM, BHD, PLCH, and FB/LIP constitute the majority of DCLDs that pulmonologists encounter in clinical practice, a variety of other disorders can present with cystic change in the lung. Together these diseases encompass varying pathophysiological mechanisms and differ in their clinical presentation and disease course. A targeted history and physical examination, survey of serologies and diagnostic biomarkers, and critical review of the HRCT form the cornerstone to establish the correct DCLD diagnosis in the majority of patients. The guiding principle in decisions regarding tissue confirmation is that the least invasive approach is preferred and that biopsy is likely required in less than 25% of DCLD cases.

This book begins with a chapter introducing the definition and classification of DCLDs. Subsequent chapters address the pathogenic mechanisms underlying pulmonary cyst formation and provide a detailed overview of the radiological and pathological features of DCLDs. The common as well as uncommon causes of DCLDs are comprehensively reviewed in individual chapters, as are the extrapulmonary manifestations and physiological consequences of atmospheric pressure changes on the DCLDs. The book culminates in a final chapter that presents a

practical algorithmic approach to diagnosis that progresses from least invasive to most invasive approaches. Our aspiration for this textbook is that it will provide a one-stop, comprehensive and integrated, clinical, radiologic, and pathologic overview of DCLDs that will be as useful to the clinical investigator as it is to the practicing clinician.

We express our sincere gratitude to all of the authors who contributed to this endeavor and remained patient with us throughout. We thank our publisher, Springer, for giving us a platform to express our ideas and experiences; our associate editor, Diane Lamsback, for keeping us on track; and our publishing editor, Margaret Moore, for her help with production. We are especially grateful to our DCLD patients who have taught us so much about this fascinating family of diseases and who inspire us on a daily basis. Finally, we thank our spouses, Christine, Tom, and Holly, who continue to offer us their unconditional love and support despite our work-related distractions, preoccupations, and obsessions.

Cincinnati, OH, USA Nishant Gupta
Cincinnati, OH, USA Kathryn A. Wikenheiser-Brokamp
Cincinnati, OH, USA Francis X. McCormack

Contents

List of Contributors

Roya Babaei-Jadidi, PhD Division of Respiratory Medicine, The University of Nottingham, Nottingham, UK

Misbah Baqir, MBBS Division of Pulmonary and Critical Care Medicine, Mayo Clinic, Rochester, MN, USA

John M. Carney, MD Department of Pathology, Duke University Medical Center, Durham, NC, USA

Debbie Clements, PhD Division of Respiratory Medicine, The University of Nottingham, Nottingham, UK

Adam G. Cole, MD Division of Pulmonary, Critical Care and Sleep Medicine, University of Kentucky College of Medicine, Lexington, KY, USA

Christian W. Cox, MD Department of Radiology, Mayo Clinic, Rochester, MN, USA

Thomas N. Darling, MD, PhD Department of Dermatology, Uniformed Services University of the Health Sciences, Bethesda, MD, USA

Gail H. Deutsch, MD Department of Pathology, University of Washington School of Medicine and Seattle Children's Hospital, Seattle, WA, USA

Daniel F. Dilling, MD Division of Pulmonary and Critical Care, Stritch School of Medicine, Loyola University Chicago, Chicago, IL, USA

Souheil El-Chemaly, MD Pulmonary and Critical Care Medicine, Department of Medicine, Brigham and Women's Hospital and Harvard Medical School, Boston, MA, USA

Nishant Gupta, MD, FCCP Division of Pulmonary, Critical Care and Sleep Medicine, University of Cincinnati College of Medicine, Cincinnati, OH, USA

Cincinnati Veterans Administration Medical Center, Cincinnati, OH, USA

Padraig E. Hawkins, MD, PhD Department of Respiratory Medicine, St. Vincent's University Hospital, Dublin, Ireland

Elizabeth P. Henske, MD Pulmonary and Critical Care Medicine, Department of Medicine, Brigham and Women's Hospital, Boston, MA, USA

Kristin B. Highland, MD, MSCR Respiratory Institute, Cleveland Clinic, Cleveland, OH, USA

Simon R. Johnson, DM, FRCP Division of Respiratory Medicine and Biomedical Research Centre, The University of Nottingham, Nottingham, UK

Robert M. Kotloff, MD Department of Pulmonary Medicine, Cleveland Clinic, Cleveland, OH, USA

Joanna E. Kusmirek, MD Department of Radiology, University of Wisconsin School of Medicine and Public Health, Madison, WI, USA

Augustine S. Lee, MD Mayo Clinic, Jacksonville, FL, USA

David A. Lynch, MB, BCh Department of Radiology, National Jewish Health, Denver, CO, USA

Cormac McCarthy, MD, PhD Department of Respiratory Medicine, St. Vincent's University Hospital, Dublin, Ireland

Francis X. McCormack, MD Division of Pulmonary, Critical Care and Sleep Medicine, University of Cincinnati College of Medicine, Cincinnati, OH, USA

Cristopher A. Meyer, MD Department of Radiology, University of Wisconsin School of Medicine and Public Health, Madison, WI, USA

Hilary Miller-Handley, MD Infectious Disease Division, University of Cincinnati College of Medicine, Cincinnati, OH, USA

Pediatric Infectious Disease Division, Cincinnati Children's Hospital Medical Center, Cincinnati, OH, USA

Joel Moss, MD, PhD National Heart, Lung, and Blood Institute, National Institutes of Health, Bethesda, MD, USA

Teng Moua, MD Division of Pulmonary and Critical Care Medicine, Mayo Clinic, Rochester, MN, USA

David J. Murphy, MB, BCh, BAO, MRCPI Department of Radiology, St. Vincent's University Hospital, Dublin, Ireland

Orla O'Carroll, MD Department of Respiratory Medicine, St. Vincent's University Hospital, Dublin, Ireland

Stephen J. Ruoss, MD Division of Pulmonary and Critical Care, Stanford University School of Medicine, Stanford, CA, USA

Jay H. Ryu, MD Division of Pulmonary and Critical Care Medicine, Mayo Clinic College of Medicine and Science, Rochester, MN, USA

Laura S. Schmidt, PhD Basic Science Program, Frederick National Laboratory for Cancer Research, Frederick, MD, USA

Urologic Oncology Branch, Center for Cancer Research, National Cancer Institute, National Institutes of Health, Bethesda, MD, USA

Kuniaki Seyama, MD, PhD Division of Respiratory Medicine, Juntendo University Faculty of Medicine and Graduate School of Medicine, Tokyo, Japan

Adrian Shifren, MBBCh Division of Pulmonary and Critical Care Medicine, Washington University School of Medicine, St. Louis, MO, USA

Abhishek Singla, MD Division of Pulmonary, Critical Care and Sleep Medicine, University of Cincinnati College of Medicine, Cincinnati, OH, USA

Maxwell L. Smith, MD Department of Pathology and Laboratory Medicine, Mayo Clinic Arizona, Scottsdale, AZ, USA

Alan George Smulian, MBBCh Infectious Disease Division, University of Cincinnati College of Medicine, Cincinnati, OH, USA

Cincinnati Veterans Administration Medical Center, Cincinnati, OH, USA

Angelo Taveira-DaSilva, MD, PhD National Heart, Lung, and Blood Institute, National Institutes of Health, Bethesda, MD, USA

Robert Vassallo, MD Department of Medicine, Mayo Clinic, Rochester, MN, USA

Kathryn A. Wikenheiser-Brokamp, MD, PhD Division of Pathology and Laboratory Medicine, Cincinnati Children's Hospital Medical Center, Cincinnati, OH, USA

Department of Pathology and Laboratory Medicine, University of Cincinnati College of Medicine, Cincinnati, OH, USA

Jie Zhang, MD Division of Pulmonary and Critical Care Medicine, Department of Medicine, Mayo Clinic College of Medicine and Science, Rochester, MN, USA

Chapter 1
Definition and Classification of Diffuse Cystic Lung Diseases

Abhishek Singla and Francis X. McCormack

Definition and Terminologies

The diffuse cystic lung diseases (DCLDs) are a diverse group of lung disorders characterized by the presence of multiple parenchymal lucencies of regular or irregular spherical shape, bordered by thin walls that form a well-defined interface with normal lung [1, 2]. At a conceptual level and for the purposes of this book, it is useful to distinguish the primary DCLDs from other diffuse lung diseases that can produce cystic change (or change that appears cystic) as part of secondary pathophysiologic process, such as emphysema or pulmonary fibrosis. In addition, we propose to define "multicystic lung diseases" that typify the DCLDs as those that produce more than ten identifiable cystic lesions on high-resolution computed tomography (HRCT), and "paucicystic lung diseases" as those that typically present with fewer than ten cysts, such as primary lung cancers and echinococcus. Five examples of prototypical DCLDs that present in a multicystic fashion are lymphangioleiomyomatosis (LAM), pulmonary Langerhans cell histiocytosis (PLCH), connective tissue-related follicular bronchiolitis (FB), Birt-Hogg-Dube syndrome (BHD), and light chain deposition disease (LCDD). Although often grouped with the interstitial lung diseases (ILDs), the differential diagnosis, pathophysiology, and presentation of the family of DCLDs are fundamentally distinct from the fibrotic lung disorders. The most common DCLDs more often affect younger rather than older adults, produce radiographic lucencies more often than densities, more often present with obstructive rather than restrictive physiology, are more commonly associated with pneumothorax, and as a group tend to be associated with slower progression and a better prognosis than the scarring lung diseases. Current thinking regarding the molecular pathophysiology of the ILDs also diverges from that of the

A. Singla (✉) · F. X. McCormack
Division of Pulmonary, Critical Care and Sleep Medicine, University of Cincinnati College of Medicine, Cincinnati, OH, USA
e-mail: abhishek.singla@uc.edu; frank.mccormack@uc.edu

N. Gupta et al. (eds.), *Diffuse Cystic Lung Diseases*, Respiratory Medicine,
https://doi.org/10.1007/978-3-030-63365-3_1

DCLDs, in that the former are commonly attributed to repeated lung micro-injury to the epithelium with impaired healing, while the latter are thought to result from destructive inflammatory processes that "dissolve" lung structures, check-valve driven overdistension, or dysregulated cell-cell adhesion. Unlike the ILDs, disease progression in the DCLDs tends to follow a slow and generally linear course, rather than one marked by acute exacerbations or a relapsing, remitting pattern, as is typical of nonspecific interstitial pneumonia (NSIP) and idiopathic pulmonary fibrosis (IPF). As with the ILDs, it is possible in some cases to be confident about the diagnosis based on clinical and imaging features without the need for tissue confirmation, and it is not always necessary to establish a certain diagnosis for disease that is mild, early, or very slowly progressive. It is important to be aware, however, that there are interventions that change disease course for at least two of the most common disorders, sirolimus for LAM and smoking cessation for PLCH, and that in some cases aggressive measures including bronchoscopic or surgical biopsy are indicated to reach a definitive diagnosis.

This introductory chapter focuses on the classification and differential of the diffuse cystic lung diseases.

Defining Cysts and Differentiating Them from Other Pulmonary Parenchymal Lucencies

Cysts should be differentiated from a variety of other air-filled intra-parenchymal lesions such as airspace dilation in emphysema, bullae, pneumatoceles, honeycombing, bronchiectasis, and cavities (Table 1.1). Cysts usually contain air and

Table 1.1 Cyst and mimics [1]

Cyst	Thin-walled (<2 mm), spherical parenchymal lucency interfaced with normal lung
Cavity	Gas-filled space within pulmonary consolidation, mass, or nodule, typically thick walled (>2 mm) and more irregularly shaped than cysts
Bulla	Spherical focal lucency, ≥1 cm in diameter, bounded by a thin wall (usually <1 mm). It is usually accompanied by emphysematous changes in the adjacent lung
Bleb	Cystic air space bounded by a thin wall adjacent to the visceral pleura, typically <1 cm in size
Emphysema	Permanently enlarged airspaces distal to the terminal bronchiole with destruction of alveolar walls. Usually without visible walls on CT
Pneumatocele	Approximately round, thin-walled, air-filled space in the lung. Most frequently caused by infections, trauma, or aspiration of hydrocarbon fluid and usually transient
Honeycombing	Clustered cystic air spaces, typically 3–10 mm in diameter but occasionally as large as 2.5 cm. Usually subpleural
Bronchiectasis	Localized or diffuse bronchial dilatation, usually resulting from chronic infection, proximal airway obstruction, or congenital bronchial abnormality

have a wall thickness of less than 2 mm, but they can occasionally contain fluid or solid material and wall thickness may vary. Pneumatoceles are true cysts, but these are usually transient and are most frequently caused by infection, trauma, or aspiration of liquid hydrocarbons. The term "honeycombing" refers to clusters of round 3- to 10-mm diameter lucencies, with 1- to 3-mm wall thickness that are often stacked on top of each other in layers [1]. It is usually subpleural, and associated with other features of pulmonary fibrosis such as traction bronchiectasis and reticulations, and as such, it is usually easily distinguished from the cystic change of the DCLDs. Bronchiectasis results in dilated, thick-walled bronchi, which can also appear cystic, and may be clustered in a manner that mimics DCLDs. It can be readily differentiated from cysts based on continuity of the dilated airspace with the airways on contiguous CT sections. Cavities are thick-walled (>2 mm) and are more irregularly-shaped than cysts. These can be found within a mass, nodule, or area of consolidation.

Differentiating DCLDs from Emphysema

Emphysema describes a group of disorders that produce airspace dilation and pulmonary parenchymal lucencies that are easily confused with the cysts that occur in DCLDs, and it is therefore prudent to enlist the help of an expert radiologist to exclude the diagnosis before embarking on a comprehensive DCLD evaluation. The most common form of pulmonary emphysema is centrilobular emphysema due to tobacco or biomass fuel exposure. The dilated airspaces in centrilobular emphysema are typically spherical or polygonal in shape, surrounded by compressed lung tissue and peri-lobular vessels rather than a well-defined wall [3] and often have internal structure such as interlobular septa or a "central dot," which represents a centrilobular artery coursing through the secondary pulmonary lobule [4]. Paraseptal emphysema involves the more distal part of the secondary pulmonary lobule, and usually presents as subpleural rows of elongated, thin-walled, air-filled structures. Alpha 1 antitrypsin deficiency is a heritable form of emphysema that is often associated with panlobular emphysema, which involves the destruction of the entire secondary pulmonary lobule, and loss of the distinction between affected and normal areas [5]. Over time, the radiographic appearance becomes one of diffuse hyperlucency, rather than of focal parenchymal lucencies. Bullae are considered to be focal emphysematous areas, and frequently abut areas of centrilobular or panlobular emphysema [1, 5]. Bullae are usually >1 cm in diameter but can vary in size, sometimes filling a large fraction of the hemithorax. Blebs are smaller in size (<1 cm) and often describe lesions that abut or are visible on the pleural surface, but use of this term is discouraged because the distinction based solely on an arbitrary size cut off is not particularly meaningful or useful [1].

Distinguishing Paucicystic Lung Disease from Multicystic Lung Disease Consistent with DCLD

A common clinical dilemma is determining the relevance of a few cysts discovered as an incidental finding on chest CT. The first consideration is whether they represent pathological versus non-pathological cysts. Pulmonary cysts apparent on chest CT can occur as part of aging-related changes of the lungs in nonsmoking individuals. Aging-related cysts are typically first seen in individuals after the age of 40 years [6], and increase in prevalence with age to 5% at 40–49 years and 13% at an age over 80 years [6]. The number of cysts that can be found on the CT of aging individuals rarely (<1%) exceed 4 [6]. Ryu et al. therefore proposed that the presence of four or more cysts is a reasonable threshold for the number of cysts that can be considered abnormal [7]. The Tuberous Sclerosis Alliance Consensus Guidelines suggest using >4 as the number of cysts that establish the diagnosis of LAM in a nonsmoking individual with tuberous sclerosis complex (TSC) [8], although this metric is entirely empiric, and European Respiratory Society guidelines suggest using >10 cysts as a cut off for diagnosing LAM in a patient with TSC [9].

Classification and Epidemiology

The DCLDs can be broadly classified according to underlying etiology as those associated with low-grade or high-grade metastasizing neoplasms, polyclonal or monoclonal lymphoproliferative disorders or plasma cell dyscrasias, infections, autoimmune or connective tissue disease, smoking, and congenital or developmental defects [2] (Table 1.2). However, as shown in Fig. 1.1**,** significant overlap exists among these etiologies. For instance, LCDD could be classified as a lymphoproliferative disorder, a plasma cell dyscrasia, or a low-grade neoplasm. The true prevalence of the DCLDs is poorly understood. Rough estimates for prevalence of LAM, BHD, and PLCH in the United States are in the neighborhood of a few persons per million, while for LCDD and FB the range is likely to be lower and higher, respectively. Although individually rare, collectively the DCLDs have a significant impact upon the population at large [10]. Lack of prospective natural history profiling or consensus guidelines for diagnosis and classification for most DCLDs further compound difficulties in ascertaining accurate, population-based epidemiological data for many of these rare disease [11]. For example, there is no widely accepted definition for how to classify lung disease in Sjögren's syndrome, a disorder that is associated with both interstitial and cystic changes. The prevalence and incidence data of some of the common causes of DCLDs are listed in Table 1.3.

Table 1.2 Classification of diffuse cystic lung diseases

- Neoplastic
  - *Low-grade malignancies*
    - Lymphangioleiomyomatosis – sporadic as well as associated with tuberous sclerosis complex
    - Histiocytosis
      - Pulmonary Langerhans cell histiocytosis
      - Non–Langerhans cell histiocytoses, such as Erdheim-Chester disease, Rosai-Dorfman disease
  - *High-grade malignancies*
    - Primary pulmonary neoplasms
      - Nonsmall cell carcinomas
      - Mesenchymal cystic hamartoma
      - Pleuropulmonary blastoma
      - Lymphoma
    - Sarcomas
      - Angiosarcomas
      - Osteosarcomas
      - Synovial cell sarcoma
      - Ewing sarcoma
      - Leiomyosarcoma
      - Rhabdomyosarcoma
      - Endometrial stromal sarcoma
      - Wilms tumor
      - Pineal teratoma
      - Other sarcomas
    - Metastatic epithelial tumors
      - Adenocarcinomas of the gastrointestinal and genitourinary tract
    - Systemic malignancies
      - Lymphoma
- Genetic/developmental/congenital
  - Birt-Hogg-Dubé syndrome
  - Phakomatoses – Cowden syndrome, neurofibromatosis, Proteus syndrome
  - Connective tissues diseases – Marfan syndrome, Ehlers-Danlos syndrome (type IV)
  - COPA syndrome
  - Down syndrome
  - Congenital pulmonary airway malformation, bronchopulmonary dysplasia, etc.
- Associated with lymphocytic infiltration, lymphoproliferative disorders, plasma cell dyscrasias
  - Lymphoid interstitial pneumonia
  - Follicular bronchiolitis
  - Castleman disease
  - Lymphomatoid granulomatosis
  - Amyloidosis
  - Light chain deposition disease
  - Hypersensitivity pneumonitis
- Infectious
  - *Pneumocystis jiroveci pneumonia*
  - Staphylococcal pneumonia
  - Recurrent respiratory papillomatosis
  - Endemic fungal diseases especially coccidioidomycosis
  - Paragonimiasis
  - Hydatid cysts (*Echinococcus*)
  - COVID-19 pneumonia

(continued)

Table 1.2 (continued)

Associated with interstitial lung diseases
Hypersensitivity pneumonitis
Desquamative interstitial pneumonia
Smoking-related
Pulmonary Langerhans cell histiocytosis
Desquamative interstitial pneumonia
Respiratory bronchiolitis/smoking-related cystic lung disease
Other/miscellaneous
Posttraumatic pseudocysts
Fire-eaters lung
Hyper IgE syndrome
Acute respiratory distress syndrome
Pulmonary alveolar microlithiasis
Cyst mimics
Emphysema/bullae
Alpha-1 antitrypsin deficiency
Bronchiectasis
Honeycombing seen in late stage scarring interstitial lung diseases

Modified from [2]

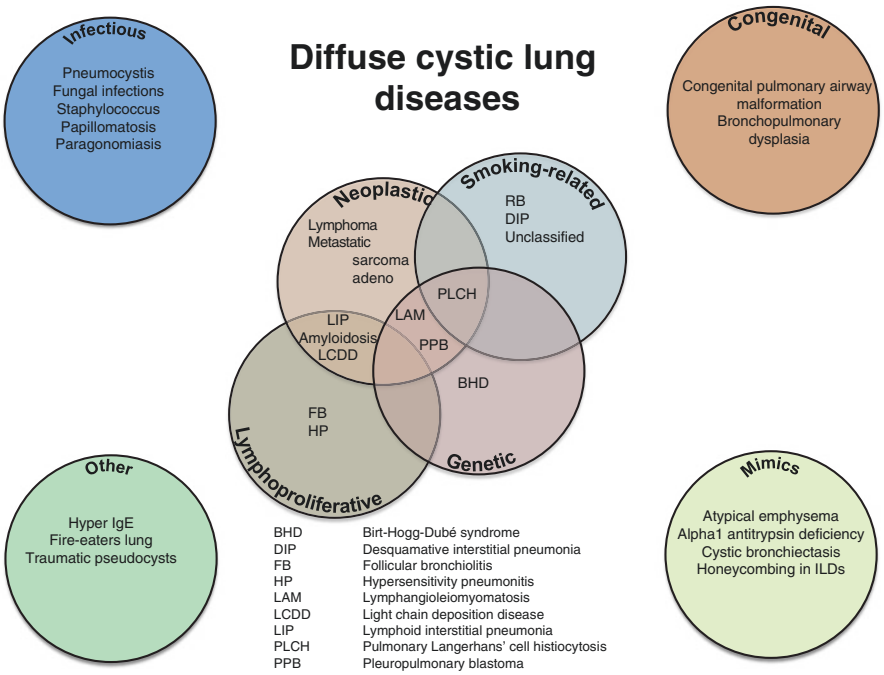

Fig. 1.1 Venn diagram of the diverse and overlapping etiologies of the DCLDs.

Table 1.3 Epidemiology of cystic lung disease

Diseases	Estimated prevalence (per million)	Estimated incidence (per million/ year)	Percentage with cysts
Lymphangioleiomyomatosis [15]	5 (3.4–7.8)[a]	0.2–0.3[a]	100%
Pulmonary Langerhans cell histiocytosis [18, 74, 75]	2.7[b]	NA	40–90%
Birt-Hogg-Dubé syndrome [27, 28, 76]	5[c]	NA	77–89%
Primary Sjögren syndrome [77–83]	608	69	10–46%
AL amyloidosis [37, 44, 84, 85]	40	10–15	<5%
Light chain deposition disease	NA	NA	<5%

AL amyloid light chain, *NA* not available
[a]in women
[b]Japanese data only in males
[c]European Data Only

Neoplastic Causes of DCLDs

Two forms of DCLD that are considered low-grade neoplasms are LAM and PLCH. LAM was historically considered to be an interstitial lung disease but has more recently been categorized as a perivascular epithelial cell (PEC) omatous mesenchymal tumor in the 2015 World Health Organization Classification of Lung Tumors [12]. LAM cells are clonal in origin, have growth-promoting biallelic mutations in the tuberous sclerosis genes, and exhibit metastatic and invasive behaviors [12, 13]. LAM can occur in sporadic form or can be inherited in up to 80% of women with TSC [14]. The estimated prevalence of sporadic LAM is reported to be approximately 5 (3.4–7.8) cases/million women with an incidence of 0.2–0.3/million women/year [15], but the true prevalence is likely greater. LAM has been recently reported to constitute 1% of the ILD population in Germany [16].

Pulmonary Langerhans cell histiocytosis is classified by the WHO as a lymphohistiocytic neoplasm. Recently, activating mutations of specific mitogen-activated protein kinases ($BRAF^{V600E}$ and others) have been found to be present in >50% of patients with PLCH [12]. PLCH most often occurs as a single organ disorder involving the lung but can also be associated with skin, bone, or pituitary involvement. Pulmonary involvement can also be seen in up to 15% of patients with systemic Langerhans cell histiocytosis, a disease that occurs more commonly in early childhood [17]. A national survey of hospital discharges conducted in Japan estimated the prevalence of PLCH to be 0.27 per 100,000 males and 0.07 per 100,000 females [18]. This is likely an underestimation as PLCH has been reported in up to 7% of patients with ILD [19, 20]. Pulmonary cysts can also occur in up to 12% of patients with non–Langerhans cell histiocytosis such as Erdheim-Chester disease [21, 22] and Rosai-Dorfman disease [23, 24].

A variety of high-grade primary and metastatic neoplasms can present with pulmonary cysts. These typically present as solid or subsolid nodules or masses that cavitate and evolve to become thin-walled cysts. Cystic changes can be seen in 1% to 4% of patients with nonsmall cell lung cancer (NSCLC) [25], with adenocarcinomas being the most common, followed by squamous cell carcinomas, and poorly differentiated carcinomas. The cystic lesions caused by primary epithelial lung tumors tend to be few in number and associated with irregular or thicker-walled cysts, consistent with a paucicystic pattern, and it is rare for this mode of neoplastic cystic remodeling in the lung to produce a multicystic pattern that closely mimics a prototypical DCLD such as LAM or BHD. In contrast, metastatic epithelial tumors from abdominal viscera (see Table 1.2) or the genitourinary tract can produce multiple cystic lesions, and pulmonary metastases from sarcomas can be associated with cystic or cavitary lesions in up to 25% of patients [26]. Indeed, metastatic endometrial stromal sarcomas and synovial sarcomas can be quite difficult to distinguish from the DCLDs. Pulmonary lymphomas are neoplasms that can also be associated with cystic lesions, but they are categorized under pulmonary lymphoproliferative disorders below.

DCLDs Caused by Genetic or Developmental Defects

Several DCLDs have a known genetic basis (Table 1.4). Those with mutations that drive cellular metastasis and invasion, such as LAM and PLCH, are listed with the neoplastic diseases above but obviously overlap with genetic causes. An example in which the cyst-causing mutations are thought to be present in resident lung cells, Birt-Hogg-Dubé syndrome, is a disorder that is associated with renal and hair follicle tumors, and cystic lung disease in approximately 77% to 89% of patients [27, 28]. BHD is caused by mutations in the folliculin (FLCN) gene encoding the tumor suppressor protein, folliculin, which plays a key role in intercellular adhesion. A variety of genetic disorders such as Marfan syndrome, Ehlers-Danlos syndrome (type IV), neurofibromatosis, Cowden syndrome, Proteus syndrome, COPA syndrome, and Down syndrome can be associated with pulmonary cysts. Cystic fibrosis was named for manifestations of fibrosis and cyst formation in the pancreas rather than the lung, where it manifests primarily as bronchiectasis [29]. Similarly, other genetic syndromes such as alpha-1 antitrypsin deficiency, cutis laxa [30], Williams-Beuren syndrome [31], and FLNA mutation [32] can also disrupt lung architecture but predominantly cause emphysema and/or bronchiectasis.

Cystic lung diseases that occur in children are commonly due to genetic mutations. Pleuropulmonary blastoma (PPB) is the most common primary pediatric lung tumor, which can manifest as a cystic neoplasm associated with mutations in the *DICER1* gene [33]. Congenital pulmonary airway malformation (CPAM) (formerly known as congenital cystic adenomatoid malformation), bronchogenic cysts, bronchopulmonary dysplasia, congenital lobar emphysema, congenital bulla, congenital bronchiectasis, and bronchial atresia can present as a DCLD in childhood. Many of these produce paucicystic rather than multicystic disease.

Table 1.4 Genetic syndromes associated with diffuse cystic lung diseases

Diseases	Associated genes	Category	Pulmonary features	Other clinical features
Syndromes associated with tumors				
Tuberous sclerosis complex [86]	*TSC1, TSC2*	AD	Pulmonary cysts (LAM) in 30–40% in females and 10–15% in men, MMPH, pleural effusions	Skin lesions, seizures, developmental delays, tumors in various organs
Birt-Hogg-Dubé syndrome [27, 28]	*FLCN*	AD	Pulmonary cysts in 77–89%	Cutaneous hamartomas, renal cysts, and renal cancers
Neurofibromatosis [87]	*NF-1, NF-2*	AD	Emphysema (25%), cysts (25%), ground-glass abnormality (37%), bullae (50%), and reticular abnormalities (50%)	Skin lesions, hamartomas, optic gliomas, and neurofibromas
Cowden syndrome [88, 89]	*PTEN*	AD	Cysts in 80%, nodules	Mucocutaneous and visceral hamartomas and an increased lifetime risk of thyroid, breast, endometrial, renal, and colon cancers
DICER1 syndrome [90]	*DICER1*	AD	Pleuropulmonary blastoma (PPB), pulmonary cysts	Thyroid gland neoplasia, ovarian tumors, and cystic nephroma
Syndromes of disordered connective tissue				
Marfan syndrome [91]	*FBN1*	AD	10% have apical blebs and bullae	Tall stature, joint laxity, aortic dilation, arachnodactyly, pectus excavatum, and ocular findings
Vascular Ehlers-Danlos syndrome [type IV] [92–94]	*COL3A1*	AD	Pulmonary blebs, cystic lesions, and hemorrhagic or fibrous nodules	Easy bruising, thin and translucent skin, and tissue fragility
Loeys-Dietz syndrome [95]	*TGFBR1, TGFBR2*	AD	Pneumothorax	Aortic dilation, skeletal deformities, bifid uvula, velvety, translucent skin

(continued)

Table 1.4 (continued)

Diseases	Associated genes	Category	Pulmonary features	Other clinical features
Cutis laxa [30]	*FBLN5, FBLN4, EFEMP2, LTBP4, ELN*	AD/AR	Emphysema; bronchiectasis	Loose, saggy, inelastic skin, hernias, visceral diverticula, joint hypermobility
FLNA mutation [32]	*FLNA*	XL	Cysts, emphysema	Intellectual disability, seizures, and cardiac valvular anomalies
Others				
Down syndrome [96, 97]	-	Chromosomal, trisomy 21	Cysts in 20–36%; usually subpleural, Sleep apnea	Dysmorphic features, developmental delay, congenital malformations
Proteus syndrome [98]	*AKT1*	Somatic mosaic mutation	Cysts in 9%	Asymmetric growth, nevi, vascular malformations
COPA Syndrome [99]	*COPA*	AD	Pulmonary cysts (80%), diffuse alveolar hemorrhage, and follicular bronchiolitis	Arthritis, proteinuria, nephropathy, autoantibodies
"Brain-thyroid-lung" syndrome [100]	*NKX2-1*	AD	Cysts, alveolar proteinosis, interstitial pneumonitis	Chorea, other neurological symptoms, hypothyroidism

AD autosomal dominant, *AR* autosomal recessive, *LAM* lymphangioleiomyomatosis, *MMPH* multifocal micronodular pneumocyte, *XL* X-linked

DCLDs Associated with Lymphoproliferative Disorders or Plasma Cell Dyscrasias

Benign lymphoproliferative disorders such as lymphoid interstitial pneumonia (LIP) and follicular bronchiolitis (FB) can be associated with cystic lung disease. Indeed, pulmonary cysts have been reported in up to 60% to 80% of patients with LIP and FB [34], but the presentation with diffuse pulmonary lucencies without significant interstitial change that is characteristic of the DCLDs is much less common. LIP is characterized by diffuse involvement of lung parenchyma with reactive pulmonary lymphoid tissue, whereas FB refers to a pattern of lymphoid follicular hyperplasia centered on airways, vessels, and interlobular septa consistent with a

lymphatic distribution, though most patients have elements of both pathologies. FB and LIP are typically associated with an underlying condition, most commonly autoimmune disorders such as Sjögren's syndrome, rheumatoid arthritis, systemic lupus erythematosus, or immunodeficiency states such as human immunodeficiency virus (HIV) and common variable immune deficiency; but they can also (rarely) be idiopathic. Malignant lymphoproliferative disorders including lymphomas can also cause cystic change in the lung [35, 36]. Moreover, marginal zone lymphoma of mucosa-associated lymphoid tissue (MALT) lymphoma can develop within pulmonary cysts and nodules in LIP, Sjögren's disease, amyloidosis, and LCDD [36–39]. Cysts have also been reported in other lymphoproliferative disorders such as Castleman disease [40, 41] and lymphomatoid granulomatosis [42], and about 13% of patients with chronic hypersensitivity pneumonitis (HP) [43].

Protein deposition diseases such as amyloid and light chain diseases can also present as DCLDs and are often associated with lymphoproliferative disorders or plasma cell dyscrasias. Amyloidosis is a group of diseases characterized by extracellular deposition of amyloid protein in an abnormal fibrillary fashion, which can occur in any organ including the lungs. The most common amyloid found in the lung is AL type in which deposition of protein derived from immunoglobulin light chains is associated with lung involvement in up to 28% of patients [44]. Pulmonary involvement in AL amyloid most commonly manifests as septal and parenchymal ground glass or nodular infiltrates, tracheobronchial disease, pleural disease, and mediastinal or hilar lymphadenopathy. Cysts in pulmonary amyloidosis occur less commonly; present in about 11% of patients, and are commonly associated with underlying connective tissue disorders, particularly Sjögren's syndrome [37]. Light chain deposition disease (LCDD) is similar to amyloidosis in that it presents with multisystem disease, but the light chain fragments do not form amyloid fibrils [45]. LCDD most commonly affects the kidneys but pulmonary predominant presentation as a DCLD has been reported, usually in association with Sjögren's syndrome, hematological malignancy (especially multiple myeloma), or lymphoma [38, 46, 47].

Smoking-Related DCLDs

There are two causes of smoking-related cystic lung disease, desquamative interstitial pneumonia (DIP) and respiratory bronchiolitis (RB). Cystic pulmonary change occurs in approximately one-third of DIP cases, usually on a background of diffuse ground-glass opacification [48]. Smoking can also lead to small airway destruction, producing a diffuse cystic pattern on chest imaging, often but not always in the setting of respiratory bronchiolitis [49–51].

ILDs Associated with Cystic Change

Cystic change in the lung has also been reported in ILDs that present with a component of fibrocystic parenchymal remodeling [52], such as sarcoidosis [53, 54] and pulmonary alveolar proteinosis (PAP) [55], IPF [56], and in late stages of pulmonary alveolar microlithiasis [57–59].

DCLDs Caused by Infections

Pneumocystis jiroveci pneumonia (PJP) is probably the most common infectious cause of DCLD and can occur in up to a third of patients [60, 61]. Cysts are much more common in PJP patients with co-existing HIV than in non-HIV PJP patients [62]. Diffuse pulmonary pneumatoceles can be seen with necrotizing bacterial infections, particularly those due to *Staphylococcus* and *Streptococcus*, and is primarily seen in children [63]. Certain parasites such as Echinococcus (hydatid cysts) and paragonimiasis are notorious for causing pulmonary cysts [64], usually in a paucicystic fashion. Respiratory papillomatosis primarily affects children and can cause cysts associated with nodules [65]. Cystic changes have recently been reported in up to 10% of patients with COVID-19 pneumonia [66]. A variety of infections such as lung abscesses, necrotizing pneumonias, septic pulmonary nodules, *Nocardia*, mycobacterial infections, and fungal pneumonias can produce radiolucencies that are usually more appropriately classified as cavities than cysts [67].

Other Causes of DCLDs

Posttraumatic pulmonary pseudocysts can occur after blunt chest trauma in up to 10% of patients, and these usually resolve over 1–6 months [68]. Accidental aspiration of petroleum derivatives during fire-eating demonstrations can also lead to development of cystic pattern on chest CT due to multiple pneumatoceles that may last for a few weeks to months [69]. Hyper-IgE syndrome (AD-HIES), formerly known as Job syndrome, is a autosomal dominant primary immunodeficiency condition characterized by markedly elevated serum IgE levels and multiple cutaneous and sinopulmonary infections that can result in pneumatoceles [70]. Subpleural cysts can also occur in patients with acute respiratory distress syndrome (ARDS), usually in late phase disease after prolonged ventilation [71]. Pulmonary vasculitidies such as granulomatosis with polyangiitis can result in cystic change, and rheumatoid nodules may cavitate and evolve to become cystic lung lesions.

Pulmonary Differential Diagnosis of Rare or Unusual Conditions

Establishing the diagnosis of a rare pulmonary disease or condition requires the formulation of a comprehensive differential diagnosis. None of us are familiar with all of the thousands of rare disorders that can present to our practices, and the correct diagnosis cannot be made if it is not considered. The history and physical exam are the cornerstones that provide the initial clues to nature of the underlying process. The CT scan of the chest has become the most useful imaging tool to develop the pulmonary differential diagnosis and pulmonary function testing can help to narrow the field by characterizing the nature of the pulmonary physiologic defect. Corroborative studies such as abdominal imaging for renal disease, serologies, sputum or pleural fluid analyses, transbronchial or surgical lung biopsy, and, most recently, genetic studies can help to establish a definitive diagnosis.

There are several resources available to obtain more information about the DCLDs. All the DCLDs meet the definition of rare or orphan diseases, whether based on the National Center for Accelerating Translational Research (NCATS) definition as a disorder with a prevalence of fewer than 200,000 affected individuals within the United States or the European ORPHANET definition of fewer than 1 in 2,000 people (www.orphanet.net) [72]. Based on the NCATs definition, there are approximately 25 million people in the United States afflicted with over 6,500 rare diseases [73]. The NCATs Genetic and Rare Disease Information Center maintains a web-based, searchable list of over 6,000 rare diseases with links to various information sources. The National Organization for Rare Diseases (www.raredisease.org) is a nongovernmental federation of organizations that seeks to expand recognition and treatment of individuals with these rare illnesses. There are several additional databases devoted to rare lung disorders, including the British Orphan Lung Disease (BOLD) register that was established in 2000 (www.britthoracic.org.uk/ClinicalInformation/RareLungDiseasesBOLD/tabid/110/Default.aspx); the British Pediatric Orphan Lung Disease (BPOLD) registry of 9 rare pediatric lung disorders in the United Kingdom (www.bpold.co.uk); and the Groupe d'Etudes et de Recherche sur les Maladies Orphelines Pulmonaires (GERM"O"P") in France (http://germop.univ-lyon1.fr/). In the United States, the NIH Rare Lung Disease Consortium (RLDC) was founded in 2003 with collaborating centers throughout the United States, Canada, and Japan. The RLDC has ongoing clinical trials and studies in several rare lung diseases including LAM, PAP, and PLCH. Several patient advocacy groups and registries provide education, support, and research funding missions for the DCLDs including the LAM Foundation (www.thelamfoundation.org), the Birt-Hogg-Dubé Foundation (www.bhdsyndrome.org), the Myrovlitis Trust (www.myrovlytistrust.org), the Pleuropulmonary Blastoma/DICER1 Registry

(https://www.ppbregistry.org), the Sjögren's Foundation (www.Sjogrens.org), and the Histiocytosis Association (www.histio.org).

The chapters that follow present the fascinating spectrum of DCLDs, many of which have provided extraordinary insight into the molecular pathogenesis of lung disease. The final chapter suggests an approach to the diagnosis and management of the DCLDs, using algorithms that favor the least invasive and most context appropriate options.

Key Learning Points

- Diffuse cystic lung diseases (DCLDs) represent a unique set of disorders characterized by thin-walled parenchymal lucencies that are fundamentally distinct from the typical interstitial lung diseases.
- While individually rare, DCLDs can be caused by a variety of neoplasms, polyclonal or monoclonal lymphoproliferative disorders or plasma cell dyscrasias, infections, autoimmune or connective tissue diseases, smoking, and genetic or developmental defects; and collectively the DCLDs occur in a substantial number of patients.
- Prototypical DCLDs that present in a multicystic fashion include lymphangioleiomyomatosis, pulmonary Langerhans cell histiocytosis (PLCH), connective tissue-related follicular bronchiolitis (FB), Birt-Hogg-Dubé syndrome (BHD), and light chain deposition disease (LCDD).
- A thorough knowledge of the presentation and key manifestations and radiographic patterns of the DCLDs is needed to arrive at an accurate diagnosis and differentiate these disorders from more common causes of parenchymal lucencies that can mimic the DCLDs such as emphysema, bronchiectasis, fibrotic lung disease, and cavitary lung diseases.

Conflicts of Interest The authors declare no conflicts of interest.

References

1. Hansell DM, Bankier AA, MacMahon H, McLoud TC, Muller NL, Remy J. Fleischner society: glossary of terms for thoracic imaging. Radiology. 2008;246(3):697–722.
2. Gupta N, Vassallo R, Wikenheiser-Brokamp KA, McCormack FX. Diffuse cystic lung disease. Part I. Am J Respir Crit Care Med. 2015;191(12):1354–66.
3. Takahashi M, Fukuoka J, Nitta N, Takazakura R, Nagatani Y, Murakami Y, et al. Imaging of pulmonary emphysema: a pictorial review. Int J Chron Obstruct Pulmon Dis. 2008;3(2):193.
4. Jawad H, Walker CM, Wu CC, Chung JH. Cystic interstitial lung diseases: recognizing the common and uncommon entities. Curr Probl Diagn Radiol. 2014;43(3):115–27.
5. Foster W Jr, Gimenez E, Roubidoux M, Sherrier R, Shannon R, Roggli V, et al. The emphysemas: radiologic-pathologic correlations. Radiographics. 1993;13(2):311–28.
6. Araki T, Nishino M, Gao W, Dupuis J, Putman RK, Washko GR, et al. Pulmonary cysts identified on chest CT: are they part of aging change or of clinical significance? Thorax. 2015;70(12):1156–62.

7. Ryu JH, Hartman TE, Torres VE, Decker PA. Frequency of undiagnosed cystic lung disease in patients with sporadic renal angiomyolipomas. Chest. 2012;141(1):163–8.
8. Northrup H, Krueger DA, Roberds S, Smith K, Sampson J, Korf B, et al. Tuberous sclerosis complex diagnostic criteria update: recommendations of the 2012 international tuberous sclerosis complex consensus conference. Pediatr Neurol. 2013;49(4):243–54.
9. Johnson SR, Cordier J-F, Lazor R, Cottin V, Costabel U, Harari S, et al. European Respiratory Society guidelines for the diagnosis and management of lymphangioleiomyomatosis. Eur Respir J. 2010;35(1):14–26.
10. Griggs RC, Batshaw M, Dunkle M, Gopal-Srivastava R, Kaye E, Krischer J, et al. Clinical research for rare disease: opportunities, challenges, and solutions. Mol Genet Metab. 2009;96(1):20–6.
11. McCarthy C, Gallego BL, Trapnell BC, McCormack FX. Epidemiology of rare lung diseases: the challenges and opportunities to improve research and knowledge. In: Rare diseases epidemiology: update and overview. New York: Springer; 2017. p. 419–42.
12. Travis WD, Brambilla E, Nicholson AG, Yatabe Y, Austin JH, Beasley MB, et al. The 2015 World Health Organization classification of lung tumors: impact of genetic, clinical and radiologic advances since the 2004 classification. Journal of thoracic oncology. 2015;10(9):1243–60.
13. McCormack FX, Travis WD, Colby TV, Henske EP, Moss J. Lymphangioleiomyomatosis: calling it what it is: a low-grade, destructive, metastasizing neoplasm. Am J Respir Crit Care Med. 2012;186(12):1210–2.
14. Cudzilo CJ, Szczesniak RD, Brody AS, Rattan MS, Krueger DA, Bissler JJ, et al. Lymphangioleiomyomatosis screening in women with tuberous sclerosis. Chest. 2013;144(2):578–85.
15. Harknett E, Chang W, Byrnes S, Johnson J, Lazor R, Cohen M, et al. Use of variability in national and regional data to estimate the prevalence of lymphangioleiomyomatosis. QJM. 2011;104(11):971–9.
16. Kreuter M, Herth F, Witt S, Kabitz H, Hagmeyer L, Hammerl P, et al. Diagnosis and management of patients with interstitial lung disease (ILD) in clinical practice in Germany: EXCITING-ILD registry. A43 ILD SCIENTIFIC ABSTRACTS: GENERAL: American Thoracic Society; 2018. p. A1670-A.
17. Haupt R, Minkov M, Astigarraga I, Schäfer E, Nanduri V, Jubran R, et al. Langerhans cell histiocytosis (LCH): guidelines for diagnosis, clinical work-up, and treatment for patients till the age of 18 years. Pediatr Blood Cancer. 2013;60(2):175–84.
18. Watanabe R, Tatsumi K, Hashimoto S, Tamakoshi A, Kuriyama T. Japan RFRGo. Clinicoepidemiological features of pulmonary histiocytosis X. Intern Med. 2001;40(10):998–1003.
19. Thomeer M, Demedts M, Vandeurzen K. Diseases VWGoIL. Registration of interstitial lung diseases by 20 centres of respiratory medicine in Flanders. Acta Clin Belg. 2001;56(3):163–72.
20. Kreuter M, Herth FJ, Wacker M, Leidl R, Hellmann A, Pfeifer M, et al. Exploring clinical and epidemiological characteristics of interstitial lung diseases: rationale, aims, and design of a nationwide prospective registry – the EXCITING-ILD registry. Biomed Res Int. 2015;2015:123–876.
21. Arnaud L, Pierre I, Beigelman-Aubry C, Capron F, Brun AL, Rigolet A, et al. Pulmonary involvement in Erdheim-Chester disease: a single-center study of thirty-four patients and a review of the literature. Arthritis Rheum. 2010;62(11):3504–12.
22. Brun A-L, Touitou-Gottenberg D, Haroche J, Toledano D, Cluzel P, Beigelman-Aubry C, et al. Erdheim-Chester disease: CT findings of thoracic involvement. Eur Radiol. 2010;20(11):2579–87.
23. Cartin-Ceba R, Golbin JM, Eunhee SY, Prakash UB, Vassallo R. Intrathoracic manifestations of Rosai–Dorfman disease. Respir Med. 2010;104(9):1344–9.
24. Gianella P, Dulguerov N, Arnoux G, Pusztaszeri M, Seebach JD. Thyroid Rosai-Dorfman disease with infiltration of IgG4-bearing plasma cells associated with multiple small pulmonary cysts. BMC Pulm Med. 2019;19(1):83.

25. Snoeckx A, Reyntiens P, Carp L, Spinhoven MJ, El Addouli H, Van Hoyweghen A, et al. Diagnostic and clinical features of lung cancer associated with cystic airspaces. J Thorac Dis. 2019;11(3):987.
26. Hoag JB, Sherman M, Fasihuddin Q, Lund ME. A comprehensive review of spontaneous pneumothorax complicating sarcoma. Chest. 2010;138(3):510–8.
27. Toro JR, Wei M-H, Glenn GM, Weinreich M, Toure O, Vocke C, et al. BHD mutations, clinical and molecular genetic investigations of Birt–Hogg–Dubé syndrome: a new series of 50 families and a review of published reports. J Med Genet. 2008;45(6):321–31.
28. Dal Sasso AA, Belém LC, Zanetti G, Souza CA, Escuissato DL, Irion KL, et al. Birt-Hogg-Dubé syndrome. State-of-the-art review with emphasis on pulmonary involvement. Respir Med. 2015;109(3):289–96.
29. Andersen DH. Cystic fibrosis of the pancreas and its relation to celiac disease: a clinical and pathologic study. Am J Dis Child. 1938;56(2):344–99.
30. Berk DR, Bentley DD, Bayliss SJ, Lind A, Urban Z. Cutis laxa: a review. J Am Acad Dermatol. 2012;66(5):842. e1–e17.
31. Wan ES, Pober BR, Washko GR, Raby BA, Silverman EK. Pulmonary function and emphysema in Williams–Beuren syndrome. Am J Med Genet A. 2010;152(3):653–6.
32. Sasaki E, Byrne AT, Phelan E, Cox DW, Reardon W. A review of filamin A mutations and associated interstitial lung disease. Eur J Pediatr. 2019;178(2):121–9.
33. Messinger YH, Stewart DR, Priest JR, Williams GM, Harris AK, Schultz KAP, et al. Pleuropulmonary blastoma: a report on 350 central pathology–confirmed pleuropulmonary blastoma cases by the international pleuropulmonary blastoma registry. Cancer. 2015;121(2):276–85.
34. Ichikawa Y, Kinoshita M, Koga T, Oizumi K, Fujimoto K, Hayabuchi N. Lung cyst formation in lymphocytic interstitial pneumonia: CT features. J Comput Assist Tomogr. 1994;18(5):745–8.
35. Honda O, Johkoh T, Ichikado K, Tomiyama N, Maeda M, Mihara N, et al. Differential diagnosis of lymphocytic interstitial pneumonia and malignant lymphoma on high-resolution CT. AJR Am J Roentgenol. 1999;173(1):71–4.
36. Hare S, Souza C, Bain G, Seely J, Frcpc GM, et al. The radiological spectrum of pulmonary lymphoproliferative disease. Br J Radiol. 2012;85(1015):848–64.
37. Zamora AC, White DB, Sykes A-MG, Hoskote SS, Moua T, Eunhee SY, et al. Amyloid-associated cystic lung disease. Chest. 2016;149(5):1223–33.
38. Baqir M, Moua T, White D, Eunhee SY, Ryu JH. Pulmonary nodular and cystic light chain deposition disease: a retrospective review of 10 cases. Respir Med. 2020;164:105896.
39. Jeong YJ, Lee KS, Chung MP, Han J, Chung MJ, Kim K-I, et al. Amyloidosis and lymphoproliferative disease in Sjögren syndrome: thin-section computed tomography findings and histopathologic comparisons. J Comput Assist Tomogr. 2004;28(6):776–81.
40. Peng M, Shi J, Feng R. Multicentric castleman disease as a rare cause of diffuse lung cysts. Am J Respir Crit Care Med. 2020;201(10):1292–3.
41. Huang H, Feng R, Li J, Song X, Li S, Xu K, et al. Castleman disease-associated diffuse parenchymal lung disease: a STROBE-compliant retrospective observational analysis of 22 cases in a tertiary Chinese hospital. Medicine. 2017;96(39):e8173.
42. Lee JS, Tuder R, Lynch DA. Lymphomatoid granulomatosis: radiologic features and pathologic correlations. Am J Roentgenol. 2000;175(5):1335–9.
43. Franquet T, Hansell DM, Senbanjo T, Remy-Jardin M, Müller NL. Lung cysts in subacute hypersensitivity pneumonitis. J Comput Assist Tomogr. 2003;27(4):475–8.
44. Berk JL, O'Regan A, Skinner M, editors. Pulmonary and tracheobronchial amyloidosis, Seminars in respiratory and critical care medicine. New York: Thieme; 2002;23(2):155–165.
45. Buxbaum JN, Chuba JV, Hellman GC, Solomon A, Gallo GR. Monoclonal immunoglobulin deposition disease: light chain and light and heavy chain deposition diseases and their relation to light chain amyloidosis: clinical features, immunopathology, and molecular analysis. Ann Intern Med. 1990;112(6):455–64.

46. Rho L, Qiu L, Strauchen JA, Gordon RE, Teirstein AS. Pulmonary manifestations of light chain deposition disease. Respirology. 2009;14(5):767–70.
47. Colombat M, Stern M, Groussard O, Droz D, Brauner M, Valeyre D, et al. Pulmonary cystic disorder related to light chain deposition disease. Am J Respir Crit Care Med. 2006;173(7):777–80.
48. Lynch DA, Travis WD, Muller NL, Galvin JR, Hansell DM, Grenier PA, et al. Idiopathic interstitial pneumonias: CT features. Radiology. 2005;236(1):10–21.
49. Gupta N, Colby TV, Meyer CA, McCormack FX, Wikenheiser-Brokamp KA. Smoking-related diffuse cystic lung disease. Chest. 2018;154(2):e31–e5.
50. Rowan C, Hansell DM, Renzoni E, Maher TM, Wells AU, Polkey MI, et al. Diffuse cystic lung disease of unexplained cause with coexistent small airway disease: a possible causal relationship? Am J Surg Pathol. 2012;36(2):228–34.
51. de Oliveira M, Dias O, Amaral A, do Nascimento E, Wanderley M, Carvalho C, et al. Diffuse cystic lung disease as the primary tomographic manifestation of bronchiolitis: a case series. Pulmonology. 2020; https://doi.org/10.1016/j.pulmoe.2020.01.006. S2531-0437(20)30024-6. Online ahead of print.
52. Akira M. Radiographic differentiation of advanced fibrocystic lung diseases. Ann Am Thorac Soc. 2017;14(3):432–40.
53. Kushima H, Ishii H, Kadota J-i, Watanabe K. Pulmonary sarcoidosis presenting with thin-walled small cysts. Intern Med. 2017;56(8):985–6.
54. Ogugua CS, Niazi M, Venkatram S. Sarcoidosis presenting with cystic lung lesions and autoimmune hemolytic anemia. J Bronchol Interven Pulmonol. 2008;15(4):273–6.
55. Kokosi M, Saunders P, Molyneaux PL, George PM, Margaritopoulos G, Kouranos V, et al. Lung cysts in pulmonary alveolar proteinosis. Eur Respir J. 2018;52(suppl 62):PA3019.
56. Ryu JH, Swensen SJ, editors. Cystic and cavitary lung diseases: focal and diffuse. Mayo Clin Proc. 2003;78(6):744–52. https://doi.org/10.4065/78.6.744.
57. Castellana G, Castellana G, Gentile M, Castellana R, Resta O. Pulmonary alveolar microlithiasis: review of the 1022 cases reported worldwide. Eur Respir Rev. 2015;24(138):607–20.
58. Deniz O, Ors F, Tozkoparan E, Ozcan A, Gumus S, Bozlar U, et al. High resolution computed tomographic features of pulmonary alveolar microlithiasis. Eur J Radiol. 2005;55(3):452–60.
59. Sumikawa H, Johkoh T, Tomiyama N, Hamada S, Koyama M, Tsubamoto M, et al. Pulmonary alveolar microlithiasis: CT and pathologic findings in 10 patients. Monaldi Arch Chest Dis. 2005;63(1):59.
60. Kuhlman JE, Kavuru M, Fishman EK, Siegelman SS. Pneumocystis carinii pneumonia: spectrum of parenchymal CT findings. Radiology. 1990;175(3):711–4.
61. Kanne JP, Yandow DR, Meyer CA. Pneumocystis jiroveci pneumonia: high-resolution CT findings in patients with and without HIV infection. Am J Roentgenol. 2012;198(6):W555–W61.
62. Hardak E, Brook O, Yigla M. Radiological features of pneumocystisjirovecii pneumonia in immunocompromised patients with and without AIDS. Lung. 2010;188(2):159–63.
63. Kunyoshi V, Cataneo DC, Cataneo AJM. Complicated pneumonias with empyema and/or pneumatocele in children. Pediatr Surg Int. 2006;22(2):186–90.
64. Kunst H, Mack D, Kon O, Banerjee A, Chiodini P, Grant A. Parasitic infections of the lung: a guide for the respiratory physician. Thorax. 2011;66(6):528–36.
65. Ruan SY, Chen KY, Yang PC. Recurrent respiratory papillomatosis with pulmonary involvement: a case report and review of the literature. Respirology. 2009;14(1):137–40.
66. Shi H, Han X, Jiang N, Cao Y, Alwalid O, Gu J, et al. Radiological findings from 81 patients with COVID-19 pneumonia in Wuhan, China: a descriptive study. Lancet Infect Dis. 2020;20(4):425–34.
67. Gafoor K, Patel S, Girvin F, Gupta N, Naidich D, Machnicki S, et al. Cavitary lung diseases: a clinical-radiologic algorithmic approach. Chest. 2018;153(6):1443–65.
68. Phillips B, Shaw J, Turco L, McDonald D, Carey J, Balters M, et al. Traumatic pulmonary pseudocyst: an underreported entity. Injury. 2017;48(2):214–20.

69. Gentina T, Tillie-Leblond I, Birolleau S, Faycal S, Saelens T, Boudoux L, et al. Fire-eater's lung: seventeen cases and a review of the literature. Medicine. 2001;80(5):291–7.
70. Chandesris M-O, Melki I, Natividad A, Puel A, Fieschi C, Yun L, et al. Autosomal dominant STAT3 deficiency and hyper-IgE syndrome molecular, cellular, and clinical features from a French national survey. Medicine. 2012;91(4):e1.
71. Gattinoni L, Caironi P, Pelosi P, Goodman LR. What has computed tomography taught us about the acute respiratory distress syndrome? Am J Respir Crit Care Med. 2001;164(9):1701–11.
72. Richter T, Nestler-Parr S, Babela R, Khan ZM, Tesoro T, Molsen E, et al. Rare disease terminology and definitions – a systematic global review: report of the ISPOR rare disease special interest group. Value Health. 2015;18(6):906–14.
73. Genetic and Rare Diseases Information Center FAQs About Rare Diseases. 2017. [Available from: https://rarediseases.info.nih.gov/diseases/pages/31/faqs-about-rare-diseases].
74. Vassallo R, Ryu JH, Schroeder DR, Decker PA, Limper AH. Clinical outcomes of pulmonary Langerhans'-cell histiocytosis in adults. N Engl J Med. 2002;346(7):484–90.
75. Kim HJ, Lee KS, Johkoh T, Tomiyama N, Lee HY, Han J, et al. Pulmonary langerhans cell histiocytosis in adults: high-resolution CT – pathology comparisons and evolutional changes at CT. Eur Radiol. 2011;21(7):1406–15.
76. Orphanet Reports Series. January 2020. [Available from: https://www.orpha.net/consor/cgi-bin/Education_Home.php?lng=EN].
77. Qin B, Wang J, Yang Z, Yang M, Ma N, Huang F, et al. Epidemiology of primary Sjögren's syndrome: a systematic review and meta-analysis. Ann Rheum Dis. 2015;74(11):1983–9.
78. Lohrmann C, Uhl M, Warnatz K, Ghanem N, Kotter E, Schaefer O, et al. High-resolution CT imaging of the lung for patients with primary Sjögren's syndrome. Eur J Radiol. 2004;52(2):137–43.
79. Watanabe M, Naniwa T, Hara M, Arakawa T, Maeda T. Pulmonary manifestations in Sjögren's syndrome: correlation analysis between chest computed tomographic findings and clinical subsets with poor prognosis in 80 patients. J Rheumatol. 2010;37(2):365–73.
80. Parambil JG, Myers JL, Lindell RM, Matteson EL, Ryu JH. Interstitial lung disease in primary Sjögren syndrome. Chest. 2006;130(5):1489–95.
81. Ito I, Nagai S, Kitaichi M, Nicholson AG, Johkoh T, Noma S, et al. Pulmonary manifestations of primary Sjogren's syndrome: a clinical, radiologic, and pathologic study. Am J Respir Crit Care Med. 2005;171(6):632–8.
82. Martínez-Balzano CD, Touray S, Kopec S. Cystic lung disease among patients with Sjögren syndrome: frequency, natural history, and associated risk factors. Chest. 2016;150(3):631–9.
83. Natalini JG, Johr C, Kreider M. Pulmonary involvement in Sjögren syndrome. Clin Chest Med. 2019;40(3):531–44.
84. Kyle RA, Larson DR, Kurtin PJ, Kumar S, Cerhan JR, Therneau TM, et al., editors. Incidence of AL amyloidosis in Olmsted County, Minnesota, 1990 through 2015. Mayo Clin Proc. 2019;94(3):465–71.
85. Quock TP, Yan T, Chang E, Guthrie S, Broder MS. Epidemiology of AL amyloidosis: a real-world study using US claims data. Blood Adv. 2018;2(10):1046–53.
86. Krueger DA, Northrup H, Roberds S, Smith K, Sampson J, Korf B, et al. Tuberous sclerosis complex surveillance and management: recommendations of the 2012 international tuberous sclerosis complex consensus conference. Pediatr Neurol. 2013;49(4):255–65.
87. Zamora AC, Collard HR, Wolters PJ, Webb WR, King T. Neurofibromatosis-associated lung disease: a case series and literature review. Eur Respir J. 2007;29(1):210–4.
88. Parvinian A, Cox CW, Hartman TE. Cowden syndrome: a cause of pulmonary cysts. J Thorac Imaging. 2018;33(6):W48–50.
89. Farooqi AO, Cham M, Zhang L, Beasley MB, Austin JH, Miller A, et al. Lung cancer associated with cystic airspaces. Am J Roentgenol. 2012;199(4):781–6.
90. Doros L, Schultz KA, Stewart DR, Bauer AJ, Williams G, Rossi CT, et al. DICER1-related disorders. GeneReviews®[Internet]. Seattle: University of Washington; 2014.

91. Karpman C, Aughenbaugh GL, Ryu JH. Pneumothorax and bullae in Marfan syndrome. Respiration. 2011;82(3):219–24.
92. Dowton SB, Pincott S, Demmer L. Respiratory complications of Ehlers-Danlos syndrome type IV. Clin Genet. 1996;50(6):510–4.
93. Kawabata Y, Watanabe A, Yamaguchi S, Aoshima M, Shiraki A, Hatamochi A, et al. Pleuropulmonary pathology of vascular Ehlers–Danlos syndrome: spontaneous laceration, haematoma and fibrous nodules. Histopathology. 2010;56(7):944–50.
94. Malfait F, Francomano C, Byers P, Belmont J, Berglund B, Black J, et al., editors. The 2017 international classification of the Ehlers–Danlos syndromes. Am J Med Genet C Semin Med Genet. 2017;175(1):8–26.
95. MacCarrick G, Black JH, Bowdin S, El-Hamamsy I, Frischmeyer-Guerrerio PA, Guerrerio AL, et al. Loeys–Dietz syndrome: a primer for diagnosis and management. Genet Med. 2014;16(8):576–87.
96. Gonzalez OR, Gomez IG, Recalde AL, Landing BH. Postnatal development of the cystic lung lesion of Down syndrome: suggestion that the cause is reduced formation of peripheral air spaces. Pediatr Pathol. 1991;11(4):623–33.
97. Biko DM, Schwartz M, Anupindi SA, Altes TA. Subpleural lung cysts in Down syndrome: prevalence and association with coexisting diagnoses. Pediatr Radiol. 2008;38(3):280–4.
98. Turner JT, Cohen MM Jr, Biesecker LG. Reassessment of the proteus syndrome literature: application of diagnostic criteria to published cases. Am J Med Genet A. 2004;130(2):111–22.
99. Tsui JL, Estrada OA, Deng Z, Wang KM, Law CS, Elicker BM, et al. Analysis of pulmonary features and treatment approaches in the COPA syndrome. ERJ Open Res. 2018;4(2):00017–2018.
100. Hamvas A, Deterding RR, Wert SE, White FV, Dishop MK, Alfano DN, et al. Heterogeneous pulmonary phenotypes associated with mutations in the thyroid transcription factor gene NKX2-1. Chest. 2013;144(3):794–804.

Chapter 2
Mechanisms of Lung Cyst Formation

Debbie Clements, Roya Babaei-Jadidi, and Simon R. Johnson

Introduction

Lung cysts are air-filled spaces with clearly defined walls of less than 2 mm surrounded by lung parenchyma. Cystic lung diseases are characterised by tens to many thousands of intrapulmonary cysts which may range in size from millimeters to centimeters. Whilst cysts are usually described as round, such as in lymphangioleiomyomatosis (LAM), in other conditions, including pulmonary Langerhans cell histiocytosis (PLCH), cysts are irregularly shaped and arise from airways rather than in the parenchyma. In this chapter, we shall describe the current thinking around mechanisms of cyst formation in four representative diseases, LAM, Birt-Hogg-Dubé syndrome (BHD), PLCH and protein deposition-related cystic lung disease. Whilst the initiating mechanism of pathologic destruction in LAM, BHD and PLCH is a consequence of dysregulation of specific molecular pathways driven by monogenic mutations, the mechanisms of parenchymal destruction in complex diseases including COPD have been more extensively studied and may help inform our understanding of mechanisms of parenchymal destruction in rare cystic lung diseases.

The lungs are constantly exposed to injurious inhaled stimuli throughout life. Loss of lung architecture by abnormally activated extracellular matrix-degrading proteases is considered to contribute to lung parenchymal destruction in a number of diseases including alpha 1 antitrypsin deficiency (A1ATD) and COPD. Whereas unregulated neutrophil elastase activity is the likely cause of degradation of elastin containing alveolar septae in A1ATD, the relationship between protease expression,

D. Clements · R. Babaei-Jadidi (✉)
Division of Respiratory Medicine, The University of Nottingham, Nottingham, UK
e-mail: debbie.clements@nottingham.ac.uk; roya.babei-jadidi@nottingham.ac.uk

S. R. Johnson
Division of Respiratory Medicine and Biomedical Research Centre, The University of Nottingham, Nottingham, UK
e-mail: simon.johnson@nottingham.ac.uk

N. Gupta et al. (eds.), *Diffuse Cystic Lung Diseases*, Respiratory Medicine,
https://doi.org/10.1007/978-3-030-63365-3_2

protease activation and parenchymal destruction in other lung diseases is less clear [1]. Further, inhibition of proteases in lung diseases, including metalloproteinase inhibition in COPD and doxycycline in LAM, has been largely unsuccessful as a treatment modality. This is likely due to the complexity of protease substrate profiles and interactions in vivo. For example, despite assignment to the family of the matrix-degrading proteases, the substrate profile of the macrophage-derived protease matrix metalloproteinase-12 (MMP-12) implicated in COPD includes a greater number of innate immune proteins, coagulation factors and bioactive molecules in addition to extracellular matrix (ECM) substrates [2]. A proteomic analysis of protease substrates in the airways of patients with COPD shows that during exacerbations, proteases cleave hundreds of non-ECM substrates, including a range of protease inhibitors, resulting in alterations in multiple protease classes and cleavage of multiple substrates [3]. Thus, inhibiting a single protease may have a large number of unpredictable and off-target effects.

Activation of proteases, reactive oxygen species and inflammatory pathways in response to a constant, low-level exposure to inhaled toxins and particles has the potential to cause lung injury. In healthy individuals, the resulting airway and alveolar damage is countered by homeostatic and repair mechanisms. Lung parenchymal loss is likely to be the result of either a large insult exceeding the lung's repair capacity, loss of protective and repair mechanisms or disease-related imbalance of injurious stimuli and repair mechanisms. Airway and alveolar progenitor/stem cells normally have the capacity to repair low-level insults caused by inhaled toxins. Repair mechanisms require the replication of alveolar or airway stem cells, including alveolar type II cells, to replace damaged alveolar epithelial type I cells. Alveolar repair is associated with the activation of alveolar developmental programs associated with lung development, particularly including the Wnt and platelet derived growth factor receptor (PDGFR) alpha pathways [4]. The replicative capacity of all cells, including alveolar stem cells, is limited. Repeated cell division and the cumulative burden of DNA mutations can predispose these cells to malignant transformation. Senescence, a mechanism which limits the absolute number of divisions made by a cell, not only protects against malignancies but also limits the capacity of tissue repair. Much of the current thinking around alveolar destruction in diseases including COPD is focused around loss of repair mechanisms by the combined impact of cell senescence and aging limiting the lungs repair capacity [5]. Senescence may occur as a response to multiple stimuli, including multiple cell divisions (replicative senescence), inflammation, reactive oxygen species or genetic activation of specific molecular pathways including the mechanistic target of rapamycin (mTOR) pathway. When alveolar epithelial cell replacement programmes are functional, the presence of an intact ECM scaffold is required for alveolar cell differentiation, survival and hence normal tissue repair.

In parenchymal lung destruction, the balance between disease-related lung injury and the efficiency of repair mechanisms is likely to maintain a balance between health, over-exuberant repair leading to fibrosis and parenchymal destruction resulting in cystic lung disease. In complex diseases such as COPD, multiple damage and repair pathways interact with each other to cause parenchymal lung damage. In rare

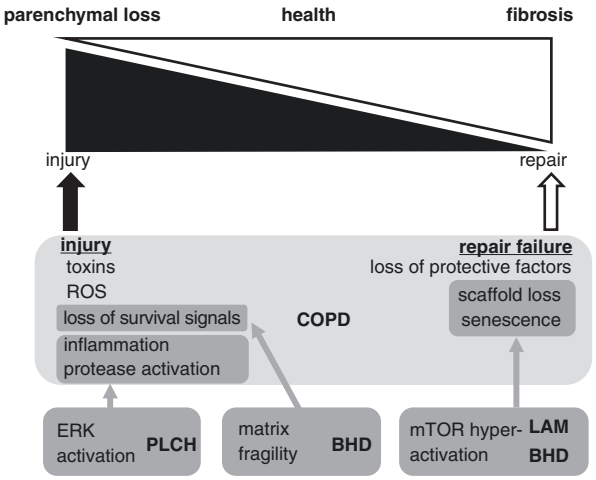

Fig. 2.1 Mechanisms of parenchymal damage in disease. Alveolar integrity in health is maintained by a balance between parenchymal injury and repair mechanisms. In diseases categorized by parenchymal destruction, including chronic obstructive pulmonary disease (COPD) or cystic lung diseases including pulmonary Langerhans cell histiocytosis (PLCH), Birt-Hogg-Dubé syndrome (BHD) or LAM, disease-related mechanisms result in parenchymal damage or impaired alveolar repair. In LAM, PLCH and BHD, specific molecular abnormalities result in primary derangement in specific processes, whereas polygenic/environmentally driven diseases such as COPD affect many injury and repair mechanisms simultaneously

diseases with a monogenic molecular etiology, disease mechanisms are likely to be more restricted to processes downstream of the molecular abnormality, such as mTOR activation in LAM and ERK activation in PLCH (Fig. 2.1).

Mechanisms of Cyst Formation in Specific Diseases

Lymphangioleiomyomatosis

Lymphangioleiomyomatosis (LAM) is a rare, multisystem disease that occurs predominantly in premenopausal women and involves the lungs and axial lymphatic system and is associated with the benign tumor angiomyolipoma [6]. It can occur sporadically (S-LAM) or in association with tuberous sclerosis complex (TSC-LAM).

The lungs and lymphatics of patients are infiltrated by smooth muscle-like ‘LAM cells’ leading to thin-walled pulmonary cysts and fluid-filled masses in the axial lymphatics [7]. Although LAM cells have a histologically benign phenotype, LAM is considered a low-grade malignant neoplasm by the World Health Organization (WHO). LAM cells can break away from the original lesion and spread (metastasize)

through the blood vessels or lymphatics [8] and can be detected in chylous fluid, blood and urine of patients [8]. The metastatic ability of the LAM cell was originally noted in patients with S-LAM, with identical *TSC2* mutations in the lung lesions and angiomyolipomas, and is also supported by the recurrence of LAM in the female recipient after transplantation from male donors [9]. Loss of lung function in patients with LAM is highly variable. The mean decline in forced expiratory volume in 1 second (FEV1) is 120–140 ml per year; some progress rapidly, whilst others can remain stable for many years [10].

LAM is often misdiagnosed and confused with other respiratory conditions [11]. Pulmonary function tests (PFTs) usually show an obstructive defect which can be mistaken for COPD or asthma. In 2010, the European Respiratory Society (ERS) laid down guidelines for the correct diagnosis of LAM and categorization of patients into three groups of definite LAM, probable LAM, and possible LAM based on high-resolution computed tomography scan (HRCT), clinical history and presentation, including a high level of the ymphangiogenic vascular endothelial vascular endothelial growth factor (VEGF-D) in the serum [12]. A recent study using unbiased serum proteomics identified that changes in vitamin D-binding protein (VTDB) and its gene, group-specific component (GC), are associated with LAM severity and survival [13].

Mechanistic target of rapamycin (mTOR) is a serine/threonine kinase member of the phosphoinositide 3-kinase (PI3K)-related kinase family. The protein is highly conserved from yeast to mammals [14]. mTOR is a component of two complexes: mTOR complex 1 (MTORC1) and mTOR complex 2 (MTORC2). mTOR complex 1 signalling regulates and promotes ribosomal biogenesis, protein synthesis, de novo lipid synthesis, nucleotide synthesis for DNA replication and proteasome-dependent proteolysis and suppresses catabolic pathways such as autophagy [15]. MTORC2 controls cell growth and survival by phosphorylating and activating PKA, PKG and other PKC protein kinases, including protein kinase B (AKT), which, when activated, facilitates proliferation, growth and cell survival [16].

Tuberous sclerosis complex (TSC) proteins 1 and 2 negatively control mTORC1. TSC is a heterotrimeric complex comprising TSC1 (hamartin), TSC2 (tuberin) and TBC1 domain family member 7 (TBC1D7) [17]. The protein complex is an upstream regulator of mTORC1, through GTPase-activating protein (GAP) for the Ras homolog enriched in the brain (Rheb) [18]. Mutations in the TSC1 and TSC2 genes result in the accumulation of active Rheb-GTP, stimulation of mTOR and phosphorylation of S6 kinase and eukaryotic initiation factor 4E-binding protein which lead to increased translation, cell size and proliferation. TSC-LAM is caused by mutations in either TSC1 or TSC2 genes [19]. In patients with TSC-LAM, a germline mutation is present in the TSC1 or TSC2 gene; the second mutation in the other TSC allele occurs in somatic tissue ('two-hit' mechanism) [20]. Although TSC-LAM occurs almost exclusively in women, it was also reported in 13%–38% of men with TSC [21, 22], albeit with milder severity than in women [22]. LAM also occurs in the absence of TSC germline mutation, in a sporadic form, caused by a somatic mutation in the TSC2 gene [23] with the second hit occurring after

conception in somatic tissues [24]. The pulmonary manifestations of S-LAM and TSC-LAM are nearly indistinguishable, although patients with TSC-LAM tend to be identified earlier, due to increased recognition of the disease or screening and as a consequence with better lung function in comparison to S-LAM [25]. S-LAM has only been reported in one male patient so far, and TSC gene mutations were not found in the lung tissue [26].

The origin of the LAM cell is unknown; these spindle-shaped cells usually can be found in small nodules in the lung in cyst walls and lymphatics. LAM cells express markers of both smooth muscle, including α-smooth muscle actin, vimentin and desmin, and melanocyte lineages such as gp100, MART-1, CD63 and PNL2 [27]. Due to the expression of melanocytic markers, it has been postulated that LAM cells originate from the neural crest [27]. LAM cells express estrogen and progesterone receptors [28] and belong to the perivascular epithelioid cell (PEC) group of neoplasms [29]. The LAM tumor is a complex structure containing TSC null ($TSC^{-/-}$) LAM cells and wild-type cells, including hyperplastic type II pneumocytes (positive for PE-10 or TTF-1 markers) lining the LAM nodules which appear to have apical microvilli and cytoplasmic projections [30]. Another cell type present in LAM lesions is the lymphatic endothelial cell, mostly located in intra-LAM lesion lymphatic channels [31]. It was once thought that the stromal cells within LAM nodules were primarily composed entirely of a single clone of LAM cells [32]; however, it is now believed that the predominant stromal cell is a wild-type fibroblast with functional TSC proteins [29] (Fig. 2.2). These LAM-associated fibroblasts (LAF) can be recruited by LAM-cell-derived chemokines, including stromal-cell-derived factor (SDF/CXCL12) and its cognate receptor, CXC chemokine receptor type 4 (CXCR4). The LAM cell/LAF association protects both cell types from apoptosis [29]. As in other 'tumor microenvironments', inflammatory cells are present in LAM nodules [33] including macrophages and mast cells [33, 34].

LAM is characterized by progressive lung cyst formation and lymphatic abnormalities. Cystic remodelling of the lung parenchyma leads to pneumothorax and

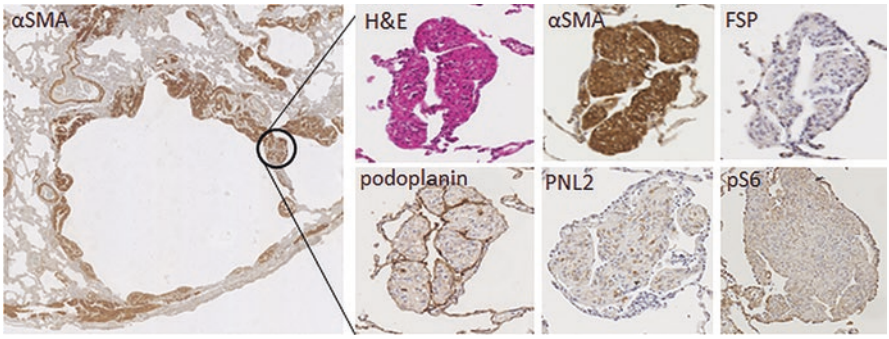

Fig. 2.2 LAM nodules contain multiple cell types. LAM nodules, identified by expression of α-smooth muscle actin (α-SMA), are composed of multiple cell types expressing fibroblast-specific protein (FSP), lymphatic endothelial cell markers (podoplanin), melanoma antigens (PNL2) on LAM cells and dysregulated mTOR signalling shown by phospho-S6 (pS6) staining

respiratory failure [5]. Lymphatic obstruction leads to chylous pleural effusions, chyloptysis and ascites [6, 35]. The mechanism of cyst formation is not fully understood, although the infiltrated LAM cells produce degrading proteases, including matrix metalloproteinases (MMP), which have been implicated in cyst formation [27]. MMPs are a family of zinc-dependent endopeptidases which were initially classified by their role in the basement membrane and ECM degradation during normal tissue turnover and growth [36]. The MMPs also have roles in the regulation of growth factors, chemokines and their ligands, inflammation and angiogenesis [37]. LAM nodules express MMP-2, MMP-9, MMP-1, MMP-13 and MMP-14 and have a reduced level of the MMP inhibitors Tissue Inhibitor of Metalloproteinases (TIMPs) 1 and 3 [38, 39]. Women with LAM have higher levels of MMP-2 in tissue and higher levels of MMP-9 in serum and urine than control women. However, two small clinical trials of the tetracycline antibiotic, doxycycline, an inhibitor of several MMPs, showed no benefit on lung function despite suppression of urinary MMP-9 [40–42], suggesting that doxycycline is not a suitable drug to target MMPs in LAM (or that other proteases are involved in the lung destruction) [42]. The serine protease plasmin is also increased in LAM lung, and its inhibitor, plasminogen activator inhibitor (PAI)-1, is reduced, as a consequence of high expression of serum response factor (SRF), leading to a proproteolytic environment [43].

Expression of another protease, cathepsin K, has been reported in LAM lesions and together with MMPs could contribute to degradation of collagen and elastic fibers [44]. Cathepsin K is a lysosomal cysteine protease predominantly expressed in osteoclasts as a bone-remodelling protease [45] and, unlike the MMPs and plasmin, is not present in normal lung parenchyma, but it is strongly expressed in LAM lung nodules [46]. Cathepsin K is also expressed in other PEComas [44], basal-like breast cancers [47] and tumor stromal fibroblasts and has been linked with tissue destruction in animal models of emphysema [48]. Cathepsin K is a potent elastase and collagenase but also selectively processes the inflammatory chemokines CXCL1, CXCL2, CXCL3, CXCL5 and CXCL8 which contain the ELR motif, enhancing their chemotactic activity and suggesting a potential role in inflammatory cell recruitment [49]. Cathepsin K is produced as a 329 amino acid proenzyme (pro-cathepsin K), which is cleaved into a 215 amino acid active form. This cleavage event requires low pH and generally occurs in the bone resorption lacunae [50]. In the cell, this usually takes place in lysosomes [51]. In tumor stroma, pro-cathepsin K activation is dependent on an acidic extracellular pH generated by membrane proton transporters, including carbonic anhydrases (CAs), vacuolar-type H^+-ATPases and sodium bicarbonate co-transporters [52]. In vitro, $TSC2^{-/-}$ cells acidify their environment in an mTOR-dependent fashion by utilizing aerobic glycolysis (also known as Warburg metabolism), which generates lactic acid, and increasing hydrogen ion exporter expression, resulting in low extracellular pH and cathepsin K activation [46]. Thus cell-cell interactions in the LAM microenvironment generate a

proteolytic environment [46]. Inhibition of cathepsin K or extracellular acidification may therefore represent a potential therapy for LAM. In bone and LAM lung, cathepsin K expression is partially mTOR dependent [53], raising the possibility that inhibition of mTOR and cathepsin K may have synergistic effects on lung destruction in LAM [46].

Whilst the mechanism underlying lung cyst formation in LAM is not completely understood, various disease-associated factors suggest that, in addition to mTOR activation, sex steroids and wild-type cells – including infiltrating immune cells – are involved in cyst formation. The gender and age prevalence of the disease implies the involvement of female hormones in LAM development and progression. Large epithelioid LAM cells around the periphery of nodules express progesterone and estrogen receptors [38]. High levels of estrogen during pregnancy [10] and in those using hormone replacement treatment [54] are associated with disease progression in LAM, and lower estrogen levels postmenopausally are associated with slower progression. In $TSC2^{-/-}$ 621–101 angiomyolipoma (AML)-derived cells, estradiol activates ERK2 to stimulate and to increase proliferation, migration and invasion [55]. Estrogen stimulation can also decrease apoptosis in vitro, by reducing BCL-2-interacting mediator of cell death (BIM) [56]. There is, however, no definite benefit of estrogen inhibition treatment in LAM [57–59]; two studies have shown no advantage in lung function decline and a significant reduction in the diffusing capacity of the lungs for carbon monoxide (DLCO) in the treated patients compared to untreated controls [10]. Moreover, the risk of osteoporosis and cardiovascular complication was increased by estrogen suppression [60]. A clinical trial of aromatase inhibition in postmenopausal women with LAM suggested that aromatase inhibition may be associated with slower loss of FEV1 [61].

The mTOR inhibitor rapamycin (sirolimus) has become the standard therapy for progressive lung disease in LAM [62]. Rapamycin treatment reduces loss of FEV1 in those treated although it may be less effective in those who have had the disease for longer and have lower pretreatment lung function [62], possibly consistent with mTOR-independent wild-type cells progressively accumulating and contributing to cyst formation.

Tumor-infiltrating immune cells, such as lymphocytes (TILs), play important roles in tumorigenesis [63]. The immune system targets and eliminates early malignant cells, but tumors may escape this immune surveillance by modulating T-cell activity. A number of checkpoints allow the immune system to promote protective immunity whilst reducing potentially harmful autoimmunity. Tumors can use these co-inhibitory pathways to prevent immune attack and elimination [63]. Targeting the immune checkpoint proteins or co-inhibitory receptors on T-cells, programmed cell death-1 (PD-1), PD-ligand 1 (PD-L1) and cytotoxic T-lymphocyte-associated antigen-4 (CTLA-4) is effective in cancer immunotherapy [63]. In models of LAM, blocking either PD-1 or CTLA-4 delays tumor growth and increases long-term survival in animals [64], suggesting a potential role of the immune system in disease progression and possibly cyst formation in LAM.

Pulmonary Langerhans Cell Histiocytosis

Pulmonary Langerhans cell histiocytosis (PLCH) (previously eosinophilic granuloma or histiocytosis X) is a rare interstitial lung disease characterised by peribronchiolar lesions containing activated dendritic cells (DC) known as Langerhans cells (LC). PLCH can occur in isolation or, less frequently, as part of a multisystem syndrome such as Hand-Schüller-Christian disease or Letterer-Siwe disease. The clinical presentation of the disease is variable and can include cough, dyspnea and pneumothorax but is sometimes an incidental finding. The disease may progress aggressively to respiratory failure although in many cases it exhibits a favorable clinical course, sometimes with spontaneous remission [65]. The precise prevalence of the disease is unknown because around one-quarter to one-third of affected individuals are asymptomatic, but it has been estimated at 0.27 and 0.07 per 100,000 in males and females, respectively [66].

PLCH can affect both children and adults; in adults, the disease generally affects both males and females aged 20–40 years and is almost exclusively associated with cigarette smoking or second-hand exposure to cigarette smoke [66–70]. On HRCT, nodules and cysts are evident in the upper and middle regions of the lung. The disease does not generally extend beyond the lung, but some patients develop bone or skin lesions or diabetes insipidus due to pituitary involvement. PLCH can be diagnosed histologically from a surgical lung biopsy or transbronchial biopsy. Langerin, CD1a and S-100 antibodies have been used in the immunohistochemical diagnosis of PLCH; langerin/CD207 and CD1a are specifically expressed in LCs [71], which also display characteristic cytoplasmic inclusions known as Birbeck granules.

Langerhans cells are a subtype of bone marrow-derived dendritic cell normally found in the skin and the bronchial epithelium. Their function in the lung is to process and present inhaled antigen followed by migration to the lymph nodes, where they mature and interact with T-cells, promoting immunity or tolerance [72]. Smoking causes Langerhans cells to accumulate in the lungs, along with T-lymphocytes, macrophages, monocytes and eosinophils. Loose nodules of inflammatory cells 1–10 mm in diameter appear in the lung parenchyma and around the bronchioles in the upper-middle portion of the lung. As the disease progresses, localized tissue destruction occurs, generating cysts.

Although the clinical presentation of the disease is not typical of cancer, there has been controversy as to whether PLCH is a reactive inflammatory disease or a neoplasm. Willman et al. and Yu et al. [73–75] demonstrated clonal proliferation of Langerhans cells in LCH, supporting the hypothesis that the disease is neoplastic. Weintraub et al. [76] subsequently showed elevated expression of p53, which can be associated with dysregulated proliferation in cancer.

A number of groups have reported frequent somatic BRAF mutations in LCH cells [77–80]. BRAF is a cytoplasmic protein kinase downstream of receptor tyrosine kinase signalling (RTK), between RAS and MEK in the MAPK signalling pathway (Fig. 2.3). The BRAF mutation most commonly found in PLCH (V600E, found in 35%–57% of patients [81]) is an activating mutation and causes dysregulated

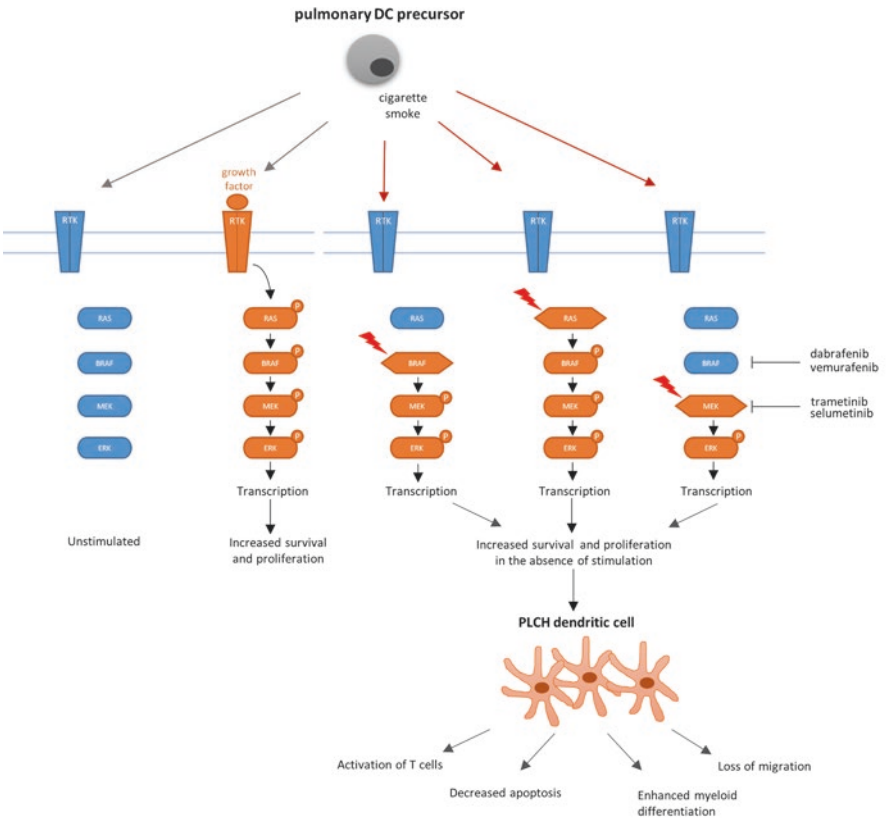

Fig. 2.3 BRAF/MEK/ERK pathway activation in Langerhans cell histiocytosis (LCH). Activating mutations in either BRAF, RAS or MEK result in ERK activation and increased dendritic cell survival and inactivation in LCH. The abnormal activation is potentially sensitive to inhibitors of BRAF and MEK

stimulation of this pathway. The RAS-RAF-MAPK pathway controls cell cycle regulation, cell proliferation, cell survival and apoptosis, and BRAF mutations have been implicated in several cancers, including melanoma, lymphoma and cancer of the lung, thyroid and colon [82–87]. Mutations in other members of the same signalling pathway have also been noted in PLCH, including *ARAF* [88], *MAP2K1* [89, 90] and *NRAS* [91]. In a recent study [91], 50% of PLCH lesions carried $BRAF^{V600E}$ mutations, and 40% harbored $NRAS^{Q61K/R}$ mutations, but these mutations were found in different clones of cells within the lesion. There is still controversy as to whether the presence of these mutations in PLCH unequivocally defines the disease as a neoplasm, given its ability to remit and resolve, but a neoplastic mechanism is currently favored.

Unlike systemic LCH, PLCH has a clear trigger, being strongly associated with cigarette smoking. Cigarette smoke causes recruitment of dendritic cells into the airways: this is an immediate response and has been observed in both mouse

models and human subjects. Cigarette smokers also display increased numbers of Langerhans cells in their airways and parenchyma [92]. Soler et al. showed a 30-fold increase in the number of Langerhans cells in the alveolar parenchyma of smokers compared with nonsmokers [93]. The mechanism by which this rapid recruitment occurs is currently unknown but may involve the induction by cigarette smoke of cytokines such as TNFα, GM-CSF, TGFβ and CCL20 in the airways.

It is not clear why LCs subsequently accumulate in the airways and parenchyma and do not migrate towards lymphoid organs. Cells harboring *BRAF* mutations could have a proliferative advantage leading to exuberant clonal expansion or could display decreased apoptosis as has been noted in melanoma and thyroid cancer. Consistent with this, Marchal et al. reported very low levels of apoptosis in the PLCH lesions and high levels of expression of the anti-apoptotic protein Bcl-xL [94]. Alternatively, trafficking to lymph nodes may be affected by altered expression of chemokine receptors such as CCR6 and 7. The consequence of this unusual behavior is the formation of characteristic PLCH lesions, containing LC, and a variable association of lymphocytes, eosinophils, fibroblasts, neutrophils, plasma cells and multinucleated giant cells. The phenotype of the LC in PLCH lesions is more typical of mature lymphostimulatory DC, normally found in the lymphoid organs, than the immature cells normally found in the airway – these mature cells are capable of initiating a significant immune response [95], perhaps targeted at the large numbers of T-cells expressing CD154 found in these lesions, a ligand expressed only transiently after T-cell activation.

As PLCH lesions are centered around bronchioles, the cysts may originate as enlarged bronchiolar lumina. However, Fukuda et al. performed a detailed ultrastructural study of early- and late-stage PLCH lung tissue and showed that around these PLCH lesions, alveolar epithelial cells show loss of attachment, their basement membranes become denuded and there is some evidence of myofibroblast recruitment in the alveolar lumen [96]. As the disease progresses, airspace enlargement and fibrosis continue; however, the contribution of S100-positive LC to the lesions appears to diminish (Fig. 2.4). There is evidence of elastin degradation and basement membrane fragmentation around the lesions leading to the suggestion that dysregulated ECM protease expression by stimulated immune cells is responsible for the breakdown of alveolar integrity. Colombat et al. also reported that almost all basement membranes had disappeared in the cyst walls and detected expression of MMP-1, MMP-2, MMP-9, MMP-12 and MMP-14 in the PLCH lesions [97]. Landi et al. used a proteomic approach to analyse bronchoalveolar lavage fluid protein composition of patients with PLCH and of controls and identified proteolytic fragments of plasma proteins (including kininogen-1 N fragments and haptoglobin) in PLCH, also suggestive of increased proteolytic activity [98].

As most patients with systemic PLCH carry a somatic activating mutation in one of the steps of the RAS-RAF-MEK-ERK signalling axis, this pathway offers an attractive target for therapy. Several reports indicate that, for patients with an identified $BRAF^{V600E}$ mutation, targeted therapy with vemurafenib, an inhibitor of mutated BRAF, results in significant clinical improvement. However, for many patients with PLCH, rather than systemic LCH, cessation of smoking results in resolution of the disease, although lung function may continue to decline as a consequence of other

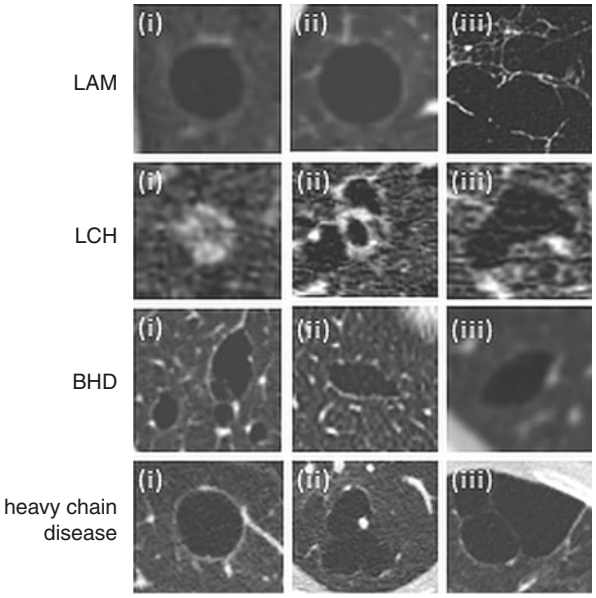

Fig. 2.4 Lung cyst morphology. Cyst characteristics among the DCLDs vary and are related to the mechanism of cyst formation. LAM: (i, ii) Cysts are round with smooth, thin walls, probably reflecting nodules surrounding cysts. Cysts are surrounded by normal lung parenchyma. (iii) In extensive disease, cysts abut each other with little intervening normal lung. PLCH: (i) Inflamed small bronchioles form nodules which cavitate. (ii) Cavitating nodules form thick-walled cysts in active disease. (iii) Later in the disease, cyst walls become less prominent, leaving irregularly shaped lucencies. BHD: (i, ii, iii) Lung cysts tend to be ovoid or lenticular, consistent with the concept that shearing mechanical forces tear apart weakened alveolar septae. Heavy chain disease: Lung cysts associated with abnormal immunoglobulin deposits have varying morphologies (i) and may be round or (ii, iii) multiple, septated and traversed by vessels

smoking-related diseases, such as COPD. Although no drug is currently approved for treatment of PLCH, cladribine, a drug used to treat the childhood form of LCH as well as multiple sclerosis and some forms of leukemia, has been reported to lead to improvement in some patients with progressive cystic PLCH [99, 100].

Birt-Hogg-Dubé Syndrome

Birt-Hogg-Dubé syndrome (BHD) is a rare autosomal dominant condition first described by Arthur R. Birt, Georgina Hogg and W. James Dubé in 1977 [101]. The disease has no gender predisposition and is characterised by fibrofolliculomas (benign hair follicle tumors) on the head and neck, pulmonary cysts and spontaneous pneumothorax. Patients with BHD can also develop kidney tumors and have a sevenfold higher lifetime risk of renal cell carcinoma than the general population [102, 103].

Pulmonary cysts in BHD are the first manifestation to appear, in early to mid adulthood, and can occur in the absence of skin and renal lesions [117]. They affect at least

80% of patients, although they do not usually affect lung function and do not appear to be correlated with smoking history. The cysts are usually small (<1 cm in diameter), bilateral, oval or irregularly shaped and in contact with the pleural surface [118–120]. They can contain residual alveolar septa, fibroblasts and lymphocytic infiltration, and it has been reported that epithelial cells, including alveolar type 2 (AT2) cells, line the cyst wall [121, 122]. Kumasaka et al. studied 229 cysts from 50 patients and noted that the cysts are bounded by normal alveolar walls, abut interlobular septa and do not contain unusual cells [118] or evidence of neoplasia (Figs. 2.4 and 2.5). In 24%–38%

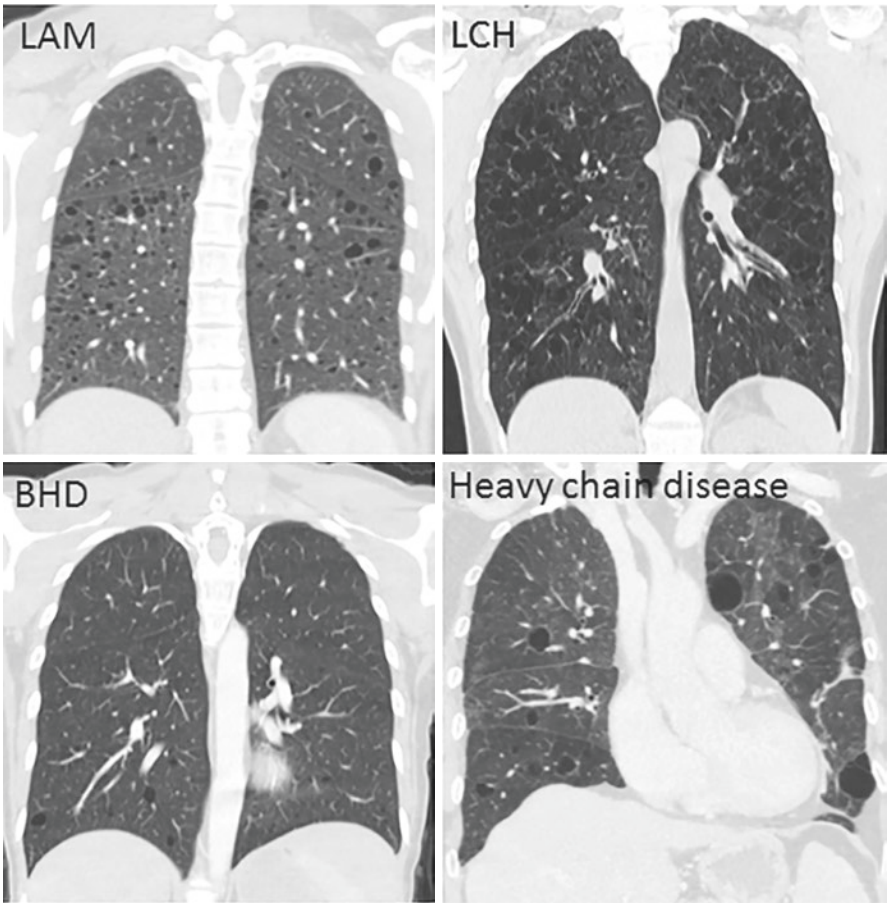

Fig. 2.5 Lung cyst distribution in specific diseases. Although speculative, it is likely that cyst distribution is related to etiology. LAM: LAM cells metastasize through blood and lymphatics resulting in a fairly homogenous distribution, perhaps tending to spare the extreme apices. PLCH: Cysts are more profuse in the upper and mid zones, perhaps reflecting the distribution of inhaled toxins including cigarette smoke. BHD: Cysts tend to be close to pleural surfaces in the mid and lower zones adjacent to the mediastinum where shear forces caused by respiratory motion are greater. Heavy chain disease: Lung cysts are randomly distributed in diffusely abnormal lung parenchyma consistent with diffuse plasma cell infiltration

of cases, they can rupture, causing pneumothorax, although the risk of pneumothorax decreases with increasing age.

In 2001, the affected locus was mapped by genetic linkage analysis to chromosome 17 and the following year to a novel gene, *folliculin (FLCN)* [104, 105], which encodes a 64 kDa cytoplasmic protein. Most of the over 100 *FLCN* mutations identified in patients with BHD are truncating, resulting in loss of function [106]. Folliculin behaves as a tumor suppressor; loss of heterozygosity of *folliculin* was identified in BHD renal lesions [107], and *flcn*+/− mice develop kidney tumors (but do not develop lung cysts) [108–110]. Fibrofolliculomas, however, do not necessarily show loss of heterozygosity of *FLCN* and may represent a haploinsufficiency phenotype [111]. The lung cysts do not appear to harbor any abnormal cells, but the high penetrance of this phenotype is also consistent with haploinsufficiency.

FLCN protein interacts with two proteins (folliculin-interacting proteins 1 and 2), which in turn interact with 5′-AMP-activated protein kinase (AMPK) [112–114]. AMPK responds to lowered intracellular ATP levels, for example, when nutrients are low, and has multiple downstream targets including the TSC2 protein, tuberin. Thus, LAM and BHD potentially share a common dysfunction – activation of the mTOR – containing protein complex MTORC1. Medvetz et al. also discovered a physical interaction between folliculin and an armadillo repeat-containing protein, plakophilin/p0071 [115]. Plakophilin is present in adherens junctions and interacts with E-cadherin, implicating loss of FLCN function in cell-cell adhesion [115, 116].

Folliculin has a widespread distribution [123]. In the lung, it is expressed in stromal cells, macrophages and alveolar epithelial cells. It has been proposed that loss of function of BHD in these cells leads to cyst formation [123], perhaps by disrupting interactions between affected epithelial and mesenchymal cells in the lung [121]. Goncharova et al. deleted *FLCN* in AT2 cells in mouse lung and demonstrated AT2 cell death, loss of epithelial integrity and airspace enlargement [124]. These effects appear to be mediated by AMPK; the knockout cells had decreased phospho-AMPK, and their phenotype was ameliorated by molecular or pharmacological AMPK activation.

As most cysts in BHD are subpleural, Graham proposed that loss of folliculin function specifically in the subpleural growth zone of the lung resulted in a failure of repair mechanisms in the lung parenchyma leading to structural fragility and cyst formation [117, 125]. Unlike PLCH and LAM, the absence of inflammation, unusual cell proliferation or unusual cell type associated with the cysts perhaps supports a model in which the alveolar septa are affected and rendered more fragile or less able to support cell adhesion. The ECM of the lung is deposited and maintained by lung fibroblasts, which express FLCN [123, 126], and is essential for attachment and survival of alveolar epithelial cells [127]. Hoshika et al. showed that lung fibroblasts from patients with BHD, carrying an identified FLCN mutation, showed reduced expression of the ECM protein fibronectin and transforming growth factor (TGF) beta, a growth factor which orchestrates tissue repair [126]. Knock down of FLCN in normal fetal lung fibroblasts showed a similar reduction in TGF beta and fibronectin expression. Both the BHD fibroblasts and the knockdown fibroblasts displayed lower chemotaxis and collagen gel contraction activity than wild-type

fibroblasts. As the BHD-derived fibroblasts still carried a functional copy of the FLCN gene, this is a phenotype associated with haplosufficiency. These data suggest that heterozygous BHD fibroblasts are deficient in key tissue repair functions, including the ability to migrate to the repair site and in the synthesis of matrix proteins.

There is no evidence that the cystic changes in BHD are a consequence of dysregulated proteolytic activity. Johannesma et al. [128] showed that cysts were stable in a 47-year-old male BHD patient for 44 months, with no increase in size or number. Further, most patients maintain normal lung function, and older patients are less likely to suffer pneumothorax, observations which are unlikely with a progressively destructive etiology. Johannesma et al. propose that loss of folliculin in the epithelial cells which have been reported to line the cysts increases cell-cell adhesion, consistent with the observations of Medvetz et al. [115, 128]. This leaves the cells less able to stretch, and under stress, the integrity of the epithelial layer is lost at its weakest point causing rupture. In this paradigm, small cysts coalesce into larger ones by rupture of the intervening septum, whilst subpleural cysts rupture into the pleural space causing pneumothorax. The idea that stretch-induced stress, combined with abnormal cell adhesion, is the causative agent in BHD lung cysts has been termed the 'Stretch hypothesis' [115, 128–130] and is consistent with the uneven spatial distribution of the cysts in BHD, where mechanical forces in the lungs may be greater in promoting cyst formation in the subpleural region.

Protein Deposition–Associated Lung Cysts

A number of diseases associated with paraprotein formation have been associated with cystic change in the lung, including light chain deposition disease (LCDD), myeloma, lymphoma, Waldenstrom macroglobulinemia and heavy chain deposition (see Figs. 2.4 and 2.5) [131]. LCDD is a rare disease, first described in 1976 by Randall et al. in two patients with renal disease [132]. LCDD is associated with overproduction of immunoglobulin light chains by plasma cells. The disease predominantly occurs in middle age and is twice as common in men [133], and around 75% of patients with LCDD have multiple myeloma or less commonly another lymphoproliferative disease, such as Waldenstrom macroglobulinemia or B-cell lymphoma. Patients with LCDD develop nonfibrillar, amorphous, eosinophilic proteinaceous deposits in multiple organs. Unlike amyloidosis, these protein deposits do not stain with Congo red and are composed of monotypic immunoglobulin light chains. The kidneys are the most commonly affected organ, but lesions can also occur in the liver, heart, small intestine, spleen, skin, nervous system and bone marrow; the lung is very rarely affected [134–136].

The initial reports of pulmonary LCDD (PLCDD) [137–142] described nodular light chain deposits in the lung. Later reports included other pulmonary features: cysts, airway involvement and bronchiectasis. The nodular form of PLCDD can be asymptomatic, but PLCDD can also take a more diffuse form, with a poor prognosis.

LCDD may rarely occur in an isolated pulmonary form without evidence of systemic B-cell proliferation. Colombat described three patients aged 28–33 years with a distinct severe cystic pulmonary phenotype associated with diffuse kappa light chain deposits but no renal manifestations of LCDD [143]. These patients were younger than typical LCDD patients, and their disease had progressed to respiratory failure. The cysts did not recur after the patients received a bilateral lung transplant, and blood and bone marrow examinations of these patients did not detect clonal plasma cell proliferation. The authors named this manifestation of LCDD *cystic lung related to LCDD* or CL-LCDD, and to date, there have been fewer than ten reports of this form of the disease. Colombat et al. demonstrated degradation of elastin fibers in alveoli, small airways and vessels in CL-LCDD and, to a lesser extent, loss of fibrillar and basement membrane collagens [97]. The authors proposed that macrophages accumulate in the vicinity of the light chain deposits and secrete an array of elastolytic and collagenolytic MMPs. Using in situ zymography, a technique which reveals localised proteolytic activity, strong gelatinolytic activity, consistent with high expression of MMP-2 and MMP-9, was detected in the vicinity of the light chain deposits.

Key Learning Points

- Cyst formation occurs when the balance of injurious environmental- and disease-related stimuli exceeds the repair capacity of the lung parenchyma.
- Dysregulation of discrete and specific signalling pathways, usually as a consequence of single gene mutations, induces injurious stimuli in rare cystic lung diseases.
- Disease-specific mechanisms causing lung damage include activation of the protease cathepsin K in lymphangioleiomyomatosis (LAM) that likely results in loss of extracellular matrix architecture, and defects in extracellular matrix attachment and repair capacity downstream of the folliculin gene in Birt-Hogg-Dubé syndrome (BHD).
- Rare diseases may share pathologic mechanisms with common diseases such as chronic obstructive pulmonary disease (COPD). mTOR-driven senescence in COPD limits alveolar repair, and mTOR-driven senescence may also contribute to cyst formation in LAM.

References

1. Taggart C, Mall MA, Lalmanach G, Cataldo D, Ludwig A, Janciauskiene S, et al. Protean proteases: at the cutting edge of lung diseases. Eur Respir J. 2017;49(2):1501200.
2. Bellac CL, Dufour A, Krisinger MJ, Loonchanta A, Starr AE, Auf dem Keller U, et al. Macrophage matrix metalloproteinase-12 dampens inflammation and neutrophil influx in arthritis. Cell Rep. 2014;9(2):618–32.
3. Mallia-Milanes B, Dufour A, Philp C, Solis N, Klein T, Fischer M, et al. TAILS proteomics reveals dynamic changes in airway proteolysis controlling protease activity and innate immunity during COPD exacerbations. Am J Physiol Lung Cell Mol Physiol. 2018;315(6):L1003–L1014.

4. Chen F, Fine A. Stem cells in lung injury and repair. Am J Pathol. 2016;186(10):2544–50.
5. Birch J, Barnes PJ, Passos JF. Mitochondria, telomeres and cell senescence: implications for lung ageing and disease. Pharmacol Ther. 2018;183:34–49.
6. McCormack FX, Travis WD, Colby TV, Henske EP, Moss J. Lymphangioleiomyomatosis: calling it what it is: a low-grade, destructive, metastasizing neoplasm. Am J Respir Crit Care Med. 2012;186(12):1210–2.
7. Johnson SR, Taveira-DaSilva AM, Moss J. Lymphangioleiomyomatosis. Clin Chest Med. 2016;37(3):389–403.
8. Crooks DM, Pacheco-Rodriguez G, DeCastro RM, McCoy JP Jr, Wang JA, Kumaki F, et al. Molecular and genetic analysis of disseminated neoplastic cells in lymphangioleiomyomatosis. Proc Natl Acad Sci U S A. 2004;101(50):17462–7.
9. Karbowniczek M, Astrinidis A, Balsara BR, Testa JR, Lium JH, Colby TV, et al. Recurrent lymphangiomyomatosis after transplantation: genetic analyses reveal a metastatic mechanism. Am J Respir Crit Care Med. 2003;167(7):976–82.
10. Johnson SR, Tattersfield AE. Decline in lung function in lymphangioleiomyomatosis: relation to menopause and progesterone treatment. Am J Respir Crit Care Med. 1999;160(2):628–33.
11. Clements D, Chang YCW, Johnson SR. Lymphangioleiomyomatosis: bench to bedside. European Respiratory Monograph. 2009;46:176–207.
12. Seyama K, Kumasaka T, Souma S, Sato T, Kurihara M, Mitani K, et al. Vascular endothelial growth factor-D is increased in serum of patients with lymphangioleiomyomatosis. Lymphat Res Biol. 2006;4(3):143–52.
13. Miller S, Coveney C, Johnson J, Farmaki AE, Gupta N, Tobin MD, et al. The vitamin D binding protein axis modifies disease severity in Lymphangioleiomyomatosis. Eur Respir J. 2018;9(13993003):00951–2018.
14. Kristof AS. mTOR signaling in lymphangioleiomyomatosis. Lymphat Res Biol. 2010;8(1):33–42.
15. Saxton RA, Sabatini DM. mTOR Signaling in growth, metabolism, and disease. Cell. 2017;168(6):960–76.
16. Sarbassov DD, Guertin DA, Ali SM, Sabatini DM. Phosphorylation and regulation of Akt/PKB by the rictor-mTOR complex. Science. 2005;307(5712):1098–101.
17. Dibble CC, Elis W, Menon S, Qin W, Klekota J, Asara JM, et al. TBC1D7 is a third subunit of the TSC1-TSC2 complex upstream of mTORC1. Mol Cell. 2012;47(4):535–46.
18. Nellist M, Sancak O, Goedbloed MA, Rohe C, van Netten D, Mayer K, et al. Distinct effects of single amino-acid changes to tuberin on the function of the tuberin-hamartin complex. Eur J Hum Genet. 2005;13(1):59–68.
19. Cudzilo CJ, Szczesniak RD, Brody AS, Rattan MS, Krueger DA, Bissler JJ, et al. Lymphangioleiomyomatosis screening in women with tuberous sclerosis. Chest. 2013;144(2):578–85.
20. Carsillo T, Astrinidis A, Henske EP. Mutations in the tuberous sclerosis complex gene TSC2 are a cause of sporadic pulmonary lymphangioleiomyomatosis. Proc Natl Acad Sci U S A. 2000;97(11):6085–90.
21. Adriaensen ME, Schaefer-Prokop CM, Duyndam DA, Zonnenberg BA, Prokop M. Radiological evidence of lymphangioleiomyomatosis in female and male patients with tuberous sclerosis complex. Clin Radiol. 2011;66(7):625–8.
22. Ryu JH, Sykes AM, Lee AS, Burger CD. Cystic lung disease is not uncommon in men with tuberous sclerosis complex. Respir Med. 2012;106(11):1586–90.
23. Astrinidis A, Khare L, Carsillo T, Smolarek T, Au KS, Northrup H, et al. Mutational analysis of the tuberous sclerosis gene TSC2 in patients with pulmonary lymphangioleiomyomatosis. J Med Genet. 2000;37(1):55–7.
24. Juvet SC, McCormack FX, Kwiatkowski DJ, Downey GP. Molecular pathogenesis of lymphangioleiomyomatosis: lessons learned from orphans. Am J Respir Cell Mol Biol. 2007;36(4):398–408.

25. Ryu JH, Moss J, Beck GJ, Lee JC, Brown KK, Chapman JT, et al. The NHLBI lymphangioleiomyomatosis registry: characteristics of 230 patients at enrollment. Am J Respir Crit Care Med. 2006;173(1):105–11.
26. Schiavina M, Di Scioscio V, Contini P, Cavazza A, Fabiani A, Barberis M, et al. Pulmonary lymphangioleiomyomatosis in a karyotypically normal man without tuberous sclerosis complex. Am J Respir Crit Care Med. 2007;176(1):96–8.
27. Henske EP, McCormack FX. Lymphangioleiomyomatosis – a wolf in sheep's clothing. J Clin Invest. 2012;122(11):3807–16.
28. Su HH, Wu W, Guo Y, Chen HD, Shan SJ. Paediatric Erdheim-Chester disease with aggressive skin manifestations. Br J Dermatol. 2018;178(1):261–4.
29. Clements D, Dongre A, Krymskaya VP, Johnson SR. Wild type mesenchymal cells contribute to the lung pathology of lymphangioleiomyomatosis. PLoS One. 2015;10(5):e0126025.
30. Matsui K. K Riemenschneider W, Hilbert Sl, Yu ZX, Takeda K, Travis WD, et al. hyperplasia of type II pneumocytes in pulmonary lymphangioleiomyomatosis. Arch Pathol Lab Med. 2000;124(11):1642–8.
31. Kumasaka T, Seyama K, Mitani K, Souma S, Kashiwagi S, Hebisawa A, et al. Lymphangiogenesis-mediated shedding of LAM cell clusters as a mechanism for dissemination in lymphangioleiomyomatosis. Am J Surg Pathol. 2005;29(10):1356–66.
32. Finlay GA. The LAM cell: what is it, where does it come from, and why does it grow? Am J Physiol Lung Cell Mol Physiol. 2004;286(4):L690-3.
33. Carbone M. Feasibility of immunotherapy for lymphangioleiomyomatosis. Am J Pathol. 2009;175(6):2252–4.
34. Edwards ST, Cruz AC, Donnelly S, Dazin PF, Schulman ES, Jones KD, et al. C-Kit immunophenotyping and metalloproteinase expression profiles of mast cells in interstitial lung diseases. J Pathol. 2005;206(3):279–90.
35. Chottanapund S, Van Duursen MB, Navasumrit P, Hunsonti P, Timtavorn S, Ruchirawat M, et al. Anti-aromatase effect of resveratrol and melatonin on hormonal positive breast cancer cells co-cultured with breast adipose fibroblasts. Toxicol In Vitro. 2014;28(7):1215–21.
36. Sorsa T, Tjaderhane L, Salo T. Matrix metalloproteinases (MMPs) in oral diseases. Oral Dis. 2004;10(6):311–8.
37. Greenlee KJ, Werb Z, Kheradmand F. Matrix metalloproteinases in lung: multiple, multifarious, and multifaceted. Physiol Rev. 2007;87(1):69–98.
38. Hayashi T, Fleming MV, Stetler-Stevenson WG, Liotta LA, Moss J, Ferrans VJ, et al. Immunohistochemical study of matrix metalloproteinases (MMPs) and their tissue inhibitors (TIMPs) in pulmonary lymphangioleiomyomatosis (LAM). Hum Pathol. 1997;28(9):1071–8.
39. Matsui K, Takeda K, Yu ZX, Travis WD, Moss J, Ferrans VJ. Role for activation of matrix metalloproteinases in the pathogenesis of pulmonary lymphangioleiomyomatosis. Arch Pathol Lab Med. 2000;124(2):267–75.
40. Golub LM, Ramamurthy NS, McNamara TF, Greenwald RA, Rifkin BR. Tetracyclines inhibit connective tissue breakdown: new therapeutic implications for an old family of drugs. Crit Rev Oral Biol Med. 1991;2(3):297–321.
41. Pimenta SP, Baldi BG, Kairalla RA, Carvalho CR. Doxycycline use in patients with lymphangioleiomyomatosis: biomarkers and pulmonary function response. J Bras Pneumol. 2013;39(1):5–15.
42. Chang WY, Cane J. L., Kumaran M, Lewis S, Tattersfield AE, Johnson SR. A 2-year randomised placebo-controlled trial of doxycycline for lymphangioleiomyomatosis. Eur Respir J. 2014;43(4):1114–23.
43. Zhe X, Yang Y, Schuger L. Imbalanced plasminogen system in lymphangioleiomyomatosis: potential role of serum response factor. Am J Respir Cell Mol Biol. 2005;32(1):28–34.
44. Chilosi M, Pea M, Martignoni G, Brunelli M, Gobbo S, Poletti V, et al. Cathepsin-k expression in pulmonary lymphangioleiomyomatosis. Mod Pathol. 2009;22(2):161–6.

45. Zhao Q, Jia Y, Xiao Y. Cathepsin K: a therapeutic target for bone diseases. Biochem Biophys Res Commun. 2009;380(4):721–3.
46. Dongre A, Clements D, Fisher AJ, Johnson SR. Cathepsin K in Lymphangioleiomyomatosis: LAM cell-fibroblast interactions enhance protease activity by extracellular acidification. Am J Pathol. 2017;187(8):1750–62.
47. Montgomery N, Hill A, McFarlane S, Neisen J, O'Grady A, Conlon S, et al. CD44 enhances invasion of basal-like breast cancer cells by upregulating serine protease and collagen-degrading enzymatic expression and activity. Breast Cancer Res. 2012;14(3):R84.
48. Zheng T, Zhu Z, Wang Z, Homer RJ, Ma B, Riese RJ, et al. Inducible targeting of IL-13 to the adult lung causes matrix metalloproteinase- and cathepsin-dependent emphysema. J Clin Invest. 2000;106(9):1081–93.
49. Repnik U, Starr AE, Overall CM, Turk B. Cysteine Cathepsins activate ELR chemokines and inactivate non-ELR chemokines. J Biol Chem. 2015;290(22):13800–11.
50. McQueney M, Amegadzie BY, D'Alessio K, Hanning CR, McLaughlin MM, McNulty D, et al. Autocatalytic activation of human cathepsin K. J Biol Chem. 1997;272(21):13955–60.
51. Turk V, Stoka V, Vasiljeva O, Renko M, Sun T, Turk B, et al. Cysteine cathepsins: from structure, function and regulation to new frontiers. Biochim Biophys Acta. 2012;1:68–88.
52. McDonald PC, Winum JY, Supuran CT, Dedhar S. Recent developments in targeting carbonic anhydrase IX for cancer therapeutics. Oncotarget. 2012;3(1):84–97.
53. Kneissel M, Luong-Nguyen NH, Baptist M, Cortesi R, Zumstein-Mecker S, Kossida S, et al. Everolimus suppresses cancellous bone loss, bone resorption, and cathepsin K expression by osteoclasts. Bone. 2004;35(5):1144–56.
54. Shen A, Iseman MD, Waldron JA, King TE. Exacerbation of pulmonary lymphangioleiomyomatosis by exogenous estrogens. Chest. 1987;91(5):782–5.
55. Gu X, Yu JI, Ilter D, Blenis N, Henske EP, Blenis J. Integration of mTOR and estrogen-ERK2 signaling in lymphangioleiomyomatosis pathogenesis. Proc Natl Acad Sci U S A. 2013;110(37):14960–5.
56. Yu JJ, Robb VA, Morrison TA, Ariazi EA, Karbowniczek M, Astrinidis A, et al. Estrogen promotes the survival and pulmonary metastasis of tuberin-null cells. Proc Natl Acad Sci U S A. 2009;106(8):2635–40.
57. Banner AS, Carrington CB, Emory WB, Kittle F, Leonard G, Ringus J, et al. Efficacy of oophorectomy in lymphangioleiomyomatosis and benign metastasizing leiomyoma. N Engl J Med. 1981;305(4):204–9.
58. Schiavina M, Contini P, Fabiani A, Cinelli F, Di Scioscio V, Zompatori M, et al. Efficacy of hormonal manipulation in lymphangioleiomyomatosis. A 20-year-experience in 36 patients. Sarcoidosis Vasc Diffuse Lung Dis. 2007;24(1):39–50.
59. Rossi GA, Balbi B, Oddera S, Lantero S, Ravazzoni C. Response to treatment with an analog of the luteinizing-hormone-releasing hormone in a patient with pulmonary lymphangioleiomyomatosis. Am Rev Respir Dis. 1991;143(1):174–6.
60. Johnson SR. Lymphangioleiomyomatosis. Eur Respir J. 2006;27(5):1056–65.
61. Lu C, Lee HS, Pappas GP, Dilling DF, Burger CD, Shifren A, et al. A phase II clinical trial of an aromatase inhibitor for postmenopausal women with Lymphangioleiomyomatosis. Ann Am Thorac Soc. 2017;14(6):919–28.
62. Bee J, Fuller S, Miller S, Johnson SR. Lung function response and side effects to rapamycin for lymphangioleiomyomatosis: a prospective national cohort study. Thorax. 2018;73(4):369–75.
63. Taveira-DaSilva AM, Hathaway O, Stylianou M, Moss J. Changes in lung function and chylous effusions in patients with lymphangioleiomyomatosis treated with sirolimus. Ann Intern Med. 2011;154(12):797–805.
64. Liu HJ, Lizotte PH, Du H, Speranza MC, Lam HC, Vaughan S, et al. TSC2-deficient tumors have evidence of T cell exhaustion and respond to anti-PD-1/anti-CTLA-4 immunotherapy. JCI Insight. 2018;3(8):98674. LID – https://doi.org/10.1172/jci.insight.98674 (doi) LID – 98674 (pii)
65. Tazi A, de Margerie C, Naccache JM, Fry S, Dominique S, Jouneau S, et al. The natural history of adult pulmonary Langerhans cell histiocytosis: a prospective multicentre study. Orphanet J Rare Dis. 2015;10:30.

66. Vassallo R, Ryu JH, Schroeder DR, Decker PA, Limper AH. Clinical outcomes of pulmonary Langerhans'-cell histiocytosis in adults. N Engl J Med. 2002;346(7):484–90.
67. Arico M, Girschikofsky M, Genereau T, Klersy C, McClain K, Grois N, et al. Langerhans cell histiocytosis in adults. Report from the international registry of the Histiocyte society. Eur J Cancer. 2003;39(16):2341–8.
68. Travis WD, Borok Z, Roum JH, Zhang J, Feuerstein I, Ferrans VJ, et al. Pulmonary Langerhans cell granulomatosis (histiocytosis X). A clinicopathologic study of 48 cases. Am J Surg Pathol. 1993;17(10):971–86.
69. Friedman PJ, Liebow AA, Sokoloff J. Eosinophilic granuloma of lung. Clinical aspects of primary histiocytosis in the adult. Medicine (Baltimore). 1981;60(6):385–96.
70. Schonfeld N, Frank W, Wenig S, Uhrmeister P, Allica E, Preussler H, et al. Clinical and radiologic features, lung function and therapeutic results in pulmonary histiocytosis X. Respiration. 1993;60(1):38–44.
71. Sholl LM, Hornick JL, Pinkus JL, Pinkus GS, Padera RF. Immunohistochemical analysis of langerin in langerhans cell histiocytosis and pulmonary inflammatory and infectious diseases. Am J Surg Pathol. 2007;31(6):947–52.
72. West HC, Bennett CL. Redefining the role of Langerhans cells as immune regulators within the skin. Front Immunol. 2017;8:1941.
73. Willman CL. Detection of clonal histiocytes in Langerhans cell histiocytosis: biology and clinical significance. Br J Cancer Suppl. 1994;23:S29–33.
74. Willman CL, Busque L, Griffith BB, Favara BE, McClain KL, Duncan MH, et al. Langerhans'-cell histiocytosis (histiocytosis X) – a clonal proliferative disease. N Engl J Med. 1994;331(3):154–60.
75. Yu RC, Chu C, Buluwela L, Chu AC. Clonal proliferation of Langerhans cells in Langerhans cell histiocytosis. Lancet. 1994;343(8900):767–8.
76. Weintraub M, Bhatia KG, Chandra RS, Magrath IT, Ladisch S. p53 expression in Langerhans cell histiocytosis. J Pediatr Hematol Oncol. 1998;20(1):12–7.
77. Badalian-Very G, Vergilio JA, Degar BA, MacConaill LE, Brandner B, Calicchio ML, et al. Recurrent BRAF mutations in Langerhans cell histiocytosis. Blood. 2010;116(11):1919–23.
78. Satoh T, Smith A, Sarde A, Lu HC, Mian S, Trouillet C, et al. B-RAF mutant alleles associated with Langerhans cell histiocytosis, a granulomatous pediatric disease. PLoS One. 2012;7(4):e33891.
79. Haroche J, Charlotte F, Arnaud L, von Deimling A, Helias-Rodzewicz Z, Hervier B, et al. High prevalence of BRAF V600E mutations in Erdheim-Chester disease but not in other non-Langerhans cell histiocytoses. Blood. 2012;120(13):2700–3.
80. Sahm F, Capper D, Preusser M, Meyer J, Stenzinger A, Lasitschka F, et al. BRAFV600E mutant protein is expressed in cells of variable maturation in Langerhans cell histiocytosis. Blood. 2012;120(12):e28–34.
81. Roden AC, Hu X, Kip S, Parrilla Castellar ER, Rumilla KM, Vrana JA, et al. BRAF V600E expression in Langerhans cell histiocytosis: clinical and immunohistochemical study on 25 pulmonary and 54 extrapulmonary cases. Am J Surg Pathol. 2014;38(4):548–51.
82. Ascierto PA, Kirkwood JM, Grob JJ, Simeone E, Grimaldi AM, Maio M, et al. The role of BRAF V600 mutation in melanoma. J Transl Med. 2012;10:85.
83. Brose MS, Volpe P, Feldman M, Kumar M, Rishi I, Gerrero R, et al. BRAF and RAS mutations in human lung cancer and melanoma. Cancer Res. 2002;62(23):6997–7000.
84. Davies H, Bignell GR, Cox C, Stephens P, Edkins S, Clegg S, et al. Mutations of the BRAF gene in human cancer. Nature. 2002;417(6892):949–54.
85. Makita Y, Narumi Y, Yoshida M, Niihori T, Kure S, Fujieda K, et al. Leukemia in cardio-facio-cutaneous (CFC) syndrome: a patient with a germline mutation in BRAF proto-oncogene. J Pediatr Hematol Oncol. 2007;29(5):287–90.
86. El-Osta H, Falchook G, Tsimberidou A, Hong D, Naing A, Kim K, et al. BRAF mutations in advanced cancers: clinical characteristics and outcomes. PLoS One. 2011;6(10):e25806.
87. Niihori T, Aoki Y, Narumi Y, Neri G, Cave H, Verloes A, et al. Germline KRAS and BRAF mutations in cardio-facio-cutaneous syndrome. Nat Genet. 2006;38(3):294–6.

88. Nelson DS, Quispel W, Badalian-Very G, van Halteren AG, van den Bos C, Bovee JV, et al. Somatic activating ARAF mutations in Langerhans cell histiocytosis. Blood. 2014;123(20):3152–5.
89. Brown NA, Furtado LV, Betz BL, Kiel MJ, Weigelin HC, Lim MS, et al. High prevalence of somatic MAP 2K1 mutations in BRAF V600E-negative Langerhans cell histiocytosis. Blood. 2014;124(10):1655–8.
90. Nelson DS, van Halteren A, Quispel WT, van den Bos C, Bovee JV, Patel B, et al. MAP 2K1 and MAP 3K1 mutations in Langerhans cell histiocytosis. Genes Chromosomes Cancer. 2015;54(6):361–8.
91. Mourah S, How-Kit A, Meignin V, Gossot D, Lorillon G, Bugnet E, et al. Recurrent NRAS mutations in pulmonary Langerhans cell histiocytosis. Eur Respir J. 2016;47(6):1785–96.
92. Lommatzsch M, Bratke K, Stoll P, Mulleneisen N, Prall F, Bier A, et al. Bronchoalveolar lavage for the diagnosis of pulmonary Langerhans cell histiocytosis. Respir Med. 2016;119:168–74.
93. Soler P, Chollet S, Jacque C, Fukuda Y, Ferrans VJ, Basset F. Immunocytochemical characterization of pulmonary histiocytosis X cells in lung biopsies. Am J Pathol. 1985;118(3):439–51.
94. Marchal J, Kambouchner M, Tazi A, Valeyre D, Soler P. Expression of apoptosis-regulatory proteins in lesions of pulmonary Langerhans cell histiocytosis. Histopathology. 2004;45(1):20–8.
95. Tazi A, Moreau J, Bergeron A, Dominique S, Hance AJ, Soler P. Evidence that Langerhans cells in adult pulmonary Langerhans cell histiocytosis are mature dendritic cells: importance of the cytokine microenvironment. J Immunol. 1999;163(6):3511–5.
96. Fukuda Y, Basset F, Soler P, Ferrans VJ, Masugi Y, Crystal RG. Intraluminal fibrosis and elastic fiber degradation lead to lung remodeling in pulmonary Langerhans cell granulomatosis (histiocytosis X). Am J Pathol. 1990;137(2):415–24.
97. Colombat M, Caudroy S, Lagonotte E, Mal H, Danel C, Stern M, et al. Pathomechanisms of cyst formation in pulmonary light chain deposition disease. Eur Respir J. 2008;32(5):1399–403.
98. Landi C, Bargagli E, Magi B, Prasse A, Muller-Quernheim J, Bini L, et al. Proteome analysis of bronchoalveolar lavage in pulmonary langerhans cell histiocytosis. J Clin Bioinforma. 2011;1:31.
99. Lorillon G, Bergeron A, Detourmignies L, Jouneau S, Wallaert B, Frija J, et al. Cladribine is effective against cystic pulmonary Langerhans cell histiocytosis. Am J Respir Crit Care Med. 2012;186(9):930–2.
100. Lorillon G, Tazi A. How I manage pulmonary Langerhans cell histiocytosis. Eur Respir Rev. 2017;26(145):170070.
101. Birt AR, Hogg GR, Dube WJ. Hereditary multiple fibrofolliculomas with trichodiscomas and acrochordons. Arch Dermatol. 1977;113(12):1674–7.
102. Toro JR, Glenn G, Duray P, Darling T, Weirich G, Zbar B, et al. Birt-Hogg-Dube syndrome: a novel marker of kidney neoplasia. Arch Dermatol. 1999;135(10):1195–202.
103. Zbar B, Alvord WG, Glenn G, Turner M, Pavlovich CP, Schmidt L, et al. Risk of renal and colonic neoplasms and spontaneous pneumothorax in the Birt-Hogg-Dube syndrome. Cancer Epidemiol Biomark Prev. 2002;11(4):393–400.
104. Nickerson ML, Warren MB, Toro JR, Matrosova V, Glenn G, Turner ML, et al. Mutations in a novel gene lead to kidney tumors, lung wall defects, and benign tumors of the hair follicle in patients with the Birt-Hogg-Dube syndrome. Cancer Cell. 2002;2(2):157–64.
105. Schmidt LS, Warren MB, Nickerson ML, Weirich G, Matrosova V, Toro JR, et al. Birt-Hogg-Dube syndrome, a genodermatosis associated with spontaneous pneumothorax and kidney neoplasia, maps to chromosome 17p11.2. Am J Hum Genet. 2001;69(4):876–82.
106. Lim DH, Rehal PK, Nahorski MS, Macdonald F, Claessens T, Van Geel M, et al. A new locus-specific database (LSDB) for mutations in the folliculin (FLCN) gene. Hum Mutat. 2010;31(1):E1043–51.
107. Vocke CD, Yang Y, Pavlovich CP, Schmidt LS, Nickerson ML, Torres-Cabala CA, et al. High frequency of somatic frameshift BHD gene mutations in Birt-Hogg-Dube-associated renal tumors. J Natl Cancer Inst. 2005;97(12):931–5.

108. Hasumi Y, Baba M, Ajima R, Hasumi H, Valera VA, Klein ME, et al. Homozygous loss of BHD causes early embryonic lethality and kidney tumor development with activation of mTORC1 and mTORC2. Proc Natl Acad Sci U S A. 2009;106(44):18722–7.
109. Hartman TR, Nicolas E, Klein-Szanto A, Al-Saleem T, Cash TP, Simon MC, et al. The role of the Birt-Hogg-Dube protein in mTOR activation and renal tumorigenesis. Oncogene. 2009;28(13):1594–604.
110. Hudon V, Sabourin S, Dydensborg AB, Kottis V, Ghazi A, Paquet M, et al. Renal tumour suppressor function of the Birt-Hogg-Dube syndrome gene product folliculin. J Med Genet. 2010;47(3):182–9.
111. van Steensel MA, Verstraeten VL, Frank J, Kelleners-Smeets NW, Poblete-Gutierrez P, Marcus-Soekarman D, et al. Novel mutations in the BHD gene and absence of loss of heterozygosity in fibrofolliculomas of Birt-Hogg-Dube patients. J Invest Dermatol. 2007;127(3):588–93.
112. Baba M, Hong SB, Sharma N, Warren MB, Nickerson ML, Iwamatsu A, et al. Folliculin encoded by the BHD gene interacts with a binding protein, FNIP1, and AMPK, and is involved in AMPK and mTOR signaling. Proc Natl Acad Sci U S A. 2006;103(42):15552–7.
113. Hasumi H, Baba M, Hong SB, Hasumi Y, Huang Y, Yao M, et al. Identification and characterization of a novel folliculin-interacting protein FNIP2. Gene. 2008;415(1–2):60–7.
114. Takagi Y, Kobayashi T, Shiono M, Wang L, Piao X, Sun G, et al. Interaction of folliculin (Birt-Hogg-Dube gene product) with a novel Fnip1-like (FnipL/Fnip2) protein. Oncogene. 2008;27(40):5339–47.
115. Medvetz DA, Khabibullin D, Hariharan V, Ongusaha PP, Goncharova EA, Schlechter T, et al. Folliculin, the product of the Birt-Hogg-Dube tumor suppressor gene, interacts with the adherens junction protein p0071 to regulate cell-cell adhesion. PLoS One. 2012;7(11):e47842.
116. Nahorski MS, Seabra L, Straatman-Iwanowska A, Wingenfeld A, Reiman A, Lu X, et al. Folliculin interacts with p0071 (plakophilin-4) and deficiency is associated with disordered RhoA signalling, epithelial polarization and cytokinesis. Hum Mol Genet. 2012;21(24):5268–79.
117. Graham RB, Nolasco M, Peterlin B, Garcia CK. Nonsense mutations in folliculin presenting as isolated familial spontaneous pneumothorax in adults. Am J Respir Crit Care Med. 2005;172(1):39–44.
118. Kumasaka T, Hayashi T, Mitani K, Kataoka H, Kikkawa M, Tobino K, et al. Characterization of pulmonary cysts in Birt-Hogg-Dube syndrome: histopathological and morphometric analysis of 229 pulmonary cysts from 50 unrelated patients. Histopathology. 2014;65(1):100–10.
119. Tobino K, Gunji Y, Kurihara M, Kunogi M, Koike K, Tomiyama N, et al. Characteristics of pulmonary cysts in Birt-Hogg-Dube syndrome: thin-section CT findings of the chest in 12 patients. Eur J Radiol. 2011;77(3):403–9.
120. Tobino K, Hirai T, Johkoh T, Fujimoto K, Kawaguchi A, Tomiyama N, et al. Difference of the progression of pulmonary cysts assessed by computed tomography among COPD, lymphangioleiomyomatosis, and Birt-Hogg-Dube syndrome. PLoS One. 2017;12(12):e0188771.
121. Furuya M, Tanaka R, Koga S, Yatabe Y, Gotoda H, Takagi S, et al. Pulmonary cysts of Birt-Hogg-Dube syndrome: a clinicopathologic and immunohistochemical study of 9 families. Am J Surg Pathol. 2012;36(4):589–600.
122. Koga S, Furuya M, Takahashi Y, Tanaka R, Yamaguchi A, Yasufuku K, et al. Lung cysts in Birt-Hogg-Dube syndrome: histopathological characteristics and aberrant sequence repeats. Pathol Int. 2009;59(10):720–8.
123. Warren MB, Torres-Cabala CA, Turner ML, Merino MJ, Matrosova VY, Nickerson ML, et al. Expression of Birt-Hogg-Dube gene mRNA in normal and neoplastic human tissues. Mod Pathol. 2004;17(8):998–1011.
124. Goncharova EA, Goncharov DA, James ML, Atochina-Vasserman EN, Stepanova V, Hong SB, et al. Folliculin controls lung alveolar enlargement and epithelial cell survival through E-cadherin, LKB1, and AMPK. Cell Rep. 2014;7(2):412–23.
125. Massaro GD, Massaro D. Postnatal lung growth: evidence that the gas-exchange region grows fastest at the periphery. Am J Phys. 1993;265(4 Pt 1):L319–22.

126. Hoshika Y, Takahashi F, Togo S, Hashimoto M, Nara T, Kobayashi T, et al. Haploinsufficiency of the folliculin gene leads to impaired functions of lung fibroblasts in patients with Birt-Hogg-Dube syndrome. Physiol Rep. 2016;4(21):e13025.
127. Dunsmore SE, Lee YC, Martinez-Williams C, Rannels DE. Synthesis of fibronectin and laminin by type II pulmonary epithelial cells. Am J Phys. 1996;270(2 Pt 1):L215–23.
128. Johannesma PC, Houweling AC, van Waesberghe JH, van Moorselaar RJ, Starink TM, Menko FH, et al. The pathogenesis of pneumothorax in Birt-Hogg-Dube syndrome: a hypothesis. Respirology. 2014;19(8):1248–50.
129. Kennedy JC, Khabibullin D, Henske EP. Mechanisms of pulmonary cyst pathogenesis in Birt-Hogg-Dube syndrome: the stretch hypothesis. Semin Cell Dev Biol. 2016;52:47–52.
130. Khabibullin D, Medvetz DA, Pinilla M, Hariharan V, Li C, Hergrueter A, et al. Folliculin regulates cell-cell adhesion, AMPK, and mTORC1 in a cell-type-specific manner in lung-derived cells. Physiol Rep. 2014;2(8):e12107.
131. Jensen L, Mann H. Cystic lung disease from protein deposition: pathogenesis and associated conditions. Curr Radiol Rep. 2018;6(3):12.
132. Randall RE, Williamson WC Jr, Mullinax F, Tung MY, Still WJ. Manifestations of systemic light chain deposition. Am J Med. 1976;60(2):293–9.
133. Pozzi C, Locatelli F. Kidney and liver involvement in monoclonal light chain disorders. Semin Nephrol. 2002;22(4):319–30.
134. Fabbian F, Stabellini N, Sartori S, Tombesi P, Aleotti A, Bergami M, et al. Light chain deposition disease presenting as paroxysmal atrial fibrillation: a case report. J Med Case Rep. 2007;1:187.
135. Gallo G, Goni F, Boctor F, Vidal R, Kumar A, Stevens FJ, et al. Light chain cardiomyopathy. Structural analysis of the light chain tissue deposits. Am J Pathol. 1996;148(5):1397–406.
136. Koopman P, Van Dorpe J, Maes B, Dujardin K. Light chain deposition disease as a rare cause of restrictive cardiomyopathy. Acta Cardiol. 2009;64(6):821–4.
137. Morinaga S, Watanabe H, Gemma A, Mukai K, Nakajima T, Shimosato Y, et al. Plasmacytoma of the lung associated with nodular deposits of immunoglobulin. Am J Surg Pathol. 1987;11(12):989–95.
138. Kijner CH, Yousem SA. Systemic light chain deposition disease presenting as multiple pulmonary nodules. A case report and review of the literature. Am J Surg Pathol. 1988;12(5):405–13.
139. Khoor A, Myers JL, Tazelaar HD, Kurtin PJ. Amyloid-like pulmonary nodules, including localized light-chain deposition: clinicopathologic analysis of three cases. Am J Clin Pathol. 2004;121(2):200–4.
140. Piard F, Yaziji N, Jarry O, Assem M, Martin L, Bernard A, et al. Solitary plasmacytoma of the lung with light chain extracellular deposits: a case report and review of the literature. Histopathology. 1998;32(4):356–61.
141. Rostagno A, Frizzera G, Ylagan L, Kumar A, Ghiso J, Gallo G. Tumoral non-amyloidotic monoclonal immunoglobulin light chain deposits ('aggregoma'): presenting feature of B-cell dyscrasia in three cases with immunohistochemical and biochemical analyses. Br J Haematol. 2002;119(1):62–9.
142. Stokes MB, Jagirdar J, Burchstin O, Kornacki S, Kumar A, Gallo G. Nodular pulmonary immunoglobulin light chain deposits with coexistent amyloid and nonamyloid features in an HIV-infected patient. Mod Pathol. 1997;10(10):1059–65.
143. Colombat M, Stern M, Groussard O, Droz D, Brauner M, Valeyre D, et al. Pulmonary cystic disorder related to light chain deposition disease. Am J Respir Crit Care Med. 2006;173(7):777–80.

Chapter 3
Radiological Evaluation of Cystic Lung Disease

Joanna E. Kusmirek, Cristopher A. Meyer, and David A. Lynch

Introduction

The diffuse cystic lung diseases (DCLDs) are a group of pathophysiologically heterogeneous disorders characterized by the presence of multiple, thin-walled, air-filled spaces in the pulmonary parenchyma [1]. The most commonly encountered DCLDs include lymphangioleiomyomatosis (LAM), pulmonary Langerhans cell histiocytosis (PLCH), and lymphoid interstitial pneumonia (LIP). However, the differential diagnosis for pulmonary cysts detected on imaging is broad and includes many less common entities, such as amyloidosis, light chain deposition disease (LCDD), Birt-Hogg-Dubé syndrome (BHD), cystic metastases, and infectious pneumatoceles, among others [2]. In a routine radiology practice, other pathologic processes are commonly encountered that mimic DCLDs such as emphysema and bronchiectasis [3]. In this chapter, the utility of chest radiographs and computed tomography (CT) in the evaluation of DCLD are reviewed. Suggested CT acquisition parameters and advanced post-processing techniques are presented to minimize radiation dose and improve the detection and characterization of lung cysts. The high-resolution CT lexicon definition for lung cysts and other similar appearing but distinct pathology in the lung parenchyma will be described. The literature defining the borderland between pathologic cysts and normal parenchymal findings is discussed. Finally, a thorough review of the imaging findings of the entities primarily

J. E. Kusmirek (✉) · C. A. Meyer
Department of Radiology, University of Wisconsin School of Medicine and Public Health, Madison, WI, USA
e-mail: CMeyer2@uwhealth.org

D. A. Lynch
Department of Radiology, National Jewish Health, Denver, CO, USA
e-mail: lynchd@njhealth.org

N. Gupta et al. (eds.), *Diffuse Cystic Lung Diseases*, Respiratory Medicine,
https://doi.org/10.1007/978-3-030-63365-3_3

associated with lung cysts will be presented with emphasis on the morphologic differences and ancillary imaging findings that allow the astute observer to differentiate the causes of DCLD.

Chest Radiography and Computed Tomography in DCLD

Radiography has low sensitivity for DCLD but is often the first imaging exam in patients that present with spontaneous pneumothorax. Radiographic findings that suggest the presence of diffuse parenchymal cysts include reticular opacities with hyperinflation (since reticulation due to fibrosis is often associated with volume loss) (Fig. 3.1). Unfortunately, these findings are nonspecific and may also be seen with emphysema or cystic fibrosis.

The presence of a spontaneous pneumothorax at radiography should initiate a search for bullae or cysts. In a patient with recurrent pneumothoraces and no known predisposing process, chest CT is indicated and typically obtained upon second presentation. In patients with apparent primary spontaneous pneumothorax, HRCT screening for BHD, LAM, and PLCH has been shown to be cost-effective [4]. CT has high sensitivity and specificity in the detection of lung cysts and is useful for further classification of DCLDs. In a study by Koyama et al. [5], two observers were able to make the correct CT diagnosis in 81% of LIP, 72% of LAM, and 72% of PLCH cases. Gupta et al. [6, 7] evaluated the accuracy of high-resolution chest computed tomography (HRCT) in diagnosing LAM and found that expert

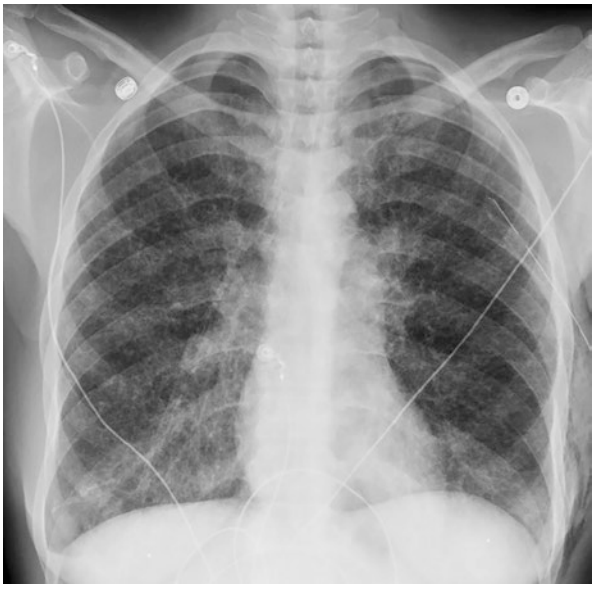

Fig. 3.1 Posteroanterior (PA) chest radiograph in a 32-year-old female with tuberous sclerosis complex and LAM, severe cystic lung disease and multiple previous bilateral spontaneous pneumothoraces reveals the typical radiographic findings of cystic lung disease with increased linear markings bilaterally and hyperinflation. A left chest tube is present for treatment of spontaneous pneumothorax

radiologists correctly diagnosed LAM in 91% of cases with a kappa of 0.82, while expert pulmonologists correctly diagnosed LAM in 86% and general pulmonologists and pulmonary fellows correctly identified LAM in 79%. Although the accuracy among expert radiologists was lower for PLCH (74%), it increased to 100% in cases rated "confident." Therefore, Gupta et al. suggest that clinicians consider tissue confirmation for PLCH in atypical cases and when considering more aggressive treatment. The American Thoracic Society/Japanese Respiratory Society LAM Clinical Practice Guideline recommends against making the final diagnosis of LAM based solely on suggestive cystic changes on HRCT if no other confirmatory clinical, radiological, or serologic features are present. In these cases, lung biopsy should be considered. Morphological characteristics important to evaluate when cysts are present include size, shape, wall regularity, relationship to vasculature, pleura, and the zonal distribution [8]. Ancillary findings at CT in the pleura, mediastinum, skin, bones, or kidneys may narrow the differential diagnosis and eliminate the need for invasive testing.

CT Technique

With current generation multidetector helical CT scanners, the entire chest can be imaged in one breath hold of typically 6 to 12 seconds, even in a dyspneic patient. Typical chest CT protocol parameters for the evaluation of DCLD are provided (Table 3.1).

Expiratory imaging may be useful in distinguishing lung cysts, which air trap from cystic bronchiectasis that will decrease in volume or collapse on expiration. Since a volumetric data set is obtained with near isotropic resolution, multiplanar reformats are routinely reconstructed. In this process, the volumetric data set is used to create nonaxial two-dimensional images, typically in coronal and sagittal planes [9], thus depicting the disease distribution in the craniocaudal orientation, which is often helpful in diffuse lung diseases, including DCLDs (Fig. 3.2). Some authors consider cyst distribution to be the most important feature in differentiating the DCLDs [10]. Orthogonal planes are also useful in distinguishing cysts from advanced cystic bronchiectasis by clearly revealing the continuity with the central airways (Fig. 3.3).

Additional volumetric reconstruction techniques that can be used include maximum intensity projection (MIP) and minimum intensity projection (MinIP) images [9]. MinIP reconstructions have been shown to improve visualization of cysts in LAM [11]. MIP images can inform the distribution of findings relative to the pulmonary vasculature and thereby help to differentiate cystic bronchiectasis from lung cysts, especially if performed along the long axis of the bronchus, in an optimized double oblique plane [12]. For differentiating emphysema from cysts, multiplanar volume rendered (VR) images are superior [12] for visualizing the "central dot" representing the centrilobular artery surrounded by emphysema. A "central dot"

Table 3.1 CT protocol for DCLD evaluation

HRCT	Evaluation of DCLD	Additional remarks
Contrast	None	–
Respiratory phase	Suspended full inspiration to total lung capacity (single breath hold for 4–6 seconds)	May add expiratory views in selected cases
Positioning	Supine	–
Slice thickness	1.0–1.25 mm	–
Slice interval	0.625–1.25 mm	–
Pitch	1.375	–
Collimation	40 mm	–
Noise index	21.5	–
Dose	As low as reasonably achievable (ALARA)	–
mAs	Recommend using automatic exposure control (AEC) to target effective dose <4 mS AEC	80 mAs or less is sufficient for most patients, except for very obese
kVp	Typically 120 (100–140)	100 kV for small adults and 140 kV for large adults
Reconstructions	Coronal and sagittal planes 1.0 × 5.0 mm	Axial MIPs or MinIPs (optional)
Reconstruction kernels	1: Standard (soft tissue) 2: High spatial frequency (Boneplus)	–

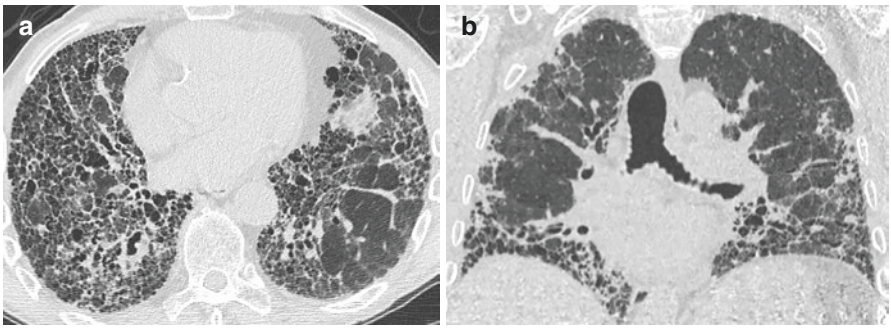

Fig. 3.2 (**a**) On a single axial CT image, there are well-demarcated lucencies diffusely at both bases right greater than left. Traction bronchiectasis is also present. The distinction of cystic lung disease from honeycomb lung may be challenging at this level. (**b**) Coronal reconstruction in the same patient reveals the basal predominant, subpleural clustering of these findings, characteristic of honeycomb lung in a patient with usual interstitial pneumonia

will be absent in lung cysts. Reconstruction kernel is important in the evaluation of the lung parenchyma (Fig. 3.4). A high spatial frequency or bone kernel improves spatial resolution and enhances edges and is preferred for lung parenchymal evaluation. A soft tissue/smooth kernel results in lung markings that are less well defined. This is the preferred reconstruction kernel for mediastinal soft tissue evaluation.

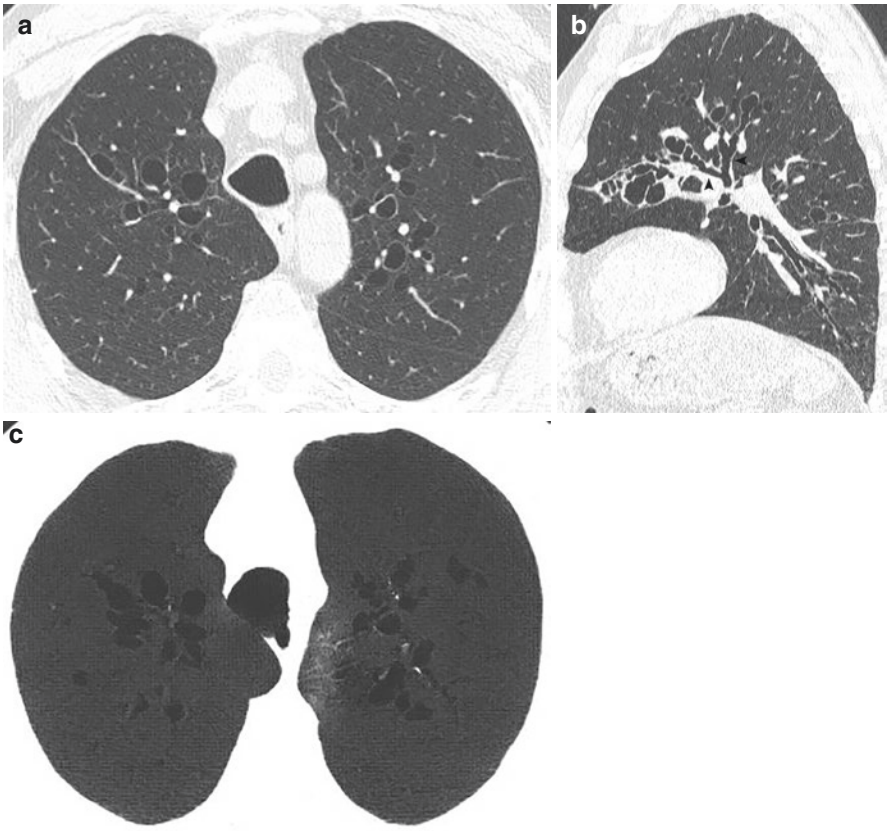

Fig. 3.3 (**a**) Axial CT image through the upper lobes reveals multiple cystic spaces associated with the pulmonary arteries. (**b**) A sagittal image demonstrates dilation of the central airways beyond the third-generation bronchi (*arrowhead*) consistent with cystic bronchiectasis of Williams-Campbell syndrome. (**c**) Minimum intensity projection image reconstruction (MinIP) is a volumetric post-processing technique that emphasizes low attenuation structures such as airways

Radiation Dose

We are all constantly exposed to natural sources of radiation. The average person in the United States receives an effective dose of about 6.2 mSv per year; half of this is from natural radiation and cosmic radiation [13]. The remainder (about 3 mSv per year) is from man-made sources, predominantly medical, but also industrial sources. People living at high altitudes such as Colorado or New Mexico receive about 1.5 mSv more per year than those living near sea level. To put these numbers in perspective, the radiation dose for an adult from a two-view chest radiograph is 0.1 mSv, which is the equivalent of approximately 10 days of natural background radiation or three coast-to-coast round-trip airline flights. CT examinations are responsible for roughly half of the radiation dose from medical imaging; in the United States, radiation dose ranges for a chest CT are typically 5 to 10 mSv [14].

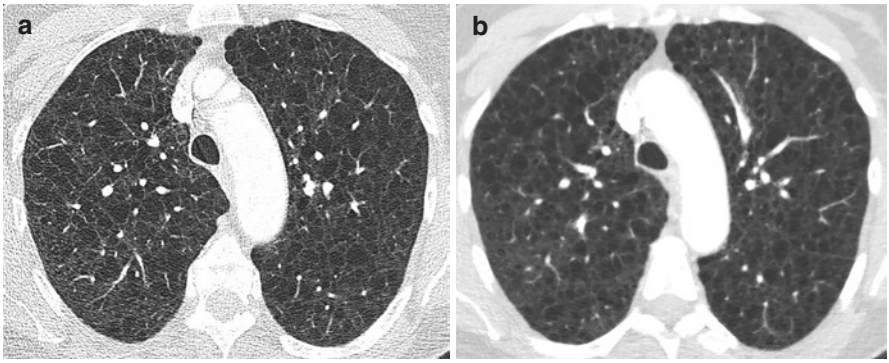

Fig. 3.4 Different reconstruction kernels. (**a**) A high spatial frequency kernel improves spatial resolution and enhances edges and is preferred for lung parenchymal evaluation. (**b**) A soft tissue/smooth kernel results in lung markings that are less well defined

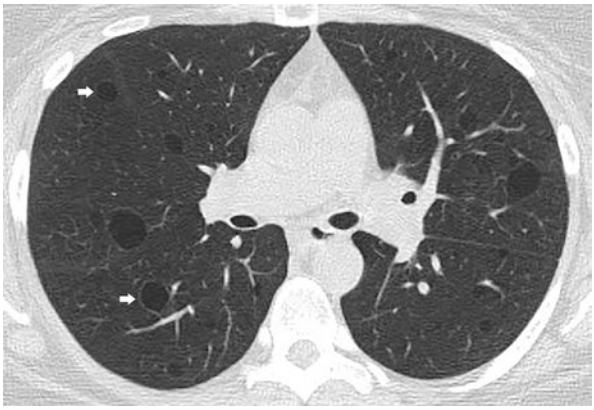

Fig. 3.5 Multiple cysts. A cyst is a round parenchymal lucency or low attenuation with a well-defined interface with normal lung and thin wall typically less than 2 mm (*arrows*)

Standard Nomenclature

A cyst is defined as any round circumscribed space that is surrounded by an epithelial or fibrous wall of variable thickness [1]. This appears as a round parenchymal lucency with a well-defined thin wall (<2 mm) (Fig. 3.5).

Emphysema is characterized by permanently enlarged airspaces distal to the terminal bronchiole with destruction of alveolar walls [1, 15]. Emphysema is classified as centrilobular, paraseptal, and panlobular (panacinar). On CT, emphysema appears as focal areas of low attenuation without visible walls [16] (Fig. 3.6).

A bulla is an airspace measuring more than 1 cm in diameter, with a thin wall (up to 1 mm in thickness) (Fig. 3.7).

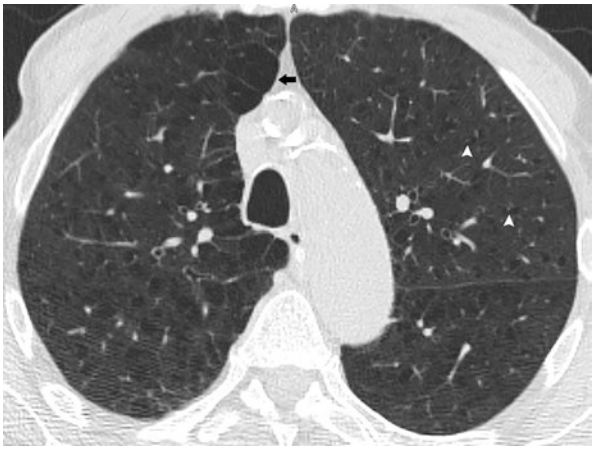

Fig. 3.6 Emphysema. Chest CT demonstrates both paraseptal and centrilobular emphysema. Paraseptal emphysema is seen as well-demarcated lucencies in the juxtapleural regions (*arrow*). Centrilobular emphysema is characterized by lucency in the core of the secondary lobule in association with a central dot (*arrowhead*) and no definable walls

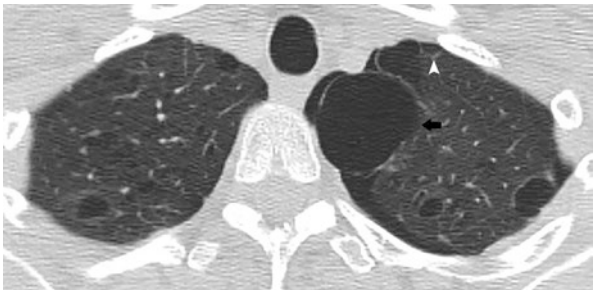

Fig. 3.7 A 52-year-old female with LAM and spontaneous left pneumothorax. CT in lung windows through the lung apices reveals a small pneumothorax on the left with a large thin-walled cystic air space protruding medially consistent with a bulla (*arrow*) and paraseptal emphysema anteriorly (*arrowhead*)

Honeycombing manifests as cysts measuring typically 3 to 10 mm (but occasionally much larger) with variable wall thickness. Honeycombing is a manifestation of end-stage fibrosis in a variety of interstitial lung diseases and is recognized as a cluster or stack of cystic air spaces, typically subpleural (Fig. 3.8).

A cavity is a gas-filled space, with distinct wall, commonly surrounded by pulmonary consolidation, or soft tissue. It may contain a fluid level (Fig. 3.9).

Pneumatocele. A thin-walled, air-filled space in the lung often associated with acute pneumonia, trauma, or aspiration of hydrocarbon fluid, which is often transient. It may contain fluid (e.g., blood products in traumatic pneumatoceles).

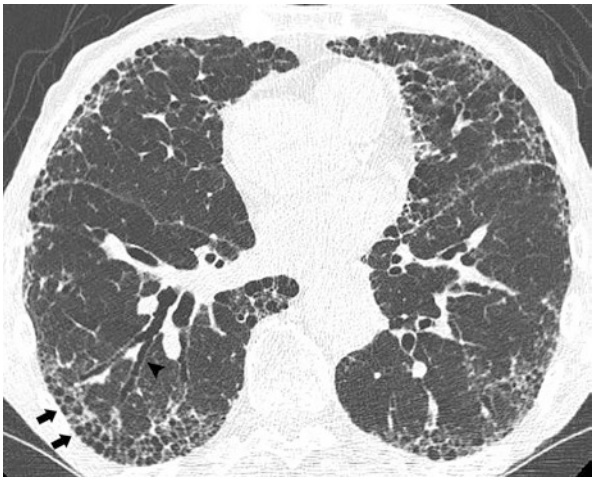

Fig. 3.8 Honeycomb lung on chest CT. Note the peripheral subpleural cystic spaces, 3 to 10 mm in size that appear stacked in geometric fashion in association with the pleura posteriorly in the right lung (*arrows*) with associated traction bronchiectasis (*arrowheads*)

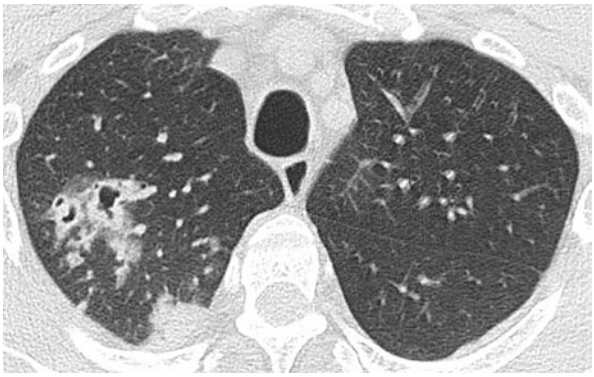

Fig. 3.9 A 42-year-old male with history of hemoptysis and MSSA bacteremia. Note the right upper lobe focus of gas with surrounding consolidation typical of necrotizing infection

Borderlands: How Many Cysts Are Too Many?

Pulmonary cysts are a common incidental finding on CT in healthy individuals. Cysts are frequently seen in the elderly; Copley et al. found cysts in 25% (10/40) of people older than 75 years, and Winter et al. reported them in 13% (6/47) of people older than 65 years. Neither authors found cysts in younger individuals [17, 18]. Araki et al. reviewed the chest CT exams of 2633 individuals and found cysts in 7.6% of participants, with the prevalence increasing with age: from 4.9% at age of 40 to 49 years to 12.9% at ages older than 80 years. No cysts were found in participants younger than 39 years [19]. In contrast, DCLDs typically affect adults in the third to fourth decade [20], including LAM [21], PLCH, and BHD [22]. Most incidentally discovered senescent pulmonary cysts remain unchanged although some may grow slowly over serial CTs. As a rule, less than five cysts in an elderly patient without concerning history or CT features are likely senescent and require no further investigation (Fig. 3.10) while the presence of cysts in a young patient and/or

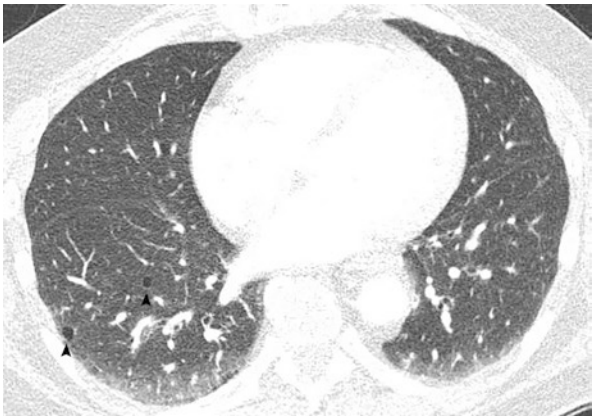

Fig. 3.10 A 66-year-old asymptomatic nonsmoking man with several incidentally discovered thin-walled cysts (*arrowheads*) in the right lower lobe

greater than five in number merit further evaluation. The tuberous sclerosis complex (TSC) guidelines specify that more than four cysts are required for diagnosis of LAM in the context of suspected TSC [23].

In the remainder of this chapter, we will describe the imaging findings associated with the DCLDs concentrating on the three most common, PLCH, LAM, and LIP followed by less frequently considered processes. Finally, several congenital and acquired processes that may mimic DCLDs will be described.

Smoking-Related DCLDs

Smoking is associated with a spectrum of diffuse lung diseases including respiratory bronchiolitis-associated interstitial lung disease (RB-ILD), desquamative interstitial pneumonia (DIP), pulmonary Langerhans cell histiocytosis (PLCH), acute eosinophilic pneumonia, and idiopathic pulmonary fibrosis (IPF) [24]. Among these, PLCH and DIP can present with cystic changes.

Pulmonary Langerhans Cell Histiocytosis

Pulmonary Langerhans cell histiocytosis (PLCH) most often affects young adults between the ages of 20 and 40 years [25], with no gender predilection and 90% to 95% of them being smokers [26]. Spontaneous pneumothorax is the first manifestation of the disease in 10% to 30% of patients [27]. Recurrent pneumothorax suggests disease progression [22]. Approximately 25% of PLCH patients are asymptomatic. The diagnosis is based on the typical imaging findings and clinical presentation. The chest radiograph may be abnormal with lung hyperexpansion and upper lobe predominant reticulonodular opacities. However, this pattern is nonspecific and can

also be seen in emphysema and LAM. PLCH is characterized by the abnormal proliferation of histiocytes in various organs. Pulmonary involvement seen in young adults is almost always associated with smoking.

By CT, the early stage of this disease manifests as centrilobular nodules, typically 1 to 5 mm in diameter, but occasionally as large as 20 mm [28] (Fig. 3.11). As the disease progresses, the nodules develop central lucencies thought to represent dilated airways and ultimately may cavitate with resultant cystic change. The cysts are variable in size, typically less than 10 mm, and often bizarre in shape (e.g., bilobed, irregular, stellate, cloverleaf, and branching). Characteristically, the process starts in the upper and mid lungs and progresses toward the bases with relative sparing of the costophrenic angles and tips of the lingula and right middle lobe [29] (Fig. 3.12). There is no central versus peripheral predilection. Initially, the cysts have thicker walls and later become thin walled with a tendency to become confluent or coalesce. The presence of coexistent centrilobular emphysema is not uncommon in these patients who typically have a strong smoking history [28]. It is notable that distinguishing PLCH from severe centrilobular emphysema can pose a diagnostic challenge in advanced cases (Fig. 3.13). The distinguishing features of emphysema include the lack of a perceptible wall and the presence of central vascular structures (central dot sign) in the emphysematous spaces [5]. PLCH is most often limited to the lungs: less commonly, extrapulmonary manifestations occur, involving the skin, bones, and hypothalamic-pituitary axis (e.g., diabetes insipidus) [30]. If a patient with multiorgan LCH has predominant lung involvement, this is considered a poor prognostic factor [31]. HRCT has a high diagnostic accuracy when classic imaging features are present (a combination of nodules and cysts in typical distribution) [25, 32]. In atypical cases, biopsy may be required.

Chest CT also has prognostic value. Severe cystic changes on initial CT correlate with higher risk of development of respiratory insufficiency [33, 34]. The utility of disease monitoring with serial CT is uncertain [5, 25, 35]. Both improvement and progression of pulmonary lesions are reported to occur during the first 14 to 22 months

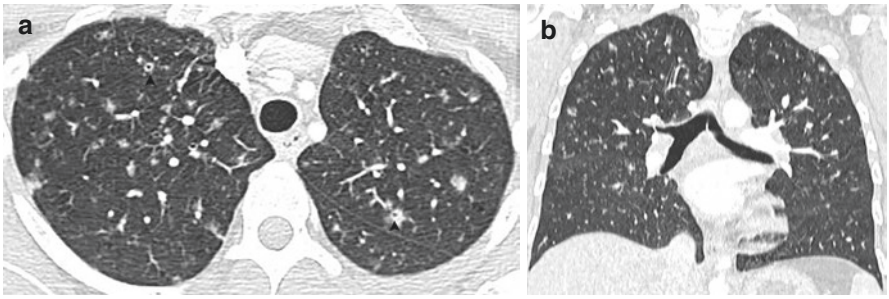

Fig. 3.11 A 44-year-old woman with heavy smoking history and bone pain and nodular changes of early PLCH. (**a**) Axial CT in lung windows through the apices shows centrilobular nodules, several with central lucency, consistent with a dilated bronchus or early cavitation (*arrowheads*). (**b**) Coronal MPR CT images show a striking upper lobe distribution with sparing of the costophrenic angles

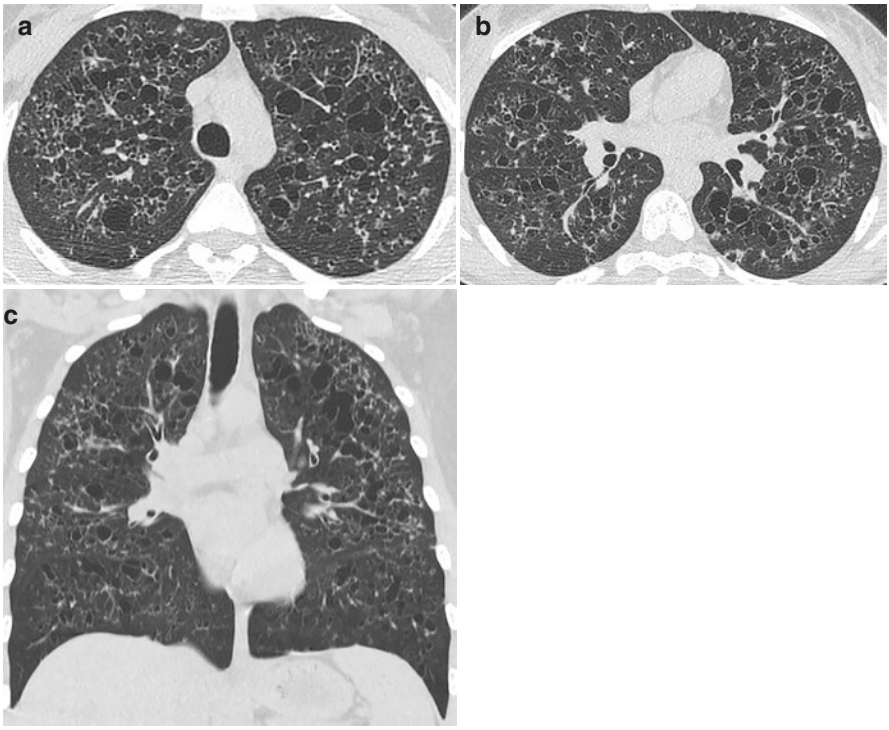

Fig. 3.12 A 34-year-old woman with tobacco use disorder, shortness of breath, and fatigue. (**a**, **b**) Axial CT is notable for bizarre shaped thin-walled cysts and nodules. (**c**) Coronal MPR illustrates the striking gradient of cystic change most severe in the upper lobes with nodules along the inferior margins and conspicuous sparing of the lung bases consistent with pulmonary Langerhans cell histiocytosis (PLCH)

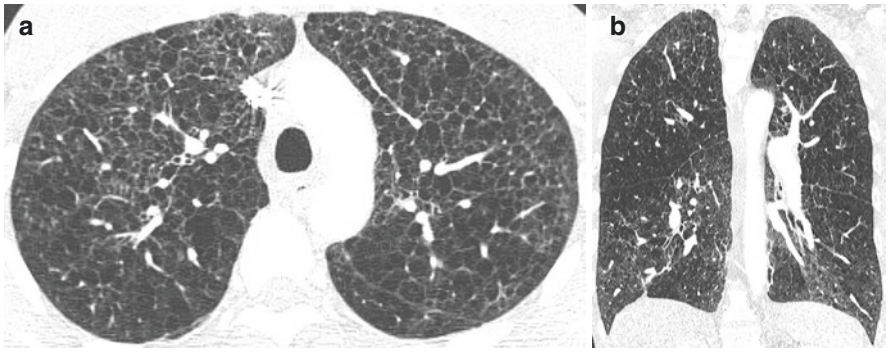

Fig. 3.13 A 51-year-old man with a greater than 30-pack-per-year smoking history presents with pulmonary hypertension and advanced confluent pulmonary Langerhans cell histiocytosis (PLCH). (**a**) Axial CT is notable for confluent cystic change in the upper lobes that is distinguished from emphysema by the lack of identifiable centrilobular core structures and the presence of definable walls. (**b**) Note that coronal MPR images reveal extensive cystic changes with a gradient from apex to base and sparing of the costophrenic angles

[26]. While smoking cessation is the mainstay of treatment, this does not slow the disease progression by imaging in all patients [32, 36, 37]. PET/CT can be used in selected cases when extrapulmonary disease is suspected, since this may change management. Positron emission tomography (PET)/CT can detect active LCH lesions with high sensitivity [38] and can be used for staging and therapy monitoring [39].

Desquamative Interstitial Pneumonia

Desquamative interstitial pneumonia (DIP) is characterized by abnormal macrophage accumulation in alveolar spaces and usually presents in middle age and older adults, more often in men. On HRCT, the hallmark finding is ground-glass opacity, typically bilateral and involving predominantly the mid and lower lungs. Centrilobular nodules may be present indicative of coexistent respiratory bronchiolitis [28]. Fibrotic changes including reticular opacities, traction bronchiectasis, and architectural distortion are also reported [40, 41]. Severe fibrosis is unusual in DIP [28]. Small cysts may be seen, usually within the areas of ground-glass abnormality. In a series of 22 patients described by Hartman et al., fibrosis was seen in 50% of patients and cysts in 32% [42] (Fig. 3.14). Akira et al. [41] found cysts in 75% of patients. Of note, there is a significant imaging, clinical, and pathologic overlap between smoking-related diseases including RB-ILD, DIP, PLCH, and emphysema. RB-ILD and DIP have similar features varying in severity, and these entities are considered to represent a spectrum of disease.

Exposure to cigarette smoke can be associated with a cystic lung appearance that can be mistaken for LAM or another diffuse cystic lung disease. There are associated features of respiratory bronchiolitis and histopathologic changes of emphysema [43]. On HRCT, emphysematous changes are typically located within the secondary pulmonary lobule, do not have well-defined walls, and demonstrate a "central dot" representing the centrilobular core structures. This finding is not seen in true cysts (Fig. 3.15).

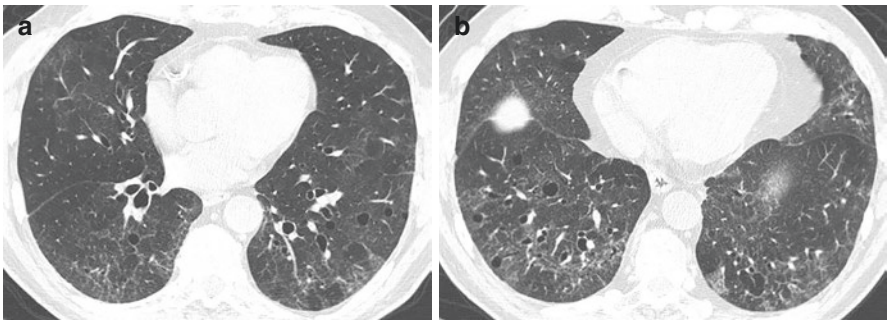

Fig. 3.14 A 67-year-old male with extensive smoking history and lung biopsy demonstrating a spectrum of smoking-related interstitial lung disease, primarily fibrosing desquamative interstitial pneumonia (DIP). (**a**, **b**) Note basilar ground-glass and reticular changes with scattered well-demarcated cysts

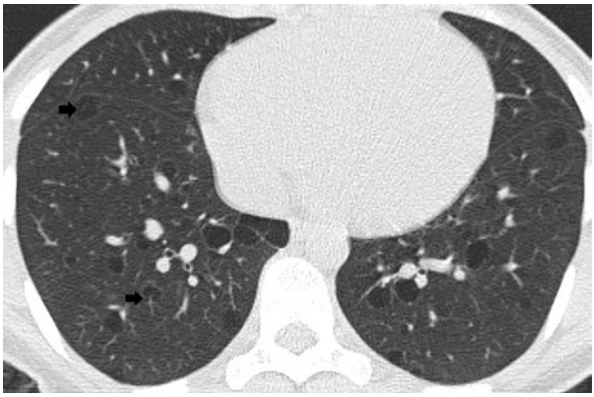

Fig. 3.15 A 19-year-old woman without identifiable tobacco smoke exposure and normal VEGF-D serology. Lung windows on chest CT revealed multiple well-demarcated lucencies with poorly defined walls. Note centrilobular structures in several of the parenchymal "cysts" (*arrows*). Open lung biopsy demonstrated focal emphysema

Lymphangioleiomyomatosis

Lymphangioleiomyomatosis (LAM) is characterized by proliferation of abnormal cells in the pulmonary interstitium affecting vessels, airways, lymphatics, alveolar septa, and pleura [2]. Proliferation around the bronchi leads to air trapping and cyst formation. Obstruction of lymphatics may cause chylous pleural effusion and ascites. In addition, venous occlusion and arterial wall thickening may occur [44]. Spontaneous pneumothorax is seen in up to 50% of patients. LAM can present in sporadic form or in association with tuberous sclerosis complex (TSC) complex, the latter being 5 to 10 times more common [45]. The sporadic form occurs most often in premenopausal women, although presentations later in life in postmenopausal women are not uncommon. Among adult women with TS, 30% to 49% have cystic pulmonary changes consistent with LAM [46, 47]. Cystic lung disease (defined as more than four cysts) is reported in up to 38% of men with TSC; however, it is usually mild [48].

CT demonstrates diffuse thin-walled cysts, typically measuring 2 to 5 mm in diameter although they can be as large as 25 to 30 mm (Fig. 3.16). The cysts are uniformly distributed and typically round or oval, but may become polygonal as disease progresses and becomes more confluent [49] (Fig. 3.17). Additional findings that have been reported include tiny centrilobular nodules, focal ground-glass opacities, and septal thickening. LAM can be mistaken with PLCH on imaging. Gupta et al. [43] suggest that the presence of internal structures or septations within the cysts should prompt an evaluation of alternative (non-LAM) etiologies of DCLD (see Fig. 3.15), particularly in patients with a history of cigarette smoke exposure. Certain features can help distinguish LAM from PLCH: LAM cysts are more regular, randomly distributed with uniform involvement from apex to base, and nodules are not typically seen [26]. Patients with TSC may have additional pulmonary and extrapulmonary findings. Hyperplasia of alveolar type 2 epithelial cells leads to the formation of 1 to 8-mm ground-glass nodules termed "multifocal micronodular pneumocyte hyperplasia" (MMPH), which can be seen in isolation or in the presence of TSC-related LAM [50, 51].

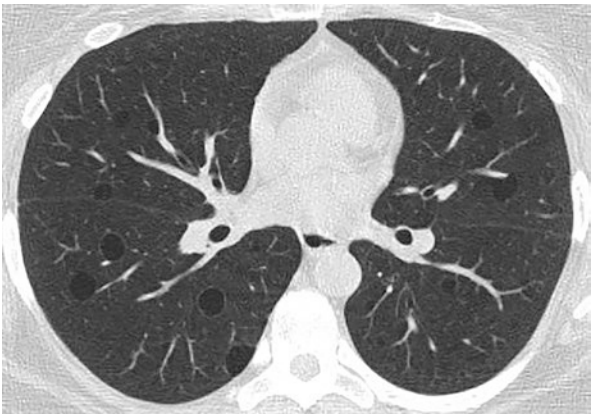

Fig. 3.16 A 63-year-old asymptomatic female with lung cysts incidentally discovered on abdominal CT. Chest CT through the mid thorax shows randomly distributed, thin-walled cysts consistent with paucicystic lymphangioleiomyomatosis (LAM)

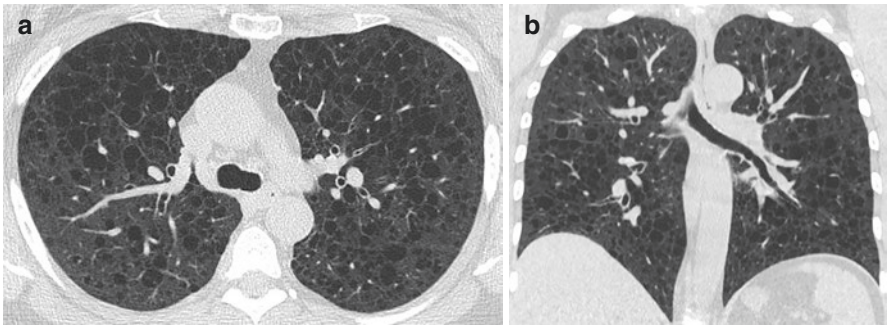

Fig. 3.17 A 48-year-old woman with minimal tobacco exposure, shortness of breath, abnormal chest CT and elevated serum VEGF-D level of 1100 pg/ml, consistent with a diagnosis of lymphangioleiomyomatosis (LAM). (**a**) Axial chest CT reveals diffuse thin-walled cysts, uniform and round or oval in shape. (**b**) Coronal MPR CT is notable for uniform involvement from apex to base

Ancillary findings that may suggest the diagnosis of LAM include renal angiomyolipomas (AMLs). Renal AMLs occur in 80% to 90% of patients with TSC-LAM and 30% to 40% of patients with sporadic LAM; about 20% of patients with AML will have TSC [52]. The presence of an AML in association with DCLD increases the diagnostic certainty of LAM. AMLs usually have a heterogeneous attenuation and enhancement on CT, with intralesional macroscopic fat. While most often asymptomatic, large lesions may hemorrhage or result in mass effect (Fig. 3.18). Intrathoracic features associated with TSC include cardiac rhabdomyomas, intramyocardial fat foci, dilatation of the aorta and pulmonary artery, and extremely rarely, mediastinal angiomyolipomas (AMLs) [53]. Other ancillary findings of TSC include giant cell astrocytomas, subependymal nodules and cortical tubers, sclerotic osseous lesions, cystic bone lesions with a sclerotic rim, renal and hepatic AMLs, and cysts (Fig. 3.19). Lymphadenopathy is seen in about 10% of patients in the mediastinum and up to 40% of patients in the retroperitoneum [52, 54] and may be mistaken for lymphoma.

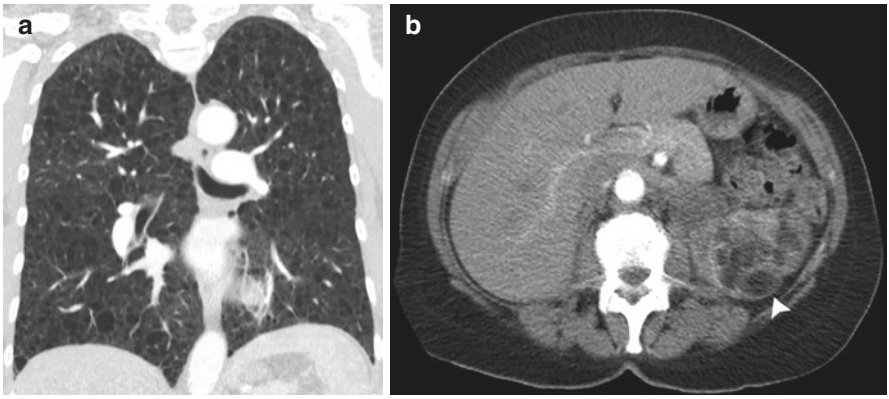

Fig. 3.18 (**a**) A 56-year-old woman with intracranial findings of tuberous sclerosis complex (TSC) and diffuse, round uniform cysts involving the costophrenic angles consistent with lymphangioleiomyomatosis (LAM). (**b**) An abdominal CT image is notable for a fat containing left renal lesion consistent with an angiomyolipoma (*arrowhead*). The combination of pulmonary cysts and renal angiomyolipoma (AML) are frequently present in S-LAM and TSC-LAM

Lymphoid Interstitial Pneumonia

Lymphoid interstitial pneumonia is characterized by polyclonal proliferation of lymphocytes and plasma cells with predominant interstitial involvement. There is hyperplasia of bronchus-associated lymphoid tissue and infiltrates in the interlobular septa and along the pleura containing lymphocytes, plasma cells, and histiocytes. LIP is categorized as both an interstitial pneumonia and a lymphoproliferative disorder [55]. The spectrum of pulmonary lymphoproliferative disorders ranges from benign airway-centered cellular infiltrates (follicular bronchiolitis), nodular lymphoid hyperplasia, LIP, diffuse lymphoid hyperplasia, to mucosa-associated lymphoid tissue (MALT) lymphoma [56]. LIP is most common in middle-aged women, occurring in association with autoimmune disorders such as Sjögren syndrome, systemic lupus erythematosus, autoimmune thyroiditis, primary biliary cirrhosis, and Castleman disease [2]. It can also be seen in patients with acquired immunodeficiency syndrome (AIDS) (especially children) and in this population is considered an AIDS-defining illness. On CT, the dominant features are ground-glass opacities, poorly defined centrilobular nodules, and thin-walled perivascular cysts [57]. The cysts vary in size, typically measuring a few millimeters to 30 mm, and are randomly distributed with a basal predominance [58]. A key feature of LIP cysts is the perivascular location with a small vascular dot visible along the wall of the cysts (Fig. 3.20a, b). The cysts generally occupy less than 10% of the lung volume [56]. New cysts may develop, usually in the areas of pre-existent centrilobular nodules or, less often, ground-glass opacities [59]. Cyst formation may be due to a partial "check-valve" effect secondary to bronchiolar obstruction [60]. Reticular opacities, interlobular septal and bronchovascular thickening, and consolidation may be associated findings. Mediastinal lymphadenopathy may be present and was seen in 15

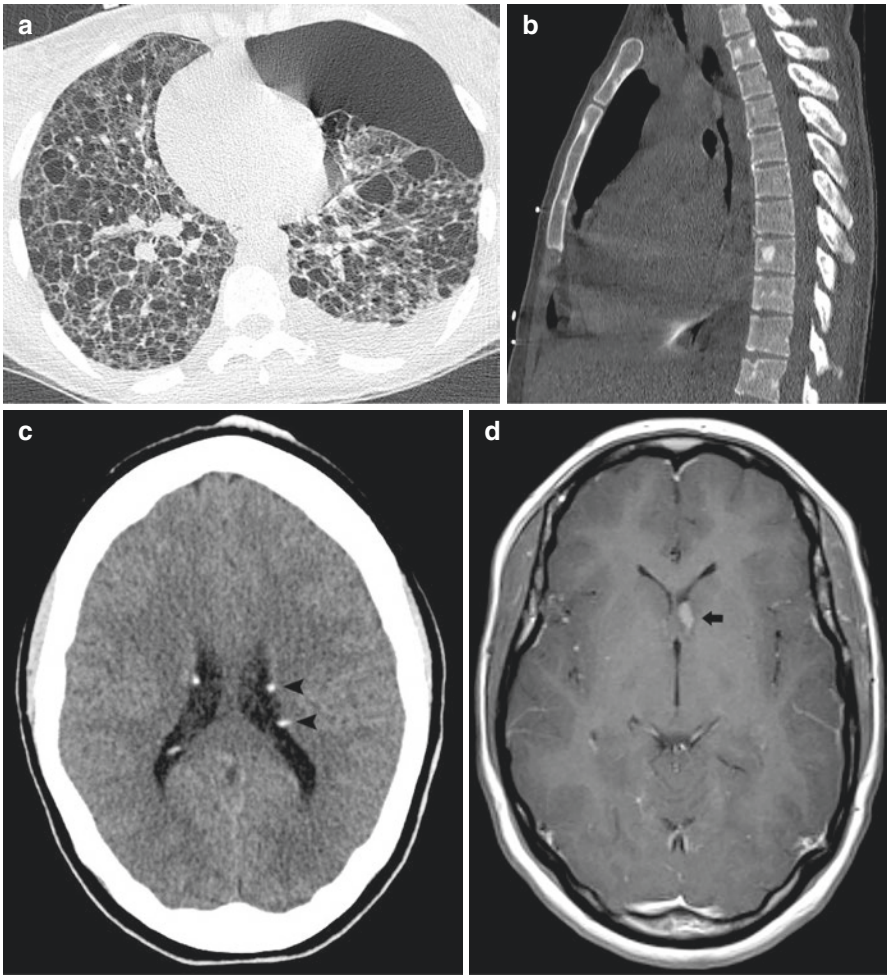

Fig. 3.19 A 32-year-old female with tuberous sclerosis complex (TSC) and severe lymphangioleiomyomatosis (LAM) with multiple bilateral spontaneous pneumothoraces (chest radiograph in Fig. 3.1). (**a**) Lung windows from chest CT reveals diffuse uniform round cysts with bilateral hydropneumothoraces left greater than right. (**b**) Sagittal MPR reconstructions in bone windows reveal multiple sclerotic bone lesions in the sternum and vertebral bodies. (**c**) Head CT at the level of the lateral ventricles with multiple subependymal nodules (*arrowheads*). (**d**) T1-weighted MRI post gadolinium reveals an enhancing mass at the foramen of Monroe consistent with a giant cell astrocytoma (*arrow*)

out of 22 patients described by Hare et al. [57]. The differential diagnosis for LIP includes MALT lymphoma; both entities may also coexist [61]. CT can help to differentiate LIP from lymphoma [57]; cysts are characteristic of LIP, whereas in large nodules exceeding 1 cm, consolidation and effusions should raise suspicion for MALT lymphoma (Fig. 3.20c).

LIP is seen in association with pulmonary amyloidosis, particularly in the context of Sjögren syndrome [62, 63] (Fig. 3.21). The presence of calcified pulmonary

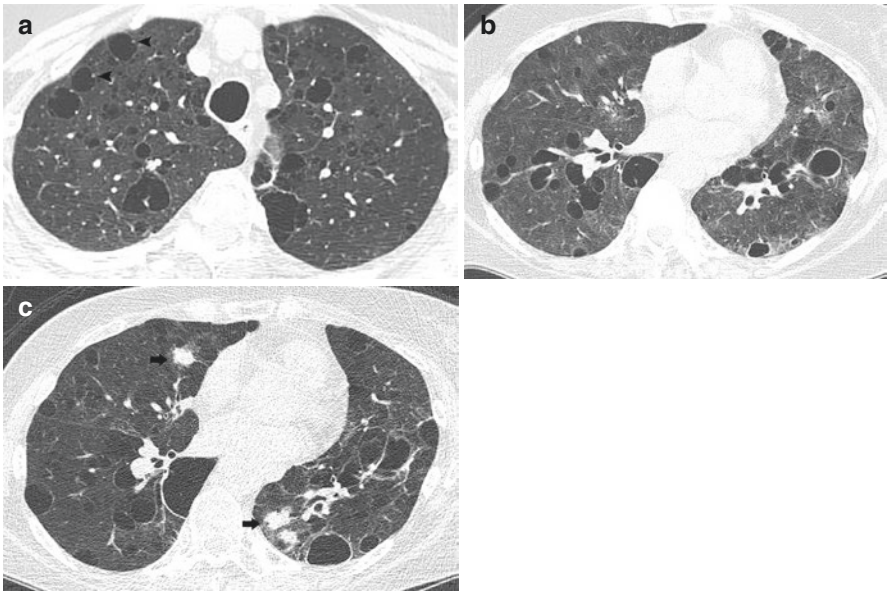

Fig. 3.20 A 71-year-old woman with Sjögren syndrome. (**a**) Baseline CT through the upper lobes is notable for perivascular cysts characteristic of lymphoid interstitial pneumonia. Note vascular "dots" on the margin of the cyst (*arrowheads*). (**b**) A more inferior CT image through the lower lobes shows additional scattered foci of ground-glass with perivascular cysts. (**c**) Follow-up CT 5 years later at the same level as part b is notable for several foci of new nodular soft tissue density exceeding 1 cm (*arrows*) consistent with MALT lymphoma proven at biopsy

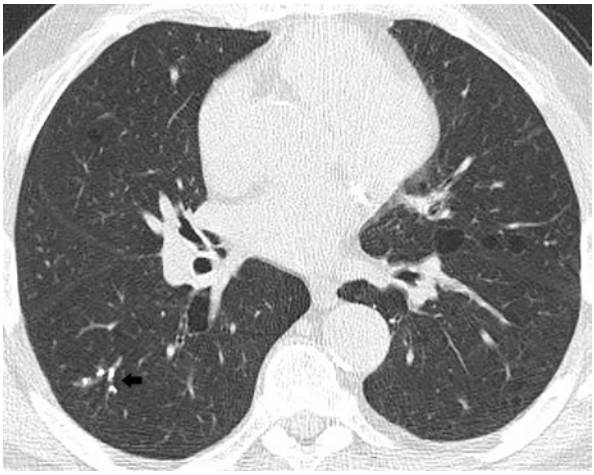

Fig. 3.21 Patient with Sjögren syndrome and amyloidosis. Bilateral cysts and right lower lobe calcified nodules (*arrow*) are present on CT

nodules in conjunction with LIP should raise suspicion of associated pulmonary amyloidosis [57]. The differentiation between LIP and cystic amyloidosis can be challenging and may require confirmation with biopsy [64, 65]. Cysts have been reported in patients with primary Sjögren syndrome and findings of nonspecific interstitial pneumonia (NSIP) without typical findings of LIP [55].

Amyloidosis and Light Chain Deposition Disease

Amyloidosis is characterized by extracellular deposition of abnormal proteins. Amyloidosis may be localized, i.e., involving a single organ (10%–20%), or systemic (80%–90%) [66], which is further classified as primary or secondary. Primary amyloidosis is seen in patients with multiple myeloma or macroglobulinemia, and secondary amyloidosis is described in various inflammatory conditions including rheumatoid arthritis, Crohn disease, cystic fibrosis, tuberculosis, and Mediterranean fever. The lungs are affected in 50% of cases and can be involved in both localized and systemic amyloidosis [67], more often in the latter form (58%-70%) [68].

HRCT findings of pulmonary amyloidosis include nodules, interlobular septal thickening, honeycombing, ground-glass opacities, and lymphadenopathy. Pulmonary cysts occur rarely and are most often described with localized amyloidosis in association with Sjögren syndrome [62]. Jeong et al. described five patients with Sjögren syndrome and amyloidosis, all of them had cysts and nodules on CT. The proposed mechanisms of cyst formation include narrowing of the airway due to inflammatory cells and amyloid deposits creating a check-valve mechanism, disruption of alveolar walls due to inflammation, amyloid deposition, and ischemia secondary to vascular amyloidosis.

Light-chain deposition disease (LCDD) occurs in middle-aged patients and commonly involves the kidneys. Lung involvement is rare; however, it can result in respiratory failure and require lung transplantation [69]. Seventy-five percent of LCDD cases occur in association with multiple myeloma or lymphoproliferative diseases, such as macroglobulinemia. The light chains accumulate in the alveolar walls, small airways, and vessels. HRCT manifestations most commonly include nodules, lymphadenopathy, and cysts (Fig. 3.22). Sheard et al. [70] described a series of 9 patients with pulmonary LCDD, all of them had thin-walled cysts on CT with mean size of 10 mm and 8 patients had nodules. Cyst formation is believed to be secondary to elastin destruction by metalloproteinases from activated macrophages. This leads to enlargement and rupture of the fragile alveoli and bronchioles [71]. The imaging features of amyloidosis and LCDD are indistinguishable and characterized by the presence of perivascular cysts and calcified and noncalcified nodules.

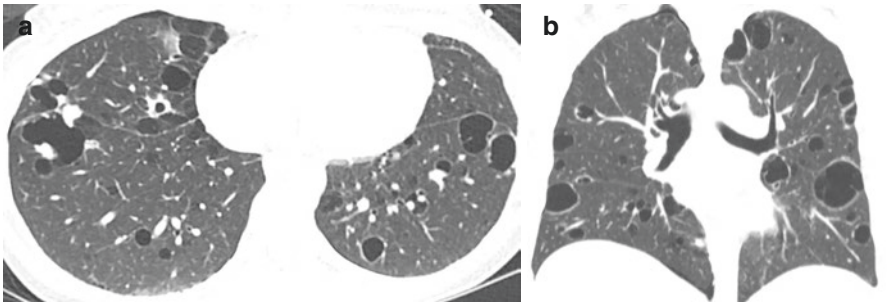

Fig. 3.22 Light-chain deposition disease (LCDD). A 32-year-old female with history of left spontaneous pneumothorax 10 years ago, now with right chest pain and small spontaneous right pneumothorax. (**a**) Axial CT image reveals multiple thin-walled cysts and adjacent nodules. (**b**) Coronal CT image is notable for diffuse involvement without zonal predilection. Case courtesy of Dr. Brett Elicker, San Francisco, CA

Birt-Hogg-Dubé Syndrome

Birt-Hogg-Dubé (BHD) syndrome is a rare autosomal dominant disorder characterized by cutaneous abnormalities, most notably fibrofolliculomas (hamartomas of the hair follicles), lung cysts, and renal tumors ranging from benign oncocytomas to renal cell carcinomas [2]. The cysts are characteristically located in the lower lungs, in subpleural, paramediastinal locations. When they are intrapulmonary, they are frequently perivenous, or oriented along the interlobular septa; they may contain internal septa [72–74]. The cysts are variable in size (from a few millimeters to 2 cm), with most cysts measuring less than 1 cm and oval or elongated. Generally, the cyst walls are thinner when compared with other DCLDs and often barely perceptible (Fig. 3.23). The total extent of lung involvement is usually less than 30%. Ayo et al. described a series of five patients with BHD and found cystic lung changes in all five patients [75]. Toro et al. reported pulmonary cysts in 89% of patients with BHD [76]. Spontaneous pneumothorax is common and can be seen in approximately 24% of patients [76]. Pulmonary cysts in BHD may develop earlier than the skin and renal manifestations and may be the presenting finding.

Hereditary Disorders

In addition to previously described TSC and BHD, there are several hereditary disorders associated with lung cysts, including neurofibromatosis type 1 (NF 1), Marfan syndrome, Ehlers-Danlos syndrome, and Proteus syndrome. These usually

present with limited number of cysts [21] and the clinical context yields the diagnosis. NF1 (von Recklinghausen's disease) is an autosomal dominant neurocutaneous disorder and can also occur as de novo mutation. The nervous system and skin are the most commonly involved, with lungs being affected in approximately 20% of patients [77]. HRCT pulmonary findings include upper lobe predominant cystic and bullous disease, ground-glass opacities, and basilar reticular abnormalities [78–80] (Fig. 3.24).

Cowden syndrome is an autosomal dominant disorder characterized by mucocutanous and visceral hamartomas and increased risk of various malignancies. In a study by Parvinian et al., pulmonary cysts were found in 75% (12/16) of patients, although typically few in number (less than 10 in 83%) and random in distribution [81]. In addition, 87% of patients had nodules.

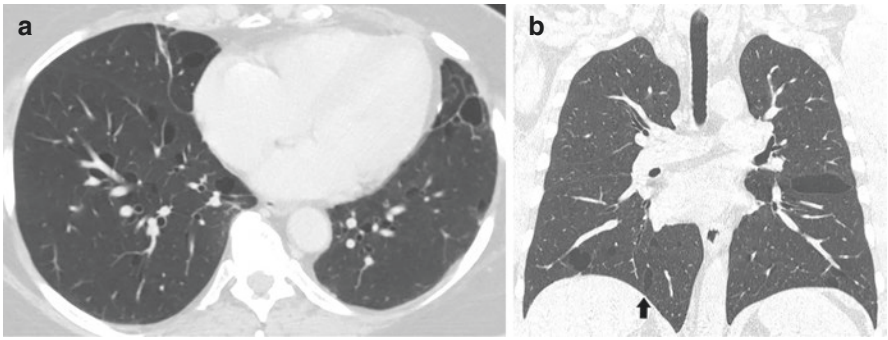

Fig. 3.23 Two cases of Birt-Hogg-Dubé syndrome (BHD). (**a**) A 67-year-old woman with exophytic renal mass and history of "blebectomy" 16 years ago. Axial CT in lung windows at the lung bases shows characteristic subpleural and perivenous cysts. (**b**) A 35-year-old man with spontaneous pneumothorax and fibrofolliculomas on neck and ears. Coronal CT reveals subpleural cysts with barely perceptible walls. Note elongated cyst at the septopleural junction, a characteristic finding of BHD cystic lung disease (*arrow*)

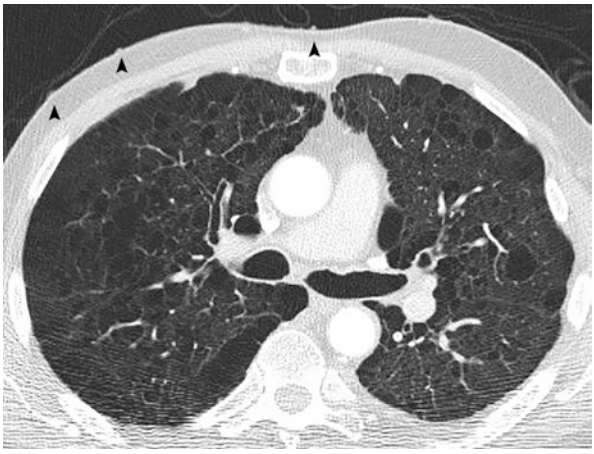

Fig. 3.24 A 56-year-old man with neurofibromatosis 1 (NF1). Note the combination of thin-walled cysts and emphysema, both reported manifestations of NF1. Small anterior cutaneous nodules are chest wall neurofibromas, an important ancillary clue to the diagnosis (*arrowheads*)

Lung Cancer Associated with Cystic Airspaces

There is increasing recognition of the association between lung cancer and cystic airspaces [82]. In some cases, the cancer appears to arise in a preexisting cyst. In others (particularly adenocarcinomas), the cyst may be preceded by a nodule, or the cyst and nodule may be present together. The cysts may be large, complex, and multiloculated. Adenocarcinoma is the usual cell type. Lung cancer should always be suspected when a cyst is present in association with a solid or ground-glass nodule. While cystic adenocarcinoma is usually unifocal, occasionally it presents with multifocal cysts associated with ground-glass nodules (Fig. 3.25). Diffuse thick-walled cystic abnormality (sometimes called "Cheerios in the chest") is a rare but recognized presentation of adenocarcinoma [83, 84] (Fig. 3.26).

Cystic Metastases

Although diffuse lung cysts are a rare presentation of metastases, in a patient with known malignancy, it is critical to consider this diagnosis (Fig. 3.27). Cystic pulmonary metastases occur most frequently in sarcomas [85–87] including angiosarcoma, osteosarcoma, synovial cell sarcoma, leiomyosarcoma, and Ewing sarcoma. Cystic metastases are less common manifestations of other primaries to include squamous cell carcinomas, gastrointestinal malignancies (e.g., colon and pancreatic [88, 89]), genitourinary adenocarcinoma [90], as well as lymphoma. Primary lung malignancies can also present with cystic metastasis, including primary lung cancer and lymphoma [91]. Cystic metastases in meningioma have also been reported [92].

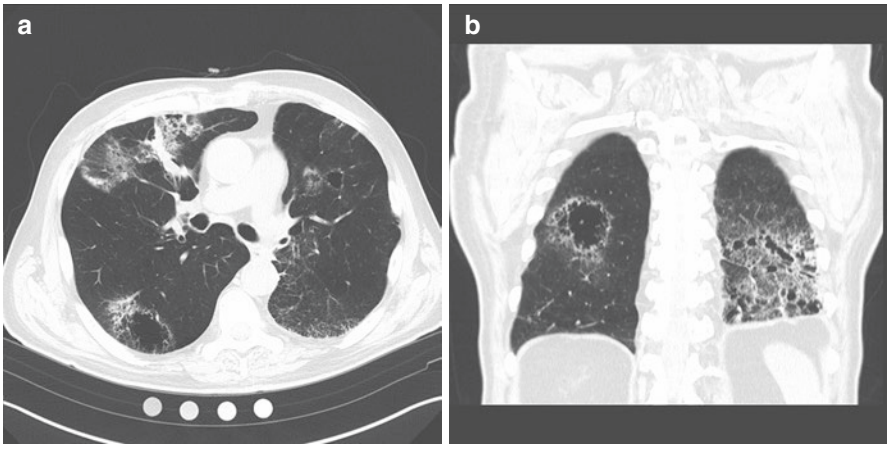

Fig. 3.25 A 60-year-old man with multifocal cystic adenocarcinoma of the lung. (**a**, **b**) Axial and coronal CT images demonstrate multifocal ground-glass abnormality associated with cysts of varying size

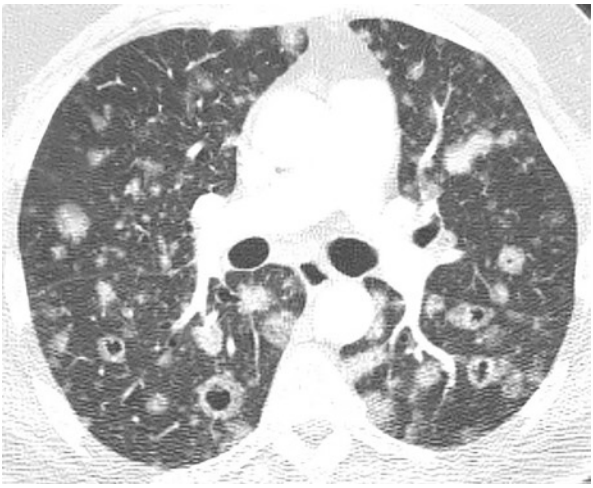

Fig. 3.26 Soggy Cheerios. A 54-year-old man with shortness of breath and hypoxia. Biopsy-proven mucinous adenocarcinoma

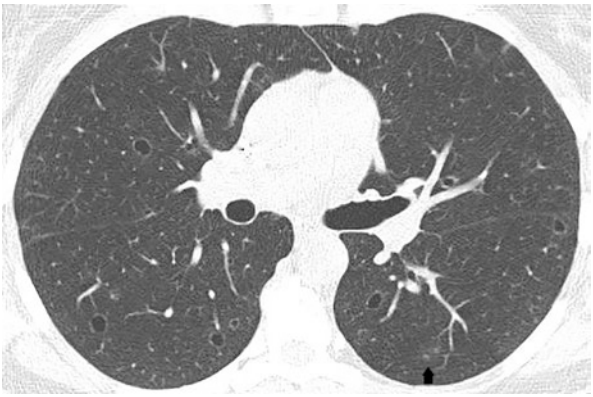

Fig. 3.27 A 45-year-old woman with colon adenocarcinoma on chemotherapy. Thin-walled cystic lung lesions in addition to several small ground-glass nodules (*arrows*) are biopsy-proven lung metastases

Several mechanisms have been proposed for the development of cystic metastases: cavitation of a previously solid lesion or infiltration of tumor cells into the walls of preexisting lung cyst. Another proposed mechanism in angiosarcoma is tumor cell proliferation forming blood-filled cystic spaces [93–95]. Cystic metastases are generally not evident on chest radiographs; therefore, a chest CT scan should be considered, especially in older patients with recurrent pneumothoraces or in settings of known primary malignancy. Cystic metastases due to sarcomas are often complicated by pneumothoraces and portend a poor prognosis [93, 96]. Endometrial stromal sarcomas have been described to result in cystic pulmonary metastases that mimic LAM [87, 97]. Moreover, cystic metastases are not flurodeoxyglucose (FDG) avid on PET scan and can be misinterpreted as benign cysts [98].

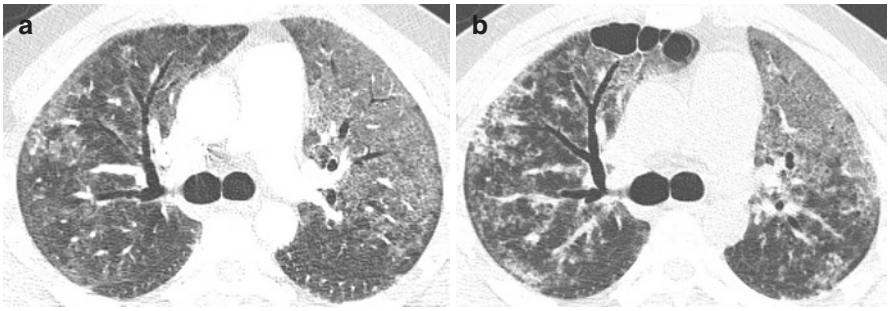

Fig. 3.28 (**a**) A 35-year-old man with HIV off antiretroviral therapy with new-onset hypoxia and shortness of breath, admitted with diffuse ground-glass opacity secondary to *Pneumocystis* pneumonia. (**b**) One week later, thin-walled cysts are present in the anterior segment right upper lobe consistent with post-infectious pneumatoceles

Infection-Related Cysts

Pneumocystis jiroveci pneumonia (PJP) is seen in immunocompromised patients and is classically associated with ground-glass opacities. Lung cysts are commonly (56%) seen in AIDS patients while rarely occurring in other patients with PJP [99]. The cysts associated with PJP are usually multiple with upper lobe predominance (Fig. 3.28). The patient may present with pneumothorax. The cysts can shrink or completely resolve with treatment [100]. Other pulmonary infections can result in necrosis and cavitation, and sometimes also cyst formation, for example, the classic "grape skin" cavity of coccidiomycoisis. Pneumatoceles are also reported in staphylococcal pneumonia [101] (see Fig. 3.9). Post-infectious pneumatoceles are generally focal abnormalities and are not a diagnostic challenge to distinguish from DCLDs.

Tracheobronchial papillomatosis is predominantly a disorder in children and less commonly young adults caused by the human papilloma virus, mainly affecting the upper airways. Rarely the disease involves the lungs resulting in multiple nodules, small cavities, and cysts [102, 103]. The cysts measure up to 5 cm and may contain fluid.

Congenital

Congenital pulmonary airway malformation (CPAM) most commonly occurs in neonates; however, it can be present in asymptomatic adults (Fig. 3.29). These are congenital abnormalities characterized by presence of disorganized lung tissue

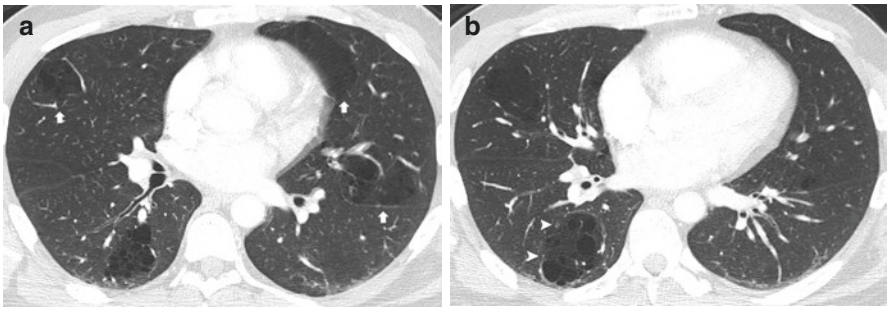

Fig. 3.29 A 32-year-old asymptomatic man. (**a**) Multiple incidentally discovered regions of lucency in several lobes on chest CT obtained for trauma after motor vehicle collision (*arrows*). (**b**) Note air trapping and focal cystic region with air trapping and a disorganized bronchovascular bundle characteristic of congential pulmonary airway malformation (CPAM) (*arrowheads*)

[104, 105]. The most common type I (70% of cases) is composed of larger cysts, 2 to 10 cm. In type II, the cysts are smaller, typically less than 2 cm. Type III contains microcysts (less than 5 mm) and may appear as consolidation on imaging. Hybrid lesions have been reported with both a component of CPAM and sequestration [106]. CPAMs are typically unilateral and more often seen in the lower lobes. In adults, they can present with recurrent pulmonary infection, pneumothorax, hemoptysis, fever, pain, and dyspnea [107, 108]. These are localized abnormalities with disorganized bronchovascular marking and are easily distinguished from DCLDs.

Other

Cysts have been reported in association with chronic and subacute hypersensitivity pneumonitis (HP); they are reported to occur in approximately 10% of patients with subacute HP [109]. With increasing recognition of chronic HP as a cause of fibrosis, in the authors' experience the prevalence is likely less than originally reported. In HP, the CT features are characterized by mosaic attenuation, air trapping, and ground-glass and ill-defined centrilobular nodules with cysts, if present, being a minor component (Fig. 3.30).

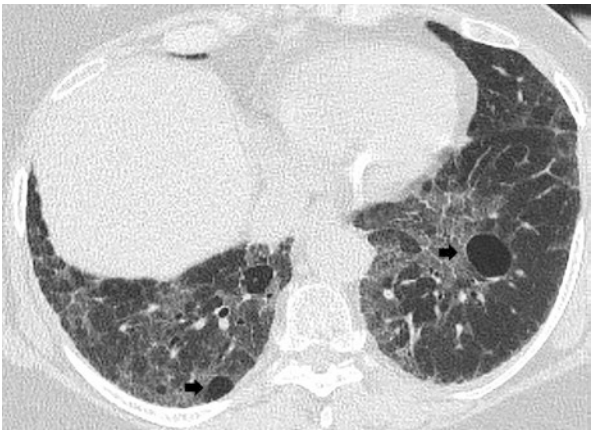

Fig. 3.30 A 74-year-old woman with shortness of breath and positive hypersensitivity panel. Chest CT shows mosaic ground-glass opacity, mild reticulation, and air trapping. Note focal cysts in both lower lobes (*arrows*)

Conclusion

With the widespread application of chest CT, cystic lung lesions are frequently encountered, sometimes incidentally. While a few cysts in an older patient are likely age-related, the presence of multiple cysts or cysts in patients aged less than 40 requires further investigation. This chapter has reviewed the CT technique recommended to investigate cystic lung disease. Initially, the mimics of true lung cysts must be excluded, mainly emphysema and bronchiectasis. The differential diagnosis for diffuse cystic lung diseases is broad and includes congenital, inflammatory, infectious, and neoplastic etiologies [75]. Several imaging characteristics will improve specificity [8] including cyst morphology, number, and distribution. The presence of additional parenchymal changes (ground-glass opacities, consolidation, nodules, reticular opacities, fibrosis, etc.) can also narrow the differential diagnosis. Finally, observation of extrapulmonary findings can be diagnostic. These are summarized in Table 3.2. As with all interstitial lung diseases, the interpretation of the imaging findings is most useful in a multidisciplinary context. In conjunction with clinical information and serology, a correct first diagnosis can be achieved in the majority of cases without further invasive testing.

Table 3.2 Clinical and CT findings in the most common DCLDs

Diagnosis	% Cysts	Clinical	Distinct HRCT features	Ancillary findings
Pulmonary Langerhans cell histiocytosis	100	Smoker	Centrilobular nodules (early), bizarre-shaped cysts (late) Costophrenic angle sparing	Enlarged main pulmonary artery, rarely bony lesions
Sporadic-LAM	100	Spontaneous pneumothorax	Diffuse uniform round or oval cysts	Chylous effusions, mediastinal and retroperitoneal adenopathy, renal angiomyolipomas
Tuberous sclerosis complex-LAM	30–50	Seizures Skin lesions Spontaneous pneumothorax	Diffuse uniform round or oval cysts Miliary nodules in multifocal micronodular pneumocyte hyperplasia (MMPH)	Renal angiomyolipomas, osteomas, rhabdomyomas, Central nervous system (CNS) giant cell astrocytomas, cortical tubers, and subependymal nodules
Lymphoid interstitial pneumonia	60–70	Sjögren syndrome AIDS Common variable immune deficiency (CVID)	Focal ground-glass opacity and perivascular cysts (vascular dot in wall)	If nodules >1 cm and effusions, consider BALT lymphoma
Amyloidosis LCDD	Rare	Sjögren syndrome Multiple myeloma and other myeloid dyscrasias	Rare nodules (often calcified) and perivascular cysts	–
Birt-Hogg-Dubé syndrome	>80	Skin lesions	Basilar, subpleural, lentiform cysts	Renal neoplasms
Cystic metastases	Rare	History of malignancy	Peripheral, hematogenous	–

Key Learning Points

- Differential diagnosis for diffuse cystic lung diseases is broad and includes congenital, inflammatory, infectious, and neoplastic etiologies.
- Chest CT is recommended to evaluate suspected or known cystic lung disease.
- Cyst mimics such as emphysema and bronchiectasis need to be excluded. This can be facilitated by the proper CT technique and additional reformats.
- Helpful clues for CT diagnosis include cyst distribution and shape, ancillary lung, and extrapulmonary findings. These should be considered in clinical context.

References

1. Hansell DM, Bankier AA, MacMahon H, McLoud TC, Müller NL, Remy J. Fleischner Society: glossary of terms for thoracic imaging. Radiology. 2008;246(3):697–722.
2. Seaman DM, Meyer CA, Gilman MD, McCormack FX. Diffuse cystic lung disease at high-resolution CT. AJR Am J Roentgenol. 2011;196(6):1305–11.
3. Kim NR, Han J. Pathologic review of cystic and cavitary lung diseases. Korean J Pathol. 2012;46(5):407–14.
4. Gupta N, Langenderfer D, McCormack FX, Schauer DP, Eckman MH. Chest computed tomographic image screening for cystic lung diseases in patients with spontaneous pneumothorax is cost effective. Ann Am Thorac Soc. 2017;14(1):17–25.
5. Koyama M, Johkoh T, Honda O, Tsubamoto M, Kozuka T, Tomiyama N, et al. Chronic cystic lung disease: diagnostic accuracy of high-resolution CT in 92 patients. AJR Am J Roentgenol. 2003;180(3):827–35.
6. Gupta N, Finlay GA, Kotloff RM, Strange C, Wilson KC, Young LR, et al. Lymphangioleiomyomatosis diagnosis and management: high-resolution chest computed tomography, Transbronchial lung biopsy, and pleural disease management. An official American Thoracic Society/Japanese respiratory society clinical practice guideline. Am J Respir Crit Care Med. 2017;196(10):1337–48.
7. Gupta N, Meraj R, Tanase D, James LE, Seyama K, Lynch DA, et al. Accuracy of chest high-resolution computed tomography in diagnosing diffuse cystic lung diseases. Eur Respir J. 2015;46(4):1196–9.
8. Baldi BG, Ribeiro Carvalho CR, Meira Dias O, Marchiori E, Hochhegger B. Diffuse cystic lung diseases: differential diagnosis. J Bras Pneumol. 2017;43(2):140–9.
9. Dalrymple NC, Prasad SR, Freckleton MW, Chintapalli KN. Introduction to the Language of Three-dimensional Imaging with Multidetector CT. Radiographics. 2005;25(5):1409–28.
10. Beddy P, Babar J, Devaraj A. A practical approach to cystic lung disease on HRCT. Insights Imaging. 2011;2(1):1–7.
11. Sabri YY, IMH I, SMT G, Assal HH. Multi-detector CT (MDCT) evaluation in interstitial lung disease (ILD): comparison of MinIP and volumetric high resolution CT (HRCT) images. Egypt J Radiol Nucl Med. 2017;48(1):87–95.
12. Beigelman-Aubry C, Hill C, Guibal A, Savatovsky J, Grenier PA. Multi–detector row CT and postprocessing techniques in the assessment of diffuse lung disease. Radiographics. 2005;25(6):1639–52.
13. NRC.GOV. [10/13/2018]. Available from: https://www.nrc.gov/about-nrc/radiation/around-us/doses-daily-lives.html
14. Huda W. Ovid Technologies Inc. Review of radiologic physics. 2010; 131.
15. Thurlbeck WM, Müller NL. Emphysema: definition, imaging, and quantification. Am J Roentgenol. 1994;163(5):1017–25.
16. Remy-Jardin M, Giraud F, Remy J, Copin MC, Gosselin B, Duhamel A. Importance of ground-glass attenuation in chronic diffuse infiltrative lung disease: pathologic-CT correlation. Radiology. 1993;189(3):693–8.
17. Copley SJ, Wells AU, Hawtin KE, Gibson DJ, Hodson JM, Jacques AE, et al. Lung morphology in the elderly: comparative CT study of subjects over 75 years old versus those under 55 years old. Radiology. 2009;251(2):566–73.
18. Winter DH, Manzini M, Salge JM, Busse A, Jaluul O, Jacob Filho W, et al. Aging of the lungs in asymptomatic lifelong nonsmokers: findings on HRCT. Lung. 2015;193(2):283–90.
19. Araki T, Nishino M, Gao W, Dupuis J, Putman RK, Washko GR, et al. Pulmonary cysts identified on chest CT: are they part of aging change or of clinical significance? Thorax. 2015;70(12):1156–62.

20. Trotman-Dickenson B. Cystic lung disease: achieving a radiologic diagnosis. Eur J Radiol. 2014;83(1):39–46.
21. Ryu JH, Tian X, Baqir M, Xu K. Diffuse cystic lung diseases. Front Med. 2013;7(3): 316–27.
22. Tazi A. Adult pulmonary Langerhans' cell histiocytosis. Eur Respir J. 2006;27(6):1272–85.
23. Northrup H, Krueger DA. International tuberous sclerosis complex consensus. Tuberous sclerosis complex diagnostic criteria update: recommendations of the 2012 International Tuberous Sclerosis Complex Consensus Conference. Pediatr Neurol. 2013;49(4):243–54.
24. Vassallo R, Harari S, Tazi A. Current understanding and management of pulmonary Langerhans cell histiocytosis. Thorax. 2017;72(10):937–45.
25. Abbott GF, Rosado-de-Christenson ML, Franks TJ, Frazier AA, Galvin JR. From the archives of the AFIP: pulmonary Langerhans cell histiocytosis. Radiographics. 2004;24(3):821–41.
26. Castoldi MC, Verrioli A, De Juli E, Vanzulli A. Pulmonary Langerhans cell histiocytosis: the many faces of presentation at initial CT scan. Insights Imaging. 2014;5(4):483–92.
27. Radzikowska E, Błasińska-Przerwa K, Wiatr E, Bestry I, Langfort R, Roszkowski-Śliż K. Pneumothorax in patients with pulmonary langerhans cell histiocytosis. Lung. 2018;196:715–20.
28. Nair A, Hansell DM. High-resolution computed tomography features of smoking-related interstitial lung disease. Semin Ultrasound CT MR. 2014;35(1):59–71.
29. Lacronique J, Roth C, Battesti JP, Basset F, Chretien J. Chest radiological features of pulmonary histiocytosis X: a report based on 50 adult cases. Thorax. 1982;37(2):104–9.
30. Earlam K, et al. Pulmonary Langerhans' cell histiocytosis and diabetes insipidus in a young smoker. Can Respir J. 2015;
31. Arico M, Egeler RM. Clinical aspects of Langerhans cell histiocytosis. Hematol Oncol Clin North Am. 1998;12(2):247–58.
32. Kim HJ, Lee KS, Johkoh T, Tomiyama N, Lee HY, Han J, et al. Pulmonary Langerhans cell histiocytosis in adults: high-resolution CT-pathology comparisons and evolutional changes at CT. Eur Radiol. 2011;21(7):1406–15.
33. Abbritti M, Mazzei MA, Bargagli E, Refini RM, Penza F, Perari MG, et al. Utility of spiral CAT scan in the follow-up of patients with pulmonary Langerhans cell histiocytosis. Eur J Radiol. 2012;81(8):1907–12.
34. Canuet M, Kessler R, Jeung MY, Métivier AC, Chaouat A, Weitzenblum E. Correlation between high-resolution computed tomography findings and lung function in pulmonary Langerhans cell histiocytosis. Respiration. 2007;74(6):640–6.
35. Delobbe A, Durieu J, Duhamel A, Wallaert B. Determinants of survival in pulmonary Langerhans' cell granulomatosis (histiocytosis X). Groupe d'Etude en Pathologie Interstitielle de la Societe de Pathologie Thoracique du Nord. Eur Respir J. 1996;9(10):2002–6.
36. Tazi A, Marc K, Dominique S, de Bazelaire C, Crestani B, Chinet T, et al. Serial computed tomography and lung function testing in pulmonary Langerhans' cell histiocytosis. Eur Respir J. 2012;40(4):905–12.
37. Mogulkoc N, Veral A, Bishop PW, Bayindir U, Pickering CA, Egan JJ. Pulmonary Langerhans' cell histiocytosis: radiologic resolution following smoking cessation. Chest. 1999;115(5):1452–5.
38. Krajicek BJ, Ryu JH, Hartman TE, Lowe VJ, Vassallo R. Abnormal fluorodeoxyglucose PET in pulmonary Langerhans cell histiocytosis. Chest. 2009;135(6):1542–9.
39. Hansen NJ, Hankins JH. Pulmonary langerhans cell histiocytosis: PET/CT for initial workup and treatment response evaluation. Clin Nucl Med. 2015;40(2):153–5.
40. Heyneman LE, Ward S, Lynch DA, Remy-Jardin M, Johkoh T, Müller NL. Respiratory bronchiolitis, respiratory bronchiolitis-associated interstitial lung disease, and desquamative interstitial pneumonia: different entities or part of the spectrum of the same disease process? AJR Am J Roentgenol. 1999;173(6):1617–22.
41. Akira M, Yamamoto S, Hara H, Sakatani M, Ueda E. Serial computed tomographic evaluation in desquamative interstitial pneumonia. Thorax. 1997;52(4):333–7.

42. Hartman TE, Primack SL, Swensen SJ, Hansell D, McGuinness G, Müller NL. Desquamative interstitial pneumonia: thin-section CT findings in 22 patients. Radiology. 1993;187(3): 787–90.
43. Gupta N, Colby TV, Meyer CA, McCormack FX, Wikenheiser-Brokamp KA. Smoking-related diffuse cystic lung disease. Chest. 2018;154(2):e31–5.
44. Abbott GF, Rosado-de-Christenson ML, Frazier AA, Franks TJ, Pugatch RD, Galvin JR. From the archives of the AFIP: lymphangioleiomyomatosis: radiologic-pathologic correlation. Radiographics. 2005;25(3):803–28.
45. McCormack FX. Lymphangioleiomyomatosis: a clinical update. Chest. 2008;133(2):507–16.
46. Avila NA, Dwyer AJ, Rabel A, Moss J. Sporadic lymphangioleiomyomatosis and tuberous sclerosis complex with lymphangioleiomyomatosis: comparison of CT features. Radiology. 2007;242(1):277–85.
47. Muzykewicz DA, Sharma A, Muse V, Numis AL, Rajagopal J, Thiele EA. TSC1 and TSC2 mutations in patients with lymphangioleiomyomatosis and tuberous sclerosis complex. J Med Genet. 2009;46(7):465–8.
48. Ryu JH, Gisele Sykes A-M, Lee AS, Burger CD. Cystic lung disease is not uncommon in men with tuberous sclerosis complex. Respir Med. 2012;106(11):1586–90.
49. Ajlan AM, Bilawich AM, Muller NL. Thoracic computed tomographic manifestations of tuberous sclerosis in adults. Can Assoc Radiol J. 2012;63(1):61–8.
50. Gupta N, Henske EP. Pulmonary manifestations in tuberous sclerosis complex. Am J Med Genet C Semin Med Genet. 2018;178:326–37.
51. Ristagno RL, Biddinger PW, Pina EM, Meyer CA. Multifocal micronodular pneumocyte hyperplasia in tuberous sclerosis. AJR Am J Roentgenol. 2005;184(3 Suppl):S37–9.
52. Tobino K, Johkoh T, Fujimoto K, Sakai F, Arakawa H, Kurihara M, et al. Computed tomographic features of lymphangioleiomyomatosis: evaluation in 138 patients. Eur J Radiol. 2015;84(3):534–41.
53. Warth A, Herpel E, Schmähl A, Hoffmann H, Herth FJ, Schirmacher P, et al. Mediastinal angiomyolipomas in a male patient affected by tuberous sclerosis. Eur Respir J. 2008;31(3): 678–80.
54. Kitaichi M, Nishimura K, Itoh H, Izumi T. Pulmonary lymphangioleiomyomatosis: a report of 46 patients including a clinicopathologic study of prognostic factors. Am J Respir Crit Care Med. 1995;151(2 Pt 1):527–33.
55. Egashira R, Kondo T, Hirai T, Kamochi N, Yakushiji M, Yamasaki F, et al. CT findings of thoracic manifestations of primary Sjögren syndrome: radiologic-pathologic correlation. Radiographics. 2013;33(7):1933–49.
56. Silva CI, Flint JD, Levy RD, Müller NL. Diffuse lung cysts in lymphoid interstitial pneumonia: high-resolution CT and pathologic findings. J Thorac Imaging. 2006;21(3):241–4.
57. Hare SS, Souza CA, Bain G, Seely JM, Gomes MM, et al. The radiological spectrum of pulmonary lymphoproliferative disease. Br J Radiol. 2012;85(1015):848–64.
58. Lynch DA. Lung disease related to collagen vascular disease. J Thorac Imaging. 2009;24(4):299–309.
59. Johkoh T, Müller NL, Pickford HA, Hartman TE, Ichikado K, Akira M, et al. Lymphocytic interstitial pneumonia: thin-section CT findings in 22 patients. Radiology. 1999;212(2): 567–72.
60. Ichikawa Y, Kinoshita M, Koga T, Oizumi K, Fujimoto K, Hayabuchi N. Lung cyst formation in lymphocytic interstitial pneumonia: CT features. J Comput Assist Tomogr. 1994;18(5):745–8.
61. Watanabe Y, Koyama S, Miwa C, Okuda S, Kanai Y, Tetsuka K, et al. Pulmonary mucosa-associated lymphoid tissue (MALT) lymphoma in Sjögren's syndrome showing only the LIP pattern radiologically. Intern Med. 2012;51(5):491–5.
62. Jeong YJ, Lee KS, Chung MP, Han J, Chung MJ, Kim KI, Seo JB, et al. Amyloidosis and lymphoproliferative disease in Sjogren syndrome: thin-section computed tomography findings and histopathologic comparisons. J Comput Assist Tomogr. 2004;28(6):776–81.

63. Marchiori E, Zanetti G, Hocchegger B, Irion KL. Cystic amyloidosis or lymphoid interstitial pneumonia associated with amyloidosis? A diagnostic challenge. Ann Thorac Surg. 2012;94(3):1041–2. author reply 1042
64. Sakai M, Yamaoka M, Kawaguchi M, Hizawa N, Sato Y. Multiple cystic pulmonary amyloidosis. Ann Thorac Surg. 2011;92(5):e109.
65. Chew KM, Clarke MJ, Dubey N, Seet JE. Nodular pulmonary amyloidosis with unusual, widespread lung cysts. Singap Med J. 2013;54(5):e97–9.
66. Desai SR, Nicholson AG, Stewart S, Twentyman OM, Flower CD, Hansell DM, et al. Benign pulmonary lymphocytic infiltration and amyloidosis: computed tomographic and pathologic features in three cases. J Thorac Imaging. 1997;12(3):215–20.
67. Aylwin AC, Gishen P, Copley SJ. Imaging appearance of thoracic amyloidosis. J Thorac Imaging. 2005;20(1):41–6.
68. Utz JP, Swensen SJ, Gertz MA. Pulmonary amyloidosis. The Mayo Clinic experience from 1980 to 1993. Ann Intern Med. 1996;124(4):407–13.
69. Colombat M, Stern M, Groussard O, Droz D, Brauner M, Valeyre D, et al. Pulmonary cystic disorder related to light chain deposition disease. Am J Respir Crit Care Med. 2006;173(7):777–80.
70. Sheard S, Nicholson AG, Edmunds L, Wotherspoon AC, Hansell DM. Pulmonary light-chain deposition disease: CT and pathology findings in nine patients. Clin Radiol. 2015;70(5):515–22.
71. Colombat M, Caudroy S, Lagonotte E, Mal H, Danel C, Stern M, et al. Pathomechanisms of cyst formation in pulmonary light chain deposition disease. Eur Respir J. 2008;32(5):1399–403.
72. Kumasaka T, Hayashi T, Mitani K, Kataoka H, Kikkawa M, Tobino K, et al. Characterization of pulmonary cysts in Birt-Hogg-Dubé syndrome: histopathological and morphometric analysis of 229 pulmonary cysts from 50 unrelated patients. Histopathology. 2014;65(1):100–10.
73. Tobino K, Gunji Y, Kurihara M, Kunogi M, Koike K, Tomiyama N, et al. Characteristics of pulmonary cysts in Birt-Hogg-Dubé syndrome: thin-section CT findings of the chest in 12 patients. Eur J Radiol. 2011;77(3):403–9.
74. Agarwal PP, Gross BH, Holloway BJ, Seely J, Stark P, Kazerooni EA. Thoracic CT findings in Birt-Hogg-Dube syndrome. AJR Am J Roentgenol. 2011;196(2):349–52.
75. Ayo DS, Aughenbaugh GL, Yi ES, Hand JL, Ryu JH. Cystic lung disease in Birt-Hogg-Dube syndrome. Chest. 2007;132(2):679–84.
76. Toro JR, Pautler SE, Stewart L, Glenn GM, Weinreich M, Toure O, et al. Lung cysts, spontaneous pneumothorax, and genetic associations in 89 families with Birt-Hogg-Dube syndrome. Am J Respir Crit Care Med. 2007;175(10):1044–53.
77. Zamora AC, Collard HR, Wolters PJ, Webb WR, King TE. Neurofibromatosis-associated lung disease: a case series and literature review. Eur Respir J. 2007;29(1):210–4.
78. Shino MY, Rabbani S, Belperio JA, Lynch JP 3rd, Weigt SS. Neurofibromatosis-associated diffuse lung disease: case report. Semin Respir Crit Care Med. 2012;33(5):572–5.
79. Nalepa P, Wolnicka M. Neurofibromatosis type 1 with interstitial pulmonary lesions diagnosed in adult patient. A case study and literature review. Pneumonol Alergol Pol. 2012;80(2):152–7.
80. Zamora AC, White DB, Sykes AM, Hoskote SS, Moua T, Yi ES, et al. Amyloid-associated cystic lung disease. Chest. 2016;149(5):1223–33.
81. Parvinian A, Cox CW, Hartman TE. Cowden syndrome: a cause of pulmonary cysts. J Thorac Imaging. 2018;33(6):W48–50.
82. Fintelmann FJ, Brinkmann JK, Jeck WR, Troschel FM, Digumarthy SR, Mino-Kenudson M, et al. Lung cancers associated with cystic airspaces: natural history, pathologic correlation, and mutational analysis. J Thorac Imaging. 2017;32(3):176–88.
83. Kho SS, Yong MC, Chan SK, Tie ST. A lung full of Cheerios. Thorax. 2018;73(10):994–5.
84. Reed SL, O'Neil KM. Cheerios in the chest. Chest. 1993;104(4):1267–8.
85. Traweek T, Rotter AJ, Swartz W, Azumi N. Cystic pulmonary metastatic sarcoma. Cancer. 1990;65(8):1805–11.
86. Chan DP, Griffith JF, Lee TW, Chow LT, Yim AP. Cystic pulmonary metastases from epithelioid cell sarcoma. Ann Thorac Surg. 2003;75(5):1652–4.

87. Aubry MC, Myers JL, Colby TV, Leslie KO, Tazelaar HD. Endometrial stromal sarcoma metastatic to the lung: a detailed analysis of 16 patients. Am J Surg Pathol. 2002;26(4):440–9.
88. Kushima H, Ishii H, Yokoyama A, Kadota J. Lung adenocarcinoma presenting with diffuse multiloculated cystic lesions. Intern Med. 2013;52(20):2375.
89. Zhang J, Zhao YL, Ye MX, Sun G, Wu H, Wu CG, et al. Rapidly progressive diffuse cystic lesions as a radiological hallmark of lung adenocarcinoma. J Thorac Oncol. 2012;7(2):457–8.
90. Imokawa S, Uehara M, Uto T, Sagisaka S, Sato J, Yasuda K, Matsushita K, et al. Pulmonary metastasis from urothelial carcinoma showing progressive multiple cystic lesions. Am J Respir Crit Care Med. 2013;188(10):1267–8.
91. Gupta N, Vassallo R, Wikenheiser-Brokamp KA, McCormack FX. Diffuse cystic lung disease. Part II. Am J Respir Crit Care Med. 2015;192(1):17–29.
92. Stefani A, Rossi G, Pecchi A, Bertolini F, Falasca A, Aramini B, et al. An unusual case of cystic interstitial lung disease. Lancet. 2013;381(9873):1246.
93. Tateishi U, Hasegawa T, Kusumoto M, Yamazaki N, Iinuma G, Muramatsu Y, et al. Metastatic angiosarcoma of the lung: spectrum of CT findings. AJR Am J Roentgenol. 2003;180(6):1671–4.
94. Yogi A, Miyara T, Ogawa K, Iraha S, Matori S, Haranaga S, et al. Pulmonary metastases from angiosarcoma: a spectrum of CT findings. Acta Radiol. 2016;57(1):41–6.
95. Aryal S, Chu C, Morehead RS. An 83-year-old man with bilateral spontaneous pneumothoraces and multiple cysts. Chest. 2011;139(6):1536–9.
96. Hoag JB, Sherman M, Fasihuddin Q, Lund ME. A comprehensive review of spontaneous pneumothorax complicating sarcoma. Chest. 2010;138(3):510–8.
97. Abrams J, Talcott J, Corson JM. Pulmonary metastases in patients with low-grade endometrial stromal sarcoma. Clinicopathologic findings with immunohistochemical characterization. Am J Surg Pathol. 1989;13(2):133–40.
98. Somasekharan Nair KK, Zabell AS, Vo KL, Shaikh MA. Pneumothorax: a classical presentation of metastatic scalp angiosarcoma. Ann Thoracic Surg. 2012;94(3):e77–8.
99. Hardak E, Brook O, Yigla M. Radiological features of Pneumocystis jirovecii pneumonia in immunocompromised patients with and without AIDS. Lung. 2010;188(2):159–63.
100. Chow C, Templeton PA, White CS. Lung cysts associated with Pneumocystis carinii pneumonia: radiographic characteristics, natural history, and complications. AJR Am J Roentgenol. 1993;161(3):527–31.
101. Erdem G, Bergert L, Len K, Melish M, Kon K, DiMauro R. Radiological findings of community-acquired methicillin-resistant and methicillin-susceptible Staphylococcus aureus pediatric pneumonia in Hawaii. Pediatr Radiol. 2010;40(11):1768–73.
102. Soldatski IL, et al. Tracheal, bronchial, and pulmonary papillomatosis in children. Laryngoscope. 2005;115(10):1848–54.
103. Zawadzka-Glos L, Jakubowska A, Chmielik M, Bielicka A, Brzewski M. Lower airway papillomatosis in children. Int J Pediatr Otorhinolaryngol. 2003;67(10):1117–21.
104. Hardee S, Tuzovic L, Silva CT, Cowles RA, Copel J, Morotti RA. Congenital cystic lung lesions: evolution from in-utero detection to pathology diagnosis-a multidisciplinary approach. Pediatr Dev Pathol. 2017;20(5):403–10.
105. Biyyam DR, Chapman T, Ferguson MR, Deutsch G, Dighe MK. Congenital lung abnormalities: embryologic features, prenatal diagnosis, and postnatal radiologic-pathologic correlation. Radiographics. 2010;30(6):1721–38.
106. Rosado-de-Christenson ML, Stocker JT. Congenital cystic adenomatoid malformation. Radiographics. 1991;11(5):865–86.
107. Shupe MP, Kwon HP, Morris MJ. Spontaneous pneumothorax in a teenager with prior congenital pulmonary airway malformation. Respir Med Case Rep. 2014;11:18–21.
108. Baral D, Adhikari B, Zaccarini D, Man Dongol R, Sah B. Congenital pulmonary airway malformation in an adult male: a case report with literature review. Case Rep Pulmonol. 2015;2015:743452.
109. Franquet T, Hansell DM, Senbanjo T, Remy-Jardin M, Müller NL. Lung cysts in subacute hypersensitivity pneumonitis. J Comput Assist Tomogr. 2003;27(4):475–8.

Chapter 4
Pathological Evaluation of Pulmonary Cysts

John M. Carney and Maxwell L. Smith

Abbreviations

A1ATD	Alpha 1 antitrypsin deficiency
BHD	Birt-Hogg-Dube syndrome
CLE	Centrilobular emphysema
CPAM	Congenital pulmonary airway malformation
CTD	Connective tissue disease
DCLD	Diffuse cystic lung disease
DIP	Desquamative interstitial pneumonia
ECD	Erdheim-Chester disease
ESS	Endometrial stromal sarcoma
GGO	Ground-glass opacities
HC	Honeycomb cysts
HP	Hypersensitivity pneumonitis
HPV	Human papilloma virus
HRCT	High-resolution computed tomography
LAM	Lymphangioleiomyomatosis
LCDD	Light chain deposition disease
LIP	Lymphoid interstitial pneumonia
MMPH	Multifocal micronodular pneumocyte hyperplasia
NSIP	Nonspecific interstitial pneumonia

J. M. Carney
Department of Pathology, Duke University Medical Center, Durham, NC, USA
e-mail: john.carney@duke.edu

M. L. Smith (✉)
Department of Pathology and Laboratory Medicine, Mayo Clinic Arizona, Scottsdale, AZ, USA
e-mail: smith.maxwell@mayo.edu

N. Gupta et al. (eds.), *Diffuse Cystic Lung Diseases*, Respiratory Medicine,
https://doi.org/10.1007/978-3-030-63365-3_4

PJP	*Pneumocystis jiroveci pneumonia*
PLCH	Pulmonary Langerhans cell histiocytosis
RB	Respiratory bronchiolitis
RRP	Recurrent respiratory papillomatosis
SRIF	Smoking-related interstitial fibrosis

Introduction

Diffuse cystic lung diseases (DCLDs) are a highly heterogeneous group of diseases with congenital, inflammatory, and neoplastic etiologies. They may present at any stage of life and involve both male and female patients. Often the clinical presentation, laboratory testing, and high-resolution computed tomography (HRCT) are sufficient to establish a diagnosis. However, some cases require pathological evaluation to clarify the diagnosis. The pathological approach to the evaluation of pulmonary cysts is covered first in this chapter, followed by detailed *pathological* descriptions of the various cystic conditions. Only clinical and radiological features that assist the pathological evaluation are discussed.

Pathological Approach to Pulmonary Cysts

The pathological approach is based primarily on the evaluation of surgical lung biopsies. In some cases, sufficient histological features are present on transbronchial forceps or cryobiopsies to allow for a definitive diagnosis (e.g., the presence of lymphangioleiomyomatosis (LAM) cell clusters), with the diagnostic utility of transbronchial biopsies dependent upon the specific lung disease. However, surgical lung biopsy remains the gold standard. A summary of the pathological approach is presented in Table 4.1.

Table 4.1 Pathological steps in the evaluation of lung biopsies for cystic lung disease

1	Recognition of a cystic structure
2	Distinction from cyst mimics
3	Evaluation of the background lung parenchyma for disease histopathology
4	Evaluation of the cyst wall for features of a specific disease
5	Correlation with clinical and radiographical features to confirm correct disease context
6	Definitive diagnosis

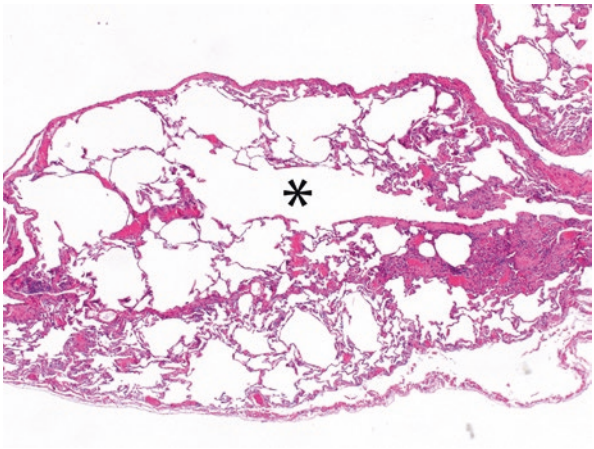

Fig. 4.1 Pulmonary cysts. In some cases of cystic lung disease, it can be very difficult to recognize the cystic structure as the lung is deflated during the biopsy procedure. In this case of BHD, a centrilobular cyst (*) can be recognized by the simplification of alveolar structure (H&E, 20X)

Surgical lung biopsies for the diagnosis of DCLDs are relatively uncommon. Without a generous clinical history, perhaps one of the more challenging tasks for the surgical pathologist is the recognition that a cyst is present. Because lung biopsies are taken with the lung deflated, the cysts are often collapsed and look quite dissimilar to their radiologic counterparts. Collapse of a cystic structure, particularly in the setting of an unremarkable cyst wall, can make cyst recognition very challenging (Fig. 4.1). In the lung, a cyst is defined by the Fleischner society (a multidisciplinary thoracic imaging group) as "a round parenchymal lucency showing a well-defined interface with normal lung in the absence of associated pulmonary emphysema" [1]. Pathologically, cysts are defined as dilated spaces, embedded in the tissue, and lined by an epithelial lining. They often contain fluid or gas. Dilated spaces not lined by epithelium are referred to as pseudocysts. Pseudocysts are mimics of true lung cysts.

Once a potential cystic structure is identified, it must be distinguished from various mimics including centrilobular emphysema (CLE), alpha 1 antitrypsin deficiency (A1ATD), bronchiectasis, cysts of honeycomb remodeling, pulmonary interstitial emphysema (PIE), and cavitary lesions.

CLE and A1ATD both result in simplification of alveolar architecture with resulting expanded airspaces, a process termed "emphysema" (Fig. 4.2a). Emphysema is identified by the radiologist and should be uncommon as the sole finding in the setting of DCLD. A frequent caveat in the setting of smoking-associated DCLD, however, is the emphysema in the background lung in addition to the presence of true cysts (e.g., of PLCH). Emphysema is encountered by the pathologist far more commonly than DCLD and is the most common cyst mimic that needs to be distinguished from a true cyst. CLE is distinguished from true cysts by the lack of a cyst wall, consisting instead of simplified alveolar wall architecture with enlarged airspaces containing isolated, "free-floating" segments of viable alveolar septal tissue

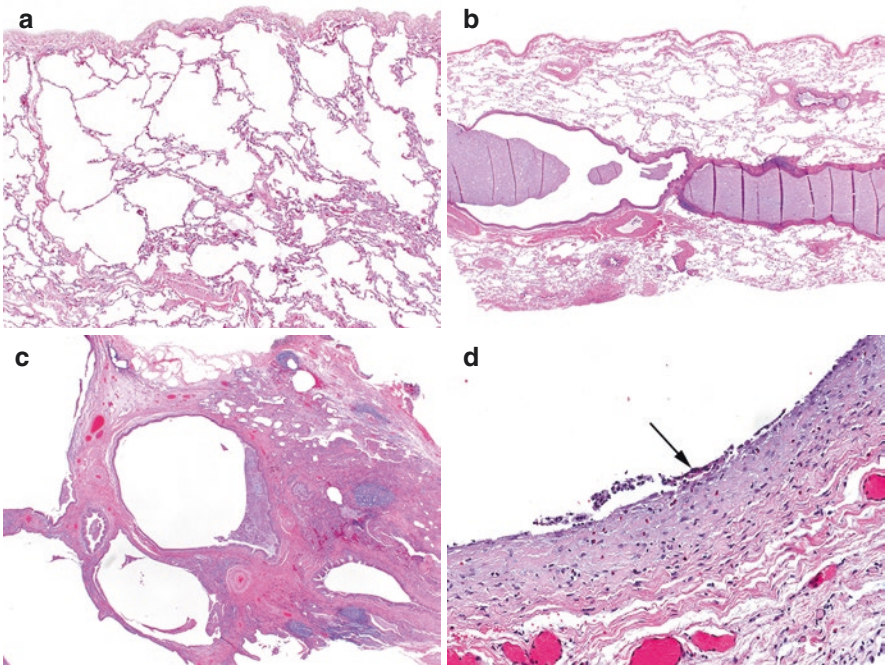

Fig. 4.2 Cyst mimics. Histological section of emphysema that shows simplification of the alveolar architecture (**a**, H&E, 20X). Bronchioloectasia characterized by a markedly dilated terminal airway with abundant luminal mucostasis mimicking a cyst (**b**, H&E, 12.5X). Occasionally, some cysts of microscopic honeycomb remodeling may be mistaken for cystic lung disease. The key to avoiding this caveat is recognizing that the cysts are embedded in advanced fibrosis (**c**, H&E, 20X). The cyst wall in the setting of pulmonary interstitial emphysema has fibrosis and is lined by histiocytes and occasional giant cells (*arrow*) without a true epithelial lining (**d**, H&E, 200X)

or cross sections of pulmonary vessels. There may be associated smoking-related changes including interstitial fibrosis, respiratory bronchiolitis, and small airway remodeling that help support an interpretation of CLE [2]. A1ATD also results in emphysema and is similarly distinguished with a more diffuse distribution than CLE, involving the entire acinus (panacinar) rather than being localized to the centriacinar region.

Bronchiectasis is an abnormal expansion of the bronchial lumen diameter, usually in response to chronic obstruction or infection. Morphologically, the ectatic airways may appear as cystic spaces. The "cyst" wall in bronchiectasis is thus comprised of the conducting airway structures including respiratory mucosa, submucosa, and cartilage allowing differentiation from true cysts. Identification of an adjacent artery present in the bronchovascular bundle is an important clue to diagnosing bronchiectasis when the conducting airway is no longer identifiable due to fibrous destruction. Ectatic bronchioles are often filled with mucus (mucostasis) associated with chronic inflammation in the accompanying respiratory mucosa (Fig. 4.2b).

Honeycomb (HC) cysts are dilated air spaces embedded in dense pulmonary fibrosis that are lined by respiratory epithelium and often filled with mucus, macrophages, and debris (Fig. 4.2c). HC cysts together with scarring fibrosis with architectural distortion represent end-stage fibrotic lung disease rather than a true DCLC. HC cysts are a significant finding in that honeycomb change is a diagnostic feature of idiopathic pulmonary fibrosis (IPF).

Pulmonary interstitial emphysema (PIE) results from the dissection of air into the interstitial space and along the bronchovascular bundles (Fig. 4.2d). Most of the time the air is absorbed and there are no residual sequelae. However, some cases become chronic and may manifest as multifocal and bilateral cysts mimicking DCLD radiographically. Histologically the dilated air spaces of PIE are distinguished by their lack of a true epithelial lining. Instead, there is often a foreign body type giant cell response to the air in the surrounding interstitium.

Finally, cavitary lesions may mimic cysts but often have very thick, fibrotic walls, lack a true epithelial lining, and are filled with inflammatory and necrotic debris. Any inflammatory or neoplastic cellular mass may undergo cavitation with a resulting cystic space. Cavities of this nature have no true cyst lining and often have a variably thickened wall. Cavitary lesions are associated with inflammatory (infection and vasculitis) and neoplastic etiologies.

Once the cyst mimics are excluded, the cyst wall provides the highest yield for diagnostic clues as to the specific type of DCLD. Specific details of the diagnostic features found in the cyst walls of the various DCLDs are covered below. Critical additional clues to the etiology of the cysts are found in the lung adjacent to the cyst. If the adjacent lung is normal, consideration should be given to LAM, metastases, infection, post-traumatic cysts, and Birt-Hogg-Dube syndrome (BHD). Prominent lymphocytic infiltration in the adjacent lung should raise concern for lymphoid interstitial pneumonia (LIP)/follicular bronchiolitis frequently associated with immunodeficiencies and connective tissue diseases particularly Sjogren syndrome, and subacute hypersensitivity pneumonitis (HP). Variable fibrosis and mixed inflammation with prominent histiocytes suggest pulmonary Langerhans cell histiocytosis (PLCH) and Erdheim-Chester disease (ECD) as potential etiologies. In congenital pulmonary airway malformation (CPAM) and other congenital abnormalities, the adjacent non-cystic lung often shows architectural abnormalities of abnormal alveolar walls, solid areas, and dilated airspaces. Finally, smoking-related changes of respiratory bronchiolitis, small airway remodeling, and smoking-related interstitial fibrosis in the background lung may point to smoking-related DCLD.

Once potential etiologies are deciphered, correlation with clinical and radiographical features can help confirm a presumptive diagnosis. Age, sex, and other comorbid diseases are important clinical features. Radiological imaging provides the best indication of the distribution, number, and size of the cysts (upper versus lower lobe; central versus peripheral; scattered versus numerous; small versus large). Table 4.2 depicts the pathological approach to the more common cystic lung diseases, comparing the specific pathological features and salient clinical and radiological findings for the diagnoses.

Table 4.2 Pathological approach to evaluation of diffuse cystic lung disease biopsies

Adjacent lung	Abnormality in adjacent lung	Contents of cyst wall	Disease	Specific pathological features	Salient clinical and radiological features
Abnormal	Lymphocytic inflammation	Lymphocytes	LIP/follicular bronchiolitis	Cellular interstitial infiltrates composed of lymphocytes, plasma cells, and macrophages Follicles with prominent germinal centers surrounding bronchioles Dilated terminal airways	Middle age, female > male. Associated CTD (especially Sjogren syndrome). HRCT is heterogeneous, normal to GGO and nodules. Cysts are randomly distributed. Peribronchovascular thickening Positive autoimmune serologies
		Lymphocytes and vague granulomas	HP	Cellular infiltrates with poorly formed granulomas in a bronchiolocentric distribution	Antigen exposure. Upper lobe distributed vague centrilobular nodules on HRCT
	Fibrosis and mixed inflammation; smoking-related changes	Histiocytes with associated mixed inflammatory cell infiltrate	PLCH	Peribronchiolar inflammation and fibrosis with Langerhans cell aggregates confirmed by CD1a immunostaining	Smoking history. Female > male. HRCT showing nodules associated with fibrosis. Variable cyst wall thickness. Upper > lower lobe cyst distribution
	Pigmented macrophages in distal airspaces	Variable chronic inflammation and fibrosis, often centrilobular	RB/DIP	Aggregates of lightly pigmented (smokers) macrophages in distal airspaces with variable collagenous interstitial fibrosis (SRIF)	HRCT shows bilateral associated GGO Smoking history Centrilobular cysts
	Deposition of amorphous eosinophilic material	Amorphous eosinophilic material	Amyloid/ LCDD	Amorphous eosinophilic material Lymphocytes and plasma cells Positive Congo red stain Light chain restriction by in situ hybridization studies Protein identification by mass spectroscopy analysis Evaluate for lymphoproliferative disease	HRCT showing cysts associated with nodules

Normal	LAM cells	LAM	Spindled and epithelioid cells in the cyst wall. Cells positive for SMA, and melanocyte markers (e.g., HMB-45)	Middle aged females. TSC-associated Diffuse randomly distributed cysts Other mesenchymal neoplasms
	Neoplastic cells	Primary and metastatic neoplasms	Variable histology depending on the tumor type (carcinoma, sarcoma, sex-cord stromal tumor, lymphoma). Immunohistochemistry often required to establish diagnosis	Metastases tend to have a lower lobe distribution on HRCT. Clinical history of malignancy is critically important
	Inflammation and/or fibrosis	Infection	Histology is variable depending on the infectious agent. Special stains for infectious microorganisms is often required. Identification of the microorganism is diagnostic	Immunosuppression increases risk of pulmonary infection
	No cyst wall with cysts lined by normal alveolar Type 1 and Type 2 epithelial cells	BHD	No specific pathologic abnormalities are diagnostic. Cystic changes are often subtle	Middle age presentation. Spontaneous pneumothorax. Associated tumors of the skin and kidney. HRCT shows a predominate basal distribution

LIP lymphoid interstitial pneumonia, *HP* hypersensitivity pneumonitis, *PLCH* pulmonary Langerhans cell histiocytosis, *RB* respiratory bronchiolitis, *DIP* desquamative interstitial pneumonia, *LAM* lymphangioleiomyomatosis, *TSC* tuberous sclerosis complex, *BHD* Birt-Hogg-Dube syndrome, *GGO* ground-glass opacity, *CTD* connective tissue disease, *HRCT* high-resolution computed tomography, *SRIF* smoking-related interstitial fibrosis

Pathology of Specific Diffuse Cystic Lung Diseases

Birt-Hogg-Dube Syndrome

Pathology

The background lung in Birt-Hogg-Dubé syndrome (BHD) is normal (Fig. 4.3a). Cysts of BHD are typically located in a peripheral, basal, and subpleural distribution. Cysts may be intraparenchymal (interstitial) (Fig. 4.3b), subpleural, or in the supporting stroma of the bronchovascular bundles or interlobular septa (Fig. 4.3c). Cysts may appear to be arising from the terminal airways or may appear randomly distributed. The cyst walls are typically thin and consist only of a thin lining of pneumocytes (Fig. 4.3d). The cyst wall often has no specific histological features, and no special stains are required for histopathological evaluation. Spontaneous pneumothorax occurs in 24% of BHD patients with pulmonary cysts [3], and thus

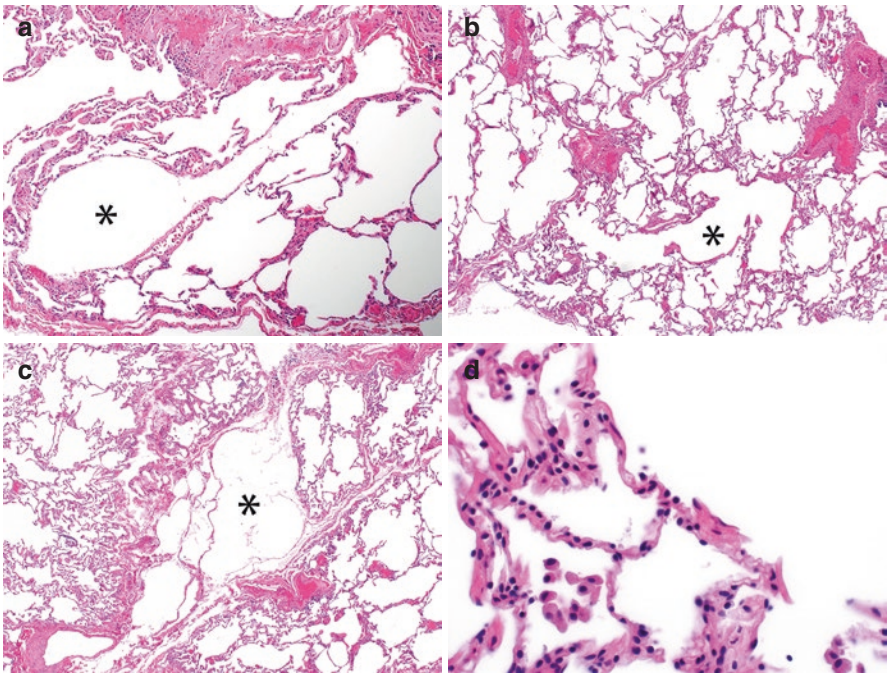

Fig. 4.3 Birt-Hogg-Dube syndrome. Cysts of BHD may be easily missed without clinical and radiographic history. The background lung parenchyma is usually unremarkable (**a**, * = cyst; H&E, 40X). The cysts (*) may be seen intraparenchymal (**b**, H&E, 20X) or in interlobular septa (**c**, H&E, 20X). The "cyst wall" in BHD is a thin delicate alveolar wall lined with unremarkable Type 1 and Type 2 pneumocytes (**d**, H&E, 400X)

reactive changes secondary to the pneumothorax may be present including pleuritis, subpleural fibrosis, vasculopathy, fibroblastic foci, chronic inflammation, and pneumocyte hyperplasia [4]. In this setting, the distinction from bullae can be challenging and a high index of suspicion is required. In suspected cases, genetic testing for mutations in the *FLCN* gene can confirm the diagnosis.

Salient Clinical and Radiological Features

The typical presentation for patients with BHD in middle age [5] is often with associated hair follicle (fibrofolliculomas) and renal neoplasms (cysts and carcinoma). Pneumothorax is a frequent presentation. On high-resolution computed tomography (HRCT), cysts of BHD show a predominant basal distribution, opposite to the upper lobe predominance of blebs and emphysema that BHD cysts most closely mimic.

Lymphoid Interstitial Pneumonia/Follicular Bronchiolitis

Pathology

The most recent consensus classification of idiopathic interstitial pneumonias defines lymphoid interstitial pneumonia (LIP) as a pattern of injury most often seen in association with other conditions such as immunodeficiencies, lymphomas, and connective tissue diseases (CTD) with only rare truly idiopathic cases [6]. LIP is characterized by diffuse alveolar septal interstitial infiltration by lymphocytes, plasma cells, and macrophages [7]. Interestingly, the pathological definition typically does not include any mention of pulmonary cysts. Radiographically, LIP presents as predominantly ground-glass opacities (GGO), correlating with the pathology definition, but also with frequent thin-walled perivascular cysts [1]. Most cases originally classified as LIP actually represented lymphoma [8]. Furthermore, the 2013 update to the American Thoracic Society/European Respiratory Society classification of the idiopathic interstitial pneumonias acknowledges most non-lymphoma LIP cases are now best classified as cellular nonspecific interstitial pneumonia (NSIP) [6].

Biopsies of LIP, although rare, show a consistently “blue” appearance at low power due to the marked lymphoid infiltrates. Biopsies contain cellular interstitial infiltrates, follicular bronchiolitis, and randomly distributed thin-walled cysts (Fig. 4.4a). The cellular interstitial infiltrates overlap with cellular NSIP except for the greater density of the lymphoplasmacytic infiltrate in LIP. Lymphoproliferative lesions and LIP can be indistinguishable based on morphology alone, and thus special studies are required to characterize the inflammatory infiltrate and assess for clonality. It is the pathologist’s responsibility to exclude lymphoma. Follicular

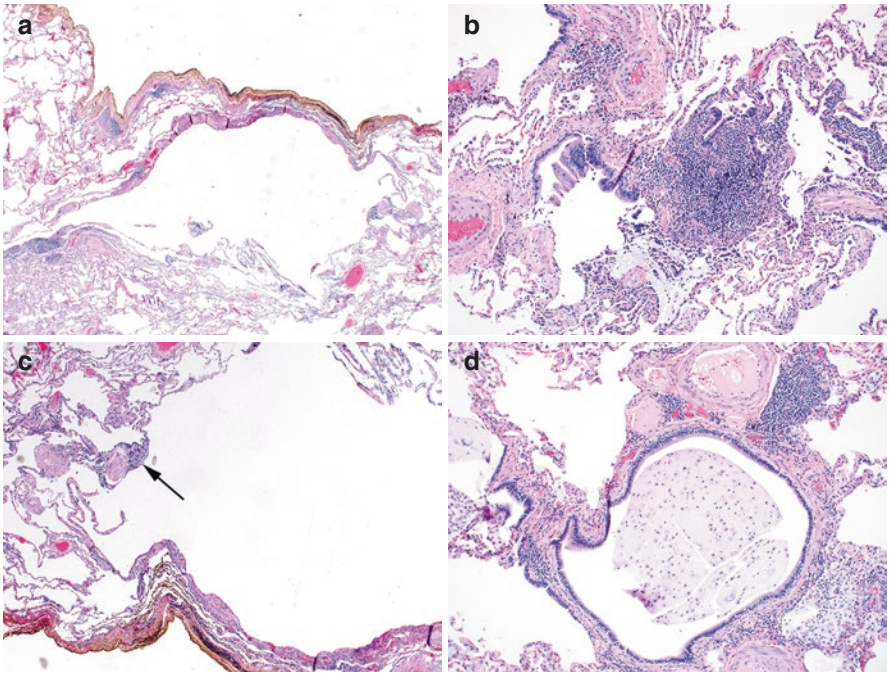

Fig. 4.4 Lymphoid interstitial pneumonia/follicular bronchiolitis. Cysts of LIP are thin walled and present within the parenchyma (**a**, H&E, 20X). Follicular bronchiolitis is a common associated finding (**b**, H&E, 200X). The cyst wall may have lymphoid infiltrates (*arrow*) (**c**, H&E, 40X). Features of chronic small airway remodeling, including bronchioloectasia, may be present (**d**, H&E, 200X)

bronchiolitis is characterized by lymphoid aggregates containing secondary follicles in an airway-centric distribution and associated with chronic bronchiolitis (Fig. 4.4b). The cysts may have a normal alveolar epithelial cell lining or may have significant lymphoid infiltrates (Fig. 4.4c). Due to the airway-centered nature of the process, histological features of chronic small airway remodeling are frequent including peribronchiolar metaplasia, bronchioloectasia, and mucostasis (Fig. 4.4d). Vague granulomas have also been described. There is variable fibrosis in the background.

Salient Clinical and Radiological Features

LIP is more frequent in middle-aged females and often associated with systemic disease symptoms. Coexisting CTD may be present and serologic testing may help confirm suspicion of a CTD. HRCT shows randomly distributed cysts of variable size. The background GGO can be helpful in establishing that the patient has a DCLD associated with background lung abnormalities.

Lymphangioleiomyomatosis

Pathology

Lymphangioleiomyomatosis (LAM) represents the prototype DCLD. Cysts in LAM are distributed diffusely through the lungs with relatively even distribution. No upper, lower, peripheral, or central predominance is seen. The background lung parenchyma has normal alveolar walls and air spaces. Significant fibrosis and inflammation are absent, except in areas of post-obstructive change. Interstitial hemosiderin deposition and hemosiderin-laden macrophages in alveolar spaces may be present in advanced stage disease. The cysts are usually of relatively uniform size and have a variably thickened wall (Fig. 4.5a, b). The histological hallmark of LAM is the presence of aggregates of spindled and epithelioid cells with a smooth muscle phenotype embedded in the cyst walls. The epithelioid cells are plump with generous eosinophilic cytoplasm, and the spindled cells have elongated nuclei with blunted nuclear tips (Fig. 4.5c). Occasionally

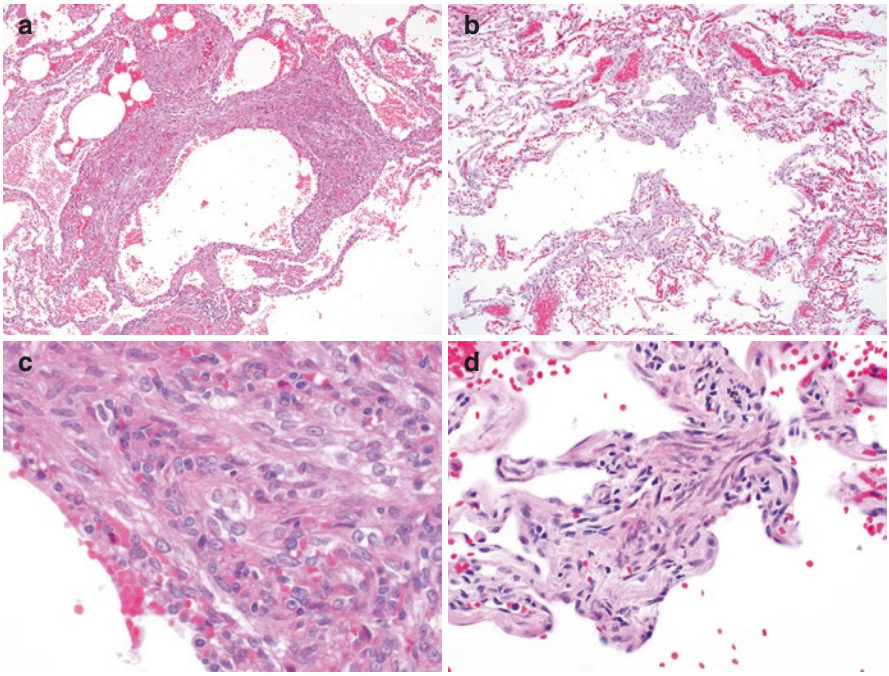

Fig. 4.5 Lymphangioleiomyomatosis. The cellularity of the cyst wall in LAM is highly variable from case to case and within cysts of the same case. The cyst wall in some cases has a marked proliferation of spindle cells (**a**, H&E, 40X), while other cysts may have very rare or no LAM cells at all (**b**, H&E, 40X). The neoplastic smooth muscle cells are large oval epithelioid cells with abundant eosinophilic or cleared cytoplasm (**c**, H&E, 400X) to spindled cells with elongated nuclei with rounded nuclear tips (**d**, H&E, 400X)

LAM cells protrude into the cyst lumen, while other times they are quite inconspicuous in the stroma of the wall. The quantity of diagnostic LAM cells can vary dramatically from cyst to cyst in the same case and from case to case. In some cases, LAM cells are quite limited and exhaustive step sections may be required for a definitive diagnosis (Fig. 4.5d). The LAM cells have a neoplastic nature and are occasionally seen outside the cyst wall in the lymphatics of the bronchovascular bundles and pleura. Involvement of local lymph nodes may also be seen. Immunohistochemical analysis demonstrates the characteristic dual melanocytic and myoid differentiation of LAM cells, which are immunopositive for smooth muscle actin and the melanocytic markers, HMB-45 (Fig. 4.6b), MITF-1 (Fig. 4.6d), and melan-A as well as for estrogen and progesterone receptors (Fig. 4.6a, c), S-100 and beta-catenin. Multifocal micronodular pneumocyte hyperplasia (MMPH) is an uncommon feature seen in patients with tuberous sclerosis complex (TSC), with or without LAM. MMPH is characterized by multiple well-demarcated nodules of cytologically bland hyperplasic Type 2 pneumocytes growing along mildly thickened alveolar walls (Fig. 4.7a, b) [9].

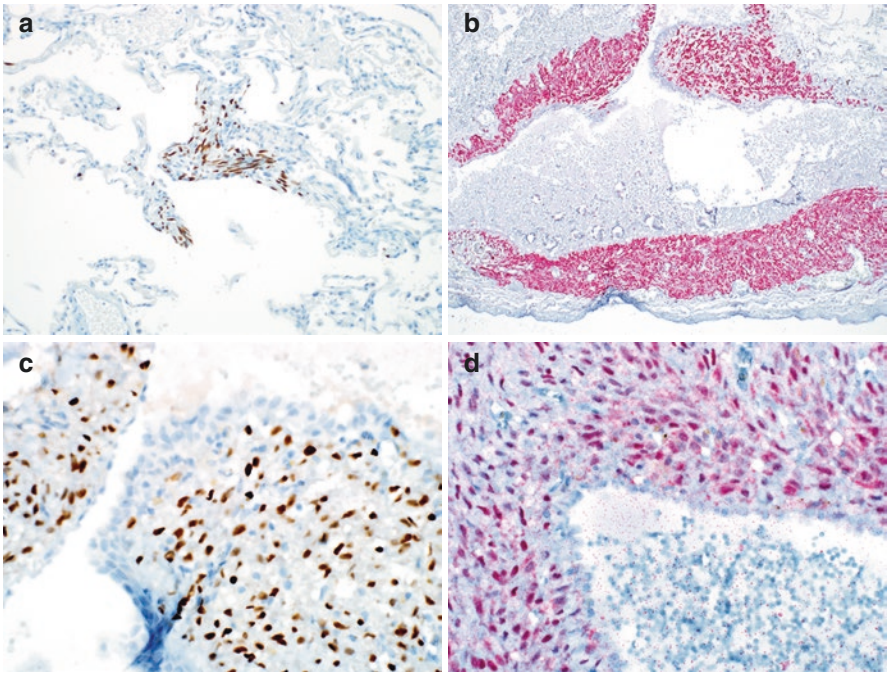

Fig. 4.6 Immunohistochemical findings in lymphangioleiomyomatosis. Dual myoid and melanocytic differentiation is seen in LAM cells, which also express hormone receptors. (**a**) Estrogen receptor, brown chromagen, 100 X. (**b**) HMB-45, red chromagen, 40X. (**c**) Progesterone receptor, brown chromagen, 200X. (**d**) MITF-1, red chromagen, 200X

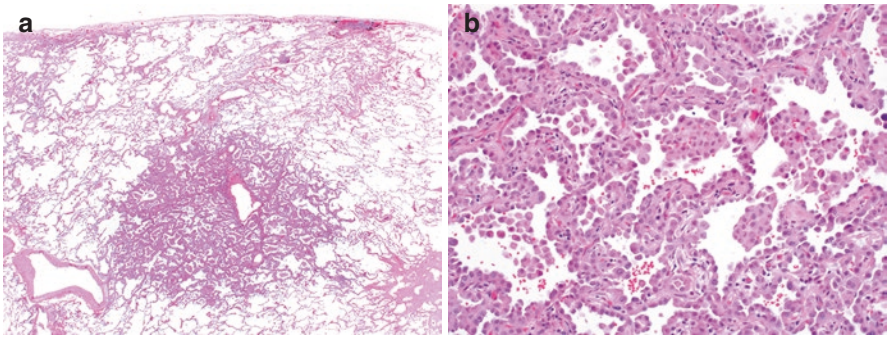

Fig. 4.7 Multifocal micronodular pneumocyte hyperplasia. MMPH may develop in patients with tuberous sclerosis complex (TSC), with or without LAM. MMPH is characterized by the nodular proliferation of hyperplastic Type 2 pneumocytes lining mildly thickened alveolar septa. Multiple nodules seen by radiographical imaging may be apparent by low power microscopic examination (**a**, H&E, 15X). The cells have bland cytologic features with abundant eosinophilic cytoplasm, round nuclei, and small nucleoli (**b**, H&E, 200X)

Salient Clinical and Radiological Features

LAM occurs in patients with TSC and as sporadic cases. LAM most commonly affects females, with only rare cases in males. LAM results from inactivating mutations in the *TSC1* or *TSC2* genes that encode the tumor suppressor proteins hamartin and tuberin, respectively. Mutations in TSC genes result in increased risk of several types of mesenchymal tumors including LAM, renal angiomyolipomas, rhabdomyoma, and angiofibroma. Genetic testing for *TSC1* and *TSC2* gene mutations can confirm the diagnosis.

Pulmonary Langerhans Cell Histiocytosis

Pathology

Pulmonary Langerhans cell histiocytosis (PLCH) was previously referred to as eosinophilic granuloma of the lung [10]. Historically a distinction was made between PLCH and systemic LCH, as the former was thought to be a reactive process to smoking and the latter a neoplastic proliferation of Langerhans cells. However, multiple studies have now detected BRAF mutations in the majority of PLCH cases, a finding routinely identified in systemic LCH counterparts [11]. The Histiocyte Society now classifies PLCH in the Langerhans group of histiocytosis, along with systemic LCH and Erdheim-Chester disease (ECD) [12]. Cysts of PLCH are classically upper lung zone predominant in distribution, as are most

inhalational-associated lung injuries. In distinction from many other DCLDs, PLCH cysts have irregularly thickened walls. There is often a centrilobular nodular component as well. Two pathologic phases of PLCH are described, cellular (proliferative) and fibrotic. In reality, many cases show a spectrum of cellular and fibrotic lesions. Lesions begin as centrilobular cellular aggregates and nodules of Langerhans cells with a mixed background inflammatory cell infiltrate (Fig. 4.8a). The presence of numerous eosinophils is particularly helpful in suggesting the diagnosis. After a period of time, the central region cavitates with resultant cyst formation (Fig. 4.8b). There is often a component of fibrosis in the cyst walls, even in the cellular phase. The background lung often shows changes associated with smoking including smoking-related interstitial fibrosis (SRIF), respiratory bronchiolitis (RB), and emphysema [13]. The presence of Langerhans cell clusters is diagnostic. Langerhans cells are a subset of macrophages with abundant cleared cytoplasm, enlarged hypochromatic nuclei with nuclear membrane grooves, folds, and irregularities (Fig. 4.8c) [14]. Langerhans cells are positive for CD68 and Factor XIIIa, general macrophage

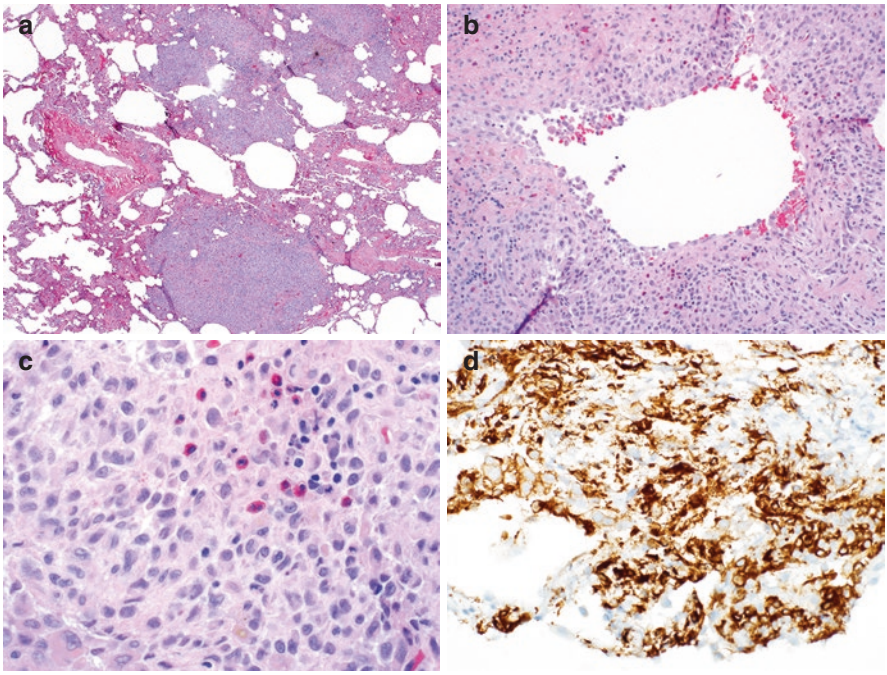

Fig. 4.8 Cellular pulmonary Langerhans cell histiocytosis (PLCH). Nodular centrilobular aggregates of Langerhans cells in a biopsy from a patient who had both cysts and nodules on radiologic imaging (**a**, H&E, 40X). The early cystic lesion in PLCH occurs during the cellular phase with central degeneration resulting in cavitary/cystic space formation (**b**, H&E, 100X). Classic morphological features of Langerhans cells include enlarged histiocytes with large nuclei, occasional nucleoli, and numerous nuclear membrane folds and grooves. A mixed background inflammatory cell infiltrate including lymphocytes and eosinophils is present in the setting of cellular PLCH (**c**, H&E, 600X). Positive reaction for CD1a by immunohistochemistry confirms the presence of Langerhans cells (**d**, CD1a, 400X)

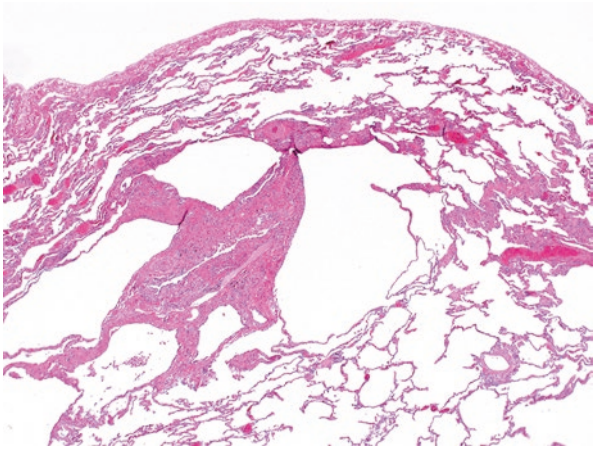

Fig. 4.9 Fibrotic pulmonary Langerhans cell histiocytosis (PLCH). In the fibrotic phase, PLCH can be recognized by the presence of cystic structures associated with stellate fibrosis. These findings correlate with the irregular cyst walls seen by radiological imaging. In this setting, Langerhans cells may be exceedingly rare or non-existent. The diagnosis is often made on H&E examination alone in conjunction with salient clinical and radiographical findings, without supportive CD1a immunohistochemistry

markers, as well as S-100 and CD1a by immunohistochemistry. The expression of CD1a is the most important feature to confirm the diagnosis (Fig. 4.8d). In the fibrotic phase of the disease, the number of Langerhans cells is markedly reduced. In fact, many cases of fibrotic PLCH no longer contain increased CD1a positive Langerhans cells, but rather are characterized by centrilobular cysts and stellate fibrotic nodules that obliterate respiratory bronchioles (Fig. 4.9) [15].

Salient Clinical and Radiological Features

Females are slightly more likely to develop PLCH compared to males. Obviously, a smoking history can be helpful in suggesting PLCH. The most valuable HRCT clues to the disease are the upper lung zone distribution of the cysts and the irregularity of the cyst walls.

Smoking-Related Cystic Lung Disease in Addition to PLCH

Pathology

Smoking produces a host of changes in the lungs in addition to PLCH including RB, desquamative interstitial pneumonia (DIP), SRIF, small airway disease, and emphysema. It is being increasingly recognized that smokers may develop DCLD even in the absence of PLCH (Fig. 4.10a) [16]. The background lung in these cases shows

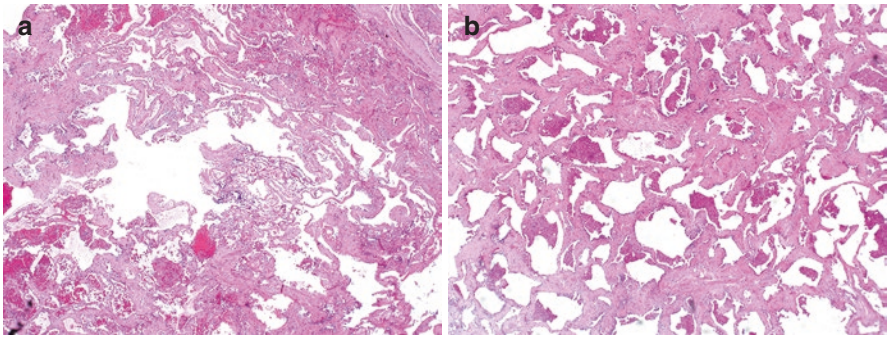

Fig. 4.10 Smoking-related cystic lung disease in addition to pulmonary Langerhans cell histiocytosis (PLCH). A partially collapsed cyst in the setting of smoking-related interstitial lung disease (**a**, H&E, 20X). The best clue to smoking as an etiology for DCLD is the presence of smoking-related changes in the background lung parenchyma. Extensive smoking-related interstitial fibrosis (SRIF) can be seen in association with respiratory bronchiolitis (RB), mimicking a desquamative interstitial pneumonia (DIP) reaction pattern (**b**, H&E, 100X)

changes typical of smoking including numerous pigmented macrophages in the airspaces (RB to DIP spectrum), variable interstitial fibrosis (SRIF), features of small airway disease (peribronchiolar metaplasia, mucostasis, bronchioloectasis), and emphysema (Fig. 4.10b). However, in a minority of cases numerous centrilobular cysts are encountered. The cyst wall often consists only of delicate alveolar septa or a terminal bronchiole. Pulmonary artery branches can be seen in the cyst wall, indicating the centrilobular location of the cysts. CD1a stains exclude cellular PLCH and the morphology of the cysts lack the stellate-shaped scarring of fibrotic PLCH [16].

Salient Clinical and Radiological Features

The clinical history of smoking is the most helpful clue to diagnosing smoking-related lung disease. HRCT shows diffuse cysts in a centrilobular distribution without an upper or lower lung zone distribution.

Amyloidosis and Light Chain Deposition Disease

Pathology

Amyloidosis and light chain deposition disease (LCDD) are rare causes of DCLD [17, 18]. Morphologically, amyloid and LCDD are indistinguishable using routine histological methods. The cysts may consist of amyloid nodules or light chains with central cavitation or may be dilatated air spaces/airways with protein deposition in the wall (Fig. 4.11a). The adjacent lung is often unremarkable or may be involved

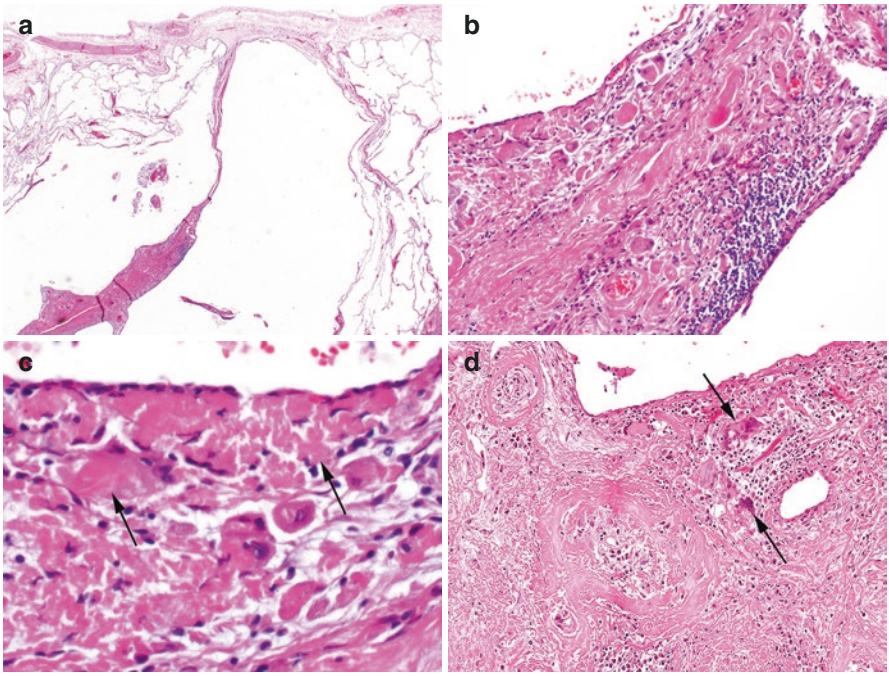

Fig. 4.11 Cystic amyloidosis and light chain deposition disease (LCDD). In cystic amyloidosis, frequently the adjacent lung parenchyma is unremarkable (**a**, H&E, 12.5X). Higher power examination of the cyst wall shows amorphous eosinophilic material (**b**, H&E, 100X; C, H&E, 400X). There are often multinucleated giant cells associated with the amyloid material (*arrows*) (**c**, H&E, 400X). LCDD can show identical histologic features including multinucleated giant cells (*arrows*) (**d**, H&E, 100X)

by diffuse amyloidosis. Both are characterized by the deposition of amorphous eosinophilic material (Fig. 4.11b). Another histological feature seen in the setting of amyloid and LCDD is a robust but variable multinucleated giant cell reaction. Giant cells are often seen attempting to engulf the amyloid material (Fig. 4.11c). Variable lymphocytic and plasma cell infiltrates are present. A variety of patterns of amyloid and LCDD have been described including diffuse, nodular, vascular, and cystic (Fig. 4.11d) [19, 20]. Cystic amyloid may occur sporadically (AA-type) in association with chronic inflammation or as a result of a lymphoproliferative process (AL-type) [21, 22]. Amyloid and LCDD are morphologically distinguished by Congo red staining based on tertiary protein folding. Amyloid folds into a beta-pleated sheet that results in Congo red reactivity while LCDD does not. Amyloid stains a salmon pink color when viewed by transmission light microscopy and has apple-green birefringence by polarization microscopy (Fig. 4.12a, b). LCDD does not stain with Congo red. By electron microscopy, amyloid is composed of randomly arranged non-branching fibrils with an average diameter of 10 nanometers [17]. In contrast, LCDD is ultrastructurally composed of punctate or powdery electron densities. Both amyloid and LCDD can be assessed with mass spectroscopy to identify the protein components present [23, 24].

Amyloid and LCDD are both often associated with lymphoproliferative disorders (predominantly MALT lymphoma) and are often seen in the setting of other DCLDs such as Sjogren syndrome, LIP, and follicular bronchiolitis (with associated accompanying pathology described previously) [25]. It is critical for the pathologist to recognize this association and thoroughly evaluate the specimen for evidence of a lymphoproliferative disorder. Additional studies may include CD3 and CD20 immunohistochemical stains, as well as kappa and lambda evaluation by in situ hybridization. If the process is associated with a lymphoproliferative disorder, light chain restriction with either kappa or lambda predominance should be detected (Fig. 4.13a, b).

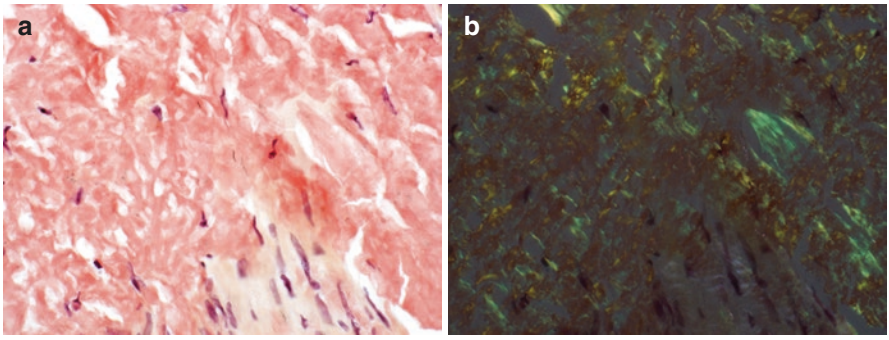

Fig. 4.12 Amyloidosis Congo red staining. A positive reaction by Congo red staining is required for the diagnosis of amyloidosis. By traditional light microscopy, amyloid has a characteristic salmon pink color (**a**, Congo red, 400X). On polarization microscopy, the apple green birefringence of the amyloid material is observed (**b**, Congo red, 400X)

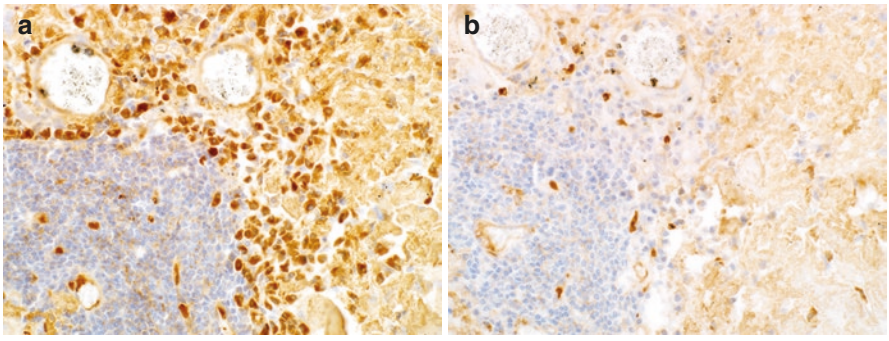

Fig. 4.13 Amyloidosis associated with lymphoproliferative disease. Once a diagnosis of amyloidosis is made, the pathologist should exclude the possibility of a lymphoproliferative process. Evaluation includes special stains assessing for kappa or lambda restriction. Although both immunohistochemistry and in situ hybridization can be used, in situ hybridization is easier to interpret. In this example, plasma cells are positive for kappa (**a**, Kappa, 200X) and negative for lambda by immunohistochemistry (**b**, Lambda, 200X)

Salient Clinical and Radiological Features

Since amyloid and LCDD are often associated with lymphoproliferative disorders, these entities tend to occur in older patients with equal sex distribution. The HRCT shows random cysts associated with nodules lacking a lobar predominance. Other clinical and radiological features are not typically contributory in narrowing the differential diagnosis.

Cystic Primary and Metastatic Neoplasms

Pathology

A wide spectrum of neoplasms has been described to involve the lung presenting as DCLD (Table 4.3) [26–34]. Neoplasms may be primary to the lung or metastases (more common in DCLD), and may be epithelial-derived carcinomas [35],

Table 4.3 Cystic neoplasms

Epithelial		
	Primary	
		Pulmonary adenocarcinoma
	Metastatic	
		Gastrointestinal adenocarcinoma
		Urothelial carcinoma
		Seminoma
		Granulosa cell tumor
		Head and neck squamous cell carcinoma
Mesenchymal		
	Primary	
		Mesenchymal cystic hamartoma
		Pleuropulmonary blastoma
	Metastatic	
		Angiosarcoma
		Osteosarcoma
		Synovial sarcoma
		Ewing sarcoma
		Leiomyosarcoma
		Rhabdomyosarcoma
		Myxosarcoma
		Endometrial stromal sarcoma
		Wilms tumor
		Pineal teratoma
Lymphoproliferative		
	Lymphoma	

Table developed based on published data [24–32]

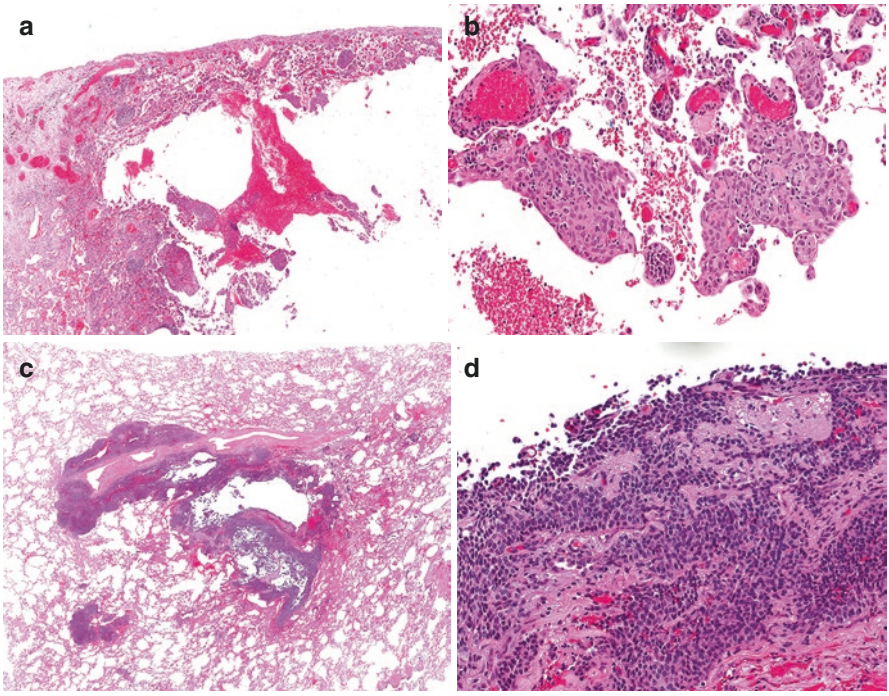

Fig. 4.14 Cystic metastatic neoplasms. Metastatic tumors presenting as multiple bilateral cystic lesions. Metastatic cystic angiosarcoma in a patient who presented initially with an atypical vascular lesion on the face (**a**, H&E, 20X). At higher power, the atypical cells and abundant red blood cells can be appreciated (**b**, H&E, 400X). The cells were immunopositive for the vascular markers CD31, ERG, and FLI-1 supporting the diagnosis. Metastatic cystic granulosa cell tumor in a patient with a previous ovarian tumor resection (**c**, H&E, 20X). At higher power the characteristic granulosa cells with scant cytoplasm, round to oval nuclei, and nuclear grooves can be seen (**d**, H&E, 400X). The cells were immunopositive for inhibin and calretinin, supporting the diagnosis

mesenchymal sarcomas (Fig. 4.14a, b) [32], sex-cord stromal tumors (Fig. 4.14c, d), or lymphomas [30]. The tumor cell of origin may be obvious by histological features; however, if this is not the case, pancytokeratin, vimentin, and CD45 immunohistochemical stains are valuable in establishing the initial differential diagnosis. Metastases have a tendency to involve the lower lung zones. Most malignant cysts are easily recognized by their cellular proliferations within the cyst walls. Unless there is an accompanying pneumothorax, the background lung is usually normal appearing. Unfortunately, especially with sarcomas, pneumothorax is a common presentation, and thus the background lung may show organizing pneumonia, fibroplasia, and inflammation.

Some neoplasms deserve specific mention. Benign metastasizing leiomyoma and metastatic endometrial stromal sarcoma (ESS) can present very similarly as LAM from a clinical, radiographical, and pathological perspective. More challenging yet is the similar immunohistochemical phenotype of positive reactivity for

estrogen receptor and SMA. Lack of expression of the melanocytic markers HMB45, S-100, and Melan-A help distinguish leiomyoma and ESS from LAM. CD10 is a consistently positive marker in ESS that is also valuable in confirming the diagnosis.

Pleuropulmonary blastoma is a primitive multipotent neoplasm found in the thorax of young pediatric patients often in the first 2 years of life. Although there are three types described, Types I and II are associated with cystic lung disease. Usually the disease is unilateral but can present as multifocal lesions in patients with a genetic tumor predisposition syndrome and *DICER1* mutations. The histological features include multiple cystic spaces lined by epithelial cells and cyst walls containing blastemal and mesenchymal elements [28, 31].

Salient Clinical and Radiological Features

Clinical history of a malignancy is the most useful clinical feature. In fact, if there is a clinical history of malignancy and a patient is found to have DCLD on imaging studies a biopsy is required to exclude a metastatic process. The HRCT findings overlap among the distinct entities and thus do not provide helpful clues to the diagnosis in this setting.

Infections

Pathology

Many infection-related cystic structures encountered in the lung are best classified as cavities according to the Fleischner Society [1]. Cavities are gas-filled lucencies with wall thicknesses >4 mm presenting within consolidated regions, mass lesions, or nodules. However, certain infectious agents may develop cysts that mimic the more classic causes of DCLD. These include *Pneumocystis jiroveci pneumonia* (PJP), human papilloma virus (HPV)-mediated recurrent respiratory papillomatosis (RRP), various *Staphylococcus* infections, Paragonimiasis, Mycobacterial infections, and *Echinococcus*.

Cystic PJP shows background lung changes typical of PJP. Abundant frothy eosinophilic material is seen in the airspaces, and there is often a brisk inflammatory cell infiltrate (Fig. 4.15a). The cysts consist of randomly dilated airspaces lined by reactive pneumocytes and inflammation. Some fibrosis may be present (Fig. 4.15b). Fungal stains are helpful in identifying the teacup-shaped organisms in the airspaces.

Recurrent respiratory papillomatosis is an HPV-mediated infectious process manifesting as numerous squamous papillomas throughout the respiratory tree. Most squamous papillomas have a typical papillary architecture; however, spread to the lungs in a minority of cases can present as cystic transformation with variably

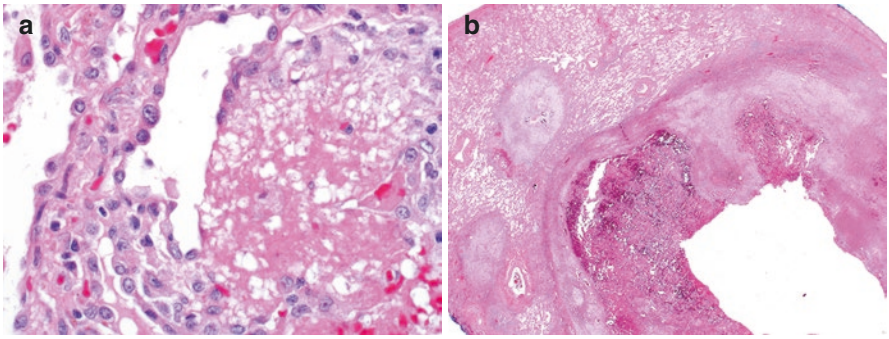

Fig. 4.15 Cystic *Pneumocystis jiroveci pneumonia*. Classic histological features of PJP include acute lung injury with frothy eosinophilic material in the air spaces (**a**, H&E, 400X). Most infectious cysts are more appropriately classified as cavities with fibrotic walls (**b**, H&E, 12.5X)

sized thin-walled cysts in a lower lung zone distribution. The cysts are lined by stratified squamous epithelium with HPV-induced koilocytic change including enlarged nuclei, irregular nuclear contours, and hyperchromasia. Rarely, malignant transformation to squamous cell carcinoma occurs.

Staphylococcus, Paragonimiasis, *Mycobacteria*, and *Echinococcus* infections can all rarely result in cystic transformation. Special stains for infectious microorganisms including tissue gram, acid-fast, and fungal stains may aid in the identification of the infectious agent.

Salient Clinical and Radiological Features

Clinical signs and symptoms of infection including fever, chills, night sweats, and leukocytosis may suggest cystic lung disease associated with infection. Development of cystic lung disease in an immunocompromised patient should also raise consideration for infection-associated DCLD.

Hypersensitivity Pneumonitis

Pathology

Cysts rarely occur in either subacute or chronic HP. Surgical lung biopsies will show the expected changes of HP including cellular interstitial infiltrates in a peribronchiolar distribution, poorly formed interstitial granulomas, chronic small airway remodeling, and variable interstitial fibrosis. In advanced cases of HP, well-established fibrosis and honeycomb cysts may develop. The cysts in HP may differ from the previously described honeycomb cysts associated with end stage

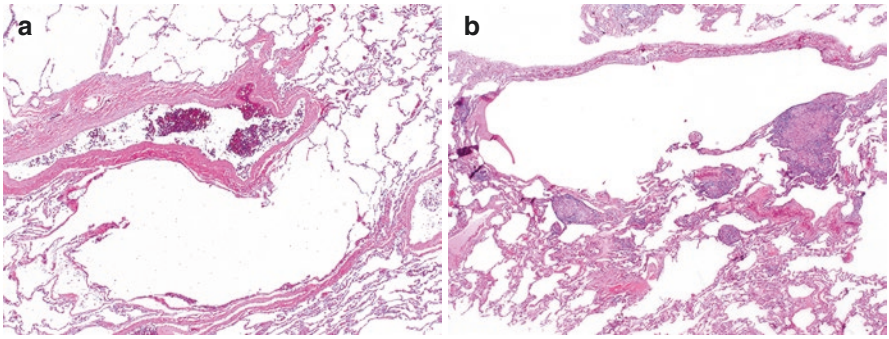

Fig. 4.16 Hypersensitivity pneumonitis. Cysts in the setting of HP may be histologically characterized by enlarged distal airspaces lined by alveolar septa (**a**, H&E, 20X) or may have chronic inflammation and poorly formed granulomas in the cyst wall (**b**, H&E, 20X)

lung disease in that these cysts may arise in areas away from advanced fibrosis. HP-related cysts appear to be localized to the centrilobular region and may represent dilated terminal or respiratory bronchioles. The cyst wall may be thin and delicate (Fig. 4.16a) but more often contains variable fibrosis, inflammation, and even granulomas and/or giant cells (Fig. 4.16b).

Salient Clinical and Radiological Features

Clinical history of exposure to an organic antigen can be helpful in narrowing the differential diagnosis. The HRCT often shows features of subacute and chronic HP including GGO, vague centrilobular nodules, mosaic attenuation, air trapping, and variable reticulation and honeycombing. The GGO seen radiographically may correlate with the histopathological finding of cellular interstitial infiltrates.

Conclusion

The pathological evaluation of DCLD involves recognizing a cystic structure, distinguishing it from cyst mimics, evaluating the sampled lung adjacent to the cysts, investigating the cyst wall for histologic clues to the diagnosis, and correlating the histopathological findings with pertinent clinical and radiological features to identify the etiology. DCLDs arise in a broad spectrum of disease categories, from congenital and infectious, to neoplastic. While many cases are diagnosed by clinical and radiological features without the need for biopsy, the pathologist plays an important role in establishing the diagnosis and etiology in those cases lacking the typical presentation for a distinct entity.

Key Learning Points

- Histopathological evaluation of the cyst wall provides the highest yield for identifying diagnostic features to establish a specific diffuse cystic lung disease diagnosis.
- Histopathological changes in the background pulmonary parenchyma may provide critical clues to the etiology of the diffuse cystic lung disease.
- Correlation with salient clinical and radiographical findings is critical to establishing the correct pathological diagnosis in diffuse cystic lung diseases.

References

1. Hansell DM, Bankier AA, MacMahon H, McLoud TC, Muller NL, Remy J. Fleischner Society: glossary of terms for thoracic imaging. Radiology. 2008;246(3):697–722.
2. Smith M, Gotway M, Larsen B, Colby T, Tazelaar H, Leslie K. Pathologic approach to cystic lung disease. AJSP: Rev Rep. 2017;22(1):36–45.
3. Toro JR, Pautler SE, Stewart L, Glenn GM, Weinreich M, Toure O, et al. Lung cysts, spontaneous pneumothorax, and genetic associations in 89 families with Birt-Hogg-Dube syndrome. Am J Respir Crit Care Med. 2007;175(10):1044–53.
4. Schneider F, Murali R, Veraldi KL, Tazelaar HD, Leslie KO. Approach to lung biopsies from patients with pneumothorax. Arch Pathol Lab Med. 2014;138(2):257–65.
5. Kunogi M, Kurihara M, Ikegami TS, Kobayashi T, Shindo N, Kumasaka T, et al. Clinical and genetic spectrum of Birt-Hogg-Dube syndrome patients in whom pneumothorax and/or multiple lung cysts are the presenting feature. J Med Genet. 2010;47(4):281–7.
6. Travis WD, Costabel U, Hansell DM, King TE Jr, Lynch DA, Nicholson AG, et al. An official American Thoracic Society/European Respiratory Society statement: update of the international multidisciplinary classification of the idiopathic interstitial pneumonias. Am J Respir Crit Care Med. 2013;188(6):733–48.
7. American Thoracic Society. European Respiratory Society international multidisciplinary consensus classification of the idiopathic interstitial pneumonias. This joint statement of the American Thoracic Society (ATS), and the European Respiratory Society (ERS) was adopted by the ATS board of directors, June 2001 and by the ERS Executive Committee, June 2001. Am J Respir Crit Care Med. 2002;165(2):277–304.
8. Nicholson AG, Wotherspoon AC, Jones AL, Sheppard MN, Isaacson PG, Corrin B. Pulmonary B-cell non-Hodgkin's lymphoma associated with autoimmune disorders: a clinicopathological review of six cases. Eur Respir J. 1996;9(10):2022–5.
9. Kobashi Y, Sugiu T, Mouri K, Irei T, Nakata M, Oka M. Clinicopathological analysis of multifocal micronodular pneumocyte hyperplasia associated with tuberous sclerosis in Japan. Respirology. 2008;13(7):1076–81.
10. Farinacci CJ, Jeffrey HC, Lackey RW. Eosinophilic granuloma of the lung; report of two cases. U S Armed Forces Med J. 1951;2(7):1085–93.
11. Favara BE, Feller AC, Pauli M, Jaffe ES, Weiss LM, Arico M, et al. Contemporary classification of histiocytic disorders. The who committee on histiocytic/reticulum cell proliferations. Reclassification Working Group of the Histiocyte Society. Med Pediatr Oncol. 1997;29(3):157–66.
12. Emile JF, Abla O, Fraitag S, Horne A, Haroche J, Donadieu J, et al. Revised classification of histiocytoses and neoplasms of the macrophage-dendritic cell lineages. Blood. 2016;127(22):2672–81.

13. Arnaud L, Pierre I, Beigelman-Aubry C, Capron F, Brun AL, Rigolet A, et al. Pulmonary involvement in Erdheim-Chester disease: a single-center study of thirty-four patients and a review of the literature. Arthritis Rheum. 2010;62(11):3504–12.
14. Colby TV, Lombard C. Histiocytosis X in the lung. Hum Pathol. 1983;14(10):847–56.
15. Travis WD, Borok Z, Roum JH, Zhang J, Feuerstein I, Ferrans VJ, et al. Pulmonary Langerhans cell granulomatosis (histiocytosis X). A clinicopathologic study of 48 cases. Am J Surg Pathol. 1993;17(10):971–86.
16. Gupta N, Colby TV, Meyer CA, McCormack FX, Wikenheiser-Brokamp KA. Smoking-related diffuse cystic lung disease. Chest. 2018;154(2):e31–e5.
17. Baqir M, Kluka EM, Aubry MC, Hartman TE, Yi ES, Bauer PR, et al. Amyloid-associated cystic lung disease in primary Sjogren's syndrome. Respir Med. 2013;107(4):616–21.
18. Colombat M, Gounant V, Mal H, Callard P, Milleron B. Light chain deposition disease involving the airways: diagnosis by fibreoptic bronchoscopy. Eur Respir J. 2007;29(5):1057–60.
19. Bhargava P, Rushin JM, Rusnock EJ, Hefter LG, Franks TJ, Sabnis SG, et al. Pulmonary light chain deposition disease: report of five cases and review of the literature. Am J Surg Pathol. 2007;31(2):267–76.
20. Desai SR, Nicholson AG, Stewart S, Twentyman OM, Flower CD, Hansell DM. Benign pulmonary lymphocytic infiltration and amyloidosis: computed tomographic and pathologic features in three cases. J Thorac Imaging. 1997;12(3):215–20.
21. Chew KM, Clarke MJ, Dubey N, Seet JE. Nodular pulmonary amyloidosis with unusual, widespread lung cysts. Singap Med J. 2013;54(5):e97–9.
22. Ohdama S, Akagawa S, Matsubara O, Yoshizawa Y. Primary diffuse alveolar septal amyloidosis with multiple cysts and calcification. Eur Respir J. 1996;9(7):1569–71.
23. Arrossi AV, Merzianu M, Farver C, Yuan C, Wang SH, Nakashima MO, et al. Nodular pulmonary light chain deposition disease: an entity associated with Sjogren syndrome or marginal zone lymphoma. J Clin Pathol. 2016;69(6):490–6.
24. Khoor A, Colby TV. Amyloidosis of the lung. Arch Pathol Lab Med. 2017;141(2):247–54.
25. Seaman DM, Meyer CA, Gilman MD, McCormack FX. Diffuse cystic lung disease at high-resolution CT. AJR Am J Roentgenol. 2011;196(6):1305–11.
26. Abrams J, Talcott J, Corson JM. Pulmonary metastases in patients with low-grade endometrial stromal sarcoma. Clinicopathologic findings with immunohistochemical characterization. Am J Surg Pathol. 1989;13(2):133–40.
27. Aubry MC, Myers JL, Colby TV, Leslie KO, Tazelaar HD. Endometrial stromal sarcoma metastatic to the lung: a detailed analysis of 16 patients. Am J Surg Pathol. 2002;26(4):440–9.
28. Hill DA, Jarzembowski JA, Priest JR, Williams G, Schoettler P, Dehner LP. Type I pleuropulmonary blastoma: pathology and biology study of 51 cases from the international pleuropulmonary blastoma registry. Am J Surg Pathol. 2008;32(2):282–95.
29. Hoag JB, Sherman M, Fasihuddin Q, Lund ME. A comprehensive review of spontaneous pneumothorax complicating sarcoma. Chest. 2010;138(3):510–8.
30. Ioachimescu OC, Sieber S, Walker MJ, Rella V, Kotch A. A 35-year-old woman with asthma and polycystic lung disease. Chest. 2002;121(1):256–60.
31. Odev K, Guler I, Altinok T, Pekcan S, Batur A, Ozbiner H. Cystic and cavitary lung lesions in children: radiologic findings with pathologic correlation. J Clin Imaging Sci. 2013;3:60.
32. Tateishi U, Hasegawa T, Kusumoto M, Yamazaki N, Iinuma G, Muramatsu Y, et al. Metastatic angiosarcoma of the lung: spectrum of CT findings. AJR Am J Roentgenol. 2003;180(6):1671–4.
33. Traweek T, Rotter AJ, Swartz W, Azumi N. Cystic pulmonary metastatic sarcoma. Cancer. 1990;65(8):1805–11.
34. Gupta N, Vassallo R, Wikenheiser-Brokamp KA, McCormack FX. Diffuse cystic lung disease. Part I. Am J Respir Crit Care Med. 2015;191(12):1354–66.
35. Farooqi AO, Cham M, Zhang L, Beasley MB, Austin JH, Miller A, et al. Lung cancer associated with cystic airspaces. AJR Am J Roentgenol. 2012;199(4):781–6.

Chapter 5
Pathophysiology of Lymphangioleiomyomatosis

Elizabeth P. Henske, Souheil El-Chemaly, Thomas N. Darling, Angelo M. Taveira-DaSilva, and Joel Moss

Lymphangioleiomyomatosis

Clinical and Pathologic Features

Lymphangioleiomyomatosis (LAM) is a rare lung disease that affects women, almost exclusively. LAM is heralded as a shining example of rapid bench to bedside progress resulting in a highly effective treatment for a rare disease. This progress has been possible because of the tightly knit LAM research community, from basic and translational scientists to clinical researchers, with strong and essential support from patients and patient advocacy organizations. LAM can occur in two settings: in women with the autosomal dominant disease tuberous sclerosis complex (TSC) and in women who do not have TSC (sporadic LAM).

E. P. Henske (✉)
Department of Medicine/Pulmonary and Critical Care, Brigham and Women's Hospital, Boston, MA, USA
e-mail: ehenske@bwh.harvard.edu

S. El-Chemaly
Pulmonary and Critical Care Medicine, Department of Medicine, Brigham and Women's Hospital and Harvard Medical School, Boston, MA, USA
e-mail: sel-chemaly@bwh.harvard.edu

T. N. Darling
Department of Dermatology, Uniformed Services University of the Health Sciences, Bethesda, MD, USA
e-mail: thomas.darling@usuhs.edu

A. M. Taveira-DaSilva · J. Moss
National Heart, Lung, and Blood Institute, National Institutes of Health, Bethesda, MD, USA
e-mail: dasilvaa@nhlbi.nih.gov; mossj@nhlbi.nih.gov

N. Gupta et al. (eds.), *Diffuse Cystic Lung Diseases*, Respiratory Medicine,
https://doi.org/10.1007/978-3-030-63365-3_5

The signs and symptoms of LAM can include dyspnea, fatigue, pneumothorax, chylothorax, retroperitoneal lymphadenopathy/lymphangioleiomyomas, and renal angiomyolipomas (AMLs) [1–3]. Symptoms of LAM typically arise in the childbearing years. A lengthy interval between initial symptoms and diagnosis is not unusual, with symptoms of exertional dyspnea and fatigue often attributed to deconditioning. Even in women who present with pneumothorax (which is a presenting symptom in about 40% of women with LAM and occurs during the disease in an even greater percentage), a delay in diagnosis can occur, since chest computed tomography (CT) screening is unfortunately not standard of care after an initial pneumothorax.

The clinical course of LAM is highly variable. In premenopausal women, progression to oxygen dependence can be rapid in the absence of therapy. However, there are women in whom LAM is detected incidentally, often during the postmenopausal years, in whom there is no evidence of lung function decline over many years. It is suspected that LAM may be present in many women at a subclinical level, with diagnoses made only in those women at the "tip of the iceberg" in terms of symptoms, or in women with incidental detection of cystic lung disease upon imaging done for another reason.

Radiographically, pulmonary LAM is characterized by bilateral, multifocal, thin-walled cystic lesions, which are usually distributed in all lobes [4]. Histologically, a diffuse proliferation of smooth muscle like LAM cells is present, accompanied by cystic alveolar destruction. An extensive network of lymphatic endothelial cells surrounds the LAM cells. Remarkably, the lymphatic vascular endothelial growth factor, VEGF-D is elevated in the serum of many LAM patients, with levels of >800 pg/mL considered diagnostic of LAM. These diagnostic levels of VEGF-D are found in about two-thirds of women with pathologically proven LAM. In women with a characteristic chest CT showing diffuse, thin-walled cysts and a VEGF-D > 800 pg/mL, a diagnosis of LAM can be made without a tissue biopsy [5].

Pathogenesis

The modern era of LAM research began in the year 2000, with the discovery of bi-allelic loss-of-function *TSC2* gene mutations in microdissected pulmonary LAM cells [6]. It was soon discovered based on work in Drosophila that the TSC proteins inhibit the mechanistic target of rapamycin (mTOR), followed by the observation that LAM cells, like other TSC2-deficient cells, have hyperphosphorylation of ribosomal protein S6 [7]. These studies paved the way for a pivotal clinical trial in which women with moderately severe LAM were randomly assigned to receive sirolimus or placebo. This study, Multicenter International LAM Efficacy of Sirolimus (MILES), clearly demonstrated that FEV1 (forced expiratory volume in 1 second) stabilized in women receiving sirolimus and continued to decline in women receiving placebo [8]. Treatment was discontinued after 1 year, and after discontinuation, lung function decline resumed in the women previously receiving sirolimus. Therefore, sirolimus appears to have a cytostatic effect in LAM and in

other manifestations of TSC, including renal AMLs [9] and subependymal giant cell astrocytomas (SEGAs) [10]; once therapy is initiated, it is unusual to discontinue treatment.

The cellular origin of LAM cells is an area of current debate and research interest [1, 11, 12]. These unusual cells express smooth muscle and melanocyte lineage markers. LAM cells appear to be histologically and genetically identical to renal AML cells. In the ~30% of women with sporadic LAM who also have renal AMLs, identical loss-of-function *TSC2* gene mutations can be found in the LAM cells and the AML cells [6], suggesting that they arise from a common progenitor cell. The possible origins of this cell include the lymphatic endothelium, the uterus, and the neural crest [11–14].

The potential role of estrogen in LAM pathogenesis is also an area of many unknowns. LAM is obviously a disease of women, and there are reports of worsening of LAM during pregnancy [15–17]. LAM cells express estrogen receptor alpha and progesterone receptor [18]. It is also known that LAM progresses more rapidly in premenopausal women when compared with postmenopausal women [19, 20]. In mouse models, estrogen can promote the survival of TSC2-deficient cells (used as a model of LAM), and can promote the spread or metastasis of TSC2-deficient cells to the lung, and the estrogen receptor antagonist Faslodex can block this metastasis [21–23]. In cellular models, estrogen activates the so-called "non-genomic" estrogen receptor pathways including MEK, to promote mesenchymal phenotypes in LAM-derived cells [22]. However, despite these findings, there are currently no prospective trials that demonstrate efficacy of hormonally targeted therapy for women with LAM, and hormonal therapy is generally not recommended for the therapy of LAM [5].

Genetics and Screening Implications

Sporadic LAM and TSC-LAM

LAM may be sporadic or occur as one manifestation of tuberous sclerosis complex (TSC-LAM). In sporadic LAM, there is no family history and negligible risk to offspring. In TSC-LAM, there may or may not be other affected individuals in the family, and there is a 50% risk of transmission of TSC to offspring [24]. TSC can impact nearly every organ of the body and usually presents in early childhood with seizures. However, some individuals with TSC remain undiagnosed until adulthood, when they present with LAM or AMLs [25]. The distinction between sporadic LAM and TSC-LAM has significant clinical implications. In those with LAM, the possibility of it occurring in the context of TSC should be considered and TSC evaluated as indicated. In women known to have TSC, they should be periodically screened for the development of LAM and other internal tumors.

Individuals with TSC are predisposed to developing hamartomatous tumors in the brain, eyes, skin, heart, kidneys, and lungs [26]. Most of these tumors have onset

in infancy or childhood, with LAM a notable exception for adult onset of symptoms. Cerebral lesions include cortical tubers, subependymal nodules, and subependymal giant cell astrocytomas (SEGAs). Seizures occur in approximately 80% of patients with onset most often within the first 3 years of life [27]. Individuals may exhibit a range of behavioral, intellectual, and psychosocial difficulties, encompassed by the term TSC-associated neuropsychiatric disorders (TAND) [27]. Retinal lesions include retinal hamartomas and retinal achromic patches. Skin lesions are observed in nearly all individuals with TSC and include hypopigmented macules and a variety of fibrous papules and plaques. Multiple cardiac rhabdomyomas are common during infancy that are often asymptomatic and spontaneously regress [26]. Renal AMLs or renal cysts develop in TSC during childhood or adolescence and are a common source of morbidity in adult patients with TSC [25]. Pulmonary involvement in TSC includes LAM and multifocal micronodular pneumocyte hyperplasia (MMPH) [24].

Screening for TSC in Those with LAM

In considering whether someone with LAM might also have TSC, it is important to recognize that the clinical picture for women newly diagnosed with TSC-LAM is often different from those diagnosed with TSC in childhood. They may present for the first time with symptoms caused by pulmonary LAM or renal AMLs and are less likely to have seizures than those diagnosed in childhood [25]. Many will have no family history of TSC at the time of diagnosis, consistent with the observation that there are no affected relatives in about two-thirds of patients with TSC [28]. Diagnosing TSC is valuable since mild severity of TSC during childhood does not spare individuals from the risk of life-threatening manifestations later in life. The diagnosis of TSC in those with LAM enables monitoring for the formation of other TSC-related tumors and provides the opportunity for patients to make informed decisions regarding childbearing [25]. It may also prevent misdiagnosis or inappropriate treatment of TSC manifestations, such as pursuing an evaluation for metastatic cancer based on MMPH, or nephrectomy when renal sparing approaches are indicated [29].

TSC is diagnosed based on clinical features or demonstration of a pathogenic mutation in *TSC1* or *TSC2* [30]. The presence of LAM with or without AMLs fulfills one major feature, so all individuals with LAM have possible TSC. The identification of one additional major feature, or two minor features, is sufficient for TSC diagnosis [30]. Initial screening for TSC in a LAM patient may include inquiry regarding personal history of seizures or other symptoms of TSC, questioning into family history of TSC or related findings, and clinical examination for TSC findings in the skin, mouth, and eyes. Complete evaluation includes additional tests and imaging detailed below [31].

Most, but not all, TSC-LAM patients have a TSC-related skin or oral finding [25]. In individuals with LAM who are yet to receive a TSC diagnosis, these skin lesions may be subtle and require skin biopsy for confirmation. For example, facial angiofibromas may appear as a few small pink- to skin-colored papules on the nose,

nasal groove, or adjacent cheeks [32]. Angiofibromas are commonly misdiagnosed as acne or warts and may have been treated in adolescence using lasers. Oral lesions are easily overlooked and include dental pitting and oral fibromas. Ungual fibromas may occur on any digit but are most common on the fifth toe where they are also inconspicuous [33]. Fibrous cephalic plaques may have been excised in childhood and hypomelanotic macules may fade in adults, so it is important to question regarding skin lesions that were excised or spontaneously resolved. An algorithm has been developed for the evaluation and differential diagnosis of these skin lesions [34]. In a LAM patient, the identification of any one of the five types of skin lesions comprising a major feature is sufficient to diagnose TSC.

Sclerotic bone lesions along the axial skeleton are associated with TSC [35, 36]. Screening for these lesions may be readily accomplished in most LAM patients by switching from pulmonary to bone window settings on existing CT scans. Sclerotic bone lesions are typically round and about 0.3 cm in diameter. They most commonly involve the spine; they may also be observed in the skull, ribs, or pelvis. It has been suggested that TSC should be suspected in those with four or more lesions in the thorax, skull, or abdomen/pelvis [35, 37].

Assuming the patient has already had high-resolution chest computed tomography (HRCT) and pulmonary function testing for evaluation of LAM, a complete TSC evaluation may also include MRI of the brain and abdomen, to examine for presence of tubers, subependymal nodules, migrational defects, subependymal giant cell astrocytoma, renal or hepatic AMLs, and renal cysts. A complete ophthalmologic evaluation including dilated fundoscopy can help assess for retinal lesions and visual field deficits. Genetic testing may be offered for family counseling or when TSC diagnosis is in question. Other tests useful as part of the initial evaluation include blood pressure, measurement of glomerular filtration rate, electrocardiogram (ECG), baseline routine electroencephalogram, and TAND evaluation [31].

Screening for LAM in Those with TSC

Women known to have TSC should be periodically screened for LAM, even if asymptomatic. LAM typically develops in women with TSC during the third or fourth decade of life, and the risk of disease increases with age. Radiographic evidence of LAM was observed in over 80% of adult females with TSC over age 40 [38]. The current recommendations are that women with TSC, 18 years or older, have baseline HRCT to screen for LAM. HRCT is also recommend for adult men with TSC if they have symptoms such as exertional dyspnea or shortness of breath, as 5–10% of adult men with TSC may also have cystic pulmonary parenchymal findings [31]. In TSC patients with no clinical symptoms and no evidence of lung cysts on their baseline HRCT, repeat HRCT imaging is recommended every 5–10 years. Low radiation imaging protocols should be used when available. In those with cysts on CT, pulmonary function testing and 6-minute walk test are recommended annually, with HRCT testing every 2–3 years. Those with more advanced TSC-LAM may need pulmonary function

testing every 3–6 months to assess disease progression [31]. Individuals with TSC should be counseled on smoking risks and women informed about possible implications of estrogen use on LAM progression [31].

Clinical Implications of TSC-LAM

Lung disease in TSC-LAM is managed like sporadic LAM. Although the severity of LAM in those with TSC may be less than those with sporadic LAM [39], there is no difference in the yearly rates of change in pulmonary function or cyst scores [40]. There is also no difference between TSC-LAM and sporadic LAM for the future risk of progression to death or transplantation [41]. Individuals with TSC-LAM need periodic monitoring for other manifestations of TSC [31]. This includes annual assessment of blood pressure and renal function, with MRI of the abdomen every 1–3 years. MRI of the brain should be performed every 1–3 years in all individuals with TSC until the age of 25 years, and those with symptomatic SEGAs should continue periodic brain MRI for life. ECG is recommended every 3–5 years to monitor for conduction defects. Clinical skin exams are performed annually and dental exams every 6 months. Eye exams are recommended annually for those with existing lesions [31]. Periodic surveillance may allow early identification of tumors or tumor progression and prompt institution of appropriate therapy.

Mosaicism

Investigations into the genetic basis for sporadic LAM and TSC-LAM uncovered the causative genes and more recently are providing clues into mosaic forms of disease [42]. TSC is caused by a pathogenic variant in one of the *TSC* genes, *TSC1* or *TSC2*. Analysis of blood DNA from patients with TSC-LAM usually reveals a pathogenic variant in one of two *TSC2* alleles. TSC tumors generally form by a somatic mutation that inactivates the second allele, a “two-hit” mechanism that is often used to define tumor suppressor genes. Individuals with sporadic LAM have a pathogenic variant in *TSC2* in LAM tumor cells but not the blood [43]. The shared genetic basis for tumor formation in TSC-LAM and sporadic LAM provides a framework for explaining many of their similarities in terms of pathogenesis and response to therapy. There are still many unanswered questions, such as the origin and timing of the mutation in sporadic LAM, as well as the cell type in which this occurs. Evidence is mounting that mosaicism is critical for understanding at least some instances of sporadic LAM.

Mosaicism occurs as a post-zygotic mutation resulting in two genetically distinct cell populations comprising the individual [44]. Mosaicism occurs in a subset of TSC patients. Because of the mixture of affected and unaffected cells comprising

their body, these individuals have a variant allele fraction (VAF) of less than 0.50 in their blood. Frequently, the VAF in the blood will be below the level of detection using standard methods of genetic analysis. In many of these individuals with no mutation identified (NMI) using standard analysis, pathogenic variants may be detected in blood using next-generation sequencing [45, 46]. Next generation sequencing may also be performed on samples from TSC skin tumors, and this may be useful in instances in which the mosaic variant is undetectable in blood [45, 47].

The timing of the post-zygotic mutation is thought to impact disease manifestations. In general, individuals with mosaic TSC tend to exhibit less severe disease with later onset than those with germline TSC [45]. Mutations occurring even later in development would be expected to impact fewer cells and cell lineages. This may result in sparing of regions of the body, as suggested by findings such as the presence of unilateral facial angiofibromas [44]. This presents the possibility for a continuum of disease, from germline TSC to mosaic TSC, including mosaic forms that may not meet diagnostic criteria for TSC, such as apparent sporadic LAM. Recently, a man presenting with sporadic LAM was shown to have mosaicism for a *TSC2* c.2320delA mutation, leading to renal AML and LAM development [48]. Such results indicate that subtle findings of TSC should not be discounted in those with apparent sporadic LAM, and that next generation sequencing of tissue samples in addition to blood may be needed to detect mosaicism.

Diagnosis of Lymphangioleiomyomatosis

A definite diagnosis of LAM can be established in women with TSC in the presence of characteristic cystic findings on chest CT scan [49]. Additional features used to support a definitive diagnosis of LAM include one of the following: the presence of renal AMLs, elevated serum VEGF-D $\geq$ 800 pg/mL, chylous effusion (pleural or ascites) confirmed by tap and biochemical analysis of the fluid, lymphangioleiomyomas, demonstration of LAM cells or LAM cell clusters on cytological examination of effusions or lymph nodes, or histopathological confirmation of LAM by lung biopsy or biopsy of retroperitoneal or pelvic masses [49].

Treatment of Lymphangioleiomyomatosis

The mainstay of pharmacological treatment of LAM is an oral mTOR inhibitor, sirolimus. Sirolimus was shown to be safe and effective for the treatment of LAM in the phase III, randomized, placebo–controlled, double-blind trial called the Multicenter International LAM Efficacy of Sirolimus (MILES) trial [8]. In the MILES trial, 89 women with LAM with FEV1 $\leq$ 70% predicted, were randomized to receive either sirolimus or placebo for 1 year followed by 1 year of observation off therapy. While patients in the placebo arm continued to decline, patients in the sirolimus

arm exhibited stabilization of their lung function decline. However, when the drug was held lung function decline resumed in both groups. The most common side effects from sirolimus were acne, mouth ulcers, nausea, diarrhea, hyperlipidemia, and lower extremity edema. Based on these results, sirolimus is now FDA approved for the treatment of LAM in the United States, and by the regulatory agencies in multiple other countries across the world including the European Union.

Other management considerations for patients with LAM include early pleurodesis following a spontaneous pneumothorax in order to prevent recurrent episodes, avoidance of estrogen, and close attention to immunizations such as annual influenza and pneumococcal vaccines. Clinical practice guidelines for the diagnosis and management of LAM have been published by the European Respiratory Society as well as the American Respiratory Society/Japanese Respiratory Society, and are an invaluable resource for practicing clinicians [4, 5, 49].

Pathophysiology of Lymphangioleiomyomatosis

Pulmonary function abnormalities in LAM are characterized by alterations in lung mechanics and impairment in gas exchange [40, 50]. The role of abnormalities in the pulmonary circulation and pulmonary hypertension at rest and during exercise in reducing oxygen transfer has not yet been well established [51]. In many ways, LAM presents unique features that mimic both obstructive and interstitial lung diseases.

Pulmonary Mechanics in LAM

Airways obstruction occurs in patients with LAM. The National Heart, Lung, and Blood Institute (NHLBI) LAM registry reported that airflow obstruction at the time of diagnosis was present in about 57% of the patients. Restrictive disease was noted in only 11% of the patients, and hyperinflation in 6% of the patients [50]. Patients with TSC-LAM had a lower prevalence of airflow obstruction than those with sporadic LAM [50]. Indeed, in a larger study involving 460 patients with sporadic LAM and 94 patients with TSC-LAM, the prevalence of airflow obstruction was 51% and 33%, respectively. Reduced DLCO was observed in 61% and 40%, respectively. Only about 20–30% of the patients with airways obstruction have a positive response to bronchodilators [52, 53].

The precise cause of airways obstruction has yet to be defined. Maximal expiratory flow is determined by the elastic recoil of the lung (P_{el}) and the frictional resistance of airways upstream (R_{us}) from an equal pressure point (EPP) where transmural airways pressure is zero [53]. Downstream from this point, there is a flow limiting segment (FLS) where flow is determined by P_{el} and R_{us} [54]. This relationship is given by Flow = $P_{el}/R_{us.}$ It is generally accepted that flow limitation

occurs at choke points throughout the lung airways where the speed of a wave propagated along the airways equals the speed of air flowing through the airways [55].

As in the case of pulmonary emphysema, a reduction in elastic recoil of the lungs could be a cause of airflow limitation in patients with LAM. However, no comprehensive studies of lung mechanics in LAM patients have so far been undertaken to test this hypothesis. To the best of our knowledge there has been only one study where the elastic recoil of the lung was found to be normal, and accordingly, it was proposed that airways obstruction in LAM was due exclusively to airways obstruction, e.g., airways disease [56]. Pathological studies have shown evidence of peripheral airways obstruction [57]. However, more comprehensive studies showed that there is scant evidence of bronchial obstruction, e.g., bronchiolitis [58], but instead, LAM cell nodular infiltrates around or in the airway walls are present and predominate in patients with lower FEV1 who exhibit a positive response to bronchodilators [59].

The site of airways obstruction and its mechanism are unclear. Flows throughout the mid (FEF50) and terminal part (FEF75) of the maximal expiratory flow volume (MEFV) curve are frequently reduced even in patients with mild obstructive disease, suggesting obstruction of the peripheral airways. However, no specific studies have been undertaken to determine the presence of small airways disease. As to the pathology of airways obstruction in LAM, a comprehensive study of lung pathology in LAM showed airway inflammation, i.e., bronchiolitis, in 47 of the 74 patients [59]. Bronchiolitis occurred in airways surrounded by heavy infiltrates of LAM cells. In most of these patients, a predominantly solid pattern of LAM lesions was observed [59]. Cystic lesions of variable severity were present in almost all patients. The most accepted hypothesis for the pathogenesis of airflow obstruction in LAM is that compression and/or infiltration of the airways and cyst walls by LAM cell clusters cause sufficient obstruction to reduce expiratory flow [60].

Gas Exchange Abnormalities in LAM

Exercise-induced hypoxemia is the major manifestation of gas exchange impairment in LAM [61, 62]. There is a broad correlation between oxygen saturation at peak exercise and lung diffusion capacity (DLCO) [62]. The assumption is that during exercise insufficient oxygen crosses the alveolar-capillary membrane to supply the oxygen demands of the skeletal and respiratory muscles. In a sub population of LAM patients, a reduced DLCO is the major functional abnormality, while flow rates, e.g., FEV1 are minimally impaired. In these patients, in the absence of imaging studies, failure to measure the DLCO, may delay the diagnosis of LAM.

Gas exchange abnormalities in LAM are related to the reduction of gas exchange surface area caused by cystic lesions, and a likely increase in extravascular lung water secondary to accumulation of chylous fluid. During exercise other factors may be contributing to worsened gas exchange, namely, alveolar hemorrhage, increased chylous fluid accumulation, and pulmonary hypertension. Therefore, it is important

not only to monitor the DLCO, but also the response to exercise as screening methods for detection of gas exchange abnormalities of what may be silent hypoxemia. Although DLCO is not a very reproducible test and has a large variability, tests performed in the same laboratory with the same equipment and trained personnel, using the same predicting equations can assist in grading disease severity and progression that may be confirmed by standard cardiopulmonary exercise testing, 6-minute walk tests, and imaging studies.

Pulmonary Hypertension

In a study comprising 120 patients with LAM, only eight were found to have an increased systolic pulmonary artery pressure (PAP) [51]. During exercise, 56 patients experienced elevation in systolic PAP > 40 mm Hg. Peak exercise oxygen saturation was the best predictor of exercise PAP. Although the prevalence of pulmonary hypertension at rest was low during exercise, it could play an important role in limiting exercise capacity, by causing right ventricular dysfunction and worsening hypoxemia.

The prevalence of pulmonary hypertension in LAM has been further studied by both echocardiographic and invasive hemodynamic techniques [63–65]. Cottin et al. [63] reported data from 29 LAM patients suspected of having pulmonary hypertension who underwent right heart catheterization. Nine patients had mean PAP between 20 and 24 mmHg and were excluded. The remaining 20 patients had a mean PAP of 32 ± 6 mmHg, and moderate to severe exercise intolerance. Compared to other LAM patients without pulmonary hypertension, LAM patients with pulmonary hypertension had more severe dyspnea, more severe airflow obstruction, more severe hypoxemia, and greater impairment in exercise capacity. Hemodynamic parameters correlated with FEV1 and DLCO. Examination of lung explants showed significant remodeling of the pulmonary arteries. Foci of LAM cells were noted to surround the pulmonary vessels [63].

In a subsequent study [64], 16 LAM patients who had echocardiographic evidence of a systolic PAP above 35 mmHg and a DLCO under 40% predicted, underwent right heart catheterization. Eight of the 16 patients (50%) had mean PAP ≥ 25 mmHg consistent with pulmonary hypertension. Six of the eight patients had pre-capillary pulmonary hypertension and the remaining two patients had post-capillary pulmonary hypertension, presumably due to left ventricular dysfunction. Patients with pulmonary hypertension had lower DLCO, lower exercise performance, and greater desaturation on 6-minute walk tests [64]. In another echocardiographic study [65], 15 LAM patients without pulmonary hypertension were compared to 15 age-matched healthy women. Doppler echocardiography was performed at rest and during graded stress echocardiography. The LAM patients experienced reduced exercise capacity, a reduction in SaO_2, and an increase in PAP, pulmonary capillary wedge pressure (PCWP), and pulmonary vascular

resistance (PVR). The elevation in PCWP was thought to be caused by left ventricular dysfunction due to dilation of the right ventricle with it displacing the interventricular septum to the left, decreasing the left ventricular dimensions, and increasing left ventricular afterload.

Exercise Limitation in LAM

Exercise limitation of various degrees of intensity is one of the most common complaints of patients with LAM. In many cases, it affects the quality of life because it interferes with activities of daily living. Four causes of exercise limitation may be postulated.

In the presence of airflow obstruction and a reduced FEV1, ventilation during exercise is limited, and as it approaches the maximal voluntary ventilation (MVV), breathing reserve is reduced and dynamic hyperinflation of the lungs may occur, leading to dyspnea and exercise cessation [66]. In normal subjects, expiratory flow limitation has been shown to reduce cardiac output by over 10%, and this effect is entirely due to a decrease in stroke volume [67, 68]. There was also a decrease in O_2 uptake that was associated with a reduction in oxygen saturation averaging 5%. Therefore, oxygen delivery to the organs and tissues declined by 15%. A competition between the skeletal and diaphragmatic muscle for the available oxygen supply would further decrease exercise performance.

A second mechanism of exercise limitation is hypoxemia. This is especially important in patients in whom lung mechanics, e.g., lung volumes and flow rates are preserved. As the oxygen requirements increase, oxygen exchange in the lungs cannot keep up with those requirements. Ventilation has to increase disproportionally with the exercise level, e.g., the ventilatory equivalent VE/VCO_2 increases, breathing reserve is reduced and oxygen supply to the muscles in insufficient, leading to early lactic acidosis and a low VO_2 anaerobic threshold.

A third mechanism is the reduction of oxygen supply to the skeletal muscles and the main respiratory muscle, the diaphragm. In a previous study [62], 28% of 217 patients who underwent exercise testing reported leg muscle fatigue as the cause of exercise cessation. As is the case with chronic obstructive pulmonary disease (COPD) and other cardiopulmonary diseases [67, 68], decreased diaphragmatic oxygen supply during exercise may be another potential cause of dyspnea during exercise, limiting exercise capacity in patients with LAM.

Finally, exercise-induced pulmonary hypertension may be occurring in patients with LAM, and this could affect gas exchange in several ways. Rapid blood flow through a reduced pulmonary vascular bed could reduce oxygen transfer by reducing contact time between alveolar gases and pulmonary capillary flow. Second, shear forces generated by blood flowing through damaged or untethered pulmonary capillaries could cause alveolar hemorrhage, which has been reported by LAM

patients during sexual intercourse, and confirmed by histopathological studies [58]. In addition, intrapulmonary arterio-venous shunts have been described in LAM patients with dyspnea [69]. Fifty percent of eight exercise intolerant LAM patients had intrapulmonary arterio-venous shunts at rest, and 62.5% had them during exercise. Three of these patients had near normal FEV1 [69].

Animal Models of Lymphangioleiomyomatosis

Animal models are critically important to understand disease pathogenesis and for the evaluation of potential therapies. Despite many efforts over the years, an animal model that faithfully replicates the human findings in LAM has not been developed. Nevertheless, existing animal models have contributed to the understanding of LAM pathogenesis and importantly allowed testing of novel therapies.

Xenograft Tumor Model

While LAM is not a solid tumor, it has been characterized as a malignancy [70]. The most commonly used animal model to study LAM is the subcutaneous tumor model, which has been successfully used as a surrogate to study the behavior of TSC-deficient tumors in vivo.

In this model, TSC2-deficient cells are transplanted under the skin of immunocompromised mice. The most commonly used mice are the severely compromised immune-deficient CD17-scid (SCID) mice, although the more severely immunodeficient NOD.*Cg-Prkdc*^{scid} *Il2rg*^{tm1Wjl}*/SzJ* (NSG) have been used as well [71]. These models are relatively inexpensive and allow the understanding of TSC-deficient cells in vivo as well as testing therapeutic targets [72]. The major limitation is the lack of an immune system in these mice, which has been shown to be important in disease pathogenesis [73, 74].

The subcutaneous xenograft model can be used to evaluate prevention of tumor growth, decrease in tumor size, or prevention of tumor regrowth. Different animal and human derived cells have been used in this model. The most commonly used human cells are derived from kidney angiomyolipoma (621–101) cells [75]. Animal derived cells include the ELT3 cells derived from uterine leiomyoma of Eker rat harboring a germline mutation in *TSC2* [76], 105 K [77] and TMKOC [78] cells derived from a renal tubular cystadenoma of a C57BL/6 J *Tsc2*$^{+/-}$ mouse. The TMKOC cells are passed through immunodeficient mice to enhance their tumorigenicity [78], which results in their ability to develop tumors in immunocompetent mice [73, 74].

Cell Homing to the Lungs

TSC-deficient cells can also be injected into the tail vein where they migrate and are entrapped into the lung. Cells can be labeled and followed by bioluminescence after injection [21, 79]. The short-term survival and homing in the lung as well as the study of factors that enhance lung entrapment such as estrogen [21] or decrease cell viability [79] can be investigated.

Tsc2-deficient cells administered through tail vein injections have been used to study the long-term consequences of the presence of TSC-deficient cells in the lungs. These data demonstrated that the presence of these cells in the lungs lead to alveolar destruction [80]. While these studies allow the evaluation of TSC-deficient cells in the lung environment, they present difficulties in longitudinal follow-up and in non-invasive monitoring. Recently, and to study disease burden in pre clinical models, Verwer et al. studied the utility of [^{18}F] Fluorocholine and [^{18}F] Fluoroacetate positron emission tomography (PET) in preclinical models of LAM, where ELT3 cells are injected into the tail vein and lung lesions were imaged 25–90 days after injection. This was followed by choline PET studies showing an increased uptake in TSC-deficient tumors [71]. This imaging modality could offer the possibility of long-term non-invasive follow-up of TSC-deficient tumors in the lungs.

Genetic Models of Lymphangioleiomyomatosis

Tsc1 *and* Tsc2 *Heterozygote Mice*

In mice, *Tsc1* or *Tsc2* disruption is embryonic lethal. Heterozygote *Tsc2*$^{+/-}$ and *Tsc1*$^{+/-}$ mice survive to adulthood. These mice develop kidney tumors by 6–12 months of age. These tumors are generally cystadenomas with rare occurrence of renal carcinomas. In addition, mice develop liver hemangiomas and occasionally paw angiosarcomas. There are minor differences in frequency of tumor development between *Tsc2*$^{+/-}$ and *Tsc1*$^{+/-}$, with *Tsc1* heterozygote mice somewhat less susceptible. However, more importantly there are strain differences in tumor development with the A/J strain the most susceptible for cystadenoma kidney tumor development. (For complete review of the genetics and phenotype of *Tsc1* and *Tsc2* heterozygote mice, see [81]).

Cell-Specific Gene Deletion

Overtime, different genetically engineered mice were generated by deleting *Tsc1, Tsc2*, or *mTOR* in multiple cell types, which resulted in different mice phenotypes, none to date faithfully recapitulating LAM lung lesions.

Klover et al. used a *Prrx1*-cre to delete *Tsc2* in the lateral plate mesoderm, which is responsible for the genesis of the limb bud and the craniofacial mesenchyme. *Prrx1* is not restricted to dermal fibroblasts but is also expressed in osteoblasts, chondrocytes, and adipocytes but not endothelial cells. *Tsc2* deletion in *Prrx1*-expressing cells resulted in hamartoma development and aberrant angiogenesis like human TSC; these lesions were associated with a response to mTOR inhibition [82].

Mesenchymal cell-specific *Tsc2* deletion using a *Dermo1*-Cre resulted in increased lethality at 3 weeks after birth and the development of polycystic kidney disease and impaired lung alveolarization [83]. The development of polycystic kidney disease was associated with increased proliferation, epithelial cell hyperplasia, and epithelial-mesenchymal transition. Paradoxically, in the lung, impaired alveolarization was attributed to decreased proliferation and altered myofibroblast differentiation [83].

In intriguing findings, *Tsc2* deletion in uterine cells using the progesterone receptor-Cre demonstrated the development of uterine leiomyomas and more importantly lung lesions at 31 weeks of age (but not younger than 24 weeks). These lesions were thought to be metastatic from the uterus and were characterized by their estrogen and progesterone receptors positivity and activated mTOR pathway [13]. In addition, these tumors were shown to be estrogen-dependent [84].

Several groups have created cell-specific *Tsc1* deletion. Silencing *Tsc1* in endothelial cells using Tie2-Cre resulted in abnormal angiogenesis and compromised cardiac development and embryonic lethality [85]. Disruption of Tsc1 in lung pulmonary artery smooth muscle cells (SM22-Cre) [86] resulted in the development of pulmonary hypertension, with smooth muscle cells showing markers of early senescence [86, 87]. Moreover, silencing Tsc1 in endothelial cells (PDGF-Cre) or epithelial cells (surfactant protein C-Cre) in mice resulted in emphysema development, in addition to pulmonary hypertension and pulmonary vascular remodeling [86]. These findings were associated with increased cell senescence and immune cell infiltration, but no associated increase in epithelial cell death. *PDGF-TSC1*$^{-/-}$ mice treated with rapamycin were protected against the development of emphysema and pulmonary hypertension [86].

This contrasts with data from Wang et al. showing that genetically deleting mTOR in bronchial (using a CC10-Cre) or alveolar (surfactant protein C-Cre) epithelial cells resulted in increased airway inflammation, and emphysema in response to cigarette smoke exposure. These findings were associated with increased epithelial cell death [88].

While the quest for an animal model completely replicating LAM remains elusive, all these models remain important in the study of LAM and TSC and can help substantially increase our understanding with regard to the pathogenesis, response to therapy, and perhaps the elusive origin of the LAM cell.

Conclusion

As we move into the next era of LAM research and clinical care, critical questions include the following: (1) What is the cellular origin of LAM cells? (2) Why does LAM affect almost exclusively women? (3) Can hormonal agents be used to selectively target LAM cells? (4) How do LAM cells recruit their extensive lymphatic network? (5) Can a genetically engineered mouse provide a robust model of LAM for use in preclinical studies? (6) What is the precise mechanism of airway obstruction in LAM? (7) What types of trial designs can be used to make further clinical progress in LAM [89]? (8) Can further biomarkers of LAM be developed that will provide early evidence of treatment efficacy and/or allow non-invasive diagnosis of LAM in women who do not have elevated serum VEGF-D [89]? Each of these questions has high-impact clinical and therapeutic implications; the answers could provide the catalyst for significant health benefits for women living with LAM.

Key Learning Points

- Lymphangioleiomyomatosis (LAM) occurs in a sporadic form (sporadic LAM) and in tuberous sclerosis complex (TSC-LAM). TSC is associated with neurologic disease and tumors of multiple organs, but some TSC patients have mild symptoms that are not obvious clinically. It is important to consider screening for TSC in women who appear to have sporadic LAM.
- Sporadic LAM is associated with renal angiomyolipomas.
- Both sporadic LAM and TSC-LAM are caused by loss-of-function mutations in the TSC1 or TSC2 gene, resulting in hyperactivation of the mechanistic target of rapamycin (mTOR), a serine/threonine kinase.
- A diagnosis of LAM can be made using varying combinations of a CT chest showing diffuse thin-walled cysts, an elevated serum vascular endothelial growth factor-D (VEGF-D) level >800 pg/ml, presence of a renal angiomyolipoma, and histologically by lung biopsy showing presence of smooth-muscle like LAM cells.
- In terms of changes in lung function, LAM can mimic both obstructive and interstitial lung disease.
- A pivotal randomized controlled clinical trial has demonstrated benefit of the oral mTOR inhibitor, sirolimus (rapamycin) for the treatment of LAM.

Acknowledgments LAM research in the Henske Lab is supported by the NHLBI, the DOD Tuberous Sclerosis Medical Research Program, and the Engles Program for TSC and LAM Research. AMTD and JM are supported by the Intramural Research Program, NIH, and NHLBI.

References

1. Henske EP, McCormack FX. Lymphangioleiomyomatosis – a wolf in sheep's clothing. J Clin Invest. 2012;122(11):3807–16.
2. Krymskaya VP, McCormack FX. Lymphangioleiomyomatosis: a monogenic model of malignancy. Annu Rev Med. 2017;68:69–83.
3. Taveira-DaSilva AM, Moss J. Epidemiology, pathogenesis and diagnosis of lymphangioleiomyomatosis. Expert Opin Orphan Drugs. 2016;4(4):369–78.
4. Johnson SR, Cordier JF, Lazor R, Cottin V, Costabel U, Harari S, et al. European Respiratory Society guidelines for the diagnosis and management of lymphangioleiomyomatosis. Eur Respir J. 2010;35(1):14–26.
5. McCormack FX, Gupta N, Finlay GR, Young LR, Taveira-DaSilva AM, Glasgow CG, et al. Official American Thoracic Society/Japanese Respiratory Society clinical practice guidelines: lymphangioleiomyomatosis diagnosis and management. Am J Respir Crit Care Med. 2016;194(6):748–61.
6. Carsillo T, Astrinidis A, Henske EP. Mutations in the tuberous sclerosis complex gene TSC2 are a cause of sporadic pulmonary lymphangioleiomyomatosis. Proc Natl Acad Sci U S A. 2000;97(11):6085–90.
7. Goncharova EA, Goncharov DA, Eszterhas A, Hunter DS, Glassberg MK, Yeung RS, et al. Tuberin regulates p70 S6 kinase activation and ribosomal protein S6 phosphorylation: a role for the TSC2 tumor suppressor gene in pulmonary lymphangioleiomyomatosis (LAM). J Biol Chem. 2002;277:30958–67.
8. McCormack FX, Inoue Y, Moss J, Singer LG, Strange C, Nakata K, et al. Efficacy and safety of sirolimus in lymphangioleiomyomatosis. N Engl J Med. 2011;364(17):1595–606.
9. Bissler JJ, McCormack FX, Young LR, Elwing JM, Chuck G, Leonard JM, et al. Sirolimus for angiomyolipoma in tuberous sclerosis complex or lymphangioleiomyomatosis. N Engl J Med. 2008;358(2):140–51.
10. Franz DN, Belousova E, Sparagana S, Bebin EM, Frost M, Kuperman R, et al. Everolimus for subependymal giant cell astrocytoma in patients with tuberous sclerosis complex: 2-year open-label extension of the randomised EXIST-1 study. Lancet Oncol. 2014;15(13):1513–20.
11. Davis JM, Hyjek E, Husain AN, Shen L, Jones J, Schuger LA. Lymphatic endothelial differentiation in pulmonary lymphangioleiomyomatosis cells. J Histochem Cytochem. 2013;61(8):580–90.
12. Delaney SP, Julian LM, Stanford WL. The neural crest lineage as a driver of disease heterogeneity in tuberous sclerosis complex and lymphangioleiomyomatosis. Front Cell Dev Biol. 2014;2:69.
13. Prizant H, Sen A, Light A, Cho SN, DeMayo FJ, Lydon JP, et al. Uterine-specific loss of Tsc2 leads to myometrial tumors in both the uterus and lungs. Mol Endocrinol. 2013;27(9):1403–14.
14. Cho JH, Patel B, Bonala S, Manne S, Zhou Y, Vadrevu SK, et al. Notch transactivates Rheb to maintain the multipotency of TSC-null cells. Nat Commun. 2017;8(1):1848.
15. Hughes E, Hodder RV. Pulmonary lymphangiomyomatosis complicating pregnancy. A case report. J Reprod Med. 1987;32(7):553–7.
16. Johnson SR, Tattersfield AE. Clinical experience of lymphangioleiomyomatosis in the UK. Thorax. 2000;55(12):1052–7.
17. Mitra S, Ghosal AG, Bhattacharya P. Pregnancy unmasking lymphangioleiomyomatosis. J Assoc Physicians India. 2004;52:828–30.
18. Logginidou H, Ao X, Russo I, Henske EP. Frequent estrogen and progesterone receptor immunoreactivity in renal angiomyolipomas from women with pulmonary lymphangioleiomyomatosis. Chest. 2000;117(1):25–30.
19. Johnson SR, Tattersfield AE. Decline in lung function in lymphangioleiomyomatosis: relation to menopause and progesterone treatment. Am J Respir Crit Care Med. 1999;160(2):628–33.

20. Taveira-DaSilva AM, Julien-Williams P, Jones AM, Stylianou M, Moss J. Rates of change in FEV1 and DLCO as potential indicators for mTOR inhibitor therapy in premenopausal lymphangioleiomyomatosis patients. Eur Respir J. 2018;51(4):1702258.
21. Yu JJ, Robb VA, Morrison TA, Ariazi EA, Karbowniczek M, Astrinidis A, et al. Estrogen promotes the survival and pulmonary metastasis of tuberin-null cells. Proc Natl Acad Sci U S A. 2009;106(8):2635–40.
22. Gu X, Yu JJ, Ilter D, Blenis N, Henske EP, Blenis J. Integration of mTOR and estrogen-ERK2 signaling in lymphangioleiomyomatosis pathogenesis. Proc Natl Acad Sci U S A. 2013;110(37):14960–5.
23. Li C, Zhou X, Sun Y, Zhang E, Mancini JD, Parkhitko A, et al. Faslodex inhibits estradiol-induced extracellular matrix dynamics and lung metastasis in a model of lymphangioleiomyomatosis. Am J Respir Cell Mol Biol. 2013;49(1):135–42.
24. Gupta N, Henske EP. Pulmonary manifestations in tuberous sclerosis complex. Am J Med Genet C Semin Med Genet. 2018;178:326–37.
25. Seibert D, Hong CH, Takeuchi F, Olsen C, Hathaway O, Moss J, et al. Recognition of tuberous sclerosis in adult women: delayed presentation with life-threatening consequences. Ann Intern Med. 2011;154(12):806–13, W-294.
26. Roach ES. Applying the lessons of tuberous sclerosis: the 2015 Hower award lecture. Pediatr Neurol. 2016;63:6–22.
27. Curatolo P, Moavero R, de Vries PJ. Neurological and neuropsychiatric aspects of tuberous sclerosis complex. Lancet Neurol. 2015;14(7):733–45.
28. Curatolo P, Moavero R, Roberto D, Graziola F. Genotype/phenotype correlations in tuberous sclerosis complex. Semin Pediatr Neurol. 2015;22(4):259–73.
29. Nathan N, Burke K, Trickett C, Moss J, Darling TN. The adult phenotype of tuberous sclerosis complex. Acta Derm Venereol. 2016;96(2):278–80.
30. Northrup H, Krueger DA. International tuberous sclerosis complex consensus G. tuberous sclerosis complex diagnostic criteria update: recommendations of the 2012 international tuberous sclerosis complex consensus conference. Pediatr Neurol. 2013;49(4):243–54.
31. Krueger DA, Northrup H. International tuberous sclerosis complex consensus G. tuberous sclerosis complex surveillance and management: recommendations of the 2012 international tuberous sclerosis complex consensus conference. Pediatr Neurol. 2013;49(4):255–65.
32. Teng JM, Cowen EW, Wataya-Kaneda M, Gosnell ES, Witman PM, Hebert AA, et al. Dermatologic and dental aspects of the 2012 international tuberous sclerosis complex consensus statements. JAMA Dermatol. 2014;150(10):1095–101.
33. Aldrich CS, Hong CH, Groves L, Olsen C, Moss J, Darling TN. Acral lesions in tuberous sclerosis complex: insights into pathogenesis. J Am Acad Dermatol. 2010;63(2):244–51.
34. Nathan N, Burke K, Moss J, Darling TN. A diagnostic and management algorithm for individuals with an isolated skin finding suggestive of tuberous sclerosis complex. Br J Dermatol. 2017;176(1):220–3.
35. Avila NA, Dwyer AJ, Rabel A, Darling T, Hong CH, Moss J. CT of sclerotic bone lesions: imaging features differentiating tuberous sclerosis complex with lymphangioleiomyomatosis from sporadic lymphangioleiomymatosis. Radiology. 2010;254(3):851–7.
36. Boronat S, Barber I, Thiele EA. Sclerotic bone lesions in tuberous sclerosis complex: a genotype-phenotype study. Am J Med Genet A. 2017;173:1891–5.
37. Brakemeier S, Vogt L, Adams LC, Zukunft B, Diederichs G, Hamm B, et al. Sclerotic bone lesions as a potential imaging biomarker for the diagnosis of tuberous sclerosis complex. Sci Rep. 2018;8(1):953.
38. Cudzilo CJ, Szczesniak RD, Brody AS, Rattan MS, Krueger DA, Bissler JJ, et al. Lymphangioleiomyomatosis screening in women with tuberous sclerosis. Chest. 2013;144(2):578–85.
39. Avila NA, Dwyer AJ, Rabel A, Moss J. Sporadic lymphangioleiomyomatosis and tuberous sclerosis complex with lymphangioleiomyomatosis: comparison of CT features. Radiology. 2007;242(1):277–85.

40. Taveira-DaSilva AM, Jones AM, Julien-Williams P, Yao J, Stylianou M, Moss J. Severity and outcome of cystic lung disease in women with tuberous sclerosis complex. Eur Respir J. 2015;45(1):171–80.
41. Gupta N, Lee HS, Ryu JH, Taveira-DaSilva AM, Beck GJ, Lee JC, et al. The NHLBI LAM registry: prognostic physiologic and radiologic biomarkers emerge from a 15-year prospective longitudinal analysis. Chest. 2019;155:288–96.
42. Peron A, Au KS, Northrup H. Genetics, genomics, and genotype-phenotype correlations of TSC: insights for clinical practice. Am J Med Genet C Semin Med Genet. 2018;178:281–90.
43. Lam HC, Nijmeh J, Henske EP. New developments in the genetics and pathogenesis of tumours in tuberous sclerosis complex. J Pathol. 2017;241(2):219–25.
44. Nathan N, Keppler-Noreuil KM, Biesecker LG, Moss J, Darling TN. Mosaic disorders of the PI3K/PTEN/AKT/TSC/mTORC1 signaling pathway. Dermatol Clin. 2017;35(1):51–60.
45. Tyburczy ME, Dies KA, Glass J, Camposano S, Chekaluk Y, Thorner AR, et al. Mosaic and intronic mutations in TSC1/TSC2 explain the majority of TSC patients with no mutation identified by conventional testing. PLoS Genet. 2015;11(11):e1005637.
46. Nellist M, Brouwer RW, Kockx CE, van Veghel-Plandsoen M, Withagen-Hermans C, Prins-Bakker L, et al. Targeted next generation sequencing reveals previously unidentified TSC1 and TSC2 mutations. BMC Med Genet. 2015;16:10.
47. Tyburczy ME, Wang JA, Li S, Thangapazham R, Chekaluk Y, Moss J, et al. Sun exposure causes somatic second-hit mutations and angiofibroma development in tuberous sclerosis complex. Hum Mol Genet. 2014;23(8):2023–9.
48. Han MK, Tyburczy ME, Darling TN, Kazerooni EA, Myers JL, McCormack FX, et al. Apparent sporadic lymphangioleiomyomatosis in a man as a result of extreme mosaicism for a TSC2 mutation. Ann Am Thorac Soc. 2017;14(7):1227–9.
49. Gupta N, Finlay GA, Kotloff RM, Strange C, Wilson KC, Young LR, et al. Lymphangioleiomyomatosis diagnosis and management: high-resolution chest computed tomography, transbronchial lung biopsy, and pleural disease management. An official American Thoracic Society/Japanese Respiratory Society clinical practice guideline. Am J Respir Crit Care Med. 2017;196(10):1337–48.
50. Ryu JH, Moss J, Beck GJ, Lee JC, Brown KK, Chapman JT, et al. The NHLBI lymphangioleiomyomatosis registry: characteristics of 230 patients at enrollment. Am J Respir Crit Care Med. 2006;173(1):105–11.
51. Taveira-DaSilva AM, Hathaway OM, Sachdev V, Shizukuda Y, Birdsall CW, Moss J. Pulmonary artery pressure in lymphangioleiomyomatosis: an echocardiographic study. Chest. 2007;132(5):1573–8.
52. Taveira-DaSilva AM, Steagall WK, Rabel A, Hathaway O, Harari S, Cassandro R, et al. Reversible airflow obstruction in lymphangioleiomyomatosis. Chest. 2009;136(6):1596–603.
53. Mead J, Turner JM, Macklem PT, Little JB. Significance of the relationship between lung recoil and maximum expiratory flow. J Appl Physiol. 1967;22(1):95–108.
54. Pride NB, Permutt S, Riley RL, Bromberger-Barnea B. Determinants of maximal expiratory flow from the lungs. J Appl Physiol. 1967;23(5):646–62.
55. Dawson SV, Elliott EA. Wave-speed limitation on expiratory flow-a unifying concept. J Appl Physiol Respir Environ Exerc Physiol. 1977;43(3):498–515.
56. Burger CD, Hyatt RE, Staats BA. Pulmonary mechanics in lymphangioleiomyomatosis. Am Rev Respir Dis. 1991;143(5 Pt 1):1030–3.
57. Sobonya RE, Quan SF, Fleishman JS. Pulmonary lymphangioleiomyomatosis: quantitative analysis of lesions producing airflow limitation. Hum Pathol. 1985;16(11):1122–8.
58. Matsui K, Beasley MB, Nelson WK, Barnes PM, Bechtle J, Falk R, et al. Prognostic significance of pulmonary lymphangioleiomyomatosis histologic score. Am J Surg Pathol. 2001;25(4):479–84.
59. Taveira-DaSilva AM, Hedin C, Stylianou MP, Travis WD, Matsui K, Ferrans VJ, et al. Reversible airflow obstruction, proliferation of abnormal smooth muscle cells, and impair-

ment of gas exchange as predictors of outcome in lymphangioleiomyomatosis. Am J Respir Crit Care Med. 2001;164(6):1072–6.
60. Argula RG, Kokosi M, Lo P, Kim HJ, Ravenel JG, Meyer C, et al. A novel quantitative computed tomographic analysis suggests how Sirolimus stabilizes progressive air trapping in lymphangioleiomyomatosis. Ann Am Thorac Soc. 2016;13(3):342–9.
61. Crausman RS, Jennings CA, Mortenson RL, Ackerson LM, Irvin CG, King TE Jr. Lymphangioleiomyomatosis: the pathophysiology of diminished exercise capacity. Am J Respir Crit Care Med. 1996;153(4 Pt 1):1368–76.
62. Taveira-DaSilva AM, Stylianou MP, Hedin CJ, Kristof AS, Avila NA, Rabel A, et al. Maximal oxygen uptake and severity of disease in lymphangioleiomyomatosis. Am J Respir Crit Care Med. 2003;168(12):1427–31.
63. Cottin V, Harari S, Humbert M, Mal H, Dorfmuller P, Jais X, et al. Pulmonary hypertension in lymphangioleiomyomatosis: characteristics in 20 patients. Eur Respir J. 2012;40(3):630–40.
64. Freitas CSG, Baldi BG, Jardim C, Araujo MS, Sobral JB, Heiden GI, et al. Pulmonary hypertension in lymphangioleiomyomatosis: prevalence, severity and the role of carbon monoxide diffusion capacity as a screening method. Orphanet J Rare Dis. 2017;12(1):74.
65. Sonaglioni A, Baravelli M, Cassandro R, Torre O, Elia D, Anza C, et al. Hemodynamic mechanisms of exercise-induced pulmonary hypertension in patients with lymphangioleiomyomatosis: the role of exercise stress echocardiography. J Am Soc Echocardiogr. 2018;31(8):888–901.
66. Baldi BG, Albuquerque AL, Pimenta SP, Salge JM, Kairalla RA, Carvalho CR. Exercise performance and dynamic hyperinflation in lymphangioleiomyomatosis. Am J Respir Crit Care Med. 2012;186(4):341–8.
67. Aliverti A, Dellaca RL, Lotti P, Bertini S, Duranti R, Scano G, et al. Influence of expiratory flow-limitation during exercise on systemic oxygen delivery in humans. Eur J Appl Physiol. 2005;95(2–3):229–42.
68. Aliverti A, Macklem PT. Last word on point:counterpoint: the major limitation to exercise performance in COPD is 1) inadequate energy supply to the respiratory and locomotor muscles, 2) lower limb muscle dysfunction, 3) dynamic hyperinflation. J Appl Physiol (1985). 2008;105(2):763.
69. Zafar MA, McCormack FX, Rahman S, Tencza C, Wikenheiser-Brokamp KA, Young LR, et al. Pulmonary vascular shunts in exercise-intolerant patients with lymphangioleiomyomatosis. Am J Respir Crit Care Med. 2013;188(9):1167–70.
70. McCormack FX, Travis WD, Colby TV, Henske EP, Moss J. Lymphangioleiomyomatosis: calling it what it is: a low-grade, destructive, metastasizing neoplasm. Am J Respir Crit Care Med. 2012;186(12):1210–2.
71. Verwer EE, Kavanagh TR, Mischler WJ, Feng Y, Takahashi K, Wang S, et al. [(18)F]Fluorocholine and [(18)F]Fluoroacetate PET as imaging biomarkers to assess phosphatidylcholine and mitochondrial metabolism in preclinical models of TSC and LAM. Clin Cancer Res. 2018;24:5925–38.
72. Cui Y, Steagall WK, Lamattina AM, Pacheco-Rodriguez G, Stylianou M, Kidambi P, et al. Aberrant SYK kinase signaling is essential for tumorigenesis induced by TSC2 inactivation. Cancer Res. 2017;77(6):1492–502.
73. Liu HJ, Lizotte PH, Du H, Speranza MC, Lam HC, Vaughan S, et al. TSC2-deficient tumors have evidence of T cell exhaustion and respond to anti-PD-1/anti-CTLA-4 immunotherapy. JCI Insight. 2018;3(8):98674.
74. Maisel K, Merrilees MJ, Atochina-Vasserman EN, Lian L, Obraztsova K, Rue R, et al. Immune checkpoint ligand PD-L1 is upregulated in pulmonary lymphangioleiomyomatosis (LAM). Am J Respir Cell Mol Biol. 2018;59:723–32.
75. Yu J, Astrinidis A, Howard S, Henske EP. Estradiol and tamoxifen stimulate LAM-associated angiomyolipoma cell growth and activate both genomic and nongenomic signaling pathways. Am J Physiol Lung Cell Mol Physiol. 2004;286(4):L694–700.

76. Howe SR, Gottardis MM, Everitt JI, Goldsworthy TL, Wolf DC, Walker C. Rodent model of reproductive tract leiomyomata. Establishment and characterization of tumor-derived cell lines. Am J Pathol. 1995;146(6):1568–79.
77. Parkhitko AA, Priolo C, Coloff JL, Yun J, Wu JJ, Mizumura K, et al. Autophagy-dependent metabolic reprogramming sensitizes TSC2-deficient cells to the antimetabolite 6-aminonicotinamide. Mol Cancer Res. 2014;12(1):48–57.
78. Atochina-Vasserman EN, Abramova E, James ML, Rue R, Liu AY, Ersumo NT, et al. Pharmacological targeting of VEGFR signaling with axitinib inhibits Tsc2-null lesion growth in the mouse model of lymphangioleiomyomatosis. Am J Physiol Lung Cell Mol Physiol. 2015;309(12):L1447–54.
79. Li C, Liu X, Liu Y, Zhang E, Medepalli K, Masuda K, et al. Tuberin regulates prostaglandin receptor-mediated viability, via Rheb, in mTORC1-hyperactive cells. Mol Cancer Res. 2017;15(10):1318–30.
80. Goncharova EA, Goncharov DA, Fehrenbach M, Khavin I, Ducka B, Hino O, et al. Prevention of alveolar destruction and airspace enlargement in a mouse model of pulmonary lymphangioleiomyomatosis (LAM). Sci Transl Med. 2012;4(154):154ra34.
81. Kwiatkowski DJ. Animal models of lymphangioleiomyomatosis (LAM) and tuberous sclerosis complex (TSC). Lymphat Res Biol. 2010;8(1):51–7.
82. Klover PJ, Thangapazham RL, Kato J, Wang JA, Anderson SA, Hoffmann V, et al. Tsc2 disruption in mesenchymal progenitors results in tumors with vascular anomalies overexpressing Lgals3. elife. 2017;6:e23202.
83. Ren S, Luo Y, Chen H, Warburton D, Lam HC, Wang LL, et al. Inactivation of Tsc2 in mesoderm-derived cells causes polycystic kidney lesions and impairs lung alveolarization. Am J Pathol. 2016;186(12):3261–72.
84. Prizant H, Taya M, Lerman I, Light A, Sen A, Mitra S, et al. Estrogen maintains myometrial tumors in a lymphangioleiomyomatosis model. Endocr Relat Cancer. 2016;23(4):265–80.
85. Ma A, Wang L, Gao Y, Chang Z, Peng H, Zeng N, et al. Tsc1 deficiency-mediated mTOR hyperactivation in vascular endothelial cells causes angiogenesis defects and embryonic lethality. Hum Mol Genet. 2014;23(3):693–705.
86. Houssaini A, Breau M, Kebe K, Abid S, Marcos E, Lipskaia L, et al. mTOR pathway activation drives lung cell senescence and emphysema. JCI Insight. 2018;3(3):93203.
87. Houssaini A, Abid S, Derumeaux G, Wan F, Parpaleix A, Rideau D, et al. Selective tuberous sclerosis complex 1 gene deletion in smooth muscle activates mammalian target of rapamycin signaling and induces pulmonary hypertension. Am J Respir Cell Mol Biol. 2016;55(3):352–67.
88. Wang Y, Liu J, Zhou JS, Huang HQ, Li ZY, Xu XC, et al. MTOR suppresses cigarette smoke-induced epithelial cell death and airway inflammation in chronic obstructive pulmonary disease. J Immunol. 2018;200(8):2571–80.
89. Nijmeh J, El-Chemaly S, Henske EP. Emerging biomarkers of lymphangioleiomyomatosis. Expert Rev Respir Med. 2018;12(2):95–102.

Chapter 6
Smoking-Induced Diffuse Cystic Lung Diseases

Jie Zhang, Christian W. Cox, and Robert Vassallo

Introduction

Cigarette smoke is a complex mixture of more than 4000 chemicals, many of which exert toxic effects on cellular function. In addition to chronic obstructive pulmonary disease (COPD) and cancer, cigarette smokers may develop diffuse interstitial and bronchiolar disorders [1–4]. These diffuse lung diseases are referred to as "smoking-related interstitial lung diseases," a term that recognizes the causal association with cigarette smoking. Several of the cigarette smoking-induced diffuse lung diseases are associated with pulmonary parenchymal cystic change. This chapter focuses on the mechanisms of cigarette smoking-induced cystic lung disease development and clinical characterization and management of smoking-induced cystic lung disease.

Cigarette Smoking and Cystic Lung Disease

While emphysematous changes are very common in smokers – even in asymptomatic cigarette smokers undergoing lung cancer screening chest computed tomography (CT) imaging – the identification of true lung cysts on imaging studies is not a frequent clinical observation. Lung cysts are air-filled lucencies (low attenuation

J. Zhang
Division of Pulmonary and Critical Care Medicine, Department of Medicine, Mayo Clinic College of Medicine and Science, Rochester, MN, USA

C. W. Cox
Department of Radiology, Mayo Clinic, Rochester, MN, USA
e-mail: cox.christian@mayo.edu

R. Vassallo (✉)
Department of Medicine, Mayo Clinic, Rochester, MN, USA
e-mail: Vassallo.Robert@mayo.edu

N. Gupta et al. (eds.), *Diffuse Cystic Lung Diseases*, Respiratory Medicine,
https://doi.org/10.1007/978-3-030-63365-3_6

area on imaging) that may be distinguished from emphysematous changes by the finding of a distinct (usually thin) wall surrounding the area of low attenuation. Radiological cystic changes in smokers will most commonly be observed in individuals with pulmonary Langerhans cell histiocytosis (PLCH), and rarely in desquamative interstitial pneumonia (DIP) [1–5]. Although not directly causative, cigarette smoking is also a risk factor for the development of idiopathic pulmonary fibrosis (IPF) [6], combined pulmonary fibrosis and emphysema (CPFE), and rheumatoid arthritis–associated diffuse lung disease [7, 8]; in these diffuse lung diseases, lung cysts may occasionally be appreciated although usually these "cyst like" abnormalities may also represent dilated airways rather than true lung cysts. Cystic lung disease may also occur in the context of cigarette smoking-induced airspace enlargement with fibrosis (AEF), as well as in some cases of tobacco-induced lung cancers originating in lung cysts [9]. Although the cigarette smoking-induced cystic lung diseases can all occur as distinct clinical/pathological entities, it is now well recognized that overlapping features may occur on both lung biopsy and chest imaging [10]. The occurrence of overlapping features of cigarette smoking-induced injury patterns reinforces the contention that these are patterns of injury associated with a common cause – cigarette smoke – that may affect an individual person in different ways. Similarly, most patients with smoking-induced cystic lung disease will have some evidence of emphysematous change, either on lung biopsy or imaging, again affirming the central role of smoking in the causation of multiple patterns of injury in the same patient.

Mechanisms by Which Tobacco Causes Cystic Lung Disease

In smokers without clinical lung disease, cigarette smoking induces inflammatory cell recruitment to small airways, consisting primarily of macrophages, neutrophils, and other immune cells [11, 12]. Although all smokers experience some degree of inflammation in small airways, as reported in autopsy studies performed on smokers without clinically evident lung disease [13], only a very small proportion develop clinically significant diffuse lung disease. The relative rarity of smoking-induced diffuse lung diseases compared to the overall prevalence of cigarette smoking suggests that cigarette smoke is only one factor responsible for the induction of these diseases, and implies that additional factors (endogenous such as genetic factors or exogenous such as infectious pathogens or allergens) are required for the induction of disease.

A characteristic morphologic feature of all smoking-related diffuse cystic lung diseases is prominent peribronchiolar inflammation [10, 14–16]. In addition, histopathological studies demonstrate increased macrophages and myeloid cells in the interstitium, airways, and alveolar spaces [14, 15, 17]. Specific mechanisms by which macrophage accumulation occurs in these conditions are not fully defined, but likely involve an increased production of macrophage recruiting and differentiating factors by airway and alveolar epithelial cells, enhanced macrophage

survival, as well as diminished apoptosis of recruited myeloid cells and macrophages [18]. In these patients, lung epithelial cells may play an important role in the inflammatory response to cigarette smoke by producing cytokines such as granulocyte-macrophage colony stimulating factor (GM-CSF), which provides proliferative and activation signals to both macrophages and dendritic cells [19, 20]. Cigarette smoke extracts have also been reported to induce transforming growth factor-beta (TGF-β) production by lung epithelial cells [21, 22]. The induction of TGF-β release is likely to be very important in immune modulation, as well as tissue remodeling and fibrosis in the airways and potentially also in the distal lung parenchyma [21]. Cigarette smoke also activates epithelial cells and macrophages to produce chemokine ligand 20 (CCL20 or Macrophage Inflammatory Protein-3 alpha) [23], tumor necrosis factor-a (TNF-α) [24], and osteopontin [25] that promote recruitment, retention, and activation of inflammatory cells, including dendritic cells.

Cigarette smoking can also directly induce abnormalities in immune cells that may be relevant to the pathogenesis of smoking-related cystic lung diseases [26–28]. Certain cigarette smoke constituents are known to activate macrophages, neutrophils, and dendritic cells in vitro, promoting generation of chemokines and cytokines that sustain local inflammation [24, 29]. It is likely that in smokers who develop diffuse lung disease, an amplified inflammatory cascade occurs within the lung that is associated with activation of multiple immune cell types, eventually leading to a chronic cycle of inflammation, further inflammatory cell recruitment, and eventually tissue remodeling and cystic change. It is possible that a secondary insult such as viral infection, other infectious processes, aspiration in the context of gastro-esophageal reflux disease, or other mechanisms of lung injury may precipitate further inflammation and airway injury that heals by fibrosis and subsequent architectural distortion, ultimately leading to cystic change. Matrix metalloproteinases (MMPs) produced by infiltrating monocytoid and myeloid cells in inflammatory nodules may play a key role in the airway remodeling and bronchiolar destruction [30]. Tissue immunohistochemical studies on PLCH biopsies have shown strong reactivity to MMP2 and MMP9, particularly in the lesional dendritic cells and macrophages, suggesting a potential direct role for these cells in local airway remodeling [31].

The anatomic reasons behind the development of cystic change in smoking-related diffuse lung diseases are still not fully appreciated, but insight has been generated on this from three-dimensional studies performed on PLCH [32]. Through study of serial histological sections of 36 lesions captured in 12 surgical specimens, Kambouchner and colleagues [32] showed that PLCH lesions center on airway lumens, and are propagated in a continuous fashion proximally and distally with the potential to involve branching bronchioles to the level of alveolar ducts. This airway-centered nature of the lesion fits very well with the link to chronic inhalation of tobacco smoke as the primary disease-inducing agent. Kambouchner and coworkers [32] showed that cavities within PLCH nodules represent airway lumens that enlarge as a result of inflammation and fibrosis of bronchiole walls. The subsequent cystic spaces that develop and progress over time, actually represent areas of

air trapping. Indeed, the observation that some of these cysts may actually shrink in size and "decompress" following chemotherapy of PLCH [33] provides additional proof that these localized areas of cystic air trapping may result from persistent small airway inflammation, which may be sufficiently improved by therapy so as to allow decompression of some of the cystic spaces.

Specific Tobacco-Induced Cystic Lung Diseases

Pulmonary Langerhans Cell Histiocytosis

Pulmonary Langerhans cell Histiocytosis (PLCH) is induced by cigarette smoke exposure in >90% of patients, and is one of the primary conditions to be considered in the evaluation of cystic lung disease, particularly in smokers [5, 15]. PLCH is an inflammatory myeloid cell neoplasm with varied biologic behavior and is characterized by accumulation of myeloid cells predominantly in peribronchiolar regions as well as other lung compartments [34]. These myeloid cells share immunohistochemical and morphological features similar to certain specific dendritic cells subtypes, namely, epithelial-associated Langerhans cells [35, 36]. Adult PLCH forms part of the histiocytic disease spectrum, which ranges from relatively benign processes such as unifocal LCH involving bone (eosinophilic granuloma) to disseminated variants associated with severe organ dysfunction [37]. PLCH is the most common of the smoking-related diffuse lung diseases, representing around 5% of the total number of diffuse lung diseases diagnosed by lung biopsy [38]. The disease usually affects young individuals in their third and fourth decades and occurs in men and women in equal proportion [5].

The overwhelming majority of adults with PLCH describe a history of active smoking or significant second-hand smoke exposure [2, 15, 38, 39]. While the pathogenesis remains incompletely understood, it is likely that cigarette smoke activates airway epithelial cells and other resident lung cells to produce cytokines that promote recruitment, activation, and retention of Langerhans-like myeloid cells in subepithelial regions of the airways [19, 20, 40]. Cigarette smoke also induces the production of cytokines with profibrotic functions, like TGF-β; this and other inflammatory mediators like GM-CSF may further promote local expansion and enhance survival of these myeloid cells. In addition, these factors may promote tissue remodeling and fibrosis, which is evident in more advanced cases [41]. The persistence of these activated myeloid cells, in the absence of overt infection or other stimulus, is likely an important mechanism by which persistent inflammation occurs and subsequent recruitment of other inflammatory cells such as T cells, plasma cells, and eosinophils, occurs. This results in inflammatory nodular lesions and the characteristic granulomatous-like inflammation (hence, the previous term "eosinophilic granuloma").

While the pathogenesis of PLCH is not fully understood, the recent identification of specific mutations in a substantial proportion of LCH and PLCH biopsies have greatly improved the understanding and biologic characterization of these histiocytic disorders. A specific mutation in the BRAF gene – the $BRAF^{V600E}$ mutation – has been described in various malignancies including melanoma, as well as some types of lung adenocarcinoma, and results in constitutive activation of the mitogen activated protein kinase (MAPK) pathway, which regulates cell differentiation and survival [34]. The $BRAF^{V600E}$ mutation occurs in 35–50% of PLCH, and at least half of systemic LCH lesions [42–45]. Recent studies also show that other members of the MAPK pathway are activated in LCH, even in the absence of $BRAF^{V600E}$ mutations, suggesting that other alterations of the MAPK pathway are involved in the pathogenesis of LCH [43].

The presenting symptoms of PLCH are nonspecific; primarily dry cough and shortness of breath, while a third of patients are asymptomatic at the time of clinical presentation and are incidentally identified on the basis of chest imaging performed for other clinical indications [5]. Constitutional symptoms occur in approximately 20–30%, while 10–20% may present with a spontaneous pneumothorax [5, 46]. Occasionally, patients will come to clinical attention because of symptoms related to skin, lymph node, or bony involvement. Pulmonary function tests may show obstructive, restrictive, mixed, or nonspecific abnormalities; pulmonary function testing may also be completely normal [5]. Physiological studies reveal limitations in exercise capacity that can occur even with relatively normal resting pulmonary function. Exercise limitation correlates with markers of pulmonary vascular dysfunction, implying vascular involvement rather than ventilatory impairment as a primary cause of exercise limitation [47].

The chest radiograph is abnormal but usually nonspecific [48]. Chest CT is essential for diagnostic evaluation and may show cystic or nodular changes or a mixture of both (Fig. 6.1). In some patients, the CT scan shows a combination of cystic and nodular lesions with prominent involvement of the mid and upper lung fields and relative sparing of the bases. In more advanced cases, but also in some patients with relatively early disease, nodular abnormalities may be minimal or absent and only cystic changes may be observed [48, 49]. Definitive diagnosis requires histopathologic confirmation by biopsy. Video-assisted thoracoscopic surgery (VATS)-guided lung biopsy is the gold standard modality for obtaining lung biopsy in patients with suspected PLCH. Bronchoscopy with transbronchial forceps biopsy may be diagnostic in up to 50% of patients, while the identification of ≥5% CD1a-positive cells on the BAL fluid may be diagnostic, although the sensitivity of this test is poor [50–54]. Bronchoscopy with transbronchial cryobiopsy is a relatively new technique that will likely have a higher diagnostic yield as compared to traditional forceps-guided transbronchial lung biopsies given the bronchiolocentric location of the lesions in PLCH. However, the safety and exact diagnostic yield of this procedure in patients with suspected PLCH remains to be systematically investigated. In centers with expertise with this technique, it may be reasonable to perform transbronchial cryobiopsy in patients with suspected PLCH, prior to performing surgical lung biopsy.

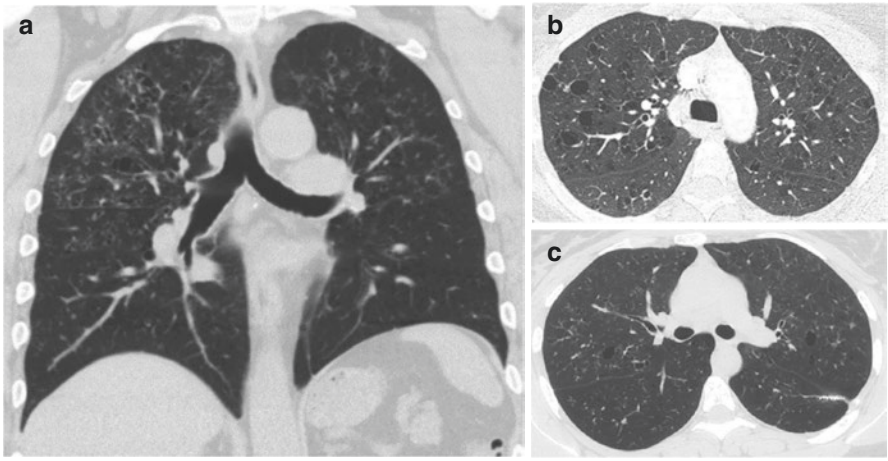

Fig. 6.1 (**a**) Coronal section from a 39-year-old smoker with biopsy proven PLCH. Note sparing of the lower lobes and upper lobe predominance of lung cysts. (**b**) Representative chest CT image from a 33-year-old smoker with PLCH showing bilateral upper lobe cystic lesions of varying sizes. (**c**) A 30-year-old smoker with biopsy proven PLCH (note surgical lung biopsy scar on left) showing discrete cystic change in both upper lobes

Histological features of early PLCH include loosely formed nodules of mixed inflammatory cells around small airways in a bronchiolocentric pattern [14]. These bronchiolocentric lesions form symmetric stellate lesions with central scarring [55]. Infiltrating "Langerhans-like" myeloid cells are abundant in early lesions and may be identified by immunohistochemical staining for CD1a or Langerin [15, 51, 55, 56]. Eosinophilic infiltration is often encountered, and may be quite extensive [15, 51, 55, 56]. Varying degrees of interstitial infiltration with macrophages, lymphocytes, and eosinophils may also be noted, and in some cases, an extensive desquamative interstitial pneumonia (DIP)-like reaction has been described [14]. Some cases are associated with extensive vascular infiltration of inflammatory cells, resulting in a proliferative vasculopathy that may involve both arteries and veins [57, 58].

The management of patients with PLCH should be individualized. All patients should undergo testing for the $BRAF^{V600E}$ mutation and other MAPK mutations by immunostaining of available biopsy tissue or gene sequencing. Many patients with mild disease or minimal symptoms do not require specific therapy other than smoking cessation and longitudinal follow-up with pulmonary function testing and chest imaging. Smoking cessation is critical for all smokers with PLCH and may be sufficient for disease remission and stabilization, particularly for individuals with milder forms of disease and with preserved lung function [5, 59–61]. A proportion of patients will require specific therapy with a trial of chemotherapy or other agents [5]. There are no biological markers to predict which patient will improve

and who will progress despite smoking cessation. The prognostic significance of $BRAF^{V600E}$ mutation status on long-term prognosis or likelihood of disease progression in adults has not been established. Although detection of specific mutations may have prognostic implications in childhood LCH, this has not been demonstrated in adult PLCH. The treatment plan should be individualized with consideration of the extent and severity of pulmonary involvement, the ability of the patient to achieve and maintain abstinence from tobacco and other inhaled product use (e.g., e-cigarettes or inhalation of other respiratory irritants such as marijuana), and patient preferences.

For patients with minimal symptoms and limited disease, observation and follow-up with longitudinal pulmonary function testing and smoking cessation may be sufficient. For symptomatic patients with more significant lung involvement, particularly if a decline in lung function is noted despite smoking cessation, systemic pharmacotherapy should be considered. Corticosteroids have historically been used to treat patients with severe or progressive disease despite a lack of supporting data [38]. Due to significant toxicity associated with high dose corticosteroid therapy and the relative lack of efficacy of this treatment, we currently do not employ corticosteroid therapy as first-line therapy. Several other immunosuppressive and chemotherapy agents have been proposed, namely, vinblastine, chlorodeoxyadenosine (also known as 2-CDA) [62], cyclophosphamide, and methotrexate [38]. Data regarding the efficacy of these agents are limited. Chlorodeoxyadenosine is effective in the management of multi-system LCH involving bone and skin with good success, and there is evidence from small case series that it may also be effective in the management of PLCH, including patients with predominantly cystic disease [62, 63]. The recognition that the vast majority of patients with PLCH have genetic mutations in the MAPK pathway, particularly $BRAF^{V600E}$, implies the potential that some patients with progressive disease and positive mutation status would benefit from targeted therapy aimed at BRAF inhibition (in patients harboring $BRAF^{V600E}$ mutation) or MEK inhibition (in patients with non-BRAF MAPK mutations). Indeed, recent reports suggest that treatment with either BRAF or MEK inhibitor therapy may be effective in progressive cases [64, 65].

Treatment of PLCH also includes management of specific complications and sequelae such as recurrent pneumothorax, pulmonary hypertension, and progressive respiratory failure [5, 35, 46, 57]. Pleurodesis should be considered for most patients with a spontaneous pneumothorax, since the recurrence rate of pneumothorax with conservative measures is high [46]. Pulmonary hypertension is another important complication [38, 57]. Overall, most patients seem to have a relatively good prognosis, particularly if smoking cessation is achieved. Some individuals may progress to extensive pulmonary scarring and emphysematous changes leading to respiratory failure [17, 38]. Lung transplant is an option with advanced PLCH. The overall survival with lung transplant is comparable to that of individuals with other indications for lung transplants [66–68].

Desquamative Interstitial Pneumonia

Desquamative interstitial pneumonia (DIP) is a primary disorder of macrophage accumulation in alveolar spaces [69] and is associated with cigarette smoking in at least two-thirds of cases [4, 70, 71]. It has also been described in the context of autoimmune diseases [72], certain infections [73], and as a drug-induced lung reaction [73, 74]. The exact pathogenesis of DIP is not well established, but a recent murine study has implicated increased GM-CSF signaling, driven by multiple external stimuli such as cigarette smoke exposure, to be a major driver of the development of DIP [75]. The clinical presentation is nonspecific, and physical examination may reveal inspiratory crackles and digital clubbing [4]. Pulmonary function testing reveals restriction in one-third of cases, normal findings in 10–20%, and a mixed defect in the remainder [4]. The lesion of respiratory bronchiolitis (RB), which is universally present on lung biopsies from cigarette smokers, represents the opposite end of the spectrum with macrophage accumulation primarily evident in respiratory bronchioles with significantly less macrophage accumulation in alveolar spaces as is more typical in DIP.

The chest radiograph shows patchy ground-glass attenuation with lower zone predominance or nonspecific linear patterns in most patients [76]. The principal abnormalities on chest high-resolution computed tomography (HRCT) include ground-glass opacities especially in the lower lung zones [77]. Irregular linear opacities and reticular patterns are frequent; however, honeycombing and significant architectural distortion are uncommon. A highly characteristic feature of DIP is the presence of small intraparenchymal cysts, often within the areas of ground-glass opacity, that can generally be distinguished from honeycombing because of their distribution within the lung parenchyma as opposed to the lung periphery (Fig. 6.2) [78]. In some instances, patients with biopsy proven DIP have been reported to develop HRCT characteristics suggestive of fibrotic nonspecific interstitial pneumonia (NSIP) following longitudinal follow-up [3].

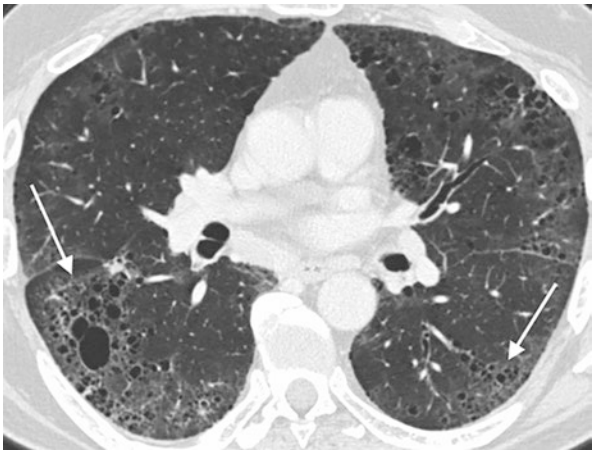

Fig. 6.2 Axial high-resolution CT image in lung window at the level of the right ventricular outflow tract of a middle-aged male smoker demonstrating intra parenchymal cystic changes in biopsy proven desquamative interstitial pneumonia (DIP). Note areas of mixed ground-glass and small cysts tracking along bronchovascular bundles (*white arrows*) in the lower lobes, characteristic of DIP

On light microscopy, lung biopsies show characteristic filling of alveolar spaces with pigmented alveolar macrophages [71]. While both respiratory bronchiolitis (RB) and DIP are associated with the accumulation of pigmented macrophages in alveolar spaces, the distribution of macrophage accumulation in RB is more bronchiolocentric and patchy, whereas in DIP it tends to be more diffuse and lacks bronchiolocentricity [10]. The extents of interstitial fibrosis, lymphoid follicles, and eosinophilic infiltration have been reported to be more prevalent in DIP than respiratory bronchiolitis-interstitial lung disease (RB-ILD) [70, 71]. Fibroblastic foci are very rarely reported, and the DIP lesion is temporally uniform [55].

Since many DIP patients are smokers, smoking cessation is an essential component of therapy. Prolonged remission of DIP after smoking cessation has also been described, but like all other smoking-related diffuse lung diseases, the effect of smoking cessation on the natural history of DIP remains poorly defined [79]. While most DIP patients have a good prognosis [80], some patients do progress to respiratory failure and premature death within 5–10 years of diagnosis [71]. Patients with DIP are frequently treated with corticosteroids, but the success with steroids is inconsistent and has not been subjected to prospective study [4]. Other immunosuppressants such as azathioprine and methotrexate have been used in anecdotal cases [81]. Lung transplant is an option for patients with progressive disease [82]. DIP can recur in the transplanted lung [83].

Airspace Enlargement with Fibrosis and Combined Pulmonary Fibrosis and Emphysema

The occurrence of lung cysts in airspace enlargement with fibrosis was nicely described in a study by Kawabata and colleagues [84], who used a large number of resected lung cancer specimens to determine histological changes more prevalent in smokers, and subsequently carefully defined the morphological attributes and correlates associated with this lesion. In that study, histopathological material from patients who had undergone lobectomy or pneumonectomy for lung cancer was reviewed, and correlations were performed between histopathological findings and smoking index (a measure of whether patients were mild, moderate, or heavy smokers). The lesion of airspace enlargement with fibrosis was noted in only 0.4% of nonsmokers, and was much more prevalent in smokers and particularly in the lobectomy specimens resected from heavy smokers (the frequency of air space enlargement with fibrosis in that study was reported as 0.4% in nonsmokers, 6.5% in mild smokers who reported smoking <25 cigarettes daily, while 21.1% of specimens from individuals who smoked >50 cigarettes daily) [84]. The cystic imaging characteristics of airspace enlargement with fibrosis have been reported in the context of this pathological lesion occurring either as a single entity, or else in association with usual interstitial pneumonia [84]. The characteristic radiologic feature of airspace

enlargement with fibrosis is the presence of multiple thin-walled cysts associated with elements of pulmonary fibrosis. The exact significance of these lesions, and distinguishing these thin-walled cysts in smokers from interstitial lung abnormalities that have been otherwise described as subclinical or asymptomatic abnormalities detected in smokers undergoing screening CT scans [85], is not clear at this time.

The term "airspace enlargement with fibrosis" is synonymous with "smoking-related interstitial fibrosis" (SRIF), which was a descriptive term first suggested by Katzenstein [86] to describe a relatively common fibrotic lesion seen exclusively in current or former smokers. Since that original description, other authors have proposed alternative names such as "RB with fibrosis," which sometimes results in confusion. The term "airspace enlargement with fibrosis" is useful because it is descriptive, does not limit this entity as being solely representative of a cigarette smoke-induced lung injury (even though most individuals with this injury will be cigarette smokers), and recognizes the fact that it may be seen in the context of pneumoconiosis or other inhalational injuries.

Histologically the lesion of airspace enlargement with fibrosis is characterized by fibrosis in the interstitial spaces with resultant remodeling, areas of emphysema, predilection to bronchiolocentric distribution, and relative absence of fibroblastic foci [84, 86]. On gross pathology, airspace enlargement with fibrosis is associated with thin-walled cysts that may be appreciated visually in lobectomy specimens. The chest CT appearance typically reveals multiple thin-walled cysts or conglomerates of cystic change along the periphery of the lung associated with focal findings of fibrosis such as architectural distortion, septal thickening, and reticulation (Fig. 6.3) [87].

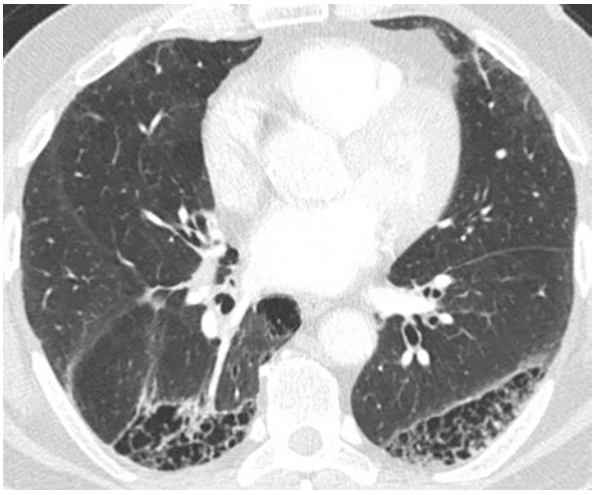

Fig. 6.3 Axial high-resolution CT image in lung window at the level of the inferior pulmonary veins in a 67-year-old male smoker demonstrating focal airspace enlargement and fibrosis (AEF) along the posterior peripheral lower lobe

It is now well appreciated that emphysema and fibrotic interstitial lung disease may coexist in the same patient; this is a clinical entity that has been given the term "combined pulmonary fibrosis and emphysema" (CPFE) [88]. This entity may occur also in individuals with autoimmune diseases such as rheumatoid arthritis, which is also more prevalent in cigarette smokers. Patients with CPFE represent a subgroup of interstitial lung disease characterized by preservation of lung volumes and disproportionate reduction in diffusing capacity of the lung for carbon monoxide (DLCO). Indeed the occurrence of both emphysema and fibrosis in the same individual reinforces the pathogenetic role of cigarette smoke as a factor that can induce both lesions. Both thin- and thick-walled cystic lesions have been described on imaging as well as histopathological sections of CPFE (Fig. 6.4). In a recent study, cystic lesions were observed in more than two-thirds of the CPFE population [89]. Whether these cystic areas represent emphysema and associated cicatricial change, or whether these represent areas of airspace enlargement with fibrosis scattered throughout emphysematous lung is not entirely clear. The diagnosis of CPFE may be challenging especially since pulmonary function tests often show preserved or slightly reduced lung volumes. In this context, the identification of velcro-like crackles on the pulmonary physical examination may be a critical clue indicating the potential for underlying fibrotic interstitial lung disease. A chest CT scan with high-resolution images is mandatory when this diagnosis is suspected. The management of CPFE patients is challenging as antifibrotic agents that are approved for the treatment of idiopathic pulmonary fibrosis have not been systematically evaluated in CPFE. Management is also challenged by the frequent occurrence of pulmonary hypertension that may be severe [89].

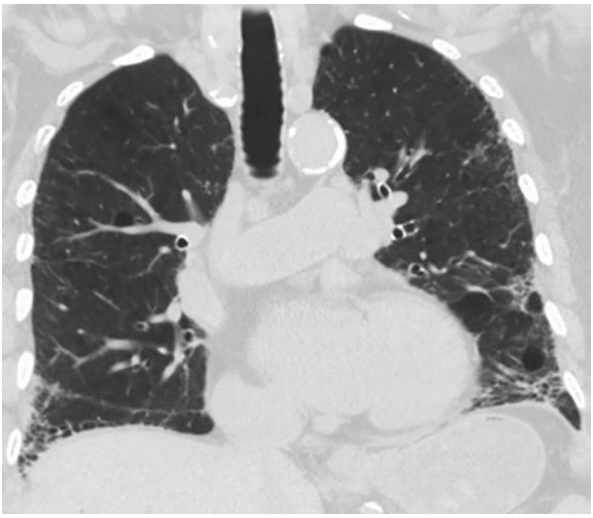

Fig. 6.4 Coronal section from a 70-year-old patient with combined pulmonary fibrosis and emphysema (CPFE) demonstrating areas of well-defined cystic change

Lung Cysts Associated with Lung Cancer in Smokers

Lung cysts have been reported in smokers with lung cancer [90, 91]. Insight into the natural history of lung cancer associated with cystic lung lesions in current or former smokers was recently provided in a study that identified nearly 3000 patients with non small cell lung cancer [90]. From this relatively large cohort of cancer patients, cystic lesions were identified in or adjacent to the primary lung cancer in 30 cases (corresponding to 1% of all of the cancer cases). Some of the lung cysts occurred in otherwise normal appearing lung. Only one individual in this cohort did not have a history of tobacco use. Over time, 20 of the reported 30 cases demonstrated increased soft tissue density in the cystic regions due to wall thickening of the cysts or increased loculations [90]. Histopathological analysis showed the presence of a check-valve mechanism involving the small airways and leading to outflow obstruction in many cases [90]. Although uncommon, the recognition that cystic lesions in smokers – particularly smokers with radiographic emphysema – may represent malignancy is important to recognize. Few studies have examined the natural history of these lesions. Fluorodeoxyglucose (FDG)-positron emission tomography (PET) may be helpful in further characterization of these lesions only if there is an associated solid component measuring >7 mm associated with the cystic lesion. In the study by Fintelmann et al. [90], some of the reported cystic cancers were preceded by a subcentimeter nodule. While specific guidelines for follow-up of indeterminate solitary cysts in smokers do not exist, in consideration of the occasional occurrence of malignancy, it is recommended that identification of a distinct solitary cyst or cluster of cysts in a smoker, particularly if accompanied by emphysema, should be followed up over time by imaging to exclude the possibility of a malignancy (Fig. 6.5).

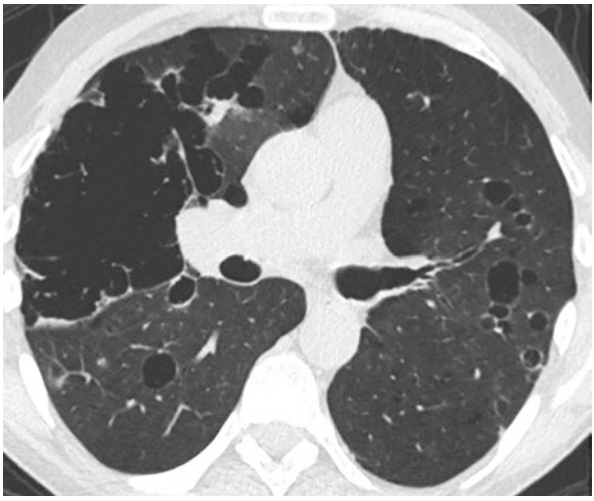

Fig. 6.5 Axial high-resolution CT image in lung window at the level of the main pulmonary artery in a 54-year-old male smoker demonstrating bilateral but right upper lobe predominant thin-walled cysts from metastatic adenocarcinoma. Some focal areas of cyst wall thickening are present with a more focal solid nodular component in the central right upper lobe

Other Smoking-Induced Diffuse Lung Diseases That May Be Associated with Cystic Change

Cigarette smoking has also been reported as the solitary etiologic factor causing diffuse cystic lung disease with imaging features that are indistinguishable from other diffuse cystic lung diseases. Gupta et al. [92] reported a series of four patients referred for evaluation and management of suspected lymphangioleiomyomatosis based on imaging characteristics. All four patients underwent lung biopsy with histopathological findings demonstrating focal alveolar destruction and chronic bronchiolitis but without diagnostic features of any other known causes of diffuse cystic lung diseases.

Key Learning Points

- Cigarette smoke exposure can lead to a variety of pulmonary diseases that can manifest as diffuse cystic lung disease on chest radiology; pulmonary Langerhans cell histiocytosis (PLCH) is the most common diffuse cystic lung disease associated with exposure to cigarette smoke.
- Mutations in the MAPK pathway, especially $BRAF_{V600E}$, in patients with PLCH have classified PLCH as an inflammatory myeloid neoplasm.
- Typical HRCT findings of PLCH include upper lobe predominant bronchiolocentric nodules, cavities, and cysts. The cysts in PLCH have a characteristic radiological appearance, are often irregular and bizarre shaped, spare the costophrenic sulci, and may be sufficient to establish a clinical diagnosis of PLCH in some instances.
- Definitive diagnosis of PLCH requires histopathological confirmation, usually by VATS-guided lung biopsy. Typical histopathological features of PLCH include the demonstration of CD1a-positive dendritic cells centered around the bronchioles admixed with a variety of other immune cells including lymphocytes, neutrophils, and eosinophils.
- Smoking cessation is of paramount importance in the management of patients with PLCH, and may lead to disease stabilization and/or regression without any other pharmacotherapy.
- Patients with PLCH should be closely followed with serial pulmonary function tests in order to select candidates that might require pharmacotherapy beyond smoking cessation alone.

Conflict of Interest The authors have no conflict of interest or any disclosures relevant to this publication. All authors have directly contributed to the content of this book chapter and reviewed the final version.

References

1. Fraig M, Shreesha U, Savici D, Katzenstein AL. Respiratory bronchiolitis: a clinicopathologic study in current smokers, ex-smokers, and never-smokers. Am J Surg Pathol. 2002;26(5):647–53.
2. Friedman PJ, Liebow AA, Sokoloff J. Eosinophilic granuloma of lung. Clinical aspects of primary histiocytosis in the adult. Medicine (Baltimore). 1981;60(6):385–96.
3. Ryu JH, Colby TV, Hartman TE, Vassallo R. Smoking-related interstitial lung diseases: a concise review. Eur Respir J. 2001;17(1):122–32.
4. Ryu JH, Myers JL, Capizzi SA, Douglas WW, Vassallo R, Decker PA. Desquamative interstitial pneumonia and respiratory bronchiolitis-associated interstitial lung disease. Chest. 2005;127(1):178–84.
5. Vassallo R, Ryu JH, Schroeder DR, Decker PA, Limper AH. Clinical outcomes of pulmonary Langerhans'-cell histiocytosis in adults. N Engl J Med. 2002;346(7):484–90.
6. Miyake Y, Sasaki S, Yokoyama T, Chida K, Azuma A, Suda T, et al. Occupational and environmental factors and idiopathic pulmonary fibrosis in Japan. Ann Occup Hyg. 2005;49(3):259–65.
7. Saag KG, Kolluri S, Koehnke RK, Georgou TA, Rachow JW, Hunninghake GW, et al. Rheumatoid arthritis lung disease. Determinants of radiographic and physiologic abnormalities. Arthritis Rheum. 1996;39(10):1711–9.
8. Klareskog L, Stolt P, Lundberg K, Kallberg H, Bengtsson C, Grunewald J, et al. A new model for an etiology of rheumatoid arthritis: smoking may trigger HLA-DR (shared epitope)-restricted immune reactions to autoantigens modified by citrullination. Arthritis Rheum. 2006;54(1):38–46.
9. Wang X, Tao YX, Zhang M, Wu WB, Yang DP, Wang M. Solitary thin-walled cystic lung cancer with extensive extrapulmonary metastasis: a case report and review of the literature. Medicine (Baltimore). 2018;97(43):e12950.
10. Vassallo R, Jensen EA, Colby TV, Ryu JH, Douglas WW, Hartman TE, et al. The overlap between respiratory bronchiolitis and desquamative interstitial pneumonia in pulmonary Langerhans cell histiocytosis: high-resolution CT, histologic, and functional correlations. Chest. 2003;124(4):1199–205.
11. Kuschner WG, D'Alessandro A, Wong H, Blanc PD. Dose-dependent cigarette smoking-related inflammatory responses in healthy adults. Eur Respir J. 1996;9(10):1989–94.
12. Casolaro MA, Bernaudin JF, Saltini C, Ferrans VJ, Crystal RG. Accumulation of Langerhans' cells on the epithelial surface of the lower respiratory tract in normal subjects in association with cigarette smoking. Am Rev Respir Dis. 1988;137(2):406–11.
13. Niewoehner DE, Kleinerman J, Rice DB. Pathologic changes in the peripheral airways of young cigarette smokers. N Engl J Med. 1974;291(15):755–8.
14. Colby TV, Lombard C. Histiocytosis X in the lung. Hum Pathol. 1983;14(10):847–56.
15. Travis WD, Borok Z, Roum JH, Zhang J, Feuerstein I, Ferrans VJ, et al. Pulmonary Langerhans cell granulomatosis (histiocytosis X). A clinicopathologic study of 48 cases. Am J Surg Pathol. 1993;17(10):971–86.
16. Myers JL, Veal CF Jr, Shin MS, Katzenstein AL. Respiratory bronchiolitis causing interstitial lung disease. A clinicopathologic study of six cases. Am Rev Respir Dis. 1987;135(4):880–4.
17. Remy-Jardin M, Remy J, Gosselin B, Becette V, Edme JL. Lung parenchymal changes secondary to cigarette smoking: pathologic-CT correlations. Radiology. 1993;186(3):643–51.
18. Tomita K, Caramori G, Lim S, Ito K, Hanazawa T, Oates T, et al. Increased p21(CIP1/WAF1) and B cell lymphoma leukemia-x(L) expression and reduced apoptosis in alveolar macrophages from smokers. Am J Respir Crit Care Med. 2002;166(5):724–31.
19. Tazi A, Bonay M, Bergeron A, Grandsaigne M, Hance AJ, Soler P. Role of granulocyte-macrophage colony stimulating factor (GM-CSF) in the pathogenesis of adult pulmonary histiocytosis X. Thorax. 1996;51(6):611–4.
20. Tazi A, Bouchonnet F, Grandsaigne M, Boumsell L, Hance AJ, Soler P. Evidence that granulocyte macrophage-colony-stimulating factor regulates the distribution and differentiated

state of dendritic cells/Langerhans cells in human lung and lung cancers. J Clin Invest. 1993;91(2):566–76.
21. Wang RD, Wright JL, Churg A. Transforming growth factor-beta1 drives airway remodeling in cigarette smoke-exposed tracheal explants. Am J Respir Cell Mol Biol. 2005;33(4): 387–93.
22. Checa M, Hagood JS, Velazquez-Cruz R, Ruiz V, Garcia-De-Alba C, Rangel-Escareno C, et al. Cigarette smoke enhances the expression of profibrotic molecules in alveolar epithelial cells. PLoS One. 2016;11(3):e0150383.
23. Bracke KR, D'Hulst AI, Maes T, Moerloose KB, Demedts IK, Lebecque S, et al. Cigarette smoke-induced pulmonary inflammation and emphysema are attenuated in CCR6-deficient mice. J Immunol. 2006;177(7):4350–9.
24. Yang SR, Chida AS, Bauter MR, Shafiq N, Seweryniak K, Maggirwar SB, et al. Cigarette smoke induces proinflammatory cytokine release by activation of NF-kappaB and posttranslational modifications of histone deacetylase in macrophages. Am J Physiol. 2006;291(1):L46–57.
25. Allen CE, Li L, Peters TL, Leung HC, Yu A, Man TK, et al. Cell-specific gene expression in Langerhans cell histiocytosis lesions reveals a distinct profile compared with epidermal Langerhans cells. J Immunol. 2010;184(8):4557–67.
26. D'Hulst AI, Vermaelen KY, Brusselle GG, Joos GF, Pauwels RA. Time course of cigarette smoke-induced pulmonary inflammation in mice. Eur Respir J. 2005;26(2):204–13.
27. Vassallo R, Tamada K, Lau JS, Kroening PR, Chen L. Cigarette smoke extract suppresses human dendritic cell function leading to preferential induction of Th-2 priming. J Immunol. 2005;175(4):2684–91.
28. Lu LM, Zavitz CC, Chen B, Kianpour S, Wan Y, Stampfli MR. Cigarette smoke impairs NK cell-dependent tumor immune surveillance. J Immunol. 2007;178(2):936–43.
29. Kode A, Yang SR, Rahman I. Differential effects of cigarette smoke on oxidative stress and proinflammatory cytokine release in primary human airway epithelial cells and in a variety of transformed alveolar epithelial cells. Respir Res. 2006;7:132.
30. Hayashi T, Rush WL, Travis WD, Liotta LA, Stetler-Stevenson WG, Ferrans VJ. Immunohistochemical study of matrix metalloproteinases and their tissue inhibitors in pulmonary Langerhans' cell granulomatosis. Arch Pathol Lab Med. 1997;121(9):930–7.
31. Zyada MM. Expression of matrix metalloproteinase-9 and significance of a macrophage assay in eosinophilic granuloma. Ann Diagn Pathol. 2009;13(6):367–72.
32. Kambouchner M, Basset F, Marchal J, Uhl JF, Hance AJ, Soler P. Three-dimensional characterization of pathologic lesions in pulmonary langerhans cell histiocytosis. Am J Respir Crit Care Med. 2002;166(11):1483–90.
33. Lorillon G, Bergeron A, Detourmignies L, Jouneau S, Wallaert B, Frija J, et al. Cladribine is effective against cystic pulmonary Langerhans cell histiocytosis. Am J Respir Crit Care Med. 2012;186(9):930–2.
34. Vassallo R, Harari S, Tazi A. Current understanding and management of pulmonary Langerhans cell histiocytosis. Thorax. 2017;72(10):937–45.
35. Vassallo R, Ryu JH, Colby TV, Hartman T, Limper AH. Pulmonary Langerhans'-cell histiocytosis. N Engl J Med. 2000;342(26):1969–78.
36. Tazi A. Adult pulmonary Langerhans' cell histiocytosis. Eur Respir J. 2006;27(6):1272–85.
37. Favara BE, Feller AC, Pauli M, Jaffe ES, Weiss LM, Arico M, et al. Contemporary classification of histiocytic disorders. The WHO Committee on histiocytic/reticulum cell proliferations. Reclassification working group of the Histiocyte Society. Med Pediatr Oncol. 1997;29(3):157–66.
38. Chaowalit N, Pellikka PA, Decker PA, Aubry MC, Krowka MJ, Ryu JH, et al. Echocardiographic and clinical characteristics of pulmonary hypertension complicating pulmonary Langerhans cell histiocytosis. Mayo Clin Proc. 2004;79(10):1269–75.
39. Delobbe A, Durieu J, Duhamel A, Wallaert B. Determinants of survival in pulmonary Langerhans' cell granulomatosis (histiocytosis X). Groupe d'Etude en Pathologie Interstitielle de la Societe de Pathologie Thoracique du Nord. Eur Respir J. 1996;9(10):2002–6.

40. Aguayo SM, King TE Jr, Waldron JA Jr, Sherritt KM, Kane MA, Miller YE. Increased pulmonary neuroendocrine cells with bombesin-like immunoreactivity in adult patients with eosinophilic granuloma. J Clin Invest. 1990;86(3):838–44.
41. Asakura S, Colby TV, Limper AH. Tissue localization of transforming growth factor-beta1 in pulmonary eosinophilic granuloma. Am J Respir Crit Care Med. 1996;154(5):1525–30.
42. Yousem SA, Dacic S, Nikiforov YE, Nikiforova M. Pulmonary Langerhans cell histiocytosis: profiling of multifocal tumors using next-generation sequencing identifies concordant occurrence of BRAF V600E mutations. Chest. 2013;143(6):1679–84.
43. Mourah S, How-Kit A, Meignin V, Gossot D, Lorillon G, Bugnet E, et al. Recurrent NRAS mutations in pulmonary Langerhans cell histiocytosis. Eur Respir J. 2016;47(6):1785–96.
44. Alayed K, Medeiros LJ, Patel KP, Zuo Z, Li S, Verma S, et al. BRAF and MAP2K1 mutations in Langerhans cell histiocytosis: a study of 50 cases. Hum Pathol. 2016;52:61–7.
45. Roden AC, Hu X, Kip S, Parrilla Castellar ER, Rumilla KM, Vrana JA, et al. BRAF V600E expression in Langerhans cell histiocytosis: clinical and immunohistochemical study on 25 pulmonary and 54 extrapulmonary cases. Am J Surg Pathol. 2014;38(4):548–51.
46. Mendez JL, Nadrous HF, Vassallo R, Decker PA, Ryu JH. Pneumothorax in pulmonary Langerhans cell histiocytosis. Chest. 2004;125(3):1028–32.
47. Crausman RS, Jennings CA, Tuder RM, Ackerson LM, Irvin CG, King TE Jr. Pulmonary histiocytosis X: pulmonary function and exercise pathophysiology. Am J Respir Crit Care Med. 1996;153(1):426–35.
48. Moore AD, Godwin JD, Muller NL, Naidich DP, Hammar SP, Buschman DL, et al. Pulmonary histiocytosis X: comparison of radiographic and CT findings. Radiology. 1989;172(1):249–54.
49. Brauner MW, Grenier P, Mouelhi MM, Mompoint D, Lenoir S. Pulmonary histiocytosis X: evaluation with high-resolution CT. Radiology. 1989;172(1):255–8.
50. Soler P, Chollet S, Jacque C, Fukuda Y, Ferrans VJ, Basset F. Immunocytochemical characterization of pulmonary histiocytosis X cells in lung biopsies. Am J Pathol. 1985;118(3):439–51.
51. Chollet S, Soler P, Bernaudin JF, Basset F. Exploratory bronchoalveolar lavage. Presse Med. 1984;13(24):1503–8.
52. Baqir M, Vassallo R, Maldonado F, Yi ES, Ryu JH. Utility of bronchoscopy in pulmonary Langerhans cell histiocytosis. J Bronchology Interv Pulmonol. 2013;20(4):309–12. https://doi.org/10.1097/LBR.0000000000000021.
53. Torre O, Harari S. The diagnosis of cystic lung diseases: a role for bronchoalveolar lavage and transbronchial biopsy? Respir Med. 2010;104(Suppl 1):S81–5. https://doi.org/10.1016/j.rmed.2010.03.021. Epub 2010 Apr 28.
54. Harari S, Torre O, Cassandro R, Taveira-DaSilva AM, Moss J. Bronchoscopic diagnosis of Langerhans cell histiocytosis and lymphangioleiomyomatosis. Respir Med. 2012;106(9):1286–92. https://doi.org/10.1016/j.rmed.2012.06.012. Epub 2012 Jul 7.
55. Aubry MC, Wright JL, Myers JL. The pathology of smoking-related lung diseases. Clin Chest Med. 2000;21(1):11–35, vii.
56. Yousem SA, Colby TV, Chen YY, Chen WG, Weiss LM. Pulmonary Langerhans' cell histiocytosis: molecular analysis of clonality. Am J Surg Pathol. 2001;25(5):630–6.
57. Fartoukh M, Humbert M, Capron F, Maitre S, Parent F, Le Gall C, et al. Severe pulmonary hypertension in histiocytosis X. Am J Respir Crit Care Med. 2000;161(1):216–23.
58. Bois MC, May AM, Vassallo R, Jenkins SM, Yi ES, Roden AC. Morphometric study of pulmonary arterial changes in pulmonary Langerhans cell histiocytosis. Arch Pathol Lab Med. 2018;142(8):929–37.
59. Negrin-Dastis S, Butenda D, Dorzee J, Fastrez J, d'Odemont JP. Complete disappearance of lung abnormalities on high-resolution computed tomography: a case of histiocytosis X. Can Respir J. 2007;14(4):235–7.
60. Abbott GF, Rosado-de-Christenson ML, Franks TJ, Frazier AA, Galvin JR. From the archives of the AFIP: pulmonary Langerhans cell histiocytosis. Radiographics. 2004;24(3):821–41.
61. Mogulkoc N, Veral A, Bishop PW, Bayindir U, Pickering CA, Egan JJ. Pulmonary Langerhans' cell histiocytosis: radiologic resolution following smoking cessation. Chest. 1999;115(5):1452–5.

62. Aerni MR, Aubry MC, Myers JL, Vassallo R. Complete remission of nodular pulmonary Langerhans cell histiocytosis lesions induced by 2-chlorodeoxyadenosine in a nonsmoker. Respir Med. 2008;102(2):316–9. PMID: 17935961 and https://doi.org/10.1016/j.rmed.2007.09.002.
63. Pardanani A, Phyliky RL, Li CY, Tefferi A. 2-Chlorodeoxyadenosine therapy for disseminated Langerhans cell histiocytosis. Mayo Clin Proc. 2003;78(3):301–6.
64. Berres ML, Lim KP, Peters T, Price J, Takizawa H, Salmon H, et al. BRAF-V600E expression in precursor versus differentiated dendritic cells defines clinically distinct LCH risk groups. J Exp Med. 2014;211(4):669–83.
65. Hyman DM, Puzanov I, Subbiah V, Faris JE, Chau I, Blay JY, et al. Vemurafenib in multiple nonmelanoma cancers with BRAF V600 mutations. N Engl J Med. 2015;373(8):726–36.
66. Dauriat G, Mal H, Thabut G, Mornex JF, Bertocchi M, Tronc F, et al. Lung transplantation for pulmonary langerhans' cell histiocytosis: a multicenter analysis. Transplantation. 2006;81(5):746–50.
67. Saleem I, Moss J, Egan JJ. Lung transplantation for rare pulmonary diseases. Sarcoidosis Vasc Diffuse Lung Dis. 2005;22(Suppl 1):S85–90.
68. Wajda N, Zhu Z, Jandarov R, Dilling DF, Gupta N. Clinical outcomes and survival following lung transplantation in patients with pulmonary Langerhans cell histiocytosis. Respirology. 2019; https://doi.org/10.1111/resp.13671. [Epub ahead of print].
69. Liebow AA, Steer A, Billingsley JG. Desquamative interstitial pneumonia. Am J Med. 1965;39:369–404.
70. Yousem SA, Colby TV, Gaensler EA. Respiratory bronchiolitis-associated interstitial lung disease and its relationship to desquamative interstitial pneumonia. Mayo Clin Proc. 1989;64(11):1373–80.
71. Craig PJ, Wells AU, Doffman S, Rassl D, Colby TV, Hansell DM, et al. Desquamative interstitial pneumonia, respiratory bronchiolitis and their relationship to smoking. Histopathology. 2004;45(3):275–82.
72. Hakala M, Paakko P, Huhti E, Tarkka M, Sutinen S. Open lung biopsy of patients with rheumatoid arthritis. Clin Rheumatol. 1990;9(4):452–60.
73. Iskandar SB, McKinney LA, Shah L, Roy TM, Byrd RP Jr. Desquamative interstitial pneumonia and hepatitis C virus infection: a rare association. South Med J. 2004;97(9):890–3.
74. Flores-Franco RA, Luevano-Flores E, Gaston-Ramirez C. Sirolimus-associated desquamative interstitial pneumonia. Respiration. 2007;74(2):237–8.
75. Suzuki T, McCarthy C, Carey B, Borchers M, Beck D, Wikenheiser-Brokamp KA, et al. Increased pulmonary GM-CSF causes alveolar macrophage accumulation: mechanistic implications for desquamative interstitial pneumonitis. Am J Respir Cell Mol Biol. 2019; https://doi.org/10.1165/rcmb.2018-0294OC. [Epub ahead of print].
76. Hansell DM, Nicholson AG. Smoking-related diffuse parenchymal lung disease: HRCT-pathologic correlation. Semin Respir Crit Care Med. 2003;24(4):377–92.
77. Heyneman LE, Ward S, Lynch DA, Remy-Jardin M, Johkoh T, Muller NL. Respiratory bronchiolitis, respiratory bronchiolitis-associated interstitial lung disease, and desquamative interstitial pneumonia: different entities or part of the spectrum of the same disease process? AJR. 1999;173(6):1617–22.
78. Mueller-Mang C, Grosse C, Schmid K, Stiebellehner L, Bankier AA. What every radiologist should know about idiopathic interstitial pneumonias. Radiographics. 2007;27(3):595–615.
79. Matsuo K, Tada S, Kataoka M, Okahara M, Hiramatsu J, Horiba M, et al. Spontaneous remission of desquamative interstitial pneumonia. Intern Med. 1997;36(10):728–31.
80. Bjoraker JA, Ryu JH, Edwin MK, Myers JL, Tazelaar HD, Schroeder DR, et al. Prognostic significance of histopathologic subsets in idiopathic pulmonary fibrosis. Am J Respir Crit Care Med. 1998;157(1):199–203.
81. Flusser G, Gurman G, Zirkin H, Prinslo I, Heimer D. Desquamative interstitial pneumonitis causing acute respiratory failure, responsive only to immunosuppressants. Respiration. 1991;58(5–6):324–6.

82. Timmer SJ, Karamzadeh AM, Yung GL, Kriett J, Jamieson SW, Smith CM. Predicting survival of lung transplantation candidates with idiopathic interstitial pneumonia: does PaO(2) predict survival? Chest. 2002;122(3):779–84.
83. Verleden GM, Sels F, Van Raemdonck D, Verbeken EK, Lerut T, Demedts M. Possible recurrence of desquamative interstitial pneumonitis in a single lung transplant recipient. Eur Respir J. 1998;11(4):971–4.
84. Kawabata Y, Hoshi E, Murai K, Ikeya T, Takahashi N, Saitou Y, et al. Smoking-related changes in the background lung of specimens resected for lung cancer: a semiquantitative study with correlation to postoperative course. Histopathology. 2008;53(6):707–14.
85. Lederer DJ, Enright PL, Kawut SM, Hoffman EA, Hunninghake G, van Beek EJ, et al. Cigarette smoking is associated with subclinical parenchymal lung disease: the Multi-Ethnic Study of Atherosclerosis (MESA)-lung study. Am J Respir Crit Care Med. 2009;180(5):407–14.
86. Katzenstein AL, Mukhopadhyay S, Zanardi C, Dexter E. Clinically occult interstitial fibrosis in smokers: classification and significance of a surprisingly common finding in lobectomy specimens. Hum Pathol. 2010;41(3):316–25.
87. Watanabe Y, Kawabata Y, Kanauchi T, Hoshi E, Kurashima K, Koyama S, et al. Multiple, thin-walled cysts are one of the HRCT features of airspace enlargement with fibrosis. Eur J Radiol. 2015;84(5):986–92.
88. Cottin V, Nunes H, Brillet PY, Delaval P, Devouassoux G, Tillie-Leblond I, et al. Combined pulmonary fibrosis and emphysema: a distinct underrecognised entity. Eur Respir J. 2005;26(4):586–93.
89. Kitaguchi Y, Fujimoto K, Hanaoka M, Kawakami S, Honda T, Kubo K. Clinical characteristics of combined pulmonary fibrosis and emphysema. Respirology. 2010;15(2):265–71.
90. Fintelmann FJ, Brinkmann JK, Jeck WR, Troschel FM, Digumarthy SR, Mino-Kenudson M, et al. Lung cancers associated with cystic airspaces: natural history, pathologic correlation, and mutational analysis. J Thorac Imaging. 2017;32(3):176–88.
91. Mascalchi M, Attina D, Bertelli E, Falchini M, Vella A, Pegna AL, et al. Lung cancer associated with cystic airspaces. J Comput Assist Tomogr. 2015;39(1):102–8.
92. Gupta N, Colby TV, Meyer CA, McCormack FX, Wikenheiser-Brokamp KA. Smoking-related diffuse cystic lung disease. Chest. 2018;154(2):e31–e5.

Chapter 7
Birt-Hogg-Dubé Syndrome

Laura S. Schmidt and Robert M. Kotloff

Introduction

Birt-Hogg-Dubé (BHD) syndrome is a rare, autosomal dominant inherited disorder that predisposes affected individuals to develop benign cutaneous papules called fibrofolliculomas, pulmonary cysts, recurrent spontaneous pneumothoraces, and kidney tumors. Germline inactivating mutations in the *folliculin* (*FLCN*) gene located on the short arm of chromosome 17 are responsible for BHD syndrome [1]. Hornstein and Knickenberg [2] were the first to describe "cutaneous perifollicular fibromatosis cutis" that appeared to be inherited in a small two-generation family. Two years later, Canadian physicians Birt, Hogg, and Dubé reported a large multi-generation family in which 15 adult members presented with facial papules histologically consistent with fibrofolliculomas that were nearly indistinguishable clinically and histologically from the perifollicular fibromas described by Hornstein and Knickenberg [3]. The segregation patterns in both of these kindreds supported an autosomal dominant mode of inheritance for the cutaneous lesions, and the disease was subsequently named Birt-Hogg-Dubé (BHD) syndrome. An association of recurrent spontaneous pneumothoraces [4, 5] and/or bilateral renal tumors [6, 7] with BHD cutaneous lesions was suggested by several early case studies. A risk assessment performed by Zbar and colleagues in a cohort of BHD-affected family members and their unaffected siblings confirmed that renal tumors and spontaneous

L. S. Schmidt (✉)
Basic Science Program, Frederick National Laboratory for Cancer Research, Frederick, MD, USA

Urologic Oncology Branch, Center for Cancer Research, National Cancer Institute, National Institutes of Health, Bethesda, MD, USA
e-mail: schmidtl@mail.nih.gov

R. M. Kotloff
Department of Pulmonary Medicine, Cleveland Clinic, Cleveland, OH, USA
e-mail: kotlofr@ccf.org

N. Gupta et al. (eds.), *Diffuse Cystic Lung Diseases*, Respiratory Medicine,
https://doi.org/10.1007/978-3-030-63365-3_7

pneumothoraces were part of the phenotypic spectrum of BHD [8]. This chapter reviews the clinical manifestations, diagnostic criteria, molecular genetics, and management of BHD syndrome.

Clinical Manifestations of BHD Syndrome

BHD syndrome is characterized by phenotypic variability. Individuals affected with BHD may present with skin, pulmonary, or renal manifestations singly or in any combination. The clinical presentation may vary among affected individuals from the same BHD family or among BHD families that inherit the identical *FLCN* mutation. Familial spontaneous pneumothorax families with germline *FLCN* mutations have been reported in which pulmonary cysts and pneumothorax were the only presenting features [9–11], and BHD families presenting with renal cancer without pulmonary or cutaneous manifestations have also been described [12].

Cutaneous

Fibrofolliculomas, trichodiscomas, and acrochordons were described by Birt and colleagues as the hallmark cutaneous features of BHD syndrome [3]. Fibrofolliculomas, the most frequently observed manifestation, will develop in over 85% of individuals affected with BHD, usually in the third decade of life. They appear as white to flesh-colored papules, 2–4 mm in size, on the face, neck, ear lobes, and upper trunk (Fig. 7.1a). They can occur singly or in numbers >100, and are neither painful nor pruritic [13]. It has been suggested that fibrofolliculomas and trichodiscomas are in

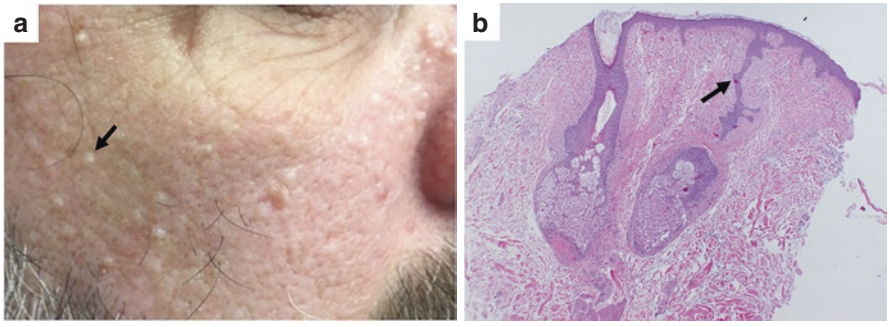

Fig. 7.1 (**a**) Multiple white, dome-shaped fibrofolliculomas (representative lesion indicated by arrow) on the face of a patient with BHD syndrome. (**b**) Hematoxylin and eosin staining of a fibrofolliculoma showing strands of epithelial cells surrounded by fibrous stroma (arrow) with adjacent hair follicle. (Adapted from Schmidt LS, Linehan WM [13])

fact the same lesion, but that different sectioning planes lead to the appearance of different histologies [14]. Acrochordons are common in the general population and, therefore, not specific for BHD syndrome. Other cutaneous manifestations reported in BHD patients include fibrous papules/angiofibromas, which are characteristically associated with tuberous sclerosis complex [15], lipomas [5, 7], perifollicular fibromas [16, 17], and papules of the oral mucosa [7].

Pulmonary

Cystic lung disease is present in approximately 90% of patients with BHD syndrome [11, 18, 19], typically appearing by the fourth decade of life, and in some cases representing the sole manifestation of the syndrome. Patients may note nonspecific respiratory symptoms including episodic chest pain, mild dyspnea, and cough [18], but it is uncertain whether symptoms are truly a consequence of the presence of cysts. Limited data on pulmonary function testing in BHD syndrome patients suggest that lung function is usually normal, though longitudinal assessment of lung function is lacking [20–23]. To date, there are no published reports of respiratory failure developing as a consequence of BHD syndrome.

As expected in the presence of cystic lung disease, spontaneous pneumothorax is relatively common in patients with BHD syndrome and is often the event that first brings them to medical attention. It has been estimated that BHD syndrome accounts for 5–10% of patients presenting with "primary" spontaneous pneumothorax [24]. The reported frequency of pneumothorax varies widely and is influenced by the particular characteristics of the study population. For example, 24% of patients at the National Institutes of Health recruited principally on the basis of dermatological manifestations had experienced at least one spontaneous pneumothorax compared to 76% of patients surveyed from the Rare Lung Diseases Clinic Network [18, 19]. The risk of pneumothorax is 50-fold higher among patients with BHD syndrome compared to unaffected family members [8].

Among BHD syndrome patients, the average age at the time of the first pneumothorax approximates 38 years [11, 18, 19], but this complication has been reported in individuals as young as 7 years of age. Total lung cyst volume, largest cyst diameter and volume, and extent of lower lung zone disease have been identified as risk factors for spontaneous pneumothorax [19, 21]. A family history of pneumothorax is elicited in up to 50% of BHD syndrome patients presenting with pneumothorax. Patients with a positive family history appear to be at greater risk for developing a spontaneous pneumothorax than those BHD syndrome patients without such a history [25]. In contrast, age, gender, smoking history, and specific *FLCN* gene mutation have not been associated with increased risk [19, 25]. For those patients experiencing an initial spontaneous pneumothorax, recurrence rates in the absence of pleurodesis are high, ranging from 42% to 86% in published series [11, 18, 19, 21].

Renal

Bilateral, multifocal renal tumors develop in up to one-third of BHD syndrome patients (range 12–35%) with a median age at diagnosis of 50–52 years [12, 25–28]. Zbar and colleagues found that BHD syndrome-affected family members had a sevenfold increased risk for developing kidney tumors when compared to their unaffected siblings [8]. BHD syndrome-affected individuals may present with a variety of histologic subtypes of renal tumors, most frequently chromophobe renal cancer and hybrid oncocytic tumors with features of chromophobe renal cancer and oncocytoma [29]. Multiple tumors with different histologies may be present in a single kidney of a BHD syndrome patient. Although quite rare, renal tumor metastases can develop in the setting of BHD syndrome [12, 27, 28].

Other Clinical Manifestations

A number of different clinical manifestations have been reported in patients with BHD syndrome including parotid gland tumors and parotid oncocytomas [26, 28, 30–32], parathyroid adenomas [5], thyroid nodules, and thyroid cancer [11, 28, 33], but whether these clinical features are part of the BHD syndrome phenotype remains to be determined.

Several early reports suggested a link between the BHD syndrome-associated cutaneous lesions and colonic polyps/cancer in BHD syndrome-affected individuals [2, 4, 34, 35]. However, a risk assessment conducted by Zbar et al. [8] in a BHD syndrome cohort from the United States did not find an increased risk for colon manifestations in BHD syndrome patients compared to their unaffected siblings. On the other hand, Nahorski et al. compared two groups of BHD syndrome patients from the United Kingdom with two different *FLCN* mutations and found a significantly greater risk for colon neoplasia in individuals with the c.1285dupC mutation relative to those with the c.610delGCinsTA mutation [36], suggesting the possibility that different *FLCN* variants may predispose to a greater or lesser risk of colon neoplasia in BHD syndrome. The lifetime risk of developing colon neoplasia by the age of 80 in the BHD syndrome cohort from the United Kingdom (n = 149) was 20% compared to a baseline of 4.9% in the unaffected population, which may suggest that additional factors affect colon polyp development in the setting of BHD syndrome including environment, population ethnicity, or *FLCN* genotypes.

Radiographic and Histologic Features of BHD Syndrome

Cutaneous

Fibrofolliculomas are characterized by centrally located, aberrant hair follicles surrounded by a moderately well-circumscribed proliferation of loose connective tissue with fine collagen fibers embedded in mucin-rich stroma (Fig. 7.1b). Anastomosing strands of epithelial cells, 2–4 cells thick, typically extend from the infundibulum of the hair follicle into the connective tissue mantle [3]. Small sebocytes are found within these epithelial structures [7]. In fact, many of the epithelial strands are continuous with the sebaceous glands, which often display hyperplasia, suggesting that fibrofolliculomas may be caused by abnormal growth and differentiation arising from the "mantle," which represents a stage in sebaceous gland morphogenesis [37].

Pulmonary

Several radiographic features visualized on high resolution computed tomography (HRCT) of the lungs may be helpful in distinguishing BHD syndrome from other etiologies of diffuse cystic lung disease [38, 39]. The cysts are thin walled, have a lower lung zone predominance, and frequently abut the pleural surface. They range in size from a few millimeters to over 2 centimeters. While smaller cysts tend to be circular, the larger cysts are often irregular or lentiform in shape and can be multiseptated (Fig. 7.2a, b). At least some of the cysts abut or incorporate proximal

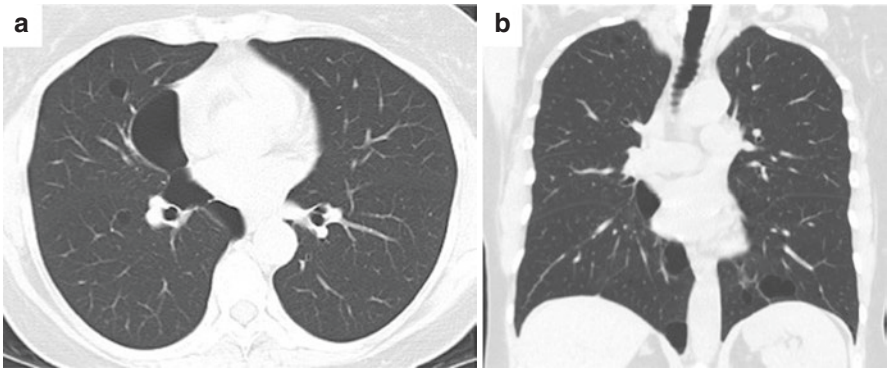

Fig. 7.2 Pulmonary manifestations of BHD syndrome. Axial (**a**) and coronal (**b**) HRCT images demonstrating the characteristic radiographic appearance of BHD lung cysts. (Note the subpleural and basilar distribution of the cysts and the subtle septations of the large cyst abutting the mediastinum on the axial image)

segments of the lower lobe pulmonary artery or vein [39]. Attesting to the distinct radiographic features of BHD syndrome, three expert thoracic radiologists presented with HRCT images from 89 patients with various cystic lung diseases were able to diagnose BHD syndrome with an accuracy of 93% [40].

In contrast, the histopathology of BHD syndrome lung cysts is not particularly distinctive and has been reported to closely resemble that of emphysematous blebs [41]. Several investigators have challenged this claim, arguing that this conclusion was based on studies of ruptured cysts in the setting of pneumothorax and that unruptured cysts must be closely scrutinized in order to appreciate the subtle differences [42, 43]. These investigators cite the absence of inflammatory infiltrates in the portion of the cyst wall remote from the subpleural region as the major feature that distinguishes BHD syndrome cysts from blebs. Because there are no pathognomonic features, however, lung biopsy cannot be used as a means to establish a diagnosis of BHD syndrome.

Renal

BHD syndrome patients present with bilateral, multifocal renal tumors that can be detected by magnetic resonance imaging (MRI) or computed tomography (CT) of the abdomen (Fig. 7.3a, b). Histologically, BHD syndrome-associated renal tumors

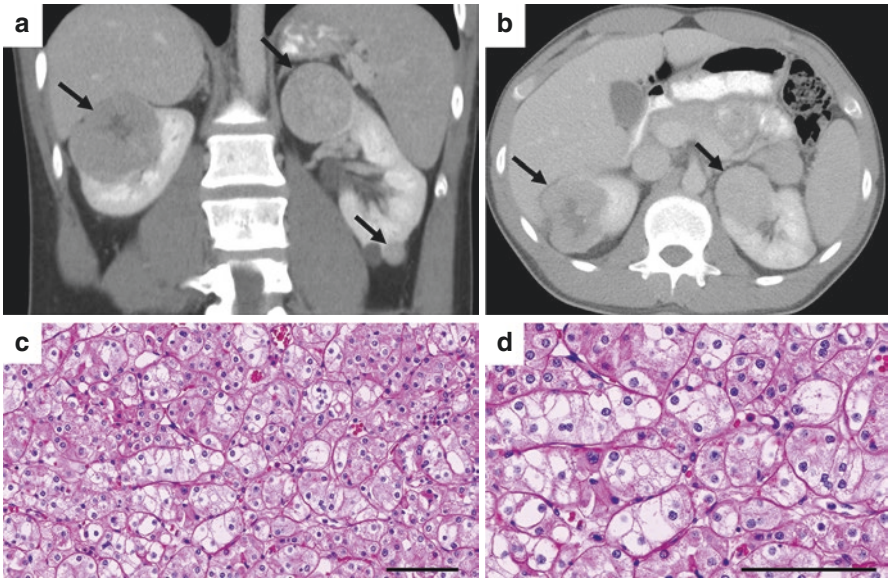

Fig. 7.3 Renal manifestations of BHD syndrome. Abdominal coronal (**a**) and axial (**b**) CT scans showing bilateral, multifocal renal tumors in a BHD patient (*arrows*). (**c**, **d**) Histology of hybrid oncocytic renal tumors that present most frequently in BHD patients. Scale bar, 100 μm. (Adapted from Schmidt LS, Linehan WM [13])

are most frequently chromophobe renal carcinoma (34%) or hybrid oncocytic tumors with features of both chromophobe renal carcinoma and oncocytoma (50%) (Fig. 7.3c, d), but clear cell renal carcinoma (9%), oncocytoma (5%) and, although rare, papillary renal cell carcinoma (2%) have also been reported [29]. Renal cysts have been documented in the setting of BHD syndrome, but no comparisons to general population-based frequencies have been performed [28, 33, 44]. Kidneys of BHD syndrome patients frequently harbor regions within the apparently normal renal parenchyma that contain microscopic foci of oncocytic cells termed "oncocytosis." Since oncocytosis develops in the kidneys of BHD syndrome patients who present with different histologic tumor subtypes, it has been suggested that renal oncocytic cells are precursors to all subtypes of renal cancer [29].

Diagnostic Criteria for BHD Syndrome

It is important to be aware of the phenotypic variability associated with BHD syndrome when evaluating the manifestations of a patient to confirm a diagnosis. Physicians should consider BHD syndrome in the differential diagnosis of a patient who presents with cutaneous papules clinically consistent with fibrofolliculomas or has a family history of these lesions. Additionally, pulmonary cysts, especially when located in the lung bases, or history of pneumothorax in a patient or as part of his/her family history, should raise suspicion for BHD syndrome. Finally, a personal or family history of bilateral or multifocal renal cancer with early age of onset (<50 years), especially with hybrid oncocytic or chromophobe histology, may be suggestive of BHD syndrome [13, 45, 46]. These characteristic features of BHD syndrome may be present singly or in any combination in a patient and his/her affected family members.

Several groups have proposed diagnostic criteria for BHD syndrome [13, 45, 46]. Two examples are presented in Tables 7.1 and 7.2; the latter is a "pulmonary-centric"

Table 7.1 Diagnostic criteria for Birt-Hogg-Dubé syndrome

Diagnosis requires one major or two minor criteria:
Major criteria
At least five fibrofolliculomas or trichodiscomas, with at least one histologically confirmed; adult onset
Pathogenic *FLCN* germline mutation
Minor criteria
Multiple lung cysts: bilateral basally located lung cysts with no other apparent cause, with or without spontaneous pneumothorax
Renal cancer: early onset (<50 years) or multifocal or bilateral renal cancer, or renal cancer of mixed chromophobe and oncocytic histology
A first-degree relative with BHD

Reprinted from Lancet Oncology, 10, Menko et al. [45], Copyright 2009, with permission from Elsevier

Table 7.2 Alternative diagnostic criteria for Birt-Hogg-Dubé syndrome

Characteristic[a] or compatible[b] lung HRCT with one of the following:
Skin biopsy positive for fibrofolliculoma or trichodiscoma
Confirmed family history of BHD in first- or second-degree family member
Histologic confirmation of chromophobe renal carcinoma or hybrid oncocytic tumor
Genetic testing positive for *FLCN* mutation

Modified from [46]

[a]Multiple thin-walled, round, elliptical, or lentiform well-defined air-filled cysts without internal structure, in a basilar, medial, and subpleural predominant distribution, with preserved or increased lung volume, and no other significant pulmonary involvement (specifically no interstitial lung disease)

[b]Thin-walled cysts without the more typical elliptical shape or subpleural distribution

schema that is applicable in the commonly encountered clinical context of the patient presenting with cystic lung disease. All the proposed criteria consider demonstration of a pathogenic *FLCN* mutation by genetic testing to be one means of confirming the diagnosis. In contrast to other cystic lung diseases (see below), lung biopsy does not provide diagnostic confirmation and should not be employed unless an alternative diagnosis is being strongly considered.

For the patient presenting with cystic lung disease, major diagnostic considerations other than BHD syndrome include lymphangioleiomyomatosis, pulmonary Langerhans cell histiocytosis, and lymphoid interstitial pneumonia. Clinical, radiographic, and laboratory features of each of these entities are summarized in Table 7.3.

Genetics of BHD Syndrome: *FLCN* Gene

FLCN Gene Discovery and Mutation Spectrum

Genetic linkage analysis in families with the cutaneous features of BHD syndrome localized the disease gene to the short arm of chromosome 17 [47, 48]. Using positional cloning strategies, Nickerson and colleagues narrowed the BHD genetic locus to chromosome 17p11.2, and subsequently identified germline protein-truncating mutations in a novel gene, *folliculin* (*FLCN*), which encodes a protein that is conserved across species [1]. In the 16 years since the *FLCN* gene was discovered, the mutation spectrum as reported in a number of large BHD cohorts [25–28, 33,

Table 7.3 Clinical, radiographic, and laboratory features of the common diffuse cystic lung diseases

Cystic lung disease	Clinical features	Typical HRCT features	Laboratory features
LAM	Almost exclusively in females (occasionally in males with TSC) Renal angiomyolipomas in up to 50% of cases Retroperitoneal or pelvic lymphangioleiomyomas Chylous effusion May be accompanied by clinical features of TSC	Small thin-walled round cysts, varying little in size or shape, uniformly distributed throughout the lungs	Serum VEGF-D > 800 pg/ml Presence of *TSC1* or *TSC2* mutation (in patients with underlying TSC) Airflow obstruction on spirometry Lung biopsy demonstrating characteristic histology with HMB-45 positive smooth muscle cells
LCH	Young adults between 20 and 40 years of age Nearly all affected adults are current or former smokers Diabetes insipidus in 15% Bone lesions in up to 15%	Early disease: nodules, some cavitary ("cheerio sign") Advanced disease: Cysts of varying size and irregular shape, with prominent walls Nodules and cysts have an upper and mid-lung zone distribution, often sparing the costophrenic angles	Bronchoalveolar lavage with ≥5% CD1a-positive cells Lung biopsy demonstrating characteristic histology with Langerhans cells staining positive for S-100 protein and CD1a
LIP	Underlying autoimmune or immunodeficiency disorder in majority of cases Sjogen's syndrome is most common underlying disorder; other disorders include lupus, HIV (typically in children), common variable immunodeficiency	Few thin-walled cysts, typically arising in areas of ground-glass opacity Often accompanied by centrilobular or subpleural nodules	Positive ANA, anti-Ro/SS-A, and/or anti-La/SS-B antibody Positive serologic test for HIV Hypogammaglobulinemia Lung biopsy demonstrating polyclonal infiltration of interstitium and alveolar air spaces with mature lymphocytes and plasma cells
BHD	Fibrofolliculomas Renal neoplasms, typically multifocal hybrid oncocytic tumors or chromophobe renal cell carcinomas Family history of pneumothorax or renal neoplasms	Bilateral thin-walled round or lentiform cysts of variable sizes, often subpleural, with a lower lung zone predominance	Genetic testing positive for *FLCN* mutation No distinctive features on lung biopsy

Abbreviations: *LAM* lymphangioleiomyomatosis; *LCH* Langerhans cell histiocytosis; *LIP* lymphoid interstitial pneumonia; *BHD* Birt-Hogg-Dubé; *TSC* tuberous sclerosis complex

49–51] now encompasses nearly 150 unique *FLCN* mutations located in all coding exons and includes all mutation types (insertion/deletion, nonsense, missense, splice site, intragenic deletions) [52]. Frameshift insertion/deletion mutations are the most frequent mutation type in BHD syndrome patients [52], and a mutation "hot spot" (c.1285dup/delC) has been reported in exon 11 in a mononucleotide run of 8 cytosines [1, 12, 26–28, 33, 51]. Due to the development of reliable methods to detect intragenic deletions/duplications (e.g., multiplex ligation-dependent probe amplification [MLPA], comparative genomic hybridization [CGH]) and more accurate DNA sequencing technologies, the mutation detection rate for *FLCN* reported in multiple BHD syndrome cohort studies is approaching 90% (range 69–88%) [25–28, 33].

Genotype-Phenotype Associations

To date, no clear association between *FLCN* mutation type or location within the gene and any of the phenotypic features of BHD has been reported; however, some interesting genotype-phenotype trends have emerged. Furuya and colleagues found the highest incidence of renal tumors in BHD syndrome patients who carried the c.1285dupC *FLCN* "hot spot" mutation (40.5%) [28], and Schmidt and coworkers saw significantly more renal cancer in c.1285dupC carriers relative to c.1285delC carriers [26]. Toro et al. reported a trend toward more pneumothoraces in individuals with *FLCN* mutations in exons 9 and 12. In addition, individuals with mutations in exons 9 and 12 had significantly more cysts, and larger cyst diameters and volumes than individuals with *FLCN* mutations in other exons [19]. Kunogi and coworkers [11] found more mutations in the 3′ end of the *FLCN* gene (exons 12 and 13; 13/25, 52%) in Japanese BHD patients, but this observation was not supported in another Japanese BHD cohort ($n = 120$) evaluated by Furuya and colleagues who found equal distribution of *FLCN* mutations along the entire length of the gene [28].

FLCN as a Tumor Suppressor Gene

Multiple lines of evidence support a role for *FLCN* as a tumor suppressor gene. The majority of *FLCN* mutations are insertion/deletion and nonsense mutations predicted to truncate the FLCN protein and lead to loss of function. *Flcn*-deficient mouse, rat, and canine models that carry a mutant or inactivated copy of the *Flcn* gene develop kidney tumors or multi-cystic kidneys subsequent to loss of the remaining wild-type *Flcn* allele [53–57]. Kidney tumors that develop in BHD syndrome patients show loss of the second copy of *FLCN* by mutation or loss of chromosome 17p sequences (loss of heterozygosity, LOH) (Fig. 7.4) [58]. Furthermore, a *FLCN*-null renal tumor cell line established from a BHD syndrome patient was tumorigenic in immunocompromised mice, but lost its oncogenic properties when wild-type *FLCN*

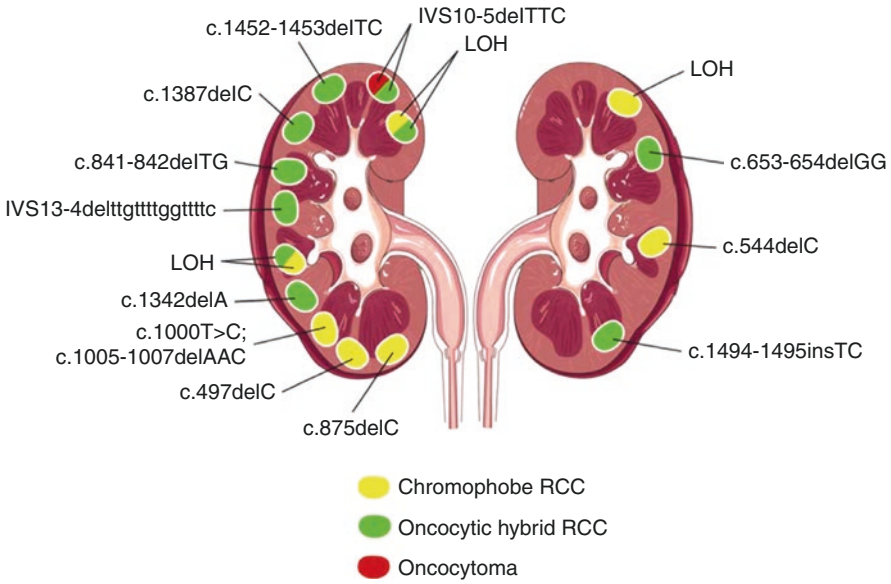

Fig. 7.4 *FLCN* is a tumor suppressor gene. Different somatic second hit *FLCN* mutations in multiple tumors that developed in the kidneys of a BHD patient with a germline *FLCN* mutation demonstrate that *FLCN* is a tumor suppressor gene. Histologic subtypes are color coded. Chromophobe renal cell carcinoma (RCC), yellow; oncocytic hybrid tumor, green; renal oncocytoma, red. LOH, loss of heterozygosity. (Reprinted with permission from Vocke CD et al. [58])

expression was restored [59, 60]. Interestingly, BHD pulmonary cysts [61] and fibrofolliculomas [62] stain positively for FLCN by immunohistochemistry raising the possibility that *FLCN* haploinsufficiency may be sufficient to trigger the aberrant cutaneous and pulmonary changes that lead to the BHD syndrome-associated phenotypes in these tissues.

Potential Functions of the FLCN Protein

The *FLCN* gene encodes a 64 kDa protein that is highly conserved across species but does not contain classical protein domains to suggest a functional role in cells. FLCN was shown to interact through its carboxy-terminus with two novel proteins, folliculin-interacting protein 1 (FNIP1) [63] and folliculin-interacting protein 2 (FNIP2) [64, 65], and with AMP-activated protein kinase (AMPK). AMPK is a critical energy and nutrient sensor in cells and an important negative regulator of mechanistic target of rapamycin (mTOR), which in turn is the master controller of cellular protein synthesis and cell growth [66]. The interaction of AMPK with FLCN and FNIP1/FNIP2 led researchers to investigate a potential role of FLCN in modulating mTOR activity.

Role of FLCN in Modulating mTOR Activity

Early work to elucidate FLCN function relied upon the development and study of *Flcn*-deficient in vivo models. Genetically engineered mouse models in which *Flcn* inactivation was targeted to the kidney developed polycystic kidneys and cystic renal tumors, which displayed activation of mTORC1 and reduced tumor/cyst formation in response to the mTOR inhibitor, rapamycin [55, 56, 67]. Renal tumors that developed in a heterozygous *Flcn* +/− mouse model subsequent to loss of the wild-type *Flcn* allele showed both mTORC1 and mTORC2 activation [57]. However, Hartman and colleagues generated a *Flcn* +/− mouse model that was also subjected to ENU mutagenesis, and the kidney cysts/tumors that developed in this model displayed mTORC1 inhibition (reduced phospho-S6 staining, a readout for mTORC1 activity) [68]. Hudon and coworkers developed another *Flcn* +/− mouse model in which phospho-S6 staining was negative in small single cysts but positive in large complex cysts, leading to the suggestion that the role of Flcn in modulating mTORC1 is complex and may be cell and context dependent [69].

Role of FLCN in Amino Acid-Dependent Regulation of mTOR Activation on the Lysosome

Functional insight has been gained from work by Nookala and colleagues who resolved the crystal structure of the carboxy-terminal half of FLCN and identified structural similarity to the differentially expressed in normal cells and neoplasia (DENN) domain proteins. DENN domain proteins are a family of Rab guanine nucleotide exchange factors (GEFs) involved in GDP-GTP exchange and an essential part of vesicle membrane transport [70]. Recent work from two independent laboratories has expanded this idea further by demonstrating that FLCN coordinates cellular responses to changes in amino acid availability through regulation of another Ras-related family of GTP-binding proteins, the heterodimers RagA/B and Rag C/D [71, 72]. mTORC1 activation by amino acids requires its recruitment to the lysosome surface, which is facilitated by a complex of lysosome-associated proteins including vacuolar adenosine triphosphatase, the Ragulator complex, RagA/B and RagC/D [73]. Petit and colleagues found that when amino acids are low, the FLCN-FNIP complex bound to RagA/B [72]; Tsun and coworkers showed that FLCN displayed GTPase activating protein (GAP) activity toward RagC/D placing it in its GDP-bound form, which is necessary for mTORC1 recruitment to the lysosome [71]. Meng and coworkers [74] have demonstrated that FLCN (in association with FNIP) binds to RagA/B only when it is in its GDP-bound state, which is achieved through the GTPase activating protein (GAP) activity of the GATOR1 complex [74]. These studies underscore a role of FLCN in amino acid-dependent regulation of mTOR activation, but the details remain to be fully elucidated.

Role of FLCN in Other Pathways Involved in Cellular Homeostasis

Experimental evidence has been presented to support a role for FLCN in regulating other important pathways and cellular processes including TFE3/TFEB transcriptional activation [72, 75, 76], canonical WNT signaling [77], regulation of PGC1α and mitochondrial biogenesis [78, 79], and autophagy [80, 81].

Role of FLCN in Maintenance of Proper Cell-Cell Adhesion and Cell Polarity

The mechanisms by which FLCN inactivation can lead to the development of pulmonary cysts and subsequent spontaneous pneumothorax remain under active investigation. Using a yeast two-hybrid approach, two independent laboratories discovered a physical interaction between FLCN and the adherens junction protein p0071 (also known as plakophilin-4), which is characterized by armadillo repeats and is a positive regulator of the small GTPase RhoA [82, 83]. However, their reports differ on whether FLCN positively or negatively affects p0071 function. Medvetz and coworkers [82] reported that downregulation of FLCN led to increased cell-cell adhesion and disruption of cell polarity, which was phenocopied by downregulation of p0071, and demonstrated that FLCN was a positive regulator of RhoA and Rho-associated kinase (ROCK) activity. Nahorski and colleagues [83] showed that FLCN colocalized with p0071 at cell junctions and the midbody during cytokinesis leading to disordered cytokinesis under conditions of FLCN deficiency. In contrast to Medvetz et al., they found that FLCN was a negative regulator of RhoA activity, and they showed that treatment of *FLCN*-deficient cells with a downstream inhibitor of ROCK activity reversed the increased cell migration phenotype [83]. Regardless of the disparate results that demonstrate both negative and positive regulation of RhoA activity by FLCN, both studies provide convincing evidence that the FLCN-p0071 interaction is important for proper cell polarity and intercellular junctions. Mice with *Flcn* inactivation targeted to the epidermal layer of the skin show a striking phenotype including skin and hair abnormalities, epidermal hyperplasia, and increased mTOR activation, providing further support for the in vitro studies that suggest that FLCN deficiency leads to deregulated cell-cell adhesion [82].

AMPK is required for cell survival and maintenance of epithelial cell junctions, and its activity is regulated through phosphorylation by the serine/threonine kinase LKB1. Localization of LKB1 to epithelial cell junctions is regulated by E-cadherin [84]. In the studies described above, Nahorski and colleagues observed a mislocalization of E-cadherin in a mouse inner medullary collecting duct-3 cell model with FLCN or p0071 knockdown [83]. A role for FLCN in regulating localization of E-cadherin was also supported by studies in a mouse model in which *Flcn*

inactivation was targeted to surfactant protein-C expressing alveolar epithelial cells (AECs) [85]. In this study, *Flcn*-deficient AECs displayed reduced AMPK phosphorylation, lowered LKB1 levels, and marked reduction of E-cadherin in the adherens junctions of cell membranes, which were reversed by Flcn expression. *Flcn* loss in AECs resulted in increased cell permeability and elevated apoptosis. Taken together these studies support a role for Flcn in the maintenance of epithelial cell-cell junctions and AEC survival, potentially through the E-cadherin-LKB1-AMPK axis, and demonstrate that *Flcn* loss may lead to alveolar airspace enlargement and cyst formation through dysregulation of this cascade.

The "stretch hypothesis" [82, 86, 87] has been proposed to explain how alveolar enlargements that produce BHD syndrome-associated pulmonary cysts develop. During respiration, cell-cell junctions allow the lung to expand and then "snap back" to its original shape and cellular structure. Defects in cell-cell adhesion under FLCN deficiency may lead to stretch-induced stress at regions with weaker cell-cell adhesion forces including interlobular septa and attachments to visceral pleura, resulting in airspace enlargement. Continued research efforts will be necessary to validate this proposed mechanism for pulmonary cyst development in BHD syndrome.

Management of BHD Syndrome

Cutaneous

Although fibrofolliculomas are not painful or pruritic, BHD syndrome patients often pursue treatment for removal of these lesions because they can be quite disfiguring. Surgical intervention using curettage and hyfrecation has provided satisfactory results in some cases [88]. Laser ablation (erbium:YAG or CO2) is another treatment option for removal of fibrofolliculomas without scarring, but partial relapse and occurrence of new lesions were noted after a period of 6 months [89]. Vernooij et al. have suggested that fibrofolliculomas may arise from abnormal growth of the sebaceous gland mantle, and since sebaceous gland growth can be inhibited by certain retinoids, topical treatment with these compounds may represent a potential therapy for the cutaneous lesions in BHD syndrome [37].

Pulmonary

HRCT is often performed as part of the diagnostic evaluation, particularly for patients whose initial presentation involved a spontaneous pneumothorax. For those patients for whom the diagnosis of BHD syndrome was based on renal or cutaneous manifestations or *FLCN* genetic testing, we recommend obtaining a baseline-HRCT, as the presence of cystic lung disease would prompt counseling the patient on the possible future occurrence of pneumothorax. We also recommend obtaining

baseline pulmonary function testing in those patients with cystic lung disease and those who report dyspnea on exertion since our current understanding of the impact of BHD syndrome on lung function is incomplete. CT scans and pulmonary function testing should be repeated only as warranted by new or worsening respiratory symptoms; there is currently no indication to perform serial testing for surveillance purposes alone.

Pulmonary management of BHD syndrome principally centers on treatment and secondary prevention of pneumothoraces. Because of the high recurrence rate with conservative management alone (i.e., chest tube thoracostomy), performance of pleurodesis following an initial spontaneous pneumothorax is generally recommended. Data on the efficacy of pleurodesis in this setting are scant, but one survey-based study suggested an ipsilateral pneumothorax recurrence rate of 33% following pleurodesis compared to 63% when pneumothorax was managed conservatively [18]. A Japanese group has developed a novel thoracoscopic approach to pneumothorax prevention, covering the entire visceral pleura with an absorbable cellulose mesh applied with fibrin glue. This not only provides an immediate seal at the site of the pleural rent but also induces fibrous thickening of the visceral pleura, without producing visceral to parietal pleural adhesions and presumably without compromising lung expansion and lung function. Among 52 BHD syndrome patients undergoing total pleural covering, none experienced a subsequent recurrent pneumothorax, with a mean follow-up period of 38 +/− 22 months [90]. However, this procedure is not widely available, and additional studies will be required before it can be recommended as an alternative to pleurodesis.

An area of uncertainty in managing BHD syndrome patients with cystic lung disease is the risk of pneumothorax associated with commercial air travel. As ambient pressure falls in a partially pressurized commercial jet flying at cruising altitude, the trapped gas within non-communicating lung cysts expands according to Boyle's Law, thus risking cyst rupture and pneumothorax. The actual risk of pneumothorax with air travel for the BHD syndrome patient is uncertain but likely small, with two survey-based studies estimating the risk to be 0.12–0.63% per flight [18, 91]. The risk is likely further mitigated following pleurodesis. Although patients should be counseled about the potential risk, air travel is not contraindicated in the absence of significantly compromised lung function (which would not be anticipated from BHD syndrome alone). Similar uncertainties exist about the risk of pneumothorax with diving, but at least one professional society considers cystic lung disease of any cause to represent an absolute contraindication [92].

Renal

Individuals with a confirmed diagnosis of BHD syndrome are at lifelong risk for the development of bilateral, multifocal renal tumors. Since renal tumors have been reported in BHD syndrome patients as young as 20 years of age [12], it is recommended that at-risk individuals undergo serial abdominal imaging every 36 months

starting at 20–21 years of age [45, 93]. CT or magnetic resonance imaging with intravenous contrast is preferred to give the best anatomic detail of the kidneys. Renal ultrasonography is not recommended because it may not detect some tumors due to small size or because of similar echogenicity of BHD-associated hybrid oncocytic or chromophobe renal tumors to the surrounding renal parenchyma. Once a renal tumor is identified, the patient is monitored closely until the tumor reaches 3 cm in maximum dimension, at which point surgical intervention is recommended. Since BHD syndrome patients are at risk for developing multiple tumors, and therefore, may undergo repeat surgeries during their lifetime, nephron sparing surgical procedures are optimal to conserve as much normal kidney parenchyma as possible. Cryotherapy or radiofrequency ablation can complicate future surgical procedures; hence, these approaches are not recommended for BHD syndrome patient management unless the patient is a poor surgical candidate [93].

Conclusion

In the 16 years since germline mutations in the novel tumor suppressor gene *FLCN* were identified as causative for BHD syndrome, we have expanded our knowledge of the BHD clinical phenotype and our understanding of the *FLCN* mutation spectrum. Through the development and study of a number of *FLCN*-deficient in vitro and in vivo models, significant advancements have been made in our understanding of the cellular pathways and processes in which FLCN may have a functional role (Fig. 7.5; extensively reviewed in Schmidt et al. [94]).

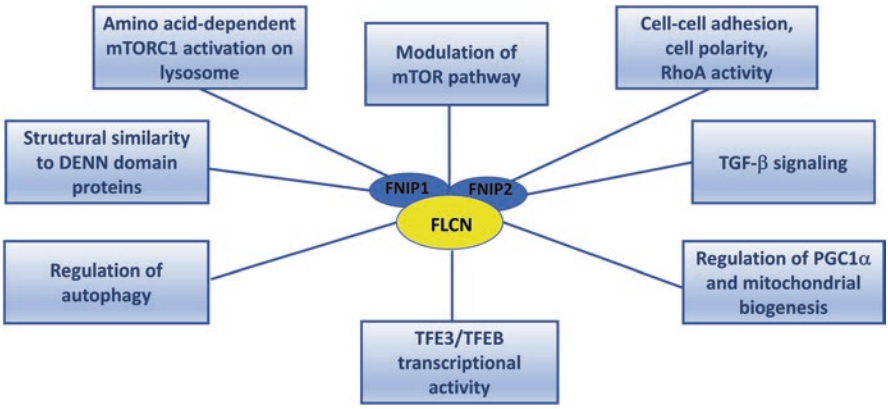

Fig. 7.5 Molecular pathways and cellular processes in which FLCN may have a functional role. (Adapted from Schmidt LS, Linehan WM [77])

However, details remain elusive as to the exact mechanisms underlying pulmonary cyst formation and kidney tumor development. Further studies are needed to identify biomarkers prognostic for more aggressive kidney cancer and to inform therapeutic drug design, and to predict those BHD syndrome-affected individuals who will be most at risk for developing pneumothoraces. Physicians need to be on high alert for the clinical manifestations and patient/family histories that would lead to suspicion for BHD syndrome. If warranted, they should recommend *FLCN* genetic diagnostic testing, and if positive, set up appropriate routine surveillance for kidney tumors and advise patients on ways to reduce recurrence of pneumothorax.

Key Learning Points

- Birt-Hogg-Dubé (BHD) syndrome is an autosomal dominant inherited disorder that predisposes at-risk individuals to develop benign cutaneous fibrofolliculomas, pulmonary cysts, recurrent spontaneous pneumothoraces, and bilateral multifocal kidney tumors.
- Germline loss-of-function mutations in the *folliculin* (*FLCN*) gene are responsible for BHD syndrome.
- Loss of heterozygosity or somatic mutation of the remaining copy of the *FLCN* gene was demonstrated in kidney tumors that develop in animal models of BHD syndrome and in BHD syndrome patients confirming a tumor suppressor role for *FLCN*.
- Evidence is emerging that FLCN may function in a number of energy and nutrient sensing pathways including the AMPK-mTOR axis, PGC1α regulation and control of mitochondrial biogenesis, amino acid-dependent activation of mTOR on the lysosomes through Rag GTPases, and cell-cell adhesion through RhoA signaling.
- Pulmonary management of patients with BHD syndrome principally centers on treatment and secondary prevention of spontaneous pneumothorax; pleurodesis following an initial episode is recommended due to the high rate of ipsilateral recurrence.
- Individuals who inherit a pathogenic *FLCN* mutation are at lifelong risk for developing kidney tumors and therefore should undergo routine abdominal imaging to monitor for tumor development.

Acknowledgments This work was supported by the Intramural Research Program of the National Institutes of Health (NIH), National Cancer Institute (NCI), Center for Cancer Research. This project has been funded in part with Federal funds from the Frederick National Laboratory for Cancer Research, NIH, under Contract HHSN261200800001E (LSS). The content of this publication does not necessarily reflect the views or policies of the Department of Health and Human Services, nor does mention of trade names, commercial products, or organizations imply endorsements by the US Government.

References

1. Nickerson ML, Warren MB, Toro JR, Matrosova V, Glenn GM, Turner ML, et al. Mutations in a novel gene lead to kidney tumors, lung wall defects, and benign tumors of the hair follicle in patients with the Birt-Hogg-Dubé syndrome. Cancer Cell. 2002;2:157–64.
2. Hornstein OP, Knickenberg M. Perifollicular fibromatosis cutis with polyps of the colon – a cutaneo-intestinal syndrome sui generis. Arch Dermatol Res. 1975;253:161–75.
3. Birt AR, Hogg GR, Dube WJ. Hereditary multiple fibrofolliculomas with trichodiscomas and acrochordons. Arch Dermatol. 1977;113:1674–7.
4. Binet O, Robin J, Vicart M, Ventura G, Beltzer-Garelly E. Fibromes perifolliculaires polypose colique familaile pneumothorax spontanes familiaux. Ann Dermatol Venereol. 1986;113:928–30.
5. Chung JY, Ramos-Caro FA, Beers B, Ford MJ, Flowers F. Multiple lipomas, angiolipomas, and parathyroid adenomas in a patient with Birt-Hogg-Dubé syndrome. Int J Dermatol. 1996;35:365–7.
6. Roth JS, Rabinowitz AD, Benson M, Grossman ME. Bilateral renal cell carcinoma in the Birt-Hogg-Dubé syndrome. J Am Acad Dermatol. 1993;29:1055–6.
7. Toro JR, Glenn G, Duray P, Darling T, Weirich G, Zbar B, et al. Birt-Hogg-Dubé syndrome: a novel marker of kidney neoplasia. Arch Dermatol. 1999;135:1195–202.
8. Zbar B, Alvord WG, Glenn GM, Turner M, Pavlovich CP, Schmidt LS, et al. Risk of renal and colonic neoplasms and spontaneous pneumothorax in the Birt-Hogg-Dubé syndrome. Cancer Epidemiol Biomark Prev. 2002;11:393–400.
9. Graham RB, Nolasco M, Peterlin B, Garcia CK. Nonsense mutations in folliculin presenting as isolated familial spontaneous pneumothorax in adults. Am J Respir Crit Care Med. 2005;172:39–44.
10. Painter JN, Tapanainen H, Somer M, Tukiainen P, Aittomäki K. A 4-bp deletion in the Birt-Hogg-Dubé gene (FLCN) causes dominantly inherited spontaneous pneumothorax. Am J Hum Genet. 2005;76:522–7.
11. Kunogi M, Kurihara M, Ikegami TS, Kobayashi T, Shindo N, Kumasaka T, et al. Clinical and genetic spectrum of Birt-Hogg-Dubé syndrome patients in whom pneumothorax and/or multiple lung cysts are the presenting feature. J Med Genet. 2010;47:281–7.
12. Benusiglio PR, Giraud S, Deveaux S, Méjean A, Correas JM, Joly D, et al. Renal cell tumour characteristics in patients with the Birt-Hogg-Dubé cancer susceptibility syndrome: a retrospective, multicentre study. Orphanet J Rare Dis. 2014;9:163.
13. Schmidt LS, Linehan WM. Molecular genetics and clinical features of Birt-Hogg-Dubé syndrome. Nat Rev Urol. 2015;12:558–69.
14. Schulz T, Hartschuh W. Birt-Hogg-Dubé syndrome and Hornstein-Knickenberg syndrome are the same: different sectioning technique as the cause of different histology. J Cutan Pathol. 1999;26:55–61.
15. Misago N, Kimura T, Narisawa Y. Fibrofolliculoma/trichodiscoma and fibrous papule (perifollicular fibroma/angiofibroma): a revaluation of the histopathological and immunohistochemical features. J Cutan Pathol. 2009;36:943–51.
16. Junkins-Hopkins JM1, Cooper PH. Multiple perifollicular fibromas: report of a case and analysis of the literature. J Cutan Pathol. 1994;21:467–71.
17. Shvartsbeyn M1, Mason AR, Bosenberg MW, Ko CJ. Perifollicular fibroma in Birt-Hogg-Dubé syndrome: an association revisited. J Cutan Pathol. 2012;39:675–9.
18. Gupta N, Kopras EJ, Henske EP, James LE, El-Chemaly S, Veeraraghavan S, et al. Spontaneous Pneumothoraces in patients with Birt-Hogg-Dube syndrome. Ann Am Thorac Soc. 2017;14(5):706–13.
19. Toro JR, Pautler SE, Stewart L, Glenn GM, Weinreich M, Toure O, et al. Lung cysts, spontaneous pneumothorax, and genetic associations in 89 families with Birt-Hogg-Dube syndrome. Am J Respir Crit Care Med. 2007;175(10):1044–53.

20. Park HJ, Park CH, Lee SE, Lee GD, Byun MK, Lee S, et al. Birt-Hogg-Dube syndrome prospectively detected by review of chest computed tomography scans. PLoS One. 2017;12(2):e0170713.
21. Skolnik K, Tsai WH, Dornan K, Perrier R, Burrowes PW, Davidson WJ. Birt-Hogg-Dube syndrome: a large single family cohort. Respir Res. 2016;17:22.
22. Tobino K, Hirai T, Johkoh T, Kurihara M, Fujimoto K, Tomiyama N, et al. Differentiation between Birt-Hogg-Dube syndrome and lymphangioleiomyomatosis: quantitative analysis of pulmonary cysts on computed tomography of the chest in 66 females. Eur J Radiol. 2012;81(6):1340–6.
23. Tomassetti S, Carloni A, Chilosi M, Maffe A, Ungari S, Sverzellati N, et al. Pulmonary features of Birt-Hogg-Dube syndrome: cystic lesions and pulmonary histiocytoma. Respir Med. 2011;105(5):768–74.
24. Johannesma PC, Reinhard R, Kon Y, Sriram JD, Smit HJ, van Moorselaar RJ, et al. Prevalence of Birt-Hogg-Dube syndrome in patients with apparently primary spontaneous pneumothorax. Eur Respir J. 2015;45(4):1191–4.
25. Toro JR, Wei MH, Glenn GM, Weinreich M, Toure O, Vocke CD, et al. BHD mutations, clinical and molecular genetic investigations of Birt-Hogg-Dubé syndrome: a new series of 50 families and a review of published reports. J Med Genet. 2008;45:321–31.
26. Schmidt LS, Nickerson ML, Warren MB, Glenn GM, Toro JR, Merino MJ, et al. Germline BHD-mutation spectrum and phenotype analysis of a large cohort of families with Birt-Hogg-Dubé syndrome. Am J Hum Genet. 2005;76:1023–33.
27. Houweling AC, Gijezen LM, Jonker MA, van Doorn MBA, Oldenburg RA, van Spaendonck-Zwarts, et al. Renal cancer and pneumothorax risk in Birt-Hogg-Dubé syndrome; an analysis of 115 FLCN mutation carriers from 35 BHD families. Br J Cancer. 2011;105:1912–9.
28. Furuya M, Yao M, Tanaka R, Nagashima Y, Kuroda N, Hasumi H, et al. Genetic, epidemiologic and clinicopathologic studies of Japanese Asian patients with Birt-Hogg-Dubé syndrome. Clin Genet. 2016;90:403–12.
29. Pavlovich CP, Walther MM, Eyler RA, Hewitt SM, Zbar B, Linehan WM, et al. Renal tumors in the Birt-Hogg-Dubé syndrome. Am J Surg Pathol. 2002;26:1542–52.
30. Liu V, Kwan T, Page EH. Parotid oncocytoma in the Birt-Hogg-Dubé syndrome. J Am Acad Dermatol. 2000;43:1120–2.
31. Maffé A, Toschi B, Circo G, Giachino D, Giglio S, Rizzo A, et al. Constitutional FLCN mutations in patients with suspected Birt-Hogg-Dubé syndrome ascertained for non-cutaneous manifestations. Clin Genet. 2011;79:345–54.
32. Lindor NM, Kasperbauer J, Lewis JE, Pittelkow M. Birt-Hogg-Dubé syndrome presenting as multiple oncocytic parotid tumors. Hered Cancer Clin Pract. 2012;10:13.
33. Kluger N1, Giraud S, Coupier I, Avril MF, Dereure O, Guillot B, et al. Birt-Hogg-Dubé syndrome: clinical and genetic studies of 10 French families. Br J Dermatol. 2010;162:527–37.
34. Rongioletti F, Hazini R, Gianotti G, Rebora A. Fibrofolliculomas, trichodiscomas and achrocordons (Birt-Hogg-Dubé) associated with intestinal polyposis. Clin Exp Dermatol. 1989;14:72–4.
35. Le Guyadec T, Dufau JP, Poulain JF, Vaylet F, Grossin M, et al. Multiple trichodiscomas associated with colonic polyposis. Ann Dermatol Venereol. 1998;125:717–9.
36. Nahorski MS, Lim DH, Martin L, Gille JJ, McKay K, Rehal PK, et al. Investigation of the Birt-Hogg-Dubé tumour suppressor gene (FLCN) in familial and sporadic colorectal cancer. J Med Genet. 2010;47:385–90.
37. Vernooij M, Claessens T, Luijten M, van Steensel MA, Coull BJ. Birt-Hogg-Dubé syndrome and the skin. Familial Cancer. 2013;12:381–5.
38. Agarwal PP, Gross BH, Holloway BJ, Seely J, Stark P, Kazerooni EA. Thoracic CT findings in Birt-Hogg-Dube syndrome. AJR Am J Roentgenol. 2011;196(2):349–52.
39. Tobino K, Gunji Y, Kurihara M, Kunogi M, Koike K, Tomiyama N, et al. Characteristics of pulmonary cysts in Birt-Hogg-Dube syndrome: thin-section CT findings of the chest in 12 patients. Eur J Radiol. 2011;77(3):403–9.

40. Gupta N, Meraj R, Tanase D, James LE, Seyama K, Lynch DA, et al. Accuracy of chest high-resolution computed tomography in diagnosing diffuse cystic lung diseases. Eur Respir J. 2015;46(4):1196–9.
41. Butnor KJ, Guinee DG Jr. Pleuropulmonary pathology of Birt-Hogg-Dube syndrome. Am J Surg Pathol. 2006;30(3):395–9.
42. Furuya M, Tanaka R, Koga S, Yatabe Y, Gotoda H, Takagi S, et al. Pulmonary cysts of Birt-Hogg-Dube syndrome: a clinicopathologic and immunohistochemical study of 9 families. Am J Surg Pathol. 2012;36(4):589–600.
43. Kumasaka T, Hayashi T, Mitani K, Kataoka H, Kikkawa M, Tobino K, et al. Characterization of pulmonary cysts in Birt-Hogg-Dube syndrome: histopathological and morphometric analysis of 229 pulmonary cysts from 50 unrelated patients. Histopathology. 2014;65(1):100–10.
44. Kluijt I, de Jong D, Teertstra HJ, Axwijk PH, Gille JJ, Bell K, et al. Early onset of renal cancer in a family with Birt-Hogg-Dubé syndrome. Clin Genet. 2009;75:537–43.
45. Menko FH, van Steensel MA, Giraud S, Friis-Hansen L, Richard S, Ungari S, et al.; European BHD Consortium. Birt-Hogg-Dubé syndrome: diagnosis and management. Lancet Oncol. 2009;10:1199–206.
46. Gupta N, Seyama K, McCormack FX. Pulmonary manifestations of Birt-Hogg-Dube syndrome. Familial Cancer. 2013;12(3):387–96.
47. Khoo SK, Bradley M, Wong FK, Hedblad MA, Nordenskjold M, Teh BT. Birt-Hogg-Dubé syndrome: mapping of a novel hereditary neoplasia gene to chromosome 17p12-q11.2. Oncogene. 2001;20:5239–42.
48. Schmidt LS, Warren MB, Nickerson ML, Weirich G, Matrosova V, Toro JR, et al. Birt-Hogg-Dubé syndrome, a genodermatosis associated with spontaneous pneumothorax and kidney neoplasia, maps to chromosome 17p11.2. Am J Hum Genet. 2001;69:876–82.
49. Leter EM, Koopmans AK, Gille JJ, van Os TA, Vittoz GG, David EF, et al. Birt-Hogg-Dubé syndrome: clinical and genetic studies of 20 families. J Invest Dermatol. 2008;128:45–9.
50. Rossing M, Albrechtsen A, Skytte AB, Jensen UB, Ousager LB, Gerdes AM, et al. Genetic screening of the FLCN gene identify six novel variants and a Danish founder mutation. J Hum Genet. 2017;62:151–7.
51. Liu Y, Xu Z, Feng R, Zhan Y, Wang J, Li G, et al. Clinical and genetic characteristics of Chinese patients with Birt-Hogg-Dubé syndrome. Orphanet J Rare Dis. 2017;12:104.
52. Lim DH, Rehal PK, Nahorski MS, Macdonald F, Claessens T, Van Geel M, et al. A new locus-specific database (LSDB) for mutations in the folliculin (FLCN) gene. Hum Mutat. 2010;31:E1043–51.
53. Okimoto K, Sakurai J, Kobayashi T, Mitani H, Hirayama Y, Nickerson ML, et al. A germ-line insertion in the Birt-Hogg-Dubé (BHD) gene gives rise to the Nihon rat model of inherited renal cancer. Proc Natl Acad Sci U S A. 2004;101:2023–7.
54. Lingaas F, Comstock KE, Kirkness EF, Sorensen A, Aarskaug T, Hitte C, et al. A mutation in the canine BHD gene is associated with hereditary multifocal renal cystadenocarcinoma and nodular dermatofibrosis in the German Shepherd dog. Hum Mol Genet. 2003;12:3043–53.
55. Baba M, Furihata M, Hong SB, Tessarollo L, Haines DC, Southon E, et al. Kidney-targeted Birt-Hogg-Dubé gene inactivation in a mouse model: Erk1/2 and Akt-mTOR activation, cell hyperproliferation, and polycystic kidneys. J Natl Cancer Inst. 2008;100:140–54.
56. Chen J, Futami K, Petillo D, Peng J, Wang P, Knol J, et al. Deficiency of FLCN in mouse kidney led to development of polycystic kidneys and renal neoplasia. PLoS One. 2008;3:e3581.
57. Hasumi Y, Baba M, Ajima R, Hasumi H, Valera VA, Klein ME, et al. Homozygous loss of BHD causes early embryonic lethality and kidney tumor development with activation of mTORC1 and mTORC2. Proc Natl Acad Sci U S A. 2009;106:18722–7.
58. Vocke CD, Yang Y, Pavlovich CP, Schmidt LS, Nickerson ML, Torres-Cabala CA, et al. High frequency of somatic frameshift BHD gene mutations in Birt-Hogg-Dubé-associated renal tumors. J Natl Cancer Inst. 2005;97:931–5.

59. Yang Y, Padilla-Nash HM, Vira MA, Abu-Asab MS, Val D, Worrell R, et al. The UOK 257 cell line: a novel model for studies of the human Birt-Hogg-Dubé gene pathway. Cancer Genet Cytogenet. 2008;180:100–9.
60. Hong SB, Oh H, Valera VA, Stull J, Ngo DT, Baba M, et al. Tumor suppressor FLCN inhibits tumorigenesis of a FLCN-null renal cancer cell line and regulates expression of key molecules in TGF-beta signaling. Mol Cancer. 2010;9:160.
61. Koga S, Furuya M, Takahashi Y, Tanaka R, Yamaguchi A, Yasufuku K, et al. Lung cysts in Birt-Hogg-Dubé syndrome: histopathological characteristics and aberrant sequence repeats. Pathol Int. 2009;59:720–8.
62. van Steensel MA, Verstraeten VL, Frank J, Kelleners-Smeets NW, Poblete-Gutiérrez P, Marcus-Soekarman D, et al. Novel mutations in the BHD gene and absence of loss of heterozygosity in fibrofolliculomas of Birt-Hogg-Dubé patients. J Invest Dermatol. 2007;127:588–93.
63. Baba M, Hong SB, Sharma N, Warren MB, Nickerson ML, Iwamatsu A, et al. Folliculin encoded by the BHD gene interacts with a binding protein, FNIP1, and AMPK, and is involved in AMPK and mTOR signaling. Proc Natl Acad Sci U S A. 2006;103:15552–7.
64. Hasumi H, Baba M, Hong SB, Hasumi Y, Huang Y, Yao M, et al. Identification and characterization of a novel folliculin-interacting protein FNIP2. Gene. 2008;415:60–7.
65. Takagi Y, Kobayashi T, Shiono M, Wang L, Piao X, Sun G, et al. Interaction of folliculin (Birt-Hogg-Dubé gene product) with a novel Fnip1-like (FnipL/Fnip2) protein. Oncogene. 2008;27:5339–47.
66. Inoki K, Kim J, Guan KL. AMPK and mTOR in cellular energy homeostasis and drug targets. Annu Rev Pharmacol Toxicol. 2012;52:381–400.
67. Chen J, Huang D, Rubera I, Futami K, Wang P, Zickert P, et al. Disruption of tubular Flcn expression as a mouse model for renal tumor induction. Kidney Int. 2015;88:1057–69.
68. Hartman TR, Nicolas E, Klein-Szanto A, Al-Saleem T, Cash TP, Simon MC, et al. The role of the Birt-Hogg-Dubé protein in mTOR activation and renal tumorigenesis. Oncogene. 2009;28:1594–604.
69. Hudon V, Sabourin S, Dydensborg AB, Kottis V, Ghazi A, Paquet M, et al. Renal tumour suppressor function of the Birt-Hogg-Dubé syndrome gene product folliculin. J Med Genet. 2010;47:182–9.
70. Nookala RK, Langemeyer L, Pacitto A, Ochoa-Montano B, Donaldson JC, Blaszczyk BK, et al. Crystal structure of folliculin reveals a hidDENN function in genetically inherited renal cancer. Open Biol. 2012;2:120071.
71. Tsun ZY, Bar-Peled L, Chantranupong L, Zoncu R, Wang T, Kim C, et al. The folliculin tumor suppressor is a GAP for the RagC/D GTPases that signal amino acid levels to mTORC1. Mol Cell. 2013;52:495–505.
72. Petit CS, Roczniak-Ferguson A, Ferguson SM. Recruitment of folliculin to lysosomes supports the amino acid-dependent activation of Rag GTPases. J Cell Biol. 2013;202:1107–22.
73. Zoncu R1, Efeyan A, Sabatini DM. mTOR: from growth signal integration to cancer, diabetes and ageing. Nat Rev Mol Cell Biol. 2011;12:21–35.
74. Meng J, Ferguson SM. GATOR1-dependent recruitment of FLCN-FNIP to lysosomes coordinates Rag GTPase heterodimer nucleotide status in response to amino acids. J Cell Biol. 2018;217:2765–76.
75. Hong SB, Oh H, Valera VA, Baba M, Schmidt LS, et al. Inactivation of the FLCN tumor suppressor gene induces TFE3 transcriptional activity by increasing its nuclear localization. PLoS One. 2010;5:e15793.
76. Wada S, Neinast M, Jang C, Ibrahim YH, Lee G, Babu A, et al. The tumor suppressor FLCN mediates an alternate mTOR pathway to regulate browning of adipose tissue. Genes Dev. 2016;30:2551–64.
77. Kennedy JC, Khabibullin D, Hougard T, Nijmeh J, Shi W, Henske EP. Loss of FLCN inhibits canonical WNT signaling via TFE3. Hum Mol Genet. 2019;28(19):3270–81.

78. Klomp JA, Petillo D, Niemi NM, Dykema KJ, Chen J, Yang XJ, et al. Birt-Hogg-Dubé renal tumors are genetically distinct from other renal neoplasias and are associated with up-regulation of mitochondrial gene expression. BMC Med Genet. 2010;3:59.
79. Hasumi H, Baba M, Hasumi Y, Huang Y, Oh HB, Hughes RM, et al. Regulation of mitochondrial oxidative metabolism by tumor suppressor FLCN. J Natl Cancer Inst. 2012;104:1750–64.
80. Dunlop EA, Seifan S, Claessens T, Behrends C, Kamps MA, Rozycka E, et al. FLCN, a novel autophagy component, interacts with GABARAP and is regulated by ULK1 phosphorylation. Autophagy. 2014;10:1749–60.
81. Possik E, Jalali Z, Nouet Y, Yan M, Gingras MC, Schmeisser K, et al. Folliculin regulates ampk-dependent autophagy and metabolic stress survival. PLoS Genet. 2014;10:e1004273.
82. Medvetz DA, Khabibullin D, Hariharan V, Ongusaha PP, Goncharova EA, Schlechter T, et al. Folliculin, the product of the Birt-Hogg-Dubé tumor suppressor gene, interacts with the adherens junction protein p0071 to regulate cell-cell adhesion. PLoS One. 2012;7:e47842.
83. Nahorski MS, Seabra L, Straatman-Iwanowska A, Wingenfeld A, Reiman A, Lu X, et al. Folliculin interacts with p0071 (plakophilin-4) and deficiency is associated with disordered RhoA signalling, epithelial polarization and cytokinesis. Hum Mol Genet. 2012;21:5268–79.
84. Sebbagh M, Santoni MJ, Hall B, Borg JP, Schwartz MA. Regulation of LKB1/STRAD localization and function by E-cadherin. Curr Biol. 2009;19:37–42.
85. Goncharova EA, Goncharov DA, James ML, Atochina-Vasserman EN, Stepanova V, Hong SB, et al. Folliculin controls lung alveolar enlargement and epithelial cell survival through E-cadherin, LKB1, and AMPK. Cell Rep. 2014;7:412–23.
86. Kennedy JC, Khabibullin D, Henske EP. Mechanisms of pulmonary cyst pathogenesis in Birt-Hogg-Dubé syndrome: the stretch hypothesis. Semin Cell Dev Biol. 2016;52:47–52.
87. Johannesma PC, Houweling AC, van Waesberghe JH, van Moorselaar RJ, Starink TM, Menko FH, et al. The pathogenesis of pneumothorax in Birt-Hogg-Dubé syndrome: a hypothesis. Respirology. 2014;19:1248–50.
88. Farrant PB, Emerson R. Letter: hyfrecation and curettage as a treatment for fibrofolliculomas in Birt-Hogg-Dube syndrome. Dermatol Surg. 2007;33:1287–8.
89. Gambichler T, Wolter M, Altmeyer P, Hoffman K. Treatment of Birt-Hogg-Dubé syndrome with erbium: YAG laser. J Am Acad Dermatol. 2000;43(5 Pt 1):856–8.
90. Mizobuchi T, Kurihara M, Ebana H, Yamanaka S, Kataoka H, Okamoto S, et al. A total pleural covering of absorbable cellulose mesh prevents pneumothorax recurrence in patients with Birt-Hogg-Dube syndrome. Orphanet J Rare Dis. 2018;13(1):78.
91. Johannesma PC, van de Beek I, van der Wel JW, Paul MA, Houweling AC, Jonker MA, et al. Risk of spontaneous pneumothorax due to air travel and diving in patients with Birt-Hogg-Dube syndrome. Springerplus. 2016;5(1):1506.
92. British Thoracic Society Fitness to Dive Group SotBTSSoCC. British Thoracic Society guidelines on respiratory aspects of fitness for diving. Thorax. 2003;58(1):3–13.
93. Stamatakis L, Metwalli AR, Middelton LA, Linehan WM. Diagnosis and management of BHD-associated kidney cancer. Familial Cancer. 2013;12:397–402.
94. Schmidt LS, Linehan WM. FLCN: the causative gene for Birt-Hogg-Dubé syndrome. Gene. 2018;640:28–42.

Chapter 8
Lymphoid Interstitial Pneumonia and Follicular Bronchiolitis

Kristin B. Highland and Augustine S. Lee

Abbreviations

AIDS	acquired immune deficiency syndrome
BAL	bronchoalveolar lavage
CVID	common variable immunoglobulin deficiency
DILS	diffuse infiltrative lymphocytic syndrome
FB	follicular bronchiolitis
GLILD	granulomatous-lymphocytic interstitial lung disease
GPA	granulomatosis with polyangiitis
HIV	human immunodeficiency virus
HRCT	high-resolution chest computed tomography
IPAF	interstitial pneumonia with autoimmune features
LDH	lactate dehydrogenase
LIP	lymphoid interstitial pneumonia
NLH	nodular lymphoid hyperplasia
PFT	pulmonary function test
RA	rheumatoid arthritis
SS	Sjögren's syndrome

K. B. Highland (✉)
Respiratory Institute, Cleveland Clinic, Cleveland, OH, USA
e-mail: highlak@ccf.org

A. S. Lee
Mayo Clinic, Jacksonville, FL, USA

N. Gupta et al. (eds.), *Diffuse Cystic Lung Diseases*, Respiratory Medicine,
https://doi.org/10.1007/978-3-030-63365-3_8

Introduction

Follicular bronchiolitis (FB) and lymphoid interstitial pneumonia (LIP) represent a pathophysiological continuum of lymphocytic infiltration from hyperplasia of bronchus-associated lymphoid tissue to cellular expansion of the interstitium with fibrosis [1]. In other words, LIP is a clinicopathologic term that describes diffuse involvement of the lung parenchyma by reactive pulmonary lymphoid tissue, whereas FB refers to a pattern of lymphoid follicular hyperplasia centered on airways, vessels, and interlobular septa consistent with a lymphatic distribution [2]. Although LIP can be difficult to distinguish from FB, we will review the clinical, radiologic, and pathologic presentation of both entities in this continuum. We will also review what little is known regarding their etiopathogenesis and treatment.

Lymphoid Interstitial Pneumonia

LIP was first described by Carrington and Liebow in 1966 [3]. It is a benign lymphoproliferative disorder that is characterized by diffuse infiltration of small mature lymphocytes, plasma cells, and histiocytes that spread diffusely into the alveolar septae.

Clinical Presentation

LIP is an uncommon disorder that is rarely idiopathic; rather, it is thought to be an expression of systemic immunologic disorders in the lung [4]. The diagnosis of LIP should be considered in anyone with lung cysts and an immunologic abnormality (Table 8.1). A thorough evaluation for an underlying systemic condition, especially autoimmune and immunodeficiency states, should be undertaken after a radiological or histopathological diagnosis of LIP is established [5].

LIP has a bimodal distribution. In children less than 13, LIP is generally associated with human immunodeficiency virus (HIV) and is an acquired immunodeficiency syndrome (AIDS)-defining illness [6]. Whereas in adults, LIP most commonly affects women in the fourth to sixth decade with an underlying autoimmune disorder or immunodeficiency [7, 8]. The female to male prevalence in adults is 2:1 [8]. Most non-HIV adults presenting with LIP are white [8], whereas in the context of HIV, LIP is more commonly seen in those of black African or Afro-Caribbean origin, particularly those from Haiti [9].

Table 8.1 Clinical and radiologic features of follicular bronchiolitis and lymphoid interstitial pneumonia

	Follicular bronchiolitis	Lymphoid interstitial pneumonia
Common associations	**Immune deficiencies** Congenital CVID HIV **Connective tissue disorders** SS RA **Interstitial pneumonias** Hypersensitivity pneumonitis LIP NSIP	**Immune deficiencies** Congenital CVID HIV **Connective tissue disorders** SS RA SLE **Interstitial pneumonias** IPAF **Viruses** EBV HIV HHV-8 Hepatitis B Hepatitis C
Pulmonary function test	Obstructive, reduced FEF25–75 Air trapping Diffusion limitation Restriction Mixed, nonspecific, or normal	Diffusion limitation Restriction
Nodules	1–3 mm common, >12 mm uncommon Centrilobular, tree-in-bud Peribronchial Ground-glass nodules	Mixed, nonspecific, or normal Micronodules, but up to 2 cm Centrilobular, subpleural, perilymphatic Ground-glass nodules
Airways	Bronchial wall thickening Bronchiolectasis Mosaicism, air trapping	Bronchial wall thickening
Cysts	Rounded or oval 5 mm to 5 cm Diffuse or basilar Perivascular, internal septation	Round, thin walled 5 mm to 5 cm <10% of parenchyma Present in 60%–80% Occur randomly in all lung zones Peribronchovascular
Septal/interstitial abnormality	Minimal or none unless coexisting with another pattern	Basilar reticulation Honeycombing rare Present in approximately 65%

CVID common variable immune deficiency, *HIV* human immunodeficiency virus, *EBV* Epstein-Barr virus; *HHV-8* human gammaherpesvirus 8, *RA* rheumatoid arthritis, *SS* Sjögren's syndrome, *SLE* systemic lupus erythematosus, *LIP* lymphoid interstitial pneumonia, *NSIP* nonspecific interstitial pneumonia, *IPAF* interstitial pneumonia with autoimmune features, *FEF25–75* forced expiratory flow at 25-75%, *mm* millimeter, *cm* centimeter

Patients may have constitutional symptoms including fevers, chills, night sweats, weight loss, and fatigue [7, 10]. Patients may also present with pleuritic chest pain possibly indicating a pneumothorax [11]. On examination, patients may have bibasilar end inspiratory crackles [12], or the chest may be silent as it often is in children. Clubbing of the fingers and toes frequently occurs in children, but may not be present in adults [13–15]. Splenomegaly is commonly associated with LIP in the setting of common variable immune deficiency (CVID) [16]. When LIP occurs in the setting of HIV, it may be associated with other features of diffuse infiltrative lymphocytic syndrome (DILS) including xerophthalmia and xerostomia, nontender parotid and salivary gland involvement, widespread lymphadenopathy, hepatosplenomegaly, or discomfort after eating if lymphocytic gastritis is a feature. There may also be facial numbness or weakness caused by seventh cranial nerve palsy. Patients may also present neck stiffness and headache due to aseptic meningitis [9].

Pulmonary function may show a restrictive ventilatory defect with a reduced diffusion [17]. Approximately 80% of patients with LIP have serum dysproteinemias; most commonly hypergammaglobulinemia [8] but hypogammaglobulinemia can occur in the setting of CVID. The cause of this is unknown but likely reflects chronic systemic autoimmune inflammation [18]. Serum lactate dehydrogenase (LDH) may be elevated, but this is a nonspecific finding [9].

Associated Conditions

Many affected patients have immune dysregulation or an underlying autoimmune disease, and thus, LIP is thought to represent a nonspecific response to multiple stimuli or antigens [7, 19]. Tertiary lymphoid neogenesis, which is associated with chronic inflammatory conditions, is seen in the distinct B- and T-cell areas of cellular proliferation found in LIP [20, 21]. Although the specific immunologic pathogenesis for LIP is unknown, an immunologic pathogenesis is further supported by an association with major histocompatibility complex antigens [9] and the presence of immune complex deposition [22].

Viral Associations

Chronic antigenic stimulation as a cause of LIP is suggested by the association of several viruses (EBV, HIV, HHV-8, hepatitis B, hepatitis C) with LIP [19, 23]. Epstein-Barr virus (EBV) is frequently found in the lungs of children and some adults with LIP [24]. EBV infects B lymphocytes, inducing proliferation of these cells, and patients with various types of immunodeficiency are at increased risk for developing a sustained EBV-related proliferation response, resulting in B-cell lymphoproliferative disorders [25]. EBV is also often found in the lungs of children with LIP and AIDS [26], and the titers of EBV antibodies are significantly higher in adult patients with AIDS and LIP compared to AIDS patients without LIP [27]. The

predilection for EBV and/or HIV being associated with LIP in children is likely due to the presence of bronchus-associated lymphoid tissue, which is less commonly seen in healthy adult lungs [15]. Viral-related LIP may be associated with a cellular immune response against the viral antigen as CD8+ lymphocytes, in particular, are considered to play a major role in the pathology of LIP, with increased CD8+ lymphocytes found in BAL fluid [15].

Autoimmune Disease

Another hypothesis suggests that LIP is due to loss of self-tolerance; a clonality of autoreactive T cells develops in response to lung antigens [28]. This is most evident by the strong association between LIP (and follicular bronchiolitis) and Sjögren's syndrome (SS): nearly 1% of adults with SS have LIP, and 30% to 60% of adults with LIP have SS [29–32]. LIP is also associated with a number of other autoimmune disorders including rheumatoid arthritis, systemic lupus erythematosus, autoimmune thyroid disease, primary biliary cirrhosis, myasthenia gravis, hemolytic and pernicious anemia, idiopathic thrombocytopenic purpura, erythrocyte sensitization syndrome, autoimmune glomerulonephritis, ulcerative colitis, celiac sprue, and diabetes mellitus [7, 8, 33–37]. Because of this strong association with autoimmune disease, the presence of LIP is one of the criteria for the new entity "interstitial pneumonia with autoimmune features (IPAF)," which describes patients with an idiopathic interstitial pneumonia and features suggestive of, but not definitive for, a connective tissue disease [38].

Immunodeficiencies

A polyclonal hypergammaglobulinemia is typically present when LIP is associated with an underlying autoimmune condition. However, LIP also occurs in the setting of other immunodeficiencies in addition to that seen in HIV/AIDS, and dysgammaglobulinemia syndrome is frequently linked to LIP.

LIP may be seen in approximately 10% of patients with CVID [16, 39]. Pathologic specimens from patients with CVID frequently contain both granulomatous and lymphoproliferative histopathologic patterns, otherwise called granulomatous-lymphocytic interstitial lung disease (GLILD). Lymphoid hyperplasia, follicular bronchiolitis, and LIP may "represent different ends of a spectrum of the same disease" [5, 16, 40]. The presence of GLILD decreases survival by 50% compared to patients with CVID and no evidence of GLILD [16].

LIP may occur after allogeneic hematopoietic stem cell transplantation, often following a viral infection or in the context of chronic graft versus host disease [41–43]. LIP may also be seen in the immunodeficiency syndrome ataxia-telangiectasia [44].

Other Associations

LIP has also been associated with Castleman disease, another rare lymphoproliferative disorder, which may result in systemic inflammatory symptoms, lymphadenopathy, and multi-organ involvement [45]. This has been reported primarily in patients with Asian ancestry [8, 53].

Radiology

The classic radiologic findings of LIP are bilateral interstitial infiltrates of the lower lobes. Alveolar and reticulonodular infiltrative patterns are also seen [8]. However, the chest radiograph is neither sensitive nor specific for LIP and may miss characteristic imaging findings that may be detected by high-resolution computed tomography (HRCT) of the chest.

HRCT typically shows a combination of ill-defined centrilobular and subpleural micronodules, ground-glass opacities, basilar reticulation, peribronchovascular interstitial thickening, and pulmonary cysts. Cysts are present in 60%–80% of patients and are thin walled and regular shaped (round) (Fig. 8.1). They vary in size and are often large (up to 3 cm) [46]. Typically, cysts comprise <10% of the lung parenchyma. They occur randomly in all lung zones but are often basilar and subpleural or along the peribronchovascular bundle [47]. Cysts are postulated to be a consequence of bronchiolar obstruction by lymphocytic infiltrates accompanied by postobstructive ectasia/dilatation [5]. Ischemia is another process that can induce cystic change in the lungs. The obstruction of small capillaries that supply the terminal bronchiole leads to necrosis of the airways and ischemic dilatation.

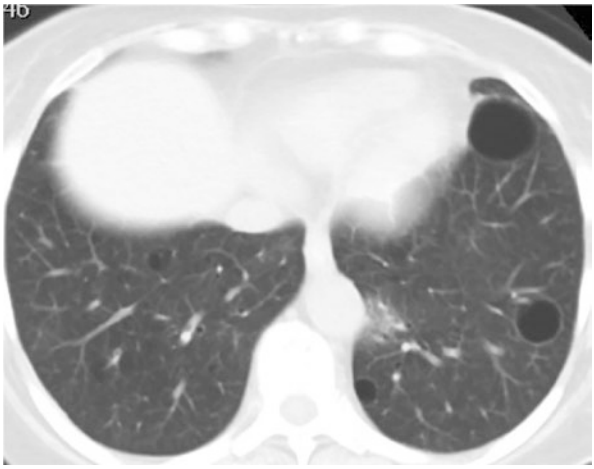

Fig. 8.1 High-resolution chest computed tomography of a patient with lymphoid interstitial pneumonia showing multiple thin-walled round cysts

Ground-glass opacities may represent areas of alveolar septal infiltrates, whereas centrilobular nodules represent foci of peribronchiolar infiltrates [13]. Although micronodules are characteristic, 40% of patients may have larger nodules up to 2 cm. Nodules are typically subpleural and in a perilymphatic distribution [48]. Ground-glass opacities and nodules may evolve into consolidation, architectural distortion, and honeycombing [9]. The reverse halo sign (atoll sign) may be seen [49]. Mediastinal and hilar adenopathy are also seen in approximately 65% of patients with LIP [13, 50–52]. The regular (as opposed to bizarre) shape of the cysts, presence of adenopathy, and septal thickening help to distinguish LIP from pulmonary Langerhans cell histiocytosis, whereas the presence of centrilobular nodules allows differentiation of LIP from lymphangioleiomyomatosis [47, 50].

Radiologic findings may wax and wane with a chronic, indolent course [5]. Radiologic findings that may be reversible include ground-glass attenuation, airspace consolidation, centrilobular small nodules, subpleural small nodules, large nodules, thickening of the interlobular septa, thickening of bronchovascular bundles, and lymph node enlargement [52], whereas cysts and architectural distortion may stay stable or progress on imaging follow-up. Often, new cysts develop in areas of previous centrilobular nodules [52].

Diagnosis

LIP should be considered when there is a characteristic HRCT in the correct clinical context. However, in the absence of a clearly diagnosed systemic disease, it is recommended that the diagnosis of LIP be confirmed histologically [2, 53].

Bronchoscopy is most useful for establishing an alternative diagnosis. Bronchoalveolar lavage (BAL) will reveal a lymphocytosis with a shift in favor of CD3 T lymphocytes, often with a mild increase in eosinophils and alveolar macrophages [33]. More importantly, the BAL should be negative for viral, bacterial, and fungal pathogens and neoplastic (clonal) cells [9].

As the yield of transbronchial biopsies is low in making a diagnosis of LIP, surgical lung biopsy (Fig. 8.2) is the procedure of choice. The macroscopic appearance of the lung may be normal, but histopathologic examination generally shows a diffuse interstitial inflammatory infiltrate composed of mature small lymphocytes, plasma cells, and occasional histiocytes [12]. This pattern is most characteristically present in the areas surrounding lymphatic channels, such as the alveolar septa, interstitial septa, peribronchovascular regions, and subpleural lung [7]. Alveolar aggregates of lymphoid tissue may cause bronchiolitis and small airway plugging leading to cysts [9]. The interstitial lymphoid cells are mainly T cells (CD3+) mixed with histiocytes and plasma cells, while B cells (CD20+) are more prominent in peribronchial germinal centers [54]. Scattered multinucleated giant cells or ill-formed granulomas are seen in the lymphoid infiltrates in about half of the cases [9, 12]. There is no evidence of vasculitis or necrosis. Hyperplasia of type II pneumocytes is commonly seen, and fibrosis may develop in more advanced cases [9, 12].

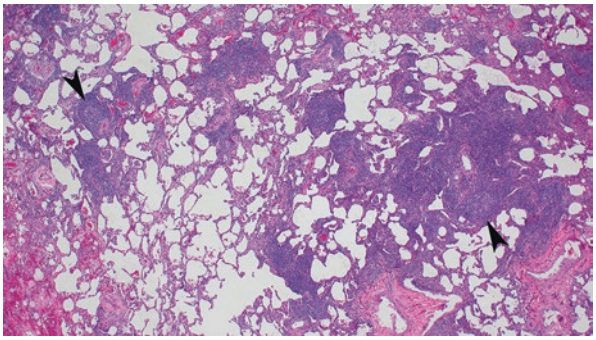

Fig. 8.2 Lymphoid interstitial pneumonia. Chronic lymphoplasmacytic inflammation extends from the bronchovascular area to the adjacent lobule. Germinal centers can be seen both around the airway and also in more distal areas of the lobule (arrowheads). Hematoxylin and eosin: 20×

The histopathologic differential diagnosis of LIP includes lymphomatoid granulomatosis, hypersensitivity pneumonitis, small lymphocytic lymphoma, and MALTomas [5, 18]. Immunohistochemical studies and flow cytometry should be performed in order to distinguish between the polyclonal populations of lymphocytes seen in LIP and a monotypic cell population seen in malignant lymphoproliferative disorders. In the past, LIP was considered a risk factor for the development of malignant lymphoma; however, many of the previously described cases were reclassified as lymphoma, and only a small number of definite LIP cases are felt to have undergone malignant transformation. Due to its association with immunocompromised states, stains for *Pneumocystis jiroveci* pneumonia (PJP) must be carried out in all patients.

Treatments

The natural history of LIP is variable, and it may often be stable for many months without specific treatment, although approximately one-third of cases may progress to pulmonary fibrosis and respiratory failure [12, 52]. The reported median survival times range from 5 years [5] to 11.5 years [53].

Patients with mild or indolent disease may not require therapy [55]. However, treatment should be considered in patients with disabling symptoms or a progressive decline in pulmonary function [39]. There are no randomized, placebo-controlled clinical trials to inform treatment decisions. Instead, treatment recommendations are based on case reports and case series. Approximately 50% to 60% of patients stabilize or improve with corticosteroids [8]. Suggested prednisone regimens range from 1 to 2 mg/kg/day for 2 to 12 weeks followed by a slow taper over another 6–12 weeks [56]. Variable improvement and treatment responses have also been reported with hydroxychloroquine, azathioprine, rituximab, cyclophosphamide, and

chlorambucil [8, 39, 55, 57–59]. There may be a role for gamma globulin therapy in patients with hypogammaglobulinemia [8, 60]. LIP associated with HIV often resolves with highly active antiretroviral drug treatment [61].

Follicular Bronchiolitis

Follicular bronchiolitis (FB) is considered one of the reactive lymphoid disorders that affect the lungs, along with nodular lymphoid hyperplasia (NLH) – which is synonymous with pseudolymphoma, and LIP [62].

Histologically, FB is characterized by nonneoplastic, polyclonal [63] lymphoid hyperplasia of the bronchus-associated lymphoid tissue (BALT). Lymphoid follicles containing reactive germinal centers lie in the walls of the small airways (<2 mm, non-cartilaginous) leading to progressive narrowing and eventual obliteration of the bronchioles. There is little to no extension to the alveolar septa and interstitium. BALT is itself not native to adult human airways and can be considered an ectopic lymphoid tissue that appears to develop as a result of antigenic stimulation [64]. This might suggest that FB reflects a pathologically exaggerated inflammatory response with BALT and lymphoplasmacytic infiltration in the susceptible host with an aberrant immune system (Table 8.1). NLH and LIP share the same reactive lymphoid and plasmacytic inflammation but are distinguished from each other based on the diffuseness and the predominant compartments of the lung affected. Whereas FB is primarily bronchiolocentric, LIP is characterized by more extensive interstitial involvement. However, these entities are not mutually exclusive, and FB may coexist with LIP and NLH, which can dominate over FB in the affected patient's clinical and radiographic presentation.

Clinical Presentation

Clinically, FB is most commonly associated with connective tissue diseases (CTD), particularly rheumatoid arthritis (RA) and Sjögren's syndrome (SS), as well as congenital and acquired immunodeficiencies such as HIV infection and CVID. Other associations include hypersensitivity reactions, diffuse panbronchiolitis, granulomatosis with polyangiitis (GPA), interstitial pneumonias, multicentric Castleman disease, infections, and bronchiectasis [65–68]. Infrequently, FB may exist in a "primary" idiopathic form without any identifiable associated conditions or derangements of the immune system [68]. However, as a result of overlapping clinical features, multiple clinical associations, and the need for a biopsy for definitive confirmation of FB, its precise prevalence and epidemiology remain unknown and are dependent on the underlying associated condition. For example, FB will be

more prevalent in the pediatric population among those with congenital immune deficiency syndromes, whereas it may be more prevalent later in life in adult women affected by SS. Most, but not all, series appear to indicate FB being identified after recognition of the associated disorder [65, 68], although FB as a presenting manifestation of SS has been described [78].

Attributable respiratory symptoms are commonly cough and dyspnea. However, they may be mild or, in some cases, asymptomatic. Among those with respiratory symptoms, evidence of small airway disease can be found in over half of the patients with SS [69, 70]; however, it is not clear how many may be asymptomatic or have only mild impairment [68, 69, 71, 72].

Pulmonary function testing (PFT) should include both lung volumes and diffusion capacity, in addition to the standard spirometry. As with other causes of bronchiolitis where the small airways are predominantly affected, obstructive physiology by classic definitions may not always be present as might be expected, but depending on the severity of the disease and the specific type of bronchiolitis, the PFTs may be normal, restricted, and nonspecific or have mixed defects [60, 68, 72, 73]. Lung volumes may demonstrate air trapping, and the diffusion capacity for carbon monoxide may be reduced, which may be the most sensitive indicator [68]. Among the newer techniques, impulse oscillometry may be a promising technique to detect peripheral airway disease, but is not readily available [74].

Radiology

Short of a lung biopsy, the most specific objective clues for FB are found radiographically. However, a plain chest radiograph is typically inadequate, as it may be normal. In the symptomatic patient suspected of, or at risk for, having bronchiolitis, HRCT imaging is required (Fig. 8.3). Micronodules ranging from 1 to 3 mm are universal, with up to half between 3 and 12 mm [75]. They can be greater than a centimeter but are less common prompting consideration for other processes. They are most commonly diffuse and less commonly basilar predominant or equally

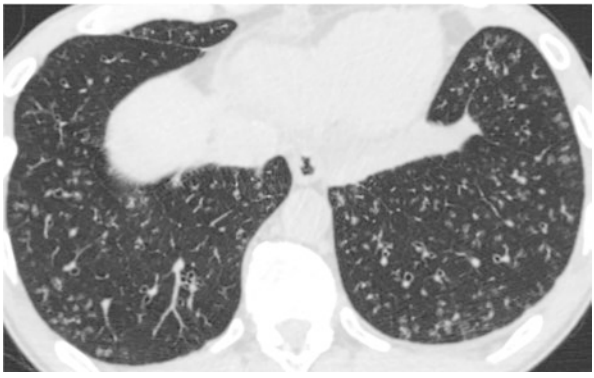

Fig. 8.3 High-resolution chest computed tomography of a patient with follicular bronchiolitis showing multiple solid and ground-glass nodules in a peribronchial distribution and tree-in-bud distribution. Bronchial wall thickening, bronciolectasis, and bronchiectasis are also present

distributed [75]. They can appear solid and also with ground-glass opacities, often in a centrilobular, tree-in-bud, or peribronchial distribution [75, 76]. Additional evidence of airway disease can be appreciated with bronchial wall thickening and dilation (i.e., bronchiolectasis), sometimes evolving into more obvious features of bronchiectasis. Indirect features of small airway disease typically include evidence of air trapping suggested by mosaicism that can be accentuated on expiratory CT imaging. Although this is fairly characteristic in constrictive bronchiolitis and bronchiolitis of hypersensitivity pneumonitis, it does not appear to be a common feature for follicular bronchiolitis [75, 77]. A more unique feature to FB and LIP among the different types of bronchiolitis and idiopathic interstitial pneumonias is that patients can present with diffuse cystic lung disease, particularly in the clinical context of SS [71, 78]. In a series of four patients with SS who presented with cystic lung disease, SSA was positive in all, and surgical lung biopsy in three showed two cases of FB and one case of LIP [78]. These rounded or oval cysts were described to be variable in size (5 mm to 5 cm), basilar predominant if not diffuse, perivascular, and sometimes with internal septations. The authors propose that these characteristic findings in established SS may obviate the need for a biopsy to confirm FB or LIP. However, lymphoma and amyloid can complicate cystic lung disease and should be considered in the context of associated nodularity [79, 80]. Cystic lung disease in FB may not be as common of a finding when associated with other disorders such as RA or in immunodeficiencies [75, 81], but is considered a common feature of LIP [52].

Diagnosis

Although the CT features in the appropriate clinical context may suggest the presence of FB, a formal diagnosis still requires a surgical lung biopsy (Fig. 8.4). The decision to do a biopsy may lie largely on the clinical context of whether alternative considerations that have important prognostic or treatment

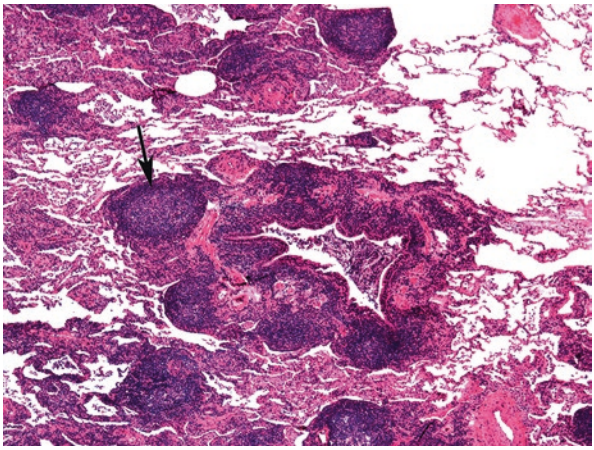

Fig. 8.4 Follicular bronchiolitis. Thoracoscopic wedge excision reveals chronic bronchiolitis with germinal centers (arrow) adjacent to small airways, features consistent with follicular bronchiolitis. Hematoxylin and eosin: 200×

implications are being considered, such as lymphoma or amyloid. Progressive disease may also prompt the need for definitive histologic diagnosis, especially if there is no specific context such as SS to guide the clinician. As surgical lung biopsy is associated with some morbidity and mortality, a period of observation may also be appropriate. Increasing expertise and availability of bronchoscopic transbronchial cryobiopsy may prove to be a more cost-effective, if not a safer, alternative to a surgical lung biopsy, particularly since the FB abnormalities are airway centered [82, 83]. The diagnostic yield may further improve with a multidisciplinary review.

If there is no clinical pressure to achieve a firm histological diagnosis, a confident working diagnosis might be achieved based on the clinical context and HRCT features, as described previously. Thus, it is imperative to evaluate thoroughly for clues to underlying connective tissue disease, immune deficiency states, hypersensitivity exposures, and other associated disorders.

Treatment

As most cases of FB are secondary to another primary disorder, treatment is often related to treating the underlying disease. Although no formal randomized controlled trials exist specifically targeting FB, there are observational data to support that treating the underlying immune derangement may be of benefit, particularly in acquired immunodeficiency syndromes such as HIV [84, 85] and CVID [86]. However, in some cases, treatment targeting the underlying disorder may be ineffective including in systemic inflammatory disorders such as in RA [73] and SS [29]. Many have treated empirically, regardless of the mechanism, with prednisone or cytotoxic agents including azathioprine, mycophenolate, and cyclophosphamide, with anecdotal benefit [64, 68, 71, 87]. As with the literature in diffuse panbronchiolitis and bronchiectasis, macrolides may be of help in idiopathic FB or possibly even when associated with other disorders [46, 68, 88–91]. Finally, there is rationale for, but little experience with, more specific targeted therapies such with rituximab and other biologic agents that target the lymphoplasmacytic inflammation [56].

Conclusion

Follicular bronchiolitis and lymphoid interstitial pneumonia represent a pathologic continuum arising from benign reactive lymphoid reaction of the BALT leading to formation of nodules and luminal narrowing and to expansion of the interstitium with fibrosis and, in some cases, cyst formation. Multiple disorders have been associated with LIP and FB including autoimmune disorders and immunodeficiencies, but they can also occur in an idiopathic form. Additionally, LIP and FB may be overshadowed by other features of these other disorders or by other injury patterns, such as interstitial pneumonias, that may coexist and

dominate the clinical and radiographic presentation. Diagnostic evaluation thus requires a careful evaluation for associated conditions, and given the variable patterns on pulmonary function testing and an insensitive chest radiograph, HRCT imaging is necessary to identify the suggestive features for FB and LIP. Cystic disease in well-established SS may be specific for FB and/or LIP, but a definitive diagnosis in most other contexts requires a surgical biopsy. Treatment should initially target any underlying conditions, and in refractory or idiopathic variants, prednisone, macrolides, cytotoxic medications, and biologic agents have been used with variable success.

Key Learning Points

- Follicular bronchiolitis and lymphoid interstitial pneumonia are characterized by polyclonal infiltration of the lung by mature lymphocytes. Follicular bronchiolitis is primarily bronchiolocentric, whereas lymphoid interstitial pneumonia extends into the interstitium with fibrosis.
- Follicular bronchiolitis and lymphoid interstitial pneumonia are rarely idiopathic and are generally associated with an immunodeficiency or autoimmune condition.
- Lymphoid interstitial pneumonia is an AIDS-defining illness in children.
- There is a strong association between lymphoid interstitial pneumonia and follicular bronchiolitis and Sjögren's syndrome with nearly 1% of Sjögren's syndrome patients having LIP or FB and 30%–60% of patients with LIP having Sjögren's syndrome.
- The diagnosis of LIP should be considered in anyone with lung cysts and an immunologic abnormality.
- The diagnosis of follicular bronchiolitis should be considered in anyone with micronodules in a peribronchial distribution with an underlying immunologic abnormality.
- Treatment of follicular bronchiolitis and lymphoid interstitial pneumonia is focused on treating the underlying/associated condition.

Conflicts of Interest Dr. Highland has received grants/contracts or honorarium from Actelion Pharmaceuticals, Bayer Healthcare, Boehringer Ingelheim, Eiger Pharmaceuticals, Genentech, Gilead Sciences, Reata Pharmaceuticals, and United Therapeutics.

References

1. Gupta N, Vassallo R, Wikenheiser-Brokamp, FX MC. Diffuse cystic lung disease. Part II. Am J Respir Crit Care Med. 2015;192(1):17–29.
2. Guinee DG Jr. Update on nonneoplastic pulmonary lymphoproliferative disorders and related entities. Arch Pathol Lab Med. 2010;134(5):691–701.
3. Carrington CB, Liebow AA. Lymphocytic interstitial pneumonia. Amer J Path. 1966;48:36a.
4. Takata T, Nagafuchi S, Tsuda H, Uehira K, Kondo S, Ueda A, et al. Lymphocytic interstitial pneumonia associated with a marked increase in monoclonal IgM-κ-type rheumatoid factor and serum CA19-9. Jpn J Med. 1991;30(1):92–6.

5. Swigris JJ, Berry GJ, Raffin TA, Kuschner WG. Lymphoid interstitial pneumonia: a narrative review. Chest. 2002;122:2150–64.
6. WHO Case definitions of HIV for surveillance and revised clinical staging and immunological classification of HIV-related disease in adults and children. WHO 2006. http://www.who.int/hiv/
7. Filipek MS, Thompson ME, Wang PL, Gosselin MV, L Primack S. Lymphocytic interstitial pneumonitis in a patient with systemic lupus erythematosus. J Thorac Imaging. 2004;19(3):200–3.
8. Strimlan CV, Rosenow EC III, Weiland LH, Brown LR. Lymphocytic interstitial pneumonitis: review of 13 cases. Ann Intern Med. 1978;88(5):616–21.
9. Doffman SR, Miller RF. Interstitial lung disease in HIV. Clin Chest Med. 2013;34(2):293–306.
10. Jawad H, Walker CM, Wu CC, Chung JH. Cystic interstitial lung diseases: recognizing the common and uncommon entities. Curr Probl Diagn Radiol. 2014;43(3):115–27.
11. Parker JS, Shellito J, Pei LA, Mason CM. Lymphocytic interstitial pneumonitis presenting as recurrent pneumothoraces. Chest. 1991;100(6):1733–5.
12. Koss MN, Hochholzer L, Langloss JM, Wehunt WD, Lazarus AA. Lymphoid interstitial pneumonia: Clinicopathological and immunopathological findings in 18 cases. Pathology. 1987;19(2):178–85.
13. Johkoh T, Műller NL, Pickford M, Hartman TE, Ichikado K, Akira M, et al. Lymphocytic interstitial pneumonia: thin-section CT findings in 22 patients. Radiology. 1999;212(2):567–72.
14. Zar HJ. Chronic lung disease in human immunodeficiency virus (HIV) infected children. Pediatr Pulmonol. 2008;43(1):1–10.
15. Saito M, Hatakeyama S, Wakabayashi Y, Yanagimoto S, Takemura T, Yotsuyanagi H. A pathologically proven case of adult-onset HIV-related lymphocytic interstitial pneumonia with acute exacerbation treated with steroid and antiretroviral therapy. J Infect Chemother. 2015;21(12):868–72.
16. Bates CA, Ellison MC, Lynch DA, Cool CD, Brown KK, Routes JM. Granulomatous-lymphocytic lung disease shortens survival in common variable immunodeficiency. J Allergy Clin Immunol. 2004;114(2):415–21.
17. Panchahbai TS, Farver C, Highland KB. Lymphocytic interstitial pneumonia. Clin Chest Med. 2016;37(3):463–74.
18. Dalvi V, Gonzalez EB, Lovett L. Lymphocytic interstitial pneumonitis (LIP) in Sjögren's syndrome: a case report and a review of the literature. Clin Rheumatol. 2007;26(8):1339–43.
19. Fishback N, Koss M. Update on lymphoid interstitial pneumonitis. Curr Opin Pulm Med. 1996;2(5):429–33.
20. Randall TD. Bronchus-associated lymphoid tissue (BALT0 structure and function). Adv Immunol. 2010;107:187–241.
21. Maglione PJ, Ko HZB, Beasley MB, Strauchen JA, Cunningham-Rundles C. Tertiary lymphoid neogenesis is a component of pulmonary lymphoid hyperplasia in patients with common variable immunodeficiency. J Allergy Clin Immunol. 2014;133(2):535–42.
22. DeCoteau WE, Tourville D, Ambrus M, Montes M, Adler R, Tomasi TB Jr. Lymphoid interstitial pneumonia and autoerythrocyte sensitization syndrome. Arch Intern Med. 1974;134(3):519–22.
23. Park JH, Levinson AI. Granulomatous-lymphocytic interstitial lung disease (GLILD) in common variable immunodeficiency (CVID). Clin Immunol. 2010;134(2):97–103.
24. Malamou-Mitsi V, Tsai M, Gal A, Koss MN, O'Leary TJ. Lymphoid interstitial pneumonia not associated with HIV infection: role of Epstein-Barr virus. Mod Pathol. 1992;5(5):487–91.
25. Mueller GA, Pickoff AS. Pediatric lymphocytic interstitial pneumonitis in an HIV-negative child with pulmonary Epstein-Barr virus infection. Pediatr Pulmonol. 2003;36(5):447–9.
26. Marzouk K, Corate L, Saleh S, Sharma OP. Epstein-Barr-virus-induced interstitial lung disease. Curr Opin Pulm Med. 2005;11(5):456–60.
27. Kramer MR, Saldana MJ, Ramos M, Pitchenik AE. High titers of Epstein-Barr virus antibodies in adult patients with lymphocytic interstitial pneumonitis associated with AIDS. Respir Med. 1992;86(1):49–52.

28. Levinson AI, Hopewell PC, Stites DP, Spitler LE, Fudenberg HH. Coexistent lymphoid interstitial pneumonia, pernicious anemia, and agammaglobulinemia. Arch Intern Med. 1976;136(2):213–6.
29. Shi JH, Liu HR, Xu WB, Feng RE, Zhang ZH, Tian XL, et al. Pulmonary manifestations of Sjögren's syndrome. Respiration. 2009;78:377–86.
30. Alkhayer M, McCann BG, Harrison BD. Lymphocytic interstitial pneumonitis in association with Sjogren's syndrome. Br J Dis Chest. 1988;82:306–9.
31. Sarkar PK, Patel N, Furie RA, Talwar A. Pulmonary manifestations of primary Sjögren's syndrome. Chest Duis Allied Sci. 2009;51:93–101.
32. Constantopoulos SH, Papadimitrioo CS, Moutsopoulos HM. Respiratory manifestations in primary Sjögren's syndrome. A clinical, functional and histologic study. Chest. 1985;88:226–9.
33. Khardori R, Eagleton LE, Soler NG. Lymphocytic interstitial pneumonitis in autoimmune thyroid disease. Am J Med. 1991;90(5):649–52.
34. Rodriguez-Rosin R, Pares A, Bruguera M, Coll J, Picado C, Agusti-Vidal A, et al. Pulmonary involvement in primary biliary cirrhosis. Thorax. 1981;36(3):208–12.
35. Schuyler MR, Niewochner DE, Inkley SR, Kohn R. Abnormal lung elasticity in juvenile diabetes mellitus. Am Rev Respir Dis. 1976;11391:37–41.
36. Garcia D, Young L. Lymphocytic interstitial pneumonia as a manifestation of SLE and secondary Sjogren's syndrome. BMJ Case Rep. 2013; https://doi.org/10.1136/bcr-2013-009598.
37. Benisch B, Peison B. The association of lymphocytic interstitial pneumonia and systemic lupus erythematosus. Mt Sinai J Med. 1979;46(4):398–01.
38. Fischer A, Antoniou KM, Brown KK, Cadranel J, Corte TJ, du Bois RM, et al. An official European Respiratory Society/American Thoracic Society research statement: interstitial pneumonia with autoimmune features. Eur Respir J. 2015;46(4):976–87.
39. Prasse A, Kayser G, Warnatz K. Common variable immunodeficiency-associated granulomatous and interstitial lung disease. Curr Opin Pulm Med. 2018;19(5):503–9.
40. Katzenstein A. Katzenstein's and Askin's surgical pathology of non-neoplastic lung disease. 3rd ed. Philadelphia: W. B. Saunders; 1997.
41. Bergeron A, Bengoufa D, Feuillet S, Meignin V, Peffault de Latour R, Rybojad M, et al. The spectrum of lung involvement in collagen vascular-like diseases following allogeneic hematopoietic stem cell transplantation. Medicine. 2011;90(2):146–57.
42. Kotloff RM, Alhya VN, Crawford SW. Pulmonary complications of solid organ and hematopoietic stem cell transplantation. Am J Respir Crit Care Med. 2004;170(1):22–48.
43. Bolaños-Meade J, Ioffe O, Hey JC, Vogelsang GB, Akpek G. Lymphocytic pneumonitis as the manifestation of acute graft-versus-host disease of the lung. Am J Hematol. 2004;79(2):132–5.
44. Tangsinmankong N, Wayne AS, Howenstine MS, Washington KR, Langston C, Gatti RA, et al. Lymphocytic interstitial pneumonitis, elevated IgM concentration, and hepatosplenomegaly in ataxia-telangiectasia. J Pediatr. 2001;138(6):939–41.
45. Chan KL, Lade S, Prince HM, Harrison SJ. Update and new approaches in the treatment of Castleman disease. J Blood Med. 2016;7:145–58.
46. Ichikawa Y, Kinoshita M, Koga T, Oizumi K, Fujimoto K, Hayabuchi N. Lung cyst formation in lymphocytic interstitial pneumonia: CT features. J Comput Assist Tomogr. 1994;18(5):745–8.
47. Baldi BG, Carvalho CRR, Dias OM, Marchiori E, Hochhegger B. Diffuse cystic lung diseases: differential diagnosis. J Bras Pneumol. 2017;43(2):140–9.
48. Becciolini V, Gudinchet F, Cheseaux JJ, Schnyder P. Lymphocytic interstitial pneumonia in children with AIDS: high-resolution /CT finings. Eur Radiol. 2001;11(6):1015–20.
49. Freeman MD, Grajo JR, Karamsadkar ND, Steffensen TS, Hazelton TR. Reversed halo sign on CT as a presentation of lymphocytic interstitial pneumonia. Radiol Case. 2013;7(10):51–6.
50. Grant LA, Babar J, Griffin N. Cysts, cavities, and honeycombing in multisystem disorders: differential diagnosis and findings on thin-section CT. Clin Radiol. 2009;64(4):439–48.
51. Desai SR, Nicholson AG, Stewart S, Twentyman OM, Flower CD, Hansell DM. Benign pulmonary lymphocytic infiltration and amyloidosis: computed tomographic and pathologic features in three cases. J Thorac Imaging. 1997;12(3):215–20.

52. Johkoh T, Ichikado K, Akira M, Honda O, Tomiyama N, Mihara N, et al. Lymphocytic interstitial pneumonia: follow-up CT findings in 14 patients. J Thorac Imaging. 2000;15(3):162–7.
53. Cha SL, Fessler MB, Cool CD, Schwarz ML, Brown KK. Lymphoid interstitial pneumonia: clinical features, associations and prognosis. Eur Respir J. 2006;28(2):364–9.
54. Nicholson AG, Wotherspoon TC, Diss DM, Hansell DM, Du Bois R, Sheppard MN, et al. Reactive pulmonary lymphoid disorders. Histopathology. 1995;26(5):405–12.
55. Parambil JG, Myers JL, Lindell RM, Matteson EL, Ryu JH. Interstitial lung disease in primary Sjögren's syndrome. Chest. 2006;130(5):1489–95.
56. Devauchelle-Pensecd V, Pennec Y, Morvan J, Pers JO, Daridon C, Jousse-Joulin S, et al. Improvement of Sjögren's syndrome after two infusions of rituximab (anti-CD20). Arthritis Rheum. 2007;57:310–7.
57. Schupp JC, Köhler T, Müller-Quernheim J. Usefulness of cyclophosphamide pulse therapy in interstitial lung diseases. Respiration. 2016;91:296–301.
58. Okada M, Suzuki K, Matsumoto M, Nakashima M, Nakanishi T, Takada K, et al. Intermittent intravenous cyclophosphamide pulse therapy for the treatment of active interstitial lung disease associated with collagen vascular diseases. Mod Rheumatol. 2007;17:131–6.
59. Swartz MA, Vivino FB. Dramatic reversal of lymphocytic interstitial pneumonitis in Sjögren's syndrome with rituximab. JCR J Clin Rheumatol. 2011;17:454.
60. Popa V. Lymphocytic interstitial pneumonia in common variable immunodeficiency. Ann Allergy. 1988;60:203–6.
61. Dufour V, Wislez M, Bergot E, Mayaud C, Cadranel J. Improvement of symptomatic human immunodeficiency virus-related lymphoid interstitial pneumonia in patients receiving highly active antiretroviral therapy. Clin Infect Dis. 2003;36:e127–30.
62. Poletti V, Ravaglia C, Tomassetti S, Gurioli C, Casoni G, Asioli S, et al. Lymphoproliferative lung disorders: clinicopathological aspects. Eur Respir Rev. 2013;22(130):427–36.
63. Tashiro K, Ohshima K, Suzumiya J, Yoneda S, Yahiro M, Sugihara M, et al. Clonality of primary pulmonary lymphoproliferative disorders; using in situ hybridization and polymerase chain reaction for immunoglobulin. Leuk Lymphoma. 1999;36(1–2):157–67.
64. Randall TD. Bronchus-associated lymphoid tissue (BALT) structure and function. Adv Immunol. 2010;107:187–241.
65. Yousem SA, Colby TV, Carrington CB. Follicular bronchitis/bronchiolitis. Hum Pathol. 1985;16(7):700–6.
66. Couture C, Colby TV. Histopathology of bronchiolar disorders. Semin Respir Crit Care Med. 2003;24(5):489–98.
67. Travis WD, Hoffman GS, Leavitt RY, Pass HI, Fauci AS. Surgical pathology of the lung in Wegener's granulomatosis. Review of 87 open lung biopsies from 67 patients. Am J Surg Pathol. 1991;15(4):315–33.
68. Aerni MR, Vassallo R, Myers JL, Lindell RM, Ryu JH. Follicular bronchiolitis in surgical lung biopsies: clinical implications in 12 patients. Respir Med. 2008;102(2):307–12.
69. Kakugawa T, Sakamoto N, Ishimoto H, Shimizu T, Nakamura H, Nawata A, et al. Lymphocytic focus score is positively related to airway and interstitial lung diseases in primary Sjogren's syndrome. Respir Med. 2018;137:95–102.
70. Kampolis CF, Fragkioudaki S, Mavragani CP, Zormpala A, Samakovli A, Moutsopoulos HM. Prevalence and spectrum of symptomatic pulmonary involvement in primary Sjogren's syndrome. Clin Exp Rheumatol. 2018.;36 Suppl;112(3):94–101.
71. Lu J, Ma M, Zhao Q, Meng F, Wang D, Cai H, et al. The clinical characteristics and outcomes of follicular bronchiolitis in Chinese adult patients. Sci Rep. 2018;8(1):7300.
72. Yuksekkaya R, Celikyay F, Yilmaz A, Arslan S, Inanir A, Inonu H, et al. Pulmonary involvement in rheumatoid arthritis: multidetector computed tomography findings. Acta Radiol. (Stockholm, Sweden: 1987. 2013;54(10):1138–49.
73. Devouassoux G, Cottin V, Liote H, Marchand E, Frachon I, Schuller A, et al. Characterisation of severe obliterative bronchiolitis in rheumatoid arthritis. Eur Respir J. 2009;33(5):1053–61.

74. McNulty W, Usmani OS. Techniques of assessing small airways dysfunction. Eur Clin Respir J. 2014;1:25898-http://dx.doi.org/10.3402/ecrj.v1.25898.
75. Howling SJ, Hansell DM, Wells AU, Nicholson AG, Flint JD, Muller NL. Follicular bronchiolitis: thin-section CT and histologic findings. Radiology. 1999;212(3):637–42.
76. Kang EY, Woo OH, Shin BK, Yong HS, Oh YW, Kim HK. Bronchiolitis: classification, computed tomographic and histopathologic features, and radiologic approach. J Comput Assist Tomogr. 2009;33(1):32–41.
77. Pipavath SJ, Lynch DA, Cool C, Brown KK, Newell JD. Radiologic and pathologic features of bronchiolitis. AJR Am J Roentgenol. 2005;185(2):354–63.
78. Gupta N, Wikenheiser-Brokamp KA, Fischer A, McCormack FX. Diffuse cystic lung disease as the presenting manifestation of Sjogren syndrome. Ann Am Thorac Soc. 2016;13(3):371–5.
79. Borie R, Wislez M, Antoine M, Copie-Bergman C, Thieblemont C, Cadranel J. Pulmonary mucosa-associated lymphoid tissue lymphoma revisited. Eur Respir J. 2016;47(4):1244–60.
80. Do KH, Lee JS, Seo JB, Song JW, Chung MJ, Heo JN, et al. Pulmonary parenchymal involvement of low-grade lymphoproliferative disorders. J Comput Assist Tomogr. 2005;29(6):825–30.
81. Weinman JP, Manning DA, Liptzin DR, Krausert AJ, Browne LP. HRCT findings of childhood follicular bronchiolitis. Pediatr Radiol. 2017;47(13):1759–65.
82. Lentz RJ, Fessel JP, Johnson JE, Maldonado F, Miller RF, Rickman OB. Transbronchial cryobiopsy can diagnose constrictive bronchiolitis in veterans of recent conflicts in the middle east. Am J Respir Crit Care Med. 2016;193(7):806–8.
83. Ussavarungsi K, Kern RM, Roden AC, Ryu JH, Edell ES. Transbronchial Cryobiopsy in diffuse parenchymal lung disease: retrospective analysis of 74 cases. Chest. 2017;151(2):400–8.
84. Rasmussen LD, Pedersen C, Madsen HD, Laursen CB. Follicular bronchiolitis in an HIV-infected individual on combination antiretroviral therapy with low CD4+ cell count but sustained viral suppression. BMJ Case Rep. 2017;2017:bcr2017221025.
85. Shipe R, Lawrence J, Green J, Enfield K. HIV-associated follicular bronchiolitis. Am J Respir Crit Care Med. 2013;188(4):510–1.
86. Tashtoush B, Memarpour R, Ramirez J, Bejarano P, Mehta J. Granulomatous-lymphocytic interstitial lung disease as the first manifestation of common variable immunodeficiency. Clin Respir J. 2018;12(1):337–43.
87. Romero S, Barroso E, Gil J, Aranda I, Alonso S, Garcia-Pachon E. Follicular bronchiolitis: clinical and pathologic findings in six patients. Lung. 2003;181(6):309–19.
88. Hayakawa H, Sato A, Imokawa S, Toyoshima M, Chida K, Iwata M. Bronchiolar disease in rheumatoid arthritis. Am J Respir Crit Care Med. 1996;154(5):1531–6.
89. Thalanayar PM, Holguin F. Follicular bronchiolitis in primary ciliary dyskinesia. Australas Med J. 2014;7(7):294–7.
90. Kobayashi H, Kanoh S, Motoyoshi K, Aida S. Tracheo-broncho-bronchiolar lesions in Sjogren's syndrome. Respirology. 2008;13(1):159–61.
91. Ichikawa Y, Ninomiya H, Koga H, Tanaka M, Kinoshita M, Tokunaga N, et al. Erythromycin reduces neutrophils and neutrophil-derived elastolytic-like activity in the lower respiratory tract of bronchiolitis patients. Am Rev Respir Dis. 1992;146(1):196–203.

Chapter 9
Amyloidosis and Immunoglobulin Deposition Disease

Misbah Baqir and Teng Moua

Abbreviations

AA	secondary amyloidosis
AL	light chain amyloidosis
ATTR	amyloidogenic transthyretin
CT	computed tomography
CTD	connective tissue disease
DLCO	diffusion capacity for carbon monoxide
FLC	free light chains
LCDD	light chain deposition disease
MGUS	monoclonal gammopathy of unknown significance
MM	multiple myeloma
SSA	senile systemic amyloidosis
TTR	transthyretin
WHO	World Health Organization

Amyloidosis

Introduction

Amyloidosis is a group of diseases characterized by the inappropriate folding and deposition of proteins in affected organs. The conversion of such proteins from their normal soluble forms to highly organized fibrillar aggregates called amyloid [1] culminates in the deposition of β-pleated (as opposed to normal alpha-helical) fibrous sheets in the extracellular space. Multiple types of proteins are capable of forming amyloid fibrils, but all share similar basic structures and histochemical

M. Baqir (✉) · T. Moua
Division of Pulmonary and Critical Care Medicine, Mayo Clinic, Rochester, MN, USA
e-mail: baqir.misbah@mayo.edu

N. Gupta et al. (eds.), *Diffuse Cystic Lung Diseases*, Respiratory Medicine,
https://doi.org/10.1007/978-3-030-63365-3_9

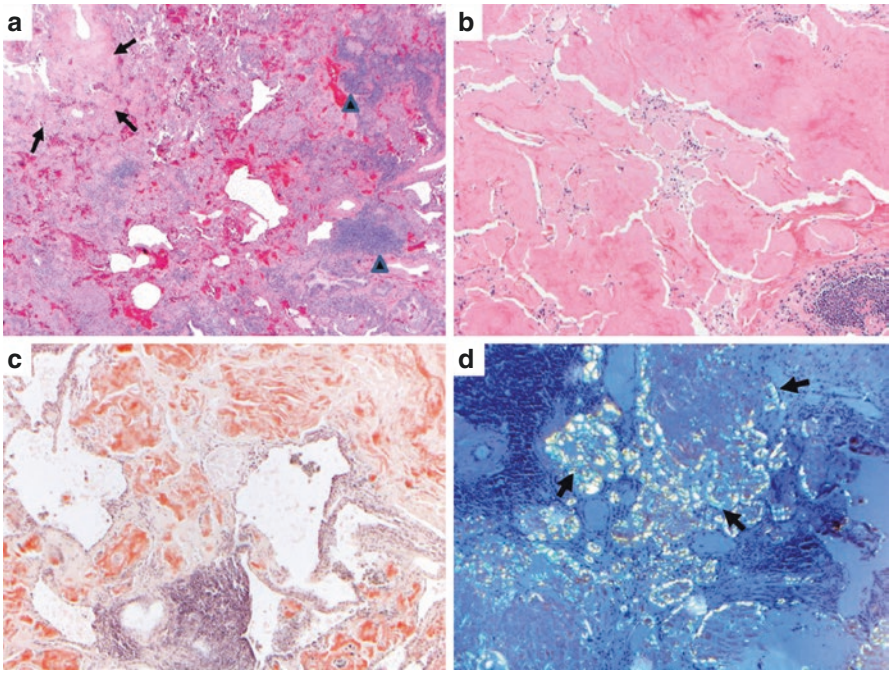

Fig. 9.1 Pulmonary amyloidosis in a 54-year-old female with longstanding Sjögren's syndrome and progressive cystic and nodular disease, who underwent resection of enlarging left lower lobe nodules. (**a**) H&E stain of amyloid deposition **(arrow)** and lymphoid aggregates **(arrowhead)** with lambda-restricted plasma cells consistent with MALT lymphoma (40×), (**b**) confluent amyloid deposition (100×), and (**c** and **d**) Congo red-stained section illuminated with plain and polarized light, respectively, revealing apple-green birefringence **(arrow)** (both 100×). (Courtesy of Dr. Joanne Yi, Department of Pathology, Mayo Clinic Rochester)

properties [2–5]. These complex structures confer resistance to proteolysis and an affinity for the diazo dye Congo red, which results in the characteristic apple-green birefringence seen under polarized light microscopy (see Figs. 9.1 and 9.2 for histopathologic case examples). These fibrillary deposits may then affect the structure and function of affected organs by mechanisms that are not clearly understood. Research from several laboratories has demonstrated that amyloidogenic light chains can be directly cytotoxic [6].

In 1993, the World Health Organization (WHO) classified amyloidosis based on two criteria, the identity of the precursor protein and whether the disease was primary or secondary to an underlying condition [7]. This classification schema is often extended to include patterns of organ involvement, rapidity of disease progression, and disease outcome (Table 9.1). Primary amyloidosis is caused by a clonal population of plasma cells and is often associated with monoclonal gammopathy of unknown significance (MGUS) or multiple myeloma (MM) that produces either monoclonal light chains of either the kappa (κ) or lambda (λ) subtypes. Light chain amyloidosis (AL) is the most common cause of amyloidosis, with a reported incidence of 8.9 per million person-years [8]. Secondary (AA) amyloidosis occurs in

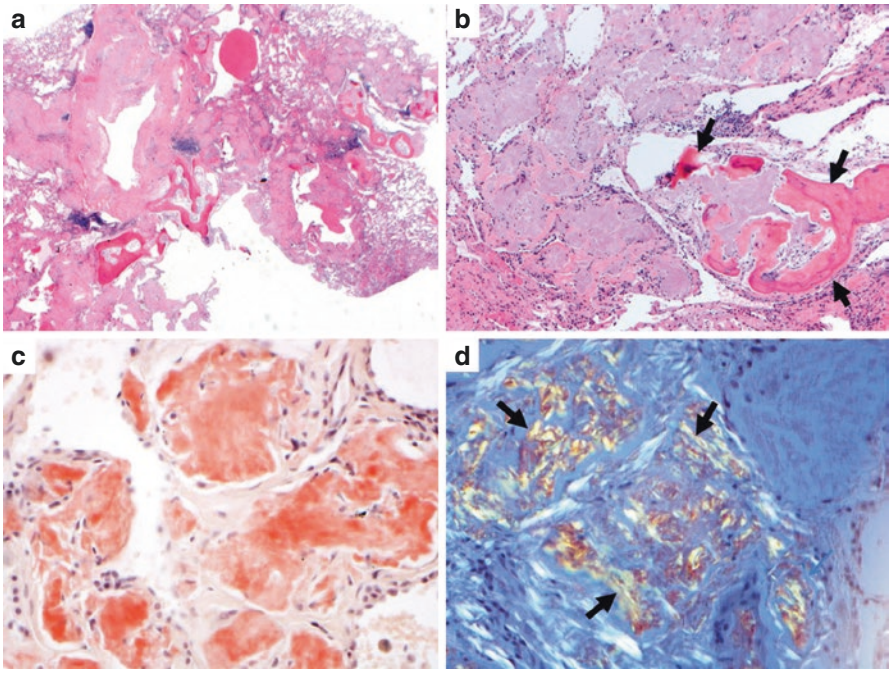

Fig. 9.2 Pulmonary amyloidoma associated with extranodal marginal zone MALT lymphoma in a 47-year-old female presenting with enlarging left lower lobe nodules. (**a**) H&E low-power view of amyloidoma (20×); (**b**) medium power (100×) view showing ossification within the amyloidoma **(arrow)**; (**c** and **d**) Congo red-stained section illuminated with plain and polarized light, respectively, revealing apple-green birefringence **(arrow)** (both 200×). (Courtesy of Dr. Joanne Yi, Department of Pathology, Mayo Clinic Rochester)

Table 9.1 Types of amyloidosis

Amyloid protein Subunit	Abbreviation	Clinical syndrome
Monoclonal light chain	AL	Systemic: primary amyloidosis, multiple myeloma, Waldenstrom's macroglobulinemia, lymphoma Localized: skin, lungs, larynx, bladder
Serum amyloid A	AA	Chronic inflammatory conditions or malignancy
Transthyretin wild type	SSA	Senile dementia and cardiomyopathy
Variant transthyretin	ATTR	Familial (mutant) cardiomyopathy and nervous system involvement
β2 microglobulin	Aβ2M	Dialysis-related disease affecting joints

the setting of chronic inflammatory conditions or malignancy. Long-term dialysis-related amyloidosis primarily affects periarticular tissues but can be systemic and is caused by deposition of β2 microglobulin. Transthyretin (TTR), a protein that transports thyroxine and retinol, is associated with a third form of the disease called senile systemic amyloidosis.

AL Amyloidosis

Diagnosis of AL amyloidosis is challenging as presentations may be variable and often mimic those of common disorders. A high index of suspicion is required in clinical scenarios that are encountered on an almost daily basis, such as nondiabetic nephrotic syndrome, nonischemic cardiomyopathy, hepatomegaly, or increased serum alkaline phosphatase in the setting of normal liver imaging [9]. Screening often begins with serum and urine immunofixation and immunoglobulin free light chain (FLC) assays [10–12]. If both immunofixation and FLC ratio are normal, AL amyloidosis is unlikely, and further evaluation should only be taken if clinical suspicion remains high [13]. Histopathologic confirmation is generally required to establish a definitive diagnosis (see Figs. 9.1 and 9.2). Bone marrow biopsy of the iliac crest combined with abdominal subcutaneous fat aspiration identifies amyloid deposits in 85% of patients [14, 15]. If both fat aspirate and bone marrow stain negative for amyloid, biopsy of clinically involved organs may be required. The next step after establishing diagnosis is the determination of local vs. systemic involvement.

Virtually, all patients with systemic AL amyloidosis require treatment at the time of diagnosis. This is often pursued and directed by an expert hematologist. Systemic amyloidosis is usually treated with bortezomib-based chemotherapy [16–18] or hematopoietic stem cell transplantation [19]. Systemic AL amyloidosis may involve multiple organs including the kidneys, heart, liver, nervous system, gastrointestinal tract, lymphoreticular system, and adrenal glands. Typical sites for localized amyloidosis include the skin [20], larynx [21], genitourinary tract [22], or lung. Pulmonary involvement in AL amyloidosis may include both vascular and parenchymal manifestations. AL amyloidosis has been reported in the walls of nearly all blood vessels at autopsy [23]. Extravascular lung involvement is seen in both localized and systemic AL disease and may be characterized as follows:

1. Diffuse interstitial opacities or alveolar-septal disease
2. Cystic lung disease
3. Nodular lung disease
4. Tracheobronchial disease
5. Mediastinal and hilar adenopathy
6. Pleural disease
7. Pulmonary hypertension

Pleural disease in the form of recurrent exudative and hemorrhagic pleural effusions has been described in case reports [24]. Effusions secondary to cardiac involvement with systemic amyloidosis have also been reported [25]. There are only a few case reports describing pulmonary arterial hypertension due to amyloidosis independent of interstitial lung disease or cardiac involvement [26, 27]. Diffuse infiltrates in the form of ground-glass opacities have been described as nonspecific additional findings on chest CT scans of patients with nodular or cystic amyloidosis [28, 29]. Mediastinal and hilar lymphadenopathy (in both systemic and localized amyloidosis) are common and may be associated with nodal calcification in

popcorn or, more rarely, egg shell patterns [30]. The presence of adenopathy should prompt a search for an underlying plasma cell dyscrasia [31–34].

Pulmonary-specific manifestations of systemic amyloidosis seem to be less apparent than those of other organ systems, including in autopsy cases where widespread amyloid deposition is found in the walls of alveoli and pulmonary blood vessels [23]. This suggests that clinically significant cardiac and renal involvement contribute more to immediate morbidity and mortality than associated pulmonary disease [35, 36]. A retrospective review of a large cohort found 138 of 492 (28%) cases of AL amyloid had clinical pulmonary findings, while only 9% of those had lone pulmonary disease in the absence of cardiac involvement [37].

Cystic Lung Disease

Zamora et al. [29] analyzed 187 cases of biopsy-proven amyloidosis and noted 21 with cystic lung disease. Cysts were described as thin-walled (<2 mm), multiple, bilateral, small (< 1 cm) to medium (1–2 cm) in size, and often in a peribronchovascular distribution with lower lobe predominance (see Fig. 9.3 for case example).

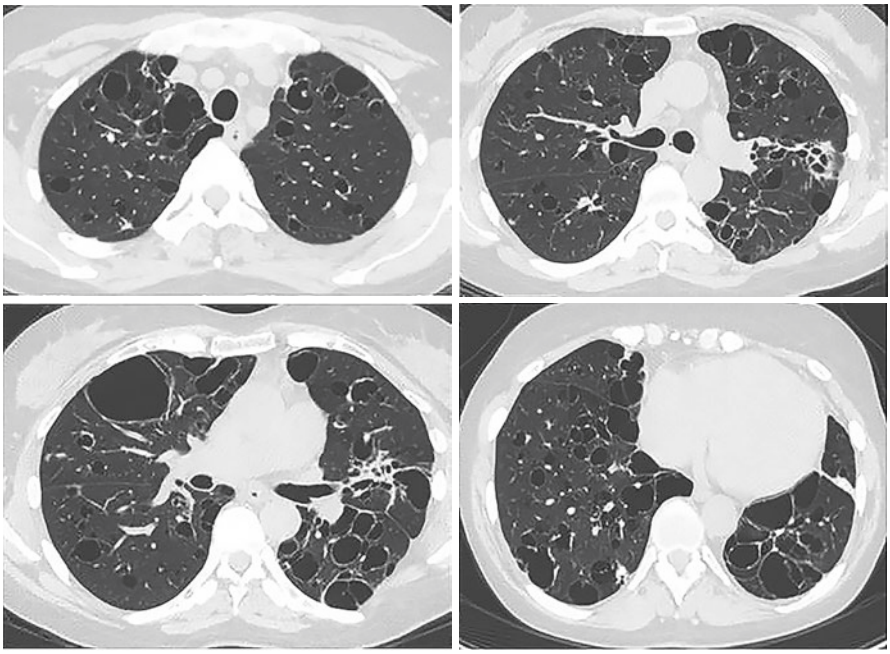

Fig. 9.3 Diffuse cystic lung disease in a 54-year-old female with longstanding Sjögren's syndrome and suspected lymphoid interstitial pneumonia (LIP). Radiologic findings progressed with enlargement of a left lower lobe nodule, which upon resection revealed pathologic features of both pulmonary amyloidoma and MALT lymphoma (see Fig. 9.1 for pathology). Patient was subsequently treated with rituximab, which produced a favorable response without evidence of relapse

Underlying autoimmune conditions, particularly Sjögren's syndrome, were described in this cohort though associations with rheumatoid arthritis, inclusion body myositis, and mixed connective tissue disease have also been reported [28, 29, 38]. In the series by Zamora et al., 81% had accompanying nodules with 33% being subsequently diagnosed with mucosa-associated lymphoid tissue (MALT) lymphoma [29]. The majority of cases associated with connective tissue disease or MALT lymphoma appeared to be focal disease involving only the lungs, though in a few cases such findings ultimately proved to represent manifestations of systemic disease [29, 38]. Baqir et al. described cystic and nodular lesions in amyloidosis associated with primary Sjögren's syndrome in eight patients, three of whom also subsequently developed MALT lymphoma [28].

Symptoms of cystic lung disease include cough and shortness of breath, though patients are often asymptomatic. Pulmonary function testing is frequently within normal limits but occasionally reveals obstruction and/or isolated reduction in diffusion capacity for carbon monoxide (DLCO) [29]. Cysts may remain stable or increase in size and number, but spontaneous radiologic resolution has not been reported [28, 29, 38].

Several theories have been suggested for the mechanism of cyst formation in amyloidosis. One involves inflammatory infiltration or amyloid deposition in the small airways, which results in airway narrowing with ball-valve effect and overinflation of distal airways with cyst development [39, 40]. Amyloid-mediated destruction of bronchoalveolar structures or capillaries [23] within the interstitium leading to ischemia and destructive remodeling of the alveolar walls has also been proposed.

Nodular Lung Disease

Nodular pulmonary amyloidosis is often a manifestation of localized AL amyloidosis but can also be seen in systemic disease. According to one study, amyloid chains differ in their composition in localized and systemic nodular amyloidosis. In 18 cases of localized nodular amyloidosis, there was a predominance of immunoglobulin light chains (12 κ, 4 λ, and 2 mixed κ and λ), with 13 also showing significant heavy chain deposition, while systemic amyloidosis was primarily caused by λ light chain infiltration with only rare involvement of heavy chains [38].

On high-resolution computed tomography (CT) scanning, amyloid nodules are typically multiple (>10 nodules), solid or semisolid density with mixed attenuation, and variable in size ranging from 5 mm to greater than 1 cm (with the majority being sub-centimeter) [28, 29]. As with cystic features, amyloid nodules tend to have a lower lobe predilection. Calcifications may be seen along with cavitation at presentation or develop over time [38]. The radiologic course of nodules varies from stable to slow growth with progressive cavitation and calcification.

In some cases, nodules may represent underlying MALT lymphoma, especially in the setting of connective tissue diseases (CTD), such as Sjögren's syndrome [28, 29]. In one study of 21 patients with amyloidosis of varying cause, six had MALT

lymphoma [29], while another study of eight Sjögren's syndrome-related amyloid reported three with MALT lymphoma [28].

To the extent that some amyloid nodules appear to represent lymphoplasmacytic neoplasms, there is interest in the role of nuclear positive emission tomography (PET) scanning. Several studies have reported PET-positive findings [41–44] associated with amyloid nodules, while others report negative or mixed results [45–47]. According to one study, PET positivity was seen in 81% of amyloid cases [42]. Another study reported PET sensitivity of 81% for systemic MALT lymphoma [48]. Potential explanations for these discrepancies include differences in the resolution and technique of PET scans in older studies [42], difficulties in discriminating tracer uptake in the tumor from background inflammation or superimposed infection [48, 49], and variable degrees of plasmacytic cell infiltration [50]. Although PET scan results may be variable, there is general consensus that an SUV uptake greater than 3.0 should raise suspicion for associated lymphoma or plasmacytoma [45].

Tracheobronchial Amyloidosis

In tracheobronchial amyloidosis, amyloid deposits occur in the trachea and typically extend into the main bronchi. Two major forms have been described, nodular, which is tumorlike, and diffuse infiltrative, which appears as diffuse plaques [31]. Common presenting symptoms include cough, dyspnea, and hemoptysis [51]. Progressive narrowing of the airways may lead to wheezing, atelectasis, lobar collapse, and recurrent pneumonia [52].

Management is often conservative, including airway clearance and antibiotics for bronchitic episodes [51]. For those with progressive disease, treatment with bronchoscopic or surgical resection [51, 53] and even laser and external beam radiotherapy (as plasma cells may be radiosensitive) may be considered [54]. Occasionally, patients require repeat bronchoscopy to reduce tumor burden or revise airway stenting. Laser therapy may involve carbon dioxide laser ablation or neodymium: yttrium-aluminum-garnet laser treatment [55]. Although tracheobronchial amyloidosis is categorized as a local disease, prognosis is poor with overall survival of only 31%–43% at 4–6 years [35, 51], especially for those with proximal or midtracheal involvement that can lead to respiratory failure. It is important to note that repeated laser treatments themselves result in injury and scarring that can lead to complications of airway stenosis. Systemic chemotherapy has not proven useful.

AA Amyloidosis

Serum amyloid A protein is an acute phase reactant [56]. Patients with chronic inflammatory or infectious conditions such as adult-onset Still's disease, ankylosing spondylitis, psoriatic arthropathy, periodic fever, bronchiectasis, inflammatory

bowel disease, and malignancy are more likely to develop AA amyloidosis [57]. Disease prevalence is difficult to determine as only a handful of cases have been reported. AA may involve any organ, but mortality appears to be most closely related to extent of renal involvement [58, 59], typically presenting as nephrotic range proteinuria. Lung involvement is rare. Radiographic abnormalities associated with AA amyloidosis are often more attributable to the underlying inflammatory condition [35], and treatment is typically focused on management of the systemic illness [58].

Transthyretin (TTR) Amyloidosis

TTR is a homotetrameric protein produced in the liver that transports thyroxine and retinol in the serum [60, 61]. It is the precursor protein in two distinctive forms of amyloidosis: (1) familial or hereditary, derived from mutant TTR [62, 63], and (2) senile systemic amyloidosis (SSA) [64, 65] caused by insoluble complexes of normal TTR. About 100 TTR mutations have been implicated in the formation of amyloidogenic TTRs (ATTRs) [66] in familial amyloidosis, while SSA, on the other hand, is an autosomal dominant inherited disease seen in less than 1 in a 100,000 people in the United States [67].

Familial ATTR is a slowly progressive systemic disease often involving the heart, peripheral nerves, eye, kidney, and gastrointestinal tract. Of these, cardiac involvement is the most significant and life-threatening [68]. Pulmonary involvement is considered rare or perhaps underestimated as cardiac symptoms may precede and eclipse pulmonary symptoms. Two autopsy studies have revealed diffuse amyloid deposits in the walls of bronchi/bronchioles and pulmonary vessels, including the pulmonary arteries and veins [68, 69]. Despite extensive pathologic findings, clinical manifestations were seen in only 5 (4.5%) of 110 patients presenting with ATTR from a large retrospective cohort, primarily manifesting as abnormal chest x-ray findings. Such findings included nonspecific interstitial infiltrates, pleural effusion, basilar opacities, and nodules [57].

The incidence of SSA appears to increase with age. According to one study, pulmonary vascular or alveolar-septal amyloid deposits occurred in 2% of patients less than 80 years old, 10% of those aged 80–84, and 20% in those greater than 84 [70]. Similar to familial ATTR, despite extensive histologic involvement on autopsy, there was often a paucity of clinical and radiologic respiratory findings. Liver transplantation corrects the mutant amyloidogenic TTR production in familial disease [71, 72] and may attenuate or halt ongoing amyloid accumulation, but does not address amyloid deposition in SSA, where the precursor protein that is deposited is a nonmutant TTR that continues to be produced by the allograft.

Light Chain Deposition Disease

LCDD was first described in 1976 by Randall et al. [73] who reported two cases of renal failure associated with multi-organ infiltration by free light (κ) chain determinants without evidence of amyloidosis. LCDD is included in the family of "monoclonal immunoglobulin (Ig) deposition diseases" according to the WHO Classification of Tumors of Hematopoietic and Lymphoid Tissues [74]. Manifestations of LCDD result from tissue deposition of monoclonal Ig-derived material (usually κ light chains) causing organ dysfunction. The incidence of LCDD is unknown. The median age at diagnosis is 58 years, and it occurs 2.5 times more commonly in men than women [75]. LCDD is often associated with other lymphoplasmacytic proliferative diseases, including MM (58%) and MGUS (17%) [74].

The serum of patients with oligosecretory diseases such as LCDD often does not contain monoclonal free light chains at a level that is sufficient for detection by either serum or urine protein electrophoresis [76, 77]. Screening tests for LCDD include either identification of a monoclonal population of bone marrow plasma cells via immunofluorescence or an altered serum-free light chain ratio. Abnormal serum-free light chain ratios are found in 88% to 100% of patients with LCDD [10, 78]. Definitive diagnosis and distinction from amyloidosis can be achieved through tissue biopsy with histologic examination including Congo red staining, immunofluorescence using anti-κ and anti-λ chain antibodies, and, when necessary, electron microscopy. Characteristic findings on histopathology include amorphous eosinophilic deposits which on Congo red staining do not exhibit apple-green birefringence under polarized light (please see Fig. 9.4 for case example). Electron microscopy reveals granular electron-dense deposits, thus excluding amyloidosis. Tissue deposits in LCDD are composed mostly of κ light chains as detected by immunofluorescence. It is unclear what determines variable deposition in fibrillary or granular patterns. Some in vitro studies suggest amino acid sequences at specific sites and net protein charge may determine the configuration of deposits [79], while others propose that variation in light chain degradation influences fibrillary vs. granular deposition [80, 81]. Both AL amyloidosis and LCDD are associated with plasma cell dyscrasias. Distinguishing characteristics are summarized in Table 9.2.

In most cases, LCDD is systemic and involves multiple organs. Renal involvement is common and characterized by proteinuria, hematuria, and progressive decline in kidney function [75]. Extrarenal sites include the liver, heart, nervous system, and lungs [82]. Other less common sites are the lymph nodes, bone marrow, spleen, pancreas, thyroid, gastrointestinal tract, adrenal glands, and skin.

Lung involvement is usually asymptomatic in LCDD. Among the parenchymal findings that have been described, nodular presentations are more common than diffuse cystic disease [83–85]. Nodules may be solitary or multiple and bilateral with an average diameter of 10 mm (range, 3–20). On histopathologic examination,

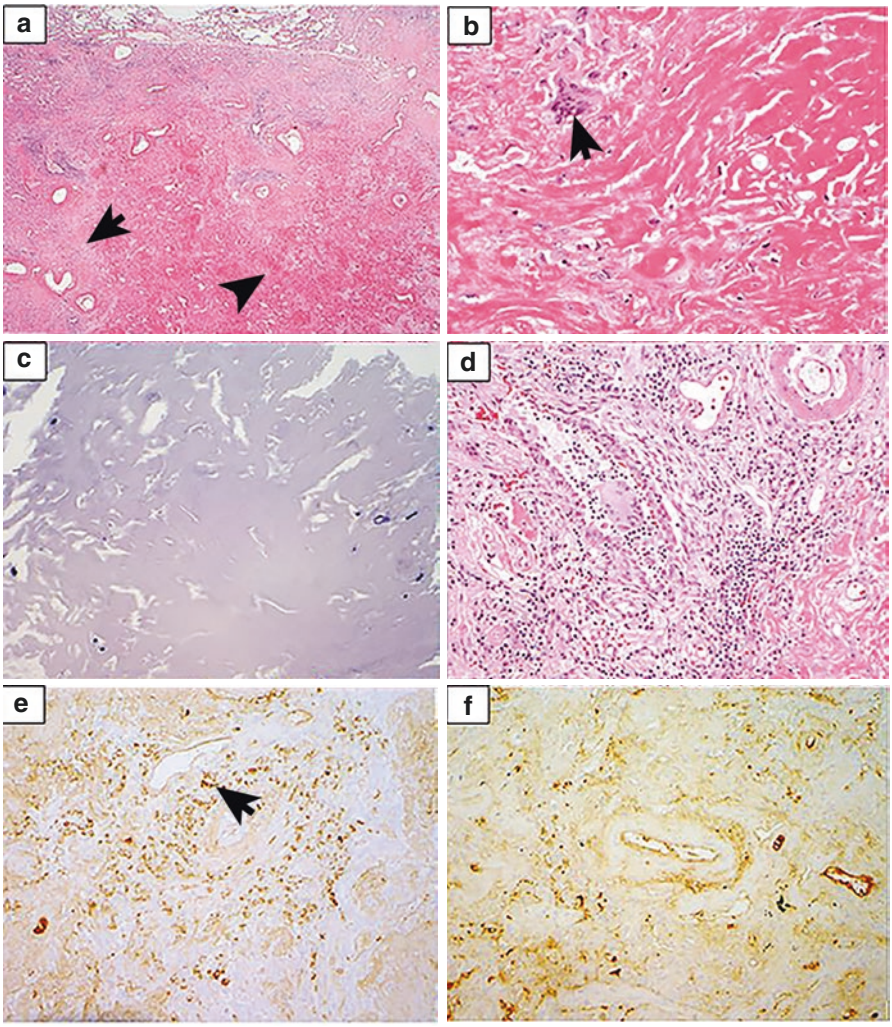

Fig. 9.4 Diffuse pulmonary nodules, ranging in size from 0.7 to 2 cm in a 62-year-old female who underwent wedge resection for suspicion of lymphoma. (**a**) Large area of amorphous pink material **(arrow)** in a background of lung parenchyma **(arrowhead)**; (**b**) occasional multinucleated giant cells **(arrow)** found within the amorphous material; (**c**) negative Congo red stain; (**d**) mild patchy chronic inflammatory infiltrate composed of small B and T cells (not shown) with monotypic kappa plasma cells **(arrow)** in (**e**), negative for lambda plasma cells (**f**). Magnification: ×20 (**a**), ×400 (**b**, **c**), and ×200 (**d**–**f**). (Courtesy of Dr. Anja C. Roden, Department of Pathology, Mayo Clinic Rochester)

Table 9.2 Comparison of AL amyloidosis and light chain deposition disease

	AL amyloid	LCDD
Type of light chain deposits	λ in 75%, κ in 25%	κ (almost always)
Appearance of deposits under electron microscope	Fibrillar	Nodular
Congo red staining	Apple-green birefringence under polarized light	Negative
Thioflavin T staining	Positive	Negative
Binding to serum amyloid P (SAP) component	Positive	Negative
Region of light chain immunoglobulin deposition	Variable	Constant

Abbreviations and symbols: *AL* light chain amyloid, *LCDD* light chain deposition disease, λ lambda, κ kappa

irregular deposits of acellular eosinophilic material surrounded by a foreign body giant cell reaction are often seen. Most cases also have clonal lymphoplasmacytic infiltrates. The proportion of plasma cell vs. lymphocytes found on pathology varies among reported cases [85–87]. LCDD of the lungs has also been reported in association with Sjögren's syndrome [86].

Pulmonary cysts in LCDD are usually thin-walled with a mean size of about 10 mm (range, 4–15) (please see Fig. 9.5 for case example). A peculiar finding of vessels traversing the cysts has been reported [85]. Most cysts are accompanied by at least one nodule. Colombat et al. described the pathology of these cysts in comparison to other cystic lung diseases such as lymphangioleiomyomatosis and Langerhans cell histiocytosis. They found that all three cystic lung diseases are associated with a paucity of elastic fibers in the cystic areas but differ in the patterns of type IV and fibrillary collagen remodeling. Light chain deposits are often surrounded by numerous macrophage-derived giant cells, which they postulated may participate in lung destruction through the production of various matrix metalloproteinases [84]. The same group described three cases of LCDD-associated cystic lung disease progressing to respiratory failure and undergoing lung transplantation at 3, 10, and 11 years after symptom onset [83].

According to a study describing lung histopathology in LCDD, the disease may be subclassified into diffuse or nodular forms. Diffuse disease is characterized by varying degrees of basement membrane thickening in involved structures, whereas nodular disease is associated with eosinophilic depositions, lymphoplasmacytic infiltrates, and giant cell reactions. The diffuse histopathologic presentation appears to be more aggressive with a median survival of 2 years from diagnosis [86]. Additional non-cystic radiologic findings include ground-glass opacities, airway narrowing, and lymph node enlargement with nodal calcification [85].

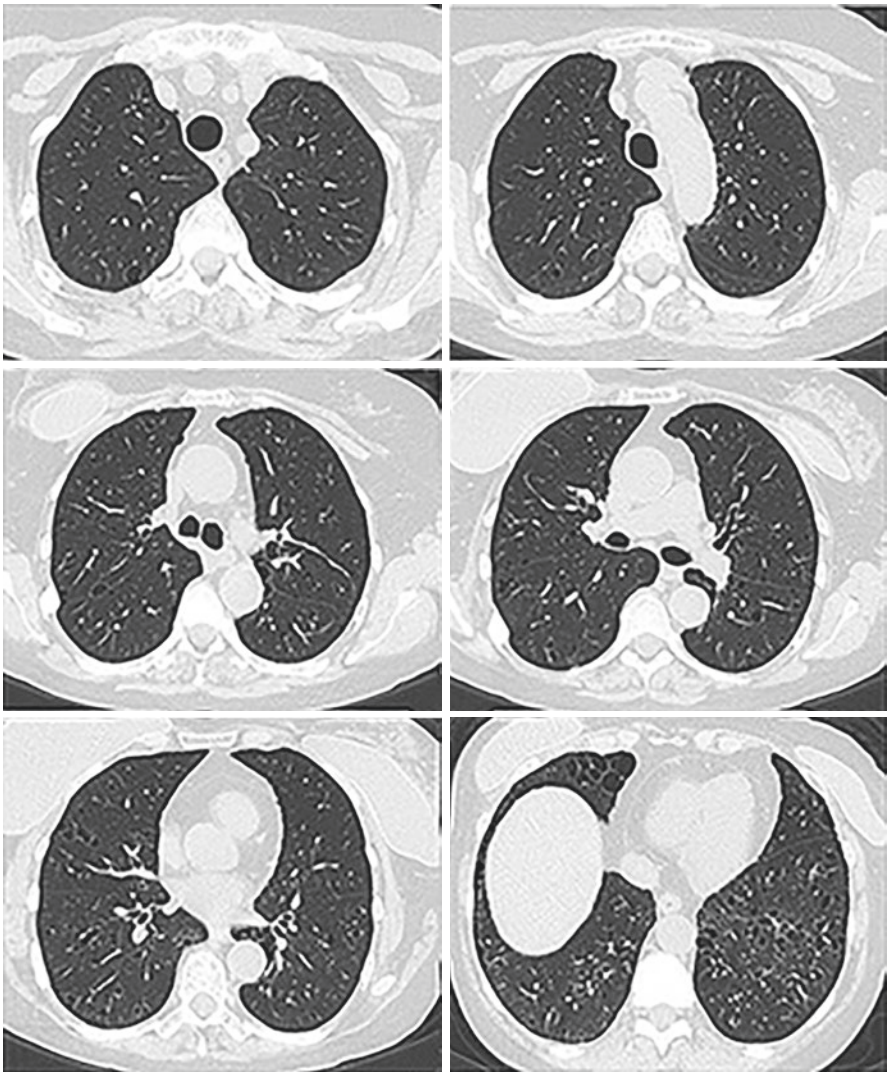

Fig. 9.5 Diffuse cystic lung disease in a 69-year-old female presenting with mild dyspnea and chronic kidney disease, confirmed on kidney and liver biopsy as LCDD. Pulmonary function testing was within normal limits except for isolated decrease in diffusion capacity for carbon monoxide (DLCO). Therapy with bortezomib and cyclophosphamide was initiated by hematology; plans for possible future stem cell transplantation were discussed

Treatment indications include systemic involvement, renal dysfunction, and the presence of MM. If LCDD is associated with MM, prognosis is often poor, and patients are treated according to MM protocols [88]. For other scenarios, there are no established or standardized regimens [89]. Empiric options that have been employed have included autologous stem cell transplantation, bortezomib, immunomodulatory drugs, and renal transplantation [90].

Key Learning Points

- Amyloidosis and LCDD should be considered in the differential of patients presenting with cystic and nodular lung disease.
- The differentiation of these disorders and definitive diagnosis typically require histopathologica verification.
- Identification of precursor proteins and distinction of limited vs. multisystemic involvement in amyloid are predictive of treatment response and prognosis.
- Morbidity in LCDD appears to be primarily attributable to renal involvement, with treatment options based on the co-existence of multiple myeloma.

References

1. Merlini G, Bellotti V. Molecular mechanisms of amyloidosis. N Engl J Med. 2003;349(6):583–96.
2. Puchtler H, Sweat F. Congo red as a stain for fluorescence microscopy of amyloid. J Histochem Cytochem. 1965;13(8):693–4.
3. Cathcart ES, Skinner M, Cohen AS. Immunogenicity of amyloid. Immunology. 1971;20(6):945–54.
4. Harada M, Isersky C, Cuatrecasas P, Page D, Bladen HA, Eanes ED, et al. Human amyloid protein: chemical variability and homogeneity. J Histochem Cytochem. 1971;19(1):1–15.
5. Serpell LC, Sunde M, Blake CC. The molecular basis of amyloidosis. Cell Mol Life Sci. 1997;53(11–12):871–87.
6. Shi J, Guan J, Jiang B, Brenner DA, Del Monte F, Ward JE, et al. Amyloidogenic light chains induce cardiomyocyte contractile dysfunction and apoptosis via a non-canonical p38alpha MAPK pathway. Proc Natl Acad Sci USA. 2010;107(9):4188–93.
7. Kazatchkine MD, Husby G, Araki S, Benditt EP, Benson MD, Cohen AS, et al. Nomenclature of amyloid and amyloidosis. Bull World Health Org. 1993;71(1):105–8.
8. Kyle RA, Linos A, Beard CM, Linke RP, Gertz MA, O'Fallon WM, et al. Incidence and natural history of primary systemic amyloidosis in Olmsted County, Minnesota, 1950 through 1989. Blood. 1992;79(7):1817–22.
9. Gertz MA. Immunoglobulin light chain amyloidosis: 2013 update on diagnosis, prognosis, and treatment. Am J Hematol. 2013;88(5):416–25.
10. Katzmann JA. Screening panels for monoclonal gammopathies: time to change. Clin Biochem Rev. 2009;30(3):105–11.
11. Shaheen SP, Levinson SS. Serum free light chain analysis may miss monoclonal light chains that urine immunofixation electrophoreses would detect. Clin Chim Acta. 2009;406(1–2):162–6.
12. Dispenzieri A, Kyle R, Merlini G, Miguel JS, Ludwig H, Hajek R, et al. International myeloma working group guidelines for serum-free light chain analysis in multiple myeloma and related disorders. Leukemia. 2009;23(2):215–24.
13. Palladini G, Russo P, Bosoni T, Verga L, Sarais G, Lavatelli F, et al. Identification of amyloidogenic light chains requires the combination of serum-free light chain assay with immunofixation of serum and urine. Clin Chem. 2009;55(3):499–504.
14. Petruzziello F, Zeppa P, Catalano L, Cozzolino I, Gargiulo G, Musto P, et al. Amyloid in bone marrow smears of patients affected by multiple myeloma. Ann Hematol. 2010;89(5):469–74.
15. van G, II, Hazenberg BP, Bijzet J, Haagsma EB, Vellenga E, Posthumus MD, et al. Amyloid load in fat tissue reflects disease severity and predicts survival in amyloidosis. Arthritis Care Res 2010;62(3):296–301.
16. Reece DE, Hegenbart U, Sanchorawala V, Merlini G, Palladini G, Blade J, et al. Efficacy and safety of once-weekly and twice-weekly bortezomib in patients with relapsed systemic AL amyloidosis: results of a phase 1/2 study. Blood. 2011;118(4):865–73.

17. Reece DE, Sanchorawala V, Hegenbart U, Merlini G, Palladini G, Fermand JP, et al. Weekly and twice-weekly bortezomib in patients with systemic AL amyloidosis: results of a phase 1 dose-escalation study. Blood. 2009;114(8):1489–97.
18. Venner CP, Lane T, Foard D, Rannigan L, Gibbs SD, Pinney JH, et al. Cyclophosphamide, bortezomib, and dexamethasone therapy in AL amyloidosis is associated with high clonal response rates and prolonged progression-free survival. Blood. 2012;119(19):4387–90.
19. Sidiqi MH, Aljama MA, Muchtar E, Buadi FK, Warsame R, Lacy MQ, et al. Autologous stem cell transplant for immunoglobulin light chain amyloidosis patients aged 70 to 75. Biol Blood Marrow Transplant. 2018;
20. Dahdah MJ, Kurban M, Kibbi AG, Ghosn S. Primary localized cutaneous amyloidosis: a sign of immune dysregulation? Int J Dermatol. 2009;48(4):419–21.
21. Gallivan GJ, Gallivan HK. Laryngeal amyloidosis causing hoarseness and airway obstruction. J Voice. 2010;24(2):235–9.
22. Javed A, Canales BK, Maclennan GT. Bladder amyloidosis. J Urol. 2010;183(6):2388–9.
23. Celli BR, Rubinow A, Cohen AS, Brody JS. Patterns of pulmonary involvement in systemic amyloidosis. Chest. 1978;74(5):543–7.
24. Sterlacci W, Veits L, Moser P, Steiner HJ, Ruscher S, Jamnig H, et al. Idiopathic systemic amyloidosis primarily affecting the lungs with fatal pulmonary haemorrhage due to vascular involvement. Pathol Oncol Res. 2009;15(1):133–6.
25. Berk JL, Keane J, Seldin DC, Sanchorawala V, Koyama J, Dember LM, et al. Persistent pleural effusions in primary systemic amyloidosis: etiology and prognosis. Chest. 2003;124(3):969–77.
26. Eder L, Zisman D, Wolf R, Bitterman H. Pulmonary hypertension and amyloidosis--an uncommon association: a case report and review of the literature. J Gen Intern Med. 2007;22(3):416–9.
27. Dingli D, Utz JP, Gertz MA. Pulmonary hypertension in patients with amyloidosis. Chest. 2001;120(5):1735–8.
28. Baqir M, Kluka EM, Aubry MC, Hartman TE, Yi ES, Bauer PR, et al. Amyloid-associated cystic lung disease in primary Sjogren's syndrome. Respir Med. 2013;107(4):616–21.
29. Zamora AC, White DB, Sykes AM, Hoskote SS, Moua T, Yi ES, et al. Amyloid-associated cystic lung disease. Chest. 2016;149(5):1223–33.
30. Gross BH. Radiographic manifestations of lymph node involvement in amyloidosis. Radiology. 1981;138(1):11–4.
31. Thompson PJ, Citron KM. Amyloid and the lower respiratory tract. Thorax. 1983;38(2):84–7.
32. Garcia Gallego F, Letter CCJL. Hilar enlargement in amyloidosis. N Engl J Med. 1974;291(10):531.
33. Zatloukal P, Bezdicek P, Schimonova M, Havlicek F, Tesarova P, Slovakova A. Waldenstrom's macroglobulinemia with pulmonary amyloidosis. Respiration. 1998;65(5):414–6.
34. Fu J, Seldin DC, Berk JL, Sun F, O'Hara C, Cui H, et al. Lymphadenopathy as a manifestation of amyloidosis: a case series. Amyloid. 2014;21(4):256–60.
35. Utz JP, Swensen SJ, Gertz MA. Pulmonary amyloidosis. The Mayo Clinic experience from 1980 to 1993. Ann Intern Med. 1996;124(4):407–13.
36. Kyle RA, Gertz MA. Primary systemic amyloidosis: clinical and laboratory features in 474 cases. Semin Hematol. 1995;32(1):45–59.
37. Berk JL, O'Regan A, Skinner M. Pulmonary and tracheobronchial amyloidosis. Semin Respir Crit Care Med. 2002;23(2):155–65.
38. Grogg KL, Aubry MC, Vrana JA, Theis JD, Dogan A. Nodular pulmonary amyloidosis is characterized by localized immunoglobulin deposition and is frequently associated with an indolent B-cell Lymphoproliferative disorder. Am J Surg Pathol. 2013;37(3):406–12.
39. Kobayashi H, Matsuoka R, Kitamura S, Tsunoda N, Saito K. Sjogren's syndrome with multiple bullae and pulmonary nodular amyloidosis. Chest. 1988;94(2):438–40.
40. Jeong YJ, Lee KS, Chung MP, Han J, Chung MJ, Kim KI, et al. Amyloidosis and lymphoproliferative disease in Sjogren syndrome: thin-section computed tomography findings and histopathologic comparisons. J Comput Assist Tomogr. 2004;28(6):776–81.

41. Currie GP, Rossiter C, Dempsey OJ, Legge JS. Pulmonary amyloid and PET scanning. Respir Med. 2005;99(11):1463–4.
42. Beal KP, Yeung HW, Yahalom J. FDG-PET scanning for detection and staging of extranodal marginal zone lymphomas of the MALT type: a report of 42 cases. Ann Oncol. 2005;16(3):473–80.
43. Zhang WD, Guan YB, Li CX, Huang XB, Zhang FJ. Pulmonary mucosa-associated lymphoid tissue lymphoma: computed tomography and (1)(8)F fluorodeoxyglucose-positron emission tomography/computed tomography imaging findings and follow-up. J Comput Assist Tomogr. 2011;35(5):608–13.
44. Ollenberger GP, Knight S, Tauro AJ. False-positive FDG positron emission tomography in pulmonary amyloidosis. Clin Nucl Med. 2004;29(10):657–8.
45. Baqir M, Lowe V, Yi ES, Ryu JH. 18F-FDG PET scanning in pulmonary amyloidosis. J Nucl Med. 2014;55(4):565–8.
46. Yadav S, Sharma S, Gilfillan I. Unusual positron emission tomography findings in pulmonary amyloidosis: a case report. J Cardiothorac Surg. 2006;1:32.
47. Hoffmann M, Wohrer S, Becherer A, Chott A, Streubel B, Kletter K, et al. 18F-Fluoro-deoxyglucose positron emission tomography in lymphoma of mucosa-associated lymphoid tissue: histology makes the difference. Ann Oncol. 2006;17(12):1761–5.
48. Alinari L, Castellucci P, Elstrom R, Ambrosini V, Stefoni V, Nanni C, et al. 18F-FDG PET in mucosa-associated lymphoid tissue (MALT) lymphoma. Leuk Lymphoma. 2006;47(10):2096–101.
49. Perry C, Herishanu Y, Metzer U, Bairey O, Ruchlemer R, Trejo L, et al. Diagnostic accuracy of PET/CT in patients with extranodal marginal zone MALT lymphoma. Eur J Haematol. 2007;79(3):205–9.
50. Woehrer S, Streubel B, Chott A, Hoffmann M, Raderer M. Transformation of MALT lymphoma to pure plasma cell histology following treatment with the anti-CD20 antibody rituximab. Leuk Lymphoma. 2005;46(11):1645–9.
51. O'Regan A, Fenlon HM, Beamis JF Jr, Steele MP, Skinner M, Berk JL. Tracheobronchial amyloidosis. The Boston University experience from 1984 to 1999. Medicine (Baltimore). 2000;79(2):69–79.
52. Cotton RE, Jackson JW. Localized amyloid 'Tumours' of the lung simulating malignant neoplasms. Thorax. 1964;19:97–103.
53. Rubinow A, Celli BR, Cohen AS, Rigden BG, Brody JS. Localized amyloidosis of the lower respiratory tract. Am Rev Respir Dis. 1978;118(3):603–11.
54. Kalra S, Utz JP, Edell ES, Foote RL. External-beam radiation therapy in the treatment of diffuse tracheobronchial amyloidosis. Mayo Clin Proc. 2001;76(8):853–6.
55. Nugent AM, Elliott H, McGuigan JA, Varghese G. Pulmonary amyloidosis: treatment with laser therapy and systemic steroids. Respir Med. 1996;90(7):433–5.
56. Yamada T. Serum amyloid a (SAA): a concise review of biology, assay methods and clinical usefulness. Clin Chem Lab Med. 1999;37(4):381–8.
57. Lachmann HJ, Hawkins PN. Amyloidosis and the lung. Chron Respir Dis. 2006;3(4):203–14.
58. Gillmore JD, Lovat LB, Persey MR, Pepys MB, Hawkins PN. Amyloid load and clinical outcome in AA amyloidosis in relation to circulating concentration of serum amyloid a protein. Lancet. 2001;358(9275):24–9.
59. Gertz MA. Secondary amyloidosis (AA). J Intern Med. 1992;232(6):517–8.
60. Blake CC, Geisow MJ, Swan ID, Rerat C, Rerat B. Structure of human plasma prealbumin at 2-5 a resolution. A preliminary report on the polypeptide chain conformation, quaternary structure and thyroxine binding. J Mol Biol. 1974;88(1):1–12.
61. Noy N, Slosberg E, Scarlata S. Interactions of retinol with binding proteins: studies with retinol-binding protein and with transthyretin. Biochemistry. 1992;31(45):11118–24.
62. Costa PP, Figueira AS, Bravo FR. Amyloid fibril protein related to prealbumin in familial amyloidotic polyneuropathy. Proc Natl Acad Sci U S A. 1978;75(9):4499–503.

63. Ando Y, Araki S, Ando M. Transthyretin and familial amyloidotic polyneuropathy. Intern Med. 1993;32(12):920–2.
64. Sletten K, Westermark P, Natvig JB. Senile cardiac amyloid is related to prealbumin. Scand J Immunol. 1980;12(6):503–6.
65. Pitkanen P, Westermark P, Cornwell GG 3rd. Senile systemic amyloidosis. Am J Pathol. 1984;117(3):391–9.
66. Connors LH, Richardson AM, Theberge R, Costello CE. Tabulation of transthyretin (TTR) variants as of 1/1/2000. Amyloid. 2000;7(1):54–69.
67. Lobato L, Beirão I, Silva M, Fonseca I, Queirós J, Rocha G, et al. End-stage renal disease and dialysis in hereditary amyloidosis TTR V30M: presentation, survival and prognostic factors. Amyloid. 2004;11(1):27–37.
68. Smith RR, Hutchins GM, Moore GW, Humphrey RL. Type and distribution of pulmonary parenchymal and vascular amyloid. Correlation with cardiac amyloid. Am J Med. 1979;66(1):96–104.
69. Ueda M, Ando Y, Haraoka K, Katsuragi S, Terasaki Y, Sugimoto M, et al. Aging and transthyretin-related amyloidosis: pathologic examinations in pulmonary amyloidosis. Amyloid. 2006;13(1):24–30.
70. Kunze WP. Senile pulmonary amyloidosis. Pathol Res Pract. 1979;164(4):413–22.
71. Suhr OB, Friman S, Ericzon BG. Early liver transplantation improves familial amyloidotic polyneuropathy patients' survival. Amyloid. 2005;12(4):233–8.
72. Ohya Y, Ando Y, Ueda M, Yamamoto H, Takeichi T, Yamashita T, et al. Long-term outcome of liver transplantation for patients with transthyretin related familial amyloid polyneuropathy (FAP). Am J Transplant. 2008;8:378.
73. Randall RE, Williamson WC Jr, Mullinax F, Tung MY, Still WJ. Manifestations of systemic light chain deposition. Am J Med. 1976;60(2):293–9.
74. McKenna RWKR, Kuehl WM, Grogan TM, Harris NL, Coupland RW. Plasma cell Neoplasm in WHO classification of tumours of haematopoietic and lymphoid tissues. Lyon: International Agency for Research on Cancer; 2008.
75. Pozzi C, D'Amico M, Fogazzi GB, Curioni S, Ferrario F, Pasquali S, et al. Light chain deposition disease with renal involvement: clinical characteristics and prognostic factors. Am J Kidney Dis. 2003;42(6):1154–63.
76. Blade J, Kyle RA. Nonsecretory myeloma, immunoglobulin D myeloma, and plasma cell leukemia. Hematol Oncol Clin N. 1999;13(6):1259.
77. Drayson M, Tang LX, Drew R, Mead GP, Carr-Smith H, Bradwell AR. Serum free light-chain measurements for identifying and monitoring patients with nonsecretory multiple myeloma. Blood. 2001;97(9):2900–2.
78. Nasr SH, Valeri AM, Cornell LD, Fidler ME, Sethi S, D'Agati VD, et al. Renal monoclonal immunoglobulin deposition disease: a report of 64 patients from a single institution. Clin J Am Soc Nephrol. 2012;7(2):231–9.
79. Kaplan B, Livneh A, Gallo G. Charge differences between in vivo deposits in immunoglobulin light chain amyloidosis and non-amyloid light chain deposition disease. Br J Haematol. 2007;136(5):723–8.
80. Picken MM, Frangione B, Barlogie B, Luna M, Gallo G. Light chain deposition disease derived from the kappa I light chain subgroup. Biochemical characterization. Am J Pathol. 1989;134(4):749–54.
81. Rostagno A, Vidal R, Kaplan B, Chuba J, Kumar A, Elliott JI, et al. pH-dependent fibrillogenesis of a VkappaIII Bence Jones protein. Br J Haematol. 1999;107(4):835–43.
82. Ronco PM, Alyanakian MA, Mougenot B, Aucouturier P. Light chain deposition disease: a model of glomerulosclerosis defined at the molecular level. J Am Soc Nephrol. 2001;12(7):1558–65.
83. Colombat M, Stern M, Groussard O, Droz D, Brauner M, Valeyre D, et al. Pulmonary cystic disorder related to light chain deposition disease. Am J Respir Crit Care Med. 2006;173(7):777–80.

84. Colombat M, Caudroy S, Lagonotte E, Mal H, Danel C, Stern M, et al. Pathomechanisms of cyst formation in pulmonary light chain deposition disease. Eur Respir J. 2008;32(5):1399–403.
85. Sheard S, Nicholson AG, Edmunds L, Wotherspoon AC, Hansell DM. Pulmonary light-chain deposition disease: CT and pathology findings in nine patients. Clin Radiol. 2015;70(5):515–22.
86. Arrossi AV, Merzianu M, Farver C, Yuan C, Wang SH, Nakashima MO, et al. Nodular pulmonary light chain deposition disease: an entity associated with Sjogren syndrome or marginal zone lymphoma. J Clin Pathol. 2016;69(6):490–6.
87. Colombat M, Gounant V, Mal H, Callard P, Milleron B. Light chain deposition disease involving the airways: diagnosis by fibreoptic bronchoscopy. Eur Respir J. 2007;29(5):1057–60.
88. Rajkumar SV. Multiple myeloma: 2011 update on diagnosis, risk-stratification, and management. Am J Hematol. 2011;86(1):57–65.
89. Lorenz EC, Gertz MA, Fervenza FC, Dispenzieri A, Lacy MQ, Hayman SR, et al. Long-term outcome of autologous stem cell transplantation in light chain deposition disease. Nephrol Dial Transplant. 2008;23(6):2052–7.
90. Gertz MA. Managing light chain deposition disease. Leuk Lymphoma. 2012;53(2):183–4.

Chapter 10
Infectious Etiologies of Diffuse Cystic Lung Diseases

Hilary Miller-Handley and Alan George Smulian

Abbreviations

COPD	Chronic obstructive pulmonary disease
CT	Computerized tomography
HIV	Human immunodeficiency virus
IPA	Invasive pulmonary aspergillosis
MRI	Magnetic resonance imaging
NTM	Nontuberculous mycobacteria
PCP	*Pneumocystis* pneumonia
TMP-SMX	Trimethoprim-sulfamethoxazole

Introduction

Infectious etiologies more typically produce single or multiple, focal or widely scattered cystic lesions than the extensive profusion of cysts that is typical for diffuse thin-walled cystic lung diseases [1, 2]. Mechanistically, three major pathways

H. Miller-Handley
Infectious Disease Division, University of Cincinnati College of Medicine, Cincinnati, OH, USA

Pediatric Infectious Disease Division, Cincinnati Children's Hospital Medical Center, Cincinnati, OH, USA

A. G. Smulian (✉)
Infectious Disease Division, University of Cincinnati College of Medicine, Cincinnati, OH, USA

Cincinnati Veterans Administration Medical Center, Cincinnati, OH, USA
e-mail: George.Smulian@uc.edu

N. Gupta et al. (eds.), *Diffuse Cystic Lung Diseases*, Respiratory Medicine,
https://doi.org/10.1007/978-3-030-63365-3_10

Table 10.1 Mechanisms of cystic and cavitary lung disease caused by infectious organisms

1. Cystic dilatation of lung structures:
(a) *Pneumocystis jirovecii*-associated cystic lung disease
(b) Cystic suppurative/necrotic bronchiectatic air space disease
2. Parenchymal necrosis:
(a) Suppurative:
(i) Lung abscess
(ii) Pneumatocele
(iii) Chronic fungal infections – aspergillosis, mucormycosis
(iv) Chronic bacterial infections – actinomycosis, nocardiosis
(b) Granulomatous – caseous/non-caseous:
(i) Tuberculous
(ii) NTM
(iii) Endemic fungal disease:
1. Histoplasmosis
2. Blastomycosis
3. Coccidioidomycosis
3. Cystic lung displacement:
(i) Hydatid cysts
(iii) Paragonimiasis

are postulated to result in infectious lung cyst formation [3], including (1) cystic dilatation of lung structures, (2) parenchymal necrosis, and (3) cystic expansion and displacement of lung structures. This classification will be used to outline the clinical and radiographic presentations of infectious cyst formation in the lung (Table 10.1).

Radiologic Definitions

As defined by the third Fleischner Society criteria [4, 5], a cyst is any low-attenuating circumscribed space, containing gas or liquid, enclosed by an epithelial or fibrous wall and with a well-defined interface with the normal lung tissue. A cavity, in contrast, is a gas-filled space within a pulmonary consolidation or mass that is characterized by thicker walls (> 4 mm) than a cyst (≤ 4 mm). Pneumatoceles are thin-walled gas-filled spaces associated with acute infection or trauma that tend to resolve over time. Other mimics of cystic lung disease include honeycombing and bronchiectasis. Viewed in certain planes, bronchiectatic air spaces may have a similar appearance to cysts; however, the presence of adjacent bronchovascular bundles can help distinguish bronchiectasis from true cysts.

Cystic Dilatation of Lung Structures

Pneumocystis jirovecii-*Associated Cystic Lung Disease*

Pneumocystis jirovecii, a human-specific fungal pathogen, is an important opportunistic pathogen in immunocompromised patients, particularly those with cell-mediated immunodeficiency [6]. *Pneumocystis* was first recognized as the pathogen that caused interstitial plasma cell pneumonia in premature, malnourished infants in European orphanages following World War II. *Pneumocystis* has since emerged as a leading cause of pneumonia in immunocompromised patients of diverse etiologies, such as those infected with the human immunodeficiency virus (HIV) [7, 8].

Pneumocystis pneumonia (PCP) is characterized by the triad of dyspnea, nonproductive cough, and fever [6]. Although a productive cough and chest tightness may occur, purulent sputum should raise suspicion of bacterial infection. HIV-infected patients frequently have prolonged prodromal periods with subtle clinical manifestations, in contrast to other immunocompromised hosts who typically have more acute symptoms of 1- or 2-week duration at presentation. Physical examination reveals varying degrees of respiratory distress. Lung auscultation is typically nonrevealing, although basilar rales may occasionally be present.

The radiographic findings seen in HIV- and non-HIV-infected individuals with PCP also differ [9]. On the chest radiograph, usual findings include diffuse infiltrates with symmetric reticular or granular opacities emanating from the perihilar regions. Patients with early disease may have a normal chest radiograph, but patchy ground-glass opacification may be detected on high-resolution computerized tomography [10]. The classical findings of extensive ground-glass opacifications are seen in both HIV-infected and non-HIV-infected individuals [11], but lung cysts occur primarily in HIV-infected patients (Fig. 10.1), perhaps related to the

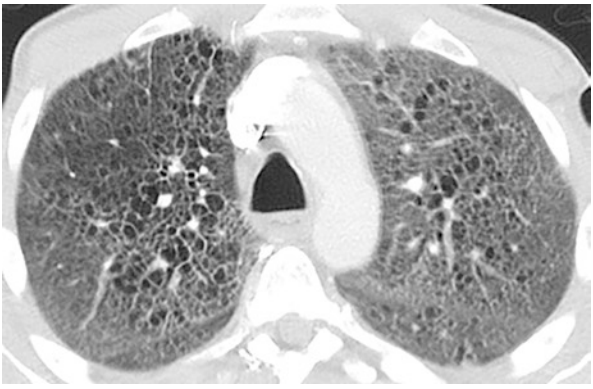

Fig. 10.1 Axial chest CT of an HIV-infected patient with *Pneumocystis jirovecii* pneumonia showing diffuse cystic changes

long-standing, low-grade inflammation that often exists before a clinical diagnosis of PCP is made in this subset of patients. This radiographic presentation has become less common due to earlier intervention with antiretroviral therapy and PCP prophylaxis. Other unusual manifestations include focal infiltrates, lobar consolidation, nodules, cavities, effusions, and lymphadenopathy. An increased frequency of pneumothorax and apical infiltrates has been noted with the administration of aerosolized pentamidine.

Risk factors for PCP include deficiency in cell-mediated immunity; prematurity and malnutrition; primary immunodeficiency disorders, particularly severe combined immunodeficiency disease; infection with HIV; and cytotoxic or immunosuppressive drugs for the treatment of cancer, transplantation, or collagen vascular disorders [8]. Studies of HIV/AIDS patients have documented a significant risk of PCP when CD4 lymphocyte counts fall below 200 cells/μL; other factors associated with a higher risk for PCP included CD4+ cell percentage < 14%, previous episodes of PCP, oral thrush, recurrent bacterial pneumonia, unintentional weight loss, and higher plasma HIV RNA [12, 13]. Corticosteroids are by far the most commonly used immunosuppressive drugs that predispose to PCP in the non-HIV-infected patients. Symptoms often begin after the steroid dose has been tapered.

The principal laboratory abnormality is arterial hypoxemia with an increased alveolar-arterial (PAO_2-PaO_2) gradient; this is often accompanied by respiratory alkalosis. Blood oxygenation may be normal early in the course of PCP, but desaturation with exercise is common at this stage. Pulmonary function tests may reveal reversible airway obstruction, airway hyperreactivity, or a restrictive abnormality, and the diffusing capacity for carbon monoxide (DL_{CO}) is sensitive in detecting alveolar-capillary block. Serum lactic dehydrogenase (LDH) levels, which reflect the degree of lung injury, increase with disease progression. 1,3-ß-D glucan has excellent sensitivity for PCP; however, it can be falsely elevated by a variety of infectious and noninfectious etiologies.

The natural history of untreated PCP in HIV-infected and other immunocompromised patients is progressive respiratory impairment ending in death. Since recovery from PCP does not confer immunity, patients are at risk of recurrence as long as the predisposing conditions exist; HIV-infected patients are at highest risk for this complication. The cystic lesions typically seen in HIV-infected individuals with late presentation of PCP may regress or disappear following treatment of the *P. jirovecii* infection and the underlying HIV [14]. Chronic airway disease can develop following PCP, which may be further complicated by bacterial infections.

Histopathologically, PCP is characterized by the presence of a foamy, vacuolated exudate filling the alveoli in lung sections stained with hematoxylin and eosin [15]. The use of stains such as methenamine silver reveals masses of *Pneumocystis* cystic forms. With severe disease, there may be interstitial fibrosis, edema, and the development of hyaline membranes. Hypertrophy of type II alveolar cells, which suggests tissue repair, is often present; however, other aspects of the host inflammatory response in HIV-infected and other immunocompromised patients are mild and nonspecific. In contrast, premature or malnourished infants display an interstitial plasma cell infiltrate, which led to the historical classification of PCP as an

interstitial plasma cell pneumonia. Extrapulmonary lesions of PCP display the typical foamy material found in the lungs [16].

Serological studies have revealed that *Pneumocystis* has a worldwide distribution and that exposure to the organism occurs early in life [17]. The HIV pandemic changed PCP from a sporadic disease to a problem of major medical and public health importance. Although the incidence of PCP has fallen with widespread chemoprophylaxis and antiretroviral therapy, the organism remains the leading cause of opportunistic infection in HIV patients in industrialized countries. Despite difficulties in obtaining accurate incidence rates in developing countries because of lack of access to medical care and the higher frequency of more virulent infections such as tuberculosis, *Pneumocystis* is now recognized with increasing frequency in tropical and developing countries, and cystic manifestations may be more prevalent in those populations given the late presentation and the prolonged duration of subclinical disease that occur in under-resourced clinical settings [18].

Trimethoprim-sulfamethoxazole (TMP-SMX), which acts by inhibiting folic acid synthesis, is considered the drug of choice for all forms of PCP [19]. Therapy is continued for 14 days in non-HIV-infected patients and for 21 days in persons infected with HIV. TMP-SMX is well tolerated by non-HIV-infected patients, whereas more than half of HIV-infected patients experience serious adverse reactions [20]. Several alternative regimens are available for the treatment of mild to moderate cases of PCP ($Pa_{O2} > 70$ mmHg or a $PA_{O2} - Pa_{O2} < 35$ mmHg on breathing room air). TMP plus dapsone and clindamycin plus primaquine are as effective as TMP-SMX [21]. Alternative regimens that are recommended for the treatment of moderate to severe PCP ($Pa_{O2} \leq 70$ mmHg or a $PA_{O2} - Pa_{O2} \geq 35$ mmHg) are parenteral pentamidine, parenteral clindamycin plus primaquine, or trimetrexate plus leucovorin [21]. Parenteral clindamycin plus primaquine may be more efficacious than pentamidine [22].

Molecular evidence of resistance to sulfonamides and to atovaquone has emerged among human *Pneumocystis* isolates [23]. Although prior sulfonamide exposure is a risk factor, this resistance has also occurred in HIV-infected patients who have never received sulfonamides. The outcome of therapy appears to be linked more strongly to traditional measures – e.g., high Acute Physiology, Age, and Chronic Health Evaluation III (APACHE III) scores, need for positive-pressure ventilation, delayed intubation, and development of pneumothorax – than to the presence of molecular markers of sulfonamide resistance [24].

Early institution of antiretroviral therapy in HIV patients presenting with PCP has been associated with improved survival, but careful attention should be devoted to the possible development of the immune reconstitution inflammatory syndrome [25]. HIV-infected patients frequently experience deterioration of respiratory function shortly after receiving anti-*Pneumocystis* drugs. The adjunctive administration of tapering doses of glucocorticoids to HIV-infected patients with moderate to severe PCP can prevent this problem and improve the rate of survival [26]. For maximal benefit, this adjunctive therapy should be started early in the course of the illness. The use of steroids as adjunctive therapy in HIV-infected patients with mild PCP or in non-HIV-infected patients is currently being evaluated.

Prophylaxis is indicated for HIV-infected patients with CD4+ T cell counts of <200/μL or a history of oropharyngeal candidiasis and for both HIV-infected and non-HIV-infected patients who have recovered from PCP [19]. Prophylaxis may be discontinued in HIV-infected patients once CD4+ T cell counts have risen to >200/uL and remained at that level for ≥3 months. Primary prophylaxis guidelines for immunocompromised hosts who are not infected with HIV are less clear. TMP-SMX is the drug of choice for primary and secondary prophylaxis [27]. This agent also provides protection against toxoplasmosis and some bacterial infections. Alternative regimens are available for individuals intolerant of TMP-SMX, including dapsone, atovaquone, or pentamidine regimens.

Cystic Suppurative/Necrotic Bronchiectatic Air Spaces

Bronchiectasis is defined as irreversible localized or diffuse bronchial dilatation usually resulting from chronic infection, airway obstruction, or congenital bronchial abnormalities. Repeated infection cycles result in failure of normal mucosal and muscular layer healing, and transmural inflammation causes destruction of supportive mural tissues such as smooth muscle and cartilage resulting in bronchomalacia and scarring. Airway dilatation can extend to the lung periphery. Cystic or saccular forms of bronchiectasis result in dilated airways that can be difficult to distinguish from true pulmonary cysts. Infections such as *Bordetella pertussis* and *Mycobacterium tuberculosis* are frequently implicated in the generation of bronchiectatic airways; secondary colonization and infection with agents such as *Pseudomonas aeruginosa*, *Staphylococcus aureus*, and *Aspergillus fumigatus* may perpetuate the infection/inflammation cycle resulting in ongoing airway damage.

Parenchymal Necrosis

Infectious cavities may occur during or following a necrotizing pneumonic process due to aerobic and anaerobic infections. Infectious cavities vary in size and number and are characterized by an area of surrounding pulmonary consolidation on chest imaging [28].

Suppurative

Lung Abscess

Lung abscesses are formed by necrosis of pulmonary parenchyma followed by expulsion or resorption of the caseous material. They are classically round or ovoid in shape with air fluid levels and thick walls and may be classified as primary or

secondary based on the presence of underlying conditions such as airway obstruction, bronchiectasis, or hematogenous spread and as acute or chronic based on the duration of symptoms prior to presentation. Pneumonia complicated by the formation of multiple small (<2 cm) abscesses is referred to as necrotizing pneumonia [28, 29]. Cavitation and abscess formation are often associated with aspiration, which results in polymicrobial infections of mixed gram-positive and gram-negative anaerobic bacteria and aerobic flora derived from the gingival crevices. Inocula that reach the lower airways may be inadequately cleared because of impaired consciousness or large, recurring bacterial challenges that can occur in the setting of swallowing disorders [28]. Cavitation may also be seen with aggressive gram-positive pathogens such as *Streptococcus pneumoniae*, *Streptococcus anginosus*, or *Staphylococcus aureus* or enteric gram-negative pathogens such as *Escherichia coli*, *Enterobacter cloacae*, *Klebsiella pneumoniae*, and *Pseudomonas aeruginosa* [30, 31]. Cavities are common features of septic embolization especially with aggressive suppurative organisms such as *Staphylococcus aureus* following tricuspid valve endocarditis or following embolization from jugular vein thrombophlebitis associated with *Fusobacterium necrophorum* in Lemierre's syndrome.

Most patients with lung abscess, especially those with anaerobic polymicrobial infections, present with indolent symptoms evolving over weeks or months. Symptoms include fever, cough, and sputum production often with evidence of chronic systemic disease such as night sweats and weight loss. Physical findings often include evidence of poor dentition, associated conditions that reduce consciousness, digital clubbing, and lung sounds reflecting parenchymal disease and/or pleural effusion.

Microbiological sampling is important in guiding therapy with the caveat that anaerobes may be difficult to isolate and the antimicrobial therapy should usually include anaerobic coverage unless a clear monobacterial process is confirmed [30]. Many empiric combinations have been used, including clindamycin, beta-lactam/beta-lactamase combinations, beta-lactams with metronidazole, or carbapenems. Targeted therapy directed at a single organism without anaerobic coverage should only be considered when no oral flora is isolated. Recent influenza infection increases the risk for a monomicrobial *Staphylococcus aureus* abscess. Duration of therapy should be at least 3 to 4 weeks, but many will continue until radiographic stability or clearance. Therapy may consist of initial intravenous therapy with conversion to an oral regimen as the infection responds. Surgery is rarely required for uncomplicated lung abscess management but may be required in patients who fail to respond to medical management, suspected malignancy, hemorrhage, extremely large abscesses, or abscesses involving highly resistant organisms [31, 32].

Postinfectious Pneumatocele

These thin-walled, air-filled cavities arise from an inflammatory process that causes central necrosis with subsequent retraction by surrounding pulmonary parenchyma [33]. The process is thought to result from parenchymal necrosis and check valve or

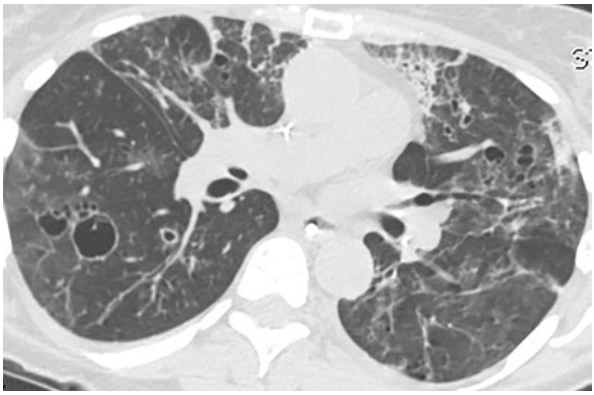

Fig. 10.2 Axial CT of a 57-year-old female with no underlying health issues following recovery from *Staphylococcus aureus* pneumonia demonstrating bilateral thin-walled pneumatoceles

ball valve obstruction resulting in air trapping. The most common cause is infection in patients with localized bacterial pneumonia although similar findings may be seen as a complication of blunt trauma or hydrocarbon aspiration [34]. Infectious pneumatoceles are most commonly seen in staphylococcal and streptococcal infections but are also reported with pneumococcal pneumonia and in association with gram-negative infections (Fig. 10.2). Management consists of appropriate treatment of the underlying infection. These transient air-filled cavities typically resolve over time and persistence should raise concern for an alternative diagnosis.

Chronic Fungal Infections

Chronic fungal infections such as pulmonary aspergillosis and pulmonary mucormycosis can result in dense focal parenchymal consolidation with cavitation [35–38]. Although the radiographic appearance of fungal cystic lesions can be similar to that of bacterial necrotizing pneumonias, fungal infections classically present with a more insidious onset and are more commonly seen in immunocompromised individuals or patients with underlying chronic lung disease. The foci of parenchymal breakdown within the area of consolidation are often small and multiple in number. Regional hilar adenopathy is not a prominent feature associated with pulmonary aspergillosis or mucormycosis. Pulmonary aspergillus infection may present with a variety of clinical syndromes that vary based on host inflammatory response and immune status. These may range from allergic bronchopulmonary aspergillosis with reactive airways, increased IgE levels, and central bronchiectasis to invasive pulmonary aspergillosis (IPA) in severely immunocompromised individuals. In invasive and semi-invasive aspergillosis, a halo of low attenuation may be seen with early invasive lesions, and this may progress to cavitary lesions with a characteristic air crescent sign due to cavitary necrosis on CT imaging [39]. These features are characteristic of IPA, but similar findings may be seen with other angioinvasive organisms including *Mucorales*, *Fusarium*, and *Scedosporium* [40]. Chronic

necrotizing aspergillosis associated with cavitary infiltrates may also be seen in individuals with chronic lung disease and lesser degrees of immunosuppression such as alcoholism or diabetes [37].

A confirmed diagnosis requires tissue biopsy showing hyphal invasion and a positive culture for the appropriate organisms, although invasive procedures to achieve this level of certainty may be contraindicated in severely ill immunosuppressed patients due to potential risks. Cultures of *Aspergillus* spp. or other invasive fungi from expectorated sputum of high-risk individuals with compatible radiographic findings are supportive of the diagnosis, although *Aspergillus* is often cultured from patients in whom no clinical illness is apparent so positive cultures with low risk for invasive fungal infection should be interpreted with caution. Antibody detection plays little role in the diagnosis of IPA as immunocompromised individuals at greatest risk may mount poor serological responses. Detection of circulating galactomannan has contributed substantially to the diagnosis of invasive aspergillosis. Studies report sensitivity of 40%–89% depending on the extent of disease, prior antifungal therapy, number of samples per patient, and other variables. Specificity is also high although false positives have been reported associated with dietary intake, antibiotics such as piperacillin/tazobactam, and bacterial infection with *Bifidobacterium.* Other potential markers such as B-glucan, approved for clinical diagnosis of invasive fungal infections, may be of value although species-specific sensitivity varies [41].

Historically, the efficacy of antifungal therapy has been poor, likely related in part to the often compromised immune status of the host and the advanced stage of infection at the time of diagnosis. Triazoles such as voriconazole, posaconazole, and isavuconazole remain primary therapy for IPA, while amphotericin B preparations remain the first line for Mucorales infections. Triazoles may also be used for these infections although experience is more limited and variable. Adjunctive measures such as reduction in immunosuppressive agents and improvement in the underlying host defenses are crucial.

Chronic Bacterial Infections

Chronic bacterial infections such as actinomycosis may present with persistent consolidation or a mass which may contain areas of cavitation [42]. Pulmonary actinomycosis is caused by microaerophilic or anaerobic actinomycetes and may cross tissue planes resulting in pleural disease or invade the chest wall resulting in pleuropulmonary fistulas and sinuses draining purulent fluid containing characteristic sulfur granules. Similar subacute presentations of pulmonary infection with cavitation may be seen with organisms such as the aerobic actinomycetes, *Nocardia*, and *Rhodococcus*. As with other suppurative cavitary infections, management requires an accurate microbiological diagnosis and prolonged antimicrobial therapy.

Granulomatous Parenchymal Necrosis

Infections resulting in granulomatous inflammatory response may manifest as nodules which cavitate during primary infections or cavitary lesions associated with postprimary infection and secondary reactivation disease. Tuberculous cavitary lesions are usually seen in postprimary disease, while cavitary nodules in nontuberculous mycobacterial infection are predominantly seen as a manifestation of progressive primary disease. Cavitation of fungal nodules may be seen during both primary infection and in reactivation disease.

Tuberculous Cavitary Lung Disease

Cavitary pulmonary tuberculous lesions are seen primarily in the apical-posterior portion of the upper lobes and less frequently in the apex of the lower lobes [43]. The pathologic features of tuberculosis are the result of the balance between the degree of tissue hypersensitivity and bacterial antigen load. When the population of activated lymphocytes and macrophages with enhanced microbicidal activity is associated with a low bacterial antigen load, highly organized collections of lymphocytes, macrophages, Langerhans giant cells, and fibroblasts form granulomas resulting in containment of infection. When both antigen load and tissue hypersensitivity are high, epithelioid and giant cells are sparse, and exudative reactions with poorly organized granulomas with central caseous necrosis form. The caseous necrosis is unstable and may liquify and discharge through the bronchial tree resulting in tuberculous cavitary disease with extremely high bacterial burdens. Apical-posterior distribution is attributed to the higher oxygen tensions and lower lymphatic flow in the apices, resulting in enhanced bacterial proliferation and bacterial antigen retention, respectively. As tissue hypersensitivity develops during postprimary infection or reactivation, the environment is conducive to tissue necrosis and cavitation. Fibrous encapsulation and inelasticity of the surrounding lung tissue prevent collapse of the cavity. The cavitary lesions may progress due to the tendency of apical foci to liquify, the high organism burden within pulmonary cavities, and the spread of caseous material through the bronchial tree. Progression from limited infiltrates to advanced cavitary disease may occur rapidly over a period of months.

Radiographic findings of patchy or nodular infiltrates in the subapical-posterior areas of the upper lobe are suggestive of tuberculosis in at-risk populations especially if bilateral and associated with cavitation. Cavities may be better visualized by CT. Air-fluid levels are uncommon in tuberculous cavitation. Active disease is often characterized by a mixture of small sharply defined granulomatous lesions, softer exudative lesions with indistinct borders, and fibrous scars with sharp borders.

The diagnosis of tuberculosis is made by the demonstration of *M. tuberculosis* by acid-fast stain or auramine-rhodamine fluorescent staining in respiratory secretions and confirmed by growth and speciation [44]. Induced sputum or bronchoscopically derived samples may increase the yield if the diagnosis is not obtained from

expectorated samples. Nucleic acid amplification tests offer an additional technique for the direct detection of *M. tuberculosis* in clinical specimens and distinction between tuberculous and nontuberculous mycobacterium cultured from clinical samples. Treatment typically consists of four drug therapy, followed by two drug-directed therapy based on sensitivities; however, the regimen may vary based on resistance patterns within the community.

Nontuberculous Mycobacterial Infections

Nontuberculous mycobacterial (NTM) infections may present with a variety of radiographic findings including bronchiectasis and fibronodular infiltrates often involving the right middle lobe and left lingular segments [43]. Cavitation of nodules is not uncommonly observed. Large thin-walled cysts may also be seen [45]. These may occur predominantly in the upper lobes in individuals with chronic underlying lung disease, chronic smokers, and alcoholics. Multiple nontuberculous mycobacterial species have been associated with chronic pulmonary infection including rapidly growing mycobacteria, such as *M. fortuitum*, *M. abscessus*, and *M. chelonae*, and slow-growing mycobacteria, such as *Mycobacterium avium* complex and *M. kansasii*. Predisposing factors for pulmonary NTM disease include underlying lung disease, alcoholism, and cystic fibrosis. *Mycobacterium avium* infection is also found in a subset of middle-aged and elderly women with no predisposing conditions (Lady Windermere syndrome, named after the leading lady in an Oscar Wilde play). The diagnosis is made based on the isolation of NTMs from multiple samples of respiratory secretions in the presence of compatible radiographic and clinical findings [46, 47]. Treatment varies based on the mycobacterium species. As environmental organisms, NTMs are not uncommonly isolated as incidental findings in individuals without compatible radiographic findings or clinical symptoms, and this asymptomatic colonization or transient infection does not warrant treatment.

Endemic Fungal Infections

Endemic pulmonary fungal infections can arise through the inhalation of fungal spores of regionally prevalent organisms such as *Histoplasma capsulatum* in the Midwest, *Coccidioides* spp. in the Southwestern United States, and *Blastomyces dermatitidis* in the Southeastern United States and upper Midwest [48–51]. Most acute pulmonary infections due to endemic fungi resolve spontaneously, but nodules and cavities may be seen as residual findings [52, 53]. Solitary peripheral nodules are seen in about 4% of individuals with coccidioidomycosis [54, 55]. These may liquify and drain resulting in a solitary thin-walled peripheral cavity which may be asymptomatic or present with cough or localized pain. About half close spontaneously over a period of years. Underlying lung disease such as COPD, chronic smoking, diabetes, and alcohol abuse predispose to the development of

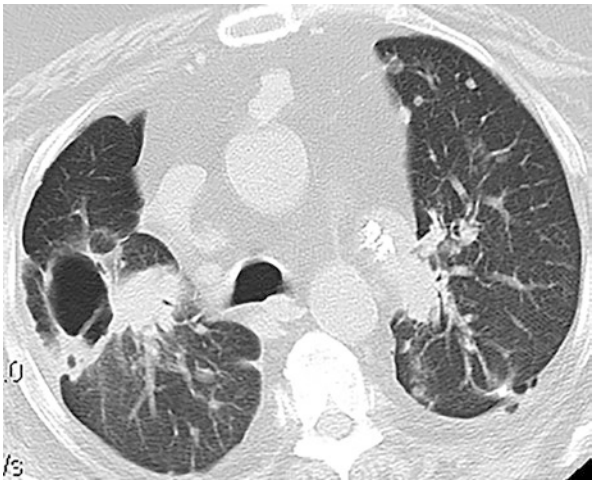

Fig. 10.3 Axial CT of a 58-year-old male with history of pulmonary blastomycosis with right-sided cystic lesion

chronic pulmonary infection, such as chronic fibrocavitary coccidioidal pneumonia or chronic cavitary or non-cavitary histoplasmosis. Blastomycosis more commonly presents as a chronic pneumonia or mass lesion and may mimic bronchogenic carcinoma [48]. Cavitation may be found with the primary lobar pneumonia, as solitary cavitary nodules or as fibronodular infiltrates with cavitation (Fig. 10.3). Similar findings may be seen in paracoccidioidosis and sporotrichosis. The diagnosis is dependent on the isolation and identification of the specific fungal pathogen, histological diagnosis, or specific serological assays [56, 57].

Cystic Expansion with Lung Displacement

Hydatid Cysts

Hydatid cysts caused by infection with the metacestode stage of *Echinococcus* tapeworms are most commonly described in sheep-raising areas and are endemic around the Mediterranean basin, Australia, and South America. Approximately 50% of detected cases occur in asymptomatic individuals, and many more cases likely remain undiagnosed [58–61]. Children and young adolescents are more likely to remain asymptomatic for reasons that are not fully clear. When symptomatic, presenting symptoms may include cough, chest pain, and hemoptysis. Hydatid cysts in the lung are characteristically smooth-walled ranging from 2 mm to 1 cm in thickness. Internal scolexes may be visible on CT imaging. Pulmonary cysts are more commonly multiple than solitary. The diagnosis is based on appropriate epidemiological exposure and supported by serological assays. Unfortunately, sensitivity of available serological assays is generally lower for pulmonary disease than hepatic disease, ranging from 51% to 84% [62]. There is no correlation between serological

results and the size or number of cysts, and negative serology does not rule out the diagnosis of echinococcosis. The principal complication of pulmonary *Echinococcus* infection is cyst rupture with spilling of cyst contents into the bronchial tree or pleural cavity. Cyst rupture may be associated with fever and acute hypersensitivity reactions or a more insidious increase in cough or chest pain with bronchial rupture and pleural effusion, empyema, or pneumothorax with pleural rupture. Management usually consists of surgical removal of the cyst in conjunction with antiparasitic therapy with albendazole or mebendazole.

Paragonimiasis

Paragonimiasis is an infection caused by the lung flukes of the *Paragonimus* genus transmitted via consumption of raw or undercooked crab or crayfish. All forms of *Paragonimus* result in similar disease and clinical presentations including *Paragonimus westermani* from Asia, *P. africanus* from West Africa, and *P. mexicanus* from Central and South America. Most infections are subclinical, but symptoms can occur with heavy organism burdens [63–65] and include fever, malaise, diarrhea, and abdominal pain, especially early in infection. Symptoms typically resolve with no therapy but may be followed by the development of chest pain and dyspnea associated with exudative eosinophilic pleural effusions. Late phases of pulmonary infection may last for many years without outward evidence of chronic illness, although recurrent hemoptysis can occur. Fever and peripheral eosinophilia are generally absent. Chest radiograph or CT may include ring shadow lesions due to the relative lucency of cystic cavities. The cystic lesions are often located peripherally and are more common in the mid and lower lung zones helping distinguish them from tuberculous cavitation. The presence of pleural effusions (reported in 20–60% of cases) in conjunction with multiple cysts is suggestive of the diagnosis. Perilesional nodules and worm migration tracts are also reported.

The diagnosis is made based on the combination of appropriate environmental exposure, positive serologies, microscopy, and imaging. Early disease may manifest with peripheral eosinophilia though this is rarely seen in later disease. Microscopic examination of expectorated sputum or bronchoalveolar lavage will usually reveal the characteristic eggs with a thick yellowish-brown shell and prominent operculum. A 24-hour sputum collection enhances the sensitivity of detection of eggs. ELISA assays are highly sensitive and specific (92% and > 90%, respectively). These assays are not useful for monitoring response to therapy as antibody levels may not decrease for many years after treatment. Therapy with praziquantel (25 mg/kg three times a day for 3 days) is the treatment of choice for all species of paragonimiasis. Treatment is indicated for symptomatic as well as asymptomatic infections, given the potential for later complications. Cure rates of pulmonary infection approach 100%. Infection can be prevented by avoiding eating raw or undercook crab and crayfish, and strict hygiene measures to prevent fecal contamination of water sources in order to limit transmission.

Conclusion

A number of infectious diseases can produce cystic changes in the lung parenchyma by a variety of pathophysiological mechanisms. While some of these disorders can mimic the common DCLDs, typically, the tempo of disease progression and other associated constitutional symptoms can provide a clue to the underlying etiology. A predominance of cavitary lesions and focal rather than diffuse cystic change can also help ascertain the underlying cause. It is important for clinicians to have a high index of suspicion for infectious etiologies, as these may persist in the chronic phase and may benefit from definite antimicrobial treatments.

Key Learning Points

- A variety of pulmonary infections can produce cystic radiologic changes that may mimic other diffuse cystic lung diseases.
- Clues that might lead clinicians to think about underlying infections may include acuity of symptoms, associated constitutional symptoms such as fever, other symptoms such as purulent sputum, underlying immunosuppressed states such as HIV, coexistence of cavitary and/or nodular lesions, and focal rather than diffuse disease.
- *Pneumocystis jirovecii* is the typical example of infectious cystic lung disease. Cystic lung disease from pneumocystis is seen more commonly in patients with HIV as opposed to other immunocompromised states and is more of a late manifestation.
- Bacterial infections such as *Staphylococcus aureus*, fungal infections such as coccidioidomycosis, and parasitic infections such as paragonimiasis are other common infectious etiologies of cystic lung disease.
- The treatment involves antimicrobials directed at the causative organisms and often leads to resolution of the radiologic findings.
- It is important for clinicians to consider infectious causes when evaluating patients with cystic lung disease as cysts may persist in the chronic phase and definitive antimicrobial treatment may be beneficial.

References

1. Ryu JH, Tian X, Baqir M, Xu K. Diffuse cystic lung diseases. Front Med. 2013;7(3):316–27.
2. Seaman DM, Meyer CA, Gilman MD, McCormack FX. Diffuse cystic lung disease at high-resolution CT. AJR Am J Roentgenol. 2011;196(6):1305–11.
3. Boddu P, Parimi V, Taddonio M, Kane JR, Yeldandi A. Pathologic and radiologic correlation of adult cystic lung disease: a comprehensive review. Pathol Res Int. 2017;2017:3502438.
4. Tuddenham WJ. Glossary of terms for thoracic radiology: recommendations of the nomenclature Committee of the Fleischner Society. AJR Am J Roentgenol. 1984;143(3):509–17.
5. Hansell DM, Bankier AA, MacMahon H, McLoud TC, Muller NL, Remy J. Fleischner society: glossary of terms for thoracic imaging. Radiology. 2008;246(3):697–722.
6. Thomas CF Jr, Limper AH. Current insights into the biology and pathogenesis of Pneumocystis pneumonia. Nat Rev Microbiol. 2007;5(4):298–308.

7. Cisse OH, Pagni M, Hauser PM. De novo assembly of the Pneumocystis jirovecii genome from a single bronchoalveolar lavage fluid specimen from a patient. MBio. 2012;4(1):e00428–12.
8. Morris A, Norris KA. Colonization by Pneumocystis jirovecii and its role in disease. Clin Microbiol Rev. 2012;25(2):297–317.
9. Hardak E, Brook O, Yigla M. Radiological features of Pneumocystis jirovecii pneumonia in immunocompromised patients with and without AIDS. Lung. 2010;188(2):159–63.
10. Huang L, Stansell J, Osmond D, Turner J, Shafer KP, Fulkerson W, et al. Performance of an algorithm to detect Pneumocystis carinii pneumonia in symptomatic HIV-infected persons. Pulmonary complications of HIV infection study group. Chest. 1999;115(4):1025–32.
11. Kanne JP, Yandow DR, Meyer CA. Pneumocystis jiroveci pneumonia: high-resolution CT findings in patients with and without HIV infection. AJR Am J Roentgenol. 2012;198(6):W555–61.
12. Kaplan JE, Hanson DL, Navin TR, Jones JL. Risk factors for primary Pneumocystis carinii pneumonia in human immunodeficiency virus-infected adolescents and adults in the United States: reassessment of indications for chemoprophylaxis. J Infect Dis. 1998;178(4):1126–32.
13. Kaplan JE, Hanson DL, Jones JL, Dworkin MS. Viral load as an independent risk factor for opportunistic infections in HIV-infected adults and adolescents. AIDS. 2001;15(14):1831–6.
14. Ferre C, Baguena F, Podzamczer D, Sanchez C, Viladrich PF, Garau J, et al. Lung cavitation associated with Pneumocystis carinii infection in the acquired immunodeficiency syndrome: a report of six cases and review of the literature. Eur Respir J. 1994;7(1):134–9.
15. Saldana MJ, Mones JM. Pulmonary pathology in AIDS: atypical Pneumocystis carinii infection and lymphoid interstitial pneumonia. Thorax. 1994;49(Suppl):S46–55.
16. Karam MB, Mosadegh L. Extra-pulmonary Pneumocystis jiroveci infection: a case report. Braz J Infect Dis. 2014;18(6):681–5.
17. Peglow SL, Smulian AG, Linke MJ, Pogue CL, Nurre S, Crisler J, et al. Serologic responses to Pneumocystis carinii antigens in health and disease. J Infect Dis. 1990;161(2):296–306.
18. Lowe DM, Rangaka MX, Gordon F, James CD, Miller RF. Pneumocystis jirovecii pneumonia in tropical and low and middle income countries: a systematic review and meta-regression. PLoS One. 2013;8(8):e69969.
19. White PL, Backx M, Barnes RA. Diagnosis and management of Pneumocystis jirovecii infection. Expert Rev Anti-Infect Ther. 2017;15(5):435–47.
20. Safrin S, Finkelstein DM, Feinberg J, Frame P, Simpson G, Wu A, et al. Comparison of three regimens for treatment of mild to moderate Pneumocystis carinii pneumonia in patients with AIDS. A double-blind, randomized, trial of oral trimethoprim-sulfamethoxazole, dapsone-trimethoprim, and clindamycin-primaquine. ACTG 108 study group. Ann Intern Med. 1996;124(9):792–802.
21. Toma E, Fournier S, Dumont M, Bolduc P, Deschamps H. Clindamycin/primaquine versus trimethoprim-sulfamethoxazole as primary therapy for Pneumocystis carinii pneumonia in AIDS: a randomized, double-blind pilot trial. Clin Infect Dis. 1993;17(2):178–84.
22. Smego RA Jr, Nagar S, Maloba B, Popara M. A meta-analysis of salvage therapy for Pneumocystis carinii pneumonia. Arch Intern Med. 2001;161(12):1529–33.
23. Kazanjian PH, Fisk D, Armstrong W, Shulin Q, Liwei H, Ke Z, et al. Increase in prevalence of Pneumocystis carinii mutations in patients with AIDS and P. carinii pneumonia, in the United States and China. J Infect Dis. 2004;189(9):1684–7.
24. Weng L, Huang X, Chen L, Feng LQ, Jiang W, Hu XY, et al. Prognostic factors for severe Pneumocystis jiroveci pneumonia of non-HIV patients in intensive care unit: a bicentric retrospective study. BMC Infect Dis. 2016;16(1):528.
25. Fei MW, Kim EJ, Sant CA, Jarlsberg LG, Davis JL, Swartzman A, et al. Predicting mortality from HIV-associated Pneumocystis pneumonia at illness presentation: an observational cohort study. Thorax. 2009;64(12):1070–6.
26. National Institutes of Health-University of California Expert Panel for Corticosteroids as Adjunctive Therapy for Pneumocystis P. Consensus statement on the use of corticosteroids as adjunctive therapy for pneumocystis pneumonia in the acquired immunodeficiency syndrome. N Engl J Med. 1990;323(21):1500–4.

27. Ahuja J, Kanne JP. Thoracic infections in immunocompromised patients. Radiol Clin N Am. 2014;52(1):121–36.
28. Pennza PT. Aspiration pneumonia, necrotizing pneumonia, and lung abscess. Emerg Med Clin North Am. 1989;7(2):279–307.
29. Landay MJ, Christensen EE, Bynum LJ, Goodman C. Anaerobic pleural and pulmonary infections. AJR Am J Roentgenol. 1980;134(2):233–40.
30. Bartlett JG. The role of anaerobic bacteria in lung abscess. Clin Infect Dis. 2005;40(7):923–5.
31. Duncan C, Nadolski GJ, Gade T, Hunt S. Understanding the lung abscess microbiome: outcomes of percutaneous lung parenchymal abscess drainage with microbiologic correlation. Cardiovasc Intervent Radiol. 2017;40(6):902–6.
32. Hirshberg B, Sklair-Levi M, Nir-Paz R, Ben-Sira L, Krivoruk V, Kramer MR. Factors predicting mortality of patients with lung abscess. Chest. 1999;115(3):746–50.
33. Al-Saleh S, Grasemann H, Cox P. Necrotizing pneumonia complicated by early and late pneumatoceles. Can Respir J. 2008;15(3):129–32.
34. Yang TC, Huang CH, Yu JW, Hsieh FC, Huang YF. Traumatic pneumatocele. Pediatr Neonatol. 2010;51(2):135–8.
35. Danion F, Aguilar C, Catherinot E, Alanio A, DeWolf S, Lortholary O, et al. Mucormycosis: new developments into a persistently devastating infection. Semin Respir Crit Care Med. 2015;36(5):692–705.
36. Gefter WB, Weingrad TR, Epstein DM, Ochs RH, Miller WT. "semi-invasive" pulmonary aspergillosis: a new look at the spectrum of aspergillus infections of the lung. Radiology. 1981;140(2):313–21.
37. Parra I, Remacha A, Rezusta A, Suarez D, Suarez J, Herreras JA, et al. Chronic necrotizing pulmonary aspergillosis. Med Mycol. 2004;42(4):369–71.
38. Soeiro Ade M, Hovnanian AL, Parra ER, Canzian M, Capelozzi VL. Post-mortem histological pulmonary analysis in patients with HIV/AIDS. Clinics (Sao Paulo). 2008;63(4):497–502.
39. Westcott J, Davis SD, Fleishon H, Gefter WB, Henschke CI, McLoud TC, et al. Acute respiratory illness in HIV-positive patients. American College of Radiology. ACR Appropriateness Criteria. Radiology. 2000;215(Suppl):649–53.
40. Rahman FU, Irfan M, Fasih N, Jabeen K, Sharif H. Pulmonary scedosporiosis mimicking aspergilloma in an immunocompetent host: a case report and review of the literature. Infection. 2016;44(1):127–32.
41. Smith JA, Kauffman CA. Pulmonary fungal infections. Respirology. 2012;17(6):913–26.
42. Smego RA Jr, Foglia G. Actinomycosis. Clin Infect Dis. 1998;26(6):1255–61. quiz 62–3
43. Goo JM, Im JG. CT of tuberculosis and nontuberculous mycobacterial infections. Radiol Clin N Am. 2002;40(1):73–87. viii
44. Nahid P, Dorman SE, Alipanah N, Barry PM, Brozek JL, Cattamanchi A, et al. Official American Thoracic Society/Centers for Disease Control and Prevention/Infectious Diseases Society of America clinical practice guidelines: treatment of drug-susceptible tuberculosis. Clin Infect Dis. 2016;63(7):e147–e95.
45. Larsson LO, Polverino E, Hoefsloot W, Codecasa LR, Diel R, Jenkins SG, et al. Pulmonary disease by non-tuberculous mycobacteria – clinical management, unmet needs and future perspectives. Expert Rev Respir Med. 2017;11(12):977–89.
46. Philley JV, DeGroote MA, Honda JR, Chan MM, Kasperbauer S, Walter ND, et al. Treatment of non-tuberculous mycobacterial lung disease. Curr Treat Options Infect Dis. 2016;8(4):275–96.
47. Haworth CS, Banks J, Capstick T, Fisher AJ, Gorsuch T, Laurenson IF, et al. British Thoracic Society guidelines for the management of non-tuberculous mycobacterial pulmonary disease (NTM-PD). Thorax. 2017;72(Suppl 2):ii1–ii64.
48. Bradsher RW Jr. Pulmonary blastomycosis. Semin Respir Crit Care Med. 2008;29(2):174–81.
49. Bradsher RW. Clinical features of blastomycosis. Semin Respir Infect. 1997;12(3):229–34.
50. Galgiani JN, Ampel NM, Blair JE, Catanzaro A, Johnson RH, Stevens DA, et al. Coccidioidomycosis. Clin Infect Dis. 2005;41(9):1217–23.

51. Kauffman CA. Endemic mycoses: blastomycosis, histoplasmosis, and sporotrichosis. Infect Dis Clin N Am. 2006;20(3):645–62. vii
52. Valdivia L, Nix D, Wright M, Lindberg E, Fagan T, Lieberman D, et al. Coccidioidomycosis as a common cause of community-acquired pneumonia. Emerg Infect Dis. 2006;12(6):958–62.
53. Kauffman CA. Histoplasmosis: a clinical and laboratory update. Clin Microbiol Rev. 2007;20(1):115–32.
54. Kim MM, Blair JE, Carey EJ, Wu Q, Smilack JD. Coccidioidal pneumonia, Phoenix, Arizona, USA, 2000–2004. Emerg Infect Dis. 2009;15(3):397–401.
55. Jude CM, Nayak NB, Patel MK, Deshmukh M, Batra P. Pulmonary coccidioidomycosis: pictorial review of chest radiographic and CT findings. Radiographics. 2014;34(4):912–25.
56. Galgiani JN, Ampel NM, Blair JE, Catanzaro A, Geertsma F, Hoover SE, et al. 2016 Infectious Diseases Society of America (IDSA) clinical practice guideline for the treatment of Coccidioidomycosis. Clin Infect Dis. 2016;63(6):e112–46.
57. Chapman SW, Dismukes WE, Proia LA, Bradsher RW, Pappas PG, Threlkeld MG, et al. Clinical practice guidelines for the management of blastomycosis: 2008 update by the Infectious Diseases Society of America. Clin Infect Dis. 2008;46(12):1801–12.
58. Arinc S, Kosif A, Ertugrul M, Arpag H, Alpay L, Unal O, et al. Evaluation of pulmonary hydatid cyst cases. Int J Surg. (London, UK. 2009;7(3):192–5.
59. Morar R, Feldman C. Pulmonary echinococcosis. Eur Respir J. 2003;21(6):1069–77.
60. Kervancioglu R, Bayram M, Elbeyli L. CT findings in pulmonary hydatid disease. Acta Radiol. 1999;40(5):510–4.
61. Santivanez S, Garcia HH. Pulmonary cystic echinococcosis. Curr Opin Pulm Med. 2010;16(3):257–61.
62. Ortona E, Rigano R, Buttari B, Delunardo F, Ioppolo S, Margutti P, et al. An update on immunodiagnosis of cystic echinococcosis. Acta Trop. 2003;85(2):165–71.
63. Lane MA, Marcos LA, Onen NF, Demertzis LM, Hayes EV, Davila SZ, et al. Paragonimus kellicotti flukes in Missouri, USA. Emerg Infect Dis. 2012;18(8):1263–7.
64. Kanpittaya J, Sawanyawisuth K, Vannavong A, Intapan PM, Maleewong W, Zhang W, et al. Different chest radiographic findings of pulmonary paragonimiasis in two endemic countries. Am J Trop Med Hyg. 2010;83(4):924–6.
65. Kim TS, Han J, Shim SS, Jeon K, Koh WJ, Lee I, et al. Pleuropulmonary paragonimiasis: CT findings in 31 patients. AJR Am J Roentgenol. 2005;185(3):616–21.

Chapter 11
Neoplasms That Present as Multicystic Lung Disease

Padraig E. Hawkins, David J. Murphy, Francis X. McCormack, Kathryn A. Wikenheiser-Brokamp, and Cormac McCarthy

Introduction

A pulmonary cyst is defined as a round, well-circumscribed space surrounded by a wall of variable thickness that may be either epithelial or fibrous [1]. Radiologically, a cyst is defined as a round parenchymal lucency or low attenuating area with a well-defined interface with normal lung [2]. Most cysts contain air, but cysts may also be fluid filled or have a solid component. Cysts can have varying wall thickness but are most often thin-walled (i.e., <2 mm). There is considerable overlap between the appearance of cysts and numerous other radiographical and pathological entities including bullae and cavities that are well described elsewhere [3]. Malignant

P. E. Hawkins
Department of Respiratory Medicine, St. Vincent's University Hospital, Dublin, Ireland

D. J. Murphy
Department of Radiology, St. Vincent's University Hospital, Dublin, Ireland
e-mail: David.murphy@svhg.ie

F. X. McCormack
Division of Pulmonary, Critical Care and Sleep Medicine, University of Cincinnati College of Medicine, Cincinnati, OH, USA
e-mail: frank.mccormack@uc.edu

K. A. Wikenheiser-Brokamp
Division of Pathology and Laboratory Medicine, Cincinnati Children's Hospital Medical Center, Cincinnati, OH, USA

Department of Pathology and Laboratory Medicine, University of Cincinnati College of Medicine, Cincinnati, OH, USA
e-mail: Kathryn.wikenheiser-brokamp@cchmc.org

C. McCarthy (✉)
Department of Respiratory Medicine, St. Vincent's University Hospital, Dublin, Ireland

School of Medicine, University College Dublin, Dublin, Ireland
e-mail: Cormac.McCarthy@UCD.ie

N. Gupta et al. (eds.), *Diffuse Cystic Lung Diseases*, Respiratory Medicine,
https://doi.org/10.1007/978-3-030-63365-3_11

processes can arise in the lung as primary cavitating lesions or as metastatic tumors that cavitate. Pulmonary cavitary lesions may contain air-fluid levels and often have thicker walls. Both cavitary and cystic lung lesions may arise from a malignant condition. In this chapter, several malignant conditions that may present as pulmonary cysts are described along with review of the limited available literature that addresses the radiological and pathological appearance as well as the management of these entities.

Primary Lung Cancer

Lung cancer has been the leading cause of cancer death in the United States for many years despite the advent of lung cancer screening programs, public health initiatives to reduce smoking, molecular profiling of lung tumors, and novel targeted therapies [4]. Primary lung cancers (bronchogenic carcinomas) cavitate relatively frequently [5]. While the majority of cavitating lung cancers are thick-walled (i.e., >4 mm), lung cancers presenting as thin-walled cavities or cysts have also been described. A cavity is generally defined as an air- or fluid-filled space with wall thickness of >4 mm [2]. Moreover, the maximal thickness of a given cavity wall around the entire circumference of the structure has been proposed as a means to differentiate benign from malignant cavitary lesions [6]. However, this benchmark is not without exception, as thin-walled cysts can be associated with malignancy. Wall thickness may also be a useful marker of neoplastic activity and malignant potential. Woodring et al. showed that 92% of solitary thin-walled cavities (≤4 mm) were of benign etiology [6]. In a series by Guo et al. only 0.46% of operable lung cancers manifested as thin-walled cysts [7]. Cancers presenting with thin-walled cysts were reported to be typically of an earlier TNM stage than similar sized cancers presenting with thick-walled cavities with lower metabolic activity and rates of vascular invasion and metastases [8].

Thin-walled cystic primary lung cancers are usually solitary and are most often adenocarcinomas [9, 10] **(**Figure 11.1a-c**).** Squamous cell lung cancers account for only 4% to 29% of cystic lung cancers [11] **(**Figure 11.1d-h**).** While a portion of these cystic lung cancers may arise de novo, in an area of previously normal lung, primary lung cancers may also arise in a pre-existing cystic airspace [10]. Protean presentations of cystic lung cancers may pose a diagnostic challenge and result in missed, erroneous, or delayed diagnoses. A cystic airspace may include a bronchiectatic airway, bullous emphysema (Figure 11.1b), congenital malformation, fibrotic cyst, or subpleural bleb. To assist physicians in determining the potential malignant nature of thin-walled cysts, Mascalchi et al. described four morphological types of pericystic lung cancers based on chest computed tomography (CT) radiographic findings: type I – a nodule abutting the external aspect of a lung cyst, type II – a nodule arising from the cyst wall and projecting to the inner surface of a cystic space, type III – cyst wall thickening, and type IV – a multicystic lesion containing areas of soft tissue attenuation [12]. In a subsequent review of cases by Xue et al., radiological signs suggestive of malignancy, including those described by Mascalchi et al., were present in all 18 individuals who were diagnosed with lung cancer presenting as a solitary thin-walled cavity [9].

Fintlemann et al. described pathologic data on 21 cystic primary lung cancers and concluded that the mechanisms of cystic airspace formation in neoplastic processes fall into one of four categories: (1) check-valve mechanisms in which proximal airway obstruction leads to dilation and ballooning of distal airspace, (2) adenocarcinomas that infiltrate around emphysematous cysts, (3) cavitation of a nodule due to central necrosis, and (4) adenocarcinomas that arise within a preexisting bulla. In this study, the authors found that 7 out of 30 patients had another cystic lesion elsewhere in the lung and that 4 out of 7 patients represented with a synchronous lung cancer [13]. Metastatic disease from cystic primary lung cancers is rare. In one cohort of 45 patients, only 3 patients had metastatic spread [5].

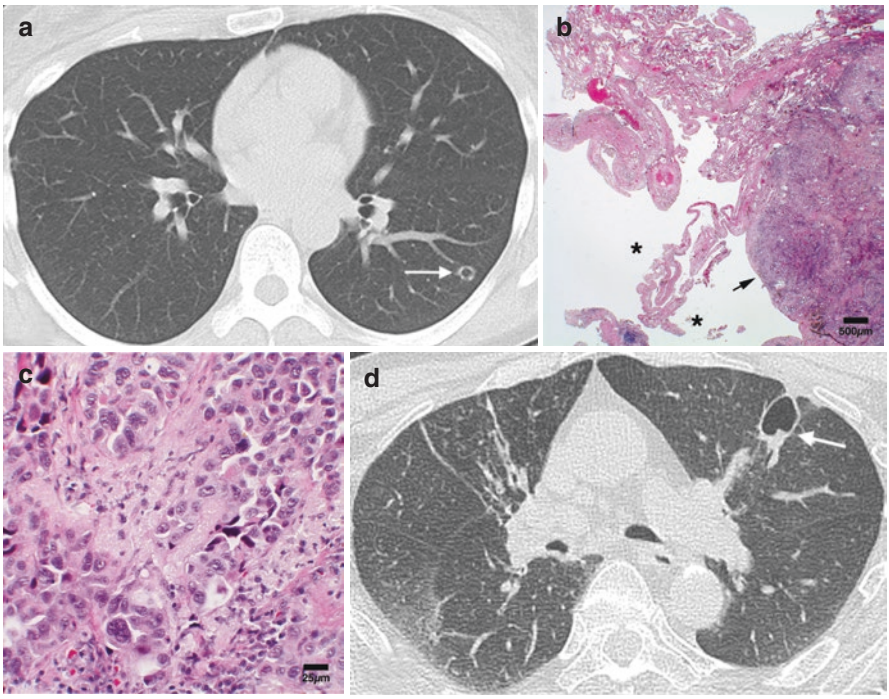

Fig. 11.1 Primary lung cancer with cavitation. (**a**) A 9 mm left lower lobe nodule with a central cystic airspace (*arrow*) identified on chest CT radiological imaging diagnosed as primary lung mucinous adenocarcinoma on biopsy. (**b**) Histologic image showing a solid nodule (*arrow*) at the periphery of bullous emphysema (*) (H&E). (**c**) Higher magnification histologic image demonstrates that the nodule is comprised of an infiltrating poorly differentiated non-small cell carcinoma found to have features of both adenocarcinoma and squamous cell carcinoma (H&E). (**d**) Chest CT image showing a 33-mm left upper lobe cavity with irregular wall thickening (*arrow*) at its posterolateral aspect, identified as pulmonary squamous cell carcinoma on biopsy. (**e**) Histological image of a subpleural cystic lesion with a peripheral solid component (*arrow*) extending into the cystic space (*) developing in a 69-year-old man with smoking-related lung disease (H&E). (**f**) A carcinoma infiltrating a reactive desmoplastic stroma comprised the nodular component (H&E). (**g**) Nests of malignant cells were also present within the cystic spaces (H&E). (**h**) Squamous cell carcinoma was diagnosed based upon morphological features including intercellular bridges (*arrow*) and keratin production (*) (H&E)

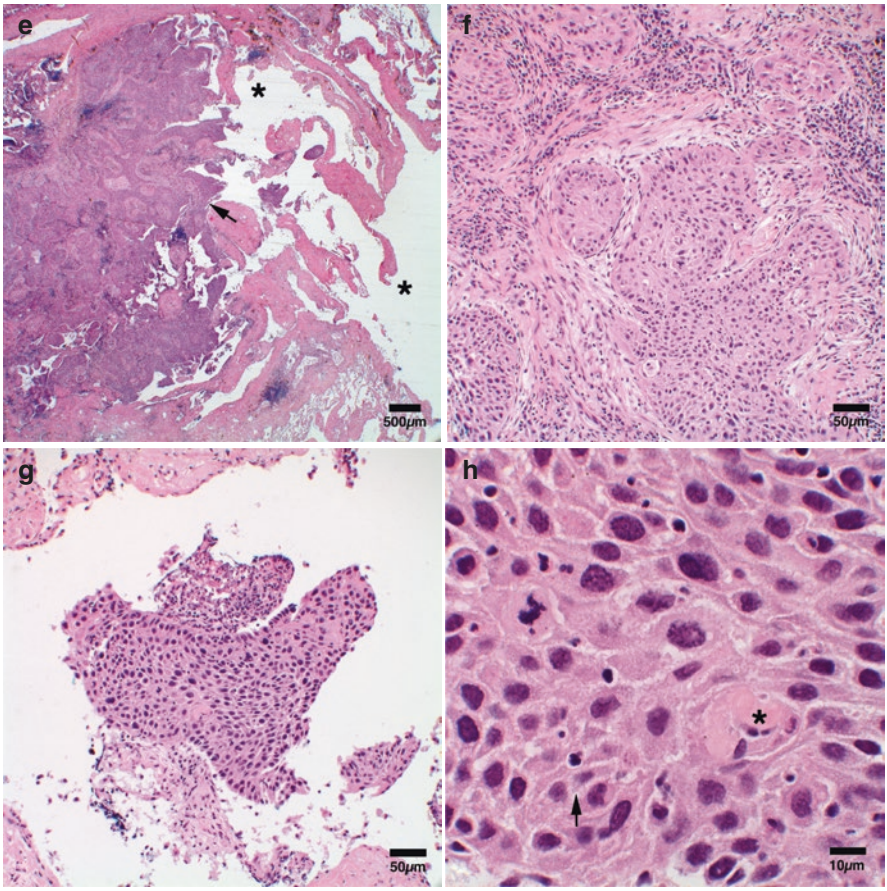

Fig. 11.1 (continued)

Farooqi et al. examined CT scans from a lung cancer screening program and found 26 cases of lung cancers (3.7%) abutting a cystic airspace. Emphysema was present in 73% of these patients [10]. With the advent of CT screening for lung cancer, it is likely that diagnosis of these thin-walled cystic lung cancers will become more common and provide insights into the pace and mechanisms of their evolution.

The diagnosis of cystic lung cancers poses other diagnostic issues for physicians. Positron emission tomography–computed tomography (PET-CT) relies on a critical mass of metabolically active cells within a confined area that is often not the case in cystic lung cancers, in which the malignant cells are less densely clustered and infiltrate along cyst wall planes. Secondly, the fact that low-grade adenocarcinomas and in situ pulmonary adenocarcinomas (formerly bronchioalveolar cell carcinomas) are the most common lung cancers associated with cystic air spaces reduces the effectiveness of PET-CT as a diagnostic modality given that these tumor types typically have lower metabolic activity and PET positivity than other lung cancer types

[10]. CT-guided biopsy of cystic lung cancers may also be associated with increased risk of complications and be technically challenging given their small size and association with cystic air spaces [11]. Nakahara et al. used a technique of percutaneous needle washing of cysts for cytological analysis which showed good diagnostic sensitivity but is not widely used and does not likely provide sufficient tissue for molecular typing [14].

Metastatic Adenocarcinoma

The majority of primary lung cancers presenting as cystic lesions are adenocarcinomas. Metastatic adenocarcinomas that arise in extrapulmonary primary sites, usually from gastrointestinal (GI) or genitourinary (GU) organs, can result in cystic pulmonary metastases as has been reported for colorectal carcinoma (Figure 11.2a), cholangiocarcinoma and pancreatic adenocarcinoma (Figure 11.2b) [15–17], and urothelial and endometrial carcinomas (Figure 11.2c) [18]. The radiological manifestations of cystic metastases can vary from isolated solitary cystic lesions to diffuse cystic lung lesions.

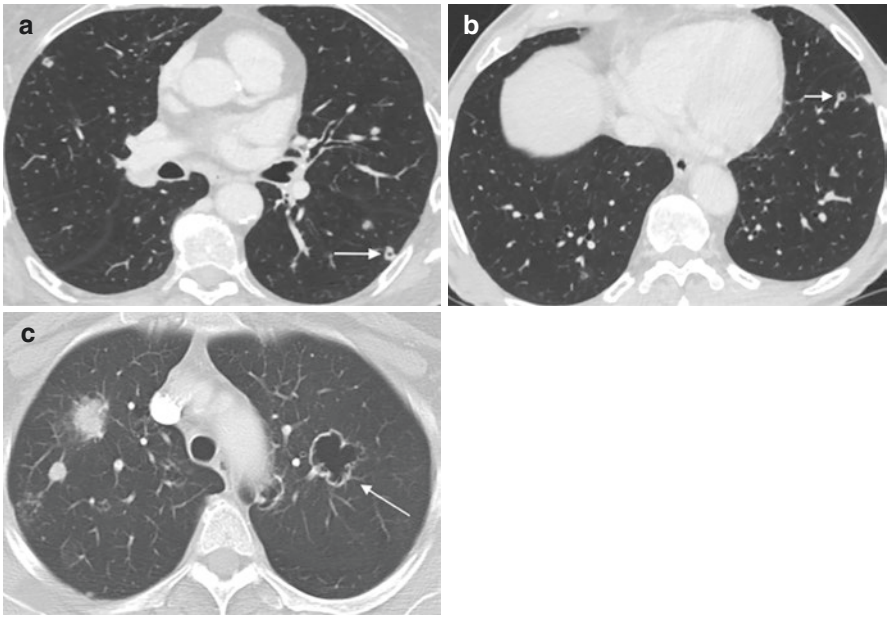

Fig. 11.2 Pulmonary cavitary metastases. (**a**) Metastatic rectal adenocarcinoma with multiple scattered subcentimeter pulmonary metastases, including an 11 mm left lower lobe nodule with a central cystic airspace (*arrow*). (**b**) Metastatic pancreatic adenocarcinoma with multiple small pulmonary metastases and a 6 mm left lower lobe nodule with central cystic airspace (*arrow*). (**c**) Cavitating pulmonary metastasis from primary endometrial carcinoma (*arrow*)

Bladder Carcinoma

The most common histological type of bladder cancer is transitional cell carcinoma (TCC), sometimes called urothelial cell carcinoma. It is the ninth most common cancer worldwide [19] and has a significant male predominance, most likely due to its association with cigarette smoking [20]. Approximately 70% of bladder cancers present as superficial disease, which, despite risk of local recurrence, rarely progress to locally invasive or metastatic disease. The most common sites of TCC metastatic spread are liver, lung, and bone. Although the usual patterns of lung involvement are solid nodules, multiple nodules, a solitary mass, pleural effusion, or interstitial micronodules [21], TCC can also rarely manifest as cavitating nodules or masses [21, 22]. Imokawa et al. reported a case of a 75-year-old man who presented with cystic metastases and bilateral pneumothoraces requiring surgical intervention [23]. On histological examination, the walls of the cyst were lined by a dense proliferation of tumor cells, and the terminal bronchioles were narrowed by the presence of tumor cells. Tumor emboli were also present in the pulmonary arteries. Hiensch et al. reported a case with both cavitary and cystic nodules in the lung due to metastatic TCC confirmed by biopsy [20]. Fiorelli et al. reported cavitary pulmonary metastases with wall thicknesses ranging from 2 mm to 5 mm in patients with TCC of the bladder [24]. Excavation of solid nodules may occur in response to chemotherapeutic treatment of metastatic TCC resulting in cavitary and cystic lung lesions (Fig. 11.3) [25].

Sarcomas

Sarcomas are rare malignant tumors originating in tissues of mesenchymal origin [26]. Sarcomas are rare in adults, representing approximately 1% of all adult malignancies. Soft tissue sarcomas of 50 histological subtypes account for 80% of these tumors. The various tumor types are named based on the tissue of origin, according to the 2013 WHO classification [27]. The most common sarcoma subtypes in adults

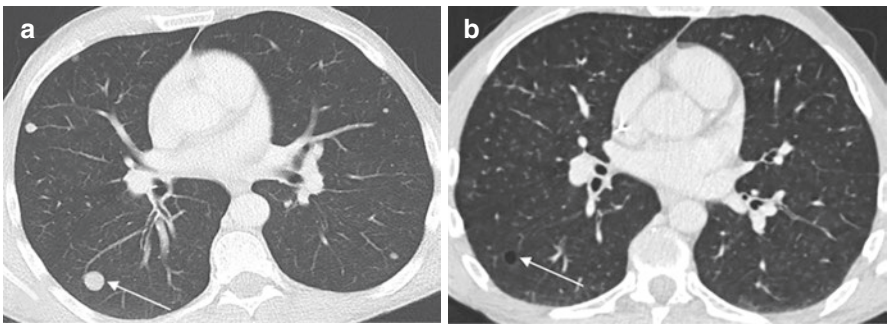

Fig. 11.3 Metastatic urothelial carcinoma. (**a**) Metastatic transitional cell carcinoma with a moderate-sized solid-appearing metastasis in the posterior right lower lobe (*arrow*). (**b**) The metastasis became cystic after systemic chemotherapy for transitional cell carcinoma (*arrow*)

are leiomyosarcoma, undifferentiated pleomorphic sarcoma, sarcoma not otherwise specified, liposarcoma, dermatofibrosarcoma, rhabdomyosarcoma, and angiosarcoma. Although most of these soft tissue sarcomas arise in the limbs, they can occur in any part of the body including visceral organs and retroperitoneal soft tissues, as well as in the thoracic and head and neck regions. The lung is the most common site of sarcoma metastasis with the majority of metastatic lesions being solid nodules, either solitary or multiple. Pulmonary metastases arising from sarcomas may also manifest as ground-glass nodules, cavitating nodules, and masses [28]. Occasionally sarcoma metastases to the lung may present as thin-walled cavities.

Epithelioid sarcoma accounts for 0.6% to 1% of sarcomas [29], and it affects mainly adolescents and young adults. The cell type of origin is unknown, and the malignancy is occasionally misdiagnosed as a benign lesion [29]. Epithelioid sarcoma may affect the fingers, hand, wrist, forearm, knee, or the lower leg. Lesions may be deep-seated, attached to tendons and bone, or superficial, presenting as firm, slow-growing, painless nodules or plaques. Epithelioid sarcoma may be solitary or multiple and tend to ulcerate. Metastases develop in up to 40% of individuals, with the lungs being the predominant site of spread. While pulmonary metastases related to epithelioid sarcoma typically present as solid nodules [28], cystic pulmonary lesions may also form [29–36]. Hoshi et al. reviewed previously reported cases of cystic pulmonary metastases from epithelioid sarcoma and found that most cases were associated with multiple bilateral metastases and frequently with pneumothorax that occurred in 85.7% of cases [29].

Angiosarcoma is a rare, malignant neoplasm of the vascular or lymphatic endothelium. The incidence of this tumor peaks in the seventh decade of life and more commonly affects males. Angiosarcomas present in two forms, cutaneous and soft tissue, and are aggressive tumors that infiltrate local lymph nodes, bone, and liver with early metastasis to the lungs. The 5-year survival of patients affected by angiosarcoma is <15% [37]. Most soft tissue angiosarcomas present in the deep muscles of the leg but may also occur in the arms, trunk, head, and neck. Cutaneous angiosarcomas most often present on the face and scalp. Von Willebrand factor is the most specific of the vascular markers for this tumor but angiosarcomas also stain positively for CD31, CD34, and D2–40 (a monoclonal antibody directed against podoplanin, a mucoprotein expressed on lymphatic endothelium) by immunohistochemical stains. The median survival for head and scalp angiosarcoma following the appearance of lung metastases is only 4 months [38–40].

Masuzawa et al. reviewed 23 cases of angiosarcoma of the scalp with metastases to the lung [41]. The patients were 59 to 94 years old with a male:female ratio of 16:7. The pulmonary metastases were multiple solid nodules in 39% of cases, multiple thin-walled cysts in 39%, a mix of cystic and nodular lesions in 13%, and ground-glass opacities in 9%. On serial CT imaging, there was no evidence of solid nodules prior to the development of cysts. Pneumothorax was common in the patient cohort with thin-walled cysts, with 11 of the 12 cases experiencing lung collapse [41]. Tateishi et al. reviewed CT findings of individuals with metastatic angiosarcoma of the lung at their institution between 1984 and 2001 [42]. Symptoms related to pulmonary metastases were present in less than half of these patients and included dyspnea, cough, hemoptysis, and chest pain. Multiple solid nodules were the most

common high-resolution CT (HRCT) presentation of pulmonary metastases from angiosarcoma (63%), while 21% had multiple thin-walled cysts representing the second most common presentation. All patients with multiple thin-walled cysts developed pneumothorax or hemothorax [42]. Indeed, pneumothorax may precede the diagnosis of the primary tumor in individuals with angiosarcoma [40].

Endometrial stromal sarcoma (ESS) accounts for 7% to 25% of all uterine mesenchymal tumors but <1% of all uterine tumors [43]. After leiomyosarcoma, ESS is the second most common type of mesenchymal neoplasm in the uterus. Based on clinical, pathological, and genetic characteristics, endometrial stromal tumors are divided into four categories: endometrial stromal nodule, undifferentiated uterine sarcoma, high-grade ESS, and low-grade ESS. Patients typically present with vaginal bleeding or pelvic pain. The lungs are a site of distant metastases in 7% to 28% of individuals [44]. Aubry et al. reported that the delay between diagnosis of uterine ESS and the establishment of a diagnosis of pulmonary metastases is a mean of 9.9 years (2.5–20 years) [44]. Xu et al. reviewed 36 cases of low-grade ESS (LGESS) reported in the literature [45]. LGESS is a slowly growing tumor with a course characterized by multiple relapses, which may be late and occur locally or at a remote site [46]. Up to 50% of pulmonary metastases from LGESS are asymptomatic. When symptoms are present, dyspnea is the most common, followed by chest pain. Regarding radiological findings, pulmonary metastases present as multiple pulmonary solid nodules in 50%, as a solitary nodule in 16.7%, as cystic lesions in 16.7%, and as pneumothorax in 19.4%.

Osteosarcoma is a primary malignant bone tumor with frequent early metastases that are found at presentation in 20% of cases. Osteosarcoma typically metastasizes to the lung, representing 85% of the metastatic disease that occurs with this cancer type [47]. Metastatic lesions from osteosarcoma most often take the form of solid nodules (up to 85%) and most (60%) are calcified [28]. While the majority of nodules are solid, there are reports of cavitation and presentation with thin-walled cavities. One case demonstrated a thin-walled cavity with nodularity in the wall that exhibited foci of calcification [48]. With its predilection for spread to the lung and the relatively high frequency of presentation as cysts, one must consider metastatic sarcoma in the broad differential of cystic lung disease. It is important to be cognizant of the potential for delayed spread of certain sarcomas and the potential of cystic metastases from these tumors to present with pneumothorax. Hoag et al. reviewed 126 cases of pneumothorax secondary to sarcomatous metastases and found that the most common sarcoma subtypes were osteogenic sarcoma (31.4%), followed by angiosarcoma (18.3%), synovial sarcoma (8.5%), and epithelioid sarcoma (1.3%). The authors concluded that transpleural rupture of subpleural cysts is the likely mechanism for the development of metastatic sarcoma–related pneumothoraces [49].

Perivascular Epithelioid Cell Neoplasms

Perivascular epithelioid cell neoplasms (PEComas) are rare mesenchymal neoplasms that can arise in diverse tissues and exhibit clinical behaviors ranging from benign to

malignant. The cell of origin is unclear, but PEComa are immunoreactive for smooth muscle and melanocytic markers [50]. PEComas are arranged around blood vessels and even within walls of small- to medium-sized blood vessels, often giving the appearance of being an integral part of these structures [51]. PEComas comprise a family of tumors that include angiomyolipoma (AML), clear cell "sugar" tumor (CCST) of the lung, lymphangioleiomyomatosis (LAM), primary extrapulmonary sugar tumor, clear cell myomelanocytic tumor of the falciform ligament/ligamentum teres (CCMMT), abdominopelvic sarcoma of PECs, and other tumors with similar features arising at various sites that are simply termed PEComa-not otherwise specified [52]. There is a strong association between the tuberous sclerosis complex (TSC), AML, and LAM in that these PEComas frequently harbor mutations in TSC genes (most often TSC2) and transcription factor E3 (TFE3) [51]. LAM is an archetypal diffuse cystic lung disease, presenting as a rare, female-predominant, low-grade, metastasizing neoplasm characterized by progressive infiltration of lung parenchyma by abnormal smooth muscle cells. The AMLs seen in LAM patients are related PEComas, which occur due to dysregulated mechanistic target of rapamycin (mTOR) signaling. The cysts in LAM are diffuse in distribution, and classically round to oval and thin-walled [53]. LAM is covered in detail in Chap. 5.

Fewer than 65 PEComas other than AML, LAM, and CCST have been reported [54]. The lung is the most common site of metastatic disease in malignant PEComas, typically presenting as discrete bilateral pulmonary nodules that rarely cavitate. Lung may be the sole site of metastatic spread, although the liver and peritoneum are additional common targets of PEComa metastases [55]. Okomato et al. described the case of a woman with a PEComa presenting with pneumothorax and persistent air leak associated with nodular, cavitary, and cystic lung metastases [56]. Tumor cells harboring loss of TSC1 heterozygosity were shown to be infiltrating the visceral pleura with disruption of elastic fibers.

Pulmonary Langerhans Cell Histiocytosis

Pulmonary Langerhans cell histiocytosis (PLCH) is a rare, progressive diffuse cystic lung disease, seen primarily in young adults with a history of smoking [57]. Peribronchiolar infiltration of inflammatory and Langerhans cells results in bronchiolocentric stellate interstitial nodules, which may cavitate and form thin-walled cysts (Figure 11.4a-b) [58]. Cysts are often irregular, bilobed, cloverleaf-shaped, or bizarrely shaped. Irregular cysts with nodules in an upper zone distribution may indicate PLCH over other diffuse cystic lung diseases [53]. The histopathological requisite diagnostic feature of PLCH is clusters of Langerhans cells with characteristic nuclear morphology and positive immunostaining for CD1a and/or S-100 antigen (Figure 11.4c-e). The natural history of PLCH is variable, and many patients experience progressive dyspnea, respiratory insufficiency [59, 60], and spontaneous pneumothoraces [61]. PLCH is discussed in greater detail in Chap. 6.

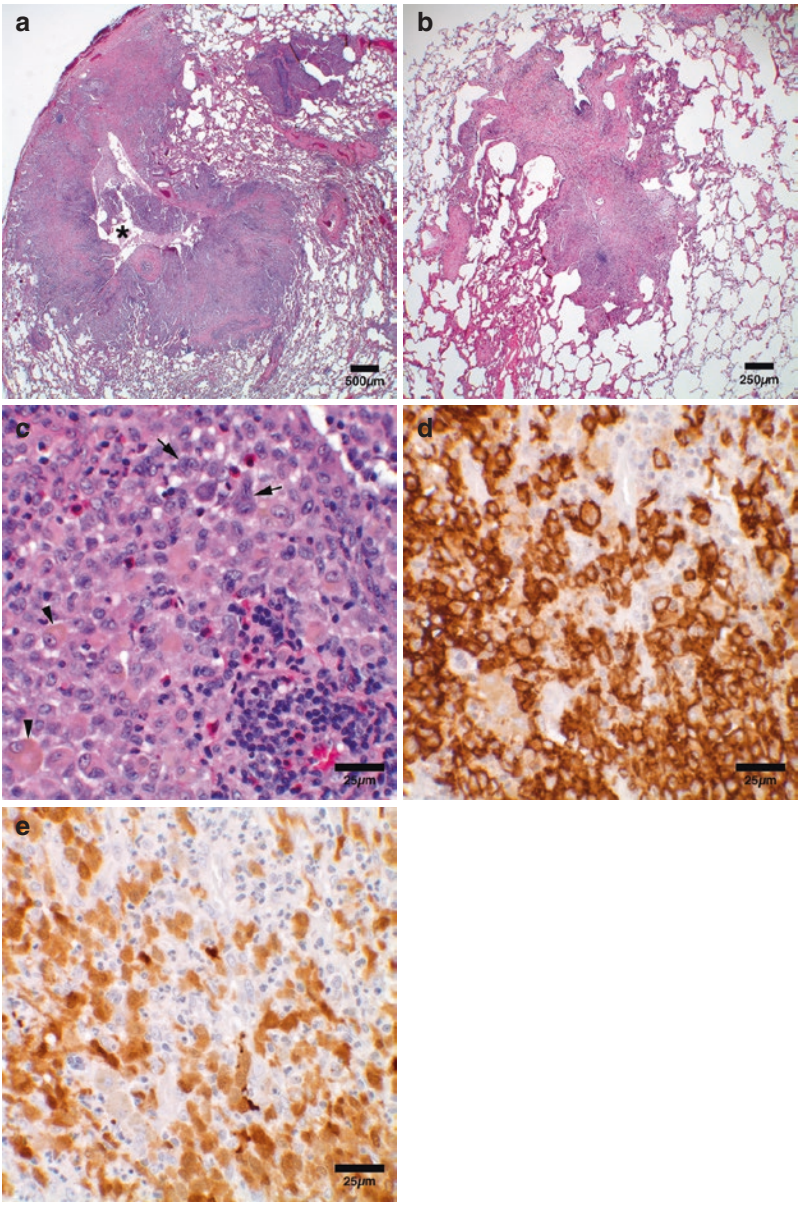

Fig. 11.4 Pulmonary Langerhans cell histiocytosis (PLCH). (**a**) Characteristic peribronchiolocentric cellular nodule of PLCH with some fibrosis. The central region (*) may appear cystic radiographically but actually represents a bronchiolar lumen with the airway wall replaced by the cellular infiltrate (H&E). (**b**) Characteristic stellate-shaped fibrotic PLCH lesion with surrounding enlarged airways formed by traction of the fibrosis (H&E). (**c**) The cellular infiltrate consists of Langerhans cells with folded or kidney-shaped nuclei (*arrows*) admixed with lymphocytes, eosinophils, and macrophages, including pigmented macrophages associated with cigarette smoking (*arrowheads*) (H&E). (**d**) The Langerhans cells have CD1a membrane staining by immunohistochemistry (CD1a). (**e**) Langerhans cells are also immunopositive for S-100 antigen (S-100)

Benign Metastasizing Leiomyoma

Uterine leiomyomas (fibroids) are the most common benign tumor of the uterus [62]. Leiomyomas typically present as multiple variably sized tumors, ranging from a few millimeters to 20 cm. Leiomyomas originate in the myometrium and are comprised of slowly growing smooth muscle cells. Up to 70% of women over the age of 50 have uterine leiomyomas on imaging with up to a third of women requesting surgery for symptoms of menorrhagia or pelvic pain [62]. Benign metastasizing leiomyoma (BML) is a rare condition that may present incidentally in women of reproductive age, often in those with a history of prior surgery for uterine leiomyoma. The interval between hysterectomy for uterine leiomyoma and diagnosis of BML ranges from 3 to 20 years [63]. Peritoneal seeding after myomectomy or hysterectomy has been suggested as a possible mechanism for development of BML as it is more often found in patients who have undergone these procedures. While the lung is the most common site of metastases, other sites that may be involved include the skin, retroperitoneum, lymph nodes, bone, mediastinum, and heart. The typical radiological appearance of BML in the lung is single or multiple pulmonary nodules ranging in size from a few millimeters to several centimeters, with sparing of the pleural surface [64]. Nodules may cavitate, although this is rare [65]. BML must be differentiated from other pulmonary smooth muscle tumors such as leiomyosarcoma as well as metastatic endometrial stromal sarcoma. The low proliferative activity and lack of local invasion aid in the differentiation of BML from other, more aggressive neoplasms.

Leiomyosarcoma may be considered the malignant counterpart of leiomyomas [66]. Leiomyosarcomas are a smooth muscle cell tumor that most commonly occur in the abdomen involving the uterus, gastrointestinal tract, or retroperitoneum but may also occur in the dermis and superficial soft tissues. Leiomyosarcomas account for approximately 25% of sarcomas with an approximately 40% risk of metastatic spread [67]. Non-cutaneous leiomyosarcoma is an aggressive tumor that is associated with a 50% 5-year mortality. Primary pulmonary leiomyosarcoma is much less common than metastatic leiomyosarcoma [68], and only the latter has been reported to be associated with cystic lung changes and pneumothorax [69, 70].

Recurrent Respiratory Papillomatosis with Pulmonary Involvement

Recurrent respiratory papillomatosis (RRP) can present with thin-walled cystic change [71]. Respiratory papillomatosis is caused by human papilloma virus (HPV), most commonly types 6 and 11, and is a condition that predominantly affects infants and adolescents. Papillomas are the most common benign tumors of the laryngotracheal region [72]. The larynx is the primary site for RRP and extension into the more distal airways is unusual. In a review of eight large case series encompassing

532 patients with laryngeal papillomatosis, only 5% had involvement of the trachea and/or proximal bronchi, and < 1% had extension into the lung parenchyma [73]. The average interval between presentation of laryngeal papillomatosis and involvement of the lung is 12 years. Distal papillomas are rare in the absence of laryngeal involvement [74].

Radiological findings of distal airway papillomatosis are varied. Tracheal and bronchial wall abnormalities may include narrowing and irregularity, and parenchymal findings of thin-walled cysts, nodules, patchy densities, or fibrosis may present contemporaneously or subsequently. A systematic review revealed that the most common radiographic presentation of lung papillomatosis was that of numerous bilateral pulmonary nodules, including cavitation in various stages of evolution, from central clearing to thin-walled cysts. Patients with RRP occasionally present with pneumothorax [71]. Pathologically, papillomas in the large airways including the trachea and bronchi are comprised of stratified squamous epithelium overlying fibrovascular cores forming exophytic projections into the airway lumen (Figure 11.5a-b). The squamous cells may have HPV-related viral cellular changes referred to as koilocytosis. Papillomas can also involve the distal airspaces as squamous epithelial nests filling and expanding alveolar airspaces (Figure 11.5c). In rare cases, malignant transformation to invasive squamous cell carcinoma occurs with invasion and destruction of the surrounding lung (Figure 11.5a and 5d). Cidofovir, an antiviral agent, has been used to empirically treat pulmonary cystic and nodular involvement by papillomas [75].

Congenital Cysts and Pediatric Cystic Lung Neoplasms

Congenital pulmonary airway malformation (CPAM), formerly known as congenital cystic adenomatoid malformation (CCAM), is a cystic developmental anomaly that is rarely associated with malignant transformation in children and adults [76]. CPAM occurs in approximately 1 in 10,000 to 25,000 live births. It is a form of congenital cystic lung disease with combined features of developmental immaturity and malformation that is characterized by varying degrees of cystic dilatation of airways, usually affecting only one lobe (Figure 11.6a-d) [77]. CPAM has a wide range of presentations clinically, from antenatal fetal demise, to severe respiratory distress in the newborn, to less life-threatening manifestations in the infant or young child such as recurrent pulmonary infections or pneumothorax. CPAMs that result in symptoms are typically removed in early life. CPAM rarely presents in adults as an incidental finding. Numerous reports have documented development of lung cancers associated with CPAM, the most common tumor types in adults being adenocarcinoma and adenocarcinoma in situ (formerly classified as bronchioloalveolar

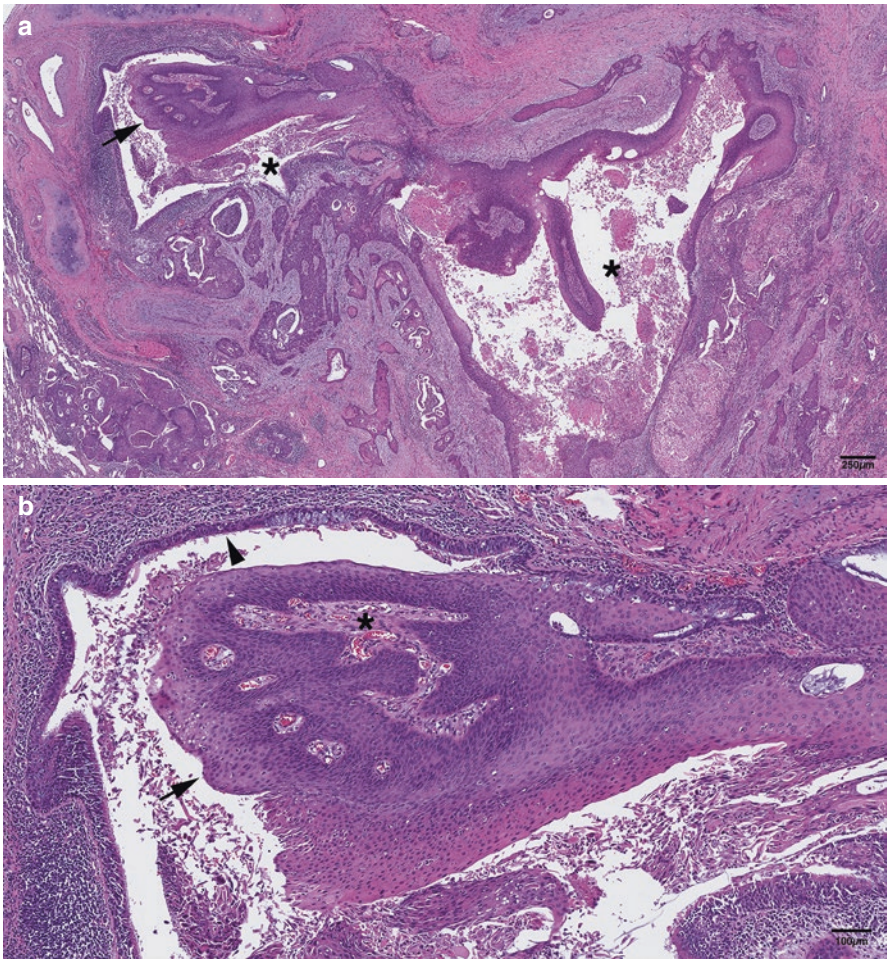

Fig. 11.5 Recurrent respiratory papillomatosis with squamous cell carcinoma. (**a**) Respiratory papillomatosis involving the bronchus with papillary structures (*arrow*) protruding into the dilated bronchiectatic airway lumen (*) appearing as a cavity (H&E). (**b**) The papillary structures are comprised of a fibrovascular core (*) lined by stratified squamous epithelium (*arrow*) that differs from the normal pseudostratified ciliated respiratory epithelium lining the bronchial lumen (*arrowhead*) (H&E). (**c**) Papillomas involve the distal lung parenchyma as squamous cell nests filling (*arrow*) and expanding (*) alveolar spaces (H&E). (**d**) In contrast to the squamous papillomas, the squamous cell carcinoma is comprised of irregular squamous cell nests (*arrows*) containing highly atypical cells (*arrowhead*) invading a desmoplastic stroma (*) (H&E)

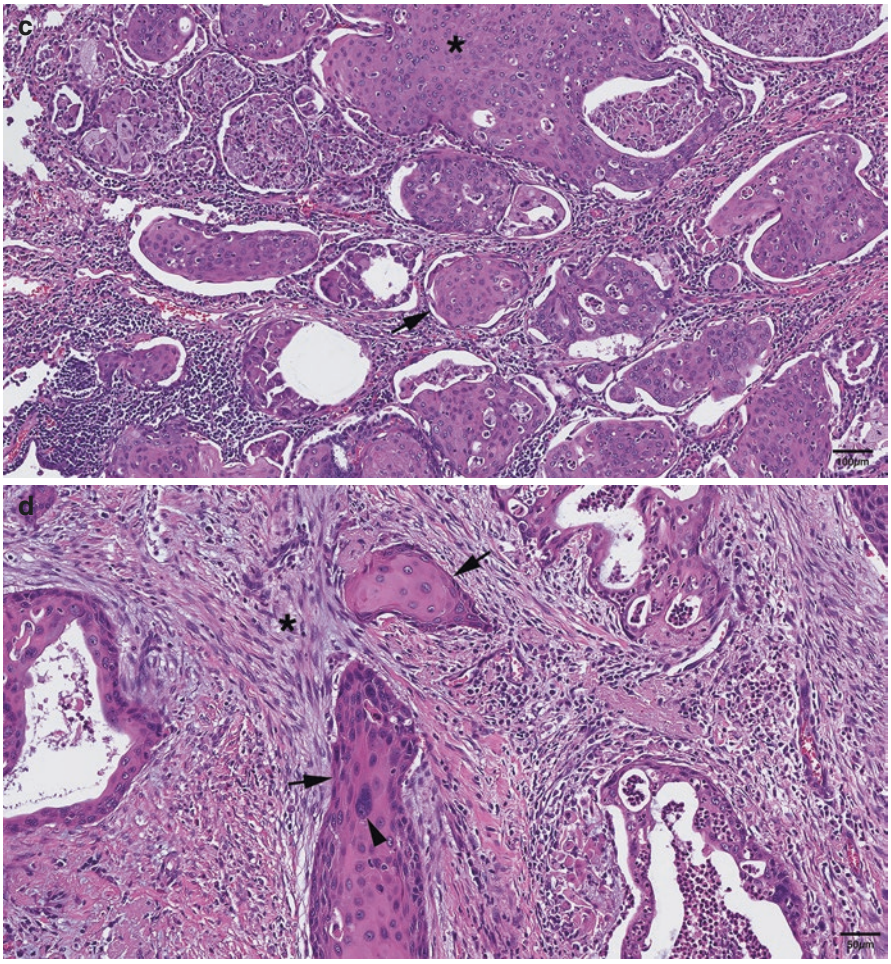

Fig. 11.5 (continued)

carcinoma) followed by squamous cell carcinoma [78]. The most common malignancies reported to be associated with CPAM in children are pleuropulmonary blastoma (PPB) and rhabdomyosarcoma, followed by adenocarcinoma and adenocarcinoma in situ [78]. It is now clear that subtypes of PPB and CPAM have indistinguishable histological and radiological features and thus represent the same entity. Malignant cells in PPB can undergo skeletal muscle differentiation resembling rhabdomyosarcoma thus requiring careful evaluation to differentiate the two entities. Moreover, it is critically important that PPB not be diagnosed as CPAM to ensure the patient receives the appropriate care and management.

Childhood primary lung tumors are rare. The most common of these, pleuropulmonary blastoma (PPB), is diagnosed by 6.8 years of age in 95% of cases

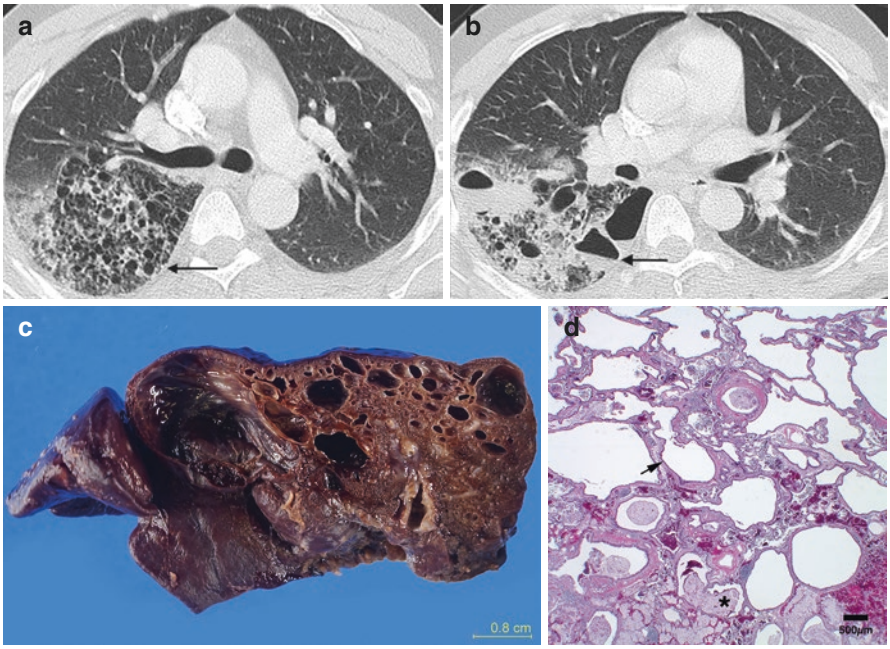

Fig. 11.6 Congenital pulmonary airway malformation (CPAM). (**a**) Large cluster of small cysts (*arrow*) is seen in the right lower lobe by chest CT, compatible with CPAM. (**b**) Note the air fluid level (*arrow*) in some of the larger cysts. (**c**) CPAM with cysts of variable size measuring up to 2.1 cm. (**d**) Histologic section of another CPAM with small cysts showing numerous bronchiole-like structures (*arrow*) that are not accompanied by arteries as is seen in the normal lung. Some of the bronchiolar structures contain intraluminal mucin (*) supporting airway obstruction as a potential mechanism for CPAM formation (H&E)

[79]. Radiological findings in PPB are varied and include solitary or multiple cysts, or a combination of solid and cystic lesions. PPB is categorized into three subtypes based on gross morphological features that represent tumor progression: type I (purely cystic), type II (solid and cystic), and type III (purely solid) (Figure 11.7a-c). Types II and III PPB are more aggressive and have the potential for both local recurrence and distant metastasis with the brain being the most common site of metastatic spread [79]. Mean 5-year, disease-free survival in patients with type I PPB is 80% to 90%, whereas patients with types II and III PPB have a mean survival of less than 50% [79]. Congenital and developmental causes of lung disease, including CPAM and PPB, are discussed in greater detail in Chap. 12.

Mesenchymal cystic hamartoma (MCH) is a rare condition, with less than 20 cases described in the literature to date [80]. It is characterized by nodular and cystic lung changes that result from the slow proliferation of immature mesenchymal cells. While it may present in childhood, it may not come to clinical attention until the third or fourth decade of life. Presenting symptoms include hemoptysis, pneumothorax, dyspnea, and potentially fatal pulmonary hemorrhage [81, 82]. Nodules

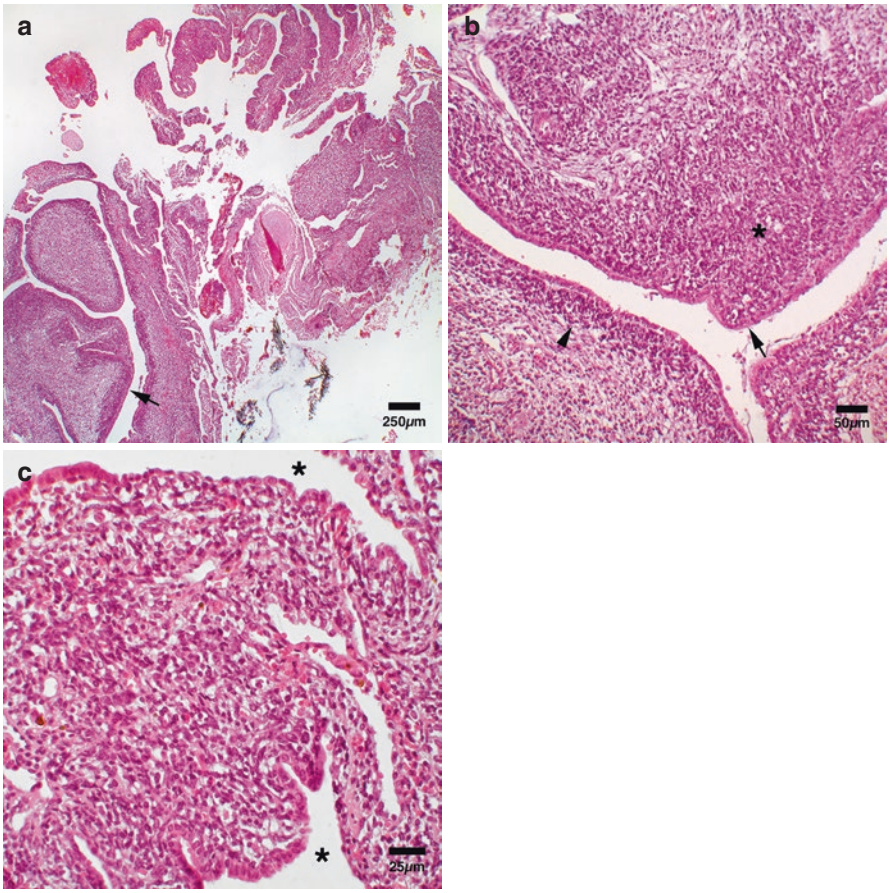

Fig. 11.7 Pleuropulmonary blastoma. (**a**) Histological sections of 4.5 cm multiloculated cyst with a focal 1 cm solid region typical of a type II PPB resected from a 2.5-year-old child with a congenital lung cyst. A multicystic mass is present with focal expansion of the cyst wall (*arrow*) (H&E). (**b**) The cyst wall is expanded by neoplastic immature mesenchymal cells (*) underlying the epithelium lining the cyst (*arrow*). The immature mesenchymal cells are focally concentrated under the epithelium (*arrowhead*) forming a cambium layer characteristic of PPB (H&E). (**c**) Higher magnification image of the neoplastic immature mesenchymal cells expanding the septa separating the cysts (*) (H&E)

tend to be small and become cystic as they enlarge (>1 cm) and are usually multifocal and bilateral, with large cysts described. Lung biopsy is generally required to make the diagnosis of MCH as it may mimic PPB, CPAM, and LAM. As this condition is generally benign and indolent, no treatment is typically required outside of management of complications, such as hemoptysis, which may require lung resection. Surveillance is advisable as there is the potential for malignant transformation to mesenchymal sarcoma as described by Hedlund et al. [83].

Lymphoproliferative Disorders

Lymphoma may involve the lung by hematogenous spread from Hodgkins or non-Hodgkin disease, local extension from mediastinal or hilar lymphoma, or by primary pulmonary involvement [84]. Lung involvement by lymphoproliferative disorders that originate outside of the lung is much more common than primary pulmonary lymphoma. Primary pulmonary lymphoma accounts for only 0.5% of all lung neoplasms [85], and it is typically classified as low-grade B cell lymphoma, lymphomatoid granulomatosis, and high-grade B cell lymphoma. Low-grade B cell lymphoma accounts for 58% to 87% of primary pulmonary lymphomas with mucosa-associated lymphoid tissue (MALT) lymphomas comprising 90% of the cases. MALT functions in mucosal defense but is not typically present in the lung under physiological circumstances. MALT lymphoma most commonly arises in the stomach in response to a chronic antigenic stimulus such as *Helicobacter pylori* that leads to the appearance of MALT with subsequent lymphomatous transformation. Eradication of *H. pylori* can result in complete remission of MALT. The antigenic stimulus that results in the formation of MALT lymphoma in the lung is not known. Half of patients with MALT lymphoma do not have symptoms and are diagnosed incidentally. Radiological findings of pulmonary MALT lymphoma include multiple, bilateral nodules that may have a bronchovascular or more random distribution. The overall 5-year survival for MALT lymphoma is >80% with no consensus regarding the treatment. Surgical resection is often performed for localized disease and chemotherapy for more widespread disease or recurrent disease, but no comparative studies have been performed to provide an evidence-based approach.

Lymphomatoid granulomatosis (LG) is a rare EBV-associated lymphoproliferative disorder with a poor prognosis [84]. The lung is invariably involved, with central nervous system involvement being common and skin involvement occurring occasionally. The vast majority of patients with LG are symptomatic presenting with respiratory or constitutional symptoms. Radiologically, the most common finding is multiple, bilateral, perivascular nodules that range in size from 1 to 8 cm and predominate in the lower lobes. The nodules may converge to form conglomerate masses. In a review of five cases, Lee et al. reported that three cases presented as thin-walled, 1 to 2 cm cystic lesions [86]. The nodules may wax and wane. Treatment generally consists of steroid therapy, cyclophosphamide, or chemotherapy [84]. Radiotherapy may be considered for localized disease.

Amyloidosis and Light Chain Deposition Disease

Amyloidosis is characterized by extracellular deposition of an insoluble fibrillary protein. It may present as a systemic condition or be confined to a specific organ, and it can be associated with an underlying malignancy [87]. Pulmonary amyloidosis may involve almost any lung structure, including the pleura, lymph nodes, tracheobronchial tree, or lung parenchyma. Amyloid deposition in the lung occurs in three main forms: tracheobronchial amyloidosis (Figure 11.8a-d), diffuse alveolar

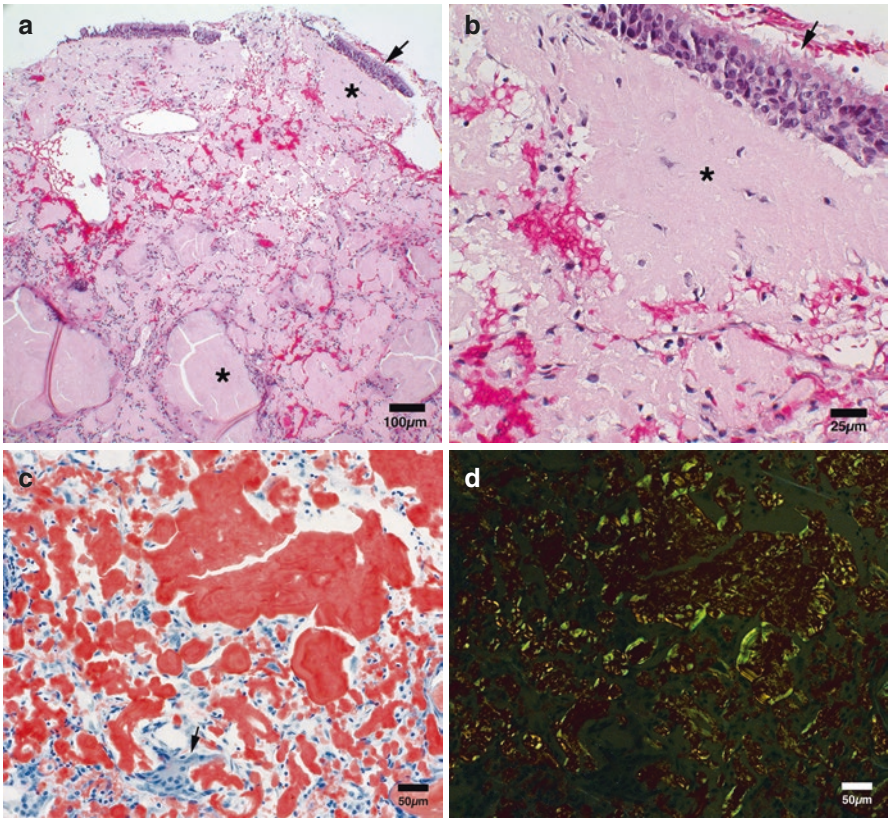

Fig. 11.8 Amyloidosis. (**a**) Histological section of a biopsy from a left hilar endobronchial lesion that may mimic a neoplasm and cause airway obstruction. The biopsy shows extensive deposits of amorphous, eosinophilic material (*) underlying the bronchial epithelium (*arrow*) and throughout the bronchial wall (H&E). (**b**) A higher magnification image shows the characteristic amorphous, eosinophilic amyloid deposits (*) underlying the bronchial epithelium (*arrow*) (H&E). (**c**) Typical orange-red appearance of amyloid with Congo red staining viewed under ordinary bright light. A multinucleated foreign body type giant cell is present engulfing the amyloid (*arrow*), a common finding in amyloidosis (Congo red). (**d**) Image of the same Congo red stained histologic section viewed under polarized light showing the characteristic apple green birefringence of amyloid (Congo red). (**e**) Histological section of a lung biopsy from a woman presenting with cystic lung disease showing cystic areas along with a parenchymal nodule (*arrow*) comprised of abundant eosinophilic material (*). Follicular bronchiolitis was also present in this biopsy from a woman who was diagnosed with Sjogren's syndrome (H&E). (**f**) Higher magnification image of the nodule shows the characteristic amorphous eosinophilic amyloid deposits involving the walls of vessels (*) within the nodule. The material stained red on Congo red staining and showed apple green birefringence with polarized light indicative of amyloid (H&E)

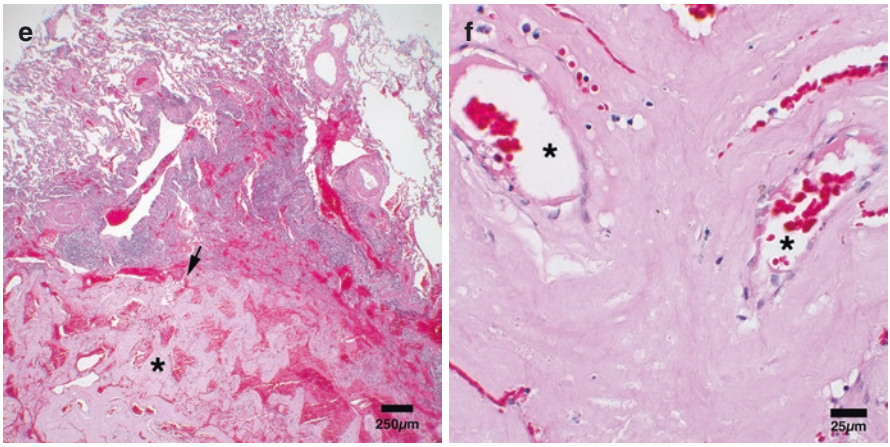

Fig. 11.8 (continued)

septal amyloidosis, and nodular amyloidosis (Figure 11.8e-f). While not widely appreciated, pulmonary amyloidosis may present as a diffuse cystic lung disease (Figure 11.8e) [88]. MALToma may be found in up to a third of subjects with amyloid-associated cystic lung disease [89, 90].

Light chain deposition disease (LCDD) is a monoclonal immunoglobulin deposition disease in which immunoglobulin light chains (as opposed to heavy chains) of a non-fibrillar form (i.e., do not stain with Congo red) are deposited in the interstitium of the kidney and/or lung. The classification of immunoglobulin deposition diseases is based on the class of immunoglobulin and the ultrastructure of the deposits. LCDD was first described in the mid-1970s. The monotypic light chain deposits in LCDD are secreted by plasma cells [91]. Up to 75% of LCDD occurs in association with multiple myeloma (MM) or a lymphoproliferative disease, in particular Waldenstrom macroglobulinaemia, but other cases have been reported to be associated with autoimmune conditions [92]. Up to 5% to 10% of MM patients have LCDD [91].

The pathogenesis of LCDD has similarities to other monoclonal immunoglobulin deposition diseases (i.e., amyloidosis, heavy chain deposition disease), in which monoclonal expansion of either a B cell or plasma cell population produces an excess of immunoglobulin polypeptides that accumulate in various tissues, leading to compromise of tissue/organ function. Renal involvement is a fairly consistent feature of LCDD [93], and cardiac and hepatic involvement are also common with consequences of organ function being much greater for the heart than for the liver. Lung involvement by LCDD is less common and typically manifests as solid nodules [94]. However, LCDD can present as cystic lung disease [95]. On HRCT, cysts associated with LCDD are generally thin-walled, roughly spherical, and diffusely distributed. Histologically there is deposition of amorphous, eosinophilic material in a perilymphatic and bronchovascular distribution. Matrix metalloproteinases may play a role in the development of cysts in LCDD [95]. In some cases, cystic destruction of the lung has progressed to respiratory failure and the need for lung transplant [92], which is the presentation that led to the discovery of the cystic form of pulmonary LCDD.

Conclusion

It is important to be aware of the broad spectrum of neoplastic conditions that may mimic the typical cystic lung diseases seen in pulmonary clinic, such Birt-Hogg-Dubé syndrome and follicular bronchiolitis/lymphoid interstitial pneumonia. Many of the pulmonary disorders associated with lung cysts, such as PLCH, LCDD, and LAM, are actually low-grade neoplasms that blur the boundaries between malignant and benign processes. Higher grade neoplasms of the lung, gastrointestinal tract, and kidneys are the most common sources of malignant pulmonary cysts with soft tissue sarcomas and lymphomas also in the differential diagnosis. With increased use of high-quality CT imaging, the identification of solitary and multiple pulmonary cysts will likely become more frequent. It is thus important for physicians to adapt a systematic approach to the diagnosis and management of cystic lung lesions, including the rare cystic neoplasms that often require targeted interventions and genetic phenotyping.

Key Learning Points

- While primary lung cancer can frequently present with cavitary lesions, true cystic lesions from primary lung cancer are uncommon and generally present as solitary lesions, with adenocarcinoma of the lung being the most common etiology.
- Metastatic adenocarcinomas and sarcomas represent the most common high-grade malignancies that can present as pulmonary cysts.
- Perivascular epithelioid cell neoplasms (PEComas) are rare mesenchymal neoplasms that frequently metastasize to the lungs and can form pulmonary cysts. Lymphangioleiomyomatosis (LAM) is a member of the PEComa family and is the prototypical diffuse cystic lung disease.
- In addition to LAM, several other common causes of diffuse cystic lung disease, such as pulmonary Langerhans cell histiocytosis (PLCH) and light chain deposition disease (LCDD), represent low-grade malignancies.
- Cystic change from underlying malignancies could also be seen in children, with the most common etiologies being malignant transformation in congenital pulmonary airway malformation (CPAM) and primary pleuropulmonary blastoma (PPB).

References

1. Genereux GP. The end-stage lung: pathogenesis, pathology, and radiology. Radiology. 1975;116(02):279–89.
2. Hansell DM, Bankier AA, MacMahon H, McLoud TC, Muller NL, Remy J. Fleischner society: glossary of terms for thoracic imaging. Radiology. 2008;246(3):697–722.
3. Jawad H, Walker CM, Wu CC, Chung JH. Cystic interstitial lung diseases: recognizing the common and uncommon entities. Curr Probl Diagn Radiol. 2014;43(3):115–27.

4. Herbst RS, Morgensztern D, Boshoff C. The biology and management of non-small cell lung cancer. Nature. 2018;553(7689):446–54.
5. Deng H, Zhang J, Zhao S, Zhang J, Jiang H, Chen X, et al. Thin-wall cystic lung cancer: a study of 45 cases. Oncol Lett. 2018;16(1):755–60.
6. Woodring JH, Fried AM, Chuang VP. Solitary cavities of the lung: diagnostic implications of cavity wall thickness. AJR Am J Roentgenol. 1980;135(6):1269–71.
7. Guo J, Liang C, Sun Y, Zhou N, Liu Y, Chu X. Lung cancer presenting as thin-walled cysts: an analysis of 15 cases and review of literature. Asia Pac J Clin Oncol. 2016;12(1):e105–12.
8. Tomizawa K, Shimizu S, Ohara S, Fujino T, Nishino M, Sesumi Y, et al. Clinical significance of tumor cavitation in surgically resected early-stage primary lung cancer. Lung Cancer. 2017;112:57–61.
9. Xue X, Wang P, Xue Q, Wang N, Zhang L, Sun J, et al. Comparative study of solitary thin-walled cavity lung cancer with computed tomography and pathological findings. Lung Cancer. 2012;78(1):45–50.
10. Farooqi AO, Cham M, Zhang L, Beasley MB, Austin JH, Miller A, et al. Lung cancer associated with cystic airspaces. AJR Am J Roentgenol. 2012;199(4):781–6.
11. Sheard S, Moser J, Sayer C, Stefanidis K, Devaraj A, Vlahos I. Lung cancers associated with cystic airspaces: Underrecognized features of early disease. Radiographics. 2018;38(3):704–17.
12. Mascalchi M, Attina D, Bertelli E, Falchini M, Vella A, Pegna AL, et al. Lung cancer associated with cystic airspaces. J Comput Assist Tomogr. 2015;39(1):102–8.
13. Fintelmann FJ, Brinkmann JK, Jeck WR, Troschel FM, Digumarthy SR, Mino-Kenudson M, et al. Lung cancers associated with cystic airspaces: natural history, pathologic correlation, and mutational analysis. J Thorac Imaging. 2017;32(3):176–88.
14. Nakahara Y, Mochiduki Y, Miyamoto Y. Percutaneous needle washing for the diagnosis of pulmonary thin-walled cavitary lesions filled with air. Intern Med. 2007;46(14):1089–94.
15. Al Attar L, Keshary A, Abu-Awwad R. Cheerios floating on lung computed tomography scan revealing cholangiocarcinoma of the lungs. Cureus. 2018;10(4):e2497.
16. Fielli M, Avila F, Saino A, Seimah D, Fernandez CM. Diffuse cystic lung disease due to pulmonary metastasis of colorectal carcinoma. Respir Med Case Rep. 2016;17:83–5.
17. Ropars C, Kerjouan M, Larible C, Llamas Gutierrez F, Lederlin M, De Latour B, et al. Lung metastases of pancreatic adenocarcinoma: watch for the second train! Rev Mal Respir. 2019;36(6):738–41.
18. Sewchuran T. Solid to cystic: a case report of imaging findings of atypical lung metastases. SA J Radiol. 2019;23(1):1663.
19. Torre LA, Bray F, Siegel RL, Ferlay J, Lortet-Tieulent J, Jemal A. Global cancer statistics, 2012. CA Cancer J Clin. 2015;65(2):87–108.
20. Hiensch R, Belete H, Rashidfarokhi M, Galperin I, Shakil F, Epelbaum O. Unusual patterns of thoracic metastasis of urinary bladder carcinoma. J Clin Imaging Sci. 2017;7:23.
21. Agrawal A, Sahni S, Vulisha AK, Gumpeni R, Shah R, Talwar A. Pulmonary manifestations of urothelial carcinoma of the bladder. Respir Med. 2017;128:65–9.
22. Rovirosa A, Salud A, Felip E, Capdevila F, Giralt J, Bellmunt J. Cavitary pulmonary metastases in transitional cell carcinoma of the urinary bladder. Urol Int. 1992;48(1):102–4.
23. Imokawa S, Uehara M, Uto T, Sagisaka S, Sato J, Yasuda K, et al. Pulmonary metastasis from urothelial carcinoma showing progressive multiple cystic lesions. Am J Respir Crit Care Med. 2013;188(10):1267–8.
24. Fiorelli A, Vicidomini G, Messina G, Santini M. Metastasis from transitional cell carcinoma of urinary bladder as cystic pulmonary lesion. J Thorac Dis. 2011;3(1):71–3.
25. Kurian A, Lee J, Born A. Urothelial bladder cancer with cavitary lung metastases. Can Respir J. 2011;18(3):e46–7.
26. Yang J, Ren Z, Du X, Hao M, Zhou W. The role of mesenchymal stem/progenitor cells in sarcoma: update and dispute. Stem Cell Investig. 2014;1:18.
27. Fletcher CD HP, Mertens F, Bridge J. WHO classification of tumours of soft tissue and bone. International agency for research on cancer 4th edition; 2013. 468 p.

28. Ciccarese F, Bazzocchi A, Ciminari R, Righi A, Rocca M, Rimondi E, et al. The many faces of pulmonary metastases of osteosarcoma: retrospective study on 283 lesions submitted to surgery. Eur J Radiol. 2015;84(12):2679–85.
29. Hoshi M, Oebisu N, Iwai T, Ieguchi M, Ban Y, Nakamura H. An unusual presentation of pneumothorax associated with cystic lung metastasis from epithelioid sarcoma: a case report and review of the literature. Oncol Lett. 2018;15(4):4531–4.
30. Hasegawa S, Inui K, Kamakari K, Kotoura Y, Suzuki K, Fukumoto M. Pulmonary cysts as the sole metastatic manifestation of soft tissue sarcoma: case report and consideration of the pathogenesis. Chest. 1999;116(1):263–5.
31. Chan DP, Griffith JF, Lee TW, Chow LT, Yim AP. Cystic pulmonary metastases from epithelioid cell sarcoma. Ann Thorac Surg. 2003;75(5):1652–4.
32. Kikuchi E, Kinoshita I, Yamazaki K, Itoh T, Shimizu T, Shimizu H, et al. Epithelioid sarcoma presenting as pulmonary cysts with cancer antigen 125 expression. Respirology. 2006;11(6):826–9.
33. Choi SY, Kim YH, Kwon JB, Suh JH, Shin OR, Hong SH. Epithelioid sarcoma metastatic to the lung as pulmonary cysts without other metastatic manifestation. J Thorac Oncol. 2008;3(5):532–3.
34. Liu Y, Ma X, Zang D, Zhou C, Zhang J. Epithelioid sarcoma with osteoporosis and pneumothorax. Eur J Dermatol. 2011;21(2):296–7.
35. Chong SG, Casserly BP. An unusual cause of spontaneous recurrent pneumothoraces. Br J Hosp Med (Lond). 2012;73(2):110–1.
36. Jeon SY, Yhim HY, Lee NR. Epithelioid sarcoma with spontaneous pneumothorax and massive pleural effusion. Korean J Intern Med. 2016;31(1):191–3.
37. Ajayi AA, Commins SV, Clarke DE. Metastatic Angiosarcoma of the scalp presenting with cystic lung lesions: a case report and review of cystic lung diseases. Perm J. 2018;22:17–168.
38. Sakurai H, Hada M, Miyashita Y, Tsukamoto K, Oyama T, Ashizawa I. Simultaneous bilateral spontaneous pneumothorax secondary to metastatic angiosarcoma of the scalp: report of a case. Surg Today. 2006;36(10):919–22.
39. May T, Blank S, Dressel D, Van der Kloot TE. Angiosarcoma with extensive pulmonary metastases, presenting with spontaneous bilateral pneumothoraces. Am J Respir Crit Care Med. 2013;188(6):749.
40. Lawton PA, Knowles S, Karp SJ, Suvana SK, Spittle MF. Bilateral pneumothorax as a presenting feature of metastatic angiosarcoma of the scalp. Br J Radiol. 1990;63(746):132–4.
41. Masuzawa M, Mikami T, Numata Y, Tokuyama W, Masuzawa M, Murakumo Y, et al. Association of D2-40 and MMP-1 expression with cyst formation in lung metastatic lesions of cutaneous angiosarcoma on the scalp: immunohistochemical analysis of 23 autopsy cases. Hum Pathol. 2013;44(12):2751–9.
42. Tateishi U, Hasegawa T, Kusumoto M, Yamazaki N, Iinuma G, Muramatsu Y, et al. Metastatic angiosarcoma of the lung: spectrum of CT findings. AJR Am J Roentgenol. 2003;180(6):1671–4.
43. Hoang L, Chiang S, Lee CH. Endometrial stromal sarcomas and related neoplasms: new developments and diagnostic considerations. Pathology. 2018;50(2):162–77.
44. Aubry MC, Myers JL, Colby TV, Leslie KO, Tazelaar HD. Endometrial stromal sarcoma metastatic to the lung: a detailed analysis of 16 patients. Am J Surg Pathol. 2002;26(4):440–9.
45. Xu Y, Liang ZX, Guo JT, Su X, Lu YL, Guan XZ. Cystic and solitary nodular pulmonary metastases in a patient with low-grade endometrial stromal sarcoma: a case report and literature review. Oncol Lett. 2019;18(2):1133–44.
46. Ali RH, Rouzbahman M. Endometrial stromal tumours revisited: an update based on the 2014 WHO classification. J Clin Pathol. 2015;68(5):325–32.
47. Isakoff MS, Bielack SS, Meltzer P, Gorlick R. Osteosarcoma: current treatment and a collaborative pathway to success. J Clin Oncol. 2015;33(27):3029–35.
48. Le Garff G, Lena H, Corbineau F, Kerbrat P, Delaval P. Unusual cause of recurrent pneumothorax: excavated metastasis of osteosarcoma. Ann Thorac Surg. 2001;72(6):2111–3.
49. Hoag JB, Sherman M, Fasihuddin Q, Lund ME. A comprehensive review of spontaneous pneumothorax complicating sarcoma. Chest. 2010;138(3):510–8.

50. Vang R, Kempson RL. Perivascular epithelioid cell tumor ('PEComa') of the uterus: a subset of HMB-45-positive epithelioid mesenchymal neoplasms with an uncertain relationship to pure smooth muscle tumors. Am J Surg Pathol. 2002;26(1):1–13.
51. Thway K, Fisher C. PEComa: morphology and genetics of a complex tumor family. Ann Diagn Pathol. 2015;19(5):359–68.
52. Martignoni G, Pea M, Reghellin D, Zamboni G, Bonetti F. PEComas: the past, the present and the future. Virchows Arch. 2008;452(2):119–32.
53. Seaman DM, Meyer CA, Gilman MD, McCormack FX. Diffuse cystic lung disease at high-resolution CT. AJR Am J Roentgenol. 2011;196(6):1305–11.
54. Folpe AL, Mentzel T, Lehr HA, Fisher C, Balzer BL, Weiss SW. Perivascular epithelioid cell neoplasms of soft tissue and gynecologic origin: a clinicopathologic study of 26 cases and review of the literature. Am J Surg Pathol. 2005;29(12):1558–75.
55. Tirumani SH, Shinagare AB, Hargreaves J, Jagannathan JP, Hornick JL, Wagner AJ, et al. Imaging features of primary and metastatic malignant perivascular epithelioid cell tumors. AJR Am J Roentgenol. 2014;202(2):252–8.
56. Okamoto S, Komura M, Terao Y, Kurisaki-Arakawa A, Hayashi T, Saito T, et al. Pneumothorax caused by cystic and nodular lung metastases from a malignant uterine perivascular epithelioid cell tumor (PEComa). Respir Med Case Rep. 2017;22:77–82.
57. Vassallo R, Harari S, Tazi A. Current understanding and management of pulmonary Langerhans cell histiocytosis. Thorax. 2017;72(10):937–45.
58. Abbott GF, Rosado-de-Christenson ML, Franks TJ, Frazier AA, Galvin JR. From the archives of the AFIP: pulmonary Langerhans cell histiocytosis. Radiographics. 2004;24(3):821–41.
59. Tazi A, de Margerie C, Naccache JM, Fry S, Dominique S, Jouneau S, et al. The natural history of adult pulmonary Langerhans cell histiocytosis: a prospective multicentre study. Orphanet J Rare Dis. 2015;10:30.
60. Vassallo R, Ryu JH, Schroeder DR, Decker PA, Limper AH. Clinical outcomes of pulmonary Langerhans'-cell histiocytosis in adults. N Engl J Med. 2002;346(7):484–90.
61. Mendez JL, Nadrous HF, Vassallo R, Decker PA, Ryu JH. Pneumothorax in pulmonary Langerhans cell histiocytosis. Chest. 2004;125(3):1028–32.
62. Williams ARW. Uterine fibroids – what's new? F1000Res. 2017;6:2109.
63. Jautzke G, Muller-Ruchholtz E, Thalmann U. Immunohistological detection of estrogen and progesterone receptors in multiple and well differentiated leiomyomatous lung tumors in women with uterine leiomyomas (so-called benign metastasizing leiomyomas). A report on 5 cases. Pathol Res Pract. 1996;192(3):215–23.
64. Abramson S, Gilkeson RC, Goldstein JD, Woodard PK, Eisenberg R, Abramson N. Benign metastasizing leiomyoma: clinical, imaging, and pathologic correlation. AJR Am J Roentgenol. 2001;176(6):1409–13.
65. Zhang J, Dong A, Cui Y, Wang Y, Chen J. Diffuse cavitary benign metastasising leiomyoma of the lung. Thorax. 2019;74(2):208–9.
66. Grossmann AH, Layfield LJ, Randall RL. Classification, molecular characterization, and the significance of pten alteration in leiomyosarcoma. Sarcoma. 2012;2012:380896.
67. Coindre JM, Terrier P, Guillou L, Le Doussal V, Collin F, Ranchere D, et al. Predictive value of grade for metastasis development in the main histologic types of adult soft tissue sarcomas: a study of 1240 patients from the French Federation of Cancer Centers Sarcoma Group. Cancer. 2001;91(10):1914–26.
68. Arnold LM 3rd, Burman SD, AH OY. Diagnosis and management of primary pulmonary leiomyosarcoma. J Am Osteopath Assoc. 2010;110(4):244–6.
69. Traweek T, Rotter AJ, Swartz W, Azumi N. Cystic pulmonary metastatic sarcoma. Cancer. 1990;65(8):1805–11.
70. Mehzad M. Leiomyosarcoma of the uterus presenting with pneumothorax. Br J Dis Chest. 1977;71(2):132–4.
71. Gelinas JF, Manoukian J, Cote A. Lung involvement in juvenile onset recurrent respiratory papillomatosis: a systematic review of the literature. Int J Pediatr Otorhinolaryngol. 2008;72(4):433–52.

72. Boddu P, Parimi V, Taddonio M, Kane JR, Yeldandi A. Pathologic and radiologic correlation of adult cystic lung disease: a comprehensive review. Pathol Res Int. 2017;2017:3502438.
73. Kramer SS, Wehunt WD, Stocker JT, Kashima H. Pulmonary manifestations of juvenile laryngotracheal papillomatosis. AJR Am J Roentgenol. 1985;144(4):687–94.
74. Godwin JD, Webb WR, Savoca CJ, Gamsu G, Goodman PC. Multiple, thin-walled cystic lesions of the lung. AJR Am J Roentgenol. 1980;135(3):593–604.
75. Dancey DR, Chamberlain DW, Krajden M, Palefsky J, Alberti PW, Downey GP. Successful treatment of juvenile laryngeal papillomatosis-related multicystic lung disease with cidofovir: case report and review of the literature. Chest. 2000;118(4):1210–4.
76. Gorospe L, Munoz-Molina GM, Ayala-Carbonero AM, Fernandez-Mendez MA, Arribas-Marcos A, Castro-Acosta P, et al. Cystic adenomatoid malformation of the lung in adult patients: clinicoradiological features and management. Clin Imaging. 2016;40(3):517–22.
77. Boucherat O, Jeannotte L, Hadchouel A, Delacourt C, Benachi A. Pathomechanisms of congenital cystic lung diseases: focus on congenital cystic Adenomatoid malformation and Pleuropulmonary Blastoma. Paediatr Respir Rev. 2016;19:62–8.
78. Casagrande A, Pederiva F. Association between congenital lung malformations and lung tumors in children and adults: a systematic review. J Thorac Oncol. 2016;11(11):1837–45.
79. Messinger YH, Stewart DR, Priest JR, Williams GM, Harris AK, Schultz KA, et al. Pleuropulmonary blastoma: a report on 350 central pathology-confirmed pleuropulmonary blastoma cases by the international Pleuropulmonary Blastoma registry. Cancer. 2015;121(2):276–85.
80. Fasanya AA, Hattab Y, Patel A, Lega M. Mesenchymal cystic hamartoma of the lung. Respir Med Case Rep. 2017;21:158–60.
81. Chadwick SL, Corrin B, Hansell DM, Geddes DM. Fatal haemorrhage from mesenchymal cystic hamartoma of the lung. Eur Respir J. 1995;8(12):2182–4.
82. Mark EJ. Mesenchymal cystic hamartoma of the lung. N Engl J Med. 1986;315(20):1255–9.
83. Hedlund GL, Bisset GS 3rd, Bove KE. Malignant neoplasms arising in cystic hamartomas of the lung in childhood. Radiology. 1989;173(1):77–9.
84. Cadranel J, Wislez M, Antoine M. Primary pulmonary lymphoma. Eur Respir J. 2002;20(3):750–62.
85. Hare SS, Souza CA, Bain G, Seely JM, Frcpc, Gomes MM, et al. The radiological spectrum of pulmonary lymphoproliferative disease. Br J Radiol. 2012;85(1015):848–64.
86. Lee JS, Tuder R, Lynch DA. Lymphomatoid granulomatosis: radiologic features and pathologic correlations. AJR Am J Roentgenol. 2000;175(5):1335–9.
87. Real de Asua D, Costa R, Galvan JM, Filigheddu MT, Trujillo D, Cadinanos J. Systemic AA amyloidosis: epidemiology, diagnosis, and management. Clin Epidemiol. 2014;6:369–77.
88. Sakai M, Yamaoka M, Kawaguchi M, Hizawa N, Sato Y. Multiple cystic pulmonary amyloidosis. Ann Thorac Surg. 2011;92(5):e109.
89. Zamora AC, White DB, Sykes AM, Hoskote SS, Moua T, Yi ES, et al. Amyloid-associated cystic lung disease. Chest. 2016;149(5):1223–33.
90. Kluka EM, Bauer PR, Aubry MC, Ryu JH. Enlarging lung nodules and cysts in a 53-year-old woman with primary Sjogren syndrome. Chest. 2013;143(1):258–61.
91. Buxbaum J, Gallo G. Nonamyloidotic monoclonal immunoglobulin deposition disease. Light-chain, heavy-chain, and light- and heavy-chain deposition diseases. Hematol Oncol Clin North Am. 1999;13(6):1235–48.
92. Colombat M, Stern M, Groussard O, Droz D, Brauner M, Valeyre D, et al. Pulmonary cystic disorder related to light chain deposition disease. Am J Respir Crit Care Med. 2006;173(7):777–80.
93. Ronco PM, Alyanakian MA, Mougenot B, Aucouturier P. Light chain deposition disease: a model of glomerulosclerosis defined at the molecular level. J Am Soc Nephrol. 2001;12(7):1558–65.
94. Bhargava P, Rushin JM, Rusnock EJ, Hefter LG, Franks TJ, Sabnis SG, et al. Pulmonary light chain deposition disease: report of five cases and review of the literature. Am J Surg Pathol. 2007;31(2):267–76.
95. Colombat M, Caudroy S, Lagonotte E, Mal H, Danel C, Stern M, et al. Pathomechanisms of cyst formation in pulmonary light chain deposition disease. Eur Respir J. 2008;32(5):1399–403.

Chapter 12
Congenital and Developmental Causes of Cystic Lung Disease

Gail H. Deutsch and Kathryn A. Wikenheiser-Brokamp

Abbreviations

CCAM	Congenital cystic adenomatoid malformation
CHAOS	Congenital high airway obstruction syndrome
CLO	Congenital lobar overinflation
CNLD	Chronic neonatal lung disease
CPAM	Congenital pulmonary airway malformation
ELS	Extralobar sequestrations
FGFR2	Fibroblast growth factor receptor 2
FLNA	Filamin A
ILS	Intralobar sequestrations
miRNAs	Micro-RNAs
NKX2–1	NK2 homeobox 1
PPB	Pleuropulmonary blastoma
TBX4	T-box transcription factor 4
TTF-1	Thyroid transcription factor 1

G. H. Deutsch (✉)
Department of Pathology, University of Washington School of Medicine and Seattle Children's Hospital, Seattle, WA, USA
e-mail: gail.deutsch@seattlechildrens.org

K. A. Wikenheiser-Brokamp
Division of Pathology and Laboratory Medicine,
Cincinnati Children's Hospital Medical Center, Cincinnati, OH, USA

Department of Pathology and Laboratory Medicine,
University of Cincinnati College of Medicine, Cincinnati, OH, USA
e-mail: Kathryn.wikenheiser-brokamp@cchmc.org

N. Gupta et al. (eds.), *Diffuse Cystic Lung Diseases*, Respiratory Medicine,
https://doi.org/10.1007/978-3-030-63365-3_12

Congenital Cystic Lung Malformations

The widespread use of antenatal ultrasound has led to increased in utero detection of congenital cystic lung malformations. These entities comprise a group of rare but clinically significant developmental abnormalities, including bronchogenic cysts, congenital pulmonary airway malformation, pulmonary sequestration, congenial lobar emphysema, and pulmonary hyperplasia. Although many of these lesions will remain asymptomatic, there is a wide range of clinical complications including hydrops fetalis, airway obstruction, infection, and rarely neoplasia [1]. Treatment of even asymptomatic congenital lung lesions is variable with some managed conservatively, while others surgically resected [2]. Many congenital lung abnormalities detected early in pregnancy will have regressed significantly by birth, further complicating management decisions [3]. While the conventional nomenclature of these malformations infers that congenital cystic lung malformations are distinct lesions, they frequently share common modes of pathogenesis and histological features [4–7]. Specifically, bronchogenic cysts and extralobar sequestration reflect abnormal foregut budding during embryonic development, while congenital cystic pulmonary airway malformations, intralobar sequestration, pulmonary hyperplasia, and congenital lobar overinflation are often related to airway obstruction, with or without secondary dysplastic changes. In an attempt to bring clarity to the origin of these lesions and guide clinical management decisions, revised classifications have been proposed based on the anatomical/pathological findings or imaging appearance of the entities [4, 8–10] (Table 12.1).

Bronchogenic Cyst

Bronchogenic or bronchial cysts arise from anomalous budding of the foregut during development. They present as unilocular fluid or mucin-filled cysts that histologically recapitulate the bronchial structure, without connection to the lung (Fig. 12.1).

Bronchogenic cysts typically occur in the mediastinum or subcarinal area but may be intraparenchymal or even subdiaphragmatic or cutaneous [11, 12]. On radiological imaging, bronchogenic cysts appear as round thin-walled cystic cavities with sharp margins that may have air-fluid levels. They do not communicate with the normal tracheobronchial tree unless they become secondarily infected, which commonly occurs in intraparenchymal cysts. The time of clinical presentation is variable and related to compression of adjacent structures (e.g., trachea, bronchi, esophagus), infection, or rupture. Patients usually present later in life with dyspnea, recurrent coughing, wheezing, dysphagia, or pneumonia, but neonatal presentation or incidental detection on imaging taken for unrelated reasons is not unusual. On pathological examination, bronchogenic cysts consist of a single cyst containing clear or turbid fluid, the latter reflective of secondary infection. Management consists of surgical resection.

Table 12.1 Langston classification and radiographic classification of congenital lung malformations

Langston classification[a]
I. Bronchopulmonary malformations
Bronchogenic cyst
Bronchial atresia
Cystic pulmonary airway malformation, large cyst type (Stocker type 1)
Isolated
With systemic arterial/venous connection (hybrid lesion/intralobar sequestration)
Cystic pulmonary airway malformation, small cyst type (Stocker type 2)
Extralobar sequestration (with/without connection to gastrointestinal tract)
Isolated
With cystic pulmonary airway malformation, small cyst type (hybrid lesion)
II. Pulmonary hyperplasia and related lesions
Congenital high airway malformation
Solid congenital pulmonary airway malformation, small cyst type (Stocker type 3)
Polyalveolar lobe
III. Congenital lobar emphysema
Radiographic Classification[b]
I. Group 1 (congenital solid/cystic lung malformation)
Cystic pulmonary airway malformation, small cyst type (Stocker type 2)
Extralobar and intralobar sequestration
Bronchial atresia
Bronchogenic cyst
Mixed malformation
II. Group 2 (congenital hyperlucent lobe)
Congenital lobar emphysema
Polyalveolar lobe
III. Group 3 (congenital small lung)
Lung/lobar agenesis
Pulmonary hypoplasia

[a]Adapted from [4]
[b]Adapted from [10]

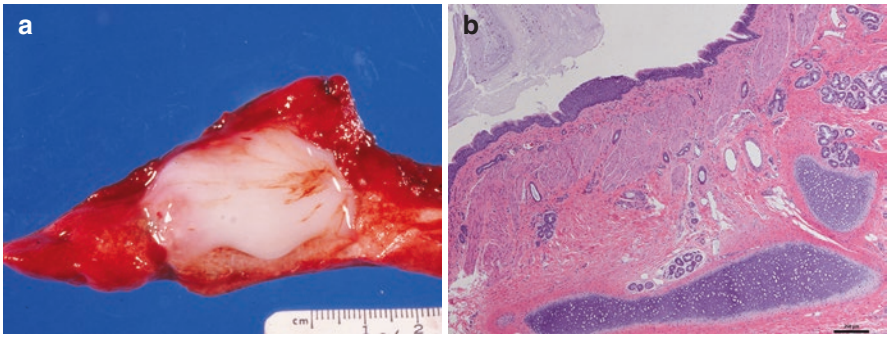

Fig. 12.1 Bronchogenic cyst. (**a**) An intraparenchymal bronchogenic cyst containing abundant mucus. (**b**) Bronchogenic cysts recapitulate the appearance of the normal bronchus lined by ciliated respiratory epithelium and containing smooth muscle, submucosal glands, and plates of cartilage in the wall (H&E)

Congenital Pulmonary Airway Malformation

Congenital pulmonary airway malformation (CPAM), previously known as congenital cystic adenomatoid malformation (CCAM), is the most common lung malformation of the lower respiratory tract [13]. CPAMs derive their blood supply from the pulmonary artery and drain via the pulmonary veins, with the exception of hybrid lesions (CPAM in pulmonary sequestrations) that have a systemic blood supply. CPAMs occur sporadically with no known genetic predilection. Mechanisms resulting in CPAM formation are debated, but the hypothesis that CPAMs arise from in utero obstruction during development has been substantiated by several studies [5–7].

Historically CPAMs have been categorized into separate subtypes in the Stocker classification, which is based upon cyst size and histological resemblance to segments of the normal respiratory tree, from trachea and large bronchi to peripheral acinar structures [14]. However, with further insights into CPAM pathogenesis, experience with the clinical behavior of this entity and frequent occurrence of hybrid lesions (CPAM in pulmonary sequestrations), the continued utility of the Stocker classification is contested [4]. Stocker type 0 CPAM is now recognized to be acinar dysplasia, a rare diffuse developmental lung disorder associated with mutations in the T-box transcription factor *TBX4* and fibroblast growth factor receptor 2 (*FGFR2*) [15, 16]. Stocker type 3 CPAM resembles pulmonary hyperplasia, and Stocker type 4 CPAM is thought to represent type I pleuropulmonary blastoma (discussed below). Langston divided the most frequent CPAMs into two types: a large cyst type (equivalent to Stocker type 1) and a small cyst type (equivalent to Stocker type 2). This terminology has in part been adapted in the radiographical literature to guide clinical management [17, 18] (see Table 12.1). By histological assessment, the small cyst type is the most common CPAM subtype [19].

Large cyst CPAM presents by radiographical imaging as a solitary lung mass containing variably sized cysts, usually measuring greater than 2 cm. The cysts replace the normal lung parenchyma and may be unilocular or multilocular and septated

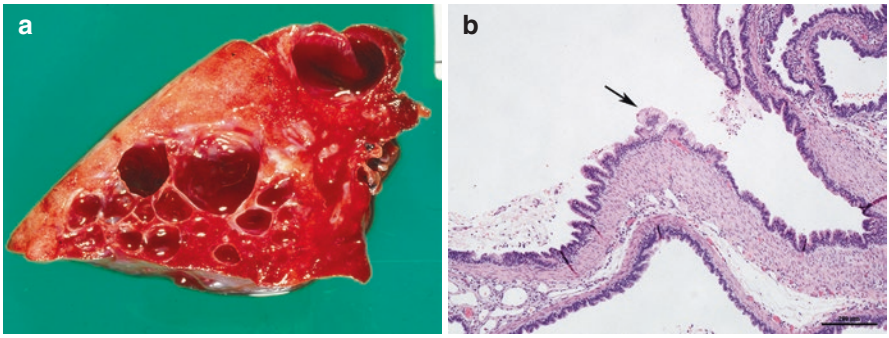

Fig. 12.2 Congenital pulmonary airway malformation (CPAM), large cyst type. (**a**) Large cyst type CPAM has cysts of variable size, usually measuring greater than 2 cm. (**b**) Microscopically, the cysts are lined by ciliated respiratory epithelium with smooth muscle in the wall; focal mucigenic epithelium is typically seen (*arrow*) (H&E)

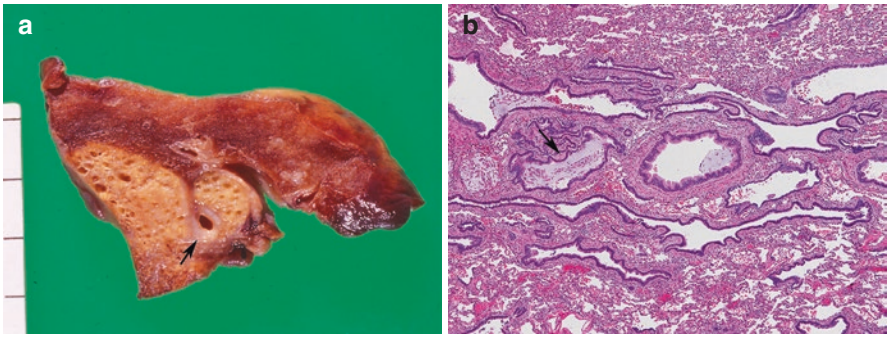

Fig. 12.3 Congenital pulmonary airway malformation (CPAM), small cyst type. (**a**) Small cyst type CPAM has multiple small cysts admixed with solid areas of parenchyma. A bronchus is present within the lesion (*arrow*). (**b**) Histologic sections show abnormally apposed bronchiole-like structures, many with intraluminal mucus providing evidence of obstruction (*arrow*) (H&E, 100×)

(Figure 12.2a). Histological examination demonstrates that the cysts are lined by ciliated respiratory epithelium, often containing clusters of mucigenic cells [19] (Figure 12.2b). Cartilage is rarely present in the cyst walls.

Small cyst CPAM is identified as an echogenic mass by ultrasound examination and is comprised of multiple small cysts, which can be heterogeneous in appearance based on the presence of cystic and solid components (Figure 12.3a). Small cyst CPAM may be associated with other congenital anomalies, including cardiovascular and renal malformations as well as diaphragmatic hernia [14]. Bronchial atresia is more frequently identified in small cyst than large cyst CPAM. Features of bronchial atresia are also commonly seen in pulmonary sequestrations with systemic blood supply [4]. Histologically a small cyst CPAM is composed of increased bronchiolar-like profiles lined by cuboidal to ciliated respiratory epithelium that, unlike normal bronchioles, are not accompanied by arteries (see Figure 12.3b).

Rhabdomyomatous differentiation with small bundles of mature skeletal muscle may be present around the cysts and is not reflective of rhabdomyosarcoma. CPAMs resected during fetal life demonstrate significant immaturity akin to the lung during early development and do not fit well into existing classification schemes [20].

The presentation of CPAMs is quite variable; patients may present with respiratory distress in early infancy or remain asymptomatic until later in life. The vast majority of cases are now detected by routine prenatal ultrasound examination. Large lesions typically cause symptoms by compromising alveolar growth during development leading to pulmonary hypoplasia. Mediastinal shift with subsequent development of polyhydramnios and hydrops may develop with rapidly enlarging lesions [21]. Expectant management is appropriate for the nonhydropic fetus, whereas survival of fetuses with hydrops may be dependent on fetal intervention, including thoracoamniotic shunt placement, percutaneous laser ablation, and rarely open fetal surgery [22]. Infants who are symptomatic postnatally are treated with surgical resection, which generally consists of lobectomy or segmental resection. Surgical intervention for a child with an asymptomatic CPAM is controversial. Recurrent infection and a small risk of neoplastic transformation have been cited as reasons for elective resection [19, 23–26]. Reported malignancies are primarily mucinous adenocarcinomas thought to arise from mucigenic epithelium which is frequently present in large cyst CPAM [27, 28]. KRAS mutations have been detected in several cases, similar to precursor adenocarcinoma lesions in the adult lung [29, 30].

Pulmonary Sequestrations

Pulmonary sequestrations are masses of nonfunctioning lung that do not connect to the normal tracheobronchial tree and have a systemic arterial blood supply, usually arising from the thoracic or abdominal aorta [31]. Occasionally, the systemic arterial supply originates from other arteries including the celiac, splenic, intercostal, subclavian, and even coronary arteries [32]. Venous drainage may occur through either a pulmonary or systemic vein. Pulmonary sequestrations are classified as intralobar sequestrations (ILS) when they occur within the visceral pleural lining of the adjacent surrounding lung, and extralobar sequestrations (ELS) when they are separate from the lung and have their own pleural lining. Sequestrations are the second most common lung lesion detected antenatally after CPAM.

ELS comprise the majority of sequestrations and are often identified in utero as a large echo-dense mass that may become smaller relative to the normal lung with advancing gestational age. ELS commonly present with respiratory distress shortly after birth. Antenatal presentation may include polyhydramnios and fetal hydrops. There is a frequent association of ELS with other congenital anomalies, especially diaphragmatic hernia, cardiac abnormalities, and other foregut duplications including bronchogenic cysts [33]. A connection to the gastrointestinal tract may be present (Figure 12.4a). Similar to bronchogenic cysts, ELS are believed to arise from a foregut-derived supernumerary lung bud, but contain distal lung parenchyma [4, 32]. While most are intrathoracic, they can also be found below the diaphragm. On gross

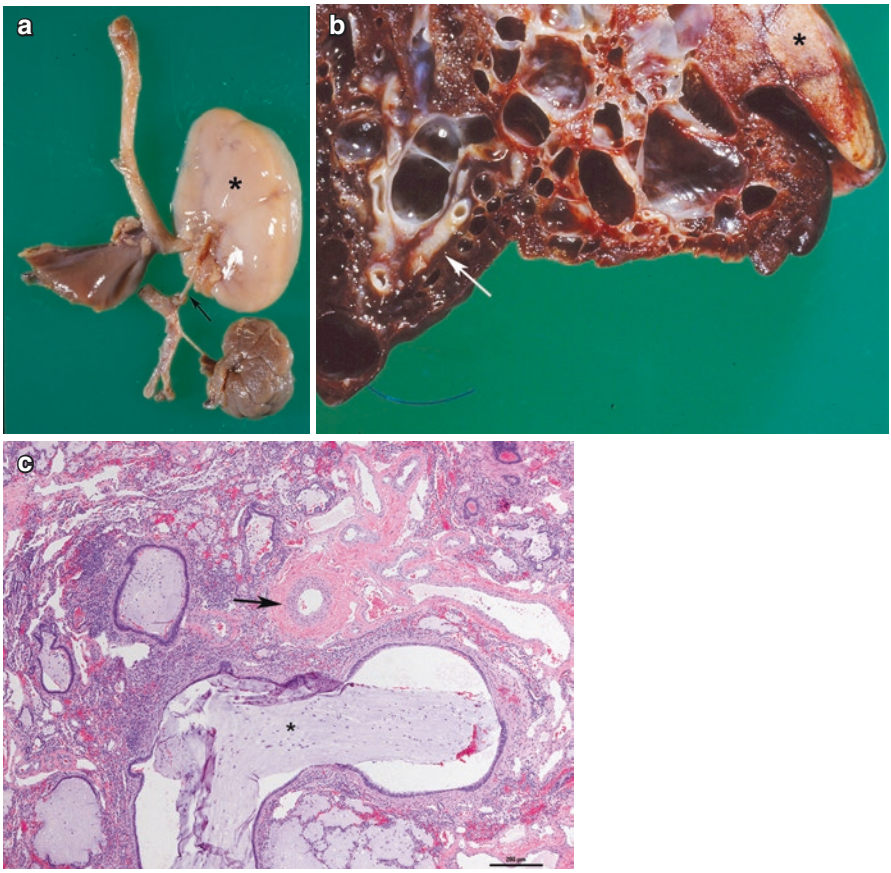

Fig. 12.4 Pulmonary sequestrations. (**a**) A large extralobar sequestration (ELS) (*) seen below the diaphragm with connection to the distal esophagus (stomach on left) and vascular supply (*arrow*) from the descending aorta; (right kidney lower right corner). (**b**) Intralobar sequestrations (ILS) are usually well-demarcated from the adjacent normal lung (*) and have thick-walled systemic arteries (*arrow*). They often resemble a congenital pulmonary airway malformation (CPAM) with cystic spaces. (**c**) Evidence of proximal airway obstruction is common in both ELS and ILS with dilated airways filled with mucus (*), identical to that seen in bronchial atresia. Arteries with medial thickening reflect systemic blood supply (*arrow*). Depending upon the age of presentation and presence of concurrent infection, inflammation and dense fibrosis may be present (H&E)

examination, ELS resemble an accessory lung lobe with its own pleura and a vascular pedicle containing a systemic artery and a draining vein. Pulmonary sequestrations are composed of lung parenchyma with enlarged and poorly subdivided airspaces, and containing abnormally large thick-walled vessels, reflective of the systemic vascular supply (Figure 12.4b). Notably, bronchial atresia with small cyst CPAM features is extremely common in both ELS and ILS [5, 34]. Depending on the presence of proximal airway obstruction, there may be associated mucus accumulation (Figure 12.4c).

ILS is defined by an isolated nonfunctioning lung segment contained within normal lung and with systemic arterial supply (see Figure 12.4b). Most ILS are located

in the lower lobes. If not detected by routine prenatal ultrasound, they present in childhood or adolescence with cough and recurrent pulmonary infections; in some cases, the lesion is detected as an incidental finding on chest radiograph [35]. Radiographically, ILS typically appears as a dense mass within the pulmonary parenchyma; infection can lead to cystic change with fluid levels.

Historically, there has been debate whether ILS is a congenital or acquired lesion. The late age of presentation and history of recurrent infection support ILS being an acquired lesion. In contrast, the frequent presence of bronchial atresia with CPAM features in ILS supports it being part of a spectrum of congenital lung malformations with or without systemic arterial supply [36].

Due to overlapping pathological features, ILS can be difficult to distinguish from a CPAM or isolated bronchial atresia in the absence of knowledge of an associated systemic arterial supply (Figure 12.4b,c). When infected, ILS may be confused with chronic pneumonia, although in chronic pneumonia there is a normal bronchial connection to the involved lung.

Pulmonary Hyperplasia and Congenital Lobar Overinflation

Pulmonary hyperplasia (also termed polyalveolar lobe) is the result of airway obstruction during development, which blocks outflow of fetal fluid leading to increased alveolar growth. Pulmonary hyperplasia has also been referred to as type 3 CPAM in the Stocker classification [37]. Upper airway obstruction, such as tracheal or laryngeal atresia, affects all lung lobes (also termed congenital high airway obstruction syndrome, or CHAOS) (Figure 12.5a,b), while bronchial atresia and stenosis result in focal hyperplasia (Figure 12.5c).

The pathogenesis of congenital lobar overinflation (CLO) is similar to pulmonary hyperplasia, in that intrinsic or extrinsic compression of an airway results in progressive lobar over expansion, albeit due to alveolar distension by air rather than increased alveolar growth as seen in pulmonary hyperplasia (Figure 12.5d). The underlying cause can be secondary to an intrinsic cartilaginous abnormality with resultant weak or absent bronchial cartilage or extrinsic compression of an airway (e.g., bronchogenic cyst or an enlarged or anomalous pulmonary artery). Intraluminal obstruction from meconium or mucus plugs is another potential etiology. In CLO, the compressed airway acts as a one-way valve, resulting in air trapping postnatally. While CLO may be referred to as congenital lobar emphysema, the term "emphysema" is inaccurate as alveolar wall destruction does not accompany the alveolar expansion.

Pulmonary hyperplasia may manifest in utero with polyhydramnios or fetal hydrops, from compression of venous return to the heart. In both pulmonary hyperplasia and CLO, newborns usually present with respiratory distress [38]. Tension pneumothorax may occur. Radiographical imaging demonstrates progressive hyperinflation or hyperlucency of a lobe. Marked overinflation may lead to compression of the adjacent lung and mediastinal shift, often necessitating lobectomy. In both

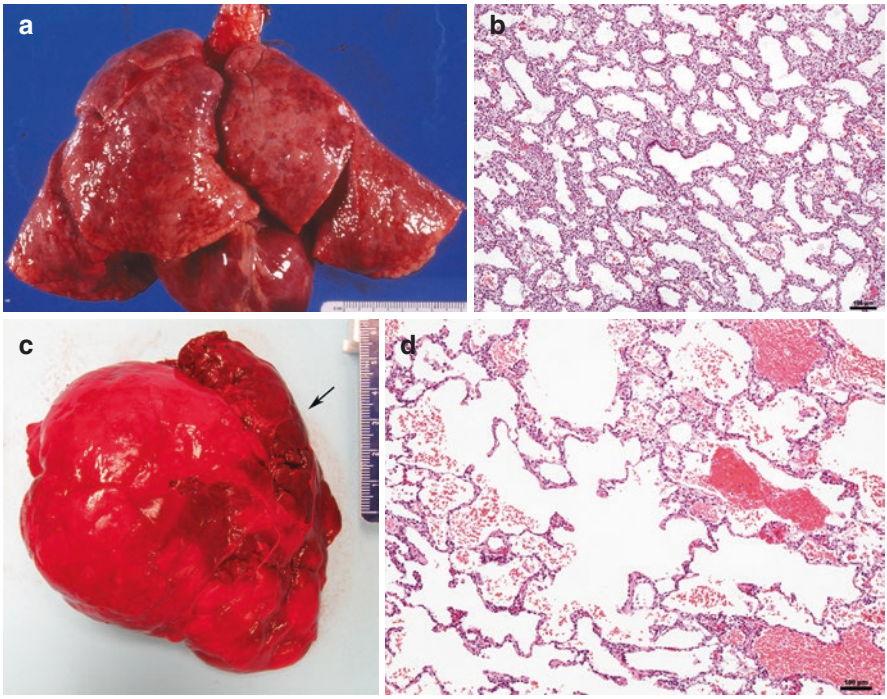

Fig. 12.5 Pulmonary hyperplasia and congenital lobar overinflation (CLO). (**a**) All lung lobes in an infant with congenital laryngeal stenosis are markedly enlarged (heart lower center). (**b**) Histologically the lungs have a striking increase in alveolar spaces compared to airways, that are often structurally abnormal (H&E). (**c**) Hyperinflation of the right middle lobe in a newborn with severe bronchial compression from a large aortopulmonary window (*arrow* denotes compressed right upper lobe). (**d**) CLO is characterized microscopically by diffuse dilatation of alveoli rather than an increase in alveolar spaces as seen in pulmonary hyperplasia (H&E)

pulmonary hyperplasia and CLO, the involved lung lobes are enlarged, bulky, and sometimes pale (see Figure 12.5a and c).

Developmental Diffuse Cystic Lung Disease

Alveolar Growth Abnormalities Presenting with Cystic Lung Disease

Alveolar growth abnormalities are characterized by impaired alveolarization with deficient alveolar septation and airspace enlargement that may be misinterpreted as "emphysematous change" on radiographical imaging and pathological evaluation [39]. While impaired lung growth is traditionally considered to occur in the context of prenatal onset pulmonary hypoplasia and chronic neonatal lung disease of

Table 12.2 Alveolar growth abnormalities presenting as diffuse cystic lung disease

I. Pulmonary hypoplasia (restriction of prenatal lung growth)
Oligohydramnios (e.g., prolonged rupture of membranes, renal dysfunction)
Restriction of thoracic volume (e.g., diaphragmatic hernia, pleural effusions, thoracic deformity from skeletal dysplasia)
Central nervous system and neuromuscular disorders resulting in decreased fetal breathing
II. Chronic neonatal lung disease of prematurity (clinical bronchopulmonary dysplasia)
III. Congenital heart disease
Cardiac anomalies with reduced pulmonary blood flow (e.g., tetralogy of Fallot, pulmonary artery stenosis/atresia, tricuspid atresia)
Cyanotic heart disease impairing postnatal alveolarization
IV. Chromosome disorders
Trisomy 21 with deficient postnatal alveolarization (often manifests with subpleural cysts on imaging)
Other chromosomal defects
V. Monogenetic disorders
FLNA (Filamin A; high phenotypic diversity including brain, cardiovascular, and gastrointestinal anomalies. Radiographical imaging may mimic congenital lobar overinflation)
NKX2.1 (NKX2.1; associated with brain-thyroid-lung syndrome)
DICER1 (DICER1; tumor predisposition syndrome with diverse manifestations most commonly including pleuropulmonary blastoma, cystic nephroma, ovarian Sertoli-Leydig cell tumors, and thyroid nodular hyperplasia/carcinoma. Radiographical imaging may mimic cystic pulmonary airway malformation)

prematurity (clinical bronchopulmonary dysplasia), it also occurs in infants with congenital heart disease as well as those with chromosomal disorders (Table 12.2) [40].

The majority of cases with pulmonary hypoplasia are secondary to congenital anomalies or pregnancy complications that inhibit lung development. As distension of the lung with liquid and fetal respiratory movements is required for prenatal lung growth, any mechanism that interferes with these processes can result in pulmonary hypoplasia. The severity of the lung growth abnormality depends on the mechanism of hypoplasia and the timing of the insult. Conditions that occur early in pregnancy (renal anomalies) may interfere with airway branching as well as alveolar formation, while later events (premature rupture of membranes) will impact only alveolar formation.

As lung maturation continues after birth, with most alveolarization occurring within the first 2 years of life [41], postnatal events can impact lung growth as well. Postnatal growth abnormalities predominate in infants with chronic neonatal lung disease (CNLD) related to prematurity, which is increasing as the survival of premature infants improves. Radiographical findings are variable based on etiology, age of the infant, and severity of the growth abnormality. Prior treatments involving high concentrations of oxygen and mechanical ventilation resulted in coarse reticular opacities, cystic lucencies, and distorted lung aeration reflecting alternating regions of

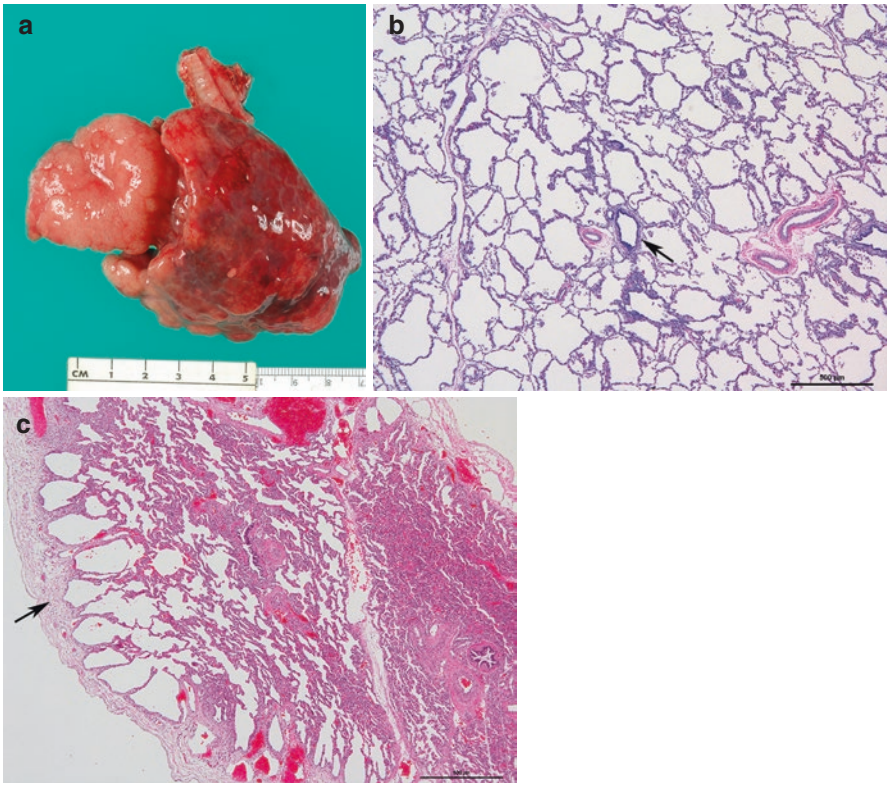

Fig. 12.6 Deficient lung growth manifesting as cystic lung disease. (**a**) Alternating areas of hyperexpansion and collapse are prominent in the left lung of an 11-week infant with severe pulmonary hypoplasia from bladder outlet obstruction. (**b**) Histologic assessment shows marked enlargement and simplification of alveoli, which normally are smaller in size than bronchioles (*arrow*) (H&E). (**c**) Deficient alveolarization is often most prominent in the subpleural space (*arrow*), as seen in the lungs from an infant with trisomy 21 (H&E)

interstitial fibrosis and atelectasis with hyperinflation on histology [42] (Figure 12.6a). Current neonatal practices including surfactant replacement and refined ventilatory strategies demonstrate more subtle radiographic imaging abnormalities, the most frequent being hyperlucent areas with linear and triangular opacities [43]. The hyperlucent areas correspond to enlarged alveoli and reduced distal vascularization (Figure 12.6b). In general, there is significant variability in the radiographical imaging findings associated with alveolar growth abnormalities, but subpleural cysts along the lung periphery, pulmonary fissures, and bronchovascular bundles can be quite characteristic, particularly in deficient lung growth associated with trisomy 21 [40, 44]. This finding correlates well with the subpleural accentuation of cystically dilated alveoli frequently seen on lung biopsy [45] (Figure 12.6c). The subpleural space is theorized to be the predominant site for late alveolar formation [46, 47].

Monogenetic Disorders Presenting with Diffuse Cystic Lung Disease

Heterozygous loss-of-function mutations in *FLNA*, which encodes the actin cross-linking protein filamin A, cause an X-linked dominant disorder with variable multi-organ involvement, including periventricular nodular heterotopias in the brain, cardiovascular anomalies, Ehlers-Danlos syndrome-like features, intestinal pseudo-obstruction, and pulmonary disease of varying severity [48–50]. Respiratory symptoms are often progressive and accompanied by severe clinical pulmonary hypertension. Age of onset of pulmonary disease associated with *FLNA* mutations occurs over a wide range but frequently presents in the first few months of life [50, 51]. Severe hyperinflation with hyperlucent cystic areas alternating with areas of atelectasis and thickening of the interlobular septa is a common appearance reported on computed tomography (CT) scan [50, 51]. The disorder may also present with severe lobar "emphysema" mimicking the localized lung malformation congenital lobar overinflation. Histologic assessment of lung tissue reveals marked alveolar enlargement and simplification reflective of a lung growth abnormality commonly combined with hypertensive changes of the pulmonary arteries, as well as abnormal muscularization of pulmonary veins and lymphatics [51, 52] (Figure 12.7a). The pathology can be similar to that of other lung disorders with deficient lung growth with pulmonary arteriopathy, which may delay diagnosis, especially in a premature infant, unless clinically suspected [52].

Diffuse cystic lung disease reflective of alveolar simplification can be the primary manifestation of pulmonary disease in individuals with heterozygous mutations in the *NKX2-1* gene (thyroid transcription factor 1, TTF-1). Cystically dilated airspaces may be accompanied by other pathologic findings including alveolar proteinosis, nonspecific interstitial pneumonitis, and fibrous remodeling [53–55]

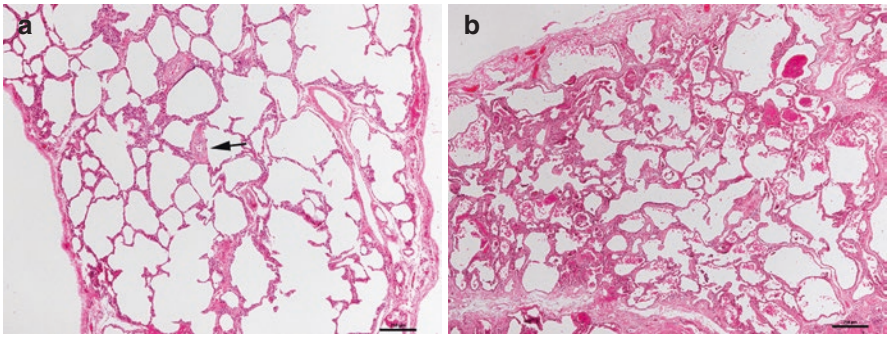

Fig. 12.7 Monogenetic disorders presenting with diffuse cystic lung disease. (**a**) A term infant with mild hypoplasia of the aortic arch and early onset respiratory distress was found to have a mutation in Filamin-A (*FLNA*) after lung biopsy (H&E). Medial hypertrophy of the pulmonary arteries (*arrow*) accompanies diffuse airspace enlargement. (**b**) Cystic dilatation of alveoli in a young child with an inherited *NKX2.1* mutation (H&E)

(Figure 12.7b). NKX2-1 is a homeobox protein critical for development and function of the lung, brain, and thyroid [56, 57]. Haploinsufficiency of *NKX2-1* due to either gene deletions or loss-of-function mutations results in "Brain-Thyroid-Lung" syndrome with individuals having a variable degree of pulmonary disease, thyroid dysfunction, and neurologic abnormalities [53, 58]. The onset of presentation is often in the newborn period or early childhood with respiratory distress syndrome progressing to interstitial lung disease and frequent pulmonary infections [53]. Recurrent spontaneous pneumothorax has also been reported [53, 54]. CT imaging demonstrates a range of findings from mild to diffuse ground-glass opacities, cysts, infiltrates, and fibrosis. Patient prognosis is variable and dependent upon the extent of lung disease.

The DICER1 tumor predisposition syndrome commonly presents as cystic lung disease. The DICER1 syndrome is an autosomal dominant condition caused by mutations in the *DICER1* gene. DICER1 is required for generation of mature microRNAs (miRNAs) that have essential regulatory roles in multiple processes including development and oncogenesis [59]. Pleuropulmonary blastoma (PPB) is the hallmark manifestation of the DICER1 syndrome and one of the most important causes of DICER1 associated morbidity and mortality [60]. Multiple other benign and malignant neoplasms are seen in the DICER1 syndrome including cystic nephroma, sarcoma and Wilms tumor of the kidney, Sertoli-Leydig cell tumor of the ovary, adenomas and carcinomas of the thyroid gland, embryonal rhabdomyosarcoma, neuroblastoma, pituitary blastoma, and pineoblastoma [60, 61]. Heterozygous germline DICER1 loss-of-function mutations were first identified in PPB in 2009 and have subsequently been identified in >70% of PPB patients [62, 63]. A somatic mutation is acquired in the second allele in DICER1 associated benign and malignant lesions, characteristically occurring in one of five hotspot codons encoding the RNase IIIb domain resulting in a dysfunctional protein [59, 61]. Genetic studies in mice demonstrate that DICER1 loss in the lung epithelium during a particular time frame during embryonic development recapitulates the PPB phenotype, and fibroblastic growth factor FGF9 overexpression in the DICER1 deficient lung epithelium promotes proliferation of the immature mesenchymal cells [64, 65]. Together, mouse models, the natural history of PPB, and tumor sequencing support DICER1 loss during lung development initiating PPB pathogenesis with tumor progression to sarcoma resulting from accumulation of additional oncogenic mutations [66, 67].

PPB manifests as three tumor subtypes representing clinicopathologic progression from a cystic (type I PPB) to a combined cystic and solid malignancy (type II PPB) to a completely solid sarcoma (type III PPB) [68]. PPB primarily affects children with >95% of cases diagnosed by 7 years of age [69]. Median ages of diagnosis are 8, 35, and 41 months for type I, type II, and type III PPBs, respectively, supporting tumor progression over time. Progression from type I to types II and III PPB are well documented in individual patients; however, not all type I PPBs progress to the more malignant subtypes [69]. Lesions with the same multilocular cystic architecture as type I PPB but lacking the primitive mesenchymal cell component that progresses to malignant sarcoma that defines PPB types II and III are identified in children as well as adults with pathologic germline DICER1 mutations [69, 70].

These lesions are presumed to be type I PPBs that have regressed and are designated type Ir PPB. Pulmonary cysts identified in adults with pathologic germline DICER1 variants are not typically resected for oncologic indications but can result in pneumothorax or symptoms related to superinfection [60]. Importantly, there are case reports of pediatric patients with type Ir PPB progressing to type II or III PPB as late as 53 months after diagnosis indicating the need for follow-up, especially when type Ir PPB is diagnosed in a young child [69].

PPB presents with variable clinical symptoms from respiratory distress to nonproductive cough, fever, and chest pain with pneumothorax being a frequent presentation of cystic type I PPB [68, 69]. A primary consideration in the radiological differential diagnosis of cystic PPB is CPAM with intrapulmonary bronchogenic cyst, pneumatocele, and pleuropulmonary synovial sarcoma representing additional considerations [61]. Radiographical features favoring a diagnosis of CPAM include prenatal detection, presence of a systemic feeding vessel, asymptomatic presentation, and hyperinflated lung [71]. These distinguishing features form the basis for an algorithm to identify children at higher risk of PPB to aid in determining cystic lesions that require resection. Two critically important points need to be highlighted regarding the differential diagnosis of cystic PPB and CPAM. First, cystic PPB and CPAM can be clinically and radiographically indistinguishable [71, 72]. Thus, frequent careful follow-up of cystic lesions in children is recommended with development of high-risk features or growth prompting consideration for resection. Second, type I PPB and type 4 CPAM in the Stocker classification system have indistinguishable histologic and radiologic features leading to the conclusion that type I PPB and type 4 CPAM represent the same entity [73–76]. It is therefore critically important that type I PPB not be diagnosed as CPAM to ensure that patients receive appropriate postoperative care and follow-up for malignancy.

Distinguishing pathological features of cystic type I PPB are the multilocular architecture and the frequent well-circumscribed border with adjacent normal lung parenchyma (Figures 12.8a,b) [70]. Key diagnostic histopathological features are collections of small primitive mesenchymal cells within the cyst walls and the cuboidal to flattened epithelial cells resembling normal alveolar epithelial cells lining the septa that separate the cysts (Figures 12.8c,d). The abundance of immature mesenchymal cells varies greatly among cases consisting of a uniform cellular cambium layer underlying the surface epithelium (see Figures 12.8c,d) to very focal, small cellular aggregates requiring examination of multiple tissue sections for identification. Lesions with the same multilocular cystic architecture but lacking a primitive cell component are designated as regressed or nonprogressed PPB type Ir. PPB progression is characterized by expansion of the primitive mesenchymal cells to form a cystic malignancy with a solid sarcomatous component (type II PPB) or an entirely solid sarcoma (type III PPB). The PPB subtype is the strongest predictor of outcome with 5-year overall survival rates of 91%, 71%, and 53% for type I, II, and III PPB, respectively [69]. These outcome data highlight the need to detect and treat PPB in its earliest, most curable, cystic type I stage. To this end, testing to identify at-risk individuals and recommended surveillance strategies have been developed [60].

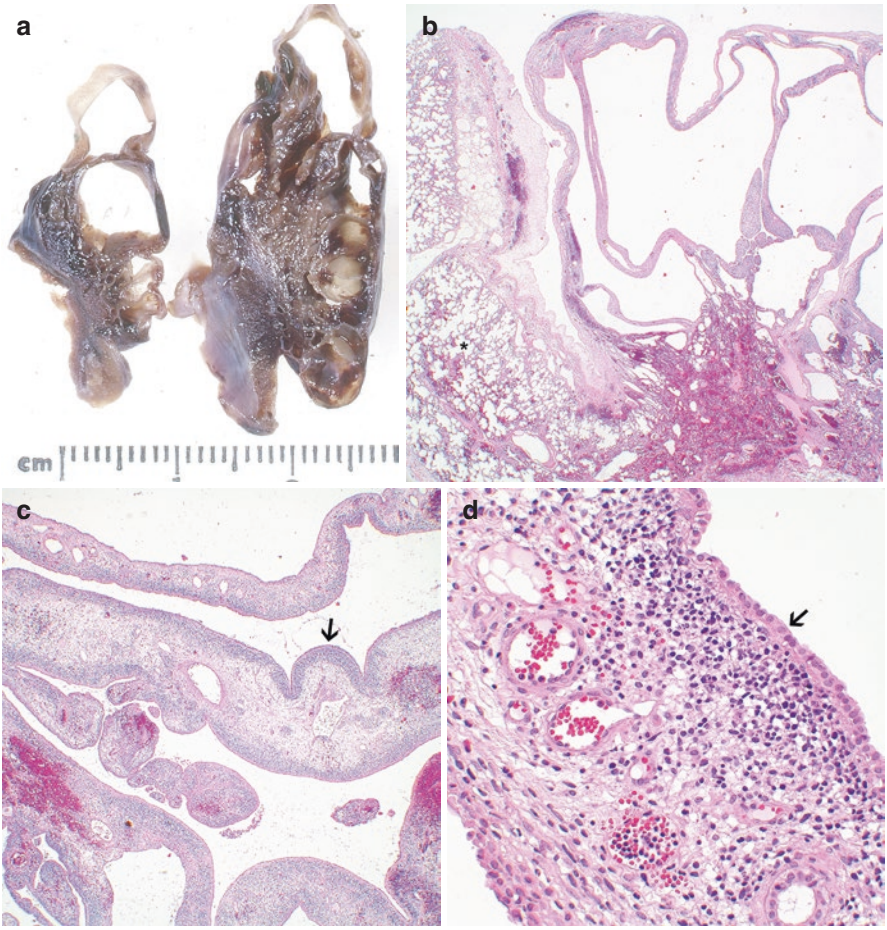

Fig. 12.8 Type I pleuropulmonary blastoma (PPB). (**a**) Lung tissue resected from a 2-year-old infant presenting with spontaneous pneumothorax containing a multiloculated cystic lesion well demarcated from the adjacent normal lung. (**b**) Microscopic examination confirms the multiloculated architecture and a well-circumscribed border with the adjacent normal lung (*) (H&E, 20×). (**c**) The cyst walls contain a cambium layer of mesenchymal cells underlying the surface epithelium (*arrow*) (H&E, 40×). (**d**) The cambium layer is comprised of small immature mesenchymal cells with the overlying epithelium (*arrow*) comprised of cuboidal cells resembling normal alveolar type 2 epithelial cells (H&E, 400×)

Conclusion

Diverse congenital and developmental entities present as cystic lung disease including lung malformations, growth abnormalities, and neoplasms. The widespread use of antenatal ultrasound has resulted in congenital lung malformations being increasingly detected in utero providing new challenges in clinical decision-making as well

as opportunities to observe lesion evolution over time. Identification of underlying mechanisms of disease, including airway obstruction and genetic alterations, has provided insights into the pathogenesis of multiple congenital and developmental lesions. A multidisciplinary approach is critical to arriving at a specific diagnosis, with integration of clinical, radiological, pathological, and frequently molecular testing required to optimize patient management.

Key Learning Points

- Airway obstruction is the etiology underlying many congenital cystic lung malformations.
- Revised pathology and radiology-based classifications have been developed for congenital cystic lung malformations to encompass pathogenesis and clinical behavior.
- Deficient lung growth can present as diffuse cystic lung disease.
- Genetic conditions can manifest as cystic lung disease.

References

1. Puligandla PS, Laberge JM. Congenital lung lesions. Clin Perinatol. 2012;39(2):331–47.
2. Stanton M, Njere I, Ade-Ajayi N, Patel S, Davenport M. Systematic review and meta-analysis of the postnatal management of congenital cystic lung lesions. J Pediatr Surg. 2009;44(5):1027–33.
3. Kunisaki SM, Ehrenberg-Buchner S, Dillman JR, Smith EA, Mychaliska GB, Treadwell MC. Vanishing fetal lung malformations: prenatal sonographic characteristics and postnatal outcomes. J Pediatr Surg. 2015;50(6):978–82.
4. Langston C. New concepts in the pathology of congenital lung malformations. Semin Pediatr Surg. 2003;12(1):17–37.
5. Riedlinger WF, Vargas SO, Jennings RW, Estroff JA, Barnewolt CE, Lillehei CW, et al. Bronchial atresia is common to extralobar sequestration, intralobar sequestration, congenital cystic adenomatoid malformation, and lobar emphysema. Pediatr Dev Pathol. 2006;9(5):361–73.
6. Kunisaki SM, Fauza DO, Nemes LP, Barnewolt CE, Estroff JA, Kozakewich HP, et al. Bronchial atresia: the hidden pathology within a spectrum of prenatally diagnosed lung masses. J Pediatr Surg. 2006;41(1):61–5. discussion-5
7. Imai Y, Mark EJ. Cystic adenomatoid change is common to various forms of cystic lung diseases of children: a clinicopathologic analysis of 10 cases with emphasis on tracing the bronchial tree. Arch Pathol Lab Med. 2002;126(8):934–40.
8. Achiron R, Hegesh J, Yagel S. Fetal lung lesions: a spectrum of disease. New classification based on pathogenesis, two-dimensional and color Doppler ultrasound. Ultrasound Obstet Gynecol. 2004;24(2):107–14.
9. Bush A. Congenital lung disease: a plea for clear thinking and clear nomenclature. Pediatr Pulmonol. 2001;32(4):328–37.
10. Seear M, Townsend J, Hoepker A, Jamieson D, McFadden D, Daigneault P, et al. A review of congenital lung malformations with a simplified classification system for clinical and research use. Pediatr Surg Int. 2017;33(6):657–64.
11. Nobuhara KK, Gorski YC, La Quaglia MP, Shamberger RC. Bronchogenic cysts and esophageal duplications: common origins and treatment. J Pediatr Surg. 1997;32(10):1408–13.
12. Zvulunov A, Amichai B, Grunwald MH, Avinoach I, Halevy S. Cutaneous bronchogenic cyst: delineation of a poorly recognized lesion. Pediatr Dermatol. 1998;15(4):277–81.

13. Gajewska-Knapik K, Impey L. Congenital lung lesions: prenatal diagnosis and intervention. Semin Pediatr Surg. 2015;24(4):156–9.
14. Stocker JT, Madewell JE, Drake RM. Congenital cystic adenomatoid malformation of the lung. Classification and morphologic spectrum. Hum Pathol. 1977;8(2):155–71.
15. Szafranski P, Coban-Akdemir ZH, Rupps R, Grazioli S, Wensley D, Jhangiani SN, et al. Phenotypic expansion of TBX4 mutations to include acinar dysplasia of the lungs. Am J Med Genet A. 2016;170(9):2440–4.
16. Barnett CP, Nataren NJ, Klingler-Hoffmann M, Schwarz Q, Chong CE, Lee YK, et al. Ectrodactyly and lethal pulmonary acinar dysplasia associated with homozygous FGFR2 mutations identified by exome sequencing. Hum Mutat. 2016;37(9):955–63.
17. Biyyam DR, Chapman T, Ferguson MR, Deutsch G, Dighe MK. Congenital lung abnormalities: embryologic features, prenatal diagnosis, and postnatal radiologic-pathologic correlation. Radiographics. 2010;30(6):1721–38.
18. Adzick NS, Harrison MR, Glick PL, Golbus MS, Anderson RL, Mahony BS, et al. Fetal cystic adenomatoid malformation: prenatal diagnosis and natural history. J Pediatr Surg. 1985;20(5):483–8.
19. Pogoriler J, Swarr D, Kreiger P, Adzick NS, Peranteau W. Congenital cystic lung lesions: redefining the natural distribution of subtypes and assessing the risk of malignancy. Am J Surg Pathol. 2019;43(1):47–55.
20. Kreiger PA, Ruchelli ED, Mahboubi S, Hedrick H, Scott Adzick N, Russo PA. Fetal pulmonary malformations: defining histopathology. Am J Surg Pathol. 2006;30(5):643–9.
21. Crombleholme TM, Coleman B, Hedrick H, Liechty K, Howell L, Flake AW, et al. Cystic adenomatoid malformation volume ratio predicts outcome in prenatally diagnosed cystic adenomatoid malformation of the lung. J Pediatr Surg. 2002;37(3):331–8.
22. Vu L, Tsao K, Lee H, Nobuhara K, Farmer D, Harrison M, et al. Characteristics of congenital cystic adenomatoid malformations associated with nonimmune hydrops and outcome. J Pediatr Surg. 2007;42(8):1351–6.
23. Ioachimescu OC, Mehta AC. From cystic pulmonary airway malformation, to bronchioloalveolar carcinoma and adenocarcinoma of the lung. Eur Respir J. 2005;26(6):1181–7.
24. Granata C, Gambini C, Balducci T, Toma P, Michelazzi A, Conte M, et al. Bronchioloalveolar carcinoma arising in congenital cystic adenomatoid malformation in a child: a case report and review on malignancies originating in congenital cystic adenomatoid malformation. Pediatr Pulmonol. 1998;25(1):62–6.
25. West D, Nicholson AG, Colquhoun I, Pollock J. Bronchioloalveolar carcinoma in congenital cystic adenomatoid malformation of lung. Ann Thorac Surg. 2007;83(2):687–9.
26. Abdallah HI, Karmazin N, Marks LA. Late presentation of misalignment of lung vessels with alveolar capillary dysplasia. Crit Care Med. 1993;21(4):628–30.
27. Lantuejoul S, Nicholson AG, Sartori G, Piolat C, Danel C, Brabencova E, et al. Mucinous cells in type 1 pulmonary congenital cystic adenomatoid malformation as mucinous bronchioloalveolar carcinoma precursors. Am J Surg Pathol. 2007;31(6):961–9.
28. Stacher E, Ullmann R, Halbwedl I, Gogg-Kammerer M, Boccon-Gibod L, Nicholson AG, et al. Atypical goblet cell hyperplasia in congenital cystic adenomatoid malformation as a possible preneoplasia for pulmonary adenocarcinoma in childhood: a genetic analysis. Hum Pathol. 2004;35(5):565–70.
29. Kim MY, Kang CH, Park SH. Multifocal synchronous mucinous adenocarcinomas arising in congenital pulmonary airway malformation: a case report with molecular study. Histopathology. 2014;65(6):926–32.
30. Sakamoto H, Shimizu J, Horio Y, Ueda R, Takahashi T, Mitsudomi T, et al. Disproportionate representation of KRAS gene mutation in atypical adenomatous hyperplasia, but even distribution of EGFR gene mutation from preinvasive to invasive adenocarcinomas. J Pathol. 2007;212(3):287–94.
31. Landing BH, Dixon LG. Congenital malformations and genetic disorders of the respiratory tract (larynx, trachea, bronchi, and lungs). Am Rev Respir Dis. 1979;120(1):151–85.

32. Newman B. Congenital bronchopulmonary foregut malformations: concepts and controversies. Pediatr Radiol. 2006;36(8):773–91.
33. Stocker JT, Kagan-Hallet K. Extralobar pulmonary sequestration: analysis of 15 cases. Am J Clin Pathol. 1979;72(6):917–25.
34. Conran RM, Stocker JT. Extralobar sequestration with frequently associated congenital cystic adenomatoid malformation, type 2: report of 50 cases. Pediatr Dev Pathol. 1999;2(5):454–63.
35. DeParedes CG, Pierce WS, Johnson DG, Waldhausen JA. Pulmonary sequestration in infants and children: a 20-year experience and review of the literature. J Pediatr Surg. 1970;5(2):136–47.
36. Holder PD, Langston C. Intralobar pulmonary sequestration (a nonentity?). Pediatr Pulmonol. 1986;2(3):147–53.
37. Stocker JT, Drake RM, Madewell JE. Cystic and congenital lung disease in the newborn. Perspect Pediatr Pathol. 1978;4:93–154.
38. Stigers KB, Woodring JH, Kanga JF. The clinical and imaging spectrum of findings in patients with congenital lobar emphysema. Pediatr Pulmonol. 1992;14(3):160–70.
39. Guillerman RP. Imaging of childhood interstitial lung disease. Pediatr Allergy Immunol Pulmonol. 2010;23(1):43–68.
40. Deutsch GH, Young LR, Deterding RR, Fan LL, Dell SD, Bean JA, et al. Diffuse lung disease in young children: application of a novel classification scheme. Am J Respir Crit Care Med. 2007;176(11):1120–8.
41. Cooney TP, Thurlbeck WM. The radial alveolar count method of Emery and Mithal: a reappraisal 2 – intrauterine and early postnatal lung growth. Thorax. 1982;37(8):580–3.
42. Northway WH Jr, Rosan RC, Porter DY. Pulmonary disease following respirator therapy of hyaline-membrane disease. Bronchopulmonary dysplasia N Engl J Med. 1967;276(7):357–68.
43. Agrons GA, Courtney SE, Stocker JT, Markowitz RI. From the archives of the AFIP: lung disease in premature neonates: radiologic-pathologic correlation. Radiographics. 2005;25(4):1047–73.
44. Biko DM, Schwartz M, Anupindi SA, Altes TA. Subpleural lung cysts in down syndrome: prevalence and association with coexisting diagnoses. Pediatr Radiol. 2008;38(3):280–4.
45. Cooney TP, Thurlbeck WM. Pulmonary hypoplasia in Down's syndrome. N Engl J Med. 1982;307(19):1170–3.
46. Massaro GD, Massaro D. Postnatal lung growth: evidence that the gas-exchange region grows fastest at the periphery. Am J Phys. 1993;265(4 Pt 1):L319–22.
47. Narayanan M, Owers-Bradley J, Beardsmore CS, Mada M, Ball I, Garipov R, et al. Alveolarization continues during childhood and adolescence: new evidence from helium-3 magnetic resonance. Am J Respir Crit Care Med. 2012;185(2):186–91.
48. Robertson SP, Twigg SR, Sutherland-Smith AJ, Biancalana V, Gorlin RJ, Horn D, et al. Localized mutations in the gene encoding the cytoskeletal protein filamin a cause diverse malformations in humans. Nat Genet. 2003;33(4):487–91.
49. Sole G, Coupry I, Rooryck C, Guerineau E, Martins F, Deves S, et al. Bilateral periventricular nodular heterotopia in France: frequency of mutations in FLNA, phenotypic heterogeneity and spectrum of mutations. J Neurol Neurosur Ps. 2009;80(12):1394–8.
50. Shelmerdine SC, Semple T, Wallis C, Aurora P, Moledina S, Ashworth MT, et al. Filamin A (FLNA) mutation-a newcomer to the childhood interstitial lung disease (ChILD) classification. Pediatr Pulmonol. 2017;52(10):1306–15.
51. Burrage LC, Guillerman RP, Das S, Singh S, Schady DA, Morris SA, et al. Lung transplantation for FLNA-associated progressive lung disease. J Pediatr. 2017;186:118–23. e6
52. Lord A, Shapiro AJ, Saint-Martin C, Claveau M, Melancon S, Wintermark P. Filamin A mutation may be associated with diffuse lung disease mimicking bronchopulmonary dysplasia in premature newborns. Respir Care. 2014;59(11):e171–7.
53. Hamvas A, Deterding RR, Wert SE, White FV, Dishop MK, Alfano DN, et al. Heterogeneous pulmonary phenotypes associated with mutations in the thyroid transcription factor gene NKX2-1. Chest.

54. Thorwarth A, Schnittert-Hubener S, Schrumpf P, Muller I, Jyrch S, Dame C, et al. Comprehensive genotyping and clinical characterisation reveal 27 novel NKX2-1 mutations and expand the phenotypic spectrum. J Med Genet. 2014;51(6):375–87.
55. Galambos C, Levy H, Cannon CL, Vargas SO, Reid LM, Cleveland R, et al. Pulmonary pathology in thyroid transcription factor-1 deficiency syndrome. Am J Respir Crit Care Med. 2010;182(4):549–54.
56. Kimura S, Hara Y, Pineau T, Fernandez-Salguero P, Fox CH, Ward JM, et al. The T/ebp null mouse: thyroid-specific enhancer-binding protein is essential for the organogenesis of the thyroid, lung, ventral forebrain, and pituitary. Genes Dev. 1996;10(1):60–9.
57. Guillot L, Carre A, Szinnai G, Castanet M, Tron E, Jaubert F, et al. NKX2-1 mutations leading to surfactant protein promoter dysregulation cause interstitial lung disease in "brain-lung-thyroid syndrome". Hum Mutat. 2010;31(2):E1146–62.
58. Krude H, Schutz B, Biebermann H, von Moers A, Schnabel D, Neitzel H, et al. Choreoathetosis, hypothyroidism, and pulmonary alterations due to human NKX2-1 haploinsufficiency. J Clin Invest. 2002;109(4):475–80.
59. Foulkes WD, Priest JR, Duchaine TF. DICER1: mutations, microRNAs and mechanisms. Nat Rev Cancer. 2014;14(10):662–72.
60. Schultz KAP, Williams GM, Kamihara J, Stewart DR, Harris AK, Bauer AJ, et al. DICER1 and associated conditions: identification of at-risk individuals and recommended surveillance strategies. Clin Cancer Res. 2018;24(10):2251–61.
61. Guillerman RP, Foulkes WD, Priest JR. Imaging of DICER1 syndrome. Pediatr Radiol. 2019;49(11):1488–505.
62. Brenneman M, Field A, Yang J, Williams G, Doros L, Rossi C, et al. Temporal order of RNase IIIb and loss-of-function mutations during development determines phenotype in pleuropulmonary blastoma / DICER1 syndrome: a unique variant of the two-hit tumor suppression model. F1000Res. 2015;4:214.
63. Hill DA, Ivanovich J, Priest JR, Gurnett CA, Dehner LP, Desruisseau D, et al. DICER1 mutations in familial pleuropulmonary blastoma. Science. 2009;325(5943):965.
64. Wagh PK, Gardner MA, Ma X, Callahan M, Shannon JM, Wert SE, et al. Cell- and developmental stage-specific Dicer1 ablation in the lung epithelium models cystic pleuropulmonary blastoma. J Pathol. 2015;236(1):41–52.
65. Yin Y, Castro AM, Hoekstra M, Yan TJ, Kanakamedala AC, Dehner LP, et al. Fibroblast growth factor 9 regulation by MicroRNAs controls lung development and links DICER1 loss to the pathogenesis of Pleuropulmonary Blastoma. PLoS Genet. 2015;11(5):e1005242.
66. Pugh TJ, Yu W, Yang J, Field AL, Ambrogio L, Carter SL, et al. Exome sequencing of pleuropulmonary blastoma reveals frequent biallelic loss of TP53 and two hits in DICER1 resulting in retention of 5p-derived miRNA hairpin loop sequences. Oncogene. 2014;33(45):5295–302.
67. Seki M, Yoshida K, Shiraishi Y, Shimamura T, Sato Y, Nishimura R, et al. Biallelic DICER1 mutations in sporadic pleuropulmonary blastoma. Cancer Res. 2014;74(10):2742–9.
68. Priest JR, McDermott MB, Bhatia S, Watterson J, Manivel JC, Dehner LP. Pleuropulmonary blastoma: a clinicopathologic study of 50 cases. Cancer. 1997;80(1):147–61.
69. Messinger YH, Stewart DR, Priest JR, Williams GM, Harris AK, Schultz KA, et al. Pleuropulmonary blastoma: a report on 350 central pathology-confirmed pleuropulmonary blastoma cases by the international Pleuropulmonary Blastoma registry. Cancer. 2015;121(2):276–85.
70. Hill DA, Jarzembowski JA, Priest JR, Williams G, Schoettler P, Dehner LP. Type I pleuropulmonary blastoma: pathology and biology study of 51 cases from the international pleuropulmonary blastoma registry. Am J Surg Pathol. 2008;32(2):282–95.
71. Feinberg A, Hall NJ, Williams GM, Schultz KA, Miniati D, Hill DA, et al. Can congenital pulmonary airway malformation be distinguished from type I pleuropulmonary blastoma based on clinical and radiological features? J Pediatr Surg. 2016;51(1):33–7.
72. Oliveira C, Himidan S, Pastor AC, Nasr A, Manson D, Taylor G, et al. Discriminating preoperative features of pleuropulmonary blastomas (PPB) from congenital cystic adenomatoid malformations (CCAM): a retrospective, age-matched study. Eur J Pediatr Surg. 2011;21(1):2–7.

73. Dehner LP, Messinger YH, Williams GM, Stewart DR, Harney LA, Schultz KA, et al. Type I Pleuropulmonary Blastoma versus congenital pulmonary airway malformation type IV. Neonatology. 2017;111(1):76.
74. Hill DA, Dehner LP. A cautionary note about congenital cystic adenomatoid malformation (CCAM) type 4. Am J Surg Pathol. 2004;28(4):554–5. author reply 5
75. MacSweeney F, Papagiannopoulos K, Goldstraw P, Sheppard MN, Corrin B, Nicholson AG. An assessment of the expanded classification of congenital cystic adenomatoid malformations and their relationship to malignant transformation. Am J Surg Pathol. 2003;27(8):1139–46.
76. Stocker JT. Cystic lung disease in infants and children. Fetal Pediatr Pathol. 2009;28(4):155–84.

Chapter 13
Rare Causes of Cystic Lung Disease

Adrian Shifren and Jay H. Ryu

COPA Syndrome

COPA syndrome is a monogenic primary immunodeficiency that was first described in 2015. COPA syndrome results in immune dysregulation and manifests clinically with autoimmune-mediated pulmonary, renal, and joint involvement. It mainly affects patients of pediatric age groups and is inherited in an autosomal dominant pattern with variable penetrance [1]. COPA syndrome results from mutations in the *COPA* gene on chromosome 1. The gene encodes a vesicular transport protein known as coatomer-associated protein subunit alpha (COPα) [2].

Molecular Pathology of COPA Syndrome

COPα is part of the coat protein complex I (COPI). COPI is a coatomer, a soluble macromolecular complex responsible for membrane trafficking and localization of vesicle-bound cargo [3]. COPI coats membrane-bound vesicles and initiates the budding process from a donor membrane on the *cis* end of the Golgi complex. These budding vesicles are responsible for retrograde transport of their cargo to the endoplasmic reticulum (ER) or other Golgi complexes for further processing. COPI is a heptameric protein assembled from seven nonidentical protein subunits (α, β, β', γ,

A. Shifren
Division of Pulmonary and Critical Care Medicine, Washington University School of Medicine, St. Louis, MO, USA
e-mail: ashifren@wustl.edu

J. H. Ryu (✉)
Division of Pulmonary and Critical Care Medicine, Mayo Clinic College of Medicine and Science, Rochester, MN, USA
e-mail: ryu.jay@mayo.edu

N. Gupta et al. (eds.), *Diffuse Cystic Lung Diseases*, Respiratory Medicine,
https://doi.org/10.1007/978-3-030-63365-3_13

δ, ε, and ζ) [4]. The COPA gene is expressed in all cell types and encodes the α subunit of COPI. COPα binds proteins bearing a carboxyl-terminal dilysine motif [5].

Four mutations are currently linked to COPA syndrome: Arg233His, Asp243Gly, Glu241Lys, and Lys230Asn [2]. All are heterozygous missense single-nucleotide polymorphisms within a 14 amino acid region encoding the WD5 and WD6 repeats of the WD40 domain of the protein. Functional analyses of these mutations demonstrate impaired binding of mutant COPA to dilysine-tagged proteins [2]. Patient-derived cells display evidence of increased ER stress, activation of the unfolded protein response (UPR), and impaired autophagic function.

COPA syndrome is marked by robust immune dysregulation. Patient-derived cells demonstrate increased transcription of IL-1β, IL-6, and IL-23, cytokines critical for the expansion of Th17 cells. In addition, patient-derived CD4+ T cells exhibit skewing toward an IL-17A-secreting Th17 phenotype, which has been strongly linked to the development of autoimmunity [6]. Most recently, activation of the type I interferon pathway, along with upregulation of interferon stimulated genes, was demonstrated in an index case of COPA syndrome and confirmed in four previously diagnosed COPA patients [7].

Clinical Characteristics of COPA Syndrome

Patients present with a syndrome of pulmonary, renal, and joint disease [1, 2, 7, 8]. The disease manifests in early childhood: 75% of patients present with signs and symptoms of disease prior to age 5, with an average onset around 3.5 years of age [1, 2]. The majority of patients are female, suggesting a female predominance for penetrance; however, larger patient cohorts are needed to corroborate this observation [1, 8]. Presenting symptoms vary widely depending on organ involvement. They include isolated joint pain and pulmonary symptoms, hemoptysis, fatigue, dyspnea at rest or with exertion, and cough [8].

Autoantibodies in COPA Syndrome

No single autoantibody has emerged as specific for, or diagnostic of, COPA syndrome. Various autoantibodies have been detected in COPA syndrome, but both the presence and titers of these autoantibodies fluctuate over time and with disease activity. Up to 86% of patients demonstrate a positive antinuclear antibody (ANA) titer ranging from 1:40 to 1:1280. Homogenous, speckled, and diffuse patterns of ANA staining have all been reported [1, 8]. Positive antineutrophil cytoplasmic antibody (ANCA) titers have been described in almost two-thirds of patients, and both cytoplasmic (cANCA) and perinuclear (pANCA) antibodies have been detected [1, 8]. Rheumatoid factor is present in 50–70% of patients, but cyclic citrullinated peptide antibodies were positive in only 20% of patients [8].

Pulmonary Manifestations of COPA Syndrome

Pulmonary disease is almost universally present in patients with COPA syndrome and is characterized by the development of diffuse parenchymal lung disease in almost all reported cases [1]. The most common pulmonary manifestations of COPA syndrome are pulmonary cysts, diffuse alveolar hemorrhage (DAH), and follicular bronchiolitis (FB). However, since COPA syndrome presents as either a diffuse cystic lung disease (DCLD) or pulmonary-renal syndrome, it can be challenging to establish the diagnosis on pulmonary findings alone.

In an international multicenter study of 14 patients with COPA syndrome, pulmonary cysts were identified in more than 80% of subjects with available CT scans [8]. The cysts tended to be thin-walled and randomly distributed throughout the lung parenchyma (Fig. 13.1). Lung biopsy samples from two female subjects with DCLD were negative for HMB-45 on immunohistochemical staining. Only one subject in the study had a history of pneumothorax.

Seven of the 14 patients (50%) patients developed DAH [8]. Hemoptysis was a presenting symptom in approximately half the cases, but marked anemia in the absence of hemoptysis was also described. Almost half of patients with DAH exhibited a pulmonary-renal syndrome with concomitant renal failure at the time of presentation. Two of three patients who underwent transbronchial lung biopsy after presenting with DAH demonstrated acute lung injury with evidence of capillaritis. All seven subjects with DAH were treated with a combination of high-dose corticosteroids and intravenous cyclophosphamide resulting in rapid resolution of DAH in six of the seven subjects. The last subject had recurrent DAH requiring additional treatment with rituximab to effect resolution. Plasmapheresis was not required for any of the subjects [8]. Maintenance immunosuppression was continued with either mycophenolate mofetil or azathioprine.

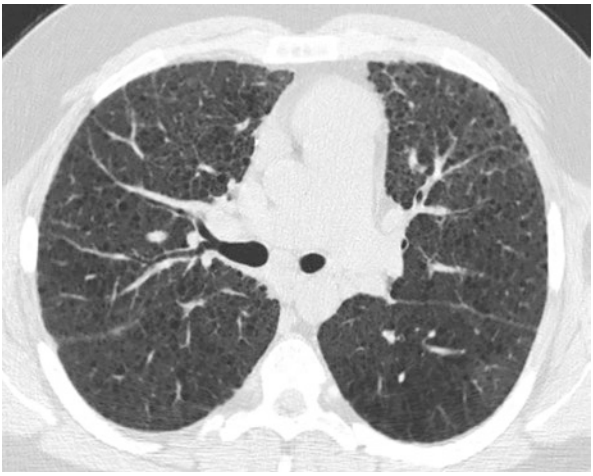

Fig. 13.1 High-resolution CT scan of the chest of a 19-year-old man with COPA syndrome. Small cysts are present throughout both lungs

Patients with long-standing COPA syndrome appear to develop interstitial lung disease (ILD). ILD appears to have a later age of onset, with patients presenting in the second decade of life [1]. FB is the most common pattern noted on lung biopsies from patients with COPA syndrome [8]. FB is the clinical and radiologic manifestation of hyperplasia of bronchus-associated lymphoid tissue (*BALT*) [9]. It typically appears as small (1–3 mm) centrilobular nodules often in association with patchy ground-glass opacities [10]. All COPA syndrome subjects with biopsy evidence of FB demonstrated ground-glass nodules and/or opacities on CT scans. Other patterns noted on CT scanning include nonspecific interstitial pneumonia (NSIP) and lymphoid interstitial pneumonia (LIP) [1]. LIP has been confirmed on lung biopsy specimens and has a known association with immune dysregulation. Diffuse interstitial pulmonary neuroendocrine cell hyperplasia (DIPNECH) has been described in two adult patients with COPA syndrome, one of whom required transplantation [11]. Whether DIPNECH is an adult manifestation of long-standing COPA syndrome is not yet known at this time.

Extrapulmonary Manifestations of COPA Syndrome

Arthritis contributes significantly to patient morbidity. Approximately 95% of patients develop arthritis. Arthritis affecting large joints (shoulders and knees), small joints (metacarpophalangeal and interphalangeal joints), and the axial skeleton (cervical spine) has been described [8]. In one series, the knees and interphalangeal joints of the hands were most frequently involved [1]. Arthritic manifestations tend to flare in conjunction with pulmonary disease and improve with immunosuppression [1, 8].

Renal disease tends to present later than musculoskeletal and pulmonary disease, with onset typically occurring in the patient's mid to late teen years [1]. Almost half of the patients had either proteinuria and/or decreased renal function, and in all patients undergoing renal biopsy, histologic features of glomerulopathy were present. Pathologic lesions on individual renal biopsies tend to be heterogeneous with positive immunofluorescence staining for IgG, IgA, IgM, C3, and C1q being described [1, 8]. While up to 75% of patients demonstrate necrotizing or crescentic lesions indicative of more severe disease, progression to hemodialysis or transplantation appears to be rare [1].

Fire-Eater's Lung

Fire-eater's lung is a unique form of exogenous lipoid pneumonia. It is the result of unintended aspiration of flammable petrochemical derivatives during fire-eating and fire-blowing [12, 13]. When blowing fire, the performer forcefully exhales a mouthful of liquid hydrocarbon (usually the petroleum derivative kerdan) against a

flaming baton, igniting an aerosol that gives the impression of breathing fire [14]. Residual oral petrochemicals are aspirated on subsequent inhalation. Following aspiration, the petrochemicals are phagocytosed by macrophages resulting in a lipoid pneumonia with granulomatous foreign body reaction. Cavitation within the lipoid pneumonia leads to the development of pneumatoceles [15].

The clinical findings of fire-eater's lung can mimic bacterial pneumonia. In a retrospective case series of 123 patients, the most frequent symptoms included cough (~50%), chest pain (~45%), fever (~35%), dyspnea (~25%), and minor hemoptysis (~10%) [13]. These findings are corroborated by a second series of 17 patients [14]. One case of respiratory failure requiring mechanical ventilation has been described [14]. CXR demonstrates pulmonary infiltrates in 80–100% of cases, most commonly (66%) in the right lower lung field as would be expected in cases of aspiration [13, 14]. CT findings include ground-glass opacities or consolidation predominantly involving the middle and lower lobes. Pneumatoceles typically occur within the ground-glass or consolidative opacities. Pneumothorax and pneumomediastinum are rare in exogenous lipoid pneumonias, and none were reported in either case series [13, 14, 16]. The optimal treatment for fire-eater's lung is unknown. Treatment with antibiotics varies widely, ranging from 22% to 75% of cases depending on the study. Similarly, corticosteroids were administered in 5–38% of cases [13, 14]. All cases showed complete clinical, physiologic, and radiologic recovery by 6 months, irrespective of the therapeutic management [13, 14]. These data suggest that supportive care for fire-eater's lung is most likely sufficient.

Recreational Drug Abuse

Recreational drug abuse is associated with a variety of lung injuries involving the airways, parenchyma, vasculature, and pleura. Drugs that are commonly abused and result in lung injury include marijuana, cocaine, and intravenously administered drugs such as heroin.

Marijuana is derived from the herbaceous flowering plant *Cannabis sativa*. Resin from the flowers, leaves, and stems contain the principal psychoactive component of marijuana, delta-9-tetrahydrocannabinol (Δ9-THC). It is usually consumed by smoking (with approximately 15–20% bioavailability) or oral ingestion (providing approximately 5% bioavailability) [17]. One form of parenchymal lung injury in marijuana users is bullae formation involving the upper lobes. This is most commonly observed in regular marijuana users [18, 19]. Most of the reported patients have been between 25 and 50 years of age. The development of these bullae is thought to be related to the large inspiratory volume and breath-holding maneuver used by marijuana smokers as well as the toxic effects of marijuana smoke itself to the lung parenchyma.

Cocaine is a stimulant drug extracted from the leaves of the *Erythroxylon coca* plant. Cocaine is either inhaled in crystalline powder form or smoked in free-base form. The crystalline form can also be used intravenously [17]. Bullous emphysema

predominantly involving the upper lobes has been associated with smoking cocaine [20]. This emphysematous process can be complicated by pneumomediastinum and pneumothorax as well as lung abscess [19, 21]. Bullous emphysema involving the upper lobes has also been associated with intravenous drug abuse [22].

Radiation Therapy

Radiation-induced lung injury is a relatively common complication of radiation therapy for chest wall and intrathoracic malignancies. Incidental irradiation of the lungs results in lung injury in 5% to 20% of patients receiving radiation for lung cancers [23]. **Radiation-induced lung injury** is variable in appearance, and dependent on imaging modality and timing of the imaging with respect to radiation therapy. Classically, early and late forms of **radiation-induced lung injury** are described, corresponding to radiation pneumonitis and radiation fibrosis, respectively. Both injuries tend to manifest imaging abnormalities conforming to the limits of the radiation port rather than respecting anatomical lung boundaries [24].

Atypical forms of radiation-induced lung injury include radiation-induced organizing pneumonia and radiation-induced eosinophilic pneumonia, both of which can involve the lung outside the field of irradiation [25, 26]. A rare case of DCLD related to radiation therapy has been reported [27]. This case involved a 4-year-old child who had undergone treatment with systemic chemotherapy along with whole lung and abdomen irradiation for metastatic Wilms tumor. Ten months after completion of her radiation therapy, she presented with persistent dyspnea and cough. Chest CT scan demonstrated scattered cystic lesions in both lungs along with diffuse ground-glass and reticular opacities. Surgical lung biopsy revealed interstitial inflammation and fibrosis felt to be consistent with radiation fibrosis. There were regions of cystic remodeling associated with pericystic fibrosis. There was no evidence of neoplasm or infection. In the following months, the parenchymal abnormalities including cystic lesions regressed.

Key Learning Points

- Cystic lung disease may include particularly rare etiologies.
- COPA syndrome
  - COPA syndrome is a monogenic primary immunodeficiency.
  - It is inherited in an autosomal dominant pattern with variable penetrance.
  - The gene encodes a vesicular transport protein known as coatomer-associated protein subunit alpha (COPα), which is expressed in all cell types and is responsible for membrane trafficking and localization of vesicle-bound cargo.
  - COPA syndrome is characterized by robust immune dysregulation.
  - The disease manifests in early childhood.
  - Patients present with a syndrome of pulmonary, renal, and joint disease.
  - Pulmonary disease is universally present in patients with COPA syndrome.
  - The most common pulmonary manifestations include pulmonary cysts, diffuse alveolar hemorrhage (DAH), and follicular bronchiolitis (FB).

  - Pulmonary cysts are identified on CT scan in >80% of subjects.
  - The cysts tended to be thin-walled and randomly distributed throughout the lung parenchyma.
  - COPA syndrome may present as a pulmonary-renal syndrome.
  - Patients with long-standing COPA syndrome may develop interstitial lung disease.
  - Follicular bronchiolitis is the most common interstitial disease noted on lung biopsy.

- Fire-eater's lung (FEL)
  - FEL is a unique form of lipoid pneumonia.
  - After blowing fire, residual oral petrochemicals are aspirated on subsequent inhalation, resulting in a lipoid pneumonia.
  - Cavitation within the lipoid pneumonia leads to the development of pneumatoceles.
  - CXR demonstrates pulmonary infiltrates in 80–100% of cases.
  - The optimal treatment for FEL is unknown.

- Recreational drug abuse
  - Marijuana users develop bullae formation involving the upper lobe.
  - This is most commonly observed in regular marijuana users.
  - The bullae are thought to arise from large volume breath holding, in combination with the toxic effects of marijuana smoke.
  - Cocaine users develop bullous emphysema predominantly involving the upper lobes.
  - The emphysematous changes can be complicated by pneumomediastinum and pneumothorax.
  - Development of emphysematous bullae is associated with both cocaine smoking and intravenous cocaine use.

- **Radiation-induced lung injury (RILI)**
  - RILI is a relatively common complication of radiation therapy for chest wall and intrathoracic malignancies.
  - A rare case of diffuse cystic lung disease related to radiation therapy has been reported.

References

1. Vece TJ, Watkin LB, Nicholas S, Canter D, Braun MC, Guillerman RP, et al. Copa syndrome: a novel autosomal dominant immune dysregulatory disease. J Clin Immunol. 2016;36(4):377–87.
2. Watkin LB, Jessen B, Wiszniewski W, Vece TJ, Jan M, Sha Y, et al. COPA mutations impair ER-Golgi transport and cause hereditary autoimmune-mediated lung disease and arthritis. Nat Genet. 2015;47(6):654–60.
3. Schekman R, Orci L. Coat proteins and vesicle budding. Science. 1996;271(5255):1526–33.

4. Dodonova SO, Diestelkoetter-Bachert P, von Appen A, Hagen WJ, Beck R, Beck M, et al. VESICULAR TRANSPORT. A structure of the COPI coat and the role of coat proteins in membrane vesicle assembly. Science. 2015;349(6244):195–8.
5. Kirchhausen T. Three ways to make a vesicle. Nat Rev Mol Cell Biol. 2000;1(3):187–98.
6. Miossec P, Korn T, Kuchroo VK. Interleukin-17 and type 17 helper T cells. N Engl J Med. 2009;361(9):888–98.
7. Volpi S, Tsui J, Mariani M, Pastorino C, Caorsi R, Sacco O, et al. Type I interferon pathway activation in COPA syndrome. Clin Immunol. 2018;187:33–6.
8. Tsui JL, Estrada OA, Deng Z, Wang KM, Law CS, Elicker BM, et al. Analysis of pulmonary features and treatment approaches in the COPA syndrome. ERJ Open Res. 2018 Jun 27;4(2):00017.
9. Tashtoush B, Okafor NC, Ramirez JF, Smolley L. Follicular bronchiolitis: a literature review. J Clin Diagn Res. 2015;9(9):OE01–5.
10. Pipavath SJ, Lynch DA, Cool C, Brown KK, Newell JD. Radiologic and pathologic features of bronchiolitis. AJR Am J Roentgenol. 2005;185(2):354–63.
11. Gomes VC, Silva MC, Maia Filho JH, Daltro P, Ramos SG, Brody AS, et al. Diagnostic criteria and follow-up in neuroendocrine cell hyperplasia of infancy: a case series. J Bras Pneumol. 2013;39(5):569–78.
12. Brander PE, Taskinen E, Stenius-Aarniala B. Fire-eater's lung. Eur Respir J. 1992;5(1):112–4.
13. Franzen D, Kohler M, Degrandi C, Kullak-Ublick GA, Ceschi A. Fire eater's lung: retrospective analysis of 123 cases reported to a National Poison Center. Respiration. 2014;87(2):98–104.
14. Gentina T, Tillie-Leblond I, Birolleau S, Saidi F, Saelens T, Boudoux L, et al. Fire-eater's lung: seventeen cases and a review of the literature. Medicine (Baltimore). 2001;80(5):291–7.
15. Cheung YK, Lau KK, Li X. Fire-eater's pneumonia. J Med Imaging Radiat Oncol. 2008;52(5):528.
16. Betancourt SL, Martinez-Jimenez S, Rossi SE, Truong MT, Carrillo J, Erasmus JJ. Lipoid pneumonia: spectrum of clinical and radiologic manifestations. AJR Am J Roentgenol. 2010;194(1):103–9.
17. Benson MK, Bentley AM. Lung disease induced by drug addiction. Thorax. 1995;50(11):1125–7.
18. Johnson MK, Smith RP, Morrison D, Laszlo G, White RJ. Large lung bullae in marijuana smokers. Thorax. 2000;55(4):340–2.
19. Hii SW, Tam JD, Thompson BR, Naughton MT. Bullous lung disease due to marijuana. Respirology. 2008;13(1):122–7.
20. van der Klooster JM, Grootendorst AF. Severe bullous emphysema associated with cocaine smoking. Thorax. 2001;56(12):982–3.
21. Mishra R, Patel R, Khaja M. Cannabis-induced bullous lung disease leading to pneumothorax: case report and literature review. Medicine (Baltimore). 2017;96(19):e6917.
22. Gurney JW, Bates FT. Pulmonary cystic disease: comparison of Pneumocystis carinii pneumatoceles and bullous emphysema due to intravenous drug abuse. Radiology. 1989;173(1):27–31.
23. Marks LB, Yu X, Vujaskovic Z, Small W Jr, Folz R, Anscher MS. Radiation-induced lung injury. Semin Radiat Oncol. 2003;13(3):333–45.
24. Choi YW, Munden RF, Erasmus JJ, Park KJ, Chung WK, Jeon SC, et al. Effects of radiation therapy on the lung: radiologic appearances and differential diagnosis. Radiographics. 2004;24(4):985–97. discussion 998
25. Cornelissen R, Senan S, Antonisse IE, Liem H, Tan YK, Rudolphus A, et al. Bronchiolitis obliterans organizing pneumonia (BOOP) after thoracic radiotherapy for breast carcinoma. Radiat Oncol. 2007;2:2.
26. Cottin V, Frognier R, Monnot H, Levy A, DeVuyst P, Cordier JF, et al. Chronic eosinophilic pneumonia after radiation therapy for breast cancer. Eur Respir J. 2004;23(1):9–13.
27. Wolf MS, Chadha AD, Carroll CM, Borinstein SC, Young LR. Unusual progression and subsequent improvement in cystic lung disease in a child with radiation-induced lung injury. Pediatr Radiol. 2015;45(7):1086–90.

Chapter 14
Mimics, Impersonators, and Semblances of Pulmonary Cysts

Orla O'Carroll, David J. Murphy, and Cormac McCarthy

Introduction

Pathologically, a cyst is defined as any round circumscribed space surrounded by a wall, either epithelial or fibrous, of varying thickness [1]. The Fleischner Society Guidelines define a pulmonary cyst radiographically as a round parenchymal lucency or low-attenuating area with a well-defined interface with normal lung [2]. Cysts can have variable wall thickness, though they are most often thin-walled with a mural diameter of less than 2 mm. Most commonly cysts contain air, but they also may be fluid-filled or contain solid material on occasion. Typically, cysts occur without associated emphysematous change.

There is considerable overlap between the radiological appearance of cysts and numerous other radiographical and pathological entities [3]. For example, a bulla is defined as a focal lucency measuring more than 1 cm in diameter, which is bordered by a thin wall no greater than 1 mm in thickness [4]. Bullae, in comparison to cysts, occur in the presence of emphysematous change. Moreover, a cavity is defined as a lucency or low-attenuation area, which tends to occur within an area of pulmonary consolidation, nodule, or mass [2]. Cavities may or may not contain air-fluid levels. Usually wall thickness of a cavity is greater than 4 mm though notably in the case of cavitating consolidation, the consolidation will often resolve leaving only a thin

O. O'Carroll
Department of Respiratory Medicine, St. Vincent's University Hospital, Dublin, Ireland
e-mail: orlaocarroll@svhg.ie

D. J. Murphy
Department of Radiology, St Vincent's University Hospital, Dublin, Ireland
e-mail: David.murphy@svhg.ie

C. McCarthy (✉)
Department of Medicine and Respiratory Medicine, Education and Research Centre, University College Dublin, St. Vincent's University Hospital, Dublin, Ireland
e-mail: Cormac.McCarthy@UCD.ie

N. Gupta et al. (eds.), *Diffuse Cystic Lung Diseases*, Respiratory Medicine,
https://doi.org/10.1007/978-3-030-63365-3_14

wall. Furthermore, a pneumatocele is a round thin-walled airspace in the lung, which occurs in response to various causative factors such as trauma, aspiration, or acute pneumonia by a process of parenchymal necrosis and check-valve airway obstruction [5].

Given the overlap with other radiological entities there is often diagnostic uncertainty in terms of the radiological diagnosis of cystic lung disease. In this chapter, we consider in more detail a range of common conditions whose radiographical features mimic those of the true diffuse cystic lung diseases (DCLDs).

Emphysema

Emphysema can be pathologically defined as a condition of the lung characterized by abnormal, permanent enlargement of airspaces distal to the terminal bronchiole, accompanied by the destruction of their walls, and without obvious fibrosis [6].

Emphysema is a term used interchangeably with chronic obstructive pulmonary disease (COPD) and is associated with a high burden of morbidity and mortality. COPD is currently the third leading cause of mortality worldwide [7, 8].

While emphysema tends to be strongly associated with smoking, there are other conditions that can cause this structural disorder in the lungs. Alpha-one antitrypsin deficiency (AATD) is a genetic disease characterized by low circulating levels of the alpha-1 antitrypsin protein (AAT) and is inherited in an autosomal co-dominant fashion. AAT is an important and potent protease inhibitor synthesized and secreted by the liver. It functions mainly in the lungs to protect elastic structures against proteases such as neutrophil elastase. Mutations in the SERPINA1 gene on chromosome 14q32, the gene that encodes for AAT, alter the configuration of the protein in multiple ways to inhibit its release from hepatocytes, thereby leading to reduced circulating levels systemically. Homozygosity for the PI*Z allele is associated with low AAT serum levels and high risk of clinical disease. The imbalance of protease and antiprotease caused by reduced AAT levels results in destruction of alveolar walls and interstitial tissues leading to early and rapidly progressive emphysema, particularly when compounded by cigarette smoking [9]. Radiologically it is associated with extensive basal-predominant panlobular emphysema [10, 11] and the distribution itself may trigger diagnosis of the disease as this is an unusual pattern in any other context [12]. Treatment options center around lifestyle modifications and treatment of ensuing COPD, cirrhosis, or panniculitis; however, intravenous AAT replacement therapy is employed in more severe cases in countries where it is available and is the only treatment known to target the underlying cause of the disease [13–15].

The radiological evaluation of emphysema involves CT as the core imaging modality. While plain chest radiography can be utilized in the early stages of workup, it does not allow advanced assessment of the extent of emphysematous changes. Several distinct morphological subtypes of emphysema exist and can be characterized on CT (Fig. 14.1). There is a degree of correlation between certain clinical features of COPD and imaging abnormalities, which can help stratify clinical risk

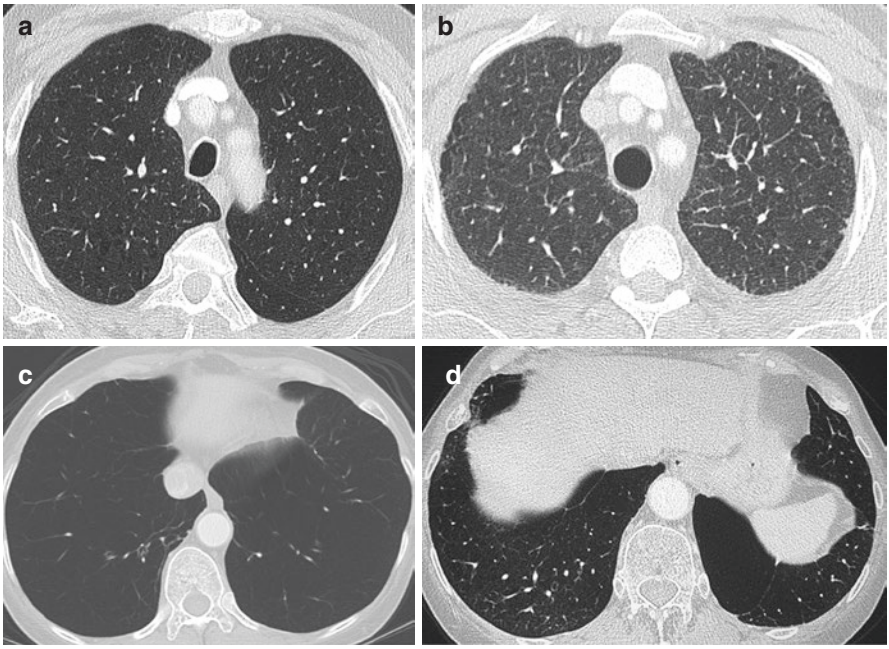

Fig. 14.1 Emphysema. Panel A illustrates centrilobular emphysema with multiple areas of low attenuation representing central destruction of the secondary pulmonary lobule. Paraseptal emphysema is visible in panel B toward the posterior pleural surface. These areas of hypoattenuation represent selective destruction of the distal acinus. Panel C shows severe panlobular emphysema with diffuse destruction of lung parenchyma across the entirety of the secondary pulmonary lobule. Panel D demonstrates a large bulla in the left lung base

for patients [16, 17]. For example, centrilobular emphysema and panlobular emphysema are associated with greater dyspnea and reduced walk distance compared to paraseptal emphysema where there can be less of a symptom burden [16].

Centrilobular emphysema, the most common emphysematous subtype, predominantly affects the upper lobes and is defined by small areas of low attenuation. Pathologically, these low attenuation areas are representative of areas of destruction in the center of the secondary pulmonary lobule and are surrounded by normal lung. These areas tend to be poorly defined due to their thin walls and are traversed by centrilobular arteries or arterioles, which mark their center. The areas can range in size from 1 to 3 mm and correlate with pathologically defined centrilobular emphysema [18]. Centrilobular emphysema tends to occur in older patients and is exquisitely associated with smoking status [19]. As the disease progresses, there is increased destruction of the lobular unit and confluence of the observed areas of low attenuation on CT. At this stage, the surrounding walls become almost imperceptible or disappear altogether, and the centrilobular distribution becomes less apparent.

Paraseptal emphysema is the pattern observed when the distal acinus is selectively destroyed [20]. Lesions form near the pleural surface and in the interlobar

fissures, and can often coalesce to form large hyperlucent areas bordered by interlobular septae, which are intact but thickened by associated fibrosis due to the high level of airway inflammation [21]. Paraseptal emphysema tends to occur in the middle and upper zone subpleural areas as well as along the mediastinal fissures. Minimal subpleural paraseptal emphysema can be encountered in nonsmokers [22]. Paraseptal emphysema can occur in rows where it can sometimes be confused with the honeycomb change characteristic of fibrotic interstitial lung diseases [23].

Panlobular emphysema refers to diffuse destruction of lung parenchyma across the entire secondary pulmonary lobule rather than the central destruction pathognomonic of centrilobular emphysema [24]. It tends to affect the lower lobes and is highly associated with AATD [25]. It can also occur in cigarette smokers, usually in combination with centrilobular emphysema, and also in those who abuse certain intravenous drugs [26].

Bullae are defined as avascular low-attenuation areas greater than 1 cm in diameter with a thin but perceptible wall [4] and are found in all subtypes of emphysema. They are most closely associated with paraseptal emphysema and are often found in the upper lobes of the lung [27]. Bullae may be associated with adjacent atelectasis whereby the bulla becomes so large it impairs the expansion of the adjacent normal lung [28].

The distinct morphological subtypes of the spectrum of emphysema on CT scanning can help to distinguish disease phenotypes as well as allow assessment of disease severity for patients [16, 17]. CT appearances of emphysema can mimic DCLDs as all subtypes are marked by hyper-lucency with some element of a surrounding wall. Careful observation of spirometric airflow limitation, documentation of patient exposure history, and assessment of symptomatic burden can lead to the correct diagnosis and identify potential treatment strategies for the patients affected by this disease.

Interstitial Lung Disease

The term "interstitial lung disease" (ILD) is a broad classification encompassing a range of lung diseases that cause diffuse alterations to the lung parenchyma over time. The term represents a diverse group of conditions of varying severity, etiology, and prognosis but which are unified by the pathophysiological end-points of acute lung injury leading to chronic interstitial inflammation, damage to parenchymal tissues, fibroblastic change, and eventual distortion of normal lung architecture [29]. Previously investigation of diffuse ILDs often required lung biopsy [30], but advanced CT techniques allow current diagnostic criteria to rely more on imaging interpretation, abrogating the need to histologically demonstrate the underlying pathology in a substantial proportion of patients [31, 32]. Fibrotic ILDs can present with numerous radiological patterns, and a number of these may involve cystic appearing structures such as honeycombing and clustered traction bronchiectasis.

Honeycombing is defined as subpleural, clustered, multi-layered, or multi-tiered cystic air spaces with well-defined walls [33]. It is often difficult to distinguish from

paraseptal emphysema. While honeycombing involves stacked cystic structures, paraseptal emphysema presents as a linear arrangement of cysts without stacking. The cystic spaces in honeycomb lung are associated with irregularly thickened walls and range in diameter from 3 to 10 mm. Pathologically these cystic areas represent dilated and thickened terminal bronchioles and most commonly occur in patients with end-stage ILD [34]. Demonstration of honeycombing in association with peripheral subpleural basal-predominant reticular opacities and traction bronchiectasis leads to a radiological diagnosis of definite usual interstitial pneumonia (UIP) and negates the need for surgical lung biopsy as a confirmatory diagnostic test [35]. Probable UIP is marked by the abovementioned features but without demonstration of honeycombing. In these cases, the clinical context is combined with imaging results, and surgical biopsy may be employed if the risk: benefit ratio is favorable for the individual [35].

UIP is the typical radiological pattern observed in idiopathic pulmonary fibrosis (IPF) (Fig. 14.2a) but can also be observed in other disease processes, including

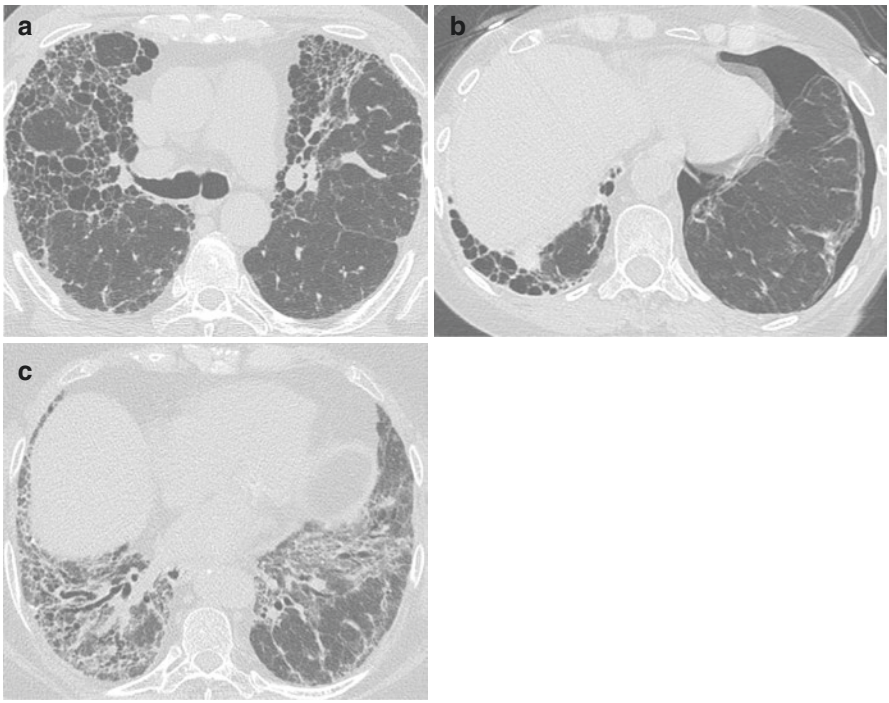

Fig. 14.2 Interstitial lung disease. Panel A demonstrates the CT findings in a patient with usual interstitial pneumonia pattern associated with idiopathic pulmonary fibrosis. The constellation of findings includes honeycombing, traction bronchiectasis, and subpleural reticular opacities thus demonstrating definite UIP. Panel B illustrates honeycombing in a patient with rheumatoid arthritis associated interstitial lung disease. Also noted is an incidental left-sided spontaneous pneumothorax. Panel C shows significant architectural distortion associated with fibrotic nonspecific interstitial pneumonitis

rheumatoid arthritis-interstitial lung disease (RA-ILD) (Fig. 14.2b), drug-related ILD, sarcoidosis, and some occupational lung diseases [36]. Furthermore, honeycombing can occur in some cases of nonspecific interstitial pneumonia (Fig. 14.2c) though it is usually a very late sign in longstanding NSIP and tends to not be the predominant feature on imaging [37, 38]. Clusters of cystic lesions seen with ILDs such as NSIP and hypersensitivity pneumonitis can often represent traction bronchiectasis rather than true honeycombing. If bronchiectasis is the cause of these clusters, the cysts tend to be larger than the cysts of honeycombing and are more regular in size [38].

Although cystic areas can be seen in a variety of fibrotic ILDs, careful demographic and clinical history-taking combined with the presence of other (noncystic) interstitial abnormalities on chest radiology often makes it rather straightforward to distinguish these ILDs from true DCLDs.

Bronchiectasis

Bronchiectasis is defined as irreversible abnormal dilatation of the bronchial tree, particularly the proximal and medium-sized bronchi [39]. Bronchiectasis most commonly occurs as a consequence of other conditions and involves destruction and weakening of the bronchial walls through multiple processes such as inflammation, edema, and fibrosis [40]. These factors combine to attract multiple pathogens to the areas of damaged lung, and over time bronchiectatic lungs can often become a nidus for colonization with resistant bacteria [41]. The end result is marked architectural distortion of lung tissue [42]. Causes of the disease are most likely infective, most notably primary lung infection, aspiration pneumonia, and immunodeficiency, but can also be caused by connective tissue disorders, genetic diseases such as cystic fibrosis, and toxin exposure [43]. Clinically bronchiectasis is suspected in patients who present with increased cough, sputum production, and hemoptysis.

Bronchiectasis is often characterized as cylindrical, cystic, or varicose, and differentiation of these three subtypes is made on CT imaging [44]. Airway dilatation is the most common finding on HRCT and can be seen either as parallel lines, so-called tram lines, or end-on where it is seen as ring-shaped shadows. If the airway diameter is more than one and a half times the accompanying vessel's diameter, this indicates the presence of cylindrical bronchiectasis. This finding is also termed the "signet-ring" sign where the dilated airway is air filled and contiguous with the small opacity of the pulmonary artery [45] (Fig. 14.3a). In addition to dilatation of the airway, lack of tapering of the bronchus and bronchial wall thickening are seen and the combination of all three features is more specific for bronchiectasis than for other conditions that can also be associated with mild bronchial dilatation such as asthma.

Varicose bronchiectasis is diagnosed wherever alternating areas of bronchial dilatation and constriction occur in nearby proximity [46]. Constricted areas can give rise to post-obstructive pneumonitis and thereby cause additional damage to

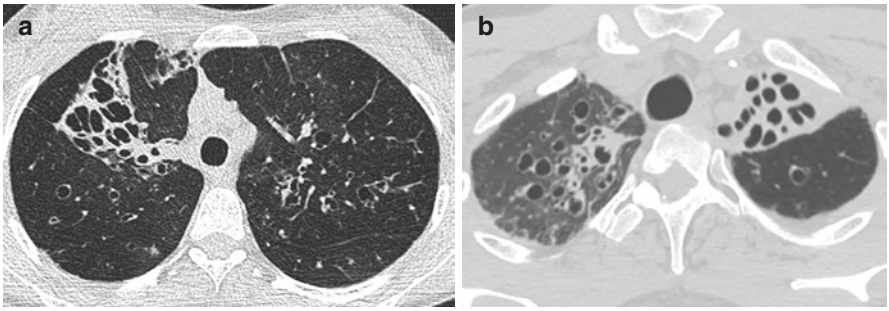

Fig. 14.3 Bronchiectasis. Panel A depicts bronchiectasis, dilated bronchioles can be seen throughout and there are examples of signet-ring formation where the dilated bronchiole is wider in diameter than the accompanying vessel. Panel B is from a patient with cystic fibrosis and demonstrates the severe apical cystic bronchiectasis associated with these cases

lung parenchyma [47]. Cystic bronchiectasis occurs in more severe cases where unchecked inflammation can result in neovascularization and angiogenesis [48]. This causes cyst-like structures to form off the damaged bronchial wall, and these tend to cluster, often into areas which resemble clusters of grapes [47]. This bronchiectasis subtype mimics DCLDs most closely [2] (Fig. 14.3b).

The distribution on HRCT of bronchiectasis can be indicative of the underlying cause [49]. Cystic fibrosis is commonly associated with upper lobe predominant findings on CT, which tend to be particularly severe in terms of the level of parenchymal distortion [50] (see Fig. 14.3b). Primary ciliary dyskinesia, which causes bronchiectasis due to impaired mucus clearance, has a predilection for middle and lower zones, while idiopathic bronchiectasis tends to occur in the lower zones [51]. There is some evidence that the extent of bronchiectasis on HRCT correlates with disease severity with evidence of mucus plugging and bronchial wall thickening correlating with decline in FEV_1 over time in a repeated measure study [52]; however, this assertion has not been borne out in subsequent studies [53]. The pattern of disease does not seem to correlate well with clinical severity measures except that cystic bronchiectasis can be associated with hemoptysis [44].

Neoplastic Processes

Cavitary and cystic change is an unusual but documented occurrence in lung neoplasms, and in certain cases cavitary lung tumors can be difficult to differentiate from DCLDs. Detailed description of the neoplastic causes of DCLDs is provided in Chap. 11 of this textbook. In those with primary lung malignancy, cavitary change has been detected in up to 22% of CT images [54, 55]. Squamous cell carcinoma accounts for the vast majority of the cases of cavitary primary lung malignancy, up to 80% in some reports [56] (Fig. 14.4). Adenocarcinoma represents the remainder of cases. In general, cavities associated with malignancy are solitary; however, very

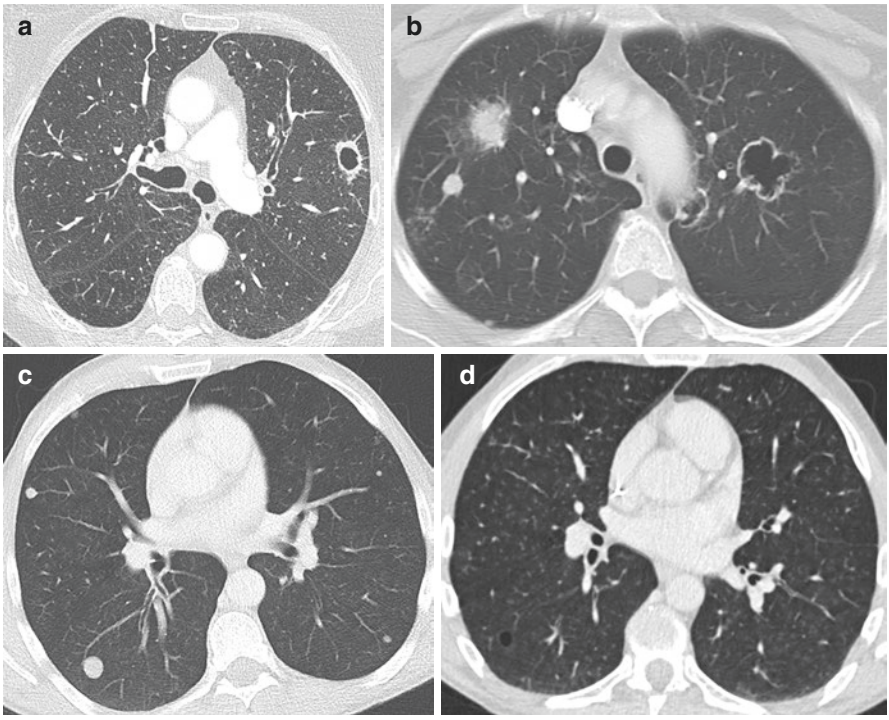

Fig. 14.4 Neoplastic processes. Panel A illustrates a cavitary mass in a patient with primary squamous cell carcinoma of the lung. Panel B illustrates a similar cyst-like structure in a patient with metastatic endometrial sarcoma. Panel C demonstrates a metastatic urothelial cancer with a moderate-sized metastasis in the posterior right lower lobe. This metastasis has become cystic after treatment of the urothelial cancer, panel D

rarely bronchoalveolar cell carcinoma can present with multiple cavitary lesions [57]. The proposed mechanism for cavity and cyst genesis in lung cancer is that unchecked rapid growth of the tumor exceeds the tumor's own blood supply and central necrosis occurs [55]. Recently it has been shown that a very high proportion of those primary tumors that cavitate exhibit overexpression of epidermal growth factor receptor (EGFR), which may contribute to their rapid growth and central necrosis and add some merit to this proposed mechanism [58]. Patients with a cavitating primary lung malignancy have a worse prognosis than those who do not have cavitary lesions, particularly for those patients with squamous cell carcinoma [59].

In addition to cavitating primary lung malignancies, cystic change can be frequently associated with metastatic malignancies, especially sarcomas arising from a variety of different sites [59]. Cystic metastases associated with sarcoma carry a particularly poor prognosis due to the lesions' tendency toward pneumothorax formation [60]. Direct extension of the metastasis to the pleural space is the most common mechanism by which this occurs. The cystic metastasis associated with rare

endometrial stromal sarcomas (see Fig. 14.4) can very closely resemble DCLDs on chest imaging, and should be a key differential diagnosis when evaluating DCLD patients [61].

Infectious and Inflammatory Causes

Multiple infectious and inflammatory processes can contribute to cyst formation (see Chap. 10 for a more in-depth discussion of the infectious etiologies of DCLDs). Many of these processes involve cavitation, which can further evolve into cystic change. The radiologic appearances of these various processes can overlap significantly with DCLDs to confer considerable diagnostic uncertainty. Cavitation can occur with a variety of organisms and form via a process of suppurative necrosis, especially in the case of bacterial pneumonia. Radiographically these cavities are surrounded by areas of consolidation and can often transform further to form lung abscesses, clearly circumscribed collections of pus occurring due to liquefactive necrosis of lung tissues [62]. Classically pulmonary abscesses are easily visualized on chest radiograph due to the presence of a thick-walled cavity containing an air-fluid level (Fig. 14.5). With treatment, the air-fluid level will resolve, consolidation

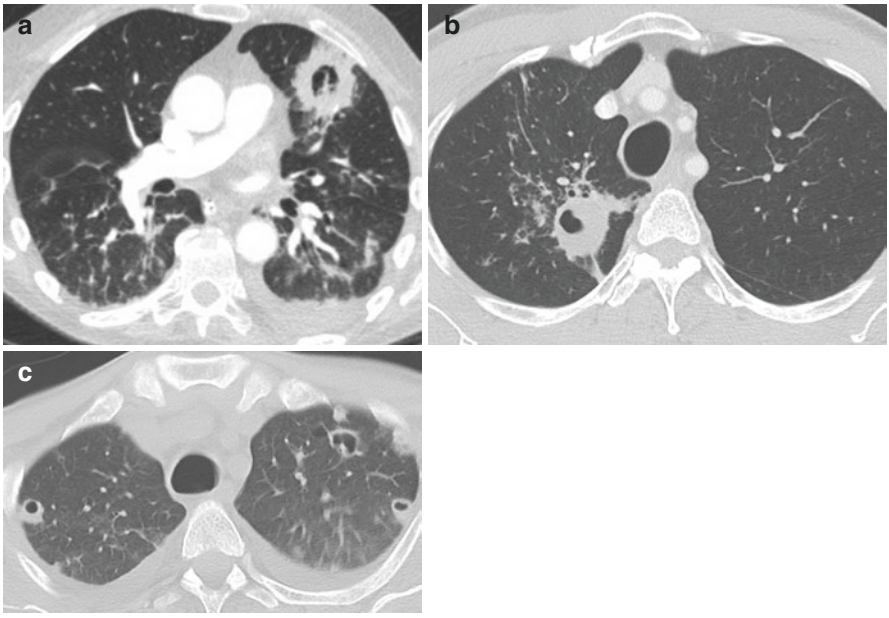

Fig. 14.5 Infectious processes. Panel A shows cavitary transformation in a case of necrotizing pneumonia due to the *Rhizopus* fungus. Panel B demonstrates a thick-walled cavity in the right upper lobe in a patient with pulmonary *Mycobacterium tuberculosis* infection. Panel C shows multiple septic emboli that have cavitated

will reduce and eventually disappear, and the wall of the cavity will become thinner. However, the cavity can persist for months after treatment of the active infection and can on occasion be mistaken for cystic lung disease [62].

Mycobacterium tuberculosis (TB), the leading cause of infectious disease mortality worldwide, is a common cause of cavitary lung disease, though TB can often take any radiographic form on imaging investigations [63]. Multiple components of the *M. tuberculosis* cell wall combine to make the bacterium highly antigenic and so a cascade of cytokines is initiated that results in formation of a protective granuloma [64]. Continual development of these TB granulomas leads to central caseating necrosis, which are the pathological hallmark of TB infection in all tissues but most notably in the lungs [65]. Cavities associated with pulmonary tuberculosis tend to be large and located in the apical regions. They are most often associated with a thick wall and surrounding consolidation and may contain an air-fluid level, which represents active infection [63] (see Fig. 14.5). Occasionally cavities can be small and numerous and over time, with treatment, may resolve their thick wall and surrounding consolidation leaving them to more closely mimic DCLDs [66]. With treatment, much of the radiographical evidence of infection will resolve, but it is common for patients to continue to display changes of pulmonary tuberculosis on imaging many years after their infection has been treated.

Septic pulmonary emboli occur when blood clots containing infectious materials embolize from their source to the lungs via the pulmonary arterial vasculature. They can occur as sequalae of a spectrum of infectious conditions; risk factors include intravenous drug use, indwelling vascular catheters, thrombophlebitis, and suppurative diseases of the head and neck [67]. The embolus itself leads to focal infarction in the pulmonary vasculature similar to nonseptic emboli [68]. However, because they contain material from an infected primary source, release of infective materials leads to the formation of a focal abscess. These tend to cavitate centrally and can be numerous giving the appearance of multiple pulmonary cysts [68] (see Fig. 14.5).

A pneumatocele is a space in the lung, which is surrounded by a thin wall and filled with gas and as such there is often very high overlap between the radiologic appearance of pneumatoceles and pulmonary cysts [2]. Most commonly, pneumatoceles occur as sequelae of infection such as *Pneumocystis jiroveci* and *Staphylococcal aureus*, but they can also occur in the setting of blunt trauma to the thorax, ingestion of hydrocarbon, and following prolonged positive pressure ventilation most commonly in neonates [69, 70]. Pneumatoceles tend to be transient and radiographically appear as smooth, rounded, thin-walled air spaces [2] (Fig. 14.6). Generally, patients with pneumatoceles are asymptomatic; however, very rarely these can rupture, resulting in pneumothorax [71]. Pneumatoceles usually resolve within 6 weeks, but rarely they can become secondarily infected and persist [72]. On a very rare occasion, pneumatoceles can cause significant tension, in which case drainage may be needed to improve hemodynamic instability [73].

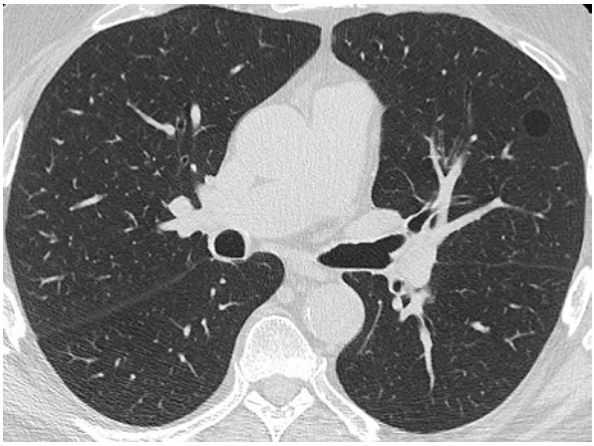

Fig. 14.6 Pneumatocele. The rounded lucency in the lung parenchyma represents a pneumatocele. It has a thin wall and is surrounded by normal lung

Conclusion

Cysts are increasingly visualized on CT imaging of the lungs and can pose a diagnostic challenge. Diagnosis involves careful attention to the existence of such cyst mimics and the knowledge that these mimics are more common than true diffuse cystic lung diseases. If these conditions have been ruled out following careful clinical and radiological correlation, patients can be investigated for processes, which cause true cystic lung disease.

Key Learning Points

- Pulmonary cysts and cyst mimics are increasingly identified due to the routine use of chest CT scanning in clinical practice.
- The most common situations where radiologic findings can mimic DCLDs include emphysema, bronchiectasis, and neoplastic and infectious etiologies.
- Certain genetic diseases such as alpha-one antitrypsin deficiency, cystic fibrosis, and primary ciliary dyskinesia can cause radiological patterns that mimic DCLDs. While alpha-one antitrypsin deficiency causes panlobular emphysema, both cystic fibrosis and primary ciliary dyskinesia can cause bronchiectasis.
- Honeycomb change and traction bronchiectasis associated with fibrotic ILDs can also mimic the cysts of DCLDs. However, the other associated radiological interstitial findings typically make it easy to distinguish between the cystic change of ILDs from the typical DCLDs.
- Pneumatoceles can be seen following certain infections, trauma, or aspiration events and tend to follow a benign course with spontaneous resolution in a few weeks.

References

1. Genereux GP. The end-stage lung: pathogenesis, pathology, and radiology. Radiology. 1975;116(02):279–89.
2. Hansell DM, Bankier AA, MacMahon H, McLoud TC, Muller NL, Remy J. Fleischner society: glossary of terms for thoracic imaging. Radiology. 2008;246(3):697–722.
3. Jawad H, Walker CM, Wu CC, Chung JH. Cystic interstitial lung diseases: recognizing the common and uncommon entities. Curr Probl Diagn Radiol. 2014;43(3):115–27.
4. Stern EJ, Frank MS. CT of the lung in patients with pulmonary emphysema: diagnosis, quantification, and correlation with pathologic and physiologic findings. AJR Am J Roentgenol. 1994;162(4):791–8.
5. Flaherty RA, Keegan JM, Sturtevant HN. Post-pneumonic pulmonary pneumatoceles. Radiology. 1960;74:50–3.
6. The definition of emphysema. Report of a National Heart, Lung, and Blood Institute, division of lung diseases workshop. Am Rev Respir Dis. 1985;132(1):182–5.
7. Murray CJ, Lopez AD. Alternative projections of mortality and disability by cause 1990-2020: global burden of disease study. Lancet. 1997;349(9064):1498–504.
8. Lozano R, Naghavi M, Foreman K, Lim S, Shibuya K, Aboyans V, et al. Global and regional mortality from 235 causes of death for 20 age groups in 1990 and 2010: a systematic analysis for the global burden of disease study 2010. Lancet. 2012;380(9859):2095–128.
9. Stoller JK, Aboussouan LS. A review of alpha1-antitrypsin deficiency. Am J Respir Crit Care Med. 2012;185(3):246–59.
10. Brantly ML, Paul LD, Miller BH, Falk RT, Wu M, Crystal RG. Clinical features and history of the destructive lung disease associated with alpha-1-antitrypsin deficiency of adults with pulmonary symptoms. Am Rev Respir Dis. 1988;138(2):327–36.
11. Gishen P, Saunders AJ, Tobin MJ, Hutchison DC. Alpha 1-antitrypsin deficiency: the radiological features of pulmonary emphysema in subjects of pi type Z and pi type SZ: a survey by the British Thoracic association. Clin Radiol. 1982;33(4):371–7.
12. American Thoracic Society, European Respiratory Society. American Thoracic Society/European Respiratory Society statement: standards for the diagnosis and management of individuals with alpha-1 antitrypsin deficiency. Am J Respir Crit Care Med. 2003;168(7):818–900.
13. Chapman KR, Burdon JG, Piitulainen E, Sandhaus RA, Seersholm N, Stocks JM, et al. Intravenous augmentation treatment and lung density in severe alpha1 antitrypsin deficiency (RAPID): a randomised, double-blind, placebo-controlled trial. Lancet. 2015;386(9991):360–8.
14. McElvaney NG, Burdon J, Holmes M, Glanville A, Wark PA, Thompson PJ, et al. Long-term efficacy and safety of alpha1 proteinase inhibitor treatment for emphysema caused by severe alpha1 antitrypsin deficiency: an open-label extension trial (RAPID-OLE). Lancet Respir Med. 2017;5(1):51–60.
15. Chapman KR, Chorostowska-Wynimko J, Koczulla AR, Ferrarotti I, McElvaney NG. Alpha 1 antitrypsin to treat lung disease in alpha 1 antitrypsin deficiency: recent developments and clinical implications. Int J Chron Obstruct Pulmon Dis. 2018;13:419–32.
16. Smith BM, Austin JH, Newell JD Jr, D'Souza BM, Rozenshtein A, Hoffman EA, et al. Pulmonary emphysema subtypes on computed tomography: the MESA COPD study. Am J Med. 2014;127(1):94.e7–23.
17. Gurney JW, Jones KK, Robbins RA, Gossman GL, Nelson KJ, Daughton D, et al. Regional distribution of emphysema: correlation of high-resolution CT with pulmonary function tests in unselected smokers. Radiology. 1992;183(2):457–63.
18. Foster WL Jr, Pratt PC, Roggli VL, Godwin JD, Halvorsen RA Jr, Putman CE. Centrilobular emphysema: CT-pathologic correlation. Radiology. 1986;159(1):27–32.
19. Cosio MG, Hale KA, Niewoehner DE. Morphologic and morphometric effects of prolonged cigarette smoking on the small airways. Am Rev Respir Dis. 1980;122(2):265–21.
20. Takahashi M, Fukuoka J, Nitta N, Takazakura R, Nagatani Y, Murakami Y, et al. Imaging of pulmonary emphysema: a pictorial review. Int J Chron Obstruct Pulmon Dis. 2008;3(2):193–204.

21. Swensen SJ, Aughenbaugh GL, Douglas WW, Myers JL. High-resolution CT of the lungs: findings in various pulmonary diseases. AJR Am J Roentgenol. 1992;158(5):971–9.
22. Mets OM, van Hulst RA, Jacobs C, van Ginneken B, de Jong PA. Normal range of emphysema and air trapping on CT in young men. AJR Am J Roentgenol. 2012;199(2):336–40.
23. Juhl KS, Bendstrup E, Rasmussen F, Hilberg O. Emphysema mimicking interstitial lung disease: two case reports. Respir Med Case Rep. 2015;15:24–6.
24. Dirksen A, Wille MM. Computed tomography-based subclassification of chronic obstructive pulmonary disease. Ann Am Thorac Soc. 2016;13(Suppl 2):S114–7.
25. Foster WL Jr, Gimenez EI, Roubidoux MA, Sherrier RH, Shannon RH, Roggli VL, et al. The emphysemas: radiologic-pathologic correlations. Radiographics. 1993;13(2):311–28.
26. Stern EJ, Frank MS, Schmutz JF, Glenny RW, Schmidt RA, Godwin JD. Panlobular pulmonary emphysema caused by i.v. injection of methylphenidate (Ritalin): findings on chest radiographs and CT scans. AJR Am J Roentgenol. 1994;162(3):555–60.
27. Goldberg C, Carey KE. Bullous lung disease. West J Emerg Med. 2013;14(5):450–1.
28. Siddiqui NA, Nookala V. Bullous emphysema. Treasure Island: StatPearls; 2019.
29. Bagnato G, Harari S. Cellular interactions in the pathogenesis of interstitial lung diseases. Eur Respir Rev. 2015;24(135):102–14.
30. Hutchinson JP, McKeever TM, Fogarty AW, Navaratnam V, Hubbard RB. Surgical lung biopsy for the diagnosis of interstitial lung disease in England: 1997–2008. Eur Respir J. 2016;48(5):1453–61.
31. Brownell R, Moua T, Henry TS, Elicker BM, White D, Vittinghoff E, et al. The use of pretest probability increases the value of high-resolution CT in diagnosing usual interstitial pneumonia. Thorax. 2017;72(5):424–9.
32. Hunninghake GW, Zimmerman MB, Schwartz DA, King TE Jr, Lynch J, Hegele R, et al. Utility of a lung biopsy for the diagnosis of idiopathic pulmonary fibrosis. Am J Respir Crit Care Med. 2001;164(2):193–6.
33. Johkoh T, Sakai F, Noma S, Akira M, Fujimoto K, Watadani T, et al. Honeycombing on CT; its definition, pathologic correlation, and future direction of its diagnosis. Eur J Radiol. 2014;83(1):27–31.
34. Wuyts WA, Cavazza A, Rossi G, Bonella F, Sverzellati N, Spagnolo P. Differential diagnosis of usual interstitial pneumonia: when is it truly idiopathic? Eur Respir Rev. 2014;23(133):308–19.
35. American Thoracic Society, European Respiratory Society. American Thoracic Society/European Respiratory Society International Multidisciplinary Consensus Classification of the Idiopathic Interstitial Pneumonias. This joint statement of the American Thoracic Society (ATS), and the European Respiratory Society (ERS) was adopted by the ATS board of directors, June 2001 and by the ERS Executive Committee, June 2001. Am J Respir Crit Care Med. 2002;165(2):277–304.
36. Chung JH, Lynch DA. The value of a multidisciplinary approach to the diagnosis of usual interstitial pneumonitis and idiopathic pulmonary fibrosis: radiology, pathology, and clinical correlation. AJR Am J Roentgenol. 2016;206(3):463–71.
37. Lee HY, Lee KS, Jeong YJ, Hwang JH, Kim HJ, Chung MP, et al. High-resolution CT findings in fibrotic idiopathic interstitial pneumonias with little honeycombing: serial changes and prognostic implications. AJR Am J Roentgenol. 2012;199(5):982–9.
38. Akira M, Inoue Y, Arai T, Okuma T, Kawata Y. Long-term follow-up high-resolution CT findings in non-specific interstitial pneumonia. Thorax. 2011;66(1):61–5.
39. Magis-Escurra C, Reijers MH. Bronchiectasis. BMJ Clin Evid. 2015:1507.
40. Boyton RJ, Altmann DM. Bronchiectasis: current concepts in pathogenesis, immunology, and microbiology. Annu Rev Pathol. 2016;11:523–54.
41. Menendez R, Mendez R, Polverino E, Rosales-Mayor E, Amara-Elori I, Reyes S, et al. Risk factors for multidrug-resistant pathogens in bronchiectasis exacerbations. BMC Infect Dis. 2017;17(1):659.
42. Ooi GC, Khong PL, Chan-Yeung M, Ho JC, Chan PK, Lee JC, et al. High-resolution CT quantification of bronchiectasis: clinical and functional correlation. Radiology. 2002;225(3):663–72.

43. Araujo D, Shteinberg M, Aliberti S, Goeminne PC, Hill AT, Fardon T, et al. Standardised classification of the aetiology of bronchiectasis using an objective algorithm. Eur Respir J. 2017;50(6):1701289.
44. Habesoglu MA, Ugurlu AO, Eyuboglu FO. Clinical, radiologic, and functional evaluation of 304 patients with bronchiectasis. Ann Thorac Med. 2011;6(3):131–6.
45. Milliron B, Henry TS, Veeraraghavan S, Little BP. Bronchiectasis: mechanisms and imaging clues of associated common and uncommon diseases. Radiographics. 2015;35(4):1011–30.
46. Cantin L, Bankier AA, Eisenberg RL. Bronchiectasis. AJR Am J Roentgenol. 2009;193(3):W158–71.
47. Moulton BC, Barker AF. Pathogenesis of bronchiectasis. Clin Chest Med. 2012;33(2):211–7.
48. Ward C, Rydell-Tormanen K, Westergren-Thorsson G, Eriksson LT, Walters H. Infection and remodelling: a 21st century model of bronchiectasis? Eur Respir J. 2011;38(4):758–60.
49. Bueno J, Flors L. The role of imaging in the diagnosis of bronchiectasis: the key is in the distribution. Radiologia. 2018;60(1):39–48.
50. Elborn JS. Cystic fibrosis. Lancet. 2016;388(10059):2519–31.
51. Robinson P, Morgan L. Bronchiectasis in PCD looks different to CF on CT scan. Multidiscip Respir Med. 2018;13(Suppl 1):24.
52. Sheehan RE, Wells AU, Copley SJ, Desai SR, Howling SJ, Cole PJ, et al. A comparison of serial computed tomography and functional change in bronchiectasis. Eur Respir J. 2002;20(3):581–7.
53. Eshed I, Minski I, Katz R, Jones PW, Priel IE. Bronchiectasis: correlation of high-resolution CT findings with health-related quality of life. Clin Radiol. 2007;62(2):152–9.
54. Mouroux J, Padovani B, Elkaim D, Richelme H. Should cavitated bronchopulmonary cancers be considered a separate entity? Ann Thorac Surg. 1996;61(2):530–2.
55. Onn A, Choe DH, Herbst RS, Correa AM, Munden RF, Truong MT, et al. Tumor cavitation in stage I non-small cell lung cancer: epidermal growth factor receptor expression and prediction of poor outcome. Radiology. 2005;237(1):342–7.
56. Chaudhuri MR. Primary pulmonary cavitating carcinomas. Thorax. 1973;28(3):354–66.
57. Edwards CW. Alveolar carcinoma: a review. Thorax. 1984;39(3):166–74.
58. Kolodziejski LS, Dyczek S, Duda K, Goralczyk J, Wysocki WM, Lobaziewicz W. Cavitated tumor as a clinical subentity in squamous cell lung cancer patients. Neoplasma. 2003;50(1):66–73.
59. Dodd GD, Boyle JJ. Excavating pulmonary metastases. Am J Roentgenol Radium Therapy, Nucl Med. 1961;85:277–93.
60. Hoshi M, Oebisu N, Iwai T, Ieguchi M, Ban Y, Nakamura H. An unusual presentation of pneumothorax associated with cystic lung metastasis from epithelioid sarcoma: a case report and review of the literature. Oncol Lett. 2018;15(4):4531–4.
61. Aubry MC, Myers JL, Colby TV, Leslie KO, Tazelaar HD. Endometrial stromal sarcoma metastatic to the lung: a detailed analysis of 16 patients. Am J Surg Pathol. 2002;26(4):440–9.
62. Gross I, Gordon O, Cohen-Cymberknoh M, Reiter J, Tsabari R, Gileles-Hillel A, et al. Giant lung cysts following necrotizing pneumonia: resolution with conservative treatment. Pediatr Pulmonol. 2019;54(6):901–6.
63. McAdams HP, Erasmus J, Winter JA. Radiologic manifestations of pulmonary tuberculosis. Radiol Clin N Am. 1995;33(4):655–78.
64. Ong CW, Elkington PT, Friedland JS. Tuberculosis, pulmonary cavitation, and matrix metalloproteinases. Am J Respir Crit Care Med. 2014;190(1):9–18.
65. Dannenberg AM Jr, Sugimoto M. Liquefaction of caseous foci in tuberculosis. Am Rev Respir Dis. 1976;113(3):257–9.
66. Ray A, Suri JC, Sen MK, Khanna A. Cystic lung disease in tuberculosis: an unusual presentation. Lung India. 2013;30(4):351–3.
67. Stawicki SP, Firstenberg MS, Lyaker MR, Russell SB, Evans DC, Bergese SD, et al. Septic embolism in the intensive care unit. Int J Crit Illn Inj Sci. 2013;3(1):58–63.
68. Jaffe RB, Koschmann EB. Septic pulmonary emboli. Radiology. 1970;96(3):527–32.

69. Arora P, Kalra VK, Natarajan G. Pneumatoceles in infants in the neonatal intensive care unit: clinical characteristics and outcomes. Am J Perinatol. 2013;30(8):689–94.
70. Hussain N, Noce T, Sharma P, Jagjivan B, Hegde P, Pappagallo M, et al. Pneumatoceles in preterm infants-incidence and outcome in the post-surfactant era. J Perinatol. 2010;30(5):330–6.
71. Thukral A, Tiwari DN, Tripathi K. Pneumatocele in an adult. J Assoc Physicians India. 2011;59:186–7.
72. Hirata S. A case of traumatic pneumatocele revealed by CT 36 years after blunt chest trauma. Nihon Kokyuki Gakkai Zasshi. 2008;46(12):1070–4.
73. Park TH, Kim JK. Nonsurgical management of an enlarging pneumatocele by fibrin sealant injection via pigtail catheter. Pediatr Pulmonol. 2016;51(2):E5–7.

Chapter 15
Extrapulmonary Manifestations of Diffuse Cystic Lung Diseases

Daniel F. Dilling and Stephen J. Ruoss

Introduction

Previous chapters in this textbook have focused on the respiratory symptoms and pulmonary features of diffuse cystic lung diseases (DCLDs). While the practicing pulmonologist is likely to feel most comfortable with the pulmonary aspects of DCLDs, these diseases often have significant extrapulmonary involvement that warrants attention and management. Such extrapulmonary aspects of the disease may even overshadow the lung disease with regard to the symptom burden or the need for ongoing testing. In this chapter, we discuss the extrapulmonary aspects in the context of the major DCLDs: Birt-Hogg-Dubé (BHD) syndrome, light chain deposition disease (LCDD), lymphocytic interstitial pneumonia/follicular bronchiolitis (LIP/FB), lymphangioleiomyomatosis (LAM), and pulmonary Langerhans cell histiocytosis (PLCH).

Lymphangioleiomyomatosis (LAM)

LAM has been characterized as a low-grade, destructive, metastasizing neoplasm [1] and can occur in patients with tuberous sclerosis complex (TSC-LAM) or in sporadic cases in the absence of TSC (S-LAM). A number of extrapulmonary manifestations have been described in patients with LAM with varying frequencies

D. F. Dilling (✉)
Division of Pulmonary and Critical Care, Stritch School of Medicine, Loyola University Chicago, Chicago, IL, USA
e-mail: ddillin@lumc.edu

S. J. Ruoss
Division of Pulmonary and Critical Care, Stanford University, Stanford, CA, USA
e-mail: ruoss@stanford.edu

N. Gupta et al. (eds.), *Diffuse Cystic Lung Diseases*, Respiratory Medicine,
https://doi.org/10.1007/978-3-030-63365-3_15

depending upon the type of LAM, TSC-LAM versus S-LAM. The most common extrapulmonary manifestation in patients with S-LAM is angiomyolipoma (AML), followed by lymphatic complications such as lymphangioleiomyomas, lymphadenopathy, or chylous effusions. While the chylous effusions commonly present with pleural involvement, chylous fluid accumulation in patients with LAM has also been described in the pericardial sac and the peritoneal cavity. Given that some patients who appear to have S-LAM may instead have subtle cases of TSC, the astute clinician may recognize some of the skin manifestations of TSC in a patient with LAM who might not previously have been recognized as having TSC (ash leaf spots, subungual fibromas, facial angiofibromas, Shagreen patches).

Angiomyolipomas

AMLs are considered to be the most common benign renal tumors, with a prevalence of less than 0.5% in the general population [2, 3]. They are more common in women than in men and are sometimes multifocal and present bilaterally (especially in cases associated with TSC) [4]. They are most often discovered incidentally, as part of imaging workup of some other condition or of an unrelated symptom [5], but also may present as a palpable mass or with hemorrhage, causing flank pain, ecchymosis, hematuria, or hemorrhagic shock. Most commonly, AMLs occur outside of the context of TSC or LAM, with such sporadic cases comprising up to 80% of all AMLs [2]. For this reason, a co-existing lung disease is often not considered at first, unless abdominal imaging reveals incidental cysts at the bases of the lungs or a clinician takes note of skin findings or neurocognitive symptoms suggestive of TSC. Considering the fact that approximately 10% of the women with AMLs may have co-existing cystic lung disease (LAM), it has been suggested that the discovery of a renal AML in females should prompt lung imaging to screen for LAM [6]. In S-LAM, AMLs are present in approximately 30–50% of the patients [7, 8] and are more often unilateral, whereas AMLs are found in approximately 80–90% of patients with TSC-LAM, and are usually multifocal and bilateral [7, 9].

The radiologic appearance of AMLs closely reflects their histologic makeup, being typically composed of areas of smooth muscle, blood vessels, and adipose tissue (Fig. 15.1). On computed tomography (CT), their appearance is often distinct enough to be pathognomonic and diagnostic, except in a small proportion of cases where the adipose tissue is insufficient to offer a definite diagnosis. The presence of an AML in a woman with diffuse, homogenous cystic lung disease is confirmatory of LAM, obviating the need for tissue to confirm the diagnosis [10]. Magnetic resonance imaging (MRI) is also useful in characterizing AMLs [11–13], although many times AMLs can be diagnosed or monitored on a serial basis with ultrasound [13].

The biology of AMLs in LAM (and TSC) has been better elucidated in the past two decades, largely as a result of the discovery of pathogenic driver mutations in TSC1 and TSC2 genes [14]. AMLs, along with LAM, are characterized as a form

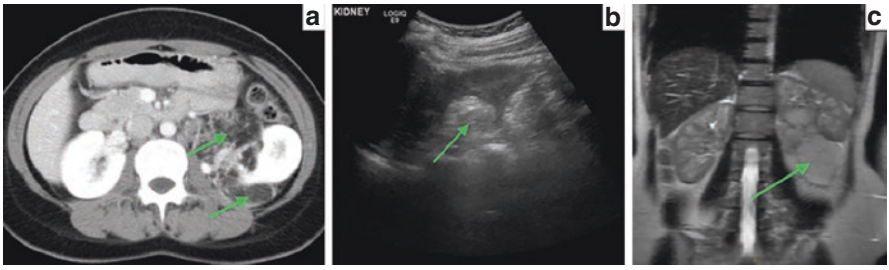

Fig. 15.1 A left renal angiomyolipoma in a single patient by (**a**) computed tomography, with arrows pointing to two hypodense areas delineating adipose tissue, (**b**) ultrasound, with arrow pointing to hyperdense tissue correlating with the tumor, and (**c**) magnetic resonance imaging, with arrow pointing to tumor that has displaced the normal kidney from its anatomical position

of perivascular epithelioid cell tumors, referred to as PEComas. They express myogenic and melanocytic markers such as actin and HMB45, respectively, and (like other PEComas) are driven by alterations in the mechanistic target of rapamycin (mTOR) pathway. This feature has been leveraged for the development of mTOR inhibition as a clinically useful treatment strategy for patients with AMLs and LAM.

In cases in which AMLs are asymptomatic and small (measuring less than 3–4 cm in diameter), no treatment is indicated. Serial imaging (by CT, MRI, or ultrasound) is adequate as a means of detecting growth, usually on an annual basis. When the diameter exceeds 3–4 cm or if aneurysmal dilation develops, consideration should be given to treatment because of a higher risk of rupture and bleed [15, 16].

Historically, treatment of large or symptomatic AMLs was limited to partial or total nephrectomy, which carries the risk for renal function loss and chronic kidney disease later in life. As such, nephron-sparing surgeries and non-surgical therapies are preferred management strategies for AMLs. Embolization of AMLs is now largely preferred to surgical options. These procedures are usually accomplished by interventional radiologists, utilizing ethanol, polyvinyl alcohol, or trisacryl gelatin microspheres as agents to eliminate blood supply to these tumors [17–19]. Embolization can be associated with a significant local inflammatory response (a so-called post-embolization syndrome) that can be quite morbid, and so it should ideally be done by experienced proceduralists and should be followed by a course of oral corticosteroids [20].

More recently, pharmacotherapy using mTOR inhibitors has garnered favor as the best initial management strategy, except in cases of intolerance of mTOR inhibitors or active or impending bleeding (where embolization may be preferred). The use of mTOR inhibitors is generally well tolerated and has been shown to durably reduce the AML size over a protracted time frame. Similar to LAM, the effect of mTOR inhibitors on AMLs is suppressive rather than curative, and durable treatment response requires long-term drug administration (Fig. 15.2) [21–25]. The mTOR inhibitor, everolimus, is now approved by the United States Food and Drug Administration for the treatment of LAM and TSC-associated AMLs.

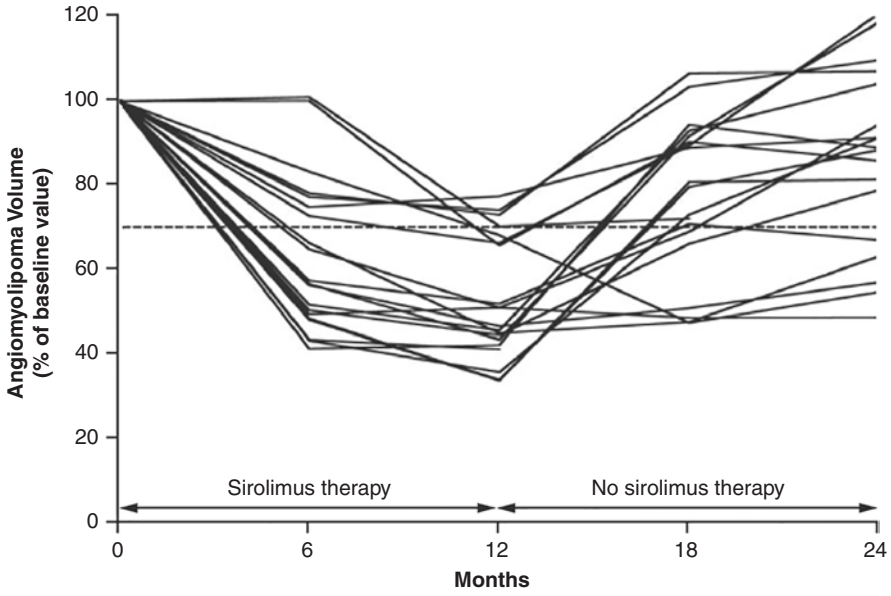

Fig. 15.2 Angiomyolipoma volume at various time points in 18 patients who completed 1 year on sirolimus followed by 1 year off of the drug in the Cincinnati Angiomyolipoma Sirolimus Trial (CAST). AML volume decreased with administration of sirolimus in the first 12 months and tended to rebound back to baseline after stopping therapy in the next 12 months. The dashed line represents 70% of the baseline value (22). (From Bissler et al. [108], Copyright © 2008 Massachusetts Medical Society. Reprinted with permission from Massachusetts Medical Society)

Lymphangioleiomyomas and Chylous Abnormalities

Extrapulmonary lymphangioleiomyomas occur infrequently in patients with LAM [26] and represent cystic masses containing chyle arising due to dilation and obstruction of the lymphatic vessels by circulating LAM cells. The presence of lymphangioleiomyomas on imaging in women with characteristic cystic lung disease on chest CT can help establish the diagnosis of LAM with certainty. Their mass may also include local enlarged lymph nodes. Their presence can sometimes be mistaken for other types of neoplasm, some of them more prototypically malignant [27, 28], and can sometimes even prompt exploratory surgery or other procedures to elicit a diagnosis. The primary danger with lymphangioleiomyomas is one of local compression on other structures, such as the vena cava, ureters, pelvic veins, bladder, and bowel. Some patients with large tumors may develop pain or uncomfortable fullness related to tumor bulk or involvement of local viscera or other structures.

Treatment of lymphangioleiomyomas is limited. De-bulking surgery or resection was used in a previous era, but chylous leaks and effusion can ensue, and tumors were often found to recur. Embolization is not effective in the same way as it may be for renal disease. Abdominal lymphangioleiomyomas respond favorably to mTOR inhibition therapy (Fig. 15.3). In a cohort of 11 women with LAM and retroperitoneal lymphangioleiomyomas treated with sirolimus therapy, nine of them

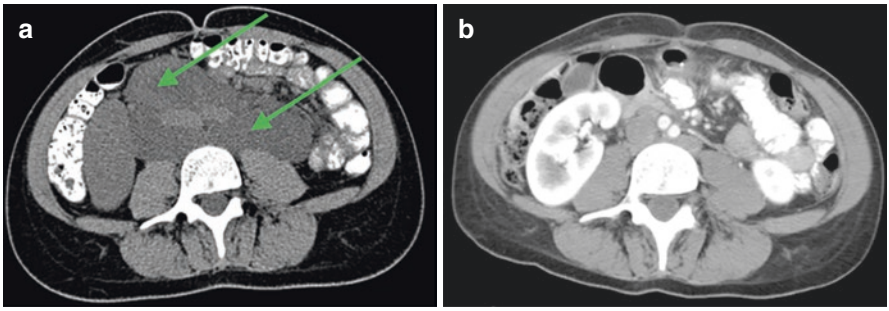

Fig. 15.3 Axial computed tomography images of a patient with sporadic LAM and a large and complex retroperitoneal lymphangioleiomyoma (arrows). (**a**) Before and **(b**) after 8 years of treatment with mTOR inhibitor, demonstrating significant reduction in size

had complete resolution and the remaining two had substantial decrease in size of the tumors over a median of 2.5 years on therapy [29]. Similar reductions in size or complete resolution of lymphangioleiomyomas have been reported in several other series and case reports [30–32]. Treatment is recommended for such lesions only if causing symptoms or if their location is threatening nearby vital structures.

Other chylous abnormalities in LAM include chylous pleural effusions, chylous pericardial effusion, chylous ascites, and chylous congestion in lung parenchyma [33]. One LAM case series included eight patients with chylous ascites, all of whom had resolution of their ascites after treatment with sirolimus [29], and other reports also show a high likelihood of resolution of chylous complications with mTOR inhibition [32, 34].

Skin Findings of Tuberous Sclerosis Complex

Because patients with sporadic LAM have TSC mutations only in diseased tissues and do not have germline mutations of *TSC1* or *TSC2*, there are no skin findings associated with LAM, per se. However, patients with TSC can have characteristic dermatological manifestations (Fig. 15.4) [35, 36], and careful physical examination for these findings can help affirm a diagnosis of TSC in a patient with apparent sporadic LAM [37]. Greater recognition of the phenomenon of TSC mosaicism has led to an approach using skin findings as part of an algorithm [38] to uncover patients with this phenotype.

Langerhans Cell Histiocytosis (LCH)

Langerhans cell histiocytosis (LCH) is a variable organ system involvement myeloid cell neoplasm. As the pathobiology of LCH has become increasingly clarified, it now seems unsurprising that the early stages of disease investigation were

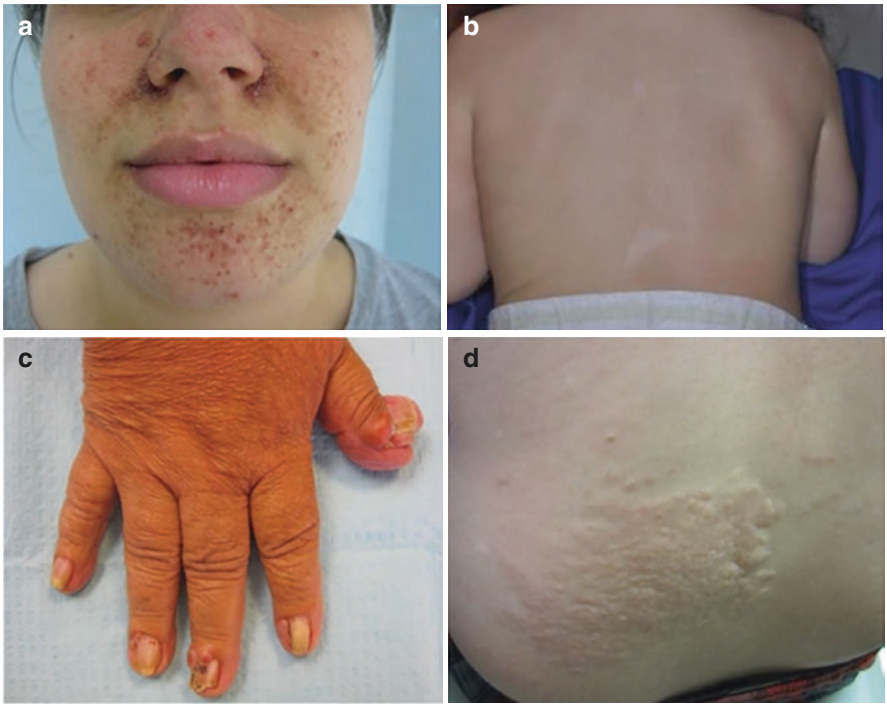

Fig. 15.4 Examples of skin manifestations of tuberous sclerosis [36]: (**a**) facial angiofibromas, (**b**) hypomelanotic macules or "ash leaf spots," (**c**) subungual fibromas, and (**d**) shagreen patch. (Adapted from Nguyen et al. [36], with permission from John Wiley and Sons)

characterized by a complex series of eponymous or pathologically incorrect labels. It is thus only fitting for a disease of such complex and multiperspective origins that its name(s) should have a similarly protean evolution. And this evolution of disease nomenclature is similarly accorded with a fascinating and progressive revelation of the now clearly neoplastic genetics and biology underlying the clinically evident disease processes.

LCH Disease Pathogenesis

From the initial collection of disease descriptions by AJ Hand (1893), A Schuller (1915), and HA Christian (1919) that provided the first eponymous name to the disease, to descriptions by E Letterer (1933) and SA Siwe (1924) adding to the clinical (and eponymous) perspective on this disease of apparent activation of histiocytes, the convergent evolution of disease nomenclature has been matched if not exceeded by progressive and important revelations regarding disease pathogenesis. The name histiocytosis X acknowledged both the apparent central role of epithelial

dendritic cells in multiorgan disease pathogenesis and the uncertainty of the ontogeny of these activated cells. Work by Langerhans in the mid-nineteenth century first characterized a population of what are now known to be epithelial dendritic cells that bear his name, and there has ensued a long, complex, and fascinating exploration of the ontogeny of these and similar dendritic cells.

Recent publications have summarized the research and current understanding of this cellular biology [39, 40], which in their sum reveal substantial insights into the significant organ involvement and disease manifestation variabilities of what is now called Langerhans cell histiocytosis (LCH).

As a brief summary of LCH pathobiology, typical cutaneous Langerhans cells (LC) are long-term resident epithelial dendritic cells whose origin is not from bone marrow-derived myeloid precursor cells but rather from yolk-sac progenitor cells that populate developing fetal skin and remain as an apparent durable and regenerating dermal dendritic cell population throughout post-fetal life [41]. These typical LC bear various cytochemical features, including the surface markers CD1a and CD207, the latter of which identifies the lectin langerin, a principal component of the Birbeck granules that initially provided a signature cytostructural feature for identification of LC, and which is now known to play important roles in LC function, including antiviral defense. In addition to these classical dermal LC, it is now known that under various pathological conditions, circulating monocyte-derived CD1a+/CD207+ cells from bone marrow origin can migrate to skin and other organs and differentiate to become Langerhans cell-like dendritic cells [42]. An analysis of pathological tissues in LCH patients has revealed that LC disease does not arise from typical epidermal LCs but instead from the influx of, and injury mediated by, activated bone marrow-derived CD1a+/CD207+ immature myeloid dendritic cells [43], and the varying numbers of T-lymphocytes, macrophages, and eosinophils they mobilize to the sites of LC-like cell-mediated inflammation.

The pathological conditions that produce activation and influx of these LC-like cells include inflammation, but also and importantly a variety of neoplastic states, with an increasingly well-characterized pattern of genetic events that produce what is now viewed as a common theme of myeloid neoplastic processes underlying LCH. As recently reviewed by Allen et al. [40], a variety of somatic mutations in the ERK and MAP kinase (MAPK) cellular signaling pathway are known to be drivers of disease evolution in a large majority of LCH cases. The ERK pathway is centrally involved in activation of myeloid lineage cells as well as neoplastic cells, with *BRAF* mutations critically participant in cancer evolution and myeloid cell dysfunction, including in LCH [44, 45]. The current conclusion from a robust body of research is that the preponderance of LCH is attributable to neoplastic activation and resulting pathology from clonal populations of bone marrow-derived CD1a+/langerin (CD207)+ LC-like cells, rather than from activation of the classical dermal LC population. The most common of the known genetic drivers of LCH disease are *BRAF* V600E and MAP2K1, with a lesser frequency of other *BRAF* mutations, *ERBB3*, and *ARAF* reported in a large single center series [46].

In addition to providing the robust body of research that has established the central role of ERK pathway mutations in the neoplastic genesis of LCH [47], the

concerted and collaborative work of a number of investigators has revealed a fascinating pattern of LCH disease. This research has led to the development of a now very robustly supported LCH disease pathogenesis model [40, 48], which these investigators describe as the **misguided myeloid differentiation model**, where LCH organ involvement and disease magnitude are not determined primarily by the specific ERK mutations but instead driven by the stage of myeloid cell differentiation at which point the ERK mutational events occur [49]. In this ERK mutation-dependent neoplastic disease model (Fig. 15.5), mutations occurring in early-stage myeloid progenitor populations will likely manifest disease that is more aggressive and/or with broader multiorgan involvement. And in contrast, ERK mutational events occurring later in myeloid progenitor differentiation, including in cases where the myeloid cells have established an organ- or tissue-restricted population before an ERK mutational event occurs, will have a more limited disease expression

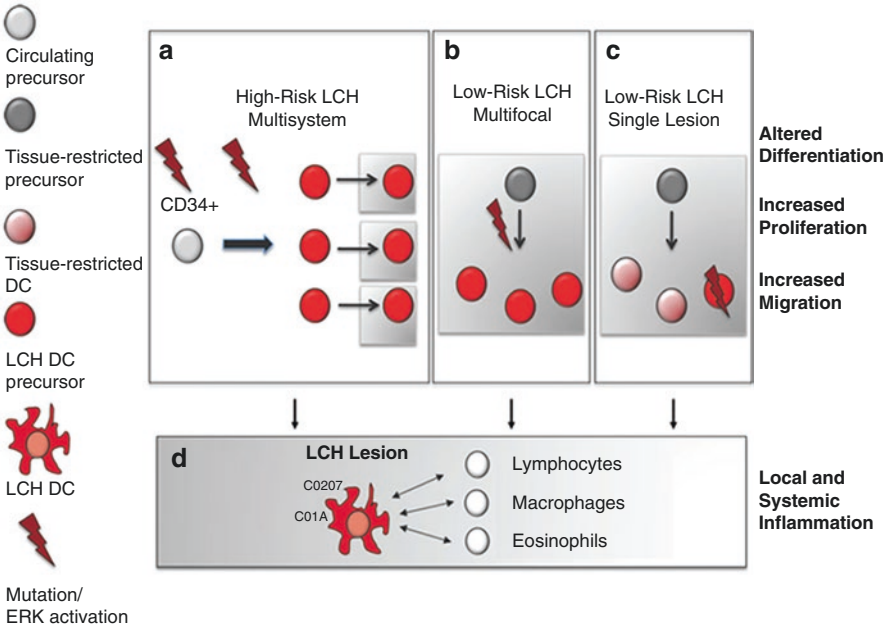

Fig. 15.5 Developmental stage of pathological DC precursor defines the extent of disease. (**a**) Somatic mutation of BRAF or other inciting event in CD34+ hematopoietic stem cells or early DC progenitors induces proliferation, maturation, and migration of pathological DCs in multiple tissues that result in high-risk multisystem LCH. (**b**) Somatic mutation of BRAF or other inciting event in a tissue-restricted DC precursor induces proliferation, maturation, and tissue-limited migration of pathological DCs that result in low-risk multisystem LCH. (**c**) Somatic mutation of BRAF or other inciting event in mature DC results in proliferation and maturation of pathological DCs leading to low-risk single lesion LCH. (**d**) Regardless of cell of origin, the pathological DCs recruit "bystander" immune cells in an inflammatory lesion characteristic of LCH. Cells in white areas indicate cells in circulation; cells in gray areas indicate cells that have migrated to tissue targets. *LCH* Langerhans cell histiocytosis, *DC* dendritic cell. (Reprinted from Berres et al. [48], with permission from John Wiley and Sons)

and magnitude, including single organ disease. And in all cases, these neoplastically activated myeloid dendritic cells recruit normal populations of inflammatory cells, including activated T-lymphocytes as well as macrophages and eosinophils, to magnify the tissue inflammatory processes.

Taking this LCH pathogenesis model of misguided myeloid differentiation as the central mechanistic pathogenesis process, we can then explore the extent of non-pulmonary LCH, with particular attention to the variations in organ involvement and disease magnitude in this neoplastic disease.

LCH Disease Clinical Manifestations

LCH is a rare disease, though somewhat more common in pediatric than adult populations. Prevalence of LCH in adults appears to be no more than 1–2 cases per million, and approximately two- to threefold higher in children [50, 51]. Organ involvement in LCH is more diverse in children than adults, whether with single system or multisystem disease. A large retrospective review of over 1700 pediatric LCH cases listed organ systems involvement, and the percentages of cases affected, which were as follows: bone, 77%; skin, 39%; lymph nodes, 19%; liver, 16%; spleen, 13%; oral mucosa, 13%; lung, 10%; and central nervous system (CNS), 6% [51]. Organ systems involvement in adults appears more restricted, though there are limited data from which these estimates are based, and ascertainment bias likely plays a role in some of the reported data [50, 52–54]. The most commonly reported organ systems involved in adults are, in decreasing order of presentation, bone, lung, pituitary gland, skin, and to a lesser extent, liver and bone marrow, with both single system and multisystem disease patterns reported [50].

LCH can have very diverse organ manifestations, from single organ involvement to very diffuse disease. Organ involvement either in single-system (SS-LCH) or multisystem (MS-LCH) disease can involve bone, skin, lymph nodes, thymus, thyroid, the gastrointestinal tract, and the central nervous system. Organ involvement can also involve bone marrow, spleen, and liver, with disease involvement in these latter three organ systems associated with greater risk of aggressive disease and mortality. Of note, while pulmonary involvement is an important focus in this book, pulmonary involvement by LCH does not appear to confer any significant overall disease prognostic import, at least as assessed in an analysis of a large European pediatric LCH cohort [55].

Constitutional symptoms in LCH can vary widely, in part dependent upon the specificity and degree of organ involvement, but the features of a chronic inflammatory state predominate. Malaise, fever, and weight loss can be common, along with pain, particularly in patients with bony disease.

Bone involvement in LCH is a classical finding of SS-LCH, although it often is seen as a manifestation of MS-LCH. The most characteristic bony involvement is of skull bones, which can involve spread into dura, and the involvement of skull base and/or maxillofacial bones carries a greater risk of CNS disease including diabetes

insipidus. Axial skeleton or long bones can be sites of significant disease. Bone pain is common at sites of disease, and vertebral compression fractures or direct CNS involvement can produce neurological impairment. Radiographically, the most common findings are lytic defects, with mixed cellular inflammatory foci accounting for the sites of bone lysis. Pathologically, the cellular features of osseous LCH disease include CD1a+ cells as well as inflammatory cells, and also includes osteoclast-like multinucleate giant cells [39].

Skin LCH disease is more commonly encountered in children and is typically rare in adults. When present in adults, the common features are of a papulonodular rash most often found often over skin folds or scalp, and with biopsies revealing LCH cells infiltrating the papillary or deeper dermis [39]. In skin as well as in other LCH-involved tissues, specific immunostaining revealing the mutant *BRAF* V600E protein in pathological tissues can confirm a LCH diagnosis [46].

Gastrointestinal tract involvement in LCH tends to be rare overall, and even more so in adults. While gastrointestinal LCH disease in pediatric patients appears to carry a worse overall prognosis and is typically associated with active features of gut involvement (malaise, weight loss, bloody diarrhea, anemia), adults are likely to have no gut-specific manifestations [56]. The most common gut LCH features reported in adults are small polyps, typically in the colon, and with typical LCH tissue pathology features including CD1a+/CD207+ cells with associated reactive cells, most often lymphocytes and to a lesser extent eosinophils and macrophages.

Central nervous system disease in LCH is less frequent than the organ systems discussed so far. It can be very problematic, with acute presentation potentially occurring early in disease, and this confers the risk for later evolution of progressive high morbidity CNS injury with poor prognosis. Again, CNS disease from LCH is significantly more common in pediatric patients than in adults. The range of manifestations of CNS disease due to LCH is broad, but a report by Grois et al. summarizes the described patterns of CNS injury into four distinct categories [57]. These are as follows: (1) hypothalamic-pituitary axis problems; (2) neuro-anatomic site-dependent findings from space-occupying lesions, such as headaches or seizures; (3) neurological dysfunction most consistent with cerebellar-pontine pathway injury, including reflex abnormalities, ataxia, intellectual impairment, tremor, or dysarthria with variable progression to severe CNS deterioration; and (4) clinical findings of overlap of one or more of the preceding patterns. Limited but revealing neuropathology reported in a more recent study by Grois and colleagues reveals patterns that suggest some variation in the mechanisms of CNS injury [58]. In a small case series of pediatric subjects, they observed three different patterns of LCH CNS disease: (a) focal granulomas involving meninges or choroid plexus, with presence of CD1a+/CD207+ cells accompanied by a marked T-lymphocyte inflammatory response; (b) granulomas occurring in brain parenchyma with marked to severe T-cell inflammation and associated severe neurodegeneration with neuronal loss; and (c) a pattern of neurodegeneration most typically involving cerebellum and brainstem, and characterized by an absence of CD1a+/CD207+, but a marked CD8+ T-cell inflammatory response with severe neuronal degeneration, microglial activation, and gliosis. On the basis of multiple features of these CNS

injury patterns, Grios et al. postulated that the pathophysiological process was most reasonably explained as a pattern of paraneoplastic encephalitis [58]. A neurodegenerative CNS disease pattern occurs infrequently in LCH patients, but it can have devastating effects, with patchy cerebral and cerebellar involvement producing symptoms including ataxia, dysmetria, dysarthria, learning problems, and behavioral abnormalities [59].

While a CD8+ T-cell dependent process may at least in part underlie the process of neurodegenerative CNS injury in LCH, more recent clinical study and animal model work appear to again more directly implicate ERK-mutation-bearing clonal myeloid progenitor cells in the process of neurodegeneration. A mouse model of *BRAF* V600E mutation insertion into myeloid progenitors produces significant neurodegeneration [60]. And a 2018 clinical study by a broad investigator collaboration has shown that cells bearing *BRAF* V600E mutations are common in patients with neurodegeneration, strongly supporting the model of LCH, including the associated neurodegenerative disease, as an ERK-mutant clonal neoplastic process [61]. That neurodegeneration can sometimes be seen well after initial LCH disease presentation is thought to be consistent with persistence of a myeloid clone that gains access to CNS to cause injury.

Lymph node involvement by LCH can be manifested by a variety of infiltrative patterns, but CD1a+/CD207+ cells are typically common, as can be giant cells. Alternatives in a reasonable differential diagnosis should include consideration of dermatopathic lymphadenopathy and anaplastic large cell lymphoma. Immunohistochemistry should identify presence of CD1a+ cells, as normal medullary sinus cells can be CD207+ [39].

High-risk organ involvement. LCH involving **bone marrow, liver, and spleen** constitutes high risk of severe disease and death from LCH. As noted above, the model of misguided myeloid differentiation proposes that LCH-initiating defects in myeloid differentiation that arise earlier in myeloid progenitor differentiation would more likely produce more severe and multiorgan disease. Pulmonary involvement by LCH does not appear to be a significant predictor of disease severity or outcome, at least in pediatric patients [62, 63].

Bone marrow involvement in LCH is clinically suggested by the presence of anemia and/or thrombocytopenia, which can range from mild to severe abnormalities [64]. The cardinal cellular features of **bone marrow involvement** in LCH are the presence of CD1a+/CD207+ cells and/or the identification of *BRAF* V600E mutations by PCR in bone marrow cells. There are cases where *BRAF* V600E mutations have not been found in CD1a+/CD207+ cells but rather in early progenitor bone marrow CD34+/CD207− cells [65], a finding quite compatible with the model of ERK-mutant misguided myeloid differentiation as the driver of disease, with variable (and in some cases early) points of myeloid differentiation being the point for disease initiation. Common associated marrow features include the presence of activated macrophages, in some cases with accompanying hemophagocytosis that underlies associated anemia or thrombocytopenia [66].

Splenic involvement in LCH, another risk organ for severe LCH disease, should be suspected when splenomegaly is noted by exam or ultrasound measurement [64].

Biopsy confirmation is often not undertaken due to biopsy-associated risks, but histological findings typically include splenic sinus involvement in LCH [39].

The clinical features of **liver involvement in LCH**, the remaining high-risk organ, generally include liver enlargement, and consensus guidelines describe the following biochemical features as consistent with LCH disease of the liver: hyperbilirubinemia (>3 times normal), hypoalbuminemia (<30 g/dl), gamma-GT increased >2 times normal, ALT or AST > 3 times normal, ascites, peripheral edema, or intra-hepatic nodular mass [64]. Histological features of liver involvement by LCH are focused on larger bile duct branch involvement with the overall histological picture one of sclerosing cholangitis, including modest presence of CD1a+/CD27+ cells infiltrating the basal cell layer of bile ducts [39].

Therapy for LCH

Historically, many drug therapy options have been tried, with limited to no significant utility achieved from a variety of immune suppressive agents including cyclophosphamide and corticosteroids. Recent therapeutic advances appear to offer more promise. Among them is vemurafenib, a small molecule direct inhibitor of the constitutively activated V600E mutant *BRAF* kinase, acting by blocking this kinase pathway in *BRAF* V600E+ cells and inducing programmed cell death, with treatment benefit seen in some LCH disease [67]. The degree to which targeting *BRAF* V600E might be overall beneficial is not yet clarified, as study data are to date limited and there are already reported mechanisms whereby cellular resistance to vemurafenib can occur. This may explain the observation of recurrence of active LCH after apparent excellent initial therapeutic responses [40].

Birt-Hogg-Dubé (BHD) Syndrome

In 1977, Arthur Birt, Georgina Hogg, and W. James Dubé described a Canadian family cohort with multiple members having skin lesions including fibrofolliculomas, trichodiscomas, and acrochordons, and with this constellation of clinical features having an apparent autosomal dominant inheritance pattern [68]. Subsequent work by multiple investigators solidified this as a neoplastic disease with multiorgan involvement, with investigation of the possible genetic basis for renal oncocytomas and chromophobe renal carcinomas establishing a familial link between these renal cancers and the skin manifestations of Birt-Hogg-Dubé syndrome (BHD) [69, 70]. Further subsequent genetic analysis of multiple kindreds affected with BHD and renal oncocytomas identified the BHD genetic locus on chromosome 17 [71], and in 2002 Nickerson et al. specifically defined the *BHD* (now *FLCN*) gene as the

causative genetic defect in BHD [72]. *FLCN* encodes the protein folliculin, a novel tumor suppressor protein that is highly conserved across species, at least from *C. elegans* to man, and interacts with other highly conserved proteins in modulating multiple cellular processes including tumor suppression, at least in part through interaction with the mTOR pathway [73].

Cellular Mechanisms for Neoplasia in BHD

The cellular mechanisms by which *FLCN* participates in the evolution of multiorgan neoplastic abnormalities of BHD are not yet fully elucidated, but many cellular pathways appear to participate in *FLCN*-mediated events in cells. Loss-of-function mutations in *FLCN* have been demonstrated to alter many cellular processes, including mitochondrial function, metabolic shifts toward oxidative phosphorylation, cellular nutrient sensing, cell-cell adhesion, ciliary function, cell-cycle progression, and altered autophagy [73]. The specific mechanisms whereby *FLCN* participates in neoplastic progression or transformation in cells remain a subject of active investigation by many [73].

A broad variety of germline *FLCN* mutations have been identified in BHD-affected families, with at least 150 separate identified *FLCN* loss-of-function mutations [72, 74–76]. A majority of known *FLCN* mutations predict folliculin truncations by sequence analysis [76]. Haploinsufficiency of normal functional *FLCN* is found in BHD cases; homozygous *FLCN* mutation appears to produce embryonic lethality, at least in animal models [72]. *FLCN* mRNA transcripts are found very broadly in tissues by northern blot analysis [72], and in situ hybridization has identified mRNA expression in skin, distal nephron of the kidney, lung stromal cells and type 1 pneumocytes, acinar cells of pancreas and parotid gland, epithelial ducts of the breast and prostate, and neurons of the cerebrum and Purkinje cells of the cerebellum. Reduced *FLCN* mRNA expression has been reported in heart, muscle, and liver [77]. The prominent expression of *FLCN* in skin, lung, and kidney supports the apparent role of loss-of-function mutations of *FLCN* in the neoplastic features of BHD in these organs.

FLCN appears to function as a tumor suppressor gene. In important investigations of BHD tumorigenesis by two groups, different and likely sequential bi-allelic mutations of *FLCN* were commonly found in tumor cells, consistent with the genetic "two-hit" model of tumor suppressor gene participation in neoplastic transformation [78, 79].

The roles of *FLCN* in cellular function are diverse, and cooperating gene products are many. The first cellular partners identified for folliculin were the folliculin interacting proteins (FNIP) 1 and 2, which, like folliculin, are highly conserved across a broad phylogenetic range. Both FNIP1 and FNIP2 appear to interact with folliculin in phosphorylation events mediated by 5'-AMP activated protein kinase

(AMPK), and perhaps mTOR as well, and the interaction of folliculin and FNIP1 may be involved in energy and/or nutrient sensing through the AMPK and mTOR signaling pathways [80]. The relationship of these specific events to cellular neoplasia is not known. But what has become clear more recently is that FNIP1 and -2 are involved with folliculin in the induction of kidney neoplasia [81]. Genetic knockout studies in a murine model revealed a clear role for the participation of functionally normal FNIP1 and -2 with folliculin in tumor suppression, and that knockout of FNIP1 and -2 induced kidney tumor evolution. In addition, FNIP1 and -2 disruption could also produce kidney cysts in the same murine model [81], suggesting potential insight into the mechanism of lung cyst development in BHD.

The roles of folliculin in mTOR-dependent cellular pathways appear complex, with both activation and suppression of mTOR activity by folliculin reported (reviewed by Schmidt and Linehan [73]). The net effect of folliculin on these events may in part depend on nutritional and/or cellular energetics. In addition, *FLCN* functional loss can activate the RAF-MEK-ERK signaling cascade to induce AKT-mTOR activation, with increased cell-cycle protein expression and cell proliferation [82]. Functional loss of *FLCN* also appears to produce changes in mitochondrial biogenesis with increased cellular mitochondrial numbers and respiratory capacity, which could also support an increased cellular proliferative state. This cellular energetic shift also appears to involve participation of the transcription factor TFE3, which is negatively regulated by *FLCN* [83]. Loss of folliculin function produces activation of TFE3, and this drives greater mitochondrial activity, among other effects. In this perspective, it is of interest that folliculin appears to interact with its cellular partners FNIP1 and FNIP2 in negative regulation of TFE3 through phosphorylation of TFE3, which induces retention of FTE3 in the cytoplasm where it is inactive [84]. Work by Betschinger et al. has revealed that this FTE3 regulation by intact folliculin-FNIP1/2 complexes has important effects on pluripotent stem cells, with normal folliculin-FNIP1/2 inducing a shift toward differentiation by stem cells [85]. And with known loss-of-function *FLCN* mutations, this promotion of cellular differentiation through a TFE3-dependent process is restricted, resulting in the preservation of the pluripotent state of stem cells [85]. Whether this process plays a role in the cellular events in BHD is at present unknown.

Recent research has revealed a fascinating added facet of the cellular and organ systems biology of folliculin, with potential direct role in the pathophysiology of BHD. Collective work by multiple investigators has established links between abnormal cilia development and function and the evolution of cysts and carcinomas in some organs, importantly kidneys (reviewed by [86]). Pursuing this link between ciliopathies and cyst and neoplasia in kidneys, Luijten and colleagues established that folliculin localizes to the primary cilium in a rat BHD model, and that altered expression of folliculin produced renal cysts as well as tumors, and in a *Wnt/beta-catenin*-dependent fashion [86]. This involvement of abnormal folliculin in primary cilium function may prove to be an important aspect of both cyst formation in organs in BHD, and the evolution of neoplasia. The answer to this question awaits future clarifying research.

Organ-Specific BHD Disease

The aberrant cellular and tissue effects of mutant *FLCN* are predominantly found in skin, lung, and kidneys, and include varying degrees of neoplastic cellular behavior. The following discussion of these abnormalities will focus primarily on skin and kidney involvement in BHD; lung disease in BHD is discussed separately in Chap. 7. Where relevant, added specific BHD-related organ pathologies will be noted.

Skin involvement in BHD involves a few well-characterized low-grade neoplastic features. These distinctive skin abnormalities were the first clue to the identification of BHD as a specific disease, and these remain cardinal features guiding the clinical diagnosis of BHD. The original report leading to the delineation of BHD as a defined disease was the description of the triad of fibrofolliculomas, trichodiscomas, and acrochordons [68]. A large body of subsequent work has now identified the **fibrofolliculoma** as the characteristic hamartomatous dermatological manifestation of BHD disease, though an alternative hypothesis for the evolution and pathology of this cutaneous abnormality has more recently been offered (see below). Trichodiscomas and perifollicular fibromas were initially considered to be separate and unique pathological processes, but these are now considered to also be indistinguishable from fibrofolliculomas [87, 88]. Acrochordons (skin tags) are not felt to be a part of the dermatopathology of BHD [89].

Fibrofolliculomas are firm, generally hypopigmented, papules typically found most prominently on the face and neck of individuals with BHD. Over 90% of Caucasians with BHD have fibrofolliculomas [90], and these are present by early adult years [87]. The frequency of fibrofolliculomas in Asian BHD populations appears to be substantially lower than in Caucasians, reported as only 27% [91].

Fibrofolliculomas are typically described pathologically as folliculo-sebaceous hamartomas arising from mesodermal and ectodermal components of the hair follicle [88]. However, some recent and fascinating work has revealed an alternative pathophysiological explanation for these papules that may reveal added insights into BHD disease evolution. In a 2013 paper, Verooij et al. reported that the pathology of fibrofolliculomas is not a hamartomatous process of the hair follicle, but rather appears to be due to hyperproliferation of epidermal cells involved in an early phase of sebaceous gland morphogenesis [92]. Their work also revealed notable activation of the canonical *Wnt* developmental signaling pathway in sebaceous tissues of fibrofolliculomas, consistent with other companion work noted earlier in this chapter suggesting the involvement of primary cilium dysregulation and dysfunction in BHD pathology, perhaps including renal cyst development as well as multiorgan neoplasia [86].

Kidney manifestations of BHD involve **neoplasia** and **cysts**, both of which are likely driven by the complex biological features that underlie the folliculin haploinsufficient state of BHD. Given the significant likelihood of malignancy when tumors are present in BHD, they represent the most clinically important aspect of BHD for clinical assessment and management.

Renal neoplasia in BHD includes a diverse array of tumor histological patterns with a significant frequency of admixture of both benign and malignant tumor cell types, as is discussed further below. The prevalence of renal tumors in BHD varies somewhat between reports, with ascertainment biases likely accounting for some of the variability. Reported renal tumor frequency in BHD cohorts ranges from 12% to 41% [75, 76, 93–96]. Renal tumor prevalence increases as a function of age. In a large cohort of 223 individuals from 33 BHD families, Zbar et al. reported an overall renal tumor prevalence of 11.9% in identified BHD subjects of age >40, compared with a 2.3% tumor prevalence in subjects with age <40 [93].

The risk of developing renal cancer is substantially higher in BHD individuals compared with the background population. When adjusted for age, the odds ratio for a BHD patient developing a renal cancer was ~sevenfold greater than in a non-BHD individual [93]. The mean age of initial diagnosis of renal tumors in BHD is from the late 40s to 50 years, with a substantial age range from 20 to the 80s [96, 97]. Interestingly, the frequency of renal tumors in BHD appears to be substantially higher in males than females, with prevalence in males as much as fivefold higher than in females [76, 97].

Multifocal and bilateral renal tumors are a common feature of BHD [70, 93, 94, 96, 97]. Renal tumors include both benign and malignant tissue types, with considerable variation noted both in and between individual patients. Given the admixed neoplasia presentations possible, careful awareness of renal status and monitoring for change are of central importance for BHD patients.

Both benign and malignant renal tumors are associated with BHD, and are commonly found concurrently in individual patients. The **benign renal neoplasms** reported in BHD are **oncocytomas** [98]. These benign tumors can exist as isolated uniform neoplasms, but do not independently constitute a large percentage of the total neoplasia noted in the kidney in BHD. More commonly, histological features of oncocytoma are found in hybrid tumors that include components of chromophobe adenocarcinoma. The **malignant renal neoplasms** are the most common tumor types associated with BHD. The malignant tumor histological types found include **chromophobe renal carcinoma**, **hybrid chromophobe-oncocytic carcinoma**, and **clear cell carcinoma** [70, 93, 94, 96, 97], the latter also termed common or conventional renal cell carcinoma [98]. In a composite review of case series of renal tumors in BHD, the relative tumor frequencies typically found are chromophobe renal carcinoma > hybrid chromophobe-oncocytic carcinoma > clear cell carcinoma, with some considerable variation in reported frequencies [93–95, 97].

Tumor genetic diversity in renal cancer in BHD is substantial, and greater than that noted in sporadic renal cancer, particularly in chromatin remodeling genes [99]. Within individual patients, there can be a rather remarkable array of second-hit mutations in renal tumors, including the full range of histological tumor types seen in BHD [79]. The frequency of second-hit genetic mutations also varies significantly between tumor types, even within individuals [78, 79].

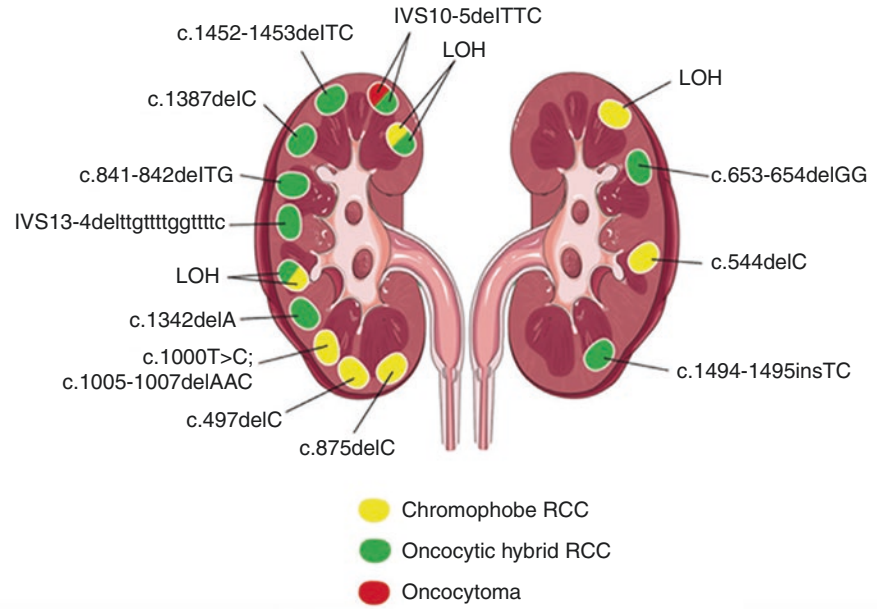

Fig. 15.6 Diagram highlighting the varying types of renal tumors and their associated mutations in a patient with BHD. LOH = Loss of heterozygosity (Adapted from Vocke et al. [79], by permission of Oxford University Press)

Clinicians should be mindful of a number of important biological and clinical aspects regarding renal tumors associated with BHD. First, the most common presentation is of multifocal tumors when neoplastic renal disease is present. Next, substantial genetic variability exists within tumors, and this can include multiple separate unique second-hit mutations in separate tumors in a single individual patient (Fig. 15.6) [79].

Accompanying the genetic variability is the common feature of admixed histological variability in individual tumors, which results in the high frequency of hybrid histology tumors noted in BHD. Coupled with this histological and genetic variability is the observation that distinguishing specific tumor types, including benign versus malignant tumors, is not possible by standard clinical imaging technologies, so that tumor growth becomes the single most important clinical determinant of the need for excision. In this regard, it should be noted that renal tumors associated with BHD are among the slowest growing tumors amid the broader array of genetically defined renal tumors. A recent report describes a median growth rate of 0.1 cm/yr (IQR, 0.04–0.24 cm/yr) in a cohort of patients with *FLCN*-deficient tumors [100]. These data may be of utility in considerations for determining the optimal frequency of surveillance imaging of tumors in BHD.

So, given these data regarding the biology and behavior of renal neoplasia in BHD, a number of clinical features need to be weighed when considering the

evaluation of BHD patients for renal abnormalities, and/or when monitoring the patient subset who have known renal tumors. These clinical parameters include the following:

- Age
- Sex
- The likelihood of malignant vs. benign tumor types
- Typical tumor growth rates

Kidney cysts are also associated with BHD, but do not manifest a malignant phenotype [101]. The evolution of renal cysts in BHD may well be linked to developmental dysregulation involving primary cilium defects under *FLCN* control [86].

Extrarenal Neoplasia Associated with BHD

Beyond kidney neoplasia, the only other significant cancer risk investigation in BHD subjects has been for colorectal neoplasia. And while there has been significant exploration of the possible participation of *FLCN* in colorectal neoplasia, the available data do not yet fully clarify this question.

In an early investigation of neoplasia in BHD subjects, Toro et al. found no colorectal cancers in a cohort of 152 individuals with BHD [70]. But that study focused primarily on renal and skin disease, and may have not identified existing colorectal neoplastic disease in that patient group. A study by Zbar et al. exploring the possible relationship of *FLCN* mutations to colorectal neoplasia in a large BHD cohort of 223 individuals from 33 families did not identify any linkage between BHD and colorectal cancer or colon polyps [93]. However, the low frequency of colorectal cancer found in the entire study population (3 colon cancers in the 111 BHD subjects and none in the 111 non-BHD subjects) raises the question of whether insufficient statistical power existed to exclude a causal relationship.

Subsequent studies have provided added insight into a possible link of *FLCN* mutations and colorectal neoplasia. Khoo et al. investigated germline *FLCN* mutational analysis in a group of 23 BHD subjects from four affected families plus four additional unrelated individuals [78]. They identified a genetic mutational hotspot in the *FLCN* exon 11 C_8 mononucleotide tract and demonstrated that these exon 11 mutant alleles appeared to function as the second-hit in BHD causation for affected subjects. Regarding the specific question of colorectal neoplasia and BHD in that same study, six of eight of their BHD subjects with exon 11 hotspot mutations had neoplastic colonic polyps, consistent with a causal role for *FLCN* mutations in colorectal neoplasia.

In a more recent study, Nahorski et al. undertook a different approach to investigate the link between *FLCN* mutations and colorectal neoplasia [102]. They studied three subject sample sets: a cohort with familial colorectal neoplasia, a 149 BHD subject cohort with well-characterized colorectal neoplasia status, and tumor DNA

from a separate group of patients with non-familial microsatellite unstable colorectal cancer. Their analysis included assessment for the presence of *FLCN* exon 11 C_8 mononucleotide tract mutations. While there were no *FLCN* exon 11 hotspot mutations identified in the familial colorectal neoplasia cohort, an association was noted between *FLCN* mutations and colorectal neoplasia in the BHD cohort. *FLCN* mutations were identified in 101 of the 149 BHD subjects, including 69 with exon 11 C_8 mononucleotide tract hotspot mutations. Of those with exon 11 hotspot mutations, the frameshift mutation c.1285dupC was significantly associated with colorectal neoplasia, with either cancer or neoplastic polyps found in 5 of the 37 individuals with that mutation, with an age-related increased risk of neoplasia. In added support of the findings in their BHD cohort, their investigation of the subjects with non-familial microsatellite unstable colorectal cancer found *FCLN* exon 11 c.1285dupC mutations in 23% (7 of 30) of the subjects, in addition to multiple other separate gene mutations, supporting the concept of participation of *FLCN* mutations in broader carcinogenesis events beyond BHD. Moreover, they also reported that the *FLCN* exon 11 mutational hotspot mapped to a potential FNIP1 interaction site in folliculin, lending added support to the concept of tumor suppressor dysfunction induced by these *FLCN* mutations [102]. Of note, a separate study of 89 BHD subjects from 51 families did not find an association between *FLCN* mutations and colorectal neoplasia, though that study was focused primarily on a familial renal neoplasia cohort and may have been limited by ascertainment bias [75].

Overall, the currently available data reveal apparent variability but also a significant causal role for *FLCN* in the genotype-phenotype relationship of the pathogenesis of colorectal neoplasia, while also acknowledging the multigenic factors participating in colorectal neoplasia.

Lymphocytic Interstitial Pneumonia/Follicular Bronchiolitis (LIP/FB)

LIP/FB can be associated with several systemic conditions such as autoimmune disorders such as Sjögren's, rheumatoid arthritis, and systemic lupus erythematosus and other immune dysregulatory conditions such as common variable immunodeficiency and human immunodeficiency virus (HIV). The most common association of LIP/FB is in the context of co-existing Sjögren's, where LIP/FB can often be the presenting disease manifestation.

Sjögren's

Sjögren's is an autoimmune disease that primarily affects salivary and lacrimal glands [103]. Interstitial lung disease (including the cystic disease that is the focus of this textbook) affects only a minority of Sjögren's patients. Sicca symptoms

present the most significant and common extrapulmonary manifestation of the disease. Treatment usually focuses on alleviating the dryness, either through artificial tears and saliva or with secretagogues [104, 105]. A systematic review of studies looking at symptoms of hyposalivation in patients with Sjögren's demonstrated that pilocarpine was superior to placebo in reducing dry mouth symptoms and that rituximab, interferon-alpha, and especially pilocarpine were more effective than placebo in increasing salivary flow [106]. The additional systemic symptoms of musculoskeletal pain and fatigue can sometimes be alleviated by use of hydroxychloroquine or through the use of other biologic agents [107]. Providers caring for patients with Sjögren's need to be cognizant of an increased potential for development of non-Hodgkin's lymphoma in this population.

Light Chain Deposition Disease

Light chain deposition disease (LCDD) is the most common form of monoclonal immunoglobulin deposition disease that can uncommonly manifest as DCLD. The source of these plasma cell-produced light chains can be multiple myeloma or other lymphoproliferative diseases – and thus there can be many extrapulmonary effects seen through these primary diseases. As far as the light chains themselves, the kidneys tend to be the most commonly affected organ, perhaps due to the fact that serum-free light chains are largely filtered by the kidneys, and thus the primary site for their deposition. This can manifest as hypertension, renal lesions, proteinuria, renal tubular acidosis, and ultimately renal failure.

Conclusion

Pulmonologists are often presented with a case of cystic lung disease and asked to make a correct diagnosis and manage the patient over time. The most common DCLDs encountered in clinical practice – LAM, BHD, PLCH, LIP/FB, and LCDD frequently have extrapulmonary manifestations that can be helpful in establishing the correct diagnosis and carry significant management implications for the patients.

Key Learning Points

- Renal AMLs and lymphatic complications such as chylous effusions, lymphadenopathy, and lymphangioleiomyomas are the most common extrapulmonary manifestations of LAM. The presence of any of these findings in women with characteristic cystic lung disease can help establish the diagnosis of LAM with certainty.
- Treatment with mTOR inhibitors is safe and effective, and the preferred mode of management rather than invasive procedures for patients with LAM and extrapulmonary manifestations.

- LCH can involve a variety of organ systems and careful consideration for systemic involvement should be given at the time of initial evaluation, as systemic involvement has implications for prognosis and overall management.
- Hair follicle tumors such as fibrofolliculomas and renal tumors are the most common extrapulmonary manifestations of BHD. All patients with BHD should undergo periodic screening for renal tumors with nephron-sparing surgery reserved for patients with tumors greater than 3 cm in size.
- LIP/FB is most commonly seen in association with autoimmune disorders, especially Sjögren's. Detailed review of systems focused on items such as sicca symptoms and other symptoms suggestive of underlying connective tissue disorders, as well as laboratory investigations for these conditions, should be obtained in patients with DCLD suggestive of LIP/FB.

References

1. McCormack FX, Travis WD, Colby TV, Henske EP, Moss J. Lymphangioleiomyomatosis – calling it what it is: a low-grade, destructive, metastasizing neoplasm. Am J Respir Crit Care Med. 2012;186(12):1210–2.
2. Fittschen A, Wendlik I, Oeztuerk S, Kratzer W, Akinli AS, Haenle MM, et al. Prevalence of sporadic renal angiomyolipoma: a retrospective analysis of 61,389 in- and out-patients. Abdom Imaging [Internet]. 2014;39(5):1009–13. Available from: https://doi.org/10.1007/s00261-014-0129-6.
3. Fujii Y, Ajima J, Oka K, Tosaka A, Takehara Y. Benign renal tumors detected among healthy adults by abdominal ultrasonography. Eur Urol. 1995;27(2):124–7.
4. Curatolo P, Bombardieri R, Jozwiak S. Tuberous sclerosis. The Lancet. 2008;372(9639):657–68.
5. Seyam RM, Bissada NK, Kattan SA, Mokhtar AA, Aslam M, Fahmy WE, et al. Changing trends in presentation, diagnosis and management of renal angiomyolipoma: comparison of sporadic and tuberous sclerosis complex-associated forms. Urology. 2008;72(5):1077–82.
6. Ryu JH, Hartman TE, Torres VE, Decker PA. Frequency of undiagnosed cystic lung disease in patients with sporadic renal angiomyolipomas. Chest. 2012;141(1):163–8.
7. Ryu JH, Moss J, Beck GJ, Lee JC, Brown KK, Chapman JT, et al. The NHLBI lymphangioleiomyomatosis registry: characteristics of 230 patients at enrollment. Am J Respir Crit Care Med. 2006;173(1):105–11.
8. Yeoh ZW, Navaratnam V, Bhatt R, McCafferty I, Hubbard RB, Johnson SR. Natural history of angiomyolipoma in lymphangioleiomyomatosis: implications for screening and surveillance. Orphanet J Rare Dis. 2014;9:151.
9. Casper KA, Donnelly LF, Chen B, Bissler JJ. Tuberous sclerosis complex: renal imaging findings. Radiology. 2002;225(2):451–6.
10. Gupta N, Finlay GA, Kotloff RM, Strange C, Wilson KC, Young LR, et al. Lymphangioleiomyomatosis diagnosis and management: high-resolution chest computed tomography, transbronchial lung biopsy, and pleural disease management an official American thoracic society/Japanese respiratory society clinical practice guideline. Am J Respir Crit Care Med. 2017;196(10):1337–48.
11. Hindman N, Ngo L, Genega EM, Melamed J, Wei J, Braza JM, et al. Angiomyolipoma with minimal fat: can it be differentiated from clear cell renal cell carcinoma by using standard MR techniques? Radiology. 2012;265(2):468–77.

12. Jinzaki M, Silverman SG, Akita H, Nagashima Y, Mikami S, Oya M. Renal angiomyolipoma: a radiological classification and update on recent developments in diagnosis and management. Abdom Imaging. 2014;39(3):588–604.
13. Park BK. Renal angiomyolipoma: radiologic classification and imaging features according to the amount of fat. AJR Am J Roentgenol. 2017;209(4):826–35.
14. Giannikou K, Malinowska IA, Pugh TJ, Yan R, Tseng YY, Oh C, et al. Whole exome sequencing identifies TSC1/TSC2 Biallelic loss as the primary and sufficient driver event for renal angiomyolipoma development. PLoS Genet. 2016;12(8):e1006242.
15. Yamakado K, Tanaka N, Nakagawa T, Kobayashi S, Yanagawa M, Takeda K. Renal angiomyolipoma: relationships between tumor size, aneurysm formation, and rupture. Radiology. 2002;225(1):78–82.
16. Seyam R, AlKhudair W, Kattan S, Alotaibi M, Alzahrani H, Altaweel W. The risks of renal angiomyolipoma: reviewing the evidence. J Kidney Cancer VHL. 2017;4(4):13–25.
17. Villalta JD, Sorensen MD, Durack JC, Kerlan RK, Stoller ML. Selective arterial embolization of angiomyolipomas: a comparison of smaller and larger embolic agents. J Urol. 2011;186(3):921–7.
18. Murray TE, Doyle F, Lee M. Transarterial embolization of angiomyolipoma: a systematic review. J Urol. 2015;194(3):635–9.
19. Urbano J, Paul L, Cabrera M, Alonso-Burgos A, Gómez D. Elective and emergency renal Angiomyolipoma embolization with ethylene vinyl alcohol copolymer: feasibility and initial experience. J Vasc Interv Radiol. 2017;28(6):832–9.
20. Bissler JJ, Racadio J, Donnelly LF, Johnson ND. Reduction of postembolization syndrome after ablation of renal angiomyolipoma. Am J Kidney Dis. 2002;39(5):966–71.
21. Bissler JJ, Kingswood JC, Radzikowska E, Zonnenberg BA, Frost M, Belousova E, et al. Everolimus for angiomyolipoma associated with tuberous sclerosis complex or sporadic lymphangioleiomyomatosis (EXIST-2): a multicentre, randomised, double-blind, placebo-controlled trial. Lancet. 2013. PMID: 23312829 Clinical Trial.
22. Bissler JJ, McCormack FX, Young LR, Elwing JM, Chuck G, Leonard JM, et al. Sirolimus for angiomyolipoma in tuberous sclerosis complex or lymphangioleiomyomatosis. N Engl J Med [Internet]. 2008;358(2):140–51. Available from: http://www.nejm.org/doi/abs/10.1056/NEJMoa063564
23. Bissler JJ, Kingswood JC, Radzikowska E, Zonnenberg BA, Belousova E, Frost MD, et al. Everolimus long-term use in patients with tuberous sclerosis complex: four-year update of the EXIST-2 study. PLoS One. 2017;12(8):e0180939.
24. Yao J, Taveira-DaSilva AM, Jones AM, Julien-Williams P, Stylianou M, Moss J. Sustained effects of sirolimus on lung function and cystic lung lesions in lymphangioleiomyomatosis. Am J Respir Crit Care Med. 2014;190(11):1273–82.
25. Hu S, Wu X, Xu W, Tian X, Yang Y, Wang ST, et al. Long-term efficacy and safety of sirolimus therapy in patients with lymphangioleiomyomatosis. Orphanet J Rare Dis. 2019;14(1):206.
26. Glasgow CG, El-Chemaly S, Moss J. Lymphatics in lymphangioleiomyomatosis and idiopathic pulmonary fibrosis. Eur Respir Rev. 2012;21(125):196–206.
27. Atallah D, Checrallah A, Rouzier R, Ghossain MA, Chahine G. Retroperitoneal lymphangioleiomyoma mimicking ovarian tumor emerging after tamoxifen therapy. Obstet Gynecol. 2006;108(3 Pt 2):762–4.
28. Jaiswal VR, Baird J, Fleming J, Miller DS, Sharma S, Molberg K. Localized retroperitoneal lymphangioleiomyomatosis mimicking malignancy: a case report and review of the literature. Arch Pathol Lab Med. 2003;127(7):879–82.
29. Taveira-Dasilva AM, Hathaway O, Stylianou M, Moss J. Changes in lung function and chylous effusions in patients with lymphangioleiomyomatosis treated with sirolimus. Ann Intern Med. 2011;154(12):797–805, W-292-3.
30. Radzikowska E, Blasinska-Przerwa K, Skronska P, Wiatr E, Switaj T, Skoczylas A, et al. Lymphangioma in patients with pulmonary lymphangioleiomyomatosis: results of Sirolimus treatment. J Cancer Sci Ther. 2016;8:9.

31. Ussavarungsi K, Laroia AT, Burger CD. Low-dose sirolimus in retroperitoneal lymphangioleiomyomas. Lung India. 2019;36(4):349–52.
32. Harari S, Elia D, Torre O, Bulgheroni E, Provasi E, Moss J. Sirolimus therapy for patients with lymphangioleiomyomatosis leads to loss of chylous ascites and circulating LAM cells. Chest. 2016;150(2):e29–32.
33. Moua T, Olson EJ, St. Jean HC, Ryu JH. Resolution of chylous pulmonary congestion and respiratory failure in lymphangioleiomyomatosis with sirolimus therapy. Am J Respir Crit Care Med. 2012;186(4):389–90.
34. Ando K, Kurihara M, Kataoka H, Ueyama M, Togo S, Sato T, et al. The efficacy and safety of low-dose sirolimus for treatment of lymphangioleiomyomatosis. Respir Investig. 2013;51(3):175–83.
35. Fitzpatrick TB, Wolff K, Goldsmith LA, Katz SI, Gilchrest BA, Paller AS, et al. Fitzpatrick's dermatology in general medicine [electronic resource]. McGraw Hill Access Medicine Clinical Library; 2008.
36. Nguyen QBD, DarConte MD, Hebert AA. The cutaneous manifestations of tuberous sclerosis complex. Am J Med Genet C Semin Med Genet. 2018;178(3):321–5.
37. Nathan N, Burke K, Moss J, Darling TN. A diagnostic and management algorithm for individuals with an isolated skin finding suggestive of tuberous sclerosis complex. Br J Dermatol. 2017;176(1):220–3.
38. Treichel AM, Kwiatkowski DJ, Moss J, Darling TN. A diagnostic algorithm for enhanced detection of mosaic tuberous sclerosis complex in adults. Br J Dermatol. 2020;182(1):235–7.
39. Picarsic J, Jaffe R. Nosology and pathology of Langerhans cell histiocytosis. Hematol Oncol Clin North Am. 2015;29(5):799–823.
40. Allen CE, Merad M, McClain KL. Langerhans-cell histiocytosis. N Engl J Med. 2018;379(9):856.
41. Hoeffel G, Wang Y, Greter M, See P, Teo P, Malleret B, et al. Adult Langerhans cells derive predominantly from embryonic fetal liver monocytes with a minor contribution of yolk sac–derived macrophages. J Exp Med. 2012;209(6):1167–81.
42. Ginhoux F, Tacke F, Angeli V, Bogunovic M, Loubeau M, Dai X-M, et al. Langerhans cells arise from monocytes in vivo. Nat Immunol. 2006;7(3):265–73.
43. Allen CE, Li L, Peters TL, Leung HE, Yu A, Man T-K, et al. Cell-specific gene expression in Langerhans cell histiocytosis lesions reveals a distinct profile compared with epidermal Langerhans cells. J Immunol. 2010;184(8):4557–67.
44. Hamdorf M, Berger A, Schüle S, Reinhardt J, Flory E. PKCδ-induced PU.1 phosphorylation promotes hematopoietic stem cell differentiation to dendritic cells. Stem Cells. 2011;29(2):297–306.
45. Davies H, Bignell GR, Cox C, Stephens P, Edkins S, Clegg S, et al. Mutations of the BRAF gene in human cancer. Nature. 2002;417(6892):949–54.
46. Simko SJ, Garmezy B, Abhyankar H, Lupo PJ, Chakraborty R, Lim KPH, et al. Differentiating skin-limited and multisystem Langerhans cell histiocytosis. J Pediatr. 2014;165(5):990–6.
47. Chakraborty R, Hampton OA, Shen X, Simko SJ, Shih A, Abhyankar H, et al. Mutually exclusive recurrent somatic mutations in MAP2K1 and BRAF support a central role for ERK activation in LCH pathogenesis. Blood. 2014;124(19):3007–15.
48. Berres ML, Merad M, Allen CE. Progress in understanding the pathogenesis of Langerhans cell histiocytosis: Back to Histiocytosis X? Br J Haematol. 2015;169:3–13.
49. Collin M, Bigley V, McClain KL, Allen CE. Cell(s) of origin of Langerhans cell histiocytosis. Hematol Oncol Clin N Am. 2015;29(5):825–38.
50. Baumgartner I, Von Hochstetter A, Baumert B, Luetolf U, Follath F. Langerhans'-cell histiocytosis in adults. Med Pediatr Oncol. 1997;28(1):9–14.
51. Grois N, Pötschger U, Prosch H, Minkov M, Arico M, Braier J, et al. Risk factors for diabetes insipidus in Langerhans cell histiocytosis. Pediatr Blood Cancer. 2006;46(2):228–33.
52. Malpas JS, Norton AJ. Langerhans cell histiocytosis in the adult. Med Pediatr Oncol. 1996;27(6):540–6.

53. Howarth DM, Gilchrist GS, Mullan BP, Wiseman GA, Edmonson JH, Schomberg PJ. Langerhans cell histiocytosis diagnosis, natural history, management, and outcome. Cancer. 1999;85(10):2278–90.
54. Aricò M, Girschikofsky M, Généreau T, Klersy C, McClain K, Grois N, et al. Langerhans cell histiocytosis in adults: report from the International Registry of the histiocyte Society. Eur J Cancer. 2003;39(16):2341–8.
55. Ronceray L, Pötschger U, Janka G, Gadner H, Minkov M, German Society for Pediatric Hematology and Oncology, Langerhans Cell Histiocytosis Study Group. Pulmonary involvement in pediatric-onset multisystem Langerhans cell histiocytosis: effect on course and outcome. J Pediatr. 2012;161(1):129–33.e1-3.
56. Singhi AD, Montgomery EA. Gastrointestinal tract langerhans cell histiocytosis: a clinicopathologic study of 12 patients. Am J Surg Pathol. 2011;35(2):305–10.
57. Grois NG, Favara BE, Mostbeck GH, Prayer D. Central nervous system disease in Langerhans cell histiocytosis. Hematol Oncol Clin North Am. 1998;12(2):287–305.
58. Grois N, Prayer D, Prosch H, Lassmann H. Neuropathology of CNS disease in Langerhans cell histiocytosis. Brain. 2005;128(4):829–38.
59. Yeh EA, Greenberg J, Abla O, Longoni G, Diamond E, Hermiston M, et al. Evaluation and treatment of Langerhans cell histiocytosis patients with central nervous system abnormalities: current views and new vistas. Pediatr Blood Cancer. 2018;65(1).
60. Mass E, Jacome-Galarza CE, Blank T, Lazarov T, Durham BH, Ozkaya N, et al. A somatic mutation in erythro-myeloid progenitors causes neurodegenerative disease. Nature. 2017;549(7672):389–93.
61. McClain KL, Picarsic J, Chakraborty R, Zinn D, Lin H, Abhyankar H, et al. CNS Langerhans cell histiocytosis: common hematopoietic origin for LCH-associated neurodegeneration and mass lesions. Cancer. 2018;124(12):2607–20.
62. Braier J, Latella A, Balancini B, Castaños C, Rosso D, Chantada G, et al. Outcome in children with pulmonary Langerhans cell histiocytosis. Pediatr Blood Cancer. 2004;43(7):765–9.
63. Odame I, Li P, Lau L, Doda W, Noseworthy M, Babyn P, et al. Pulmonary Langerhans cell histiocytosis: a variable disease in childhood. Pediatr Blood Cancer. 2006;47(7):889–93.
64. Haupt R, Minkov M, Astigarraga I, Schäfer E, Nanduri V, Jubran R, et al. Langerhans cell histiocytosis (LCH): guidelines for diagnosis, clinical work-up, and treatment for patients till the age of 18 years. Pediatr Blood Cancer. 2013;60(2):175–84.
65. Berres ML, Lim KPH, Peters T, Price J, Takizawa H, Salmon H, et al. BRAF-V600E expression in precursor versus differentiated dendritic cells defines clinically distinct LCH risk groups. J Exp Med. 2014;211(4):669–83.
66. Galluzzo ML, Braier J, Rosenzweig SD, Garcia de Dávila MT, Rosso D. Bone marrow findings at diagnosis in patients with multisystem langerhans cell histiocytosis. Pediatr Dev Pathol. 2010;13(2):101–6.
67. Diamond EL, Subbiah V, Craig Lockhart A, Blay JY, Puzanov I, Chau I, et al. Vemurafenib for BRAF V600-mutant erdheim-chester disease and langerhans cell histiocytosis analysis of data from the histology-independent, phase 2, open-label VE-BASKET study. JAMA Oncol. 2018;4(3):384–8.
68. Birt AR, Hogg GR, Dubé WJ. Hereditary multiple fibrofolliculomas with trichodiscomas and acrochordons. Arch Dermatol. 1977;113(12):1674–7.
69. Weirich G, Glenn G, Junker K, Merino M, Storkel S, Lubensky I, et al. Familial renal oncocytoma: clinicopathological study of 5 families. J Urol. 1998;160(2):335–40.
70. Toro JR, Glenn G, Duray P, Darling T, Weirich G, Zbar B, et al. Birt-Hogg-Dube syndrome. A novel marker of kidney neoplasia. Arch Dermatol. 1999;135(10):1195–202.
71. Schmidt LS, Warren MB, Nickerson ML, Weirich G, Matrosova V, Toro JR, et al. Birt-Hogg-Dubé syndrome, a genodermatosis associated with spontaneous pneumothorax and kidney neoplasia, maps to chromosome 17p11.2. Am J Hum Genet. 2001;69(4):876–82.

72. Nickerson ML, Warren MB, Toro JR, Matrosova V, Glenn G, Turner ML, et al. Mutations in a novel gene lead to kidney tumors, lung wall defects, and benign tumors of the hair follicle in patients with the Birt-Hogg-Dubé syndrome. Cancer Cell. 2002;2(2):157–64.
73. Schmidt LS, Linehan WM. FLCN: the causative gene for Birt-Hogg-Dubé syndrome. Gene. 2018;640:28–42.
74. Lim DHK, Rehal PK, Nahorski MS, Macdonald F, Claessens T, Van Geel M, et al. A new Locus-Specific Database (LSDB) for mutations in the folliculin (FLCN) gene. Hum Mutat. 2010;31(1):E1043–51.
75. Toro JR, Wei MH, Glenn GM, Weinreich M, Toure O, Vocke C, et al. BHD mutations, clinical and molecular genetic investigations of Birt-Hogg-Dubé syndrome: a new series of 50 families and a review of published reports. J Med Genet. 2008;45(6):321–31.
76. Schmidt LS, Nickerson ML, Warren MB, Glenn GM, Toro JR, Merino MJ, et al. Germline BHD-mutation spectrum and phenotype analysis of a large cohort of families with Birt-Hogg-Dubé syndrome. Am J Hum Genet. 2005;76(6):1023–33.
77. Warren MB, Torres-Cabala CA, Turner ML, Merino M, Matrosova VY, Nickerson ML, et al. Expression of Birt-Hogg-Dube gene mRNA in normal and neoplastic human tissues. Mod Pathol. 2004;17(8):998–1011.
78. Khoo SK, Giraud S, Kahnoski K, Chen J, Motorna O, Nickolov R, et al. Clinical and genetic studies of Birt-Hogg-Dubé syndrome. J Med Genet. 2002;39(12):906–12.
79. Vocke CD, Yang Y, Pavlovich CP, Schmidt LS, Nickerson ML, Torres-Cabala CA, et al. High frequency of somatic frameshift BHD gene mutations in Birt-Hogg-Dubé-associated renal tumors. J Natl Cancer Inst. 2005;97(12):931–5.
80. Baba M, Hong SB, Sharma N, Warren MB, Nickerson ML, Iwamatsu A, et al. Folliculin encoded by the BHD gene interacts with a binding protein, FNIP1, and AMPK, and is involved in AMPK and mTOR signaling. Proc Natl Acad Sci U S A. 2006;103(42):15552–7.
81. Hasumi H, Baba M, Hasumi Y, Lang M, Huang Y, Oh HBF, et al. Folliculin-interacting proteins FNIP1 and FNIP2 play critical roles in kidney tumor suppression in cooperation with FLCN. Proc Natl Acad Sci U S A. 2015;112(13):E1624–31.
82. Baba M, Furihata M, Hong SB, Tessarollo L, Haines DC, Southon E, et al. Kidney-targeted Birt-Hogg-Dubé gene inactivation in a mouse model: Erk1/2 and Akt-mTOR activation, cell hyperproliferation, and polycystic kidneys. J Natl Cancer Inst. 2008;100(2):140–54.
83. Wada S, Neinast M, Jang C, Ibrahim YH, Lee G, Babu A, et al. The tumor suppressor FLCN mediates an alternate mTOR pathway to regulate browning of adipose tissue. Genes Dev. 2016;30(22):2551–64.
84. Hong S-B, Oh H, Valera VA, Baba M, Schmidt LS, Linehan WM. Inactivation of the FLCN tumor suppressor gene induces TFE3 transcriptional activity by increasing its nuclear localization. Bryk M, editor. PLoS One. 2010;5(12):e15793.
85. Betschinger J, Nichols J, Dietmann S, Corrin PD, Paddison PJ, Smith A. Exit from pluripotency is gated by intracellular redistribution of the bHLH transcription factor Tfe3. Cell. 2013;153(2):335–47.
86. Luijten MNH, Basten SG, Claessens T, Vernooij M, Scott CL, Janssen R, et al. Birt-Hogg-Dube syndrome is a novel ciliopathy. Hum Mol Genet. 2013;22(21):4383–97.
87. Tong Y, Schneider JA, Coda AB, Hata TR, Cohen PR. Birt–Hogg–Dubé syndrome: a review of dermatological manifestations and other symptoms. Am J Clin Dermatol. 2018;19(1):87–101.
88. Schulz T, Hartschuh W. Birt-Hogg-Dube-syndrome and Hornstein-Knickenberg-syndrome are the same. Different sectioning technique as the cause of different histology. J Cutan Pathol. 1999;26(1):55–61.
89. De la Torre C, Ocampo C, Doval IG, Losada A, Cruces MJ. Acrochordons are not a component of the Birt-Hogg-Dubé syndrome: does this syndrome exist? Case reports and review of the literature. Am J Dermatopathol. 1999;21(4):369–74.
90. Toro JR, Pautler SE, Stewart L, Glenn GM, Weinreich M, Toure O, et al. Lung cysts, spontaneous pneumothorax, and genetic associations in 89 families with Birt-Hogg-Dubé syndrome. Am J Respir Crit Care Med. 2007;175(10):1044–53.

91. Murakami Y, Wataya-Kaneda M, Tanaka M, Takahashi A, Tsujimura A, Inoue K, et al. Two Japanese cases of birt-hogg-dubé syndrome with pulmonary cysts, fibrofolliculomas, and renal cell carcinomas. Case Rep Dermatol. 2014;6(1):20–8.
92. Vernooij M, Claessens T, Luijten M, Van Steensel MAM, Coull BJ. Birt-Hogg-Dubé syndrome and the skin. Familial Cancer. 2013;12(3):381–5.
93. Zbar B, Alvord WG, Glenn G, Turner M, Pavlovich CP, Schmidt L, et al. Risk of renal and colonic neoplasms and spontaneous pneumothorax pneurnothorax in the Birt-Hogg-Dubé syndrome. Cancer Epidemiol Biomark Prev. 2002;11(4):393–400.
94. Houweling AC, Gijezen LM, Jonker MA, Van Doorn MBA, Oldenburg RA, Van Spaendonck-Zwarts KY, et al. Renal cancer and pneumothorax risk in Birt-Hogg-Dubé syndrome; An analysis of 115 FLCN mutation carriers from 35 BHD families. Br J Cancer. 2011;105(12):1912–9.
95. Pavlovich CP, Grubb RL, Hurley K, Glenn GM, Toro J, Schmidt LS, et al. Evaluation and management of renal tumors in the Birt-Hogg-Dubé syndrome. J Urol. 2005;173(5):1482–6.
96. Benusiglio PR, Giraud S, Deveaux S, Méjean A, Correas JM, Joly D, et al. Renal cell tumour characteristics in patients with the Birt-Hogg-Dubé cancer susceptibility syndrome: a retrospective, multicentre study. Orphanet J Rare Dis. 2014;9:163.
97. Pavlovich CP, Walther MM, Eyler RA, Hewitt SM, Zbar B, Linehan WM, et al. Renal tumors in the Birt-Hogg-Dubé syndrome. Am J Surg Pathol. 2002;26(12):1542–52.
98. Kovacs G, Akhtar M, Beckwith BJ, Bugert P, Cooper CS, Delahunt B, et al. The Heidelberg classification of renal cell tumours. J Pathol. 1997;183(2):131–3.
99. Hasumi H, Furuya M, Tatsuno K, Yamamoto S, Baba M, Hasumi Y, et al. BHD-associated kidney cancer exhibits unique molecular characteristics and a wide variety of variants in chromatin remodeling genes. Hum Mol Genet. 2018;27(15):2712–24.
100. Ball MW, An JY, Gomella PT, Gautam R, Ricketts CJ, Vocke CD, et al. Growth rates of genetically defined renal tumors: implications for active surveillance and intervention. J Clin Oncol. 2020;38(11):1146–53. https://doi.org/10.1200/JCO.19.02263.
101. Furuya M, Yao M, Tanaka R, Nagashima Y, Kuroda N, Hasumi H, et al. Genetic, epidemiologic and clinicopathologic studies of Japanese Asian patients with Birt–Hogg–Dubé syndrome. Clin Genet. 2016;90(5):403–12.
102. Nahorski MS, Lim DHK, Martin L, Gille JJP, McKay K, Rehal PK, et al. Investigation of the Birt-Hogg-Dubé tumour suppressor gene (FLCN) in familial and sporadic colorectal cancer. J Med Genet. 2010;47(6):385–90.
103. Romão VC, Talarico R, Scirè CA, Vieira A, Alexander T, Baldini C, et al. Sjögren's syndrome: state of the art on clinical practice guidelines. RMD Open. 2018;4(Suppl 1):e000789.
104. Foulks GN, Forstot SL, Donshik PC, Forstot JZ, Goldstein MH, Lemp MA, et al. Clinical guidelines for management of dry eye associated with Sjögren disease. Ocul Surf. 2015;13(2):118–32.
105. Zero DT, Brennan MT, Daniels TE, Papas A, Stewart C, Pinto A, et al. Clinical practice guidelines for oral management of Sjögren disease: dental caries prevention. J Am Dent Assoc. 2016;147(4):295–305.
106. Al Hamad A, Lodi G, Porter S, Fedele S, Mercadante V. Interventions for dry mouth and hyposalivation in Sjögren's syndrome: a systematic review and meta-analysis. Oral Dis. 2019;25(4):1027–47.
107. Carsons SE, Vivino FB, Parke A, Carteron N, Sankar V, Brasington R, et al. Treatment guidelines for rheumatologic manifestations of Sjögren's syndrome: use of biologic agents, management of fatigue, and inflammatory musculoskeletal pain. Arthritis Care Res (Hoboken). 2017;69(4):517–27.
108. Bissler JJ, McCormack FX, Young LR, et al. Sirolimus for Angiomyolipoma in Tuberous Sclerosis Complex or Lymphangioleiomyomatosis. N Engl J Med. 2008;358(2):140–51.

Chapter 16
Pleural Disease in Diffuse Cystic Lung Diseases

Kuniaki Seyama and Masatoshi Kurihara

Abbreviations

ATS	American Thoracic Society
BHDS	Birt-Hogg-Dubé syndrome
BTS	British Thoracic Society
DCLD	Diffuse cystic lung disease
JRS	Japanese Respiratory Society
LAM	Lymphangioleiomyomatosis
LCC	LAM cell cluster
LPC	Lower pleural covering
NBI	Narrow-band imaging
ORC	Oxidized regenerated cellulose
PGA	Polyglycolic acid sheets
PLCH	Pulmonary Langerhans cell histiocytosis
PSP	Primary spontaneous pneumothorax
SSP	Secondary spontaneous pneumothorax
TPC	Total pleural covering
VATS	Video-assisted thoracoscopic surgery
VIC	Polyglactin 910 mesh

K. Seyama (✉)
Division of Respiratory Medicine, Juntendo University Faculty of Medicine and Graduate School of Medicine, Tokyo, Japan
e-mail: kseyama@juntendo.ac.jp

M. Kurihara
Pneumothorax Research Center and Department of General Thoracic Surgery, Nissan Tamagawa Hospital, Institute of Medicine, Tokyo, Japan
e-mail: kuri@tf6.so-net.ne.jp

N. Gupta et al. (eds.), *Diffuse Cystic Lung Diseases*, Respiratory Medicine,
https://doi.org/10.1007/978-3-030-63365-3_16

Introduction

Spontaneous pneumothorax, a condition in which air exists between the lung and the chest wall, is a representative pleural disease associated with diffuse cystic lung diseases (DCLDs). Not all DCLDs are complicated by a spontaneous pneumothorax, but pneumothoraces frequently occur in patients with lymphangioleiomyomatosis (LAM), Birt-Hogg-Dubé syndrome (BHDS), and pulmonary Langerhans cell histiocytosis (PLCH). Accordingly, the occurrence of a pneumothorax means that some DCLDs affect not only lung parenchyma to form air-filled cysts but also visceral pleura to cause air leakage into the pleura space. Due to the diffuse nature of visceral pleural lesions, a pneumothorax can occur repeatedly and is often intractable to treat. A pneumothorax can be also seen in patients with metastatic malignant neoplasms to the lungs, those forming nodular, cavitary, or cystic metastatic lesions in lung parenchyma, as well as metastatic pleural invasion. Another pleural manifestation associated with DCLDs is chylous pleural effusion. It is a characteristic and almost pathognomonic indicator of LAM. Comprehensive review articles regarding the epidemiology, pathogenesis, and clinical manifestations of DCLDs have recently been published [1–3]. This chapter expands upon those reviews and describes content not seen in the peer-reviewed literature.

Spontaneous Pneumothorax Associated with Diffuse Cystic Lung Diseases

Etiology of Pneumothorax

In contrast to the etiology for a primary spontaneous pneumothorax, where the rupture of blebs or subpleural bullae is usually located in the apices of the lung (Fig. 16.1a), different etiologic factors leading to fragile visceral pleura are involved in various DCLDs. Furthermore, affected areas exist diffusely all over the entire surface of the visceral pleura (Fig. 16.1b, c, and d). For example, LAM is a neoplastic disease characterized by proliferation of smooth muscle-like cells (LAM cells) in lung parenchyma, along bronchioles and axial lymphatics. Proliferating LAM cells can also be seen on visceral pleura. Accordingly, multiple, dome-shaped, thin-walled cysts are found on the visceral pleura when LAM patients undergo open thoracic or video-assisted thoracoscopic surgery (VATS) (see Fig. 16.1b). The exact mechanisms for numerous thin-walled cysts to be generated on visceral pleura remain undetermined, but LAM cells produce and secrete MMP-2, MMP-9, and cathepsins, and these proteases are believed to be involved in the cyst formation [4–6].

BHDS is a rare, inherited autosomal dominant genodermatosis caused by a germline mutation in the folliculin (*FLCN*) gene, and was first reported in 1975 and 1977 [7, 8]. The three major manifestations of BHDS are fibrofolliculomas and

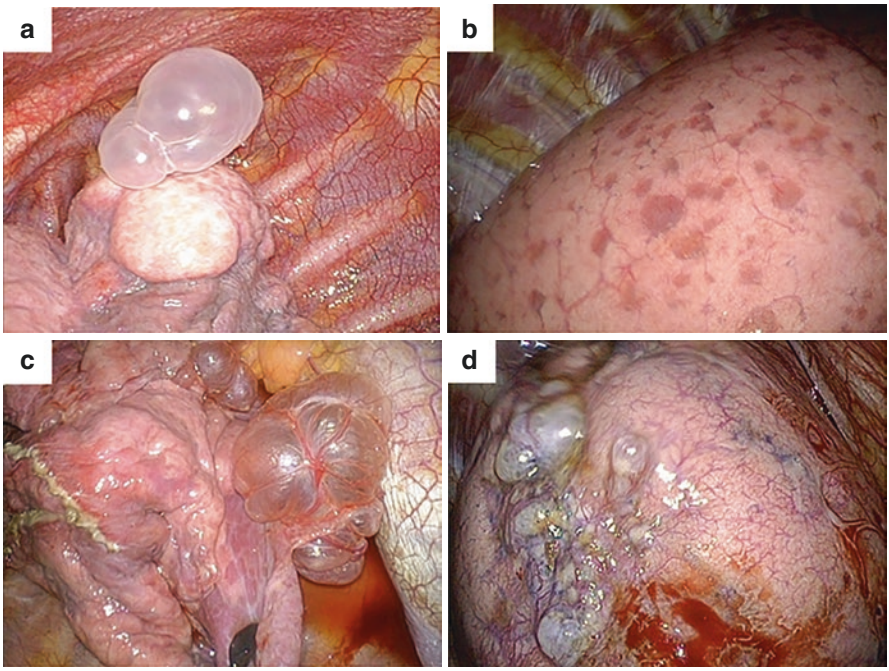

Fig. 16.1 Thoracoscopic findings of lung surface in patients with primary PSP (**a**), LAM (**b**), BHDS (**c**), and PLCH (**d**). In PSP, a transparent white bulla is protruding from the apical part of the upper lobe. Bullae can be identified at the apical segment of lower lobes and multiple bullae are often present. In LAM, numerous brown spots scattered over the entire lung surface are noted when the lungs are deflated. When the lung is more inflated, multiple, transparent, thin-walled cysts with a wide base on the lung surface can be recognized. In BHDS, bullae are usually identified on the basilar and medial areas of lower lobes. They have a transparent, thin wall with a wide base on the lung surface. Some of them are huge and lobulated with a bundle of connective tissue septa and small blood vessels. In PLCH, anthracosis due to smoking habits is noted in the area of multiple bullae and other parts of the lung surface. Conglomerated bullae with various sizes are found and some have a thin wall

trichodiscomas of the skin, renal tumors, and multiple lung cysts with or without a pneumothorax [9]. On high-resolution computed tomography of the lungs, the pulmonary cysts in BHDS have thin walls, are oval to irregular in shape, and vary in size. They are predominantly located in the basal and the lower medial zones, and approximately 40% of cysts are located alongside pleural surfaces and often abut peripheral pulmonary vessels [10, 11]. When BHDS patients undergo surgery because of a pneumothorax, thoracoscopy reveals multiple, huge bullae protruding from the lung surface (see Fig. 16.1c). These bullae are usually distributed among lower lung and the interlobar regions, but these are not solely confined to the lower lobes of the lungs. Narrow-band imaging (NBI) modes (filtered xenon light with emission bands at 415 nm and at 540 nm) produced by high-definition thoracoscopy clearly reveals numerous small and flat bullae contiguous to the interlobular septa. These are observed over the entire visceral pleura, aside from the multiple

protuberant cysts typically identified in the lower lobes, which are difficult to detect by standard white-light imaging (unfiltered xenon light) [12].

The mechanisms for bullae formation remain undetermined in BHDS, but several different mechanisms may be involved. The results of histopathological examination of 229 pulmonary cysts from 50 unrelated patients found that 54.9% of cysts examined had no inflammation [13]. This histopathological study indicated that BHDS cysts are likely to develop in the periacinar region, an anatomically weak site in a primary lobule, where alveoli attach to connective tissue septa [13]. Recently, the analyses of FLCN haploinsufficient lung fibroblasts isolated from BHDS patients demonstrated functional impairment *in vitro*. BHDS lung fibroblasts showed a marked diminution in their abilities to migrate, contract, and produce extracellular matrix proteins, which might lead to impaired tissue repair and organ fragility [14]. Another study reported the importance of alveolar epithelial cell apoptosis in cyst formation. Increased alveolar epithelial cell apoptosis was demonstrated in the BHDS lungs and conditional *flcn* knockdown in the mouse lung epithelium leads to cell apoptosis, alveolar enlargement, and an impairment of both epithelial barrier and overall lung function [15].

Pneumothorax is relatively common in PLCH and thoracoscopic findings of PLCH patients who have a pneumothorax clearly reveal the formation of multiple bullae (see Fig. 16.1d). PLCH is characterized by proliferation of specialized mucosa-associated dendritic cells known as Langerhans cells along the airways and in lung parenchyma [16]. Cigarette smoking appears to be an important factor promoting the accumulation and activation of Langerhans cells and other immune cells. Recently, *BRAF* or *MAP2K1* mutations in Langerhans cells were identified in about 40–50% of patients with PLCH [17, 18], indicating that some were polyclonal reactive proliferations induced by cigarette smoke exposure, whereas the remaining were neoplasms driven by *BRAF* or *MAP2K1* mutations. Matrix metalloproteases produced by accumulating immune or inflammatory cells are believed to contribute to bronchiolar destruction and cyst formation [19].

Clinical Manifestations and Prevalence

The clinical manifestations of spontaneous pneumothorax are similar across the various DCLDs. Sudden-onset chest pain and dyspnea either on exertion or at rest are common. In certain instances, however, patients may be asymptomatic or unaware, and the existence of a pneumothorax is incidentally discovered at a regular health check-up or an evaluation of other conditions. The prevalence of a pneumothorax in the context of an underlying DCLD is quite different. Among various DCLDs, LAM, BHDS, and PLCH are most frequently complicated by a pneumothorax. Conversely, for example, patients with Sjögren's syndrome seldom develop a pneumothorax.

Approximately 50–70% of LAM patients are reported to experience at least one spontaneous pneumothorax in their lifetime. A pneumothorax often becomes a

Table 16.1 Salient features of spontaneous pneumothoraces in DCLDs compared to PSP

Condition	Median age of first pneumothorax (years)	Recurrence rate, if managed conservatively (%)	Recurrence rate following pleurodesis (%)
PSP	15–34	30	<5%
LAM	35	71	32
BHD	37	73	35
PLCH	29	56	0–20

BHDS Birt-Hogg-Dube syndrome, *DCLD* diffuse cystic lung disease, *PLCH* pulmonary Langerhans cell histiocytosis, *PSP* primary spontaneous pneumothorax
Adapted from Gupta [20], with permission from John Wiley and Sons

presenting feature leading to the diagnosis of LAM. Patients usually have the first pneumothorax in their late 20s, with a median age of 35 years (Table 16.1) [20]. The recurrence rate of a pneumothorax for LAM patients is quite as high with an approximate rate of 70%, if managed conservatively [20]. A pneumothorax and chylothorax can occur concurrently.

BHDS patients share similar clinical features, age at onset, and recurrence rate of pneumothorax as patients with LAM (see Table 16.1). An epidemiological survey demonstrated that patients with BHDS have a 50-fold likelihood of developing a pneumothorax as compared to age-matched controls [9]. A pneumothorax can occur as early as 7 years of age [21], or as late as 73 years of age [22]. Among the three characteristic manifestations of BHDS (i.e., fibrofolliculomas of the skin, pulmonary cysts with or without a pneumothorax, and renal neoplasms), a pneumothorax can occur earliest [9]. Accordingly, a pneumothorax can become a key event for establishing the diagnosis of BHDS, and pulmonologists play an important role in making a timely diagnosis. It is necessary to determine whether any hereditary conditions exist, which may predispose certain patients to renal neoplasms. A family history of spontaneous pneumothorax is one of the specific features to distinguish BHDS from other DCLDs [11, 23].

About 15–20% of patients with PLCH are reported to experience a pneumothorax. The reported median age of the first pneumothorax in PLCH patients is 29 years old [20], and younger than those in LAM and BHDS patients (see Table 16.1). The recurrence rate of pneumothoraces in PLCH patients is less than that observed in LAM and BHD patients, and approximately half of PLCH patients are reported to experience a recurrence if managed conservatively [20]. However, the prevalence of a pneumothorax in PLCH is likely to be influenced by the study cohort. LCH is now recognized as a myeloid neoplastic disorder driven by an activated MAPK pathway, which causes misguided myeloid differentiation with the extent of disease determined by the cell of origin in which activating MAPK somatic mutations arise [24]. Additionally, ethnic difference in susceptibility to LCH and the response to therapy is suggested to exist [24]. Some PLCH patients show a very mild phenotype. Successful smoking cessation can effectively manage disease activity in a large proportion of patients with PLCH. Pulmonary cysts can disappear in some patients after smoking cessation.

Treatment of Pneumothorax

General Considerations

Treatment for a spontaneous pneumothorax in patients with DCLDs has two objectives: (1) to identify the area of visceral pleura causing air leakage into pleural space and repair it, and (2) to prevent or decrease the likelihood of recurrence. Although DCLDs consist of heterogeneous disorders with each having a different pathophysiological mechanism for forming cysts and developing a pneumothorax, controlled studies regarding these two objectives are rare in the literature for both individual disorders and collectively for secondary spontaneous pneumothorax (SSP).

The 2010 British Thoracic Society (BTS) Guidelines [25] state the following: (1) the management of SSP requires the insertion of a small-bore chest drain in most patients, (2) all patients with SSP will require early referral to a chest physician, and (3) a persistent air leak should be discussed with a thoracic surgeon after 48 hours. Simple aspiration is typically less likely to be successful in SSP as compared to PSP [25]. A substantial percentage of air leaks was reported to cease by 7 days even in patients with SSP [26] when managed by conservative tube drainage (61% for SSP vs. 75% for PSP). However, surgical intervention becomes the treatment of choice if air leaks continue beyond 7 days. Another study recommended considering surgery earlier, after 48 hours rather than 7 days, to increase the efficacy of surgery and reduce incidence of complications, as well as increase the likelihood of maximal healing [27]. If tube drainage fails to stop air leaks, either open thoracotomy with pleurectomy or VATS with pleurectomy and pleural abrasion is recommended; both can attain the two objectives described above simultaneously and effectively. However, the first objective of identifying the area of visceral pleura causing air leakage into pleural space and repairing it is often difficult to achieve in DCLDs. Since the lung surface is often very fragile in DCLDs, as represented by the LAM lungs in which there are multiple transparent, tiny cysts scattered over the visceral pleura (see Fig. 16.1b), surgical manipulation itself often causes *de novo* air leakage. To achieve the second objective of preventing or decreasing the likelihood of recurrence, surgical chemical pleurodesis can be chosen instead of pleurectomy and pleural abrasion. The use of graded talc is recommended in the BTS guidelines based on a systematic review of uncontrolled trials showing a success rate of 87% [28]. The ATS/JRS LAM Clinical Practice Guidelines recommend that VATS-guided pleural abrasion is the first-line method to achieve pleurodesis following an episode of spontaneous pneumothorax, with talc reserved for intractable episodes despite careful pleural abrasion [29].

Special Considerations Regarding the Treatment of a Pneumothorax Complicated by Diffuse Cystic Lung Diseases

Even following “the standard approach” to treating SSP described above, a high recurrence rate of pneumothorax has been reported in DCLDs. For various DCLDs, the recurrence rates of pneumothorax if managed conservatively are summarized in

Table 16.1 [20]: 71% for LAM, 73% for BHDS, and 56% for PLCH. Even after pleurodesis, the recurrence rate was found to be high: 32% for LAM, 35% for BHDS, and 0–20% for PLCH. These figures are remarkably high compared to those found in PSP: 30% of recurrence with conservative management and < 5% if pleurodesis is performed. Based on these circumstances, particularly the high recurrence rates of a pneumothorax, the American Thoracic Society (ATS)/Japanese Respiratory Society (JRS) guidelines for pleural disease management in LAM recommended that LAM patients be offered ipsilateral pleurodesis after the initial pneumothorax rather than waiting for a recurrence to intervene with a pleural symphysis procedure [29]. No such guidelines for the management of a pneumothorax in other DCLDs are currently available. This recommendation may be applicable for the other DCLDs with high recurrence rates of pneumothorax such as BHDS and PLCH.

Several precautions are required for applying the above-mentioned recommendations in routine practice not only for LAM patients but also for patients with other DCLDs that show high recurrence rates of a pneumothorax [29]. First, the decision to perform pleurodesis and the type of pleurodesis (chemical vs. surgical) should be based on shared decision-making between clinicians and patients, after discussing the various management options. The high recurrence rates after pleurodesis must also be considered [20]. Second, the approach to offer ipsilateral pleurodesis after the initial pneumothorax is based on the high recurrence rates and the overall balance between desirable and undesirable consequences [29]. Since pooled data from primarily observational studies usually do not describe the rates, types, and severity of complications due to pleurodesis, the possibility of a publication bias in favor of pleurodesis cannot be excluded. In reality, the extent and area of pleural symphysis may not be fully controllable, and symphysis may not occur uniformly in the entire hemithorax as we might expect. Due to the respiratory movement of the lungs and the continuous heartbeats, the mediastinal and interlobar areas may fail to form close apposition resulting in partial symphysis, which can lead to recurrent/chronic pneumothoraces (Fig. 16.2). These complications can render further interventions such as simple aspiration more difficult to perform, and may also cause residual restrictive ventilatory impairment. Third, regarding LAM treatment, circumstances have dramatically changed from the era when there was no established therapy to the current times with effective molecular targeted therapy using sirolimus to suppress disease progression [30]. Currently there are no good quality data regarding the impact and role of sirolimus in the occurrence and recurrence of a pneumothorax, and the difference in cost-effectiveness between conservative management of pneumothorax followed by the initiation of sirolimus versus the current standard management of performing early pleurodesis after the initial pneumothorax. Determining the effect of sirolimus on the future risk of pneumothoraces in patients with LAM is a high priority future research question.

Pleurodesis was originally invented by Spengler in 1906 to induce adhesive pleuritis with the use of silver nitrate [31]. Pleurodesis still works well for PSP patients, together with improvement of irritating agents, probably because the area of fragile visceral pleura and underlying lung tissue is limited in PSP as compared to DCLDs.

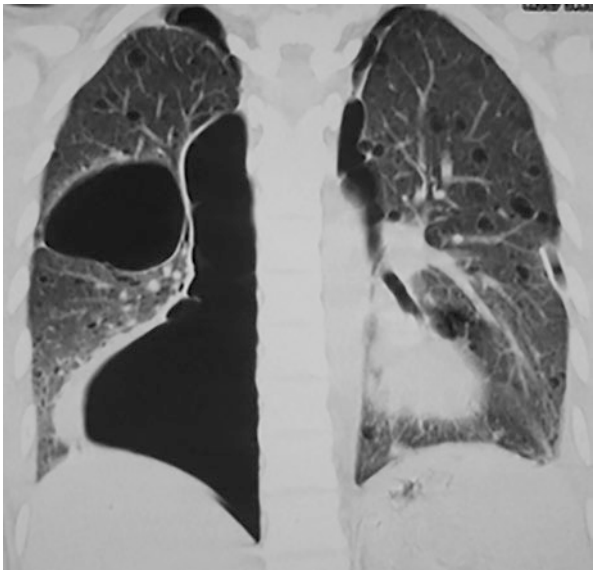

Fig. 16.2 A chronic pneumothorax due to partial pleural symphysis, developed after a repeat pleurodesis. A coronal re-formatted view of a 22-year-old female with tuberous sclerosis complex-associated LAM showed abnormal airspaces in both the mediastinal side and the interlobar area of the right hemithorax. Note that there was no way to reach the airspace since firm pleural symphysis had developed, primarily in the lateral side of the right hemithorax. Although the extent of cystic destruction of the lung is mild, this patient suffered from a severe degree of dyspnea on exertion

However, other methods besides pleurodesis to prevent or decrease the likelihood of recurrence are needed, particularly for pneumothoraces in patients with DCLDs. The recurrence rates after pleurodesis are unacceptably high, and there may be undesirable complications if pleurodesis fails to attain its intended aim.

Alternative Methods to Manage Pneumothorax in Patients with Diffuse Cystic Lung Diseases

There are two desirable features that alternative methods should fulfill. First, the target of treatment should be confined to the visceral pleura without involving healthy parietal pleura. This is important to keep the pleural physiology as normal as possible. Second, treatment should be individualized depending on the pathophysiologic condition of each underlying disease since DCLDs are heterogeneous disorders.

A technique of total pleural covering (TPC) to wrap the entire visceral pleura with sheets of oxidized regenerated cellulose (ORC) mesh, a bioabsorbable material, was initially invented for pneumothorax in LAM patients (Fig. 16.3) [32], and later applied for pneumothorax in BHDS patients [12]. The concept of TPC is to reinforce the diffusely diseased visceral pleura over its entire surface without severe

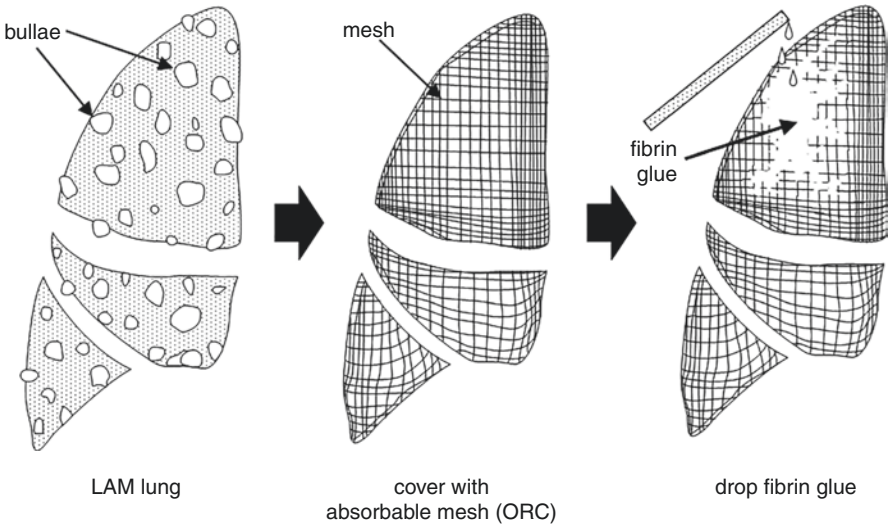

Fig. 16.3 Schematic presentation of TPC workflow. TPC procedure for a LAM lung consisting of covering the lung's entire visceral pleura with sheets of ORC mesh and subsequently spreading drops of fibrin glue. The entire procedure is performed under VATS. Adapted from Kurihara et al. [32]. Copyright: © 2016 Kurihara et al. This is an open access article distributed under the terms of the Creative Commons Attribution License, which permits unrestricted use, distribution, and reproduction in any medium, provided the original author and source are credited

pleural symphysis (ideally with no pleural symphysis). By adhering to this concept, a potential risk of intra- or postoperative massive hemorrhage and other complications is likely to be avoided when LAM patients undergo lung transplantation surgery in future. The technique almost fulfills the two requirements described above and is specifically suited for a pneumothorax developing in patients with DCLDs. To meet the first objective, there should be no involvement of the parietal pleura and few pleural symphyses after the application of TPC; the choice of covering material to reinforce the affected visceral pleura is quite critical [12, 32]. There are three different covering materials that are commercially available for reinforcing the staple line after a partial resection of the lungs with Endo-staplers: ORC (Ethicon SURGICEL®, absorbable Hemostat gauze, Johnson & Johnson, Brunswick, NJ, USA), polyglactin 910 mesh (VIC) (Vicryl™, Johnson & Johnson, Brunswick, NJ, USA), and polyglycolic acid sheets (PGA) (NEOVEIL® sheet, Gunze, Tokyo, Japan). Among these, experiments using canine models revealed that both VIC mesh and PGA sheets induced extensive pleural symphysis accompanying fibroblast proliferation and collagen deposition, whereas ORC sheets induced the visceral pleura to thicken five times more than the normal pleura without severe adhesion to parietal pleura. In this context, if VIC mesh or PGA sheets were utilized for TPC, it could lead to significant restrictive ventilatory impairment in patients. When ORC sheets were applied to reinforce staple line after bullous parts of the lung were resected, it was confirmed that the visceral pleura in the covered area was

truly thickened more than the normal visceral pleura. Histopathological examinations of lung specimens from patients with PSP who had surgery due to the recurrence of a pneumothorax (after staple line covering with ORC) showed that the thickness of the visceral pleura was approximately four times greater at 3 months and three to nine times thicker at 1 year than that of normal visceral pleura [33].

The results of TPC when performed in 43 LAM patients (applied for 54 hemithoraces) showed that a pneumothorax recurred in 14 hemithoraces (25.9%) from 11 patients (25.6%). Kaplan-Meier estimates of recurrence-free hemithoraces were 80.8% at 2.5 years, 71.7% at 5 years, and 61.4% at 9 years [32]. The recurrence-free hemithoraces in LAM patients for whom 10 or more ORC sheets were used to cover the visceral pleura (n, 39 hemithoraces) were much better than those where fewer than 10 sheets were used (n, 15 hemithoraces). In this cohort of LAM patients, TPC significantly reduced the frequency of a pneumothorax from 0.544 ± 0.606 episode/month (mean ± SD) to 0.008 ± 0.019. Grade IIIa postoperative complications were reported in 13 TPC surgeries (24.1%) such as insertion of a chest tube or other managements of delayed occurrence of air leakage, insertion of a chest tube for pleural effusion, or wound infection. Post-TPC lung function did not show apparent restrictive ventilatory impairments, and postoperative vital capacity was more than 80% of the predicted value even in LAM patients who had bilateral TPC.

The results of TPC applied for 81 BHDS patients (90 hemithoraces) were also reported recently [12]. In this study, although it is retrospective and observational, the results of a lower pleural covering (LPC) (n, 38 hemithoraces) by which only the affected area (usually lower part of the lungs) was covered with ORC were compared to those using TPC (n, 52 hemithoraces). Pneumothorax recurrence rates after LPC at 2.5, 5, and 7.5 years postoperatively were 5.4%, 12%, and 42%, respectively, whereas none of the patients who had undergone TPC developed postoperative pneumothorax recurrences. The difference in recurrence rates between LPC and TPC clearly illustrates that the entire area of visceral pleura in BHDS patients is affected by the inherent disease process, who are prone to develop pneumothoraces. As previously described, this has been confirmed when BHDS lungs have been carefully observed by thoracoscopic NBI modes. As shown by the low recurrence rates in both LAM and BHDS patients who had undergone TPC, the concept that the target of pneumothorax treatment should be the visceral pleura to reinforce its fragility is likely to be applicable to other DCLDs. However, like for any given surgical procedure, the outcomes are better if performed by experienced personnel, and this technique needs to be carefully validated at external sites prior to widespread utilization for all patients with DCLDs.

Issues Specific to Pneumothorax in Diffuse Cystic Lung Diseases

A pneumothorax is usually not a life-threatening condition, and pneumothoraces can be managed by various means. In this context, the primary outcome measure of

pneumothorax treatment is not overall survival as is the case with fatal diseases such as lung cancer, but rather should include various measures of treatment efficacy, such as length of hospital stay, recurrence rate, treatment-related morbidity or adverse effects, cost-benefit balance, and patient's health-related quality of life after treatment. The significance and implications of these outcome measures will be profoundly influenced by culture, economy, medical insurance systems, and availability or feasibility of treatment in various countries. For example, the ATS/JRS guidelines for LAM place a higher value on the reduction of morbidity and costs associated with recurrent pneumothoraces, but a lower value on the adverse effects of pleurodesis. However, in light of the benefit-adverse effect balance of pleurodesis, the recommendation "performing pleurodesis after an initial pneumothorax" may not be suitable for all situations. For example, the advent of sirolimus as an effective molecular targeted agent for LAM might reduce the likelihood of future pneumothoraces [34], and is quite likely to influence the management approach of pneumothorax in LAM patients.

Other Pleural Manifestations in Diffuse Cystic Lung Diseases

Chylothorax in Lymphangioleiomyomatosis

Chylothorax is a type of pleural effusion in which chyle is accumulated in the pleural space. Chyle has a distinctive white, odorless, and milky appearance. The diagnosis of chylothorax is established if the pleural fluid triglyceride level is above 110 mg/dL and the ratio of pleural fluid to serum cholesterol is less than 1.0. The cholesterol ratio is used to exclude pseudochylothorax, the condition in which the long-standing accumulation of pleural effusions produces a chyliform effusion with large amounts of cholesterol or lecithin-globulin complexes.

Among various diseases classified in DCLDs, chylothorax is a well-recognized complication of LAM and can be diagnostic of LAM when occurring in the right clinical context, typically a young-middle-aged female with characteristic cystic change on chest CT [29]. Chylous pleural effusion in LAM often shows a reddish-milk appearance indicating contamination with a small amount of blood. The literature describes the prevalence of chylothorax in LAM patients to be approximately 10–20% [35, 36]. In most instances, chylothorax is unilateral without a side preference, and may accompany chylous ascites or chylous pericardial effusion. Chylothorax, with or without progressive dyspnea, can occur as a presenting feature or an event leading to the diagnosis of LAM. It can also develop during the clinical course of the disease after the establishment of a LAM diagnosis. Chylothorax can occur during pregnancy [37] or develop in the hemithorax where a lung transplantation was performed; it is one of the most frequent complications after lung transplantation [38].

The precise mechanisms for chylothorax to develop in LAM patients remains unknown, but it is generally believed that it results from obstruction of lymphatic

vessels by the infiltration of proliferating LAM cells [39]. Histopathological examinations of axial lymphatics including the thoracic duct suggest that LAM-associated lymphangiogenesis also plays a role in chyle leakage [40, 41]. LAM cells proliferate in retroperitoneal lymph nodes and the walls of lymphatic vessels to form cystic dilation of lymphatic vessels. Each extrapulmonary LAM lesion has abundant lymphatic vessels, which can be demonstrated by the examination of the wall of lymphatic vessels and the interstitial tissue around the lymphatic vessels. Not only is the increased pressure in lymphatic vessels due to obstruction of lymphatics by the proliferation LAM cells, but the extra connection between lymphatics and the surrounding interstitial tissues due to LAM-associated lymphangiogesis are also likely to be involved in chyle leaks in LAM patients [40, 41]. It has also been reported that a direct communication between pleural and peritoneal cavities through diaphragmatic LAM lesions and associated abundant lymphatic vessels can contribute to the simultaneous occurrence of chylothorax and chylous ascites [42].

Chylous pleural effusion provides a unique opportunity to make a diagnosis of LAM without histopathological confirmation via invasive biopsies. LAM cell clusters (LCC), a well-organized, globular cluster consisting of LAM cells enveloped by a monolayer of lymphatic endothelial cells, can be identified if processed properly; preparation of a cell-block or collection of LCC by passing chylous effusion through a 40 μm pore-sized filter usually facilitates the detection of LCC [43]. The detection rate of LCC accumulated in chyle is likely to be higher when the earlier the fluid is obtained; the number of LCC in fluid will decrease after repeated drainage since the rate of LCC shedding via LAM-associated lymphangiogenesis is expected to not be very high.

Management of Lymphangioleiomyomatosis-Associated Chylous Pleural Effusion with Sirolimus Therapy

Before the era of sirolimus, the management of chylothorax was problematic. Nutritional approaches to try to reduce the amount of chyle leaks revealed varying degree of efficacy, including fat-restricted diets, the substitution of long-chain dietary fats with medium-chain triglycerides, or total parenteral nutrition. Repeated aspiration or continuous chest tube drainage can ameliorate symptoms related to chylothorax, but this approach is prone to lead to malnutrition as well as secondary immunodeficiency due to loss of abundant nutrients and lymphocytes in chyle, respectively. To avoid these risks, chemical or surgical pleurodesis used to be the chosen methods to manage chylothorax. However, sirolimus therapy has recently been shown to be very effective in managing LAM-associated chylous leaks, lymphatic congestion or lymphedema, and lymphangioleiomyomas [30, 44–46]. Accordingly, the official ATS/JRS LAM clinical practice guidelines recommend that LAM patients with symptomatic chylous fluid accumulations (e.g., chylous effusions and chylous ascites) be treated with sirolimus prior to invasive

management (e.g., intermittent percutaneous drainage and insertion of indwelling drainage devises) [47]. Findings to date have indicated that sirolimus therapy has been very effective in managing chyle leaks in LAM patients, and this drug appears to be durable for patients who have been on sirolimus therapy [44, 45].

Key Learning Points

- Pneumothorax is often a sentinel event for the diagnosis of diffuse cystic lung diseases, especially lymphangioleiomyomatosis, Birt-Hogg-Dubé syndrome, and Langerhans cell histiocytosis, as a consequence of disease involvement in visceral pleura.
- Controlled studies regarding the treatment for pneumothorax associated with diffuse cystic lung diseases are rare in the literature. However, two objectives should be born in mind: to identify the air-leakage point and repair it and to prevent or decrease the likelihood of recurrence.
- Chylothorax is a pleural disease peculiar to lymphangioleiomyomatosis and can be mostly managed with sirolimus.

References

1. Cooley J, Lee YCG, Gupta N. Spontaneous pneumothorax in diffuse cystic lung diseases. Curr Opin Pulm Med. 2017;23(4):323–33.
2. Gupta N, Vassallo R, Wikenheiser-Brokamp KA, McCormack FX. Diffuse cystic lung disease. Part II. Am J Respir Crit Care Med. 2015;192(1):17–29.
3. Gupta N, Vassallo R, Wikenheiser-Brokamp KA, McCormack FX. Diffuse cystic lung disease. Part I. Am J Respir Crit Care Med. 2015;191(12):1354–66.
4. Dongre A, Clements D, Fisher AJ, Johnson SR. Cathepsin K in Lymphangioleiomyomatosis: LAM cell-fibroblast interactions enhance protease activity by extracellular acidification. Am J Pathol. 2017;187(8):1750–62.
5. Hayashi T, Fleming MV, Stetler-Stevenson WG, Liotta LA, Moss J, Ferrans VJ, et al. Immunohistochemical study of matrix metalloproteinases (MMPs) and their tissue inhibitors (TIMPs) in pulmonary lymphangioleiomyomatosis (LAM). Hum Pathol. 1997;28(9):1071–8.
6. Matsui K, Takeda K, Yu ZX, Travis WD, Moss J, Ferrans VJ. Role for activation of matrix metalloproteinases in the pathogenesis of pulmonary lymphangioleiomyomatosis. Arch Pathol Lab Med. 2000;124(2):267–75.
7. Birt AR, Hogg GR, Dube WJ. Hereditary multiple fibrofolliculomas with trichodiscomas and acrochordons. Arch Dermatol. 1977;113(12):1674–7.
8. Hornstein OP, Knickenberg M. Perifollicular fibromatosis cutis with polyps of the colon – a cutaneo-intestinal syndrome sui generis. Arch Dermatol Res. 1975;253(2):161–75.
9. Zbar B, Alvord WG, Glenn G, Turner M, Pavlovich CP, Schmidt L, et al. Risk of renal and colonic neoplasms and spontaneous pneumothorax in the Birt-Hogg-Dube syndrome. Cancer Epidemiol Biomarkers Prev. 2002;11(4):393–400.
10. Tobino K, Gunji Y, Kurihara M, Kunogi M, Koike K, Tomiyama N, et al. Characteristics of pulmonary cysts in Birt-Hogg-Dube syndrome: thin-section CT findings of the chest in 12 patients. Eur J Radiol. 2011;77(3):403–9.
11. Tobino K, Hirai T, Johkoh T, Kurihara M, Fujimoto K, Tomiyama N, et al. Differentiation between Birt-Hogg-Dube syndrome and lymphangioleiomyomatosis: quantitative analysis of pulmonary cysts on computed tomography of the chest in 66 females. Eur J Radiol. 2012;81(6):1340–6.

12. Mizobuchi T, Kurihara M, Ebana H, Yamanaka S, Kataoka H, Okamoto S, et al. A total pleural covering of absorbable cellulose mesh prevents pneumothorax recurrence in patients with Birt-Hogg-Dube syndrome. Orphanet J Rare Dis. 2018;13(1):78.
13. Kumasaka T, Hayashi T, Mitani K, Kataoka H, Kikkawa M, Tobino K, et al. Characterization of pulmonary cysts in Birt-Hogg-Dube syndrome: histopathological and morphometric analysis of 229 pulmonary cysts from 50 unrelated patients. Histopathology. 2014;65(1):100–10.
14. Hoshika Y, Takahashi F, Togo S, Hashimoto M, Nara T, Kobayashi T, et al. Haploinsufficiency of the folliculin gene leads to impaired functions of lung fibroblasts in patients with Birt-Hogg-Dube syndrome. Physiol Rep. 2016;4(21):e13025.
15. Goncharova EA, Goncharov DA, James ML, Atochina-Vasserman EN, Stepanova V, Hong SB, et al. Folliculin controls lung alveolar enlargement and epithelial cell survival through E-cadherin, LKB1, and AMPK. Cell Rep. 2014;7(2):412–23.
16. Vassallo R, Ryu JH, Schroeder DR, Decker PA, Limper AH. Clinical outcomes of pulmonary Langerhans'-cell histiocytosis in adults. N Engl J Med. 2002;346(7):484–90.
17. Mourah S, How-Kit A, Meignin V, Gossot D, Lorillon G, Bugnet E, et al. Recurrent NRAS mutations in pulmonary Langerhans cell histiocytosis. Eur Respir J. 2016;47(6):1785–96.
18. Roden AC, Hu X, Kip S, Parrilla Castellar ER, Rumilla KM, Vrana JA, et al. BRAF V600E expression in Langerhans cell histiocytosis: clinical and immunohistochemical study on 25 pulmonary and 54 extrapulmonary cases. Am J Surg Pathol. 2014;38(4):548–51.
19. Hayashi T, Rush WL, Travis WD, Liotta LA, Stetler-Stevenson WG, Ferrans VJ. Immunohistochemical study of matrix metalloproteinases and their tissue inhibitors in pulmonary Langerhans' cell granulomatosis. Arch Pathol Lab Med. 1997;121(9):930–7.
20. Gupta N. Primary spontaneous pneumothorax: looking beyond the usual. Acad Emerg Med. 2018;25(4):470–2.
21. Bessis D, Giraud S, Richard S. A novel familial germline mutation in the initiator codon of the BHD gene in a patient with Birt-Hogg-Dube syndrome. Br J Dermatol. 2006;155(5):1067–9.
22. Kunogi Okura M, Yae T, Nagashima O, Hirai S, Kumasaka T, Iwase A. Pneumothorax developing for the first time in a 73-year-old woman diagnosed with Birt-Hogg-Dube syndrome. Intern Med. 2013;52(21):2453–5.
23. Ebana H, Mizobuchi T, Kurihara M, Kobayashi E, Haga T, Okamoto S, et al. Novel clinical scoring system to identify patients with pneumothorax with suspicion for Birt-Hogg-Dube syndrome. Respirology. 2018;23(4):414–8.
24. Allen CE, Merad M, McClain KL. Langerhans-cell histiocytosis. N Engl J Med. 2018;379(9):856–68.
25. MacDuff A, Arnold A, Harvey J, Group BTSPDG. Management of spontaneous pneumothorax: British thoracic society pleural disease guideline 2010. Thorax. 2010;65(Suppl 2):ii18–31.
26. Chee CB, Abisheganaden J, Yeo JK, Lee P, Huan PY, Poh SC, et al. Persistent air-leak in spontaneous pneumothorax – clinical course and outcome. Respir Med. 1998;92(5):757–61.
27. Schoenenberger RA, Haefeli WE, Weiss P, Ritz RF. Timing of invasive procedures in therapy for primary and secondary spontaneous pneumothorax. Arch Surg. 1991;126(6):764–6.
28. Kennedy L, Sahn SA. Talc pleurodesis for the treatment of pneumothorax and pleural effusion. Chest. 1994;106(4):1215–22.
29. Gupta N, Finlay GA, Kotloff RM, Strange C, Wilson KC, Young LR, et al. Lymphangioleiomyomatosis diagnosis and management: high-resolution chest computed tomography, Transbronchial lung biopsy, and pleural disease management. An official American thoracic society/Japanese respiratory society clinical practice guideline. Am J Respir Crit Care Med. 2017;196(10):1337–48.
30. McCormack FX, Inoue Y, Moss J, Singer LG, Strange C, Nakata K, et al. Efficacy and safety of sirolimus in lymphangioleiomyomatosis. N Engl J Med. 2011;364(17):1595–606.
31. Grossman LA. Recurrent bilateral spontaneous pneumothorax treated with artificial hemothorax. Ann Intern Med. 1953;39(6):1303–7. (Note; Since Spengler's work from 1906 is not only old but also in German, here listed the Grossman's article in which Spengler's work from 1906 was cited.)

32. Kurihara M, Mizobuchi T, Kataoka H, Sato T, Kumasaka T, Ebana H, et al. A total pleural covering for lymphangioleiomyomatosis prevents pneumothorax recurrence. PLoS One. 2016;11(9):e0163637.
33. Ebana H, Hayashi T, Mitani K, Kobayashi E, Kumasaka T, Mizobuchi T, et al. Oxidized regenerated cellulose induces pleural thickening in patients with pneumothorax: possible involvement of the mesothelial-mesenchymal transition. Surg Today. 2018;48(4):462–72.
34. Zhou L, Ouyang R, Luo H, Ren S, Chen P, Peng Y, et al. Efficacy of sirolimus for the prevention of recurrent pneumothorax in patients with lymphangioleiomyomatosis: a case series. Orphanet J Rare Dis. 2018;13(1):168.
35. Almoosa KF, McCormack FX, Sahn SA. Pleural disease in lymphangioleiomyomatosis. Clin Chest Med. 2006;27(2):355–68.
36. Hayashida M, Seyama K, Inoue Y, Fujimoto K, Kubo K. Respiratory failure research Group of the Japanese ministry of health L, welfare. The epidemiology of lymphangioleiomyomatosis in Japan: a nationwide cross-sectional study of presenting features and prognostic factors. Respirology. 2007;12(4):523–30.
37. Johnson SR, Taveira-DaSilva AM, Moss J. Lymphangioleiomyomatosis. Clin Chest Med. 2016;37(3):389–403.
38. Oishi H, Watanabe T, Matsuda Y, Noda M, Ejima Y, Saiki Y, et al. Single lung transplantation for lymphangioleiomyomatosis: a single-center experience in Japan. Surg Today. 2018;48(10):944–50.
39. Graham ML 2nd, Spelsberg TC, Dines DE, Payne WS, Bjornsson J, Lie JT. Pulmonary lymphangiomyomatosis: with particular reference to steroid-receptor assay studies and pathologic correlation. Mayo Clin Proc. 1984;59(1):3–11.
40. Kumasaka T, Seyama K, Mitani K, Sato T, Souma S, Kondo T, et al. Lymphangiogenesis in lymphangioleiomyomatosis: its implication in the progression of lymphangioleiomyomatosis. Am J Surg Pathol. 2004;28(8):1007–16.
41. Kumasaka T, Seyama K, Mitani K, Souma S, Kashiwagi S, Hebisawa A, et al. Lymphangiogenesis-mediated shedding of LAM cell clusters as a mechanism for dissemination in lymphangioleiomyomatosis. Am J Surg Pathol. 2005;29(10):1356–66.
42. Takagi Y, Sato T, Morio Y, Kumasaka T, Mitani K, Miyamoto H, et al. A pleuro-peritoneal communication through the diaphragm affected with lymphangioleiomyomatosis. Intern Med. 2010;49(5):439–45.
43. Mitani K, Kumasaka T, Takemura H, Hayashi T, Gunji Y, Kunogi M, et al. Cytologic, immunocytochemical and ultrastructural characterization of lymphangioleiomyomatosis cell clusters in chylous effusions of patients with lymphangioleiomyomatosis. Acta Cytol. 2009;53(4):402–9.
44. Taveira-DaSilva AM, Hathaway O, Stylianou M, Moss J. Changes in lung function and chylous effusions in patients with lymphangioleiomyomatosis treated with sirolimus. Ann Intern Med. 2011;154(12):797–805. W-292-793
45. Yao J, Taveira-DaSilva AM, Jones AM, Julien-Williams P, Stylianou M, Moss J. Sustained effects of sirolimus on lung function and cystic lung lesions in lymphangioleiomyomatosis. Am J Respir Crit Care Med. 2014;190(11):1273–82.
46. Moua T, Olson EJ, Jean HC, Ryu JH. Resolution of chylous pulmonary congestion and respiratory failure in lymphangioleiomyomatosis with sirolimus therapy. Am J Respir Crit Care Med. 2012;186(4):389–90.
47. McCormack FX, Gupta N, Finlay GR, Young LR, Taveira-DaSilva AM, Glasgow CG, et al. Official American thoracic society/Japanese respiratory society clinical practice guidelines: lymphangioleiomyomatosis diagnosis and management. Am J Respir Crit Care Med. 2016;194(6):748–61.

Chapter 17
Air Travel in Diffuse Cystic Lung Diseases

Adam G. Cole and Nishant Gupta

Introduction

Air travel is associated with increased risk for patients with chronic lung disease. In the absence of lung disease, the body's compensatory response to the hypobaric hypoxic environment of air travel is adequate, and respiratory symptoms account for only 10–15% of in-flight medical emergencies [1]. Much of the available literature regarding the clinical assessment of a patient's fitness to fly has focused on the risk of in-flight hypoxemia [2, 3]. In addition to hypoxemia, patients with diffuse cystic lung diseases (DCLDs) may also face an increased risk of in-flight pneumothorax. In this chapter, we discuss the physiologic changes that occur with air travel and their clinical implications for patients with DCLD.

Physiologic Response to Altitude

Though the cruising altitude of commercial aircrafts may vary from 14,875 feet to 47,000 feet, the Federal Aviation Administration (FAA) regulations require that commercial aircraft cabins be pressurized to an altitude of 8000 feet or 2438 meters [4, 5]. Barometric pressure at this elevation is 565 millimeters of mercury (mmHg),

A. G. Cole (✉)
Division of Pulmonary, Critical Care and Sleep Medicine, University of Kentucky College of Medicine, Lexington, KY, USA
e-mail: Adam.Cole@uky.edu

N. Gupta
Division of Pulmonary, Critical Care and Sleep Medicine, University of Cincinnati College of Medicine; Cincinnati Veterans Affairs Medical Center, Cincinnati, OH, USA
e-mail: guptans@UCMAIL.UC.EDU

N. Gupta et al. (eds.), *Diffuse Cystic Lung Diseases*, Respiratory Medicine,
https://doi.org/10.1007/978-3-030-63365-3_17

and the partial pressure of inspired oxygen (P_IO_2) is 100–105 mmHg, which is the equivalent of breathing 15.1% oxygen at sea level. In healthy individuals, this will result in a partial pressure of arterial oxygen (P_aO_2) of 60–70 mmHg, which is generally tolerated well, as would be expected based on the oxygen-hemoglobin dissociation curve (Fig. 17.1). Beginning at an altitude of 5000 feet night vision is affected, an effect most important for pilots. Per FAA regulations, pilots must use supplemental oxygen during nocturnal flights at altitudes above 5000 feet. Other than night vision impairment, healthy individuals do not usually have any symptoms of hypoxia below 12,000 feet. Between 12,000 and 15,000 feet, various central nervous system (CNS) effects occur, including euphoria, headache, mild cognitive impairment, drowsiness, dizziness, and headache. Above 15,000 feet, cognitive function can deteriorate significantly and quickly, with a pilot's ability to operate an aircraft substantially impaired in as little as 15 min. In addition, peripheral vision becomes severely impaired (tunnel vision) at 15,000 feet, and above 20,000 feet unconsciousness can occur in as quickly as 12 min [6, 7]. From a pulmonary standpoint, the physiologic response to hypoxia is to increase alveolar ventilation, thus minimizing the reduction in alveolar PO_2. This hypoxic ventilatory response is mediated by peripheral chemoreceptors in the carotid body [8]. In extreme

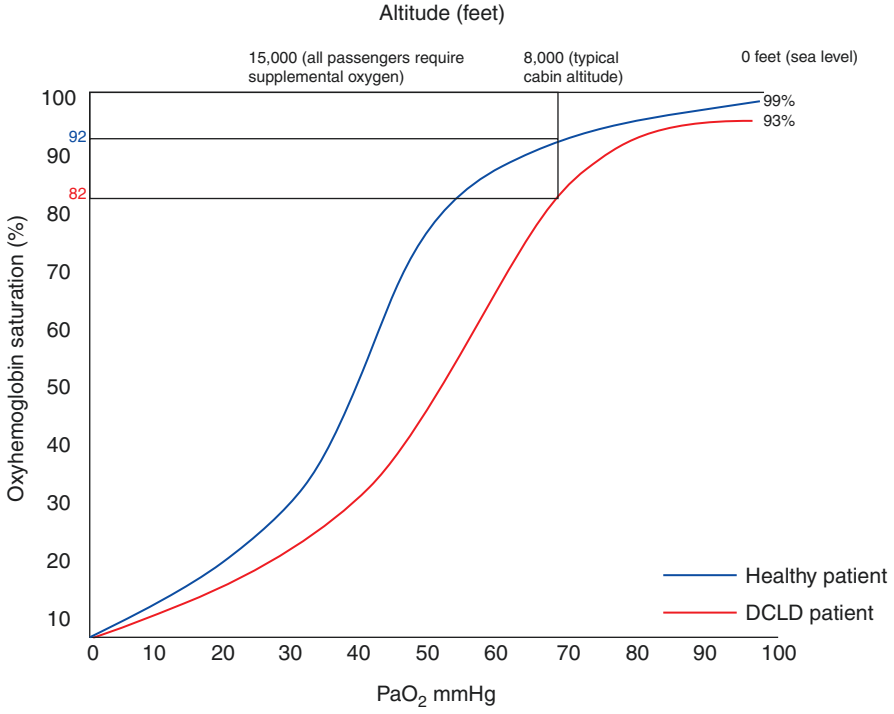

Fig. 17.1 Oxygen-hemoglobin dissociation curve for healthy individuals and patients with diffuse cystic lung disease at the equivalent altitude of a commercial airline cabin. DCLD diffuse cystic lung disease, PaO_2 arterial oxygen tension

scenarios, this response can be dramatic. For example, a study examined the arterial blood gas data from a simulated climb to the summit of Mt. Everest (through exposure to reduced PiO_2) and found the lowest $PaCO_2$ to be 9.8 mmHg. The average pH among that group was 7.53. These data demonstrate the significant hypoxic ventilatory response that could occur at high altitude, such as the hypobaric hypoxic environment of an airplane cabin [9]. In addition to the augmentation of minute ventilation mediated by the hypoxic ventilatory response, the pulmonary vasoconstriction caused by hypoxia leads to a redistribution of blood flow in the lungs in an attempt to improve ventilation-perfusion matching [10]. Finally, the diffusion of oxygen across the alveolar-capillary membrane is limited at altitude by multiple factors. The decrease in barometric pressure and consequent drop in alveolar partial pressure of oxygen (PAO_2) diminishes the pressure gradient for the diffusion of oxygen. This is especially notable with exercise, as the increase in cardiac output leads to a reduction in transit time for red blood cells through the pulmonary capillary bed, which exacerbates the diffusion impairment. Furthermore, the decreased PaO_2 at altitude lands on the steep portion of the oxygen-hemoglobin dissociation curve (see Fig. 17.1), which leads to a proportionally greater reduction in oxygen uptake [11]. Consequentially, small reductions in PaO_2 at altitude result in a significant reduction in oxygen delivery.

In the hypoxic environment at high altitude, cardiac output increases to maintain oxygen delivery to the peripheral tissues. This is mediated primarily through an increase in heart rate [12]. Stroke volume is actually decreased with exposure to altitude, possibly due to decreased LV preload as a result of the increased RV afterload from the hypoxic pulmonary vasoconstriction [13, 14]. Myocardial contractility appears to be maintained even at extreme altitude [13, 14].

The physiologic stress induced by the hypoxia of altitude is magnified in patients with underlying cardiopulmonary diseases. In certain cases, the attempts at compensation may be problematic. For example, a patient with obstructive lung disease may experience progressive expiratory flow limitation with attempts to increase minute ventilation, leading to dynamic hyperinflation and air trapping resulting in severe dyspnea. In patients with significant underlying lung disease and baseline gas exchange abnormalities, minimal exertion (e.g., ambulating to the lavatory) in the airplane could result in significant hypoxemia. For patients with cardiovascular disease, meeting the required augmentation in cardiac output may be difficult, potentially resulting in tissue hypoperfusion. Patients with pulmonary hypertension are at risk for the negative impact of hypoxia on the pulmonary vasculature and the potential increased right ventricular afterload (Fig. 17.2).

Physiologic Implications of Diving

Underwater diving results in exposure to increased pressure that is directly proportional to the depth of the dive, creating a hyperbaric environment in contrast to the hypobaric conditions encountered during air travel. This results in an increased risk

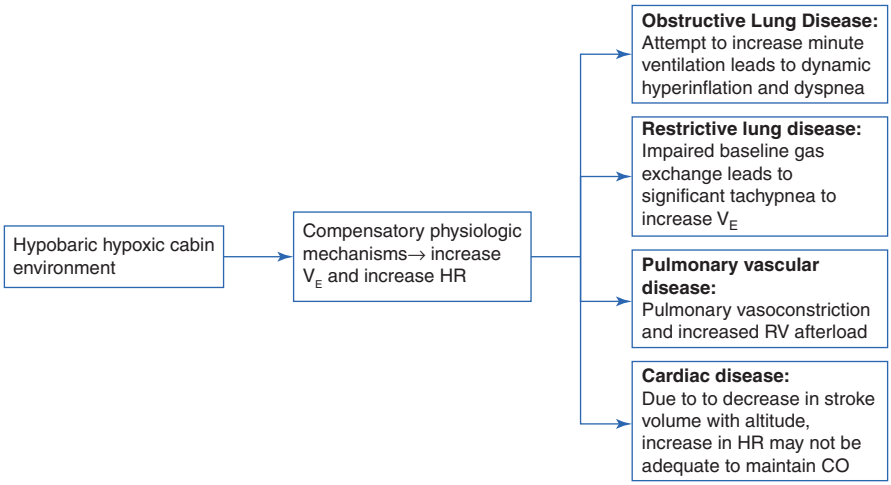

Fig. 17.2 Physiologic consequences of the hypobaric hypoxic cabin environment during commercial air travel in patients with underlying lung disease. CO cardiac output, HR heart rate, RV right ventricle, V_E minute ventilation

of pulmonary barotrauma, which could occur either during descent or ascent. For patients with DCLD, this barotrauma may manifest in the form of cyst rupture leading to a spontaneous pneumothorax. Divers breathe compressed gas that is pressurized to ambient pressure so that during descent the pressure gradients for the gas are not significantly altered. During ascent, the expansion of gas within the lungs can lead to increased transpulmonary pressures, which can lead to barotrauma. This effect is amplified by inadequate exhalation, which could be a result of breath holding or may occur because of underlying airway obstruction in patients with asthma, chronic obstructive pulmonary disease (COPD), certain DCLDs, etc. Immersion in water results in increased hydrostatic pressure, decreasing blood pooling in the peripheral circulation and therefore increasing venous return, central venous pressure, and cardiac output. Energy requirements for diving are substantial. Swimming even at slow nautical speeds requires significant oxygen consumption (VO_2). Divers with a peak $VO_2 < 20$ mL/kg/min may rapidly exceed their anaerobic threshold during a dive and develop severe dyspnea while underwater [15].

Clinical Implications

Hypoxia and Air Travel in DCLD

DCLD patients, similar to patients with other lung diseases, are at risk for worsening gas exchange during air travel due to the hypobaric hypoxic cabin environment. However, predicting the severity of in-flight hypoxia is challenging, and most

studies on this issue have focused on patients with COPD. Among DCLD patients, those with room air hypoxia or baseline long-term oxygen therapy (LTOT) requirement have the highest risk of in-flight hypoxia.

Pneumothorax and Air Travel in DCLD

The physiologic changes that occur with air travel raise a particular concern for in-flight pneumothorax in patients with DCLD. Boyle's law states that, assuming a constant temperature, the pressure and volume of a gas are inversely proportional. Therefore, as atmospheric pressure falls with air travel, gas volume expands. As noted by Baumann, this concept can be appreciated by observing a bag of potato chips during air travel – with ascent the expansion of the air in the sealed bag gives it the appearance of an inflated balloon [16].

If a parenchymal cyst has no communication with the tracheobronchial tree, significant volume expansion (up to 40%) can occur in flight [17], potentially leading to rupture of the cyst, which could cause a pneumothorax if the visceral pleura is disrupted. Postmus and colleagues postulate that variability in the size of the visceral pleural defect could affect the timing of pneumothorax development after flight. Smaller defects may result in the slow accumulation of air in the pleural space leading to a delayed presentation of pneumothorax. Furthermore, small defects may be asymptomatic and spontaneously seal. There have been some reports of patients with DCLD developing pneumothoraces several days after air travel, suggesting the possibility of this delayed presentation [18], although it is possible that these represent incidental events in a population enriched for spontaneous pneumothoraces, and are entirely unrelated to the air travel.

While the risk of hypoxia with air travel has been extensively addressed in the literature, there is comparatively little data available with respect to pneumothorax. The incidence of in-flight pneumothorax in the general population appears to be extremely low. A prospective multicenter observational study examining air travel outcomes for patients with lung disease found symptoms of in-flight respiratory distress reported by 18% of patients, but there were no in-flight pneumothoraces [19, 20]. In a retrospective analysis of 10,189 cases of in-flight medical emergencies on two European airlines, Sand and colleagues found no cases of pneumothorax [21]. Additionally, neither an analysis of 11,920 medical emergencies on multiple commercial airlines nor a recent systematic review of in-flight medical emergencies mentioned any cases of pneumothorax [22, 23]. However, given the physiologic possibility of cyst expansion during air travel, there is clinical concern for an increased risk of in-flight pneumothorax in patients with DCLD, and clinicians often are asked to provide counseling in this area. Although the data on the risk of development of spontaneous pneumothorax associated with air travel remain relatively sparse, there have been some studies examining the risk of pneumothorax with air travel in patients with certain DCLDs.

Lymphangioleiomyomatosis

Lymphangioleiomyomatosis (LAM) is a rare DCLD characterized by infiltration of the lung parenchyma with abnormal smooth muscle-like cells harboring mutations in the Tuberous Sclerosis Complex genes. This disease occurs almost exclusively in women, and it tends to be worse in premenopausal women as compared to postmenopausal women [24]. LAM is associated with a high risk of spontaneous pneumothorax, with 55–73% of patients experiencing at least one episode of pneumothorax in their lifetime [25]. Several studies have examined the issue of air travel–associated spontaneous pneumothorax in patients with LAM.

Pollock-BarZiv and colleagues surveyed LAM patients in the United States and the United Kingdom to ascertain the risk of air travel–associated spontaneous pneumothorax. Of the 276 women with LAM who had ever flown for a total of 454 flights, 10 women reported experiencing an air travel–related spontaneous pneumothorax, equating to a per-flight pneumothorax risk of 2.2%. However, in five of these patients, the symptoms of pneumothorax were present prior to boarding the plane, thus suggesting the pneumothorax occurred prior to initiation of air travel and that the actual risk of air travel–related pneumothorax in LAM may be closer to ~1% as compared to ~2% [26].

In another study, LAM patients traveling to the National Institutes of Health were assessed for the presence of pneumothorax at arrival to the center. Similar estimates were also generated for patients traveling to the NIH with other interstitial lung diseases such as idiopathic pulmonary fibrosis and sarcoidosis. A total of 281 LAM patients were evaluated in this study, and 16 arrived with a radiographically documented pneumothorax. In contrast, none of the patients with idiopathic pulmonary fibrosis or sarcoidosis had radiographic evidence of pneumothorax on arrival. In 9 out of the 16 LAM patients, the pneumothorax had preceded the study visit. From the remaining 7 patients, the authors estimated that the per-flight risk of air travel–related spontaneous pneumothorax in LAM is ~1%, and that the presence of pneumothorax after travel may be more related to the baseline increased risk of pneumothorax in LAM as opposed to a true travel-related increase in risk. Patients with reduced FEV1 and larger cysts on chest CT scans may be at higher risk of developing air travel–related spontaneous pneumothorax [27].

In the most recent study evaluating the relationship between air travel and risk of pneumothorax in LAM, Gonano and colleagues conducted a survey-based assessment of 145 LAM patients across multiple countries in the European Union and the United Kingdom. The authors calculated an estimate of ~3% per-flight risk of development of spontaneous pneumothorax in patients with LAM. Notable difference in this study as compared to the prior investigations is that any pneumothorax occurring within 30 days following air travel was considered to be related to air travel, thus likely leading to an over-estimation of the risk [28].

Birt-Hogg-Dubé Syndrome

Birt-Hogg-Dubé (BHD) syndrome is a rare autosomal dominant disorder caused by a germline mutation in the folliculin (*FLCN*) gene. BHD results in the development of hair follicle tumors (fibrofolliculomas), pulmonary cysts, and renal neoplasms. Lung cysts are usually lentiform and have a basilar distribution. The risk of spontaneous pneumothorax in BHD is approximately 50 times greater than the general population after adjusting for age [29]. In a retrospective survey-based analysis of 145 BHD patients who had flown at least once in their lifetime, Johannesma and colleagues estimated the risk of air travel and scuba diving–related spontaneous pneumothorax to be 0.63% and 0.33%, respectively. The risk of air travel–related pneumothorax was proportional to the number of cysts on chest CT [30]. In another survey-based assessment of 104 BHD patients recruited from the Rare Lung Diseases Clinic Network and the BHD Foundation, Gupta et al. estimated the air travel–related pneumothorax risk at 0.12 events per 100 flights (0.1%) [31].

Pulmonary Langerhans Cell Histiocytosis

Pulmonary Langerhans cell histiocytosis (PLCH) is a DCLD that results from the peribronchiolar accumulation of dendritic cells harboring activating mutations in the mitogen-activating protein kinase pathway, and it is strongly associated with exposure to cigarette smoke [32]. Spontaneous pneumothorax occurs in approximately 15–20% of patients with PLCH (27). In a recently published study, Singla and colleagues performed a survey-based assessment of 94 patients with PLCH. Eighty-two subjects had flown at least once in their lifetime for an estimated total of 742 flights. Two patients experienced an in-flight pneumothorax, amounting to an air travel–related pneumothorax risk of 0.27 per 100 flights (~0.3%). Individual-level risk factors that could portend a higher risk of air travel–related pneumothorax were not determined in this analysis owing to the lack of chest CT and pulmonary function test data on the subjects [33].

Air Travel Following an Episode of Spontaneous Pneumothorax

There is a paucity of evidence regarding when patients can safely undertake air travel following an episode of spontaneous pneumothorax. We follow the recommendations put forth by the British Thoracic Society and the International Air Transport Association, which suggest that air travel be delayed for 7 days following radiographic resolution of a spontaneous pneumothorax and 14 days following radiographic resolution of a traumatic pneumothorax [34, 35]. This duration may be shorter in patients who can travel with a Heimlich valve chest tube [36].

Summary of Air Travel–Related Spontaneous Pneumothorax in DCLDs

In general, the risk of spontaneous pneumothorax associated with air travel for patients with LAM, BHD, and PLCH appears to be low (~1 episode of spontaneous pneumothorax per 100 flights). Disease-specific risk of spontaneous pneumothorax with other DCLDs has not been estimated; however, it is likely that the risk is similar to the abovementioned estimates seen in the three major DCLDs. In general, the risk of pneumothorax with air travel should not be considered prohibitive for most DCLD patients, except perhaps for those with very limited respiratory reserves. The risks should be discussed in a pre-flight clinical assessment, which should also include counseling on concerning symptoms that might prompt a medical evaluation prior to undertaking air travel (Table 17.1).

Diving Risk and DCLD

Although there are no reports of diving-related complications in patients with DCLDs, there is the possibility of cyst rupture associated with pressure changes that could lead to the development of barotrauma complications such as pneumothorax and pneumomediastinum with ascent. Such complications due to barotrauma during a dive could be fatal, and management of a pneumothorax could be difficult at a remote diving site. As such, we recommend that patients with DCLD not attempt underwater diving.

Table 17.1 Checklist of items for pre-flight assessment of DCLD patients

Educate patients about the signs and symptoms of spontaneous pneumothorax such as sudden onset shortness of breath and pleuritic chest pain
Counsel patients to seek medical evaluation and not board the plane if they experience symptoms suggestive of pneumothorax prior to air travel
Reassure patients that the overall risk of air travel–related pneumothorax is low (~1 per 100 flights) and that majority of the DCLD patients are able to fly safely
Consider individualizing the counseling regarding pneumothorax and air travel based on patient's underlying disease severity taking into account the following risk factors: age and overall functional status, cardiopulmonary reserve to tolerate a pneumothorax, pulmonary function tests, number and size of cysts on chest CT scan, prior history of pneumothorax, and prior pleurodesis
Suggest patients wait for 7 days following radiographic resolution of a spontaneous pneumothorax prior to undertaking air travel
Assess patients for the need for in-flight supplemental oxygen as per the algorithm in Fig. 17.3

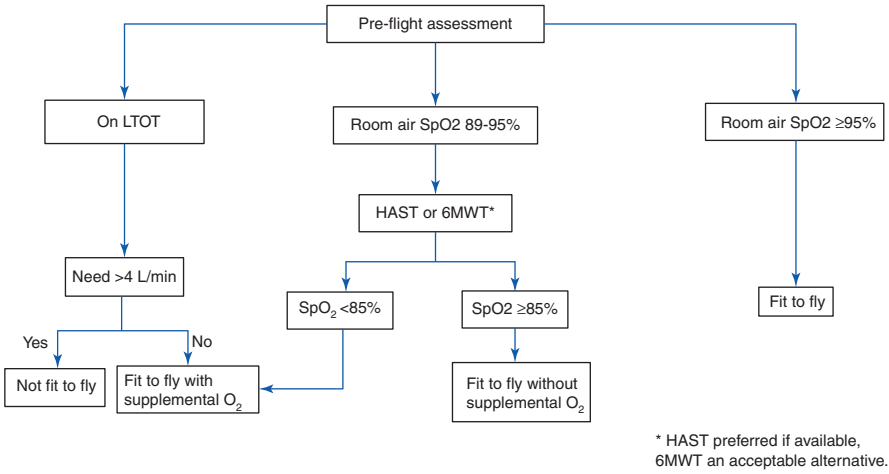

Fig. 17.3 Algorithm for the assessment of oxygenation and fitness to fly in patients with diffuse cystic lung diseases. * If available, HAST is preferred, but 6MWT is a reasonable substitute given the limited availability of HAST. 6MWT six-minute walk test, HAST hypoxia-altitude simulation test, LTOT long-term oxygen therapy

Fitness to Fly in DCLD

Most of the medical literature examining the fitness of patients with pulmonary disease to tolerate commercial air travel is derived from patients with COPD and is focused on evaluating the risk for in-flight hypoxemia. The first step in this evaluation is room air pulse oximetry. In general, if the room air SpO2 is ≥95%, the risk of in-flight hypoxia is low, and further evaluation is not generally indicated [2]. In a study examining the effect of exposure to 15% supplemental oxygen on peripheral oxygen saturation, there no was no decrease in SpO_2 to <90% during hypoxic exposure in patients who had a sea-level SpO_2 of >95% [37]. If the oxygen saturation is <95% on room air, further evaluation is needed. Pre-flight arterial blood gas analysis can sometimes be helpful, though for practical reasons pulse oximetry is more commonly used. A sea-level room air $PaO_2 \geq 70$ mmHg is the threshold used by the Aerospace Medical Association to determine fitness to fly without the need for supplemental oxygen [38]. Similar to room air SpO_2, the predictive power of room air PaO_2 for in-flight PaO_2 is questionable, though it has had good correlation with PaO_2 during the hypoxia-altitude simulation test (HAST) in some studies [2, 3].

Consideration of the patient's overall risk is an important part of the pre-flight assessment, as the correlation between room air pulse oximetry and in-flight desaturation has not been consistent in the literature [19]. For example, patients with

impaired physiologic measurements (spirometry, diffusing capacity) or severe functional limitations may warrant further pre-flight investigation even if their room air SpO_2 is ≥95%.

For patients with a room air SpO_2 less than 95% or significant overall risk, HAST can be considered. A hypobaric hypoxic challenge test would be ideal when assessing fitness to fly, as this would most closely simulate the cabin environment. However, this is not practical clinically as hypobaric simulation capabilities are not widely available. Therefore, the normobaric HAST originally described by Gong and colleagues remains the standard and simulates the hypoxic environment of altitude using 15% oxygen in nitrogen, which approximates the FiO_2 at 8000 feet. HAST is performed by having the patient breathe 15% FiO_2 for 20 min or until a steady state is reached, defined as SpO_2 within ±2% for at least 2 min. If the SpO_2 falls below 85% during the test, the subject would likely benefit from supplemental in-flight oxygen [17, 39]. If a patient does drop below 85% during the test, then supplemental oxygen can be administered by nasal cannula and titrated during the test, and it is typically titrated to achieve $SpO_2 \geq 90\%$ [40]. If supplemental oxygen titration is not available and the patient drops below 85% on HAST, then the British Thoracic Society Guidelines recommend prescribing supplemental oxygen at 2 L/min for in-flight use [17].

There is emerging evidence to suggest that the 6-min walk test (6MWT) may be a useful surrogate of HAST for pre-flight evaluation. The utility of 6MWT to conduct functional and physiologic assessment in lung disease is well established and has particular prognostic implications in certain diffuse parenchymal lung diseases. HAST is not as widely available as the 6MWT, and given the pragmatic and logistical challenges of routine HAST administration, 6MWT may be considered a reasonable substitute during the pre-flight assessment of patients with DCLD. Chetta et al. found that desaturation during 6MWT correlated with hypoxemia during HAST [41]. In a study by Edvardsen and colleagues, in subjects with a room air SpO_2 92–95%, oxygen saturation during 6MWT showed good predictive value for in-flight desaturation (area under curve 0.8). In this study, the optimal cut-off value for predicting in-flight desaturation appeared to be $SpO_2 < 84\%$ [3]. In contrast, 6-min walk distance and forced expiratory volume in 1 s (FEV_1) had weak correlation with in-flight hypoxemia.

In general, for patients who are not on LTOT but are determined after evaluation to require supplemental O_2 during air travel, most clinicians will prescribe 2 L/min if titration during testing is not available. For patients on LTOT, many clinicians will double their flow rate for air travel (e.g., increasing to 4 L/min from baseline requirement of 2 L/min). Guidelines suggest an increase in flow rate by 1–2 L/min for patients on LTOT may be sufficient [17].

As with all patients with lung disease, the severity of their physiologic impairment should be taken into consideration while making decisions regarding air travel. If their cardiopulmonary reserve is so poor that they would develop severe acute

respiratory failure with a symptomatic pneumothorax, then the risk of flying is likely prohibitive. Also, if their baseline supplemental oxygen requirement at rest is ≥4 L/min, oxygen concentrators may not be reliably able to deliver an acceptable oxygen concentration to render flying safe, and such patients should be considered unfit to fly. Unique considerations for DCLD patients include their individual risk for pneumothorax, which is likely influenced by their specific disease process and the underlying degree of cyst profusion. Additionally, whether they have previously had pleurodesis should be considered. Our approach to the pre-flight assessment of patients with DCLD includes the checklist in Table 17.1 as well as the algorithm illustrated in Fig. 17.3.

Conclusion

Evaluation of fitness to fly in patients with DCLD is complex. In addition to the concerns regarding in-flight hypoxemia, DCLD patients must be assessed for their risk for pneumothorax. Insights from recent studies regarding the risk of in-flight pneumothorax provide some guidance for clinicians. In general, the risk of air travel–related spontaneous pneumothorax is low, and most patients with DCLDs should be able to undertake air travel safely. Adjunctive physiologic testing (6MWT, HAST) is helpful for evaluating the risk of in-flight hypoxemia. An overall risk assessment of individual DCLD patients remains a crucial step in the pre-flight work-up. A checklist is presented for the pre-flight assessment of DCLD patients that integrates the risk of in-flight pneumothorax and hypoxemia.

Key Learning Points

- Pre-flight safety assessment of patients with DCLDs requires consideration of the risk for in-flight hypoxemia as well as the potential to develop spontaneous pneumothorax.
- The risk of air travel–related spontaneous pneumothorax is approximately 1 event per 100 flights in patients with DCLDs, and it is not prohibitive for majority of the patients.
- DCLD patients should be educated about the signs and symptoms of spontaneous pneumothorax and counseled to not board the plane if they experience these symptoms prior to boarding.
- Assessment of resting and exercise pulse oximetry may be a reasonable substitute for high-altitude simulation test for assessment of the need for in-flight supplemental oxygen.
- DCLD patients should be counseled to avoid scuba diving.

Conflicts of Interest The authors declare no conflicts of interest.

References

1. Nicholson TT, Sznajder JI. Fitness to fly in patients with lung disease. Ann Am Thorac Soc. 2014;11(10):1614–22.
2. Ergan B, Akgun M, Pacilli AMG, et al. Should I stay or should I go? COPD and air travel. Eur Respir Rev. 2018;27:180030 [https://doi.org/10.1183/16000617.0030-2018].
3. Edvardsen A, Akerø A, Christensen CC, Ryg M, Skjønsberg OH. Air travel and chronic obstructive pulmonary disease: a new algorithm for pre-flight evaluation. Thorax. 2012;67(11):964–9.
4. Administration FA. Electronic code of regulations. Available from: https://www.ecfr.gov/cgi-bin/text-idx?SID=5d81fa48525f27650d68094055dc543a&mc=true&node=se14.1.25_1841&rgn=div8
5. Electronic code of federal regulations [Available from: https://www.ecfr.gov/cgi-bin/text-idx?SID=5d81fa48525f27650d68094055dc543a&mc=true&node=se14.1.25_1841&rgn=div8
6. Administration FA. Medical facts for Pilots. Available from: https://www.faa.gov/air_traffic/publications/atpubs/aim_html/chap8_section_1.html
7. Chapter 8: Medical facts for Pilots [Available from: https://www.faa.gov/air_traffic/publications/atpubs/aim_html/chap8_section_1.html
8. Albert TJ, Swenson ER. Peripheral chemoreceptor responsiveness and hypoxic pulmonary vasoconstriction in humans. High Alt Med Biol. 2014;15(1):15–20.
9. Malconian MK, Rock PB, Reeves JT, Cymerman A, Houston CS. Operation Everest II: gas tensions in expired air and arterial blood at extreme altitude. Aviat Space Environ Med. 1993;64(1):37–42.
10. Khan M, Sharma S. Physiology, pulmonary vasoconstriction. [Updated 2020 Mar 25]. In: StatPearls [Internet]. Treasure Island (FL): StatPearls Publishing; 2020 Jan-. Available from: https://www.ncbi.nlm.nih.gov/books/NBK499962/.
11. West JB, Wagner PD. Predicted gas exchange on the summit of Mt. Everest Respir Physiol. 1980;42(1):1–16.
12. West JB. Respiratory and circulatory control at high altitudes. J Exp Biol. 1982;100:147–57.
13. Seccombe LM, Peters MJ. Physiology in medicine: acute altitude exposure in patients with pulmonary and cardiovascular disease. J Appl Physiol (1985). 2014;116(5):478–85.
14. Stembridge M, Ainslie PN, Hughes MG, Stöhr EJ, Cotter JD, Tymko MM, et al. Impaired myocardial function does not explain reduced left ventricular filling and stroke volume at rest or during exercise at high altitude. J Appl Physiol (1985). 2015;119(10):1219–27.
15. Bove AA. Diving medicine. Am J Respir Crit Care Med. 2014;189(12):1479–86.
16. Baumann MH. Pneumothorax and air travel: lessons learned from a bag of chips. Chest. 2009;136(3):655–6.
17. Ahmedzai S, Balfour-Lynn IM, Bewick T, Buchdahl R, Coker RK, Cummin AR, et al. Managing passengers with stable respiratory disease planning air travel: British Thoracic Society recommendations. Thorax. 2011;66(Suppl 1):i1–30.
18. Postmus PE, Johannesma PC, Menko FH, Paul MA. In-flight pneumothorax: diagnosis may be missed because of symptom delay. Am J Respir Crit Care Med. 2014;190(6):704–5.
19. Coker RK, Shiner R, Partridge MR. Is air travel safe for those with lung disease? Eur Respir J. 2008;32(5):1423–4.
20. Coker RK, Shiner RJ, Partridge MR. Is air travel safe for those with lung disease? Eur Respir J. 2007;30(6):1057–63.
21. Sand M, Bechara FG, Sand D, Mann B. Surgical and medical emergencies on board European aircraft: a retrospective study of 10189 cases. Crit Care. 2009;13(1):R3.
22. Peterson DC, Martin-Gill C, Guyette FX, Tobias AZ, McCarthy CE, Harrington ST, et al. Outcomes of medical emergencies on commercial airline flights. N Engl J Med. 2013;368(22):2075–83.
23. Martin-Gill C, Doyle TJ, Yealy DM. In-flight medical emergencies: a review. JAMA. 2018;320(24):2580–90.

24. Gupta N, Vassallo R, Wikenheiser-Brokamp KA, McCormack FX. Diffuse cystic lung disease. Part I. Am J Respir Crit Care Med. 2015;191(12):1354–66.
25. Cooley J, Lee YCG, Gupta N. Spontaneous pneumothorax in diffuse cystic lung diseases. Curr Opin Pulm Med. 2017;23(4):323–33.
26. Pollock-BarZiv S, Cohen MM, Downey GP, Johnson SR, Sullivan E, McCormack FX. Air travel in women with lymphangioleiomyomatosis. Thorax. 2007;62(2):176–80.
27. Taveira-DaSilva AM, Burstein D, Hathaway OM, Fontana JR, Gochuico BR, Avila NA, et al. Pneumothorax after air travel in lymphangioleiomyomatosis, idiopathic pulmonary fibrosis, and sarcoidosis. Chest. 2009;136(3):665–70.
28. Gonano C, Pasquier J, Daccord C, Johnson SR, Harari S, Leclerc V, et al. Air travel and incidence of pneumothorax in lymphangioleiomyomatosis. Orphanet J Rare Dis. 2018;13(1):222.
29. Gupta N, Vassallo R, Wikenheiser-Brokamp KA, McCormack FX. Diffuse cystic lung disease. Part II. Am J Respir Crit Care Med. 2015;192(1):17–29.
30. Johannesma PC, van de Beek I, van der Wel JW, Paul MA, Houweling AC, Jonker MA, et al. Risk of spontaneous pneumothorax due to air travel and diving in patients with Birt-Hogg-Dubé syndrome. Springerplus. 2016;5(1):1506.
31. Gupta N, Kopras EJ, Henske EP, James LE, El-Chemaly S, Veeraraghavan S, et al. Spontaneous pneumothoraces in patients with Birt-Hogg-Dubé syndrome. Ann Am Thorac Soc. 2017;14(5):706–13.
32. Shaw B, Borchers M, Zander D, Gupta N. Pulmonary langerhans cell histiocytosis. Semin Respir Crit Care Med. 2020;41(2):269–79.
33. Singla A, Kopras EJ, Gupta N. Spontaneous pneumothorax and air travel in pulmonary langerhans cell histiocytosis: a patient survey. Respir Investig. 2019;57(6):582–9.
34. MacDuff A, Arnold A, Harvey J. Management of spontaneous pneumothorax: British thoracic society pleural disease guideline 2010. Thorax. 2010;65(Suppl 2):ii18–31.
35. Association IAT. Medical manual 2020. Available from: https://www.iata.org/en/publications/medical-manual/
36. Wajda N, Gupta N. Air travel-related spontaneous pneumothorax in diffuse cystic lung diseases. Curr Pulmonol Rep. 2018;7(2):56–62.
37. Robson AG, Lenney J, Innes JA. Using laboratory measurements to predict in-flight desaturation in respiratory patients: are current guidelines appropriate? Respir Med. 2008;102(11):1592–7.
38. Association AM. Medical guidelines for airline travel. 2nd ed; 2003.
39. Gong H Jr, Tashkin DP, Lee EY, Simmons MS. Hypoxia-altitude simulation test. Evaluation of patients with chronic airway obstruction. Am Rev Respir Dis. 1984;130(6):980–6.
40. Cramer D, Ward S, Geddes D. Assessment of oxygen supplementation during air travel. Thorax. 1996;51(2):202–3.
41. Chetta A, Castagnetti C, Aiello M, Sergio F, Fabiano N, Tzani P, et al. Walking capacity and fitness to fly in patients with chronic respiratory disease. Aviat Space Environ Med. 2007;78(8):789–92.

Chapter 18
Approach to the Diagnosis and Management of Diffuse Cystic Lung Diseases

Abhishek Singla and Nishant Gupta

Introduction

Diffuse cystic lung diseases (DCLDs) are a heterogeneous group of diseases that differ significantly with respect to pathogenesis, clinical course, treatment, and prognosis. Underlying DCLD is usually discovered in one of the following scenarios:

1. Patients presenting with chronic respiratory symptoms such as cough and/or dyspnea on exertion.
2. Patients presenting with acute onset symptoms due to complications such as spontaneous pneumothorax.
3. Screening in at-risk populations such as adult women with tuberous sclerosis complex (TSC) or those with personal or family history of other genetic conditions such as Birt-Hogg-Dubé (BHD) syndrome.
4. Incidentally discovered abnormalities on chest or abdomen imaging done for other reasons.

Patients with DCLDs can have respiratory symptoms such as cough and dyspnea, and it is not uncommon to misdiagnose patients as having one of the more prevalent diseases such as chronic obstructive pulmonary disease or asthma. Pneumothorax is another common complication and can be the presenting

A. Singla (✉)
Division of Pulmonary, Critical Care and Sleep Medicine, University of Cincinnati College of Medicine, Cincinnati, OH, USA
e-mail: abhishek.singla@uc.edu

N. Gupta
Division of Pulmonary, Critical Care and Sleep Medicine, University of Cincinnati College of Medicine, Cincinnati, OH, USA

Cincinnati Veterans Administration Medical Center, Cincinnati, OH, USA

N. Gupta et al. (eds.), *Diffuse Cystic Lung Diseases*, Respiratory Medicine,
https://doi.org/10.1007/978-3-030-63365-3_18

manifestation of underlying DCLDs, thereby confusing the picture with primary spontaneous pneumothorax [1]. A detailed knowledge about these diseases is thus necessary for proper management of these patients. Chest high-resolution computed tomography (HRCT) remains the single most useful noninvasive diagnostic test for the evaluation of suspected DCLDs. DCLDs often have characteristic imaging findings, which can help narrow the differential diagnoses. Frequently, a confident diagnosis can be made based on CT findings and integration with clinical information. However, confirmatory tests, by either laboratory testing, tissue biopsy, or genetic analysis may be required in some cases, where clinico-radiological information is not sufficient to establish a confident diagnosis.

In this chapter, we summarize the approach toward the proper diagnosis and management of patients presenting with DCLD. In particular, we focus on the major causes of DCLDs that are most likely to be encountered in clinical practice: lymphangioleiomyomatosis (LAM), BHD, pulmonary Langerhans cell histiocytosis (PLCH), lymphocytic interstitial pneumonia (LIP)/follicular bronchiolitis (FB), amyloidosis/light chain deposition disease (LCDD), and malignancy.

Clinical Evaluation

History

A thorough and comprehensive history may provide invaluable information that can help identify the underlying etiology of DCLDs. The development of acute, rapidly progressive cystic change is usually suggestive of an infectious, inflammatory, or traumatic origin, whereas chronic processes are more likely to be secondary to neoplastic, congenital, lymphoproliferative, or other slowly progressive disorders [2].

Patient demographics may make certain diseases more likely than others. Diseases such as congenital pulmonary airway malformation (CPAM), bronchopulmonary dysplasia, and other congenital malformations are seen primarily in childhood but can uncommonly present de novo in the adult [3, 4]. Sporadic LAM is almost exclusively seen in women. While approximately 10–15% of men with TSC can have pulmonary cysts characteristic of LAM, symptomatic LAM in TSC is almost exclusively restricted to women. There is a strong association between cigarette smoking and diseases that can present with cystic changes in the lungs such as PLCH, desquamative interstitial pneumonia (DIP), and respiratory bronchiolitis, such that the presence of these diseases is unlikely in a never-smoker.

Detailed family history is an important component of history taking when evaluating patients with DCLDs. Family history of pulmonary cysts on chest imaging, pneumothoraces, skin lesions, or renal tumors can be suggestive of BHD or TSC-LAM. A history of pneumothorax within the second-degree relatives is much more suggestive of BHD than LAM [5].

Common respiratory symptoms attributable to DCLDs include cough and dyspnea on exertion. Cough is usually nonproductive; however, hemoptysis and chyloptysis can occur in a small proportion of patients with LAM [6]. Dyspnea is rare in patients where cysts or other parenchymal abnormalities are limited such as in BHD. Dyspnea can however develop or worsen acutely due to a spontaneous pneumothorax. Spontaneous pneumothorax is more common in patients with LAM, BHD and PLCH, as opposed to the other DCLDs, and usually presents in the third or fourth decade of life similar to the overall demographic of patients with a primary spontaneous pneumothorax. However, in contrast to primary spontaneous pneumothorax, DCLD patients presenting with a spontaneous pneumothorax have a much higher risk of recurrence if treated conservatively [7]. Pneumothorax can also occur in patients with *Pneumocystis jiroveci* pneumonia (PJP), connective tissue disorders such as Marfan and Ehlers-Danlos syndrome, and patients with cystic pulmonary metastases especially from underlying sarcomas such as osteogenic sarcoma, angiosarcoma, and synovial cell sarcoma with higher reported rates in patients on chemotherapy [8].

A complete review of systems is essential and often provides helpful diagnostic clues. The presence of sicca symptoms, dental caries, increased thirst, arthritis/synovitis, skin rash, and/or Raynaud's can suggest autoimmune LIP/FB as the cause of the DCLD. Frequent infections might suggest underlying immune deficiency states such as HIV and common variable immune deficiency (CVID), which are associated with LIP/FB. History of bone pain, skeletal lesions, and/or polydipsia may be a feature of extrapulmonary involvement due to histiocytic disorders such as PLCH and Erdheim-Chester disease. A subset of LAM patients may experience chylous discharge through urine, stool, or vagina. Cyclical variation of symptoms in conjunction with their menstrual cycles and post-coital hemoptysis may also be present in a subset of LAM patients.

Presence of certain diseases or manifestations can help narrow down the differential diagnosis (Table 18.1). Skin lesions and/or renal tumors can be seen in patients with BHD and in patients with TSC-LAM. Presence of DCLD in patients with TSC is highly suggestive of LAM. Similarly, the presence of renal angiomyolipomas or co-existing chylous effusions in women with characteristic cystic change on chest CT is considered diagnostic for LAM. FB/LIP is associated with a wide variety of underlying systemic autoimmune diseases, lymphoproliferative diseases, and immunodeficiency states (e.g., common variable immunodeficiency, HIV). Pulmonary amyloidosis and LCDD are commonly associated with underlying plasma cell dyscrasias or connective-tissue disorders, particularly Sjögren's, where MALT lymphoma may also be seen [9–11]. Common clinical features of systemic amyloidosis include nephrotic syndrome with or without renal insufficiency, congestive cardiomyopathy, sensorimotor and/or autonomic peripheral neuropathy, hepatomegaly, macroglossia, and hemostatic abnormalities [12]. Patients with LCDD often have co-existing renal involvement, usually in conjunction with hematological malignancies such as multiple myeloma or lymphoma [13, 14].

Table 18.1 Clinical features of diffuse cystic lung diseases

Organ system involved	Typical manifestations	DCLD associations
Dermatologic	Hypomelanotic macules, ash-leaf spots, shagreen patch, subungual fibromas, skin tags, and café au lait spots	TSC-LAM
	Fibrofolliculomas	BHD
	Papulonodular rash	PLCH
	Petechiae, purpura, nail dystrophy	Amyloidosis
Nervous system/ ocular	Cognitive impairment, seizures, subependymal giant cell astrocytomas, cortical glioneuronal hamartomas, subependymal nodules, retinal phakomas	TSC-LAM
	Diabetes insipidus	PLCH
	Neuropathy	Amyloidosis
Cardiac	Cardiomyopathy	Amyloidosis
Thoracic	Pneumothorax	LAM, BHD, PLCH
	Chylous pleural effusions	LAM
Abdominal/GI/ GU	Angiomyolipomas	LAM
	Chylous ascites	LAM
	Renal neoplasms: hybrid oncocytic tumors, chromophobe renal cell carcinomas, clear cell renal cell carcinomas, and renal oncocytomas	BHD
	Splenomegaly	CVID/LIP
	Hepatomegaly	Amyloidosis
	Proteinuria, renal failure	LCDD, amyloidosis
Musculoskeletal	Lytic bone lesions	PLCH
	Sclerotic bone lesions	TSC-LAM, ECD
	Raynaud's phenomenon	LIP/FB secondary to CTD
Others	Fatigue	LAM, PLCH, autoimmune and immune dysregulatory disorders such as Sjögren's, lupus, and CVID
	Sicca symptoms	Sjögren's, amyloidosis
	Lymphadenopathy	PLCH, LAM, amyloidosis, other lymphoproliferative disorders
	Lymphangioleiomyomas	LAM
	Macroglossia	Amyloidosis

BHD Birt-Hogg-Dubé syndrome, *CTD* connective tissue disease, *CVID* common variable immune deficiency, *DCLD* diffuse cystic lung diseases, *ECD* Erdheim-Chester disease, *FB* follicular bronchiolitis, *GI* gastrointestinal, *GU* genito-urinary, *LAM* lymphangioleiomyomatosis, *LCDD*, light chain deposition disease, *LIP* lymphocytic interstitial pneumonia, *PLCH* pulmonary Langerhans cell histiocytosis, *TSC* tuberous sclerosis complex

Physical Examination

Pulmonary exam is usually not specific enough to help ascertain a diagnosis in patients with DCLDs. Wheezing is rare in DCLDs and if present usually suggests underlying COPD or asthma. Bibasilar rales can be heard in patients with LIP or other ILDs with interstitial infiltrates or fibrosis. A high-pitched blowing sound termed "amphoric breathing" can sometimes be heard in cases of large cysts communicating with the bronchus due to turbulent airflow [15]. Diminished breath sounds on one side compared to the contralateral side might suggest the presence of a pneumothorax.

In contrast to the limited utility of pulmonary examination in patients with suspected DCLDs, extrapulmonary findings can often provide clinically useful diagnostic clues. Clubbing is rare and, if present, can be suggestive of underlying malignancy. Particular attention must be paid to the signs of underlying connective tissue disease or skin findings suggestive of BHD or TSC. Patients with BHD often have characteristic skin fibrofolliculomas, which are white to flesh-colored papules, 2–4 mm in size, on the face, neck, ear lobes, and upper trunk, and are not painful or pruritic. These lesions can be difficult to differentiate from perifollicular fibroma and angiofibromas, which are more commonly seen in TSC [16, 17]. Uncommonly, skin lesions presenting as brown to purplish papules and eczematoid or seborrhea-like lesions can be seen in patients with PLCH [18]. Petechiae, purpura, and nail dystrophy can be seen in patients with systemic amyloidosis [19]. Presence of connective tissue disorders such as skeletal anomalies, hyperextensibility, and distinct facial features could suggest a genetic syndrome such as Marfan or Ehlers-Danlos syndrome.

Diagnostic Evaluation

Laboratory testing can be a useful adjunct to aid in establishing the diagnosis of DCLDs (Table 18.2)**.** Serum vascular endothelial growth factor-D (VEGF-D) levels are elevated in women with sporadic LAM compared to healthy controls and patients with other DCLDs, and serum VEGF-D levels ≥800 pg/mL are considered diagnostic in patients with typical CT features [20, 21]. A probable diagnosis of LAM based on serum VEGF-D levels ≥600 pg/mL may be sufficient in some situations, such as for patients who have a low burden of disease that would not justify treatment, or those who are not interested in therapies or interventions [21]. It is critical to not confuse VEGF-D quantification with the more commonly commercially available VEGF quantification. In the United States, serum VEGF-D testing performed in a manner meeting College of American Pathologists (CAP)/Clinical Laboratory Improvements Amendments (CLIA) standards is only available at the

Table 18.2 Useful laboratory tests for patients with diffuse cystic lung diseases

Laboratory test	Indication	Interpretation
ANA, anti-Ro/SSA and anti-La/SSB antibodies, RF, anti-CCP	Suspected CTD	High titers suggest underlying CTD. CTD can be associated with LIP
Serum immunoglobulins	Suspected LIP, immunodeficiencies	Hypergammaglobulinemia in LIP associated with autoimmune conditions such as Sjögren's; Hypogammaglobulinemia can occur in the setting of CVID; High serum IgE in hyper IgE syndrome
Serum protein electrophoresis, serum immunofixation, and serum-free light chain quantification	Suspected amyloidosis, LCDD	Combined testing increases sensitivity; Addition of urine immunofixation and urine protein electrophoresis can further increase sensitivity; Altered free light chain ratio can be present in patients with LCDD; Can be positive in a variety of plasma cell dyscrasias and lymphoproliferative disorders
HIV	Suspected HIV	HIV can be associated with LIP or infections such as PJP
Serum VEGF-D	Suspected LAM	Serum VEGF-D $\geq$ 800 pg/mL is highly specific for the diagnosis of sporadic LAM in women with compatible radiologic features

BHD Birt-Hogg-Dubé syndrome, *CTD* connective tissue disease, *CVID* common variable immune deficiency, *DCLD* diffuse cystic lung diseases, *ECD* Erdheim-Chester disease, *FB* follicular bronchiolitis, *GI* gastrointestinal, *GU* genito-urinary, *LAM* lymphangioleiomyomatosis, *LCDD* light chain deposition disease, *LIP* lymphocytic interstitial pneumonia, *PLCH* pulmonary Langerhans cell histiocytosis, *TSC* tuberous sclerosis complex, *ANA* anti-nuclear antibody, *CCP* cyclic citrullinated peptide, *HIV* human immunodeficiency virus, *PJP Pneumocystis jiroveci* pneumonia, *VEGF-D* vascular endothelial growth factor-D

Translational Trial Development and Support Laboratory based at Cincinnati Children's Hospital Medical Center. Directions for test requisition, sample processing, and shipment are available here: https://www.testmenu.com/cincinnatichildrens/Tests/665748.

Autoimmune panel can suggest underlying rheumatological disease, particularly Sjögren's, which can be associated with FB/LIP. Approximately 80% of patients with FB/LIP also have serum dysproteinemias; most commonly hypergammaglobulinemia, but hypogammaglobulinemia can occur in the setting of CVID [22]. Screening for monoclonal proteins should be pursued in patients suspected to have amyloidosis or LCDD. A comprehensive panel that includes serum immunofixation (IFE), serum protein electrophoresis (SPEP), and serum free light chain (FLC) should be ordered to ensure adequate sensitivity [23, 24]. Addition of urine IFE and UPEP can further increase sensitivity particularly in LCDD [24]. Attention should

be paid to the free light chain ratio as this may be the only abnormality present on screening in some patients [25].

Besides the abovementioned labs, genetic analyses can be useful in certain patients. For instance, *FLCN* mutation analysis is available as a diagnostic test and detects mutations in ~90% of patients with BHD and should be considered in patients with family history of pneumothorax, renal tumors, skin lesions, or patients with feature, suggestive of BHD in the absence of a positive family history [26]. Similarly, detection of *TSC1/TSC2* mutations can help confirm the presence of underlying TSC in cases where the clinical criteria for TSC have not been met and there is high clinical suspicion [27].

Pulmonary Function Testing

Pulmonary function testing (PFT) in patients with DCLDs can be normal, or demonstrate obstructive, restrictive, or mixed abnormalities depending on cause and extent of disease. Patients with LAM, PLCH and FB most often have obstructive defects. PFTs are often normal in patients with BHD. While PFTs do not have diagnostic value, they have been shown to correlate with extent of disease on CT and serve as the primary modality used to monitor disease course and response to therapy in patients with DCLDs [28, 29]. In addition, the rate of change in PFTs is a commonly utilized end point in clinical trials aiming to develop novel therapeutic options for DCLD patients.

Radiological Assessment

Chest X-rays are usually not helpful in detailed evaluation of pulmonary cysts but can reveal the presence of pneumothorax or pleural effusions, which can sometimes be seen in patients with DCLDs and may warrant intervention. HRCT scanning is crucial in the evaluation of patients with DCLD. Critical review of the HRCT for cyst characteristics such as shape, size, wall thickness, and distribution, as well as other co-existing findings can reveal patterns that can help accurately diagnose the underlying condition in greater than two-thirds of patients [30–32], and substantially narrow the differential in the rest. The CT features of various DCLDs have been discussed in detail in Chap. 3, and key features are summarized in Tables 18.3 and 18.4, and Fig. 18.1.

Evaluation of cystic lung disease begins with ascertaining that the lesions on HRCT scan are true cysts and not mimics such as cavities, emphysema, and cystic bronchiectasis as discussed in Chap. 14. However, occasionally true cysts and cyst mimics may co-exist in the same patient. Solitary cysts are usually congenital,

Table 18.3 Diagnostic consideration based on CT chest findings

CT findings		DCLD associations
Cyst distribution	Diffuse	LAM
	Upper lobe predominance	PLCH
	Lower lobe predominance	BHD, LIP, amyloidosis/LCDD[a]
Cyst morphology	Smooth, round	LAM
	Lentiform	BHD
	Irregular, dumbbell, bizarre	PLCH
	Internal structures/ septations	BHD, FB/LIP, amyloidosis, malignancy
Associated findings	Nodules	PLCH, cystic metastases, amyloidosis, LCDD, LIP
	Ground-glass opacities	PJP, DIP, LIP
	Lymphadenopathy	LIP, LAM, amyloidosis, LCDD, cystic metastases
	Pleural effusions	LAM, lymphomas, cystic metastases

BHD Birt-Hogg-Dubé syndrome, *CTD* connective tissue disease, *CVID* common variable immune deficiency, *DCLD* diffuse cystic lung diseases, *ECD* Erdheim-Chester disease, *FB* follicular bronchiolitis, *GI* gastrointestinal, *GU* genito-urinary, *LAM* lymphangioleiomyomatosis, *LCDD* light chain deposition disease, *LIP* lymphocytic interstitial pneumonia, *PLCH* pulmonary Langerhans cell histiocytosis, *TSC* tuberous sclerosis complex, *ANA* anti-nuclear antibody, *CCP* cyclic citrullinated peptide, *HIV* human immunodeficiency virus, *PJP Pneumocystis jiroveci* pneumonia, *VEGF-D* vascular endothelial growth factor-D, *CT* computed tomography, *DIP* desquamative interstitial pneumonia

[a]Can also be diffuse

age-related phenomenon or may be a remnant of prior trauma or infection. Age-related cysts are mostly 1–5 in number, in the peripheral area of the lower lobes and remain unchanged or slightly increase in size over time [33]. These can be seen in people above 40 years old, and the prevalence increases with age. However, all solitary cysts should not be ignored, as malignancy can also present as a solitary cyst. One helpful clue to distinguish between age-related benign solitary/few cysts from malignancy associated-cysts can be the wall thickness; increased wall thickness has been associated with increasing chances of malignancy. However, the reliance on wall thickness is not 100% sensitive or specific as early cancers can present with cystic airspaces that are initially thin but became thicker overtime. Lesions can also develop nodules (endophytic or exophytic) or increase in nodule size or density over time with a consequent decrease in airspace size; however, this is not a consistent feature [34]. Other features suggestive of malignancy are nonuniform cystic walls, cyst septations, ground-glass opacity around the cyst and irregular margins, lymphadenopathy, and presence of solid or nonsolid tissue intermixed with cysts [35–37].

Cysts in LAM are numerous and are uniformly round or oval and diffusely distributed throughout the pulmonary parenchyma. BHD cysts have a lower lung zone predominance, and frequently abut the pleural surface and proximal segments of the lower lobe pulmonary artery or veins. The larger cysts are often irregular or lentiform in shape and can be multiseptated. Another key feature of BHD is the elliptical

Table 18.4 Summary of clinical, radiological, and pathologic features of major DCLDs

	LAM	PLCH	BHD	LIP/FB	Amyloidosis/LCDD
Clinical features					
Clinical features	Dyspnea, Pneumothorax, Chylothorax	Dyspnea, Cough, Pneumothorax, Constitutional symptoms such as fatigue, weight loss, and fever	Pneumothorax, Family history of pneumothorax	Dyspnea, Symptoms suggestive of underlying etiologies such as sicca symptoms associated with Sjögren's	Dyspnea
Typical age at diagnosis (years)	20–40	20–40	30–40	Variable	Variable
Gender	F>> > M	F = M	F = M	F> > M	Unknown
Smoking	–	+++	–	–	–
Family history	+/– Absent in sporadic LAM. Autosomal dominant in TSC	–	++ (autosomal dominant)	–	–
Pneumothorax	+++	++	+++	Unknown, almost certainly less than LAM, BHD, and PLCH	Unknown, almost certainly less than LAM, BHD, and PLCH
Extrapulmonary manifestations	AMLs, lymphadenopathy, lymphangioleiomyomas, chylous effusions; TSC and its associated systemic manifestations such as seizures, cognitive impairment, and skin lesions	Diabetes insipidus, Lytic bone lesions, Skin rash	Skin fibrofolliculomas, Renal tumors	Sicca symptoms, Other varying manifestations according to underlying disease such as arthralgia, synovitis, skin rash, Raynaud's, and frequent infections	Lymphoproliferative disorders, renal failure, systemic amyloidosis, hematologic malignancies

(continued)

Table 18.4 (continued)

	LAM	PLCH	BHD	LIP/FB	Amyloidosis/LCDD
HRCT features					
Cysts					
Distribution	Diffuse, random	Upper and middle lung zones; spares costophrenic angles	Basilar, subpleural especially the paramediastinal regions, also tend to abut vessels	Diffuse, random, often with eccentric vessels	Diffuse, random
Shape	Round, uniform	Bizarre, irregular, variable wall thickness	Elliptical, lentiform	Round, variable; may contain internal structure/ septations	Round, variable
Size	2 mm to 2 cm	Variable, 2 mm to >2 cm	Mostly <1 cm	Variable, 3 mm to >3 cm	Mostly <2 cm
Nodules	+/− Absent in sporadic LAM. Common in patients with TSC-LAM where they represent a benign condition known as multifocal micronodular pneumocyte hyperplasia (MMPH)	++ Micro and macro nodules with or without cavitation	−	+/− Centrilobular, usually micronodules. Larger nodules may be suggestive of underlying MALT lymphoma	+++ Nodules – can be large
Ground-glass opacities	− Except in rare circumstances where they may represent chylous congestion of the pulmonary parenchyma	− Except in patients with concomitant smoking-related pathologies such as DIP	−	+++	−
Other HRCT findings	Pleural effusions in ≤20% of patients. More common in sporadic LAM than TSC-LAM	Reticulations	−	Interlobular septal thickening Air-trapping	Lymphadenopathy

Diagnostic testing					
Laboratory	Serum VEGF-D	Serum and urine studies for diabetes insipidus	–	Polyclonal dysproteinemia ANA, anti-SSA, anti SSB (Sjögren's) HIV, quantitative immunoglobulins	Monoclonal dysproteinemia Light chain immunoglobulins
Genetic testing	Typically not needed for the diagnosis of sporadic LAM. Germline *TSC* mutations in TSC-LAM	*BRAF* and other *MAPK* pathway mutations such as NRAS and MAP2K1	Germline *FLCN* gene mutations	–	–
Diagnostic yield of TBBx	>50%	30–50%	0	Unknown, likely <30%	Unknown, likely not helpful
Typical histopathological findings on lung biopsy	Infiltration by HMB-45 + ve LAM cells with smooth muscle phenotype	S100- and CD1a-positive Langerhans cells with intracellular Birbeck granules by electron microscopy; stellate fibrotic scars in late stages	Intra-parenchymal and subpleural cysts abutting interlobular septae and lacking abnormal cell proliferations or significant fibro-inflammatory component	LIP: diffuse interstitial polyclonal lymphocytic infiltrate FB: Peribronchiolar polyclonal follicular lymphoid hyperplasia with germinal centers	Amyloid: amorphous protein deposits with fibrillar ultrastructure and apple-green birefringence by Congo red stain viewed under polarized light LCDD: typically monotypic kappa light chain deposition with finely granular ultrastructure lacking apple-green birefringence by Congo red stain and polarized light

(continued)

Table 18.4 (continued)

	LAM	PLCH	BHD	LIP/FB	Amyloidosis/LCDD
Other histopathological features			Skin biopsy showing fibrofolliculomas	Lip biopsy showing focal lymphocytic sialadenitis in Sjögren's	Abdominal fat pad or bone marrow biopsy showing amyloid or light chain deposition

Modified from Gupta et al. [2]

BH Birt-Hogg-Dubé syndrome, *CTD* connective tissue disease, *CVID* common variable immune deficiency, *DCLD* diffuse cystic lung diseases, *ECD* Erdheim-Chester disease, *FB* follicular bronchiolitis, *GI* gastrointestinal, *GU* genito-urinary, *LAM* lymphangioleiomyomatosis, *LCDD* light chain deposition disease, *LIP* lymphocytic interstitial pneumonia, *PLCH* pulmonary Langerhans cell histiocytosis, *TSC* tuberous sclerosis complex, *ANA* anti-nuclear antibody, *CCP* cyclic citrullinated peptide, *HIV* human immunodeficiency virus, *PJP Pneumocystis jiroveci* pneumonia, *VEGF-D* vascular endothelial growth factor-D, *CT* computed tomography, *DIP* desquamative interstitial pneumonia, *AML* angiomyolipoma, *BRAF* v-Raf murine sarcoma viral oncogene homolog B, *F* female, *HMB* human melanoma black, *M* male, *MALT* mucosa-associated lymphoid tissue, *MAPK* mitogen-activated protein kinase

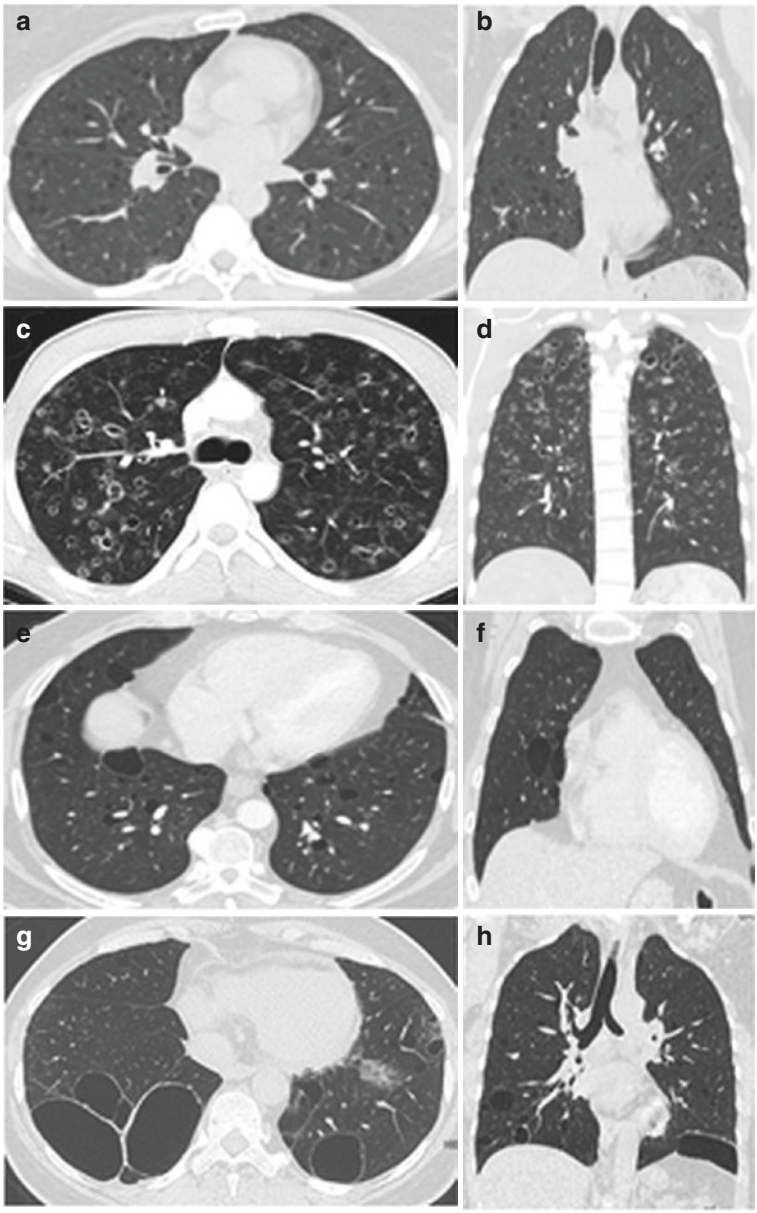

Fig. 18.1 Chest computed tomography images of common diffuse cystic lung diseases. (**a**) Axial and (**b**) coronal cuts on high-resolution chest computed tomography (HRCT) of a patient with lymphangioleiomyomatosis showing multiple smooth, round, thin-walled parenchymal cysts. (**c**) Axial and (**d**) coronal cuts on HRCT chest of a patient with pulmonary Langerhans cell histiocytosis showing multiple nodules and cysts. (**e**) Axial and (**f**) coronal cuts on HRCT chest of a patient with Birt-Hogg-Dubé syndrome showing lentiform cysts in a basilar distribution. (**g**) Axial and (**h**) coronal cuts on HRCT chest of a patient with lymphocytic interstitial pneumonia in a patient with showing multiple cysts of varying sizes and ground-glass opacities

(floppy) paramediastinal cysts; the presence of three or more elliptical paramediastinal cysts or disproportionate paramediastinal cysts is considered to be pathognomonic of BHD [38]. Recently, a quantitative analysis using paired inspiratory and expiratory CTs for estimating the extent of cyst-airway communication has been found to be useful in distinguishing BHD from other DCLDs [39].

The cysts in PLCH have varying sizes and shapes, with a predominance in the mid and upper lung fields and relative sparing of the lung bases and costophrenic angles. FB/LIP cysts vary in size and can be >50–70 mm in diameter and often have eccentric vessels at the periphery. The cysts in LIP are randomly distributed with a slight basal predominance. Lymphoma can complicate cystic lung disease in LIP and should be considered if there is associated nodularity especially large nodules, consolidation, and/or effusions [40]. Cysts in amyloidosis and LCDD are thin-walled, multiple, bilateral, small to medium in size, and often in a peribronchovascular distribution with lower lobe predominance [9, 10, 41].

Besides detailed evaluation of cysts, attention should also be paid to ancillary findings such as nodules, ground-glass opacities, lymphadenopathy, and pleural effusions. Nodules can be seen in PLCH, cystic metastases, LIP, amyloidosis, and LCDD. The presence of calcified nodules is a fairly characteristic finding seen in amyloidosis but not in LCDD and can be used to differentiate between the two conditions [9, 10]. Nodules in LIP are generally small and centrilobular. Ground-glass opacities are often seen in patients with PJP, DIP, and LIP. Due to the presence of smoking exposure in the vast majority of patients with PLCH, co-existing RB/DIP-like changes are commonly seen in PLCH and can cause the appearance of ground-glass attenuation on HRCT [42]. Mediastinal and hilar lymphadenopathy can be seen in LIP, amyloidosis, and cystic metastases. Lymphadenopathy can be bulky and associated with calcification in amyloidosis [43]. Lymphadenopathy can also be seen in patients with LAM; however, the lymphadenopathy in LAM generally tends to follow a reverse cranio-caudal gradient such that the biggest lymph nodes are in the pelvic region and tend to get progressively less bulky along the thoracic duct. Intervening lung parenchyma between cysts appears grossly normal in LAM and BHD. This is especially true for patients with sporadic LAM. Patients with TSC-LAM, however, can have multiple bland appearing nodules in addition to the cystic change. These micronodular changes most commonly represent a benign condition known as multifocal micronodular pneumocyte hyperplasia (MMPH). MMPH does not tend to progress or cause physiological impairment in these subjects [44]. It must be noted that cystic metastasis particularly from endometrial stromal sarcomas can also present exclusively as pulmonary cysts without any other radiographic abnormality [45].

Other radiological imaging may also help in clinching the diagnosis in DCLDs. Abdominal imaging can show renal tumors, which can be suggestive of LAM or BHD. AMLs are pathognomonic of LAM [46], and majority can be easily identified on CT scan and MRI due to their high fat content [47]. Identification of extrapulmonary neoplasms can be suggestive of cystic metastasis. The renal tumors in BHD can be bilateral and multifocal and provide a clue to the underlying diagnosis [48].

18-Fluoro deoxy (FDG) positron emission tomography (PET) scan can sometimes be useful in evaluation of cystic lung lesions. FDG-PET is often positive in lung cancers and metastases but given that lesions smaller than 1 cm may fall below the sensitivity threshold for FDG-PET, it can yield false-negative results when solid components, such as wall thickness or nodule size, are below this threshold [49, 50]. Moreover, FDG-PET is often negative in tumors with low metabolic activity such as low-grade adenocarcinomas and in situ pulmonary adenocarcinomas. FDG-PET may be helpful in assessing extrapulmonary disease activity in patients with PLCH and amyloidosis [51–53]. Within the lungs, a positive FDG-PET scan in PLCH is more likely in patients with early disease associated with predominantly nodular chest CT scan findings and can at times be difficult to differentiate from malignancy [51, 52]. Results for PET-CT in amyloidosis are also variable but a standardized uptake value (SUV) uptake greater than 3.0 should raise suspicion for malignancies or associated lymphoma or plasmacytoma [53]. PET-CT can also be helpful in evaluation for malignancy in patients with Sjögren's where a SUV max in the parotid gland of $\geq$4.7 and/or the presence of focal pulmonary lesions can be highly suggestive of lymphoma [54].

Pathological Evaluation

Pathologic evaluation may be required in patients where diagnosis remains uncertain after a thorough review of the clinical and radiological data. Bronchoalveolar lavage (BAL) has limited diagnostic utility and is primarily useful to rule out infectious etiologies such as PJP. The presence of more than 5% CD1a cells on BAL has been proposed as a confirmatory diagnostic finding in patients with suspected PLCH but is limited by its lack of sensitivity and is not clinically useful in most patients [55]. Bronchoscopy with transbronchial lung biopsy can be helpful in establishing the diagnosis in cases of LAM and PLCH with the diagnostic yield being more than 50% in patients with LAM and 30–50% in patients with PLCH [2]. Transbronchial lung cryobiopsy is a relatively new technique that involves freezing the lung tissue with compressed cold gas and allows the extraction of larger pieces of tissue than the traditional forceps-guided transbronchial lung biopsy. The safety and diagnostic yield of transbronchial lung cryobiopsy in patients with DCLD has not been systematically evaluated. As such, its use is perhaps best reserved in centers with expertise in the technique. Anecdotal evidence suggests that transbronchial lung cryobiopsy may be a potentially useful modality to obtain tissue in DCLD patients and is likely to have better diagnostic yield than conventional transbronchial lung biopsy [56, 57]. Video-assisted thoracoscopic surgery (VATS)-guided surgical lung biopsy remains the gold standard modality to obtain tissue for histopathological confirmation.

On pathology, true cysts have an epithelial cell lining compared to discontinuous epithelial lining resulting from parenchymal loss as seen in emphysema or

post-traumatic pseudocysts. Histological features of BHD cysts are generally not distinctive and may be indistinguishable from those of emphysema, but can include hyperplastic type II pneumocyte-like cells and positive staining for PCNA and p-S6 [58]. LAM, PLCH, amyloidosis, LCDD, and metastatic disease may show diagnostic cellular proliferations or material deposition. Proliferation of spindle cells that stain positive for HMB-45, smooth muscle actin, and estrogen and progesterone receptors is characteristic of LAM, while infiltration with Langerhans cells positive for CD1a, Langerin, and S100 is seen in PLCH [59]. Amorphous eosinophilic material is seen in amyloidosis and LCDD, and distinction can be made based on Congo red staining or material deposition seen on electron microscopy [59]. Cellular interstitial infiltrates are seen in patients with FB/LIP. Immunohistochemical studies and flow cytometry should be performed in order to distinguish between the polyclonal populations of lymphocytes seen in LIP and a monotypic cell population seen in malignant lymphoproliferative disorders.

Occasionally, the diagnosis may be established by biopsy of an involved site outside the thorax. Biopsy of skin fibrofolliculomas can establish the diagnosis of BHD and is particularly important as lung biopsy in patients with BHD is not pathognomonic. Bone biopsy can be pursued for suspected lesions in PLCH. Lip biopsy is usually the procedure of choice in the diagnosis of suspected Sjögren's. Subcutaneous abdominal fat aspirate and bone marrow biopsy may be examined for suspected amyloid, but a negative result does not necessarily exclude pulmonary amyloidosis [12].

Diagnostic Approach

While a large proportion of patients may present with symptoms secondary to DCLDs, it is not uncommon for patients to present with mild or no symptoms. A considerable subgroup of patients with DCLDs, especially those without underlying high-grade malignancies, may remain stable and not warrant any therapy. Moreover, pulmonary cysts can develop normally in some individuals, as an age-related phenomenon, and do not always represent a true pathology. Thus, the diagnostic algorithm and management must be tailored according to the individual patient's presentation, risks and preferences. For instance, it may be reasonable to pursue serial longitudinal monitoring of the clinical course in a patient with mild DCLD due to uncertain cause as long as there are minimal or no symptoms, and pursue invasive diagnostic testing if and when patient is at risk of morbidity or mortality due to disease. On the other hand, if there is a suspicion for high-grade malignancy – further evaluation with biopsy, FGD-PET, and/or serial CT scans should be pursued regardless of symptoms. We usually tend to follow the clinical course in asymptomatic or minimally symptomatic patients who do not have substantial physiological (normal PFTs) or radiological disease burden ($\leq$10 cysts on CT).

We tend to approach evaluation of DCLDs in a stepwise manner where the first step is to decipher whether the parenchymal lucencies represent true cysts or other noncystic parenchymal opacities. Once we identify true cysts, we categorize the patients on the basis of underlying cyst profusion into pauci-cystic (≤10 cysts) or multi-cystic (>10 cysts) (Fig. 18.2). Age-related cysts and a variety of diseases such as parasitic infections, traumatic pneumatoceles, primary lung cancers, and congenital cysts generally present with pauci-cystic disease. It is worth mentioning, however, that occasionally the diseases typically associated with multi-cystic chest radiology may be detected very early in the disease course at a pauci-cystic stage, highlighting the importance of continued longitudinal monitoring of patients with cystic lung disease. A proposed algorithm for work-up of patients with pauci-cystic and multi-cystic DCLDs is shown in Figs. 18.3 and 18.4.

Diagnosis of DCLD involves a detailed clinical and radiological assessment as discussed previously, with the need for invasive biopsies considered on a case-by-case basis depending upon the disease and symptom burden and the patient/physician's desire to establish a certain diagnosis. Key clinical, radiological, and pathological features of common causes of DCLDs are summarized in Table 18.4. Disease-specific diagnostic guidelines are available for a few diseases such as LAM and BHD and also for diseases associated with DCLDs such as TSC (associated with LAM) and Sjögren's (associated with LIP, amyloidosis, and/or LCDD), and are summarized in Table 18.5.

Management

Screening for DCLDs

Screening for DCLDs with CT scan of chest should be pursued in certain situations. While all cases of recurrent spontaneous pneumothorax should undergo evaluation by CT scan, preferably after re-expansion of the lung, the role of CT scan after the first episode of spontaneous pneumothorax remains unclear. It is advisable to consider chest CT imaging in first-time spontaneous pneumothorax if there is a positive family history or if the patient is female, because the discovery of either BHD or LAM, respectively, has important management implications [26]. We follow the approach of performing CT scan after first episode of an apparent primary spontaneous pneumothorax in all patients as this approach can lead to timely diagnosis of underlying conditions and allow the pursuit of appropriately aggressive interventions to reduce the pneumothorax recurrence risk. The strategy to pursue screening chest CT scan to evaluate for DCLDs in patients presenting with an apparent primary spontaneous pneumothorax has been demonstrated to be cost-effective in a recent analysis [1, 60].

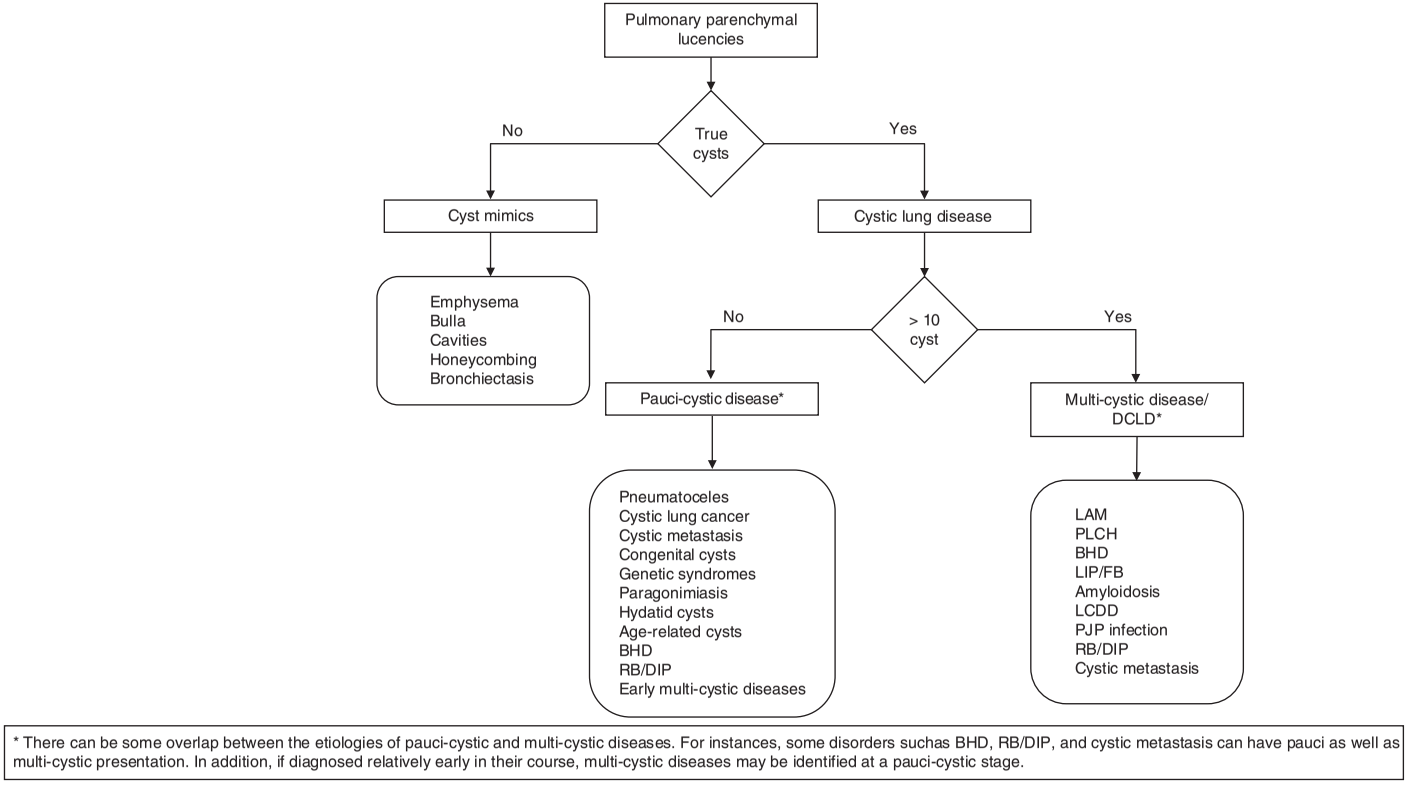

Fig. 18.2 Algorithm to classify cystic lung diseases based on chest computed tomography. BHD Birt-Hogg-Dubé syndrome, DIP desquamative interstitial pneumonia, FB follicular bronchiolitis, LAM lymphangioleiomyomatosis, LCDD light chain deposition disease, LIP lymphocytic interstitial pneumonia, PLCH pulmonary Langerhans cell histiocytosis, PJP pneumocystis jiroveci pneumonia, RB respiratory bronchiolitis

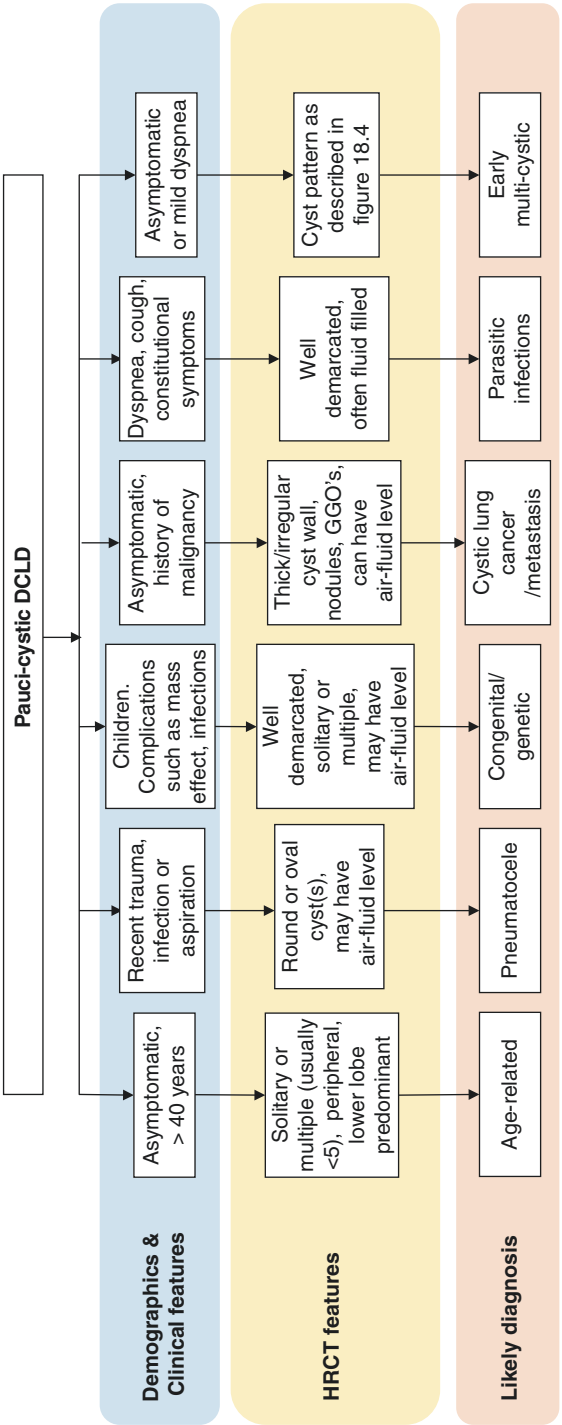

Fig. 18.3 Algorithm to guide approach to the diagnosis of pauci-cystic lung diseases. GGOs ground-glass opacities

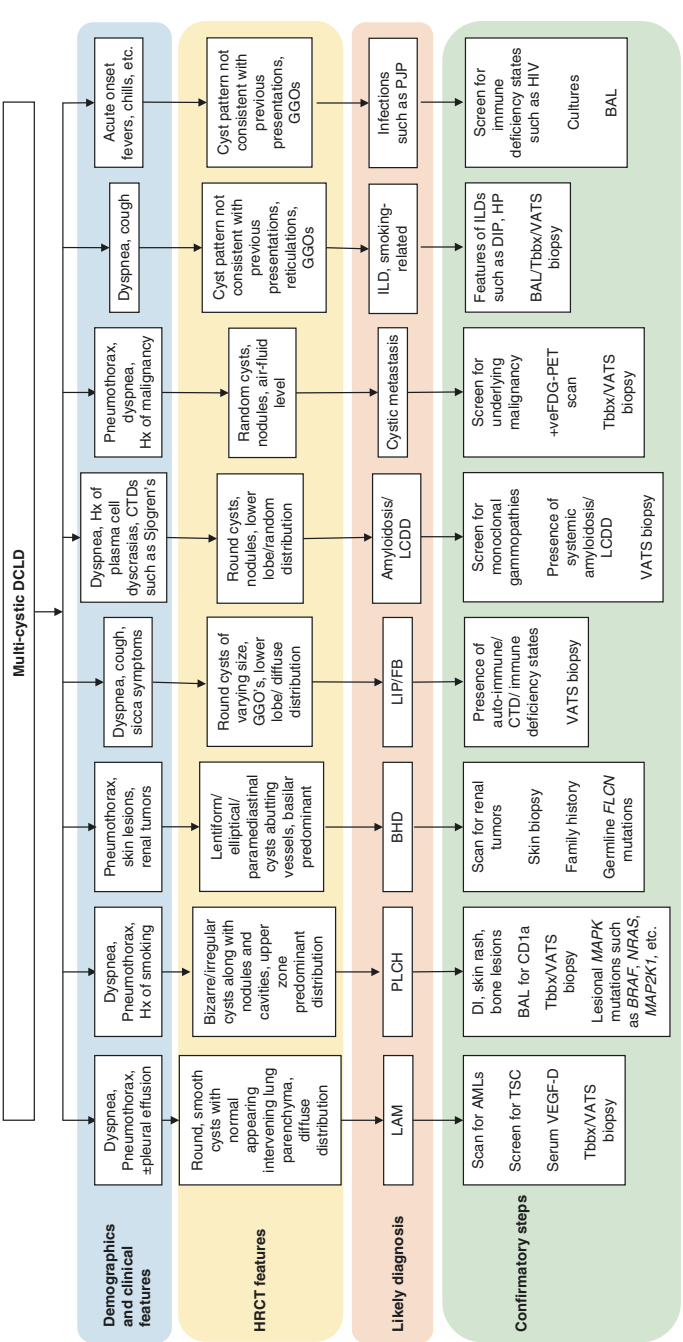

Fig. 18.4 Algorithm to guide approach to the diagnosis of diffuse multi-cystic lung diseases. AML angiomyolipoma, BAL broncheoalveolar lavage, BHD Birt-Hogg-Dubé syndrome, BRAF v-Raf murine sarcoma viral oncogene homolog B, CT computed tomography, CTD connective tissue diseases, DCLD diffuse cystic lung disease, DI diabetes insipidus, DIP desquamative interstitial pneumonia, FB follicular bronchiolitis, FDG-PET 18-Fluoro deoxy positron emission tomography, FLCN folliculin, GGOs ground-glass opacities, HRCT high-resolution computed tomography, HP hypersensitivity pneumonitis, ILD interstitial lung disease, LAM lymphangioleiomyomatosis, LCDD light chain deposition disease, LIP lymphoid interstitial pneumonia, MAPK mitogen-activated protein kinase, PLCH pulmonary Langerhans cell histiocytosis, SS Sjögren syndrome, Tbbx transbronchial biopsy, TSC tuberous sclerosis complex, VATS video-assisted thoracoscopic surgery, VEGF-D vascular endothelial growth factor-D. (Modified from Gupta et al. [2])

Certain high-risk patient groups warrant screening CT scans to evaluate for underlying DCLDs. Given the high prevalence of LAM in women with TSC, all women with TSC should undergo a baseline chest HRCT starting at the age of 18 years, regardless of pulmonary symptoms. In cases where the screening CT is negative, repeat imaging can be performed every 5 years, or sooner as dictated by pulmonary symptoms [61]. For TSC women with documented evidence of LAM on chest CT, the repeat HRCT interval can be reduced to every 2–3 years in order to gauge the trajectory of disease progression. These follow-up CT scans can be done using low-dose radiation protocols. In addition, these patients should undergo periodic (at least annual) pulmonary function testing. Sporadic renal AMLs (without TSC) can be associated with LAM in approximately 10% of the patients and discovery of renal AMLs should prompt consideration of screening for LAM with chest CT [62].

Table 18.5 Diagnostic criteria for key DCLDs and their underlying disease associations

Disease	Diagnostic criteria
LAM [20]	Compatible clinical history and characteristic HRCT of the chest + one or more of the following features: 1. Presence of TSC 2. Renal angiomyolipoma(s) 3. Elevated serum VEGF-D ≥800 pg/ml 4. Chylous effusion (pleural or ascites) confirmed by tap and biochemical analysis of the fluid. 5. Lymphangioleiomyomas (lymphangiomyomas) 6. Demonstration of LAM cells or LAM cell clusters on cytological examination of effusions or lymph nodes 7. Histopathological confirmation of LAM by lung biopsy or biopsy of retroperitoneal or pelvic masses
BHD [91, 92]	Diagnosis requires one major or two minor criteria: **Major criteria** 1. At least five fibrofolliculomas or trichodiscomas, at least one histologically confirmed, of adult onset 2. Pathogenic *FLCN* germline mutation **Minor criteria** 1. Multiple lung cysts: bilateral basally located lung cysts with no other apparent cause, with or without spontaneous pneumothorax 2. Renal cancer: early onset (<50 years) or multifocal or bilateral renal cancer, or renal cancer of mixed chromophobe and oncocytic histology 3. A first-degree relative with BHD ***Alternative diagnostic criteria in patients with lung cysts*** Characteristic or compatible lung HRCT with one of the following: 1. Skin biopsy positive for fibrofolliculoma 2. Confirmed family history of BHD in first- or second-degree family member 3. Histologic confirmation of chromophobe renal carcinoma or hybrid oncocytic tumor 4. Genetic testing positive for *FLCN* mutation

(continued)

Table 18.5 (continued)

Disease	Diagnostic criteria
TSC [27]	Major features 1. Hypomelanotic macules (≥3, at least 5-mm diameter) 2. Angiofibromas (≥3) or fibrous cephalic plaque 3. Ungual fibromas (≥2) 4. Shagreen patch 5. Multiple retinal hamartomas 6. Cortical dysplasias 7. Subependymal nodules 8. Subependymal giant cell astrocytoma 9. Cardiac rhabdomyoma 10. Lymphangioleiomyomatosis (LAM) 11. Angiomyolipomas (≥2) Minor features 1. "Confetti" skin lesions 2. Dental enamel pits (>3) 3. Intraoral fibromas (≥2) 4. Retinal achromic patch 5. Multiple renal cysts 6. Nonrenal hamartomas Definite diagnosis: Two major features (except for a combination of LAM and angiomyolipomas without other features) or one major feature with ≥2 minor features or identification of either a TSC1 or TSC2 pathogenic mutation in DNA from normal tissue Possible diagnosis: Either one major feature or ≥ 2 minor features.
Sjögren's[a] [93]	1. Labial salivary gland with focal lymphocytic sialadenitis and focus score of ≥1 foci/4 mm2 (weight /score = 3) 2. Anti-SSA/Ro-positive (weight /score = 3) 3. Ocular staining score ≥ 5 (or van Bijsterveldscore ≥4) in at least one eye (weight /score = 1) 4. Schirmer's test ≤5 mm/5 min in at least one eye (weight /score = 1). 5. Unstimulated whole saliva flow rate ≤ 0.1 mL/min (weight /score = 1) Diagnosis of Sjögren's requires a score of ≥4 and exclusion of history of head and neck radiation treatment, active hepatitis C infection, AIDS, sarcoidosis, amyloidosis, graft-versus-host disease, and IgG4-related disease

BHD Birt-Hogg-Dubé syndrome, *CTD* connective tissue disease, *CVID* common variable immune deficiency, *DCLD* diffuse cystic lung diseases, *ECD* Erdheim-Chester disease, *FB* follicular bronchiolitis, *GI* gastrointestinal, *GU* genito-urinary, *LAM* lymphangioleiomyomatosis, *LCDD* light chain deposition disease, *LIP* lymphocytic interstitial pneumonia, *PLCH* pulmonary Langerhans cell histiocytosis, *TSC* tuberous sclerosis complex, *ANA* anti-nuclear antibody, *CCP* cyclic citrullinated peptide, *HIV* human immunodeficiency virus, *PJP Pneumocystis jiroveci* pneumonia, *VEGF-D* vascular endothelial growth factor-D, *CT* computed tomography, *DIP* desquamative interstitial pneumonia, *AML* angiomyolipoma, *BRAF* v-Raf murine sarcoma viral oncogene homolog B, *F* female; *HMB* human melanoma black, *M* male, *MALT* mucosa-associated lymphoid tissue, *MAPK* mitogen-activated protein kinase, *AIDS* acquired immunodeficiency syndrome, *HRCT* high-resolution computed tomography, *Ig* immunoglobulin

[a]Associated with LIP, amyloidosis, and/or LCDD

General Management

As with any other chronic lung disease, it advisable to quit smoking and inhalation of any potentially harmful agents such as vaping and marijuana. Smoking (and marijuana) cessation is the cornerstone of treatment in patients with PLCH and can lead to disease regression or stabilization in a substantial proportion of patients. Patients should be advised to stay up to date with influenza and pneumococcal vaccines. Pulmonary rehabilitation could be an effective intervention to improve symptoms, health-related quality of life, and functional status in patients with impaired exercise tolerance [63, 64]. General recommendations applicable to all DCLD patients are highlighted in Table 18.6.

Spontaneous pneumothorax is common in DCLD patients, particularly in patients with LAM, BHD and PLCH, and carries a very high risk of recurrence [7]. Patients should be made aware of symptoms suggestive of pneumothorax, and an action plan should be formulated in case of emergency. In contrast to patients with primary spontaneous pneumothorax, given the high risk of recurrence, patients with DCLDs (especially LAM, BHD, and PLCH) presenting with a spontaneous pneumothorax should undergo pleurodesis to reduce the recurrence risk following the first episode of spontaneous pneumothorax rather than waiting for a recurrent event [20, 65, 66]. We prefer VATS-guided mechanical pleurodesis as the initial modality. It is worth mentioning that prior pleurodesis is not a contraindication for future lung transplantation [67] and that when making the decision whether to pursue pleurodesis or not, generally more weight should be assigned to the reduction in morbidity arising from recurrent spontaneous pneumothoraces as opposed to the possibility of future technical difficulties in case there is need for lung transplantation.

Situations leading to increase in cyst size or pressure can predispose patients to develop pneumothorax. In accordance with the Boyle's law of inverse relationship between pressure and volume, lung cysts have the potential to expand in size when exposed to atmospheric pressure changes such as during air travel or deep-sea diving. It is usually advised to avoid deep-sea diving as development of pneumothorax

Table 18.6 General recommendations applicable to all patients with DCLDs

Smoking cessation
Stay up to date on vaccination including annual influenza vaccination and both pneumococcal (PPSV23 and PCV13) vaccines
Air travel is safe for most patients with DCLDs. The risk of inflight pneumothorax is approximately 1 per 100 flights. Patients should be educated about the typical symptoms of pneumothorax and instructed to seek medical attention if they have new-onset symptoms suggestive of a pneumothorax
Advise against scuba diving due to the potential risk of spontaneous pneumothorax
Patients should be aware of symptoms of pneumothorax and have an action plan. Pleurodesis should be considered following the first episode of pneumothorax. Prior pleurodesis is not a contraindication for lung transplantation [94].

Modified from Obaidat et al. [95]
PCV pneumococcal conjugate vaccine, *PPSV* pneumococcal polysaccharide vaccine

in these situations can potentially become life-threatening [68]. Air travel has been shown to have a low risk (~1 episode of spontaneous pneumothorax per 100 flights) particularly in patients with LAM, BHD, and PLCH. This risk of pneumothorax with air travel is usually not considered prohibitive unless the patient has severely reduced cardiopulmonary reserve and cannot tolerate a pneumothorax. Patients should be counselled about this risk and educated about concerning symptoms that might prompt appropriate medical evaluation prior to undertaking air travel. In addition to the risk of pneumothorax associated with air travel, DCLD patients should also undergo evaluation for the need of supplemental oxygen during air travel. These issues have been covered in detail in Chap. 17 of this textbook.

Specific Treatment

Inhaled bronchodilators can be tried, especially in patients with reversible airflow obstruction on pulmonary function testing and in patients who report symptomatic benefit from a bronchodilator trial [55, 69, 70]. Concomitant asthma may be present in some patients, and inhaled corticosteroids may be beneficial in this subset.

Disease-modifying therapies for LAM, PLCH, FB/LIP, and amyloidosis are available and should be considered if patients develop significant symptoms or exhibit a progressive decline in pulmonary function (Table 18.7). Use of the mechanistic target of rapamycin (mTOR) inhibitor, sirolimus, has been shown to stabilize lung function decline and improve the quality of life in patients with LAM, and is recommend for patients with abnormal lung function as defined by forced expiratory volume in one-second (FEV1) less than or equal to 70% predicted [46]. Sirolimus has also been shown to be effective in LAM patients with chylous complications such as chylous effusions, lymphangioleiomyomas, and in patients with rapidly declining lung function. mTOR inhibitors are efficacious and safe in controlling AML burden in patients with TSC, while preserving the renal parenchyma [71, 72]. Cladribine (2-chlorodeoxyadenosine) has been shown to be helpful in refractory systemic LCH and has also been used in isolated PLCH with reported improvement [73–75]. Multiple other chemotherapeutic regimens have been tried in patients with PLCH with limited success. Targeted treatment of PLCH with BRAF or MEK inhibition may be a promising therapeutic approach in the near future [76]. Treatment of FB/LIP relies on managing the underlying cause. Immunosuppression can be helpful in idiopathic LIP and LIP associated with autoimmune disease [77]. Clinical and radiological resolution of LIP has been reported with the use of antiretroviral drugs in cases of LIP secondary to HIV [78]. Treatment of amyloidosis and LCDD depends on the extent of organ involvement and options include autologous stem cell transplantation and a variety of chemotherapeutic drugs [79]. Solitary malignancy and some congenital lesions such as CPAM and bronchogenic cysts may be amenable to surgical resection because of their propensity to enlarge and to

Table 18.7 Disease-specific management considerations for common DCLDs

Disease	Disease-modifying therapy	Other management considerations
LAM	mTOR inhibitors (sirolimus, everolimus). Typically prescribed to patients with abnormal lung function (FEV1 <70% predicted), substantial disease burden (need for supplemental oxygen, DLCO <60%), evidence of accelerated disease progression (FEV1 decline >100 ml/year), or patients with problematic chylous complications such as chylous pleural effusions	Screen for renal angiomyolipomas; Obtain detailed history and perform physical examination to look for underlying TSC; Evaluate for PH in advanced disease, patients with hypoxemic respiratory failure, clinical signs suggestive of right ventricular strain, or out of proportion reduction in DLCO
PLCH	Smoking cessation. Typically, the first and only management option for a substantial proportion of patients with PLCH Cladribine/Cytarabine MEK/BRAF inhibitors	Enquire about symptoms suggestive of extrapulmonary involvement such as lytic bone lesions and diabetes insipidus; Evaluate for PH in patients with hypoxemic respiratory failure, clinical signs suggestive of right ventricular strain, or out of proportion reduction in DLCO
BHD	None	Periodic longitudinal screening for renal tumors; Screen family members for the presence of BHD
LIP/FB	Immunosuppression, especially in patients with other noncystic parenchymal abnormalities such as ground-glass opacities	Evaluate for underlying autoimmune disease and immunodeficiencies; Consider biopsy for suspicious lesions suggestive of lymphoma such as pulmonary nodules with increasing size
Systemic amyloidosis/ LCDD	Chemotherapy Bone marrow transplantation	Evaluate for underlying lymphoproliferative diseases and plasma cell dyscrasias as well as other extrapulmonary organ involvement

BHD Birt-Hogg-Dubé syndrome, *CTD* connective tissue disease, *CVID* common variable immune deficiency, *DCLD* diffuse cystic lung diseases, *ECD* Erdheim-Chester disease, *FB* follicular bronchiolitis, *GI* gastrointestinal, *GU* genito-urinary, *LAM* lymphangioleiomyomatosis, *LCDD* light chain deposition disease, *LIP* lymphocytic interstitial pneumonia, *PLCH* pulmonary Langerhans cell histiocytosis, *TSC* tuberous sclerosis complex, *ANA* anti-nuclear antibody, *CCP* cyclic citrullinated peptide, *HIV* human immunodeficiency virus, *PJP Pneumocystis jiroveci* pneumonia, *VEGF-D* vascular endothelial growth factor-D, *CT* computed tomography, *DIP* desquamative interstitial pneumonia, *AML* angiomyolipoma; *BRAF* v-Raf murine sarcoma viral oncogene homolog B, *F* female, *HMB* human melanoma black, *M* male, *MALT* mucosa-associated lymphoid tissue, *MAPK* mitogen-activated protein kinase, *DLCO* diffusing capacity of the lung for carbon monoxide, *FEV1* forced expiratory volume in 1 second, *MEK* mitogen-activated protein kinase kinase, *mTOR* mechanistic target of rapamycin, *PH* pulmonary hypertension

become infected as well as the potential risk for transformation into malignancy [80]. Lung transplantation remains a viable management option for patients with advanced DCLDs with patients having post-transplant survival either similar to (in case of PLCH) or better than (in case of LAM) the patients undergoing lung transplantation for other pulmonary disorders [81–85]; however, recurrence of disease in allograft can occur in some patients with LAM and PLCH [86].

Active surveillance and management for co-existing conditions or complications is warranted for certain DCLDs. Patients with LAM should be evaluated for presence of TSC and AMLs [61]. Serial screening of renal tumors in BHD is recommended [48]. Development of lymphoma is the most dreaded complications of Sjögren's and can occur in ~5% of patients [77]. Although guidance on appropriate screening of lymphoma in these patients is lacking, development of three or more risk factors such as salivary gland enlargement, lymphadenopathy, Raynaud phenomenon, anti-Ro/SSA or/and anti-La/SSB autoantibodies, rheumatoid factor positivity, monoclonal gammopathy, and C4 hypocomplementemia have been associated with development of lymphoma [87]. Pulmonary hypertension is known to occur in patients with DCLDs, particularly LAM and PLCH [88–90], which may need further evaluation.

Conclusion

The combined synergy between scientists, clinicians, and patient advocacy organizations (Table 18.8) has enabled transformative progress in our understanding of the molecular pathogenesis and the development of novel therapeutic options in patients with DCLDs. The recent progress in LAM is perhaps the best exemplar of the abovementioned synergy driving meaningful progress. In a relatively short time span of approximately two decades, the collaborative effort between patients and scientists has led to major scientific breakthroughs in LAM, including identification of the causative gene, clear understanding of the disease pathogenesis, discovery of a blood-based biomarker that aids noninvasive diagnosis, and the development of FDA-approved treatment. Active efforts are underway to emulate the example of LAM and apply similar approaches to drive progress in other DCLDs. In conclusion, we submit that the DCLDs represent a unique set of disorders that are fundamentally distinct from the typical interstitial lung diseases in almost every aspect including the pathophysiology, radiological features, clinical phenotypes, natural history, and management strategies. Although rare individually, collectively DCLDs represent a substantial minority of the pulmonary practice and are being increasingly identified due to widespread use of CT scans and increased awareness. Knowledge regarding the nuances of appropriately diagnosing and treating DCLDs for clinicians is critical in order to provide optimal care to these patients. Finally, the discoveries made in this field are not only impacting the lives of patients with DCLDs but are also providing crucial insights into the pathobiology of more common conditions.

Table 18.8 Key organizations focused on advancing healthcare and research for patients with DCLDs and related rare diseases

Lymphangioleiomyomatosis/ tuberous sclerosis	The Lymphangioleiomyomatosis (LAM) Foundation (https://www.thelamfoundation.org) Tuberous Sclerosis Alliance (http://www.tsalliance.org)
Birt-Hogg-Dubé syndrome	BHD Foundation (https://www.bhdsyndrome.org) Myrovlytis Trust (www.myrovlytistrust.org)
Pulmonary Langerhans cell histiocytosis	Histiocytosis Association (https://www.histio.org)
Amyloidosis/LCDD	Amyloidosis Foundation (https://amyloidosis.org)
Sjögren's	Sjögren's Foundation (https://www.sjogrens.org)
Other organizations focused on rare diseases	Rare Lung Diseases Consortium (https://www.rarediseasesnetwork.org/cms/rld) National Organization for Rare Disorders (NORD) (http://www.rarediseases.org) International Rare Disease Research Consortium (IRDiRC) (http://www.irdirc.org) Orphanet (http://www.orpha.net) The European Organisation for Rare Diseases (http://www.eurordis.org)

BHD Birt-Hogg-Dubé syndrome, *CTD* connective tissue disease, *CVID* common variable immune deficiency, *DCLD* diffuse cystic lung diseases, *ECD* Erdheim-Chester disease, *FB* follicular bronchiolitis, *GI* gastrointestinal, *GU* genito-urinary, *LAM* lymphangioleiomyomatosis, *LCDD* light chain deposition disease, *LIP* lymphocytic interstitial pneumonia, *PLCH* pulmonary Langerhans cell histiocytosis, *TSC* tuberous sclerosis complex, *ANA* anti-nuclear antibody, *CCP* cyclic citrullinated peptide, *HIV* human immunodeficiency virus, *PJP Pneumocystis jiroveci* pneumonia, *VEGF-D* vascular endothelial growth factor-D

Key Learning Points

- When evaluating a patient with cystic change on chest imaging, a detailed history with particular attention to demographics, inhaled exposures such as smoking, family history, and search for extrapulmonary features, including cutaneous, pleural, and intra-abdominal manifestations, can provide crucial insight into the underlying diagnosis.
- High-resolution computed tomography is an essential component of the evaluation process, and careful evaluation of the cyst characteristics, such as profusion, distribution, and morphology, combined with ancillary pulmonary and extrapulmonary findings, can help differentiate between the various causes of cystic lung diseases in a large proportion of patients.
- Laboratory analysis can provide valuable information in patients with suspected DCLDs, and can sometimes be diagnostic such as elevated VEGF-D in LAM or establishment of diagnosis of Sjögren's in a patient suspected to have FB/LIP.
- Invasive procedures such as lung biopsy may be needed in some patients after exhausting the noninvasive diagnostic work-up. The decision to pursue invasive diagnostic procedures should be taken with careful consideration of future management implications and the knowledge that the diagnosis of DCLDs can generally be established by noninvasive means in over two-thirds of the patients.

- Management of patients with DCLDs includes attention to the prevention and management of complications such as spontaneous pneumothorax. There is a high risk of recurrence of pneumothorax in these patients, and pleurodesis should be considered following the initial episode of spontaneous pneumothorax rather than waiting for a recurrent episode.
- Disease-modifying therapies are available for certain DCLDs, such as mTOR inhibitors for LAM, with lung transplantation reserved for patients with advanced disease.

Conflicts of Interest The authors declare no conflicts of interest.

References

1. Gupta N. Primary spontaneous pneumothorax: looking beyond the usual. Acad Emerg Med. 2018;25(4):470–2.
2. Gupta N, Vassallo R, Wikenheiser-Brokamp KA, McCormack FX. Diffuse cystic lung disease. Part II. Am J Respir Crit Care Med. 2015;192(1):17–29.
3. Shanmugam G. Adult congenital lung disease. Eur J Cardiothorac Surg. 2005;28(3):483–9.
4. Hamanaka R, Yagasaki H, Kohno M, Masuda R, Iwazaki M. Congenital cystic adenomatoid malformation in adults: report of a case presenting with a recurrent pneumothorax and a literature review of 60 cases. Respir Med Case Rep. 2019;26:328–32.
5. Tobino K, Hirai T, Johkoh T, Kurihara M, Fujimoto K, Tomiyama N, et al. Differentiation between Birt–Hogg–Dubé syndrome and lymphangioleiomyomatosis: quantitative analysis of pulmonary cysts on computed tomography of the chest in 66 females. Eur J Radiol. 2012;81(6):1340–6.
6. Ryu JH, Moss J, Beck GJ, Lee J-C, Brown KK, Chapman JT, et al. The NHLBI lymphangioleiomyomatosis registry: characteristics of 230 patients at enrollment. Am J Respir Crit Care Med. 2006;173(1):105–11.
7. Cooley J, Lee YG, Gupta N. Spontaneous pneumothorax in diffuse cystic lung diseases. Curr Opin Pulm Med. 2017;23(4):323.
8. Hoag JB, Sherman M, Fasihuddin Q, Lund ME. A comprehensive review of spontaneous pneumothorax complicating sarcoma. Chest. 2010;138(3):510–8.
9. Zamora AC, White DB, Sykes A-MG, Hoskote SS, Moua T, Eunhee SY, et al. Amyloid-associated cystic lung disease. Chest. 2016;149(5):1223–33.
10. Baqir M, Moua T, White D, Eunhee SY, Ryu JH. Pulmonary nodular and cystic light chain deposition disease: a retrospective review of 10 cases. Respir Med. 2020;164:105896.
11. Jeong YJ, Lee KS, Chung MP, Han J, Chung MJ, Kim K-I, et al. Amyloidosis and lymphoproliferative disease in Sjögren syndrome: thin-section computed tomography findings and histopathologic comparisons. J Comput Assist Tomogr. 2004;28(6):776–81.
12. Gillmore JD, Wechalekar A, Bird J, Cavenagh J, Hawkins S, Kazmi M, et al. Guidelines on the diagnosis and investigation of AL amyloidosis. Br J Haematol. 2015;168(2):207–18.
13. Rho L, Qiu L, Strauchen JA, Gordon RE, Teirstein AS. Pulmonary manifestations of light chain deposition disease. Respirology. 2009;14(5):767–70.
14. Colombat M, Stern M, Groussard O, Droz D, Brauner M, Valeyre D, et al. Pulmonary cystic disorder related to light chain deposition disease. Am J Respir Crit Care Med. 2006;173(7):777–80.
15. Saraya T, Fujiwara M, Mikura S, Fukuda N, Ishii H, Takizawa H. Answer found in a blowing sound: Amphoric breathing due to cyst formation in pulmonary adenocarcinoma. Intern Med. 2019;58(3):423–5.

16. Misago N, Kimura T, Narisawa Y. Fibrofolliculoma/trichodiscoma and fibrous papule (perifollicular fibroma/angiofibroma): a revaluation of the histopathological and immunohistochemical features. J Cutan Pathol. 2009;36(9):943–51.
17. Nathan N, Burke K, Moss J, Darling T. A diagnostic and management algorithm for individuals with an isolated skin finding suggestive of tuberous sclerosis complex. Br J Dermatol. 2017;176(1):220–3.
18. Vassallo R, Ryu JH, Schroeder DR, Decker PA, Limper AH. Clinical outcomes of pulmonary Langerhans'-cell histiocytosis in adults. N Engl J Med. 2002;346(7):484–90.
19. Schreml S, Szeimies R-M, Vogt T, Landthaler M, Schroeder J, Babilas P. Cutaneous amyloidoses and systemic amyloidoses with cutaneous involvement. Eur J Dermatol. 2010;20(2):152–60.
20. Gupta N, Finlay GA, Kotloff RM, Strange C, Wilson KC, Young LR, et al. Lymphangioleiomyomatosis diagnosis and management: high-resolution chest computed tomography, Transbronchial lung biopsy, and pleural disease management. An official American Thoracic Society/Japanese respiratory society clinical practice guideline. Am J Respir Crit Care Med. 2017;196(10):1337–48.
21. Young LR, VanDyke R, Gulleman PM, Inoue Y, Brown KK, Schmidt LS, et al. Serum vascular endothelial growth factor-D prospectively distinguishes lymphangioleiomyomatosis from other diseases. Chest. 2010;138(3):674–81.
22. Strimlan CV, Rosenow EC III, Weiland LH, Brown L. Lymphocytic interstitial pneumonitis: review of 13 cases. Ann Intern Med. 1978;88(5):616–21.
23. Dispenzieri A, Kyle R, Merlini G, Miguel J, Ludwig H, Hajek R, et al. International myeloma working group guidelines for serum-free light chain analysis in multiple myeloma and related disorders. Leukemia. 2009;23(2):215–24.
24. Katzmann JA. Screening panels for monoclonal gammopathies: time to change. Clin Biochem Rev. 2009;30(3):105.
25. Nasr SH, Valeri AM, Cornell LD, Fidler ME, Sethi S, D'Agati VD, et al. Renal monoclonal immunoglobulin deposition disease: a report of 64 patients from a single institution. Clin J Am Soc Nephrol. 2012;7(2):231–9.
26. Boone PM, Scott RM, Marciniak SJ, Henske EP, Raby BA. The genetics of pneumothorax. Am J Respir Crit Care Med. 2019;199(11):1344–57.
27. Northrup H, Krueger DA, Roberds S, Smith K, Sampson J, Korf B, et al. Tuberous sclerosis complex diagnostic criteria update: recommendations of the 2012 international tuberous sclerosis complex consensus conference. Pediatr Neurol. 2013;49(4):243–54.
28. Paciocco G, Uslenghi E, Bianchi A, Mazzarella G, Roviaro GC, Vecchi G, et al. Diffuse cystic lung diseases: correlation between radiologic and functional status. Chest. 2004;125(1):135–42.
29. Avila NA, Chen CC, Chu SC, Wu M, Jones EC, Neumann RD, et al. Pulmonary lymphangioleiomyomatosis: correlation of ventilation-perfusion scintigraphy, chest radiography, and CT with pulmonary function tests. Radiology. 2000;214(2):441–6.
30. Koyama M, Johkoh T, Honda O, Tsubamoto M, Kozuka T, Tomiyama N, et al. Chronic cystic lung disease: diagnostic accuracy of high-resolution CT in 92 patients. Am J Roentgenol. 2003;180(3):827–35.
31. Sundaram B, Gross BH, Martinez FJ, Oh E, Müller NL, Schipper M, et al. Accuracy of high-resolution CT in the diagnosis of diffuse lung disease: effect of predominance and distribution of findings. Am J Roentgenol. 2008;191(4):1032–9.
32. Gupta N, Meraj R, Tanase D, James LE, Seyama K, Lynch DA, et al. Accuracy of chest high-resolution computed tomography in diagnosing diffuse cystic lung diseases. Eur Respir J. 2015;46(4):1196–9.
33. Araki T, Nishino M, Gao W, Dupuis J, Putman RK, Washko GR, et al. Pulmonary cysts identified on chest CT: are they part of aging change or of clinical significance? Thorax. 2015;70(12):1156–62.
34. Farooqi AO, Cham M, Zhang L, Beasley MB, Austin JH, Miller A, et al. Lung cancer associated with cystic airspaces. Am J Roentgenol. 2012;199(4):781–6.

35. Tan Y, Gao J, Wu C, Zhao S, Yu J, Zhu R, et al. CT characteristics and pathologic basis of solitary cystic lung cancer. Radiology. 2019;291(2):495–501.
36. Mascalchi M, Attinà D, Bertelli E, Falchini M, Vella A, Pegna AL, et al. Lung cancer associated with cystic airspaces. J Comput Assist Tomogr. 2015;39(1):102–8.
37. Fintelmann FJ, Brinkmann JK, Jeck WR, Troschel FM, Digumarthy SR, Mino-Kenudson M, et al. Lung cancers associated with cystic airspaces: natural history, pathologic correlation, and mutational analysis. J Thorac Imaging. 2017;32(3):176–88.
38. Escalon JG, Richards JC, Koelsch T, Downey GP, Lynch DA. Isolated cystic lung disease: an algorithmic approach to distinguishing Birt-Hogg-Dubé syndrome, Lymphangioleiomyomatosis, and lymphocytic interstitial pneumonia. Am J Roentgenol. 2019;212(6):1260–4.
39. Suzuki K, Seyama K, Ebana H, Kumasaka T, Kuwatsuru R. Quantitative analysis of cystic lung diseases by use of paired inspiratory and expiratory CT: estimation of the extent of cyst-airway communication and evaluation of diagnostic utility. Radiology: Cardiothorac Imag. 2020;2(2):e190097.
40. Hare S, Souza C, Bain G, Seely J, Frcpc, Gomes M, et al. The radiological spectrum of pulmonary lymphoproliferative disease. Br J Radiol. 2012;85(1015):848–64.
41. Sheard S, Nicholson A, Edmunds L, Wotherspoon A, Hansell D. Pulmonary light-chain deposition disease: CT and pathology findings in nine patients. Clin Radiol. 2015;70(5):515–22.
42. Vassallo R, Jensen EA, Colby TV, Ryu JH, Douglas WW, Hartman TE, et al. The overlap between respiratory bronchiolitis and desquamative interstitial pneumonia in pulmonary Langerhans cell histiocytosis: high-resolution CT, histologic, and functional correlations. Chest. 2003;124(4):1199–205.
43. Czeyda-Pommersheim F, Hwang M, Chen SS, Strollo D, Fuhrman C, Bhalla S. Amyloidosis: modern cross-sectional imaging. Radiographics. 2015;35(5):1381–92.
44. Konno S, Shigemura M, Ogi T, Shimizu K, Suzuki M, Kaga K, et al. Clinical course of histologically proven multifocal micronodular pneumocyte hyperplasia in tuberous sclerosis complex: a case series and comparison with lymphangiomyomatosis. Respiration. 2018;95(5):310–6.
45. Aubry M-C, Myers JL, Colby TV, Leslie KO, Tazelaar HD. Endometrial stromal sarcoma metastatic to the lung: a detailed analysis of 16 patients. Am J Surg Pathol. 2002;26(4):440–9.
46. McCormack FX, Gupta N, Finlay GR, Young LR, Taveira-DaSilva AM, Glasgow CG, et al. Official American Thoracic Society/Japanese respiratory society clinical practice guidelines: lymphangioleiomyomatosis diagnosis and management. Am J Respir Crit Care Med. 2016;194(6):748–61.
47. Campbell S, Uzzo RG, Allaf ME, Bass EB, Cadeddu JA, Chang A, et al. Renal mass and localized renal cancer: AUA guideline. J Urol. 2017;198(3):520–9.
48. Stamatakis L, Metwalli AR, Middelton LA, Linehan WM. Diagnosis and management of BHD-associated kidney cancer. Familial Cancer. 2013;12(3):397–402.
49. Sheard S, Moser J, Sayer C, Stefanidis K, Devaraj A, Vlahos I. Lung cancers associated with cystic airspaces: underrecognized features of early disease. Radiographics. 2018;38(3):704–17.
50. Gottumukkala RV, Fintelmann FJ, Keane FK, Shepard J-AO. Cystic lesions on lung Cancer screening chest computed tomography: when should we be concerned? Ann Am Thorac Soc. 2018;15(2):263–5.
51. Lee HJ, Ahn B-C, Lee S-W, Lee J. The usefulness of F-18 fluorodeoxyglucose positron emission tomography/computed tomography in patients with Langerhans cell histiocytosis. Ann Nucl Med. 2012;26(9):730–7.
52. Krajicek BJ, Ryu JH, Hartman TE, Lowe VJ, Vassallo R. Abnormal fluorodeoxyglucose PET in pulmonary Langerhans cell histiocytosis. Chest. 2009;135(6):1542–9.
53. Baqir M, Lowe V, Eunhee SY, Ryu JH. 18F-FDG PET scanning in pulmonary amyloidosis. J Nucl Med. 2014;55(4):565–8.
54. Keraen J, Blanc E, Besson FL, Leguern V, Meyer C, Henry J, et al. Usefulness of 18F-labeled Fluorodeoxyglucose–positron emission tomography for the diagnosis of lymphoma in primary Sjögren's syndrome. Arthritis Rheumatol. 2019;71(7):1147–57.
55. Tazi A. Adult pulmonary Langerhans' cell histiocytosis. Eur Respir J. 2006;27(6):1272–85.

56. Fruchter O, Fridel L, El Raouf BA, Abdel-Rahman N, Rosengarten D, Kramer MR. Histological diagnosis of interstitial lung diseases by cryo-transbronchial biopsy. Respirology. 2014;19(5):683–8.
57. Babiak A, Hetzel J, Krishna G, Fritz P, Moeller P, Balli T, et al. Transbronchial cryobiopsy: a new tool for lung biopsies. Respiration. 2009;78(2):203–8.
58. Furuya M, Tanaka R, Koga S, Yatabe Y, Gotoda H, Takagi S, et al. Pulmonary cysts of Birt-Hogg-Dubé syndrome: a clinicopathologic and immunohistochemical study of 9 families. Am J Surg Pathol. 2012;36(4):589–600.
59. Smith ML, Gotway MB, Larsen BT, Colby TV, Tazelaar HD, Leslie KO. Pathologic approach to cystic lung disease. AJSP Rev Rep. 2017;22(1):36–45.
60. Gupta N, Langenderfer D, McCormack FX, Schauer DP, Eckman MH. Chest computed tomographic image screening for cystic lung diseases in patients with spontaneous pneumothorax is cost effective. Ann Am Thorac Soc. 2017;14(1):17–25.
61. Krueger DA, Northrup H, Roberds S, Smith K, Sampson J, Korf B, et al. Tuberous sclerosis complex surveillance and management: recommendations of the 2012 international tuberous sclerosis complex consensus conference. Pediatr Neurol. 2013;49(4):255–65.
62. Ryu JH, Hartman TE, Torres VE, Decker PA. Frequency of undiagnosed cystic lung disease in patients with sporadic renal angiomyolipomas. Chest. 2012;141(1):163–8.
63. Nakazawa A, Cox NS, Holland AE. Current best practice in rehabilitation in interstitial lung disease. Therapeut Adv Respir Dis. 2017;11(2):115–28.
64. Araujo MS, Baldi BG, Freitas CS, Albuquerque AL, da Silva CCM, Kairalla RA, et al. Pulmonary rehabilitation in lymphangioleiomyomatosis: a controlled clinical trial. Eur Respir J. 2016;47(5):1452–60.
65. Gupta N, Kopras EJ, Henske EP, James LE, El-Chemaly S, Veeraraghavan S, et al. Spontaneous pneumothoraces in patients with Birt–Hogg–Dubé syndrome. Ann Am Thorac Soc. 2017;14(5):706–13.
66. Singla A, Kopras EJ, Gupta N. Spontaneous pneumothorax and air travel in pulmonary Langerhans cell histiocytosis: a patient survey. Respir Investig. 2019;57(6):582–9.
67. Weill D, Benden C, Corris PA, Dark JH, Davis RD, Keshavjee S, et al. A consensus document for the selection of lung transplant candidates: 2014 – an update from the pulmonary transplantation Council of the International Society for heart and lung transplantation. J Heart Lung Transplant. 2015;34(1):1–15.
68. Godden DJ, Currie G, Denison D, Farrell P, Ross JA, Stephenson R, et al. British Thoracic Society guidelines on respiratory aspects of fitness for diving. Thorax. 2003;58(1):3–13.
69. Taveira-DaSilva AM, Steagall WK, Rabel A, Hathaway O, Harari S, Cassandro R, et al. Reversible airflow obstruction in lymphangioleiomyomatosis. Chest. 2009;136(6):1596–603.
70. Tazi A, De Margerie C, Naccache JM, Fry S, Dominique S, Jouneau S, et al. The natural history of adult pulmonary Langerhans cell histiocytosis: a prospective multicentre study. Orphanet J Rare Dis. 2015;10(1):30.
71. Bissler JJ, McCormack FX, Young LR, Elwing JM, Chuck G, Leonard JM, et al. Sirolimus for angiomyolipoma in tuberous sclerosis complex or lymphangioleiomyomatosis. N Engl J Med. 2008;358(2):140–51.
72. Bissler JJ, Kingswood JC, Radzikowska E, Zonnenberg BA, Frost M, Belousova E, et al. Everolimus for angiomyolipoma associated with tuberous sclerosis complex or sporadic lymphangioleiomyomatosis (EXIST-2): a multicentre, randomised, double-blind, placebo-controlled trial. Lancet. 2013;381(9869):817–24.
73. Grobost V, Khouatra C, Lazor R, Cordier J-F, Cottin V. Effectiveness of cladribine therapy in patients with pulmonary Langerhans cell histiocytosis. Orphanet J Rare Dis. 2014;9(1):191.
74. Epaud R, Le Pointe HD, Fasola S, Ploussard S, Delestrain C, Sileo C, et al. Cladribine improves lung cysts and pulmonary function in a child with histiocytosis. Eur Respir J. 2015;45(3):831–3.
75. Lorillon G, Bergeron A, Detourmignies L, Jouneau S, Wallaert B, Frija J, et al. Cladribine is effective against cystic pulmonary Langerhans cell histiocytosis. Am J Respir Crit Care Med. 2012;186(9):930–2.

76. Haroche J, Cohen-Aubart F, Emile J-F, Arnaud L, Maksud P, Charlotte F, et al. Dramatic efficacy of vemurafenib in both multisystemic and refractory Erdheim-Chester disease and Langerhans cell histiocytosis harboring the BRAF V600E mutation. Blood. 2013;121(9):1495–500.
77. Swigris JJ, Berry GJ, Raffin TA, Kuschner WG. Lymphoid interstitial pneumonia: a narrative review. Chest. 2002;122(6):2150–64.
78. Dufour V, Wislez M, Bergot E, Mayaud C, Cadranel J. Improvement of symptomatic human immunodeficiency virus-related lymphoid interstitial pneumonia in patients receiving highly active antiretroviral therapy. Clin Infect Dis. 2003;36(10):e127–e30.
79. Palladini G, Merlini G. What is new in diagnosis and management of light chain amyloidosis? Blood. 2016;128(2):159–68.
80. Trotman-Dickenson B. Congenital lung disease in the adult: guide to the evaluation and management. J Thorac Imaging. 2015;30(1):46–59.
81. Khawar MU, Yazdani D, Zhu Z, Jandarov R, Dilling DF, Gupta N. Clinical outcomes and survival following lung transplantation in patients with lymphangioleiomyomatosis. J Heart Lung Transplant. 2019;38(9):949–55.
82. Wajda N, Zhu Z, Jandarov R, Dilling DF, Gupta N. Clinical outcomes and survival following lung transplantation in patients with pulmonary Langerhans cell histiocytosis. Respirology. 2019 Jun;25(6):644–50.
83. Hirschi S, Colombat M, Kessler R, Reynaud-Gaubert M, Stern M, Chenard MP, et al. Lung transplantation for advanced cystic lung disease due to nonamyloid kappa light chain deposits. Ann Am Thorac Soc. 2014;11(7):1025–31.
84. Boehler A. Editor lung transplantation for cystic lung diseases: lymphangioleiomyomatosis, histiocytosis x, and sarcoidosis. Semin Respir Crit Care Med. 2001;22(5):509–16.
85. Benden C, Rea F, Behr J, Corris PA, Reynaud-Gaubert M, Stern M, et al. Lung transplantation for lymphangioleiomyomatosis: the European experience. J Heart Lung Transplant. 2009;28(1):1–7.
86. Collins J, Hartman MJ, Warner TF, Muller NL, Kazerooni EA, McAdams HP, et al. Frequency and CT findings of recurrent disease after lung transplantation. Radiology. 2001;219(2):503–9.
87. Fragkioudaki S, Mavragani CP, Moutsopoulos HM. Predicting the risk for lymphoma development in Sjogren syndrome: an easy tool for clinical use. Medicine. 2016;95(25):e3766.
88. Cottin V, Harari S, Humbert M, Mal H, Dorfmüller P, Jaïs X, et al. Pulmonary hypertension in lymphangioleiomyomatosis: characteristics in 20 patients. Eur Respir J. 2012;40(3):630–40.
89. Le Pavec J, Lorillon G, Jaïs X, Tcherakian C, Feuillet S, Dorfmüller P, et al. Pulmonary Langerhans cell histiocytosis-associated pulmonary hypertension: clinical characteristics and impact of pulmonary arterial hypertension therapies. Chest. 2012;142(5):1150–7.
90. Wu X, Xu W, Wang J, Tian X, Tian Z, Xu K. Clinical characteristics in lymphangioleiomyomatosis-related pulmonary hypertension: an observation on 50 patients. Front Med. 2019;13(2):259–66.
91. Menko FH, Van Steensel MA, Giraud S, Friis-Hansen L, Richard S, Ungari S, et al. Birt-Hogg-Dubé syndrome: diagnosis and management. Lancet Oncol. 2009;10(12):1199–206.
92. Gupta N, Seyama K, McCormack FX. Pulmonary manifestations of Birt-Hogg-Dubé syndrome. Familial Cancer. 2013;12(3):387–96.
93. Shiboski CH, Shiboski SC, Seror R, Criswell LA, Labetoulle M, Lietman TM, et al. 2016 American College of Rheumatology/European league against rheumatism classification criteria for primary Sjögren's syndrome: a consensus and data-driven methodology involving three international patient cohorts. Ann Rheum Dis. 2017;76(1):9–16.
94. Travis WD, Costabel U, Hansell DM, King TE Jr, Lynch DA, Nicholson AG, et al. An official American Thoracic Society/European Respiratory Society statement: update of the international multidisciplinary classification of the idiopathic interstitial pneumonias. Am J Respir Crit Care Med. 2013;188(6):733–48.
95. Obaidat B, Yazdani D, Wikenheiser-Brokamp KA, Gupta N. Diffuse cystic lung diseases. Respir Care. 2020;65(1):111–26.

Index

N. Gupta et al. (eds.), *Diffuse Cystic Lung Diseases*, Respiratory Medicine,
https://doi.org/10.1007/978-3-030-63365-3